STRESS-DEFORMATION THEORIES FOR THE ANALYSIS OF STEEL BEAMS REINFORCED WITH GFRP PLATES

By

Phe Pham Van

A thesis submitted to the University of Ottawa
in partial fulfillment of the requirements for
Masters of Applied Science in Civil Engineering

Department of Civil Engineering
Faculty of Engineering
University of Ottawa

Abstract

A theory is developed for the analysis of composite systems consisting of steel wide flange sections reinforced with GFRP plates connected to one of the flanges through a layer of adhesive. The theory is based on an extension of the Gjelsvik theory and thus incorporates local and global warping effects but omits shear deformation effects. The theory captures the longitudinal transverse response through a system of three coupled differential equations of equilibrium and the lateral-torsional response through another system of three coupled differential equations. Closed form solutions are developed and a super-convergent finite element is formulated based under the new theory.

A comparison to 3D FEA results based on established solid elements in Abaqus demonstrates the validity of the theory when predicting the longitudinal-transverse response, but showcases its shortcomings in predicting the torsional response of the composite system. The comparison sheds valuable insight on means of improving the theory.

A more advanced theory is subsequently developed based on enriched kinematics which incorporates shear deformation effects. The shear deformable theory captures the longitudinal-transverse response through a system of four coupled differential equations of equilibrium and the lateral-torsional response through another system of six coupled differential equations.

A finite difference approximation is developed for the new theory and a new finite element formulation is subsequently to solve the new system of equations. A comparison to 3D FEA illustrates the validity of the shear deformable theory in predicting the longitudinal-transverse response as well as the lateral-torsional response.

Both theories are shown to be computationally efficient and reduce the modelling and running time from several hours per run to a few minutes or seconds while capturing the essential features of the response of the composite system.

Acknowledgements

My special thanks go to my supervisor Professor Magdi Mohareb for his great support, advice, and patience. With his academic excellence and fun character, I always believe him and try my best to become a person like him in future.

My master program is fully supported by a program of Vietnamese Government named "Project 322". The financial support is greatly acknowledged. It motivates me to have contribution to the development of my home country in future.

I would like to thank to the Department of Civil Engineering for financial support via teaching assistant positions.

My deep thanks go to my family for their moral support. The patience and sacrifice of my mothers, my fathers, my older brother's small family, my wife throughout my study are forever in my heart.

My deepest thanks go to my 2-year-old son- Lam Pham-Thanh. I miss him every second during my study abroad. His smile and innocent speaking give me responsibility and strength to overcome any difficulty.

TABLE OF CONTENT

CHAPTER 1–INTRODUCTION

TABLE OF CONTENT

CHAPTER 4–

VALIDATION OF RESULTS BASED ON NON-SHEAR DEFORMABLE THEORY

CHAPTER 5–SHEAR DEFORMABLE THEORY-FORMULATION

TABLE OF CONTENT

CHAPTER 8–VALIDATION OF RESULTS FOR SHEAR-DEFORMABLE THEORY

CHAPTER 9 – SUMMARY, CONCLUSIONS AND RECOMMENDATIONS

APPENDIX A5–SHAPE FUNCTION PLOTS FOR LONGITUDINAL–TRANSVERSE RESPONSE

APPENDIX A6–SHEAR DEFORMABLE THEORY–TOTAL POTENTIAL ENERGY

APPENDIX A7– SHEAR DEFORMABLE THEORY-VARIATION AND INTEGRATION BY PARTS OF THE TOTAL POTENTIAL ENERGY

APPENDIX A8 – SHEAR DEFORMABLE THEORY-FORMULATION OF STIFFNESS MATRICES

APPENDIX B1 – PROGRAMMING OF PROBLEM 1 IN CHAPTER 4

APPENDIX B2 – PROGRAMMING OF PROBLEM 2 IN CHAPTER 4

APPENDIX B3 – PROGRAMMING OF PROBLEMS 3 AND 4 IN CHAPTER 4

APPENDIX B4 – PROGRAMMING OF PROBLEM 1 IN CHAPTER 8

TABLE OF CONTENT

LIST OF FIGURES

Introduced in Chapter 2

Introduced in Chapter 4

LIST OF FIGURES

LIST OF TABLES

LIST OF SYMBOLS

Introduced in Chapter 2

A_a, A_b, A_p	: Cross-section area of the adhesive layer, wide flange beam and GFRP plate, respectively.
$A_{1i}, A_{2i}, A_{3i}, A_{4i}, A_{5i}, A_{6i}$	: Assumed constants of the displacement roots $W_b, W_p, V, U_b, U_p, \theta$ respectively obtained from equilibrium equation system and boundary conditions.
$\{a_a\}_{6\times1}$	: A vector of constants c_1, c_2, c_3 and *x*- coordinate.
$\{a_{a1}\}_{3\times1}$	: A vector of constants c_1, c_2, c_3
$B(0), B(L)$	: Resultant bi-moments at $z-$coordinates 0 and L, respectively.
$B_{i,i=\overline{1,12}}$	: Constant factors of equilibrium equation system as defined in Appendix A3.
b_b	: Flange width of the wide flange beam.
b_p	: Width of the GFRP plate and Adhesive layer.
$C_1,\ldots,C_8$	: Eight integration constants of in-plane governing displacement functions
$Cnsz$	: A local coordinate system within the thin-walled member, where C is on the contour of cross-section, n – axis is normal to tangent of contour at Point C, s – axis coincides with tangent at point C, and z – axis is parallel to Z – axis.
$C_a n_a s_a z$	: A local coordinate system within the adhesive layer, where C_a is on the contour of cross-section, n_a – axis is normal to tangent of contour at Point C_a, s_a – axis coincides with tangent at point C_a, and z – axis is parallel to Z – axis.
$C_b n_b s_b z$	: A local coordinate system within the beam, where C_b is on the contour of cross-section, n_b – axis is normal to tangent of contour at Point C_b, s_b – axis coincides with tangent at point C_b, and z – axis is parallel to Z – axis.
$C_p n_p s_p z$	: A local coordinate system within the GFRP plate, where C_p is on the contour of cross-section, n_p – axis is normal to tangent of contour at Point C_p, s_p – axis coincides with tangent at point C_p, and z – axis is parallel to Z – axis.
c_1, c_2, c_3	: Constants determined as in Eq.(2.34).

LIST OF SYMBOLS

D	: Symbol of first derivative with respect to *z*.
$D_1,\ldots,D_{12}$	: Twelve integration constants in out-of-plane governing displacement functions
E_a, E_b, E_p	: Modules of elasticity of adhesive, wide flange beam, GFRP plate, respectively.
G_a, G_b, G_p	: Shear modules of adhesive, wide flange beam, GFRP plate, respectively.
$\left[H_{a1}\right]_{2\times 2}, \left[H_{a2}\right]_{3\times 3}, \left[H_{a4}\right]_{3\times 3}$	: Matrices derived from expression of internal strain energy of adhesive layer as in the item 2.5.5.2.
$\left\{H_{a3}\right\}_{2\times 1}$	: A vector derived from expression of internal strain energy of adhesive layer as in the item 2.5.5.2.
h	: Total height of cross-section of the beam.
h_b	: Height taken from the center line of top flange to that of bottom flange of cross-section of the wide flange beam.
I_{yya}	: Moment of inertia of cross-section of the adhesive layer about Y_a-axis.
I_{xxb}, I_{yyb}	: Moments of inertia of cross section of the wide flange beam about *Y*- axis, *X*-axis, respectively.
I_{xxp}, I_{yyp}	: Moments of inertia of cross section of the GFRP plate about X_p- axis, Y_p-axis, respectively.
$I_{\omega\omega b}$	: Warping constant of cross-section of the wide flange beam.
$I_{\omega\omega p}$	: Warping constant of cross-section of the GFRP plate.
J_a	: Torsion constant of cross-section of the adhesive layer.
J_b	: St. Venant torsion constant of cross-section of the wide flange beam.
J_p	: St. Venant torsion constant of cross-section of the GFRP plate.
$k_i (i = 5,\ldots,10)$	: Non-zero roots of characteristic equation defined in A3.45 of Appendix A3.
L	: Length of the member.
$M_x(0), M_x(L)$	: Resultant moments about $X-$direction at $z-$coordinates 0 and L, respectively.
$M_y(0), M_y(L)$	: Resultant moments about $Y-$direction at $z-$coordinates 0 and L, respectively.
m_1, m_2	: Non-zero roots of characteristic equation defined in Eq. A3.5 of Appendix A3.
$N(0), N(L)$	: Longitudinal resultant forces at $z-$coordinates 0 and L, respectively.

LIST OF SYMBOLS

$OXYZ$: Global coordinate system used for general case and for wide flange beam cross-section.

$O_p X_p Y_p Z_p$: Global coordinate system used for GFRP plate cross-section.

$O_a X_a Y_a$: In-plane coordinate system used for adhesive cross-section.

$p_u(s_b, n_b, z), p_v(s_b, n_b, z), p_z(s_b, n_b, z)$: Tractions applied to the wide flange beam in $n-, s-, z-$ directions, respectively.

$Q_x(0), Q_x(L)$: Resultant forces in $X-$direction at $z-$coordinates 0 and L, respectively.

$Q_y(0), Q_y(L)$: Resultant forces in $Y-$direction at $z-$coordinates 0 and L, respectively.

$q(s)$: Distance from the Pole P to the line normal to tangent of contour at point C.

$q_{zb}(z), q_{xb}(z), q_{yb}(z), m_{zb}(z)$: Distributed line loads defined in Eq. (2.43).

$r(s)$: Distance from the Pole P to the tangent of contour at point C.

$T(0), T(L)$: Resultant moments about $Z-$direction at $z-$coordinates 0 and L, respectively.

t_1 : Thickness of the GFRP plate.

t_2 : Thickness of the Adhesive layer.

t_3 : Thickness of the flanges of wide flange beam.

t_w : Thickness of the web of wide flange beam.

$U(z)$: Lateral displacement of shear center O of a generic cross-section along the X direction.

$U_b(z)$: Lateral displacement of shear center O of wide flange beam.

$\{U_O\}_{3\times1}$: Displacement vector including three displacements $U_b(z),\ U_p(z),\ \theta(z)$

$\{U_L\}_{2\times1}$: Displacement vector including three displacements $W_b(z),\ \mathrm{W}_p(z)$

$U_p(z)$: Lateral displacement of shear center O of GFRP plate.

$u(s,z,n)$: Displacement of an arbitrary Point B within a cross-section along n- axis direction of the $Cnsz$ coordinate system.

$u_a(s_a, n_a, z)$: Displacement of an arbitrary Point B within a cross-section of the adhesive layer along n_a-axis direction of the $C_a n_a s_a z$ coordinate system.

LIST OF SYMBOLS

$u_b(s_b, n_b, z)$: Displacement of an arbitrary Point *B* within a cross-section of the beam along n_b-axis direction of the $C_b n_b s_b z$ coordinate system.

$u_p(s_p, n_p, z)$: Displacement of an arbitrary Point *B* within a cross-section of the GFRP plate along n_p-axis direction of the $C_p n_p s_p z$ coordinate system.

$\bar{u}(s, z)$: Displacement in the direction normal to tangent of contour at point *C*.

$V(z)$: Transversal displacement of shear center *O* of generic cross-section. This is also the transversal displacement of shear center *O* and O_p in problem of GFRP bonded to wide flange beam by weak adhesive.

$v(s, z, n)$: Displacement of an arbitrary Point *B* within a generic cross-section along *s*- axis of *Cnsz* coordinate system.

$\bar{v}(s, z)$: Displacement in the tangent direction of contour at point *C*.

$v_a(s_a, n_a, z)$: Displacement of an arbitrary Point *B* within a cross-section of the adhesive layer along v_a-axis direction of the $C_a n_a s_a z$ coordinate system.

$v_b(s_b, n_b, z)$: Displacement of an arbitrary Point *B* within a cross-section of the beam along v_b-axis direction of the $C_b n_b s_b z$ coordinate system.

$v_p(s_p, n_p, z)$: Displacement of an arbitrary Point *B* within a cross-section of the GFRP plate along v_p-axis direction of the $C_p n_p s_p z$ coordinate system.

$W(z)$: Longitudinal displacement of shear center *O* of a generic cross-section along the *Z* direction.

$W_b(z)$: Longitudinal displacement of shear center *O* of wide flange beam.

$W_p(z)$: Longitudinal displacement of shear center *O* of GFRP plate.

$w(s, z, n)$: Displacement of an arbitrary Point *B* within a generic cross-section along *z*- axis of *Cnsz* coordinate system.

$\bar{w}(s, z)$: Displacement in the z- axis direction at point *C* of contour.

$w_a(s_a, n_a, z)$: Displacement of an arbitrary Point *B* within a cross-section of the adhesive layer along z-axis direction of the $C_a n_a s_a z$ coordinate system.

LIST OF SYMBOLS

$w_b(s_b, n_b, z)$: Displacement of an arbitrary Point *B* within a cross-section of the beam along z-axis direction of the $C_b n_b s_b z$ coordinate system.

$w_p(s_p, n_p, z)$: Displacement of an arbitrary Point *B* within a cross-section of the GFRP plate along z-axis direction of the $C_p n_p s_p z$ coordinate system.

$X\left(s_b, n_b\right)$: *X*- coordinate of an arbitrary Point B_b within the beam. It's a function of $x(s_b), n_b, \alpha(s_b)$.

$Y\left(s_b, n_b\right)$: *Y*- coordinate of an arbitrary Point B_b within the beam. It's a function of $y(s_b), n_b, \alpha(s_b)$.

$x(s), y(s)$: In-plane coordinates of the Point *C* within a generic member in *OXYZ* coordinate system.

$x_a(s_a), y_a(s_a)$: In-plane coordinates of an arbitrary Point D_a within adhesive layer.

$x(s_b), y(s_b)$: In-plane coordinates of the Point *C* within the beam.

x_o, y_o : Coordinates of Pole *P* of a generic member in *OXYZ* coordinate system.

$x_p(s_p), y_p(s_p)$: In-plane coordinates of the Point *C* within GFRP plate.

z : Coordinate of the Point *C* in longitudinal direction.

$\alpha(s)$: Angle between tangent of contour at Point C and positive direction of X axis. This angle is positive if it rotates clockwise about origin *O*.

$\left\{\Delta_{b1}\right\}_{4\times1}$: Vector containing derivatives of displacement fields of the Shear Center *O* as defined in Appendix 1, item A1.1.

$\left\{\Delta_{p1}\right\}_{4\times1}$: Vector containing derivatives of displacement fields of the Shear Center O_p as defined in Appendix 1, item A1.2.

δ : Symbol of the first variation.

ε_{na}, ε_{sa}, ε_{za}, γ_{sza}, γ_{sna}, γ_{zna} : Strain components of a point within adhesive layer in local coordinate system *Cnsz*.

ε_{nb}, ε_{sb}, ε_{zb}, γ_{nsb}, γ_{znb}, γ_{szb} : Strain components of a point within wide flange beam in local coordinate system *Cnsz*.

ε_{np}, ε_{sp}, ε_{zp}, γ_{nsp}, γ_{znp}, γ_{szp} : Strain components of a point within GRFP plate in local coordinate system *Cnsz*.

LIST OF SYMBOLS

$\eta(s,z)$: Transversal displacement of a point *C* of contour in *OXYZ* coordinate system.

$\theta_z(z)$: Rotation angle about *Z*-axis at shear center *O* of cross-section, it is positive when the angle rotates clockwise.

$\xi(s,z)$: Lateral displacement of a point *C* of contour in *OXYZ* coordinate system.

π : Total potential energy.

$\sigma_z(s_b,n_b,0),\sigma_z(s_b,n_b,L)$: Tractions in $z-$direction applied to two cross-sections $Z=0$ and $Z=L$, respectively.

$\tau_u(s_b,n_b,0),\tau_u(s_b,n_b,L)$: Tractions in $n-$direction applied to two cross-sections $Z=0$ and $Z=L$, respectively.

$\tau_v(s_b,n_b,0),\tau_v(s_b,n_b,L)$: Tractions in $s-$direction applied to two cross-sections $Z=0$ and $Z=L$, respectively.

$\omega(s)$: Sectorial area at point C of contour with shear center *O*. The point *C* has an *s* – coordinate from origin C_o and *s* is positive if OC_o rotates clockwise to *OC*.

$\Omega(s,n)$: Total sectorial area of an arbitrary Point B_b within the beam, which includes effects of both global and local warpings.

$\widetilde{U}_a$: Internal strain energy of Adhesive layer.

$\widetilde{U}_{a1}$: Internal strain energy caused by shear strain γ_{sna} within Adhesive layer.

$\widetilde{U}_{a2}$: Internal strain energy caused by shear strain γ_{zna} within Adhesive layer.

$\widetilde{U}_{a3}$: Internal strain energy caused by St. Venant shear strain γ_{szp} within Adhesive layer.

$\widetilde{U}_b$: Internal strain energy of W beam.

$\widetilde{U}_{b1}$: Internal strain energy caused by axial strain within wide flange beam.

$\widetilde{U}_{b2}$: Internal strain energy caused by St. Venant shear strain γ_{szp} within wide flange beam.

$\widetilde{U}_p$: Internal strain energy of GFRP plate.

$\widetilde{U}_{p1}$: Internal strain energy caused by axial strain within GFRP plate.

$\widetilde{U}_{p2}$: Internal strain energy caused by St. Venant shear strain γ_{szp} within GFRP plate.

$\widetilde{V}$: Total load potential energy loss.

LIST OF SYMBOLS

$\tilde{V}_1$: Total load potential energy loss by end tractions.

$\tilde{V}_2$: Total load potential energy loss by member tractions.

Introduced in Chapter 3

$\{\overline{C}\}_{8\times1}$: Vector of eight integration constants in in-plane problem

$\{\overline{D}\}_{12\times1}$: Vector of twelve integration constants in out-of-plane problem

$\left[\overline{H}_{a1}\right]_{3\times3}, \left[\overline{H}_{a2}\right]_{3\times3}$: Matrices of constants c_1, c_2, c_3 defined in the Item 3.2.

$\left[\widetilde{K}_1\right]_{8\times8}, \left[\widetilde{K}_2\right]_{8\times8}, \left[\widetilde{K}_3\right]_{8\times8}$: Element stiffness matrices for longitudinal-transversal response, which are contributed by wide flange beam, GFRP plate and adhesive layer, respectively.

$\left[\widetilde{K}_4\right]_{8\times8}, \left[\widetilde{K}_5\right]_{8\times8}, \left[\widetilde{K}_6\right]_{8\times8}$: Element stiffness matrices for lateral-torsional response, which are contributed by wide flange beam, GFRP plate and adhesive layer, respectively.

$[L_1]_{8\times8}$: Matrices of constants defined in Eq. (3.6)

$[L_2]_{12\times12}$: Matrices of constants defined in Eq. (3.17)

$[N_1(z)]_{4\times8}$: Matrix of shape functions of in-plane problem

$[N_2(z)]_{6\times12}$: Matrix of shape functions of out-of-plane problem

N_{ij} : A shape function located at row i^{th} and column j^{th}

$\{\widetilde{p}_1\}_{3\times1}$: Distributed line load vector defined in 3.3.3.

$\{\widetilde{p}_2\}_{4\times1}$: Distributed line load vector defined in 3.4.3.

$[P_i]_{3\times3}, i = 1,5$: Matrices of constants which are defined in the item 3.2.3.1

$\{\widetilde{Q}_1\}_{8\times1}$: Element load vector for longitudinal-transversal response.

$\{\widetilde{Q}_2\}_{12\times1}$: Element load vector for lateral-torsional response.

$\approx{Q}_{11}, \approx{Q}_{12}$: Nodal load vectors for longitudinal-transversal and lateral-torsional responses, respectively

$\approx{Q}_{21}, \approx{Q}_{22}$: Equivalent load vectors for longitudinal-transversal and lateral-torsional responses, respectively

$[T]_{8\times8}$: A matrix which is defined in the item 3.2.3.1

$[Z_1(z)]_{4\times8}$, $[Z_2(z)]_{4\times12}$: Matrices including elements which are functions of z-coordinate

$\{\Delta_1(z)\}_{3\times1}$: Vector of governing displacement fields defined in Eq. (3.4)

$\{\Delta_2(z)\}_{3\times1}$: Vector of governing displacement fields defined in Eq.(3.15)

$\{\Delta_{1N}\}_{8\times1}$: Element nodal displacement vector defined in Eq.(3.5)

$\{\Delta_{2N}\}_{12\times1}$: Element nodal displacement vector defined in Eq.(3.16)

$\{\rho_1\}_{4\times1},\{\rho_2\}_{4\times1},\{\rho_3\}_{4\times1}$: Unit vectors defined in Eq. (3.8)

$\{\rho_4\}_{4\times1},\{\rho_5\}_{4\times1},\{\rho_6\}_{4\times1}$: Unit vectors defined in Eq. (3.19)

Introduced in Chapters 5 and 6

A_{bw}, A_{bf} : Cross-section area of web and one flange of the wide flange beam, respectively.

$\{a_{a1}\}_{8\times1}$: A vector of constants c_1,c_2,c_3 and *x*- coordinate defined in Eq.(5.19).

$\{a_{a2}\}_{3\times1}$: A vector of constants c_1,c_2,c_3 defined in Eq.(5.19).

$\{a_{a3}(n_a)\}_{6\times1}$: A vector $n_a -$coordinate defined in Eq. (5.19).

$B_1(0), B_1(L)$: Resultant bi-moments corresponding to θ_z' at two member ends, respectively.

$B_2(0), B_2(L)$: Resultant bi-moments corresponding to ψ_b at two member ends, respectively.

$b_b(z), m_{xb}(z), m_{yb}(z), m_{zb}(z), q_{xb}(z), q_{yb}(z), q_{zb}(z)$: Distributed line loads defined in Eq.(5.30)

$b_{b(i)}, m_{xb(i)}, m_{yb(i)}, m_{zb(i)}, q_{xb(i)}, q_{yb(i)}, q_{zb(i)}$: Values of $b_b(z), m_{xb}(z), m_{yb}(z)$, $m_{zb}(z), q_{xb}(z), q_{yb}(z)$, $q_{zb}(z)$ at point i in finite difference solution, respectively.

c_1,c_2,c_3 : Constants defined in Eq.(5.20).

c_4,c_5,c_6 : Constants defined in Eq.(5.20).

$[\widetilde{H}_{a11}]_{4\times4}, [\widetilde{H}_{a12}]_{4\times4}, [\widetilde{H}_{a2}]_{3\times3}, [\widetilde{H}_{a3}]_{6\times6}$: Matrices derived from expression of internal strain energy of adhesive layer as defined in Eq.(5.24).

LIST OF SYMBOLS

h_w : Web height of the wide flange beam.

$I_{xxb1}, I_{yybf}, I_{ssbf}, I_{ssbw}$: Moments of inertia of cross section of the wide flange beam defined in Eq.(5.22).

$I_{\omega\omega bg}, I_{\omega\omega bl}$: Global and local warping constant of cross-section of the wide flange beam, respectively.

$I_{\omega\omega p}$: Warping constant of cross-section of the GFRP plate as defined in Eq.(5.23).

J_b : St. Venant torsion constant of cross-section of the wide flange beam defined in Eq.(5.22).

J_p : St. Venant torsion constant of cross-section of the GFRP plate as defined in Eq.(5.23).

$M_{x1}(0), M_{x1}(L)$: Resultant moments about $X-$direction corresponding to V' at $z-$coordinates 0 and L, respectively.

$M_{x2}(0), M_{x2}(L)$: Resultant moments about $X-$direction corresponding to θ_{xb} at $z-$coordinates 0 and L, respectively.

$M_{y1}(0), M_{y1}(L)$: Resultant moments about $Y-$direction corresponding to U_b' at $z-$coordinates 0 and L, respectively.

$M_{y2}(0), M_{y2}(L)$: Resultant moments about $Y-$direction corresponding to θ_{yb} at $z-$coordinates 0 and L, respectively.

n : Number of intervals selected in finite difference solution.

$U_{b(i)}$: A value of lateral displacement $U_b(z)$ at point i in finite difference solution.

$U_{p(i)}$: A value of lateral displacement $U_p(z)$ at point i in finite difference solution.

$V_{(i)}$: A value of transversal displacement $V(z)$ at point i in finite difference solution.

$W_{b(i)}$: A value of longitudinal displacement $W_b(z)$ at point i in finite difference solution.

$W_p(z)$: Longitudinal displacement of shear center O of GFRP plate.

$W_{p(i)}$: A value of longitudinal displacement $W_p(z)$ at point i in finite difference solution.

Δ :Distance between two continuous points in finite difference solution, defined as $\Delta = L/n$

LIST OF SYMBOLS

$\{\Delta_{a1}\}_{8\times1}$: A vector containing governing displacement fields as defined in Eq. (5.19)

$\{\Delta_{a2}\}_{3\times1}$: Displacement vector including $U_b(z),\ U_p(z),\ \theta(z)$ defined in Eq. (5.19)

$\{\Delta_{a3}\}_{6\times1}$: A vector including $U_b(z),\ U_p(z),\ \theta(z)$ and its derivatives defined in Eq. (5.19)

$\gamma_{sza(i)}$, $\gamma_{sna(i)}$, $\gamma_{zna(i)}$: Values of γ_{sza} , γ_{sna} , γ_{zna} at point i in finite difference solution, respectively.

$\varepsilon_{zb(i)}$, $\gamma_{szb(i)}$: Values of ε_{zb} and γ_{szb} at point i in finite difference solution, respectively.

$\varepsilon_{zp(i)}$, $\gamma_{szp(i)}$: Values of ε_{zp} and γ_{szp} at point i in finite difference solution, respectively.

$\theta_{xb(i)},\theta_{yb(i)}$: Values of $\theta_{xb}(z),\theta_{yb}(z)$ at point i in finite difference solution, respectively.

$\theta_{xp(i)},\theta_{yp(i)}$: Values of $\theta_{xp}(z),\theta_{yp}(z)$ at point i in finite difference solution, respectively.

$\theta_{z(i)}$: Values of $\theta_z(z)$ at point i in finite difference solution.

ψ_b,ψ_p : Functions that characterizes the global warping deformation of the beam and GFRP plate, respectively.

Introduced in chapter 7

$\left[\widetilde{A}_i\right]_{i=1,9}$: Matrices of parameters as defined in Eqs.(7.5) and (7.10).

$\{D_V\}_{4\times1},\{D_{wb}\}_{2\times1},\{D_{wp}\}_{2\times1},\{D_{\theta xb}\}_{2\times1}$: Element nodal displacement vector defined in Eq.(7.3).

$H_1(z),H_2(z),H_3(z),H_4(z)$: Hermitian interpolation shape functions defined in Eq.(7.3).

$\{H(z)\}_{4\times1}$: Vector of Hermitian interpolation shape functions.

$[K_i]_{i=1,10}$: Stiffness matrix components defined in Eq. (7.4).

$\left[\overline{K_i}\right]_{i=1,21}$: Stiffness matrix components defined in Eq.(7.10).

$\left[\overline{\overline{K}}_1\right]_{10\times10}$: Element stiffness matrix for longitudinal-transversal response defined in Eq.(7.8).

$\left[\overline{\overline{K}}_2\right]_{16\times16}$: Element stiffness matrix for lateral-torsional response defined in Eq.(7.13).

$L_1(z),L_2(z)$: Linear shape functions defined in Eq.(7.3).

$\{L(z)\}_{2\times1}$: Vector of linear shape functions $L_1(z),L_2(z)$.

LIST OF SYMBOLS

$\{\overline{Q}_1\}_{8\times1}$: Element load vector for longitudinal-transversal response.

$\{\overline{Q}_2\}_{12\times1}$: Element load vector for lateral-torsional response.

$\overline{\overline{Q}}_{11}, \overline{\overline{Q}}_{12}$: Nodal load vectors for longitudinal-transversal and lateral-torsional responses, respectively.

$\overline{\overline{Q}}_{21}, \overline{\overline{Q}}_{22}$: Equivalent load vectors for longitudinal-transversal and lateral-torsional responses, respectively.

$\{\Delta_1\}_{10\times1}$: Element nodal displacement vector for longitudinal-transversal response.

$\{\Delta_2\}_{16\times1}$: Element nodal displacement vector for lateral-torsional response.

π_1 : Total potential energy for longitudinal-transversal response.

π_2 : Total potential energy for lateral-torsional response.

CHAPTER 1: INTRODUCTION

1.1. Introduction and Motivation

Carbon Fiber Reinforced Plastic (CFRP) and Glass Fiber Reinforced Plastic (GFRP) plates are increasingly being used as retrofit materials for steel members because of their high strength-to-weight ratio, high corrosion resistance, and quick installation. FRP plates are bonded to external surfaces of steel beams to increase their stiffness and strength. Thus, they help improve flexural and shear capacities of steel beams. The main difference between the two materials is that CFRP has a high modulus of elasticity (ranging from 112 GPa to 330 GPa) and is typically used in thin-layers ($1.3-12$ mm), while GFRP materials possess a lower modulus of elasticity (ranging from 17.2 GPa and 13.8 GPa to 42 GPa) and is typically used in thicker layers ($1.5-19$ mm). In a state of the art review, Harris and El Tawil (2008), recognized the potential of FRP as a retrofitting material for structural steel structures and mention that the application of FRP in steel structures is currently in its infancy, much like concrete/FRP application were in the late 1980s.

The reliable analysis of such composite systems presently necessitates the development of time consuming 3D finite element models, and thus represents an obstacle in the effective design of such systems. As such, the development of analytical and numerical analysis tools that are both (a) accurate and (b) relatively simple would be an important step towards the effective design of FRP reinforced steel members.

1.2. Scope of Research

Within the above context, the present thesis aims at developing analytical and numerical solutions for the analysis of composite systems consisting of structural steel beams reinforced with GFRP plate bonded together with an adhesive layer.

1.3. Overview of material properties

Unlike structural steel, FRP material properties exhibit large variability. This is illustrated in Table 1 which provides a summary of mechanical properties of FRP material which are used in researchers' studies. Column (1) lists the relevant references. Column (2) provides the type of FRP. Column (3) provides the modulus of elasticity. The tensile strength of FRP material is listed in the Column (4) while the Poisson ratio is listed in Column (5). Column (6) is the source of information for the mechanical properties of FRP.

Table 1.1 Mechanical properties of FRPs

Reference (1)	Material Type (2)	Young Modulus (GPa) (3)	Tensile Strength (MPa) (4)	Poisson's Ratio (5)	Source (6)
El. Damatty et al. (2003), (2012), (2013)	GFRP (EXTREN500)	17.2; 13.8	206.8	0.33; 0.31	Manufacturer Specifications
Jun Deng et al. (2004)	CFRP	E_3=310 E_1= E_2=10	-	$\nu_{12} = 0.3$ $\nu_{13} = 0.0058$ $\nu_{23} = 0.0058$	Not mentioned
Linghoff et al. (2010)	CFRP 1	200	3300	-	Manufacturer Specification
	CFRP 2	330	1500	-	
	CFRP 3	165	3100	-	
Tavakkolizadeh and Saadtmanesh (2010)	CFRP	144	2137	0.34	Tests
Miller el al. (2001)	CFRP	112	930	0.37	Manufacturer Specifications
Kent and Sherif (2008)	HS-CFRP(*)	166	3048	-	Not mentioned
	HM-CFRP(**)	207	2896	-	
	UHM-CFRP(***)	304	1448	-	
	GFRP	42	896	-	

(*) HS-CFRP: High strength CFRP; (**) HM-CFRP: High modulus CFRP; (***) UHM-CFRP: Ultra-high modulus CFRP

Also, the adhesive material used in bonding steel and FRP exhibit large variability. Table 2 provides a summary of mechanical properties of adhesive materials which are used to bond FRP material to steel beams. Column (1) lists the relevant references. The adhesive designations are given in Column (2). Column (3) lists the modulus of elasticity and shear modulus of adhesive material while Column (5) provides the Poisson's ratio. Columns (4), (6), and (7) are tensile strength, shear strength and peeling strength, respectively. Columns (8) and (9), are virtual spring stiffnesses in shear and peeling directions, respectively, as proposed by Siddique and El Damatty (2013), while Column (10) provides the source of the FRP product. In all studies, the adhesive is considered as an isotropic elastic material.

Table 1.2 Mechanical properties of adhesives

Author (1)	Type (2)	E,G, GPa (3)	σ_f, MPa (4)	ν (5)	σ_{sa}, MPa (6)	σ_{pa}, N/mm^2 (7)	K_s, N/mm^3 (8)	K_p, N/mm^3 (9)	Source (10)
El. Damatty et al. (2003), (2012), (2013)	MA 420	-	-	-	15.5	4.0	21.79	2.26	Manufacturer Tests (K_p, K_s) [7]
Jun Deng et al. (2004)	-	10,-	-	0.3	-	-	-	-	Not mentioned
Linghoff et al. (2010)	Epoxy 1	7,-	25	-	-	-	-	-	Manufacturer
	Epoxy 2	4.5,-	30	-	-	-	-	-	
Miller el al. (2001)	AV8113/ HV8113:	107, 296	-	-	13.8-17.2	-	-	-	Manufacturer
	Plexus MA555:	-	-	-	8.6-10.3	-	-	-	
Kent and Sherif (2008)	High modulus	4.5,-	25	-	24.8	-	-	-	Not mentioned
	Low modulus	0.4,-	4.8	-	9.0	-	-	-	

1.4. Literature Review

The literature review is subdivided into four subtitles: a) Studies aimed at identifying mechanical properties (Section 1.2.1), b) Analytical and computational studies for beams reinforced with GFRP plates (Section 1.2.2), c) Experimental studies on beams reinforced with GFRP plates (Section 1.3), and d) Analytical an computational models for other composite systems (Section 1.2.4).

1.4.1. Review of Studies aimed at Identifying Mechanical Properties

Miller et al. (2001) conducted a study on the application of advanced composites for steel bridge girder rehabilitation. His work involved (1) the selection of rehabilitation materials; (2) the development of an application procedure; (3) the demonstration of the repair effectiveness; and (4) the investigation of the bond between the advanced composite and the steel in terms of force transfer and durability.

A CFRP with a modulus of elasticity of 112 GPa and 5.25 mm thickness was bonded to steel girder by using either the two-part high-strength epoxy Araldite AV8113/ HV8113, provided by Ciba-Geigy Corp., Madison Heights, Mich. (Ciba-Ceigy 1999) with a shear strength of 13.8 – 17.2 MPa, or a methcrylate adhesive ITW Plexus MA555, provided by Danvers, Mass. (ITW 2000) with a shear strength of 8.6 – 10.3 MPa.

The authors provided the rehabilitating steps and requirements in details. Four full-scale bridge girders were investigated to evaluate the effectiveness of the system in terms of stiffness and strength enhancement. The results showed that CFRP retrofit resulted in an increase in the elastic stiffness ranging from 10% to 37%. Also, they resulted in an increase in the ultimate capacity increases of the two girders tested to failure by17% and 25% over the predicted deteriorated capacities. Tensile specimen tests and adhesive shear strength were conducted and force transfer and bond durability were qualified. In conclusion, the authors indicated that the application of CFRP bonded to steel beam was promising as rehabilitation method.

Zhao and Zhang (2007) conducted a comprehensive review of previous research on FRP strengthened steel structures. Four bond testing methods were investigated. In these methods, (i) Loading was indirectly applied to the FRP and the steel plate in a beam, (ii) Loading was directly applied to the steel element without gap, (iii) Loading was directly applied to the steel element with a gap, and (iv) Loading was directly applied to the FRP. The study showed that failure modes depended upon the modulus of elasticity of FRP and adhesive type and thickness. The bond-slip relationship between FRP and steel was also investigated. It was also indicated that strains in FRP and adhesive layers should be carefully quantified when strengthening steel structures with FRP as well as designing new steel structures bonded with FRP.

Harris and El-Tawil (2008) performed another state-of-the-art review on the progress in Steel-FRP composite structural systems. The review concentrated on (1) strengthening steel structures with FRP, (2) stabilizing buckling-critical steel elements with FRP, (3) relieving fatigue or fracture-critical conditions and (4) bonding FRP with steel. They summarized manufacturing information of typical mechanical properties of GFRP, CFRP, adhesive and structural steel.

1.4.2. Review of Analytical and Computational Studies for beams reinforced with GFRP

Taljsten (1997) adopted two elastic analytical models to determine the shearing and peeling stresses of the adhesive layer in a beam strengthened by a plate bonded to its bottom surface. In his first model, it was assumed that (i) the bending stiffness of the beam was much greater than that of the strengthening plate, and thus the bending stiffness of the plate was considered negligible, and (ii) The stresses in the adhesive layer were assumed constant across the thickness. As a result, bending moments of the plate and normal stresses within the adhesive were neglected. Based on these assumptions, expressions for shear stresses along the span were derived using force equilibrium equations. The second model accounted for the bending moments within the plate while adopting the shear stress distribution obtained from the first model to derive an expression for the peeling stresses. An expression for the deflection of the beam was directly derived by using moment-deflection relationship. The deflection function of the plate was obtained from a differential equation for a beam on an elastic foundation. The deflections of the beam and plate obtained were then used to determine the peeling stresses along the span. An example was investigated for a solid rectangular cross-section strengthened with plates bonded at its bottom. The stresses obtained compared well with finite-element solution using ANSYS (1994).

El Damatty and Abushagur (2003) conducted shear lap tests on eight types of adhesive for predicting the shear and peel behaviours of the adhesive systems used to bond steel sections and pultruted GFRP sheets. Test results showed that, in general, methacrylate products achieved the highest load resistance with the highest performance for the MA 420 product. Analytical models were then developed based on beam on elastic foundation analogies in order to quantify the shear and peeling spring stiffnesses from test data. The maximum shear stresses ranged from 20.9 to 34.3 MPa while the maximum peeling stresses ranged from 0.72 to 6.01 MPa.

Jun Deng et al. (2004) performed a stress analysis for the flexural behaviour of simply supported W-steel beams reinforced with CFRP plate. The CFRP was bonded only to the bottom flange of the beam. By writing the equilibrium condition, a mathematical model was developed to determine shear and normal stresses along interfaces of the adhesive layer. The model was based on force equilibrium of CFRP, steel and adhesive elements. The assumptions made were: (i) all materials were linearly elastic, (ii) plane sections remained plane, (iii) the shear and the normal stresses in the adhesive layer did not vary throughout the thickness, (iv) shear deformations in the CFRP plate and steel beams were neglected, (v) bending deformations of the adhesive were neglected, and (vi) in calculating the interfacial shear stress, bending of the CFRP plate was ignored, while it was included when calculating the interfacial normal stress. Comparisons with experimental results have shown good agreement. The model was validated by comparisons with a shell based FEA using the S4R shell elements in ABAQUS.

Linghoff et al. (2010) and Linghoff and Al-Emrani (2010) determined the performance of steel beams strengthened with CFRP laminates using laboratory tests, a simplified analytical solution and FE analysis. In their simplified analytical solution, four assumptions were made: (i) steel material was assumed to have a linearly-elastic perfectly-plastic response, (ii) both the CFRP and the epoxy were assumed to be linearly elastic until failure, (iii) strain distribution along the depth of the cross-section was assumed to be linear, and (iv) full interaction was assumed between the steel and the laminates, i.e., perfect bond was assumed between the CFRP laminate and the steel substrate.

Siddique and Damatty (2012) developed a finite element model for studying the enhancement of the buckling capacity of steel plates bonded with GFRP plates. The numerical model was based on a 13-node consistent degenerated triangular sub-parametric shell element that was developed by Koziey and Mirza (1997) and was extended to include the effects of geometric and material nonlinearities by Siddique and Damatty. The mid-surfaces of both the steel and GFRP plates were modeled using an assembly of consistent shell elements which was free from the shear-locking. For modeling the adhesive layer, a two-dimensional distributed spring element was formulated to represent the shear behavior and the springs along the transverse direction represented the peeling behavior. As a result, a 26-node contact element was proposed for modeling the adhesive between the steel-GFRP plates.

Siddique and El Damatty (2013) developed a finite element model for analyzing wide flange steel beams bonded with GFRP plates. Members analyzed include W- steel beams strengthened with GFRP plates bonded only to the compression flange covering the entire span. The GFRP plates were manufactured using the pultrusion process and had a tensile-compressive bending strength = 206.8 MPa, flexural modulus = 17,200 MPa, and Poisson's ratio = 0.33. The adhesive used to bond GFRP to steel beam was methacrylate (MA420) with a thickness of 0.79 mm. The shear strength of the adhesive was 15.5 MPa and the peeling strength was 4.0 N/mm, respectively. Four failure modes were observed. These were (i) buckling of the system, (ii) shear failure of the adhesive, (iii) peeling failure of the adhesive, and (iv) GFRP failure. Load improvement factors were developed to quantify the effect of GFRP strengthening, effects of strain hardening of steel, geometric imperfections, residual stresses, and span on the capacities of the retrofitted beams.

1.4.3. Review of Experimental Studies on Composite Beams

El Damatty et al. (2003) experimentally investigated the effect of Glass Fiber Reinforced Plastic (GFRP) sheets on enhancing the flexural capacity of wide flange steel beams. Nineteen millimeter-thick GFRP sheets were bonded both to top and bottom flanges by using the methacrylate adhesive system. Experimental results showed that a steel beam with GFRP sheets provided an increase of about 15% in stiffness, 23% in yielding moment, and 78% in ultimate moment compared to a steel beam without GFRP sheets. The authors also reported an excellent performance of the adhesive layer and observed that failure of the steel beams occurred when the tensile stresses in the GFRP sheet reached their ultimate values.

Tavakkolizadeh and Saadatmanesh (2003) conducted three experiments on composite steel-concrete girders strengthened with CFRP sheets. The CFRP was bonded to the tension flange of the steel beam. The authors observed that: (a) the ultimate load-carrying capacities of the girders significantly increased by 44%, 51%, and 76% respectively for a single layer, three-layer, and five-layer retrofitting systems, and (b) the effect of CFRP bonding on the elastic stiffness of the girders was not significant, given the flexibility of the adhesive.

Schnerch et al. (2006) conducted flexural and tensile experiments to evaluate bond behaviour of wide flange steel beams reinforced with steel plate at the compression flange and CFRP at the bottom flange. His study indicated that the adhesive types tested were able to fully develop the strength of the CFRP.

1.4.4. Analytical and Computational Models for other Composite Systems

Ditaranto (1973) developed a model for the static analysis of three-layer composite beams with a weak middle layer bent in a single plane. A kinematic model was proposed in which the top and bottom layers were assumed to behave as Bernoulli–Euler beams. The principle of minimum total potential energy was used to formulate the equilibrium equations and boundary conditions. By solving the resulting equations, closed form solutions were obtained for the displacement fields.

Based on the principle of stationary total potential energy, Vallabhan et al. (1993) formulated the governing nonlinear equilibrium equations for laminated plates consisting of two thin glass plates bonded together by a thin interlayer subjected to bending. Plane sections initially normal to the mid-surface were assumed to remain plane and normal to the mid-surface during bending for each glass layer but not for the whole unit. Shear strain in the interlayer was linearly interpolated from longitudinal in-plane displacement fields of top and bottom glass layers and vertical deflection of the structure. The bending and membrane internal strain energies for both plates were included in the formulation, whereas for the interlayer, only the shear strain energy was included. Using the finite difference technique, solutions of the resulting coupled nonlinear differential equations were solved numerically. The results of the model were observed to agree well with those based on experimental results.

Suresh and Shive (1999) expressed the dynamic equilibrium equations and boundary conditions for laminated composite open sections based on a first order shear deformable theory. The kinematic assumptions were based on the Gjelsvik theory (Gjelsvik 1981) in order to account for global and local warping effects. The mid-surface in-plane shear deformation effects were neglected while the through-thickness shear strain was incorporated and assumed to have a linear distribution. The internal strain energy for each ply of the laminated composite open sections was derived based on an orthotropic constitutive material model.

Dall'Asta (2001) developed a model for the torsional and flexural analysis of two-layer composite beams with weak shear connection at the interface. A discontinuity of longitudinal displacement fields at the connection plane was assumed while twisting was assumed identical for both layers. The system of equilibrium equations and boundary conditions was derived by using the virtual work principle.

Lee et al. (2002) developed a model for the lateral buckling of I-section composite beams. The assumptions were identical to those in Lee and Lee (2004). The principle of stationary potential energy was applied at the onset of buckling and the equilibrium equations were formulated. A finite element formulation was developed and the results compared well with those of Lin et al. (1996).

Lee and Lee (2004) developed a theory for the flexural-torsional behaviour of thin-walled composite beams. In their paper, basic assumptions regarding to the kinematics of thin-walled composites were (i) the contour of the thin wall beam did not deform in its own plane, (ii) the shear strain γ_{sz} within the middle surface was zero in each element, (iii) the Kirchhoff-Love assumption of the classical plate theory remained valid, and (iv) perfect bond was assumed in between plies. The equilibrium equation system was obtained and a finite element model was developed to numerically solve the problem.

Nowzartash and Mohareb (2005) developed a theory for the analysis of sandwich beams with large cores of soft material, in which the core was assumed to be incompressible in the transverse direction so that the distance between two interfaces remained unchanged throughout deformation. The core layer was treated as a Timoshenko beam. Starting with the principle of minimum potential energy, the authors formulated the governing equations and boundary conditions and developed a finite element solution.

Based on the kinematics assumed in Vallaabhan et al. (1993), Asik and Tezcan (2005) formulated the governing equilibrium equations and associated boundary conditions for laminated glass beams. The internal strain energy of the system consisted of bending and membrane strain components for the glass layers and shear strain energy of the interlayer. Through variational procedures, the authors derived the governing equilibrium equations and boundary conditions. Closed form solutions were provided for specific boundary conditions and comparisons were made with experimental results. Using the finite difference technique, the field equations were also solved for more general nonlinear cases.

Gara et al. (2006) proposed an analytical model for the analysis of two-layer composite beams with relative longitudinal slip and vertical uplift. The governing equations thus consisted of two longitudinal displacement fields and two transverse displacements for both layers.

Girhammar and Pan (2007) developed first-and second-order theories for the analysis of composite beams with deformable shear connectors subjected to distributed transverse and axial loads. Based on the principle of minimum potential energy, the authors formulated the equilibrium equations and boundary conditions. By comparing first order to second order analysis results, the study quantified second order effects due to axial forces.

Koutsawa and Daya (2007) developed a mathematical model for the analysis of three-layer laminated glass beams based on the assumptions that (i) plane sections remained plane and normal to middle surfaces under bending for each glass plies but not for entire cross-section, (ii) the transverse normal stresses were small compared to axial normal stresses, (iii) the transversal displacement of three layers were identical, (iv) no slip was assumed to take place at the interfaces, and (v) the interlayer only transferred shear stresses and its compressive stresses in transverse direction (i.e. the peeling stresses) was negligible. The principle of virtual work was used to obtain the governing differential equations and boundary conditions. The normal stress fields within the upper and lower plies and shear strain within the interlayer were obtained analytically. A simply supported beam subjected to uniform distributed load was analyzed and the results were validated against the solution of Asik and Tezcan (2005).

Challamel (2009), Challamel et al. (2010) and Challamel and Girhammar (2012) investigated the out-of-plane vibration analysis and lateral torsional buckling behaviour of (a) partially composite sandwich beams with faces bonded through a weak shear layer and (b) un-bonded layered beams.

The kinematic assumptions were based on (i) a discontinuity in the lateral and longitudinal displacement fields at the interface; (ii) equal twisting angles for the two components.

Table 1.3 provides a comparative summary of the various theories discussed in section in terms of cross-section geometry, materials involved, type of response, type of analysis, effects accounted within the assumed kinematics, the formulation type and/or variational principle, and solution types.

1.5. Scope of the present study

The present study develops two theories predicting the static response of steel wide flange beam reinforced with GFRP plate which captures the effects of warping and shear deformations. The effect of local warping is dominant in thick walled beams such as those having a rectangular, or circular cross-section, while the effects of local and global warping are important in thin-walled beams. For a composite system consisting of FRP plate, adhesive layer, and thin walled beam, both types of warping should be incorporated into the analysis.

The effect of shear deformation is quantified by comparing the results of the first theory which neglects the effect of shear deformation and the second theory which incorporates the effect of shear deformation. Both theories capture the longitudinal transverse response as well as the lateral torsional response. Closed form solutions are obtained for the non-shear deformable theory, while a finite difference solution is developed for shear deformable theory. In addition a finite element formulation is developed under both theories.

Table 1.3 Comparative Review of analytical and computation studies on composite systems (1)

Source	Cross-section Geometry	Materials	Longitudinal transverse response	Lateral torsional response	Types of Analysis				Effects				Formulation type/Variational principle				Solution types		
					Linear	Dynamic	Buckling	Non-linear	Global warping	Local warping	In-plane shear deformation	Through-thickness shear deformation	Virtual work	Total potential energy	Hamilton functional	Direct Force Equilibrium	Closed-Form	Finite Difference	Finite Element
Taljsten, 1997	T or R +R	General	✓	-	✓	-	-	-	-	-	-	-	-	-	-	✓	✓	-	-
Deng et al., 2004	W+R	S+ CFRP	✓	-	✓	-	-	-	-	-	-	-	-	-	-	✓	✓	✓	-

Table 1.3 Comparative Review of analytical and computation studies on composite systems (2)

Source	Cross-section Geometry	Materials	Longitudinal transverse response	Lateral torsional response	Types of Analysis				Effects				Formulation type/Variational principle				Solution types		
					Linear	Dynamic	Buckling	Non-linear	Global warping	Local warping	In-plane shear deformation	Through-thickness shear deformation	Virtual work	Total potential energy	Hamilton functional	Direct Force Equilibrium	Closed-Form	Finite Difference	Finite Element
Linghoff et al. 2010	W+R	Steel + CFRP	✓	-	✓	-	-	✓	-	-	-	-	-	-	-	✓	✓	-	✓
Siddique and El Damatty, 2012	P+P	GFRP + S	N/A		✓	-	✓	✓	N/A		✓	-	-	-	-	-	-	-	✓
Ditaranto, 1973	R+R	General	✓	-	✓	-	-	-	-	-	-	-	-	✓	-	-	✓	-	-
Vallabhan et al., 1993	P+P	G+G	N/A		✓	-	-	✓	N/A		✓	-	-	✓	-	-	-	✓	-
Suresh and Shive, 1999	TWB	LC	✓	✓	-	✓	-	-	✓	✓	-	✓	-	✓	✓	-	-	-	-
Dall'Asta, 2001	General	General	✓	✓	✓	-	-	-	✓	✓	-	-	✓	-	-	-	✓	-	-
Lee et al.,2002	W	LC	✓	✓	✓	-	✓	-	✓	✓	-	-	-	✓	-	-	✓	-	✓
Nowzartash and Mohareb, 2005	R+R	General	✓	-	✓	-	-	-	-	-	-	✓	-	✓	-	-	✓	-	✓
Asik and Tezcan, 2005	R+R	G+G	✓	-	✓	-	-	✓	-	-	-	-	-	✓	-	-	✓	✓	-
Girhammar and Pan, 2007	R+R	General	✓	-	✓	-	-	-	-	-	-	-	-	-	-	✓	✓	-	-
Koutsawa,Y and Daya, EM, 2007	R+R	G+G	✓	-	✓	✓	-	-	-	-	-	-	✓	-	-	-	✓	-	✓
Challamel et al., 2009	R+R	LC or TLSB	-	✓	✓	✓	-	-	✓	-	-	-	-	✓	✓	-	✓	-	-
Challamel et al., 2010	R+R	LC or TLSB		✓	✓	✓	-	-	✓	-	-	-	-	✓	✓	✓	✓	-	✓
Challamel et al., 2012	R+R	LC or TLSB	✓	✓	✓	-	✓	-	-	-	-	-	-	✓	-	-	✓	-	-
Present Study-Theory 1	P + W	GFRP +S	✓	✓	✓	-	-	-	✓	✓	-	-	-	✓	-	-	✓	-	✓
Present Study Theory 2	P + W	GFRP +S	✓	✓	✓	-	-	-	✓	✓	✓	-	-	✓	-	-	-	✓	✓

T=tee shaped section; R=rectangular cross-section; W=wide flange beam; TWB=thin-walled beam

TLSB=three-layer sandwich beam; P=plate; G=glass; S=steel; LC=layered composite

1.6. Layout of the thesis

Following the present introductory chapter, Chapter 2 develops a non-shear deformable theory for the analysis of composite beams with wide flange steel sections reinforced with a GFRP plate. The governing differential equations of equilibrium and boundary conditions are presented in this chapter. Chapter 3 develops a finite element solution under the same assumptions of the formulation. The element is based on shape functions which satisfy the homogeneous form of the equilibrium equations. Chapter 4 applies the new theory to solve four examples. A comparison against 3D FEA under Abaqus is also presented in the chapter. The examples showcase the strength and identify the shortcomings of the theory and set the stage for developing an improved theory. A new shear deformable theory is then developed under Chapter 5, which provides the governing field equations and possible boundary conditions under the improved theory. Chapter 6 presents a finite difference discretization for the new shear deformable theory, while Chapter 7 develops a finite element formulation based on the new shear deformable theory. Chapter 8 then presents a few examples solved under the new theory and provides an assessment of the validity of its predictions through a comparison to 3D FEA models under Abaqus. A summary, conclusions, and recommendations based on the study are then provided in Chapter 9.

The main chapters of the thesis involving derivations were concisely presented while the lengthy details of the formulations were presented in Appendices A1 through A9. Also, as part of the study, several computer programs were coded under Matlab. The listings of these programs are presented in Appendices B1 through B5.

CHAPTER 2. NON-SHEAR DEFORMABLE THEORY - FORMULATION

2.1. Introduction

The kinematics of thin walled beam theories (Vlasov (1961) and Gjelsvik (1981)) are reviewed in this Chapter. The Gjelsvik theory is then extended for the analysis of composite sections consisting of a wide flange beam reinforced with a GFRP through an adhesive material. The principle of stationary total potential energy is applied to formulate the governing differential equations of the equilibrium for the systems and the associated boundary conditions. Closed-form solutions for the homogeneous form of the governing equations are then provided. The new theory captures the transverse-longitudinal response as well as the lateral-torsional response.

2.2. Overview of Thin Walled Beam Theories

2.2.1. Introduction

In the Vlasov thin-walled beam theory (Vlasov, 1961), displacement fields of a point lying on the middle surface of a thin-walled member are related to those of an arbitrarily chosen pole, commonly taken to coincide with the shear center. Because the Vlasov theory assumes the member to have negligible thickness compared to characteristic dimensions of the section (such as flange width or web height in a wide flange section), the displacement fields of points within the cross-section that are offset from the mid-surface are not defined and are assumed to be equal to those of a point on the middle surface. As a result, the Vlasov theory suffers from two restrictions a) It does not capture local warping effects and b) the Saint-Venant shear contribution is added to a formulation as an ad-hoc effect. The Gjelsvik theory (Gjelsvik 1981) is an extension of Vlasov theory in which the thickness effect is incorporated and thus remedies both deficiencies by capturing local warping effects and captures the Saint-Venant shear effects in a seamless manner.

2.2.2. Overview of the Gjelsvik Beam

The Gjelsvik theory is based on the following kinematic assumptions:

(i) The contour does not deform in its own plane,

(ii) The shear strain γ_{sz} of the middle surface is zero, and

(iii) Each element behaves as a thin shell. This implies the Kirchhoff assumption remains valid, i.e., straight lines original normal to the section contour remains normal to the section contour after a deformation.

Assumptions (i) and (ii) are identical to those of the Vlasov theory, while Assumption (iii) is in line with the thin plate (or shell) Kirchoff theory.

2.2.3. Coordinates and Sign Conventions

A general prismatic member with an open thin walled cross section and a fixed left-handed Cartesian coordinate system *OXYZ* is considered and shown as in Fig.2.1. The member is placed with its generator parallel to the Z axis. A plane normal to the Z axis cuts the middle surface in a line called the contour of the cross section.

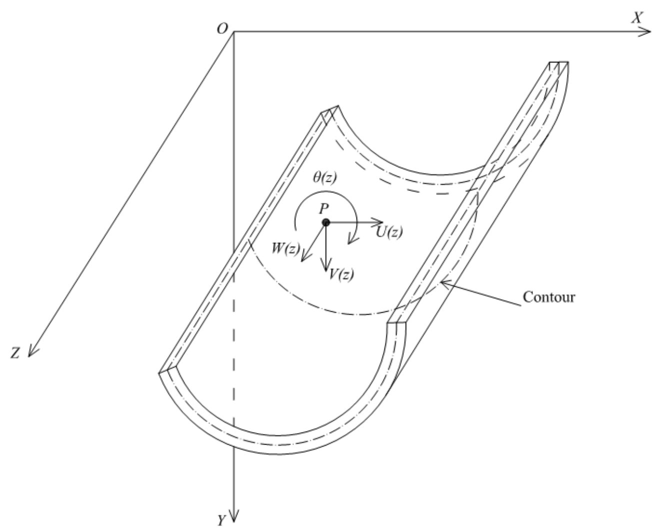

Figure 2.1. Prismatic member with an open, thin-walled cross section

Displacement fields $U(z)$, $V(z)$ of an arbitrarily chosen pole $P(x_o, y_o)$ are in the *X, Y* directions. The section is assumed to undergo a twisting rotation $\theta(z)$ that is positive when rotating clockwise when looking from the positive *Z* direction in to negative *Z* direction. Point C_o is the origin of axes.

An arbitrary Point $C(x(s), y(s))$ on the contour is offset from a Sectorial Origin C_0 by a curvilinear distance s . Coordinate s is positive when Point C rotates clockwise relative to point C_0 when looking from the positive *Z* direction into the negative *Z* direction. The tangent to the contour at point *C* makes an angle $\alpha(s)$ with the positive direction of the *X*-axis. A local left-handed coordinate system C_{nsz} is defined at point C where C_s is oriented in the tangential direction (positive in the direction of increase of s), C_n is oriented in the normal direction, and C_z is parallel to OZ (Fig. 1.2). The displacement fields of the Point C in the coordinate system C_{nsz} are termed $\bar{u}$, $\bar{v}$ and $\bar{w}$, respectively.

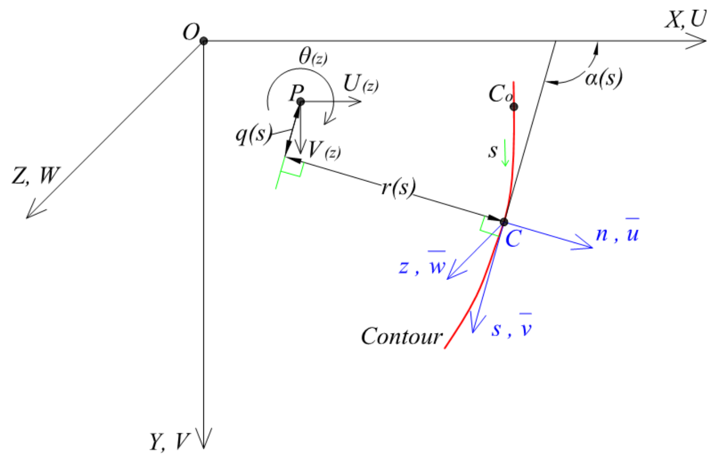

Figure 2.2. Sign convention and symbols

A point C and neighboring point C' on the section contour placed a distance *ds* apart on the contour (Fig.1.3) are considered to derive the following geometrical relationships (Gjelsvik 1981).

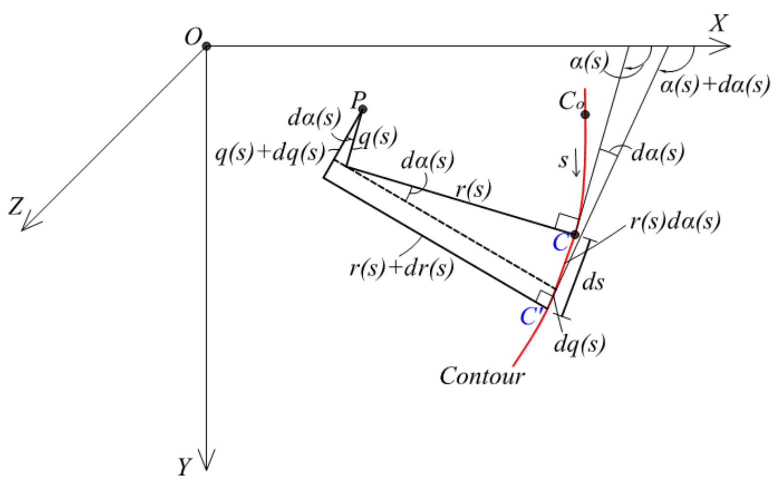

Figure 2.3. Contour geometry

$$
\begin{aligned}
dr(s) &= q(s)d\alpha(s) \\
ds &= dq(s) + r(s)d\alpha(s) \\
dx(s) &= ds\cos\alpha(s) \\
dy(s) &= ds\sin\alpha(s)
\end{aligned}
$$

$$x(s)-x_o=q(s)\cos\alpha(s)+r(s)\sin\alpha(s) \tag{2.1}$$

$$y(s)-y_o=q(s)\sin\alpha(s)-r(s)\cos\alpha(s) \tag{2.2}$$

Equations (2.1) and (2.2) are solved for $q(s)$ and $r(s)$, yielding

$$q(s)=\left[x(s)-x_o\right]\cos\alpha(s)+\left[y(s)-y_o\right]\sin\alpha(s) \tag{2.3}$$

$$r(s)=\left[x(s)-x_o\right]\sin\alpha(s)-\left[y(s)-y_o\right]\cos\alpha(s) \tag{2.4}$$

In Eq. (2.3), $q(s)$ is the distance from the pole to the point of interest in the tangential direction and $r(s)$ is distance from the pole to the point of interest in the normal direction.

2.2.4. In-plane displacement fields of a point lying on contour

Under the action of external causes such as external forces or imposed displacements, points on a cross-section are displaced in its plane according to Assumption (i) under item 2.2.2. The in-plane displacement fields at Point C can be related to the displacement fields of Pole P in the global coordinate system and the angle of twist $\theta_z(s)$ through:

$$\xi(s,z)=U(z)-\left[y(s)-y_o\right]\theta_z(z) \tag{2.5}$$

$$\eta(s,z)=V(z)+\left[x(s)-x_o\right]\theta_z(z) \tag{2.6}$$

The displacements in the global coordinate direction given in Eqs. (2.5) and(2.6) can be resolved along the tangent and normal directions at Point C yielding

$$\bar{u}(x,y,z)=\xi(x,y,z)\sin\alpha(s)-\eta(x,y,z)\cos\alpha(s) \tag{2.7}$$

$$\bar{v}(x,y,z)=\xi(x,y,z)\cos\alpha(s)+\eta(x,y,z)\sin\alpha(s) \tag{2.8}$$

From Eqs. (2.5) and (2.6), by substituting into Eqs. (2.7) and (2.8), one can express the in-plane displacements of Point C along the local coordinate system C_{nsz}, yielding

$$\bar{u}(s,z)=U(z)\sin\alpha(s)-V(z)\cos\alpha(s)-q(s)\theta_z(z) \tag{2.9}$$

and

$$\bar{v}(s,z)=U(z)\cos\alpha(s)+V(z)\sin\alpha(s)+r(s)\theta(z) \tag{2.10}$$

2.2.5. In-plane displacement fields of a Point *B* offset from middle surface

From Assumption (iii) under item (2.2.2), one can express the displacements of an arbitrary Point $B(s,n,z)$ that is offset from the section contour in terms of the displacements of the corresponding Point $C(s,z)$ on the contour as:

$$u(s,z,n)=\bar{u}(s,z) \tag{2.11}$$

$$v(s,z,n)=\bar{v}(s,z)-n\frac{\partial\bar{u}(s,z)}{\partial s} \tag{2.12}$$

From Eqs. (2.9) and (2.10), by substituting into (2.11) and (2.12), one obtains:

$$u(s,z,n)=U(z)\sin\alpha(s)\ \text{-}\ V(z)\cos\alpha(s)-q(s)\theta(z) \tag{2.13}$$

and

$$v(s,z,n)=\{1-n[\alpha'(s)]\}U(z)\cos\alpha(s)+\{1-n[\alpha'(s)]\}V(z)\sin\alpha(s)+\theta(z)[r(s)+nq'(s)] \tag{2.14}$$

2.2.6. Expressing the Longitudinal Displacement

2.2.6.1. At a Point lying on The Contour

From Assumption (ii) in item (2.2.2), the longitudinal displacement at a generic Point $C(s,z)$ lying on contour of the cross-section is given from the relation

$$\frac{\partial\bar{w}(s,z)}{\partial s}+\frac{\partial\bar{v}(s,z)}{\partial z}=0$$

which leads to

$$\bar{w}(s,z)=-\int_s\frac{\partial\bar{v}(s,z)}{\partial z}ds \tag{2.15}$$

From Eq. (2.10), by substituting into Eq. (2.15) and integrating with respect to z, one obtains:

$$\bar{w}(s,z)=W(z)-U'(z)x(s)-\ V'(z)y(s)-\omega(s)\theta_z'(z) \tag{2.16}$$

in which the sectorial coordinate $\omega(s)=\int_0^s\left[\left(x(s)-x_o\right)\sin\alpha(s)-\left(y(s)-y_o\right)\cos\alpha(s)\right]ds=\int_0^s r(s)ds$ has been defined.

2.2.6.2. At a Point offset from the Contour

From Assumption (iii) under item (2.2.2), the longitudinal displacement at a Point $B(s,n,z)$ offset from the section contour is given from the relation (Fig.2.4):

$$w(s,z,n)=\bar{w}(s,z)-n\frac{\partial\bar{u}(s,z)}{\partial z} \tag{2.17}$$

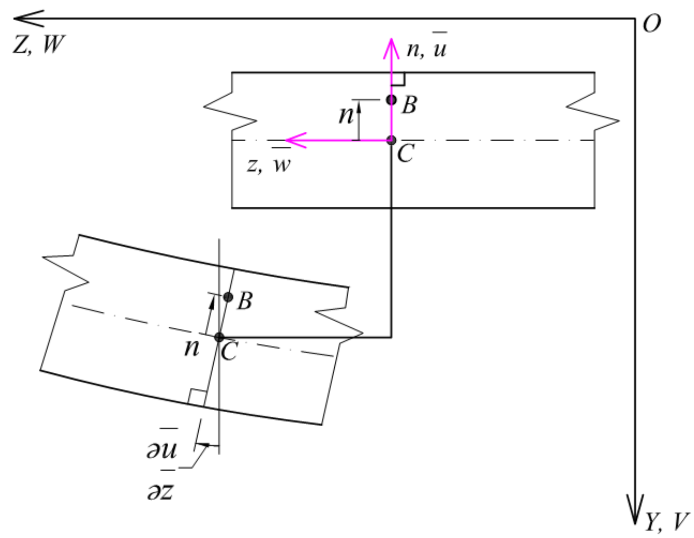

Figure 2.4. Geometrical expression for longitudinal displacement

In Eq. (2.17), the second term of the right hand side is expressed as:

$$\begin{aligned} n\frac{\partial\bar{u}}{\partial z} &= U'(z)\left[n\sin\alpha(s)\right] - V'(z)\left[n\cos\alpha(s)\right]+ \\ &\quad -n\left[\left(x(s)-x_o\right)\cos\alpha(s)+\left(y(s)-y_o\right)\sin\alpha(s)\right]\theta_z'(z) \end{aligned} \tag{2.18}$$

From Eqs. (2.16) and (2.18), by substituting into (2.17), longitudinal displacement of Point B is obtained as:

$$w(s,z,n)=W(z)-U'(z)\left[x(s)+n\sin\alpha(s)\right]-V'(z)\left[y(s)-n\cos\alpha(s)\right]-\theta_z'(z)\left[\omega(s)-nq(s)\right] \tag{2.19}$$

2.3. Composite Beam Analysis-Statement of the Problem

A steel wide flange section reinforced with a GFRP plate to one of the flanges is assumed to be subject to general loads. The GFRP plate is assumed to be connected to the steel section through a thin layer of adhesive. It is required to formulate the governing field equations and boundary conditions. The assumptions of the formulation are presented in Section 2.4. The details of the formulation are presented in Section 2.5 while closed form solutions are provided in Section 2.5.7.

2.4. Assumptions

The wide flange steel beam and the GFRP plates are considered as two Gjelsvik beams. For each of the two components, the following assumptions are made

(i) The contour does not deform in its own plane,

(ii) The shear strain γ_{sz} of the middle surface is zero,

(iii) Each element behaves as a thin shell. This is in line of the Kirchhoff assumption of straight lines remaining normal to the section contour during a deformation.

In addition, the following assumptions are made regarding the adhesive material

(iv) Perfect bond is assumed at interfaces between the adhesive and the GFRP plate and between the adhesive and the wide flange beam,

(v) The adhesive is assumed to act as a weak elastic material with a small modulus of elasticity when compared to those of the beam or GFRP. As a result, longitudinal stresses are considered negligible compared to the normal stresses in the GFRP plate and steel section,

(vi) The thickness of the adhesive layer is assumed to remain constant throughout deformation,

(vii) Displacement fields at any Point within the Adhesive layer are linearly interpolated from those at the bottom surface of the GFRP plate and those at the top flange of the beam.

In addition the following assumption is made regarding the constitutive behaviour of the materials

(viii) All materials used are considered to be isotropic linearly elastic.

2.5. Formulation

2.5.1. Kinematics

A coordinate $OXYZ$ system is chosen for the wide flange beam as shown in Fig. 2.5 where Origin O is selected to coincide with the centroid and shear center of the beam. Point $C_b(x(s_b), y(s_b))$ is a generic point lying on the section contour. Three local left-handed coordinate systems $C_b n_b s_b z$ are defined, where the s_b axis is tangent to the contour at Point C_b, while the n_b axis is normal to the contour and the z axis is parallel to the Z axis.

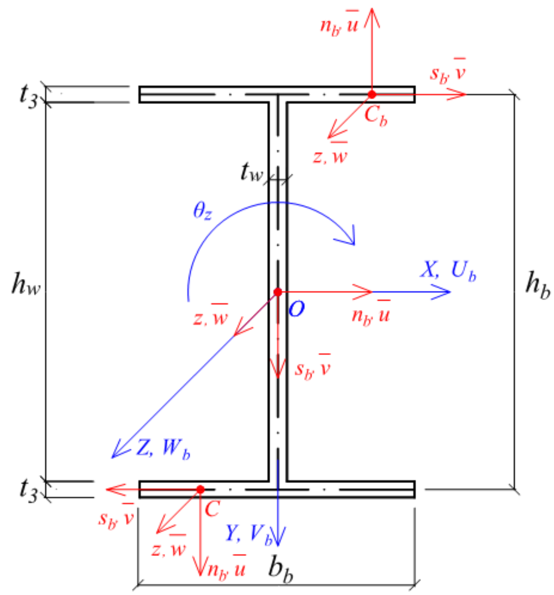

Figure 2.5. Local and global coordinates and dimensions of wide flange beam section

A similar $O_p X_p Y_p Z_p$ coordinate system is chosen for the GFRP plate as shown in the Fig. 2.6, where Origin O_p is selected to coincide with the centroid and the shear center of the GFRP plate. Point $C_p(x_p(s_p), y_p(s_p))$, in which $-b_p/2 \leq x_p \leq b_p/2$, lies is on the section mid-surface of GFRP plate. A local left-handed coordinate system $C_p n_p s_p z$ is defined, where the s_p axis coincides with the tangential direction while n_p axis is normal to the contour, and the z_p axis is parallel to the Z axis.

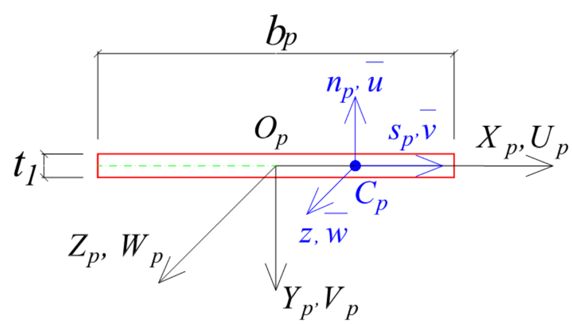

Figure 2.6. Local and global coordinates and dimensions of GFRP plate section

Under the action of external causes such as forces or displacements, the composite beam is displaced to a new position (Fig.2.7). An elevation view (a) shows the cross-section of the composite beam before and after deformation, while a plan view (b) shows the plane segments in different lengths of the GFRP and the I-shaped beam before and after deformation. Displacement fields of the shear center O of the beam in X, Y directions are $U_b(z)$, $V(z)$, respectively. Because the wide flange section is doubly symmetric, the shear center of the beam coincides with the section centroid. Also, the longitudinal displacement $W_b(z)$ is that of the section centroid/shear centre. Displacement fields of the shear center/centroid O_p of the GFRP plate in X_p, Y_p, Z_p directions are $U_p(z), V(z), W_p(z)$. The longitudinal displacement of the shear centre/centroid $W_p(z)$ is distinct from that of the wide flange displacement $W_b(z)$. One recalls that the adhesive layer is assumed to be incompressible (Assumption vi). Thus, the vertical displacement $V(z)$ of the beam and the GFRP plate are considered to be approximately equal. Also, both the wide flange beam and GFRP plate are assumed to undergo the same twisting rotation $\theta_z(z)$ that is positive when rotating clockwise when looking from the positive Z direction in to negative Z direction.

Given that the adhesive layer has a small thickness, the displacement fields of a point D_a within the adhesive layer will be linearly interpolated between the displacement fields of the corresponding point at the underside of the GFRP plate D_p and the top of the steel section D_b (Fig. 2.8). All three points D_a, D_b, D_p initially lie on the same vertical line.

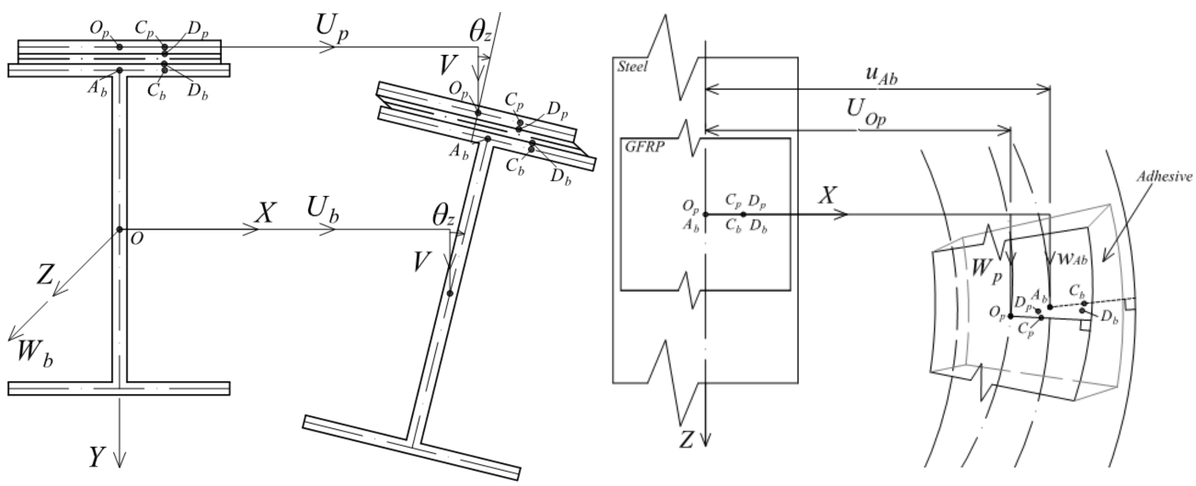

Figure 2.7. Kinematics of a GFRP strengthened wide flange beam
(a) Elevation View, and (b) Plan View

A global coordinate system $O_a X_a Y_a$ with Origin O_a is chosen at the Centroid of adhesive (Fig.2.8). Point $C_a(x_a(s_a), y_a(s_a))$, in which $-b_p/2 \le x_a \le b_p/2$, lies on the mid-surface of the adhesive layer. A local left-handed coordinate system $C_a n_a s_a z$ is selected for the layer, where coordinate s_a

coordinate is oriented along the X_a direction, the n_a coordinate is normal to the contour, and the z coordinate is oriented along the Z axis. A transverse coordinate n_a , oriented upwards is taken from centre line of the layer to a generic Point D (Fig 2.8).

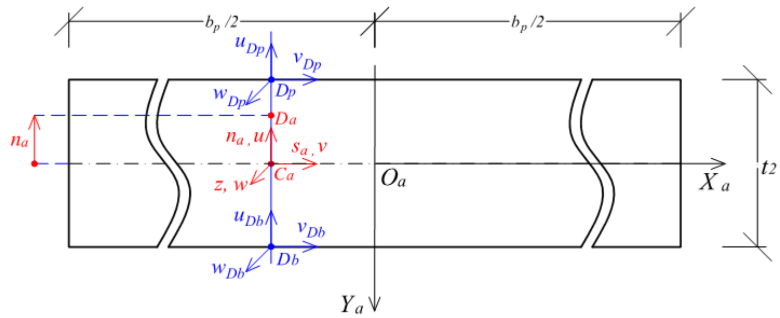

Figure 2.8. Cross-section of Adhesive layer and its coordinate system

2.5.2. Expression for Displacement Fields

2.5.2.1. Wide Flange Beam

From Eqs. (2.13), (2.14), (2.19) and to specialize them for the beam by setting $U = U_b, W = W_b$, one expresses the displacement fields for Point $B_b(s_b, n_b, z)$ offset from the section contour as:

$$u_b(s_b,n_b,z)=U_b(z)\sin\alpha(s_b)-V(z)\cos\alpha(s_b)-\theta_z(z)q(s_b) \tag{2.20}$$

$$v_b(s_b,n_b,z)=U_b(z)\cos\alpha(s_b)+V(z)\sin\alpha(s_b)+\theta_z(z)\left[r(s_b)+n_b q'(s_b)\right] \tag{2.21}$$

$$w_b(s_b,n_b,z)=W_b(z)-U_b'(z)X(s_b,n_b)-V'(z)Y(s_b,n_b)-\theta_z'(z)\Omega(s_b,n_b) \tag{2.22}$$

in which

$$X(s_b,n_b)=x(s_b)+n_b\sin\alpha(s_b);\quad Y(s_b,n_b)=y(s_b)-n_b\cos\alpha(s_b)\ ;\quad \Omega(s_b,n_b)=\omega_b(s_b)-n_b q(s_b);$$

$$q(s_b)=x(s_b)\cos\alpha(s_b)+y(s_b)\sin\alpha(s_b)\ ;\quad r(s_b)=x(s_b)\sin\alpha(s_b)-y(s_b)\cos\alpha(s_b);$$

In a matrix form, one has:

$$\begin{Bmatrix} u_b \\ v_b \\ w_b \end{Bmatrix}=\begin{Bmatrix} 0 & \sin\alpha(s_b) & -\cos\alpha(s_b) & -q(s_b) \\ 0 & \cos\alpha(s_b) & \sin\alpha(s_b) & \left[r(s_b)+n_b q'(s_b)\right] \\ 1 & -X(s_b,n_b)D & -Y(s_b,n_b)D & -\Omega(s_b,n_b)D \end{Bmatrix}\begin{Bmatrix} W_b(z) \\ U_b(z) \\ V(z) \\ \theta_z(z) \end{Bmatrix} \tag{2.23}$$

in which the operator $D=\partial/\partial z$ has been defined. By applying Eq. (2.23) for Point $D_b(s_b,\frac{t_3}{2},z)$ lying on top surface of the beam section ($\alpha=0^o$), one obtains

$$\begin{Bmatrix} u_b \\ v_b \\ w_b \end{Bmatrix}_{\left(n_b=\frac{t_3}{2}\right)} = \begin{bmatrix} 0 & 0 & -1 & -x(s_b) \\ 0 & 1 & 0 & \left(\frac{h_b+t_3}{2}\right) \\ 1 & -x(s_b)D & \left(\frac{h_b+t_3}{2}\right)D & -\left[\left(\frac{h_b-t_3}{2}\right)x(s_b)\right]D \end{bmatrix} \begin{Bmatrix} W_b(z) \\ U_b(z) \\ V(z) \\ \theta_z(z) \end{Bmatrix} \tag{2.24}$$

2.5.2.2. GFRP Plate

From Eqs. (2.13), (2.14), by substituting into (2.19), and setting $U=U_p, W=W_p$, one expresses the displacement fields for Point $B_p(s_p,n_p,z)$ offset from the section contour within the GFRP plate as

$$u_p(s_p,n_p,z)=-V(z)-\theta_z(z)x_p(s_p) \tag{2.25}$$

$$v_p(s_p,n_p,z)=U_p(z)+\theta_z(z)n_p \tag{2.26}$$

$$w_p(s_p,n_p,z)=W_p(z)-U_p'(z)x_p(s_p)+V'(z)n_p+\theta_z'(z)\left[n_p x_p(s_p)\right] \tag{2.27}$$

In a matrix form, one has:

$$\begin{Bmatrix} u_p \\ v_p \\ w_p \end{Bmatrix} = \begin{bmatrix} 0 & 0 & -1 & -x_p(s_p) \\ 0 & 1 & 0 & n_p \\ 1 & -x_p(s_p)D & n_pD & n_p x_p(s_p)D \end{bmatrix} \begin{Bmatrix} W_p(z) \\ U_p(z) \\ V(z) \\ \theta_z(z) \end{Bmatrix} \tag{2.28}$$

Therefore, displacements for Point $D_p(s_p,-\frac{t_1}{2},z)$ lying on bottom surface of the GFRP plate ($\alpha=0^o$) are given by

$$\begin{Bmatrix} u_p \\ v_p \\ w_p \end{Bmatrix}_{\left(n_p=-\frac{t_1}{2}\right)} = \begin{bmatrix} 0 & 0 & -1 & -x_p(s_p) \\ 0 & 1 & 0 & -\frac{t_1}{2} \\ 1 & -x_p(s_p)D & -\frac{t_1}{2}D & -\frac{t_1}{2}x_p(s_p)D \end{bmatrix} \begin{Bmatrix} W_p(z) \\ U_p(z) \\ V(z) \\ \theta_z(z) \end{Bmatrix} \tag{2.29}$$

2.5.2.3. Adhesive Layer

Coordinate n_a will be used to linearly interpolate displacement fields of the Point D_a as a function of point D_p and D_b as shown in Fig.2.8. Since origins O, O_p , O_a are chosen to lie along the same vertical line, one has $s_a = s_b = s_p$, and thus $x_a(s_a) = x(s_b) = x_p(s_p) = x(s)$, where $-b_p/2 \le x(s) \le b_p/2$.

As stated under Section 2.5, the displacement fields $\langle u_a \quad v_a \quad w_a \rangle^T$ of a Point D_a within the adhesive layer are determined by linear interpolation across the layer thickness, yielding

$$\begin{Bmatrix} u_a \\ v_a \\ w_a \end{Bmatrix} = \left(\frac{1}{2} + \frac{n_a}{t_2}\right) \begin{Bmatrix} u_p \\ v_p \\ w_p \end{Bmatrix}_{\left(n_p = -\frac{t_1}{2}\right)} + \left(\frac{1}{2} - \frac{n_a}{t_2}\right) \begin{Bmatrix} u_b \\ v_b \\ w_b \end{Bmatrix}_{\left(n_b = \frac{t_3}{2}\right)} \tag{2.30}$$

From Eqs. (2.24) and (2.29), by substituting into (2.30), the displacement fields at Point D_a are expressed as

$$\begin{aligned} u_{Da}(s_a, n_a, z) &= \left(\frac{1}{2} + \frac{n_a}{t_2}\right) u_p(s_p, \frac{t_3}{2}, z) + \left(\frac{1}{2} - \frac{n_a}{t_2}\right) u_b(s_b, -\frac{t_1}{2}, z) \\ &= \left(\frac{1}{2} + \frac{n_a}{t_2}\right)\left[-V(z) - \theta_z(z)x(s)\right] + \left(\frac{1}{2} - \frac{n_a}{t_2}\right)\left[-V(z) - \theta_z(z)x(s)\right] \end{aligned}$$

$$\begin{aligned} v_a(s_z, n_a, z) &= \left(\frac{1}{2} + \frac{n_a}{t_2}\right) v_p(s_p, \frac{t_3}{2}, z) + \left(\frac{1}{2} - \frac{n_a}{t_2}\right) v_b(s_b, -\frac{t_1}{2}, z) \\ &= \left(\frac{1}{2} + \frac{n_a}{t_2}\right)\left[U_p(z) - \theta_z(z)\left(\frac{t_1}{2}\right)\right] + \left(\frac{1}{2} - \frac{n_a}{t_2}\right)\left[U_b(z) + \theta_z(z)\left(\frac{h_b + t_3}{2}\right)\right] \end{aligned}$$

$$\begin{aligned} w_{Da}(s_a, n_a, z) &= \left(\frac{1}{2} + \frac{n_a}{t_2}\right) w_{Dp}(s_p, \frac{t_3}{2}, z) + \left(\frac{1}{2} - \frac{n_a}{t_2}\right) w_{Db}(s_b, -\frac{t_1}{2}, z) \\ &= \left(\frac{1}{2} + \frac{n_a}{t_2}\right)\left\{W_p(z) - U_p'(z)x(s) - V'(z)\frac{t_1}{2} - \theta_z'(z)\left[\frac{t_1}{2}x(s)\right]\right\} \\ &\quad + \left(\frac{1}{2} - \frac{n_a}{t_2}\right)\left\{W_b(z) - U_b'(z)\, x(s) + V'(z)\left(\frac{h_b + t_3}{2}\right) - \theta_z'(z)\left[\left(\frac{h_b - t_3}{2}\right)x(s)\right]\right\} \end{aligned}$$

2.5.3. Expressions for Strains

2.5.3.1. Wide Flange Beam

From the displacement fields expressed in the Eqs. (2.20), (2.21), and (2.22), the strain components are given by

$$\varepsilon_{nb} = \varepsilon_{sb} = \gamma_{nsb} = \gamma_{znb} = 0 \ ,$$

$$\gamma_{szb} = \frac{\partial v_b}{\partial z} + \frac{\partial w_b}{\partial s} = 2n_b \theta_z'(z), \text{ and}$$

$$\varepsilon_{zb} = W_b'(z) - U_b''(z) X(s_b, n_b) - V''(z) Y(s_b, n_b) - \theta_z''(z) \Omega(s_b, n_b) \tag{2.31}$$

2.5.3.2. GFRP Plate

From the displacement fields expressed in the Eqs.(2.25), (2.26) and(2.27), the strain components are

$$\varepsilon_{np} = \varepsilon_{sp} = \gamma_{nsp} = \gamma_{znp} = 0 \ ,$$

$$\gamma_{szp} = \frac{\partial v_p}{\partial z} + \frac{\partial w_p}{\partial s} = 2n_p \theta_z'(z), \text{ and}$$

$$\varepsilon_{zp} = W_p'(z) - U_p''(z) x_p + V''(z) n_p + \theta_z''(z) n_p x_p \tag{2.32}$$

2.5.3.3. Adhesive Layer

Because the cross sectional area A_a and module of elasticity E_a of the adhesive layer are very small compared to those of the GFRP plate and the wide flange beam, the bending capacity of the layer is considered negligible. Therefore, the normal stresses $\sigma_{na}, \sigma_{za}, \sigma_{za}$ are considered negligible. Thus, the corresponding strains $\varepsilon_{na}, \varepsilon_{za}, \varepsilon_{za}$ will be assumed to have a negligible contribution to the strain energy expression. The remaining strains within the layer are shear strains are given from displacement fields given in 2.5.2.3 as

$$\gamma_{zna} = \langle a_a \rangle_{1\times6}^{\mathrm{T}} \{\Delta_a\}_{6\times1}; \quad \gamma_{sna} = \langle a_{a1} \rangle_{1\times3}^{\mathrm{T}} \{U_o\}_{3\times1} \quad ; \quad \gamma_{sza} = -f(n_a)\theta'(z) \tag{2.33}$$

in which

$$\langle a_a \rangle_{1\times6}^{\mathrm{T}} = \langle -c_1 \quad c_1 \quad -c_2 \quad c_1 x \quad -c_1 x \quad -c_3 x \rangle, \quad \langle a_{a1} \rangle_{1\times3}^{\mathrm{T}} = \langle -c_1 \quad c_1 \quad -c_2 \rangle,$$
$$\langle \Delta_a \rangle_{1\times6}^{\mathrm{T}} = \langle W_b \quad W_p \quad V' \quad U_b' \quad U_p' \quad \theta_z' \rangle, \qquad \langle U_o \rangle_{1\times3}^{\mathrm{T}} = \langle U_b \quad U_p \quad \theta_z \rangle$$

with $$c_1 = \frac{1}{t_2},\ c_2 = \frac{t_1 + 2t_2 + t_3 + h_b}{2t_2},\ c_3 = \frac{t_1 + 2t_2 + t_3 - h_b}{2t_2},\ f(n_a) = \frac{(t_1 + t_3) n_a}{t_2} + \frac{t_1 - t_3}{2} \tag{2.34}$$

2.5.4. Expressions for Stresses

The non-zero stresses can be related to the strains through

$$\sigma_{zb} = E_b \varepsilon_{zb}\ ;\ \tau_{szb} = G_b \gamma_{szb}\ ;\ \sigma_{zp} = E_p \varepsilon_{zp}\ ;\ \tau_{szp} = G_p \gamma_{szp}\ ; \tau_{sza} = G_a \gamma_{sza}\ ;\ \tau_{sna} = G_a \gamma_{sna}\ ;\ \tau_{zna} = G_a \gamma_{zna} \tag{2.35}$$

2.5.5. Variational Principle

2.5.5.1. General

The total potential energy π is the sum of internal strain energies stored within the steel beam U_b the GFRP plate U_p ,adhesive layer U_a plus the load potential energy loss by tractions at member ends V_1 and member tractions within the member V_2 , i.e.,

$$\pi = U_b + U_p + U_a - V_1 - V_2 \tag{2.36}$$

2.5.5.2. Internal Strain Energy

Contribution of the beam

The internal strain energy stored in the steel beam (Eq. A1.4) is given by

$$U_b = \frac{1}{2} E_b \int_L \left(A_b\ W_b'^2 + I_{yyb} U_b''^2 + I_{xxb} V_b''^2 + I_{\omega\omega b} \theta_z''^2 \right) dz + \frac{1}{2} G_b \int_L J_b \theta_z'^2 dz \tag{2.37}$$

in which the following section properties are defined

$$A_b = \int_{A_b} dA_b = \sum_{i=1,3} b_{ib} t_{ib}\ ;\quad I_{yyb} = \int_{A_b} X(s_b, n_b)^2\, dA_b\ ;\ I_{xxb} = \int_{A_b} Y(s_b, n_b)^2\, dA_b\ ; I_{\omega\omega b} = \int_{A_b} \Omega(s_b, n_b)^2\, dA_b$$

$J_b = \int_{A_b} 4 n_b^2 dA_b = \sum_{i=\overline{1,3}} \int_{-\frac{t_i}{2}}^{\frac{t_i}{2}} \left(4 t_{ib}^2 b_{ib} \right) dt_{ib} = \sum_{i=\overline{1,3}} \frac{b_{ib} t_{ib}^3}{3}$ and $i = 1,2,3$ denote both flanges and the web.

Contribution of the plate

The internal strain energy stored in the GFRP plate (Eq. A1.7) is given by

$$U_p = \frac{1}{2} E_p \left(\int_L A_p W_p'^2 + I_{yyp} U_p''^2 + I_{xxp} V''^2 + I_{\omega\omega p} \theta_z''^2 \right) dz + \frac{1}{2} G_p \int_L J_p \theta_z'^2 dz \qquad (2.38)$$

in which the following section properties are defined

$$A_p = b_p t_p \, ; I_{yyp} = \int_{A_p} x_p^2 dA_p \, ; \; I_{xxp} = \int_{A_p} n_p^2 dA_p \, ; \; I_{\omega\omega p} = \int_{A_p} \left[n_p x_p \left(s_p \right) \right]^2 dA_p \, ;$$

$$J_p = \int_{A_p} 4n_p^2 dA_p = \int_{-\frac{t_1}{2}}^{\frac{t_1}{2}} \left(4t_p^2 b_p \right) dt_p = \frac{b_p t_p^3}{3}$$

Contribution of the adhesive layer

The internal strain energy stored in the adhesive layer (Eq. A1.12) is given by

$$\begin{aligned} U_a = & \frac{1}{2} G_a A_a \int_L c_1^2 \langle U_L \rangle_{1\times 2}^T \left[H_{a1} \right]_{2\times 2} \{ U_L \}_{2\times 1} dz + \frac{1}{2} G_a A_a \int_L \left[2c_1 c_2 V' \left(W_b - W_p \right) + c_2^2 \left(V' \right)^2 \right] dz \\ & + \frac{1}{2} G_a I_{yya} \int_L \langle U_O \rangle_{1\times 3}'^{\mathrm{T}} \left[H_{a2} \right]_{3\times 3} \{ U_O \}' dz + \frac{1}{2} G_a A_a \int_L \langle U_O \rangle_{1\times 3}^{\mathrm{T}} \left[H_{a4} \right]_{3\times 3} \{ U_O \} dz + \frac{1}{2} G_a J_a \int_L \theta_z'^2 dz \end{aligned} \qquad (2.39)$$

in which we define the following displacement vectors,

$$\langle U_L \rangle^T = \langle W_b \quad W_p \rangle, \langle U_O \rangle^T = \langle U_b \quad U_p \quad \theta_z \rangle \; ,$$

the following matrices,

$$\left[H_{a1} \right]_{2\times 2} = \begin{bmatrix} 1 & -1 \\ -1 & 1 \end{bmatrix}, \left[H_{a2} \right]_{3\times 3} = \begin{bmatrix} c_1^2 & -c_1^2 & -c_1 c_3 \\ -c_1^2 & c_1^2 & c_1 c_3 \\ -c_1 c_3 & c_1 c_3 & c_3^2 \end{bmatrix}, \left[H_{a4} \right]_{3\times 3} = \begin{bmatrix} c_1^2 & -c_1^2 & c_1 c_2 \\ -c_1^2 & c_1^2 & -c_1 c_2 \\ c_1 c_2 & -c_1 c_2 & c_2^2 \end{bmatrix}$$

in which c_1, c_2, c_3 have been defined in Eq. (2.34), and the sectional properties

$$A_a = \int_{A_a} dA = b_a t_a \, , J_a = \frac{\left(t_1^2 - t_1 t_3 + t_3^2 \right) A_a}{3} \quad I_{yya} = \int_{A_a} x^2 dA$$

2.5.5.3. Load Potential

The total potential energy loss $\tilde{V}$ is the sum of the potential energy $\tilde{V}$ lost by end tractions $\sigma_z \left(s_b, n_b, 0 \right), \; \tau_u \left(s_b, n_b, 0 \right), \tau_v \left(s_b, n_b, 0 \right), \sigma_z \left(s_b, n_b, L \right), \tau_u \left(s_b, n_b, L \right), \tau_v \left(s_b, n_b, L \right)$ at $z = 0, L$ (defined in

Fig. 2.9) and the potential energy $\tilde{I}$ lost by the member tractions $p_u(s_b,n_b,z)$, $p_v(s_b,n_b,z)$, $p_z(s_b,n_b,z)$.

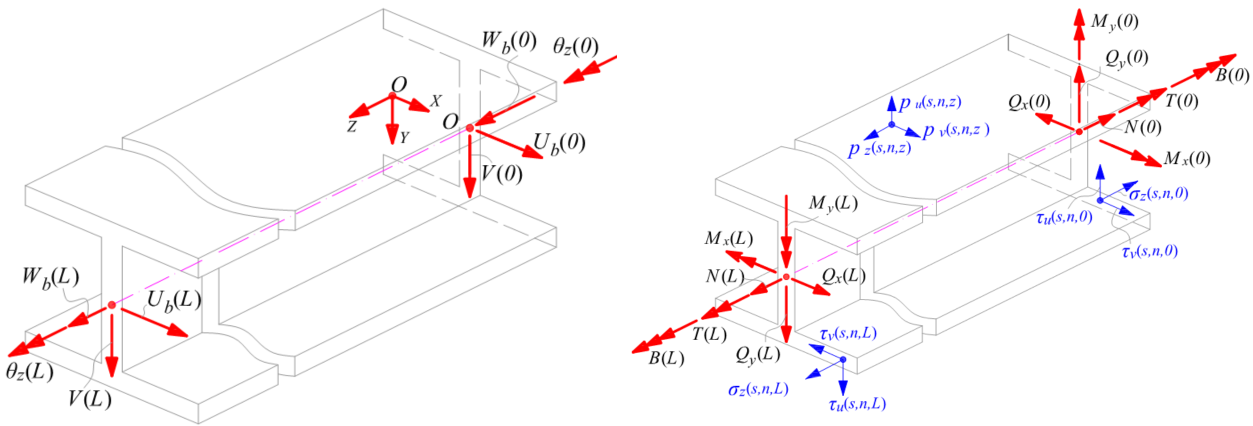

Figure 2.9. End and Member Tractions

Contribution of end loads

The total potential energy loss $\tilde{I}$ due to loads at the member ends (Section A1.4.1) are

$$
\begin{aligned}
V_1 = -\big[& N(0)W_b(0) + Q_x(0)U_b(0) + Q_y(0)V(0) + M_x(0)V'(0) + M_y(0)U_b'(0) + \\
& + T(0)\theta_z(0) + B(0)\theta_z'(0) - N(L)W_b(L) - Q_x(L)U_b(L) - Q_y(L)V(L) + \\
& - M_x(L)V'(L) - M_y(L)U_b'(L) - T(L)\theta_z(L) - B(L)\theta_z'(L)\big]
\end{aligned}
\tag{2.40}
$$

in which

$$
\begin{Bmatrix} N(Z_e) \\ Q_x(Z_e) \\ Q_y(Z_e) \\ M_x(Z_e) \\ M_y(Z_e) \\ T(Z_e) \\ B(Z_e) \end{Bmatrix} = \int_A \begin{Bmatrix} \sigma_z(s_b,n_b,Z_e) \\ \tau_v(s_b,n_b,Z_e)\cos\alpha(s_b) + \tau_u(s_b,n_b,Z_e)\sin\alpha(s_b) \\ \tau_v(s_b,n_b,Z_e)\sin\alpha(s_b) - \tau_u(s_b,n_b,Z_e)\cos\alpha(s_b) \\ -\sigma_z(s_b,n_b,Z_e)Y(s_b,n_b) \\ -\sigma_z(s_b,n_b,Z_e)X(s_b,n_b) \\ \tau_v(s_b,n_b,Z_e)\left[r(s_b) + nq'(s_b)\right] - \tau_u(s_b,n_b,Z_e)q(s_b) \\ -\sigma_z(s_b,n_b,Z_e)\Omega(s_b,n_b) \end{Bmatrix} dA, \quad Z_e = 0, L \tag{2.41}
$$

Contribution of member tractions

The total potential energy loss $\tilde{I}$ due to member tractions $p_u(s_b,n_b,z)$, $p_v(s_b,n_b,z)$, $p_z(s_b,n_b,z)$ is

$$V_2 = \int_L q_{zb}(z) W_b(z) dz + \int_L q_{xb}(z) U_b(z) dz + \int_L q_{yb}(z) V(z) dz + \int_L m_{zb}(z) \theta_z(z) dz \tag{2.42}$$

(Section A1.4.2) in which the distributed members loads are related to the applied member tractions through the contour integrals

$$\begin{Bmatrix} q_{zb}(z) \\ q_{xb}(z) \\ q_{yb}(z) \\ m_{zb}(z) \end{Bmatrix} = \int_{s_b} \begin{Bmatrix} p_z(s_b, z) \\ p_v(s_b, z)\cos\alpha(s_b) + p_u(s_b, z)\sin\alpha(s_b) + \left[\partial p_z(s_b, z)/\partial z\right] X(s_b, n_b) \\ p_v(s_b, z)\sin\alpha(s_b) - p_u(s_b, z)\cos\alpha(s_b) + \left[\partial p_z(s_b, z)/\partial z\right] Y(s_b, n_b) \\ p_v(s_b, z)\left[r(s_b) + nq'(s_b)\right] - p_u(s_b, z) q(s_b) + \left[\partial p_z(s_b, z)/\partial z\right] \Omega(s_b, n_b) \end{Bmatrix} ds_b \tag{2.43}$$

From Eqs. (2.37) through (2.42). By substituting into Eq. (2.36) and evoking the stationary condition $\delta\pi = 0$, one obtains

$$\begin{aligned}
\delta\pi = & \int_L \left[E_b A_b W_b' \delta W_b' + E_p A_p W_p' \delta W_p' + \left(E_b I_{xxb} + E_p I_{xxp}\right) V'' \delta V'' + G_a A_a c_2^2 V' \delta V' \right] dz \\
& + G_a A_a \int_L \left\{ c_1^2 \langle U_L \rangle_{1\times2}^T \left[H_{a1}\right]_{2\times2} \delta\{U_L\}_{2\times1} + c_1 c_2 \left[V' \delta\left(W_b - W_p\right) + \left(W_b - W_p\right)\delta V' \right] \right\} dz \\
& + \int_L \left[E_b I_{yyb} U_b'' \delta U_b'' + E_p I_{yyp} U_p'' \delta U_p'' + \left(E_b I_{\omega\omega b} + E_p I_{\omega\omega p}\right) \theta_z'' \delta\theta_z'' + \left(G_b J_b + G_p J_p + G_a J_a\right) \theta_z' \delta\theta_z' \right] dz \\
& + G_a \int_L \left\{ I_{yya} \langle U_O \rangle_{1\times3}'^{\mathrm{T}} \left[H_{a2}\right]_{3\times3} \delta\{U_O\}_{3\times1}' + A_a \langle U_O \rangle_{1\times3}^{\mathrm{T}} \left[H_{a4}\right]_{3\times3} \delta\{U_O\}_{3\times1} \right\} dz \\
& - \int_L q_z(z) W_b(z) dz - \int_L q_{xb}(z) U_b(z) dz - \int_L q_{yb}(z) V(z) dz - \int_L m_{zb}(z) \theta_z(z) dz \\
& + \left[Q_x(0) U_b(0) + Q_y(0) V(0) + T(0)\theta_z(0) + N(0) W_b(0) + M_y(0) U_b'(0) + \right. \\
& + M_x(0) V'(0) + B(0)\theta_z'(0) - Q_x(L) U_b(L) - Q_y(L) V(L) - T(L)\theta_z(L) + \\
& \left. - N(L) W_b(L) - M_y(L) U_b'(L) - M_x(L) V'(L) - B(L)\theta_z'(L) \right] = 0
\end{aligned} \tag{2.44}$$

2.5.6. Equilibrium equations and boundary conditions

From Eq. (2.44), all variations of displacement derivatives under integrals are integrated by parts. (Appendix A2). One obtains two sets of coupled equations and their corresponding boundary conditions. The first set of coupled equations governs the longitudinal-transverse response of the composite system and takes the form

$$\left[\begin{array}{c:c:c} -E_bA_bD^2+c_1^2G_aA_a & -c_1^2G_aA_a & c_1c_2G_aA_aD \\ \hdashline -c_1^2G_aA_a & -E_pA_pD^2+c_1^2G_aA_a & -c_1c_2G_aA_aD \\ \hdashline -c_1c_2G_aA_aD & c_1c_2G_aA_aD & \left(E_bI_{xxb}+E_pI_{xxp}\right)D^4-c_2^2G_aA_aD^2 \end{array}\right]\begin{Bmatrix} W_b \\ W_p \\ V \end{Bmatrix}=\begin{Bmatrix} q_{zb}(z) \\ 0 \\ q_{yb}(z) \end{Bmatrix} \quad (2.45)$$

with the corresponding boundary conditions

$$-\left[E_bA_bW_b'(0)-N(0)\right]\delta W_b(0)=0$$

$$\left[E_bA_bW_b'(L)-N(L)\right]\delta W_b(L)=0$$

$$-E_pA_pW_p'(0)\delta W_p(0)=0$$

$$E_pA_pW_p'(L)\delta W_p(L)=0$$

$$-\left[\left(E_bI_{xxb}+E_pI_{xxp}\right)V''(0)-M_x(0)\right]\delta V'(0)=0$$

$$\left[\left(E_bI_{xxb}+E_pI_{xxp}\right)V''(L)-M_x(L)\right]\delta V'(L)=0$$

$$-\Big[c_1c_2G_aA_aW_b(0)-c_1c_2G_aA_aW_p(0)-\left(E_bI_{xxb}+E_pI_{xxp}\right)V'''(0)+c_2^2G_aA_aV'(0)-Q_y(0)+$$
$$+\int_{s_b}p_z(s_b,0)Y(s_b,n_b)ds_b\Big]\delta V(0)=0$$

$$\Big[c_1c_2G_aA_aW_b(L)-c_1c_2G_aA_aW_p(L)-\left(E_bI_{xxb}+E_pI_{xxp}\right)V'''(L)+c_2^2G_aA_aV'(L)-Q_y(L)$$
$$+\int_{s_b}p_z(s_b,L)Y(s_b,n_b)ds_b\Big]\delta V(L)=0$$

The second system of equations governs the lateral torsional response of the system and takes the form

$$\left[\begin{array}{c:c:c} \begin{array}{c} E_bI_{yyb}D^4-c_1^2G_aI_{yya}D^2 \\ +c_1^2G_aA_a \end{array} & c_1^2G_aI_{yya}D^2-c_1^2G_aA_a & c_1c_3G_aI_{yya}D^2+c_1c_2G_aA_a \\ \hdashline c_1^2G_aI_{yya}D^2-c_1^2G_aA_a & \begin{array}{c} E_pI_{yyp}D^4-c_1^2G_aI_{yya}D^2 \\ +c_1^2G_aA_a \end{array} & -c_1c_3G_aI_{yya}D^2-c_1c_2G_aA_a \\ \hdashline c_1c_3G_aI_{yya}D^2+c_1c_2G_aA_a & -c_1c_3G_aI_{yya}D^2-c_1c_2G_aA_a & \begin{array}{c} \left(E_bI_{\omega\omega b}+E_pI_{\omega\omega p}\right)D^4 \\ -\chi D^2+c_2^2G_aA_a \end{array} \end{array}\right]\begin{Bmatrix} U_b \\ U_p \\ \theta_z \end{Bmatrix}=\begin{Bmatrix} q_{xb}(z) \\ 0 \\ m_{zb}(z) \end{Bmatrix} \quad (2.46)$$

in which $\chi = \left(G_b J_b + G_p J_p + G_a J_a + c_3^2 G_a I_{yya}\right)$. The corresponding boundary conditions are

$$-\left[E_b I_{yyb} U_b''(0) - M_y(0)\right]\delta U_b'(0) = 0$$
$$\left[E_b I_{yyb} U_b''(L) - M_y(L)\right]\delta U_b'(L) = 0$$

$$-\left[-E_b I_{yyb} U_b'''(0) + c_1^2 G_a I_{yya} U_b'(0) - c_1^2 G_a I_{yya} U_p'(0) - c_1 c_3 G_a I_{yya} \theta_z'(0) + \right.$$
$$\left. -Q_x(0) + \int_{s_b} p_z(s_b, 0) X(s_b, n_b) ds_b \right]\delta U_b(0) = 0$$

$$\left[-E_b I_{yyb} U_b'''(L) + c_1^2 G_a I_{yya} U_b'(L) - c_1^2 G_a I_{yya} U_p'(L) - c_1 c_3 G_a I_{yya} \theta_z'(L) + \right.$$
$$\left. -Q_x(L) + \int_{s_b} p_z(s_b, L) X(s_b, n_b) ds_b \right]\delta U_b(L) = 0$$

$$-E_p I_{yyp} U_p''(0)\delta U_p'(0) = 0$$
$$E_p I_{yyp} U_p''(L)\delta U_p'(L) = 0$$

$$-\left[-c_1^2 G_a I_{yya} U_b'(0) - E_p I_{yyp} U_p'''(0) + c_1^2 G_a I_{yya} U_p'(0) + c_1 c_3 G_a I_{yya} \theta_z'(0)\right]\delta U_p(0) = 0$$

$$\left[-c_1^2 G_a I_{yya} U_b'(L) - E_p I_{yyp} U_p'''(L) + c_1^2 G_a I_{yya} U_p'(L) + c_1 c_3 G_a I_{yya} \theta_z'(L)\right]\delta U_p(L) = 0$$

$$-\left[\left(E_b I_{\omega\omega b} + E_p I_{\omega\omega p}\right)\theta_z''(0) - B(0)\right]\delta\theta_z'(0) = 0$$

$$\left[\left(E_b I_{\omega\omega b} + E_p I_{\omega\omega p}\right)\theta_z''(L) - B(L)\right]\delta\theta_z'(L) = 0$$

$$-\left[-c_1 c_3 G_a I_{yya} U_b'(0) + c_1 c_3 G_a I_{yya} U_p'(0) - \left(E_b I_{\omega\omega b} + E_p I_{\omega\omega p}\right)\theta'''(0) + \chi\theta_z'(0) + \right.$$
$$\left. -T(0) + \int_{s_b} p_z(s_b, 0)\Omega(s_b, n_b) ds_b \right]\delta\theta_z(0) = 0$$
$$\left[-c_1 c_3 G_a I_{yya} U_b'(L) + c_1 c_3 G_a I_{yya} U_p'(L) - \left(E_b I_{\omega\omega b} + E_p I_{\omega\omega p}\right)\theta'''(L) + \chi\theta_z'(L) + \right.$$
$$\left. -T(L) + \int_{s_b} p_z(s_b, L)\Omega(s_b, n_b) ds_b \right]\delta\theta_z(L) = 0$$

2.5.7. Homogeneous solutions of equilibrium equations

2.5.7.1. First set of equilibrium equation system

The solution of equilibrium equation system (2.45) are expressed as

$$W_b(z) = C_1 + C_2 z + C_3 z^2 + C_4 e^{m_1 z} + C_5 e^{m_2 z}$$

$$W_p(z) = C_6 + C_7 z + C_3\left(-\frac{E_b A_b}{E_p A_p}\right) z^2 + C_4\left(-\frac{E_b A_b}{E_p A_p}\right) e^{m_1 z} + C_5\left(-\frac{E_b A_b}{E_p A_p}\right) e^{m_2 z}$$

$$V(z) = -C_1 \frac{c_1}{c_2} z - C_2 \frac{c_1}{2c_2} z^2 + C_7 \frac{c_1}{2c_2} z^2 + C_6 \frac{c_1}{c_2} z + C_3\left[\frac{2E_b A_b}{c_1 c_2 G_a A_a} z - c_1\left(\frac{E_b A_b + E_p A_p}{3c_2 E_p A_p}\right) z^3\right] + \tag{2.47}$$

$$+ C_4\left[m_1 \frac{E_b A_b}{c_1 c_2 G_a A_a} - c_1\left(\frac{E_b A_b + E_p A_p}{m_1 c_2 E_p A_p}\right)\right] e^{m_1 z} + C_5\left[m_2 \frac{E_b A_b}{c_1 c_2 G_a A_a} - c_1\left(\frac{E_b A_b + E_p A_p}{m_2 c_2 E_p A_p}\right)\right] e^{m_2 z} + C_8$$

in which $m_1 = -m_2 = \sqrt{\dfrac{c_1^2 G_a A_a\left(E_b A_b + E_p A_p\right)\left(E_b I_{xxb} + E_p I_{xxp}\right) + c_2^2 G_a A_a E_b A_b E_p A_p}{E_b A_b E_p A_p\left(E_b I_{xxb} + E_p I_{xxp}\right)}}$

The details of developing the solution are presented in Appendix A3. In Equations 2.41, the eight unknown factors including $C_i, i = 1,...,8$ are determined based on the corresponding boundary conditions.

2.5.7.2. Second set of equilibrium equation system

The solution of the equilibrium equation system (2.46) is expressed as (Appendix A3)

$$U_b = D_1 + D_2 z + D_3 z^2 + D_4 z^3 + \sum_{i=5}^{10} D_i e^{k_i z}$$

$$U_p = A_{51} + A_{52} z + D_3 z^2 + D_4 z^3 - \sum_{i=5}^{10} D_i \frac{E_b I_{yyb}}{E_p I_{yyp}} e^{k_i z} \tag{2.48}$$

$$\theta_z = -D_1 \frac{c_1}{c_2} - D_2 \frac{c_1}{c_2} z + D_{11} \frac{c_1}{c_2} + D_{12} \frac{c_1}{c_2} z + \sum_{i=5}^{10} D_i f_{6i} e^{k_i z}$$

in which

$$f_{6i} = \left[\frac{-E_b I_{yyb} E_p I_{yyp} k_i^4 + c_1^2 G_a I_{yya}\left(E_b I_{yyb} + E_p I_{yyp}\right) k_i^2 - c_1^2 G_a A_a\left(E_b I_{yyb} + E_p I_{yyp}\right)}{E_p I_{yyp}\left(c_1 c_3 G_a I_{yya} k_i^2 + c_1 c_2 G_a A_a\right)}\right],\ i = 5, 6, 7,\ 8,\ 9,\ 10$$

and the values of k_i are obtained from the sixth order equation

$$k^6 + F_1 k^4 + F_2 k^2 + F_3 = 0 \tag{2.49}$$

$$F_1 = -\frac{c_1^2 G_a I_{yya}\left(E_b I_{\omega\omega b} + E_p I_{\omega\omega p}\right)\left(E_b I_{yyb} + E_p I_{yyp}\right) + E_b I_{yyb} E_p I_{yyp}\left(G_b J_b + G_p J_p + G_a J_a + c_3^2 G_a I_{yya}\right)}{E_b I_{yyb} E_p I_{yyp}\left(E_b I_{\omega\omega b} + E_p I_{\omega\omega p}\right)};$$

$$F_2 = \frac{\left(E_b I_{yyb} + E_p I_{yyp}\right)\left[c_1^2 G_a A_a\left(E_b I_{\omega\omega b} + E_p I_{\omega\omega p}\right) + c_1^2 G_a I_{yya}\left(G_b J_b + G_p J_p + G_a J_a\right)\right] + c_2^2 G_a A_a E_b I_{yyb} E_p I_{yyp}}{E_b I_{yyb} E_p I_{yyp}\left(E_b I_{\omega\omega b} + E_p I_{\omega\omega p}\right)}$$

$$F_3 = -\frac{\left[c_1^2 G_a A_a\left(G_b J_b + G_p J_p + G_a J_a\right) + c_1^2\left(c_2 + c_3\right)^2 G_a A_a G_a I_{yya}\right]\left(E_b I_{yyb} + E_p I_{yyp}\right)}{E_b I_{yyb} E_p I_{yyp}\left(E_b I_{\omega\omega b} + E_p I_{\omega\omega p}\right)}.$$

The 12 unknown factors including $D_i, i = 1,\ldots,12$ will be determined based on 12 corresponding boundary conditions.

2.6. Summary

This chapter has developed a theory for the analysis of composite steel wide flange section reinforced with a GFRP plate connected to one of the flanges through an adhesive layer. The theory is based on an extension of the Gjelsvik theory to accommodate the composite system while allowing relative lateral and longitudinal displacements between the top of the steel beam and the underside of the GFRP plate. The resulting equilibrium conditions consist of two sets of coupled differential equations. The first set describes the longitudinal-transverse response and involves three field variables (the longitudinal displacement at the centroid of the beam, that of the plate and the transverse displacement). The second set of coupled differential equations describes the torsional-flexural response and involves three fields. These are the lateral displacements at the centroid of the steel beam, the lateral displacement at the centroid of the GFRP and the angle of twist of the composite system. The possible boundary condition expressions for both systems have also been formulated. Closed form expressions are then provided for all six displacement fields in terms of integration constants.

The closed form solutions derived are suitable for problems involving single span but are complicated to implement for problems involving multiple spans. Therefore, development of finite elements based on these closed form solutions is necessary and feasible. This will be the scope of Chapter 3.

CHAPTER 3 – NON-SHEAR DEFORMABLE THEORY-FINITE ELEMENT FORMULATION

3.1 Scope

In this Chapter, a finite element formulation is developed based on the non-shear deformable theory introduced in Chapter 2. The formulation is based on shape functions which exactly meet the homogeneous form of the equilibrium conditions developed in Chapter 2.

3.2 Expression for Total Potential Energy

From Eq. 2.36 in Chapter 2, the total potential energy π can be expressed as the sum of the total potential energy based on longitudinal-transverse response $\pi_1 = \pi_1\left(W_b, W_b', W_p, W_p', V, V', V''\right)$ and that based on the lateral torsional response $\pi_2 = \pi_2\left(U_b, U_b', U_b'', U_p, U_p', U_p'', \theta_z, \theta_z', \theta_z''\right)$. , i.e.,

$$\pi = \pi_1 + \pi_2$$

in which

$$\begin{aligned}\pi_1 &= \frac{1}{2}\int_L \left(E_b A_b W_b'^2 + E_b I_{xxb} V''^2\right) dz + \frac{1}{2}\int_L \left(E_p A_p W_p'^2 + E_p I_{xxp} V''^2\right) dz \\ &+ \frac{1}{2} G_a A_a \int_L \left[c_2^2 V'^2 + c_1^2 W_b^2 + c_1^2 W_p^2 - 2c_1^2 W_b W_p + 2c_1 c_2 V'\left(W_b - W_p\right)\right] dz + \\ &+ N(0) W_b(0) + Q_y(0) V(0) + M_x(0) V'(0) - N(L) W_b(L) - Q_y(L) V(L) - M_x(L) V'(L) + \\ &- \int_L \langle W_b \quad V \quad V' \rangle_{1\times 3} \int_{s_b} \begin{Bmatrix} p_z(s_b, z) \\ p_v(s_b, z)\sin\alpha(s_b) - p_u(s_b, z)\cos\alpha(s_b) \\ -p_z(s_b, z) Y(s_b, n_b) \end{Bmatrix}_{3\times 1} ds_b\, dz\end{aligned} \tag{3.1}$$

with $c_1 = \dfrac{1}{t_2}$, $c_2 = \dfrac{t_1 + 2t_2 + t_3 + h_b}{2t_2}$; and

$$\begin{aligned}\pi_2 &= \frac{1}{2}\int_L \left(E_b I_{yyb} U_b''^2 + E_b I_{\omega\omega b} \theta_z''^2 + G_b J_b \theta_z'^2\right) dz + \frac{1}{2}\int_L \left(E_p I_{yyp} U_p''^2 + E_p I_{\omega\omega p} \theta_z''^2 + G_p J_p \theta_z'^2\right) dz + \\ &+ \frac{1}{2}\int_L \left\{G_a J_a \theta'^2 + G_a I_{yya} \langle U_O \rangle_{1\times 3}'^{\mathrm{T}} \left[\overline{H}_{a1}\right]_{3\times 3} \{U_O\}' + G_a A_a \langle U_O \rangle_{1\times 3}^{\mathrm{T}} \left[\overline{H}_{a2}\right]_{3\times 3} \{U_O\}\right\} dz + \\ &+ Q_x(0) U_b(0) + M_y(0) U_b'(0) + T(0)\theta_z(0) + B(0)\theta_z'(0) - Q_x(L) U_b(L) - M_y(L) U_b'(L) - T(L)\theta_z(L)\end{aligned}$$

$$-B(L)\theta_z'(L)+\int_0^L \langle U_b \quad U_b' \quad \theta_z \quad \theta_z' \rangle \int_{s_b} \begin{Bmatrix} p_v(s_b,z)\cos\alpha(s_b)+p_u(s_b,z)\sin\alpha(s_b) \\ -p_z(s_b,z)X(s_b,n_b) \\ p_v(s_b,z)\left[r(s_b)+nq'(s_b)\right]-p_u(s_b,z)q(s_b) \\ -p_z(s_b,z)\Omega(s_b,n_b) \end{Bmatrix} ds_b dz \tag{3.2}$$

with $\langle U_O \rangle^T = \langle U_b \quad U_p \quad \theta_z \rangle, \left[\overline{H}_{a1}\right]_{3\times3} = \begin{bmatrix} c_1^2 & -c_1^2 & -c_1c_3 \\ -c_1^2 & c_1^2 & c_1c_3 \\ -c_1c_3 & c_1c_3 & c_3^2 \end{bmatrix}, \left[\overline{H}_{a2}\right]_{3\times3} = \begin{bmatrix} c_1^2 & -c_1^2 & c_1c_2 \\ -c_1^2 & c_1^2 & -c_1c_2 \\ c_1c_2 & -c_1c_2 & c_2^2 \end{bmatrix}$

3.3 Formulation for Longitudinal-Transverse Response

3.3.1 Closed Form Solution

One recalls that the closed form solution for the longitudinal response as provided in Eqs. 2.47 are

$$W_b(z)=C_1+C_2z+C_3z^2+C_4e^{m_1z}+C_5e^{m_2z}$$

$$W_p(z)=C_6+C_7z+C_3\left(-\frac{E_bA_b}{E_pA_p}\right)z^2+C_4\left(-\frac{E_bA_b}{E_pA_p}\right)e^{m_1z}+C_5\left(-\frac{E_bA_b}{E_pA_p}\right)e^{m_2z}$$

$$V(z)=-C_1\frac{c_1}{c_2}z-C_2\frac{c_1}{2c_2}z^2+C_7\frac{c_1}{2c_2}z^2+C_6\frac{c_1}{c_2}z+C_3\left[\frac{2E_bA_b}{c_1c_2G_aA_a}z-c_1\left(\frac{E_bA_b+E_pA_p}{3c_2E_pA_p}\right)z^3\right]+$$

$$+C_4\left[m_1\frac{E_bA_b}{c_1c_2G_aA_a}-c_1\left(\frac{E_bA_b+E_pA_p}{m_1c_2E_pA_p}\right)\right]e^{m_1z}+C_5\left[m_2\frac{E_bA_b}{c_1c_2G_aA_a}-c_1\left(\frac{E_bA_b+E_pA_p}{m_2c_2E_pA_p}\right)\right]e^{m_2z}+C_8 \tag{3.3}$$

in which $m_1=-m_2=\sqrt{\dfrac{c_1^2G_aA_a\left(E_bA_b+E_pA_p\right)\left(E_bI_{xxb}+E_pI_{xxp}\right)+c_2^2G_aA_aE_bA_bE_pA_p}{E_bA_bE_pA_p\left(E_bI_{xxb}+E_pI_{xxp}\right)}}$

3.3.2 Formulation of exact shape function

The three field displacements $W_b, W_p,$ and V in Eqs. (3.3) are expressed in a matrix form along with the first derivative of the transverse displacement with respect to z as

$$\left\{\Delta_1(z)\right\}_{4\times1}=\left[Z_1(z)\right]_{4\times8}\left\{\overline{C}\right\}_{8\times1} \tag{3.4}$$

in which $\left\langle \Delta_1(z)\right\rangle_{1\times4}^T=\left\langle W_b(z) \quad W_p(z) \quad V(z) \quad V'(z)\right\rangle$,

$\left\langle \overline{C}\right\rangle_{1\times8}^T=\left\langle C_1 \quad C_2 \quad C_3 \quad C_4 \quad C_5 \quad C_6 \quad C_7 \quad C_8\right\rangle$ is the vector of integration constants, and

$$
\left[Z_1(z)\right]_{4\times 8}=\left[\begin{array}{c|c|c|c|c|c|c|c}
1 & z & z^2 & e^{m_1 z} & e^{m_2 z} & 0 & 0 & 0\\ \hline
0 & 0 & -f_1 z^2 & -f_1 e^{m_1 z} & -f_1 e^{m_2 z} & 1 & z & 0\\ \hline
-f_2 z & -f_2 z^2/2 & 2f_3 z-f_4 z^3 & f_5 e^{m_1 z} & f_6 e^{m_2 z} & f_2 z & f_2 z^2/2 & 1\\ \hline
-f_2 & -f_2 z & 2f_3-3f_4 z^2 & f_5 m_1 e^{m_1 z} & f_6 m_2 e^{m_2 z} & f_2 & f_2 z & 0
\end{array}\right]
$$

with $f_1=\dfrac{E_b A_b}{E_p A_p}, f_2=\dfrac{c_1}{c_2}, f_3=\dfrac{E_b A_b}{c_1 c_2 G_a A_a}, f_4=\dfrac{c_1\left(E_b A_b+E_p A_p\right)}{3c_2 E_p A_p}, f_5=m_1\dfrac{E_b A_b}{c_1 c_2 G_a A_a}-\dfrac{c_1\left(E_b A_b+E_p A_p\right)}{m_1 c_2 E_p A_p},$

$f_6=m_2\dfrac{E_b A_b}{c_1 c_2 G_a A_a}-\dfrac{c_1\left(E_b A_b+E_p A_p\right)}{m_2 E_p A_p}$

By substituting $z=0$ and $z=L$ into Eq. (3.4), one obtains

$$
\left\{\Delta_{1N}\right\}_{8\times 1}=\left[L_1\right]_{8\times 8}\left\{\overline{C}\right\}_{8\times 1} \tag{3.5}
$$

in which $\left\langle\Delta_{1N}\right\rangle_{1\times 8}^{T}=\left\langle W_b(0)\quad W_p(0)\quad V(0)\quad V'(0)\quad W_b(L)\quad W_p(L)\quad V(L)\quad V'(L)\right\rangle$ is the vector of nodal displacements, and

$$
\left[L_1\right]_{8\times 8}=\left[\begin{array}{c}\left[Z_1(0)\right]_{4\times 8}\\ \hdashline \left[Z_1(L)\right]_{4\times 8}\end{array}\right] \tag{3.6}
$$

By inverting Eq. (3.5), i.e., $\left\{\overline{C}\right\}_{8\times 1}=\left[L_1\right]_{8\times 8}^{-1}\left\{\Delta_{1N}\right\}_{8\times 1}$ and substituting into Eq.(3.4), one obtains

$$
\left\{\Delta_1(z)\right\}_{4\times 1}=\left[N_1(z)\right]_{4\times 8}\left\{\Delta_{1N}\right\}_{8\times 1} \tag{3.7}
$$

in which $\left[N_1(z)\right]_{4\times 8}=\left[Z_1(z)\right]_{4\times 8}\left[L_1\right]_{8\times 8}^{-1}$ is the matrix of shape functions which satisfy the homogeneous form of the equilibrium equations. The displacement fields are extracted from Eq. (3.7) through

$$
\left(W_b(z),W_p(z),V(z)\right)=\left(\left\langle\rho_1\right\rangle_{1\times 4}^{T},\left\langle\rho_2\right\rangle_{1\times 4}^{T},\left\langle\rho_3\right\rangle_{1\times 4}^{T}\right)\left[N_1(z)\right]_{4\times 8}\left\{\Delta_{1N}\right\}_{8\times 1} \tag{3.8}
$$

in which vectors $\left\langle\rho_1\right\rangle_{1\times 4}^{T}=\left\langle 1\quad 0\quad 0\quad 0\right\rangle,\left\langle\rho_2\right\rangle_{1\times 4}^{T}=\left\langle 0\quad 1\quad 0\quad 0\right\rangle$, and $\left\langle\rho_3\right\rangle_{1\times 4}^{T}=\left\langle 0\quad 0\quad 1\quad 0\right\rangle$ have been defined.

3.3.3 Formulation of discrete equilibrium conditions

From Eq. (3.8), by substituting into Eq. (3.1), the discretized form of the first variation of the total potential energy is expressed as

$$\delta\pi_1 = \langle \delta\Delta_{1N} \rangle^T \left(\left(\left[K_1 \right]_{8\times8} + \left[K_2 \right]_{8\times8} + \left[K_3 \right]_{8\times8} \right) \{ \Delta_{1N} \}_{8\times1} - \left\{ Q_1 \right\}_{8\times1} \right) = 0 \tag{3.9}$$

in which $\left[K_1 \right]_{8\times8}$ is the stiffness contribution of wide flange beam, determined from Eq. A4.7 in Appendix A4 as

$$\begin{aligned}\left[K_1 \right]_{8\times8} = E_b \left[L_1 \right]_{8\times8}^{-1\,T} \Bigg[& A_b \int_L \left[Z_1(z) \right]_{8\times4}^{\prime T} \{ \rho_1 \}_{4\times1} \langle \rho_1 \rangle_{1\times4}^T \left[Z_1(z) \right]_{4\times8}^{\prime} dz + \\ & + I_{xxb} \int_L \left[Z_1(z) \right]_{8\times4}^{\prime\prime T} \{ \rho_3 \}_{4\times1} \langle \rho_3 \rangle_{1\times4}^T \left[Z_1(z) \right]_{4\times8}^{\prime\prime} dz \Bigg] \left[L_1 \right]_{8\times8}^{-1}\end{aligned}, \tag{3.10}$$

$\left[K_2 \right]_{8\times8}$ is the stiffness contribution of GFRP plate, determined from Eq. A4.8 in Appendix A4 as

$$\begin{aligned}\left[K_2 \right]_{8\times8} = E_p \left[L_1 \right]_{8\times8}^{-1\,T} \Bigg[& A_p \int_L \left[Z_1(z) \right]_{8\times4}^{\prime T} \{ \rho_2 \}_{4\times1} \langle \rho_2 \rangle_{1\times4}^T \left[Z_1(z) \right]_{4\times8}^{\prime} dz + \\ & + I_{xxp} \int_L \left[Z_1(z) \right]_{8\times4}^{\prime\prime T} \{ \rho_3 \}_{4\times1} \langle \rho_3 \rangle_{1\times4}^T \left[Z_1(z) \right]_{4\times8}^{\prime\prime} dz \Bigg] \left[L_1 \right]_{8\times8}^{-1}\end{aligned}, \tag{3.11}$$

and $\left[K_3 \right]_{8\times8}$ is the stiffness contribution of adhesive layer, determined from Eq. A4.19 in Appendix A4

$$\begin{aligned}\left[K_3 \right]_{8\times8} = {} & c_2^2 G_a A_a \left[L_1 \right]_{8\times8}^{-1\,T} \left[\int_L \left[Z_1(z) \right]_{8\times4}^{\prime T} \{ \rho_3 \}_{4\times1} \langle \rho_3 \rangle_{1\times4}^T \left[Z_1(z) \right]_{4\times8}^{\prime} dz \right] \left[L_1 \right]_{8\times8}^{-1} \\ & + c_1^2 G_a A_a \left[L_1 \right]_{8\times8}^{-1\,T} \left[\int_L \left[Z_1(z) \right]_{8\times4}^T \left[\{ \rho_1 \}_{4\times1} \;\vdots\; \{ \rho_2 \}_{4\times1} \right] \begin{bmatrix} 1 & -1 \\ -1 & 1 \end{bmatrix} \begin{bmatrix} \langle \rho_1 \rangle_{1\times4}^T \\ \hdashline \langle \rho_2 \rangle_{1\times4}^T \end{bmatrix} \left[Z_1(z) \right]_{4\times8} dz \right] \left[L_1 \right]_{8\times8}^{-1} \\ & + \left[M \right]_{8\times8} + \left[M \right]_{8\times8}^T\end{aligned} \tag{3.12}$$

with $\left[M \right]_{8\times8} = c_1 c_2 G_a A_a \int_L \left\{ \left[N_1(z) \right]_{8\times4}^{\prime T} \left[\{ \rho_3 \}_{4\times1} \left(\langle \rho_1 \rangle_{1\times4}^T - \langle \rho_2 \rangle_{1\times4}^T \right) \right] \left[N_1(z) \right]_{4\times8} \right\} dz$, and

and $\left\{ Q_1 \right\}_{8\times1}$ is the energy equivalent load vector, given by

$$\left\{ Q_1 \right\}_{8\times1} = \left\{ Q_{11} \right\}_{8\times1} + \left\{ Q_{21} \right\}_{8\times1} \tag{3.13}$$

where $\left\langle Q_{11} \right\rangle_{1\times8}^T = \langle -W_b(0) \quad 0 \quad -Q_y(0) \quad -M_x(0) \quad W_b(L) \quad 0 \quad Q_y(L) \quad M_x(L) \rangle$, and

$\left\{ Q_{21} \right\} = \int_L \left[\left[N_1(z) \right]_{8\times4}^T \{ \rho_1 \}_{4\times1} \;\vdots\; \left[N_1(z) \right]_{8\times4}^T \{ \rho_3 \}_{4\times1} \;\vdots\; \left[N_1(z) \right]_{8\times4}^{\prime T} \{ \rho_3 \}_{4\times1} \right] \left\{ p_1 \right\}_{3\times1} dz$ with

$$\left\{ p_1 \right\}_{3\times1} = \int_{s_b} \left\{ \begin{array}{c} p_z(s_b, z) \\ \hdashline p_v(s_b, z) \sin\alpha(s_b) - p_u(s_b, z) \cos\alpha(s_b) \\ \hdashline -p_z(s_b, z) Y(s_b, n_b) \end{array} \right\} ds_b$$

3.4 Finite Element Formulation for Lateral-Torsional Response

3.4.1 Closed Form Solution

One recalls that the closed form solution as provide in Eqs. 2.48 is

$$
\begin{aligned}
U_b &= D_1 + D_2 z + D_3 z^2 + D_4 z^3 + \sum_{i=5}^{10} D_i e^{k_i z} \\
U_p &= A_{51} + A_{52} z + D_3 z^2 + D_4 z^3 - \sum_{i=5}^{10} D_i \frac{E_b I_{yyb}}{E_p I_{yyp}} e^{k_i z} \\
\theta_z &= -D_1 \frac{c_1}{c_2} - D_2 \frac{c_1}{c_2} z + D_{11} \frac{c_1}{c_2} + D_{12} \frac{c_1}{c_2} z + \sum_{i=5}^{10} D_i f_{8i} e^{k_i z}
\end{aligned}
\tag{3.14}
$$

in which

$$
f_{8i} = \left[\frac{-E_b I_{yyb} E_p I_{yyp} k_i^4 + c_1^2 G_a I_{yya} \left(E_b I_{yyb} + E_p I_{yyp} \right) k_i^2 - c_1^2 G_a A_a \left(E_b I_{yyb} + E_p I_{yyp} \right)}{E_p I_{yyp} \left(c_1 c_3 G_a I_{yya} k_i^2 + c_1 c_2 G_a A_a \right)} \right], \; i = 5, \ldots
$$

3.4.2 Formulation of exact shape functions

Equations (3.14) are expressed in a matrix form along with the fist derivatives U_b', U_p', θ_z' as

$$
\left\{ \Delta_2(z) \right\}_{6\times1} = \left[Z_2(z) \right]_{6\times12} \left\{ \overline{D} \right\}_{12\times1} \tag{3.15}
$$

in which $\left\langle \Delta_2(z) \right\rangle_{1\times6}^T = \left\langle U_b(z) \quad U_b'(z) \quad U_p(z) \quad U_p'(z) \quad \theta_z(z) \quad \theta_z'(z) \right\rangle$ and

$\left\langle \overline{D} \right\rangle_{1\times12}^T = \left\langle D_1 \quad D_2 \quad D_3 \quad D_4 \quad D_5 \quad D_6 \quad D_7 \quad D_8 \quad D_9 \quad D_{10} \quad D_{11} \quad D_{12} \right\rangle$ is the vector of integration constants, and

$\left[Z_2(z) \right]_{3\times12} =$

$$
\begin{bmatrix}
1 & z & z^2 & z^3 & e^{k_7 z} & e^{k_8 z} & e^{k_9 z} & e^{k_{10} z} & e^{k_{11} z} & e^{k_{12} z} & 0 & 0 \\
0 & 1 & 2z & 3z^2 & k_7 e^{k_7 z} & k_8 e^{k_8 z} & k_9 e^{k_9 z} & k_{10} e^{k_{10} z} & k_{11} e^{k_{11} z} & k_{12} e^{k_{12} z} & 0 & 0 \\
0 & 0 & z^2 & z^3 & -f_7 e^{k_7 z} & -f_7 e^{k_8 z} & -f_7 e^{k_9 z} & -f_7 e^{k_{10} z} & -f_7 e^{k_{11} z} & -f_7 e^{k_{12} z} & 1 & z \\
0 & 0 & 2z & 3z^2 & -f_7 k_7 e^{k_7 z} & -f_7 k_8 e^{k_8 z} & -f_7 k_9 e^{k_9 z} & -f_7 k_{10} e^{k_{10} z} & -f_7 k_{11} e^{k_{11} z} & -f_7 k_{12} e^{k_{12} z} & 0 & 1 \\
-f_2 & -f_2 z & 0 & 0 & f_{87} e^{k_7 z} & f_{88} e^{k_8 z} & f_{89} e^{k_9 z} & f_{810} e^{k_{10} z} & f_{811} e^{k_{11} z} & f_{812} e^{k_{12} z} & f_2 & f_2 z \\
0 & -f_2 & 0 & 0 & f_{87} k_7 e^{k_7 z} & f_{88} k_8 e^{k_8 z} & f_{89} k_9 e^{k_9 z} & f_{810} k_{10} e^{k_{10} z} & f_{811} k_{11} e^{k_{11} z} & f_{812} k_{12} e^{k_{12} z} & 0 & f_2
\end{bmatrix}
$$

with $f_7 = E_b I_{yyb} / E_p I_{yyp}$.

By substituting $z = 0$ and $z = L$ into Eq. (3.15), one obtains

$$
\left\{ \Delta_{2N} \right\}_{12\times1} = \left[L_2 \right]_{12\times12} \left\{ \overline{D} \right\}_{12\times1} \tag{3.16}
$$

in which

$\langle \Delta_{2N} \rangle_{1\times12}^{T} =$

$\langle U_b(0) \quad U_b'(0) \quad U_p(0) \quad U_p'(0) \quad \theta_z(0) \quad \theta_z'(0) \quad U_b(L) \quad U_b'(L) \quad U_p(L) \quad U_p'(L) \quad \theta_z(L) \quad \theta_z'(L) \rangle$

, and

$$[L_2]_{12\times12} = \begin{bmatrix} [Z_2(0)]_{6\times12} \\ \hdashline [Z_2(L)]_{6\times12} \end{bmatrix} \tag{3.17}$$

By inverting Eq. (3.16), i.e., $\{\overline{D}\}_{12\times1} = [L_2]_{12\times12}^{-1}\{\Delta_{2,0}\}_{12\times1}$ and substituting into Eq. (3.15), one obtains

$$\{\Delta_2(z)\}_{6\times1} = [N_2(z)]_{6\times12}\{\Delta_{2N}\}_{12\times1} \tag{3.18}$$

in which the 72 elements of the matrix $[N_2(z)]_{6\times12} = [Z_2]_{6\times12}[L_2]_{12\times12}^{-1}$ are shape functions which satisfy the homogeneous form of the equilibrium equations. The displacement fields are extracted from Eq. (3.18)through

$$\left(U_b(z), U_p(z), \theta(z)\right) = \left(\langle \rho_4 \rangle_{1\times6}^T, \langle \rho_5 \rangle_{1\times6}^T, \langle \rho_6 \rangle_{1\times6}^T\right)[N_2]_{6\times12}\{\Delta_{2N}\}_{12\times1} \tag{3.19}$$

in which vectors $\langle \rho_4 \rangle_{1\times6}^T = \langle 1 \quad 0 \quad 0 \quad 0 \quad 0 \quad 0 \rangle$, $\langle \rho_5 \rangle_{1\times6}^T = \langle 0 \quad 0 \quad 1 \quad 0 \quad 0 \quad 0 \rangle$, and $\langle \rho_6 \rangle_{1\times6}^T = \langle 0 \quad 0 \quad 0 \quad 0 \quad 1 \quad 0 \rangle$ have been defined.

3.4.3 Formulation of discrete equilibrium conditions

From Eq. (3.19), by substituting into Eq. (3.2), the discretized first variation of the total potential energy is expressed as

$$\delta\pi_2 = \langle \delta\Delta_{2N} \rangle^T \left\{ \left([K_4]_{12\times12} + [K_5]_{12\times12} + [K_6]_{12\times12} \right) \{\Delta_{2N}\}_{12\times1} - \{Q_2\}_{12\times1} \right\} = 0 \tag{3.20}$$

in which:

$[K_4]_{12\times12}$ is the stiffness contribution of wide flange beam, as determined in A4.27 in Appendix A4 as

$$\begin{aligned}
[K_4]_{12\times12} = [L_2]_{12\times12}^{-1\,T} \Big\{ & E_b I_{yyb} \int_L [Z_2(z)]_{12\times6}''^T \{\rho_4\}_{6\times1} \langle \rho_4 \rangle_{1\times6}^T [Z_2(z)]_{6\times12}'' dz \\
& + E_b I_{\omega\omega b} \int_L [Z_2(z)]_{12\times6}''^T \{\rho_6\}_{6\times1} \langle \rho_6 \rangle_{1\times6}^T [Z_2(z)]_{6\times12}'' dz \quad , \\
& + G_b J_b \int_L [Z_2(z)]_{12\times6}'^T \{\rho_6\}_{6\times1} \langle \rho_6 \rangle_{1\times6}^T [Z_2(z)]_{6\times12}' dz \Big\} [L_2]_{12\times12}^{-1}
\end{aligned} \tag{3.21}$$

$[K_5]_{12\times12}$ is the stiffness contribution of GFRP plate, as determined in A4.28 in Appendix A4 as

$$\left[K_5\right]_{12\times12} = \left[L_2\right]^{-1\,T}_{12\times12}\left[E_p I_{yyp}\int_L \left[Z_2(z)\right]''^{T}_{3\times12}\{\rho_5\}_{6\times1}\langle\rho_5\rangle^{T}_{1\times6}\left[Z_2(z)\right]''_{3\times12}dz\right.$$

$$+E_p I_{\omega\omega p}\int_L \left[Z_2(z)\right]''^{T}_{3\times12}\{\rho_6\}_{6\times1}\langle\rho_6\rangle^{T}_{1\times6}\left[Z_2(z)\right]''_{3\times12}dz \qquad , \qquad (3.22)$$

$$\left.+G_p J_p\int_L \left[Z_2(z)\right]'^{T}_{3\times12}\{\rho_6\}_{6\times1}\langle\rho_6\rangle^{T}_{1\times6}\left[Z_2(z)\right]'_{3\times12}dz\right]\left[L_2\right]^{-1}_{12\times12}$$

$\left[K_6\right]_{12\times12}$ is the stiffness contribution of adhesive layer, as determined in A4.29 in Appendix A4 as

$$\left[K_6\right]_{12\times12} = \left[L_2\right]^{-1\,T}_{12\times12}\left[G_a J_a\int_L \left[Z_2\right]'^{T}_{3\times12}\{\rho_5\}_{6\times1}\langle\rho_5\rangle^{T}_{1\times6}\left[Z_2\right]'_{3\times12}dz\right.$$

$$+G_a I_{yya}\int_L \left[Z_2\right]'^{T}_{12\times3}\left[\overline{\rho}\right]^{T}_{6\times3}\left[\overline{H}_{a1}\right]_{3\times3}\left[\overline{\rho}\right]_{3\times6}\left[Z_2\right]'_{3\times12}dz \qquad (3.23)$$

$$\left.+G_a A_a\int_L \left[Z_2\right]^{T}_{12\times3}\left[\overline{\rho}\right]^{T}_{6\times3}\left[\overline{H}_{a2}\right]_{3\times3}\left[\overline{\rho}\right]_{3\times6}\left[Z_2\right]_{3\times12}dz\right]\left[L_2\right]^{-1}_{12\times12}$$

in which $\left[\overline{\rho}\right]^{T}_{6\times3} = \left[\{\rho_4\}_{6\times1} \,\vdots\, \{\rho_5\}_{6\times1} \,\vdots\, \{\rho_6\}_{6\times1}\right]$ and $\{Q_2\}_{12\times1}$ is the element load vector given by

$$\{Q_2\}_{12\times1} = \{Q_{12}\}_{12\times1} + \{Q_{22}\}_{12\times1} \qquad (3.24)$$

where

$$\langle Q_{12}\rangle^{T}_{1\times12} = \langle -Q_x(0)\quad -M_y(0)\quad 0\quad 0\quad -T(0)\quad -B(0)\quad Q_x(L)\quad M_y(L)\quad 0\quad 0\quad T(L)\quad B(L)\rangle$$

$$\{Q_{22}\} = -\int_0^L \left\langle \left[N_2(z)\right]^{T}_{12\times6}\{\rho_4\}^{T}_{6\times1} \,\vdots\, \left[N_2(z)\right]'^{T}_{12\times6}\{\rho_4\}^{T}_{6\times1} \,\vdots\, \left[N_2(z)\right]^{T}_{12\times6}\{\rho_6\}^{T}_{6\times1} \,\vdots\, \left[N_2(z)\right]'^{T}_{12\times6}\{\rho_6\}^{T}_{6\times1}\right\rangle \{p_2\}_{4\times1}dz$$

with $\{p_2\}_{4\times1} = \int_{s_b}\left\{\begin{array}{c} p_v(s_b,z)\cos\alpha(s_b) + p_u(s_b,z)\sin\alpha(s_b) \\ \hdashline -p_z(s_b,z)X(s_b,n_b) \\ \hdashline p_v(s_b,z)\left[r(s_b)+nq'(s_b)\right] - p_u(s_b,z)q(s_b) \\ \hdashline -p_z(s_b,z)\Omega(s_b,n_b) \end{array}\right\}ds_b$

3.5 Strain and Stress expressions

3.5.1 Longitudinal Normal Stress for Wide Flange Beam

In Eq. 2.31, the longitudinal normal strain is determined by

$$\varepsilon_{zb} = W_b'(z) - U_b''(z)X(s_b,n_b) - V''(z)Y(s_b,n_b) - \theta_z''(z)\Omega(s_b,n_b) \qquad (3.25)$$

In the present formulation, functions W_b, U_b, V, θ_z as determined from Eq. (3.3) and (3.14) are based on the homogeneous solution of the equilibrium equations and thus do not account for the particular solution due to member traction. The direct substitution of these functions into Eq. (3.25) for cases where tractions are non-vanishing would lead to erroneous results. Thus, in the following, an algorithm is developed to determine the strain ε_{zb} based on the nodal displacements and nodal forces of a given finite element.

From the boundary conditions in Eqs. 2.45-2.46, expressions for the higher order derivatives of displacements at the element nodes can be developed by evaluating the vector of nodal forces $\left\{Q_1\right\}_{8\times 1}$ for the element through the matrix multiplications $\left[K_{el1}\right]_{8\times 8}\left\{\Delta_{1N}\right\}_{8\times 1}$ in which $\left[K_{el1}\right]_{8\times 8}$ is the longitudinal-transverse element stiffness matrix. Also, the vector of nodal forces $\left\{Q_2\right\}_{12\times 1}$ is calculated from $\left[K_{el2}\right]_{12\times 12}\left\{\Delta_{2N}\right\}_{12\times 1}$ in which $\left[K_{el2}\right]_{12\times 12}$ is the lateral-torsional element stiffness matrix. Once $\left\{Q_1\right\}_{8\times 1}$ and $\left\{Q_2\right\}_{12\times 1}$ are determined, and thus $\left\{Q_{11}\right\}_{8\times 1}$, $\left\{Q_{12}\right\}_{12\times 1}$ nodal vectors are also determined from Eqs. (3.13) and (3.24), respectively, the higher order derivatives at the nodal displacements can be determined as follows:

The first derivative of W_b' can be obtained from

$$W_b'(0)=\frac{N(0)}{E_b A_b},W_b'(L)=\frac{N(L)}{E_b A_b} \tag{3.26}$$

Also, the second derivative of U_b'' is given by

$$U_b''(0)=\frac{M_y(0)}{E_b I_{yyb}},U_b''(L)=\frac{M_y(L)}{E_b I_{yyb}} \tag{3.27}$$

The second derivative of V'' can be obtained as

$$V''(0)=\frac{M_x(0)}{E_b I_{xxb}+E_p I_{xxp}},V''(L)=\frac{M_x(L)}{E_b I_{xxb}+E_p I_{xxp}} \tag{3.28}$$

And the second derivative of θ_z'' is

$$\theta_z''(0)=\frac{B(0)}{E_b I_{\omega\omega b}+E_p I_{\omega\omega p}},\theta_z''(L)=\frac{B(L)}{E_b I_{\omega\omega b}+E_p I_{\omega\omega p}} \tag{3.29}$$

Equations (3.26)-(3.29) are substituted into Eq. (3.25) and by setting $z=0,L$, one obtains

$$\begin{aligned}\varepsilon_{zb}(0)&=\frac{N_b(0)}{E_bA_b}-\frac{M_y(0)}{E_bI_{yyb}}X(s_b,n_b)-\frac{M_x(0)}{E_bI_{xxb}+E_pI_{xxp}}Y(s_b,n_b)-\frac{B(0)}{E_bI_{\omega\omega b}+E_pI_{\omega\omega p}}\Omega(s_b,n_b)\\ \varepsilon_{zb}(L)&=\frac{N_b(L)}{E_bA_b}-\frac{M_y(L)}{E_bI_{yyb}}X(s_b,n_b)-\frac{M_x(L)}{E_bI_{xxb}+E_pI_{xxp}}Y(s_b,n_b)-\frac{B(L)}{E_bI_{\omega\omega b}+E_pI_{\omega\omega p}}\Omega(s_b,n_b)\end{aligned}\tag{3.30}$$

and the longitudinal stresses at the nodes are obtained by

$$\sigma_{zb}(0)=E_b\varepsilon_{zb}(0),\sigma_{zb}(L)=E_b\varepsilon_{zb}(L)\tag{3.31}$$

3.5.2 Longitudinal Normal Stress for GFRP plate

As shown in Eq. 2.32, the longitudinal normal stress for the GFRP plate is expressed as

$$\varepsilon_{zp}=W_p'(z)-U_p''(z)x_p+V''(z)n_p+\theta_z''(z)n_px_p\tag{3.32}$$

In the present developments, no tractions were assumed to act on the GFRP plate. Thus the loads $N_p(0)=N_p(L)=M_{yp}(0)=M_{yp}(L)=0$ do not appear in the boundary terms. If one incorporates these stress resultants in the finite element solution, the following equations would arise

$$W_p'(0)=\frac{N_p(0)}{E_pA_p},W_p'(L)=\frac{N_p(L)}{E_pA_p}\tag{3.33}$$

and

$$U_p''(0)=\frac{M_{yp}(0)}{E_pI_{yyp}},U_p''(L)=\frac{M_{yp}(L)}{E_pI_{yyp}}\tag{3.34}$$

The derivatives of, while $V''(z)$ can be expressed as

$$V''(0)=\frac{M_x(0)}{E_bI_{xxb}+E_pI_{xxp}},V''(L)=\frac{M_x(L)}{E_bI_{xxb}+E_pI_{xxp}}\tag{3.35}$$

The second derivative of θ_z'' can be obtained as

$$\theta_z''(0)=\frac{B(0)}{E_bI_{\omega\omega b}+E_pI_{\omega\omega p}},\theta_z''(L)=\frac{B(L)}{E_bI_{\omega\omega b}+E_pI_{\omega\omega p}}\tag{3.36}$$

Equations (3.35)-(3.36) are substituted into Eq.(3.32) and by setting $z=0,L$, one obtains

$$\begin{aligned}\varepsilon_{zp}(0)&=\frac{N_p(0)}{E_pA_p}-\frac{M_y(0)}{E_pI_{yyp}}x_p+\frac{M_x(0)}{E_bI_{xxb}+E_pI_{xxp}}n_p+\frac{B(0)}{E_bI_{\omega\omega b}+E_pI_{\omega\omega p}}n_px_p\\ \varepsilon_{zp}(L)&=\frac{N_p(L)}{E_pA_p}-\frac{M_y(0)}{E_pI_{yyp}}x_p+\frac{M_x(L)}{E_bI_{xxb}+E_pI_{xxp}}n_p+\frac{B(L)}{E_bI_{\omega\omega b}+E_pI_{\omega\omega p}}n_px_p\end{aligned}\tag{3.37}$$

and the longitudinal stresses at the nodes are obtained by

$$\sigma_{zp}(0) = E_p \varepsilon_{zp}(0), \sigma_{zp}(L) = E_p \varepsilon_{zp}(L) \tag{3.38}$$

3.5.3 Shear stresses within the adhesive layer

Shear strains are expressed in Eqs. 2.33 can be expanded as

$$\begin{aligned} \gamma_{zna} &= -c_1 W_b + c_1 W_p - c_2 V' + c_1 x U_b' - c_1 x U_p' - c_3 x \theta_z' \\ \gamma_{sna} &= -c_1 U_b + c_1 U_p - c_2 \theta_z \\ \gamma_{sza} &= -\left[\frac{(t_1 + t_3) y_a}{t_2} + \frac{t_1 - t_3}{2} \right] \theta_z' \end{aligned} \tag{3.39}$$

At both element ends, one has

$$\begin{aligned} \gamma_{zna}(0) &= -c_1 W_b(0) + c_1 W_p(0) - c_2 V'(0) + c_1 x U_b'(0) - c_1 x U_p'(0) - c_3 x \theta_z'(0) \\ \gamma_{sna}(0) &= -c_1 U_b(0) + c_1 U_p(0) - c_2 \theta_z(0) \\ \gamma_{sza}(0) &= -\left[\frac{(t_1 + t_3) y_a}{t_2} + \frac{t_1 - t_3}{2} \right] \theta_z'(0) \end{aligned} \tag{3.40}$$

and

$$\begin{aligned} \gamma_{zna}(L) &= -c_1 W_b(L) + c_1 W_p(L) - c_2 V'(L) + c_1 x U_b'(L) - c_1 x U_p'(L) - c_3 x \theta_z'(L) \\ \gamma_{sna}(L) &= -c_1 U_b(L) + c_1 U_p(L) - c_2 \theta_z(L) \\ \gamma_{sza}(L) &= -\left[\frac{(t_1 + t_3) y_a}{t_2} + \frac{t_1 - t_3}{2} \right] \theta_z'(L) \end{aligned} \tag{3.41}$$

The displacement fields $W_b(Z_e), W_p(Z_e), V'(Z_e), U_b'(Z_e), U_p'(Z_e), \theta_z(Z_e), \theta_z'(Z_e)$ with $Z_e = 0, L$ are determined from the finite element solution. The shear stresses at the nodes are obtained by

$$\begin{aligned} \tau_{sza}(0) = G_a \gamma_{sza}(0), \tau_{sna}(0) = G_a \gamma_{sna}(0), \tau_{zna}(0) = G_a \gamma_{zna}(0) \\ \tau_{sza}(L) = G_a \gamma_{sza}(L), \tau_{sna}(L) = G_a \gamma_{sna}(L), \tau_{zna}(L) = G_a \gamma_{zna}(L) \end{aligned} \tag{3.42}$$

3.6 Summary

This chapter has developed a finite element formulation for the longitudinal-transverse response and torsional-flexural response for a wide flange steel beam reinforced with a GFRP plate connected to through an adhesive layer. The formulation is based on shape functions which exactly satisfy the equilibrium conditions developed in Chapter 2. The stiffness matrices and energy equivalent load vectors were developed. A finite element program based on the formulations developed in this Chapter is implemented under Matlab. Appendices B1-B3 provide the listing of the problems. Results based on the present solution and comparisons against other 3D finite element solutions are presented in Chapter 4.

CHAPTER 4: VALIDATION OF RESULTS BASED ON NON-SHEAR-DEFORMABLE THEORY

4.1 Introduction

This chapter aims to assess the validity of the non-shear-deformable theory developed in Chapter 2 and the corresponding finite element solution developed in Chapter 3. Four examples for composite systems are considered. These are: 1) A cantilever subject to transverse load acting at the tip, 2) A simply supported beam under uniformly distributed load, 3) A cantilever subject to a tip lateral load acting at the centroid of the steel section, and 4) A cantilever subject to a twisting moment acting at the tip.

The first example is aimed at assessing the validity of the longitudinal transverse response. Towards this goal, the closed form solutions developed in Chapter 2 are specialized for the case of a cantilever. The second example illustrates the ability of the finite element solution to account for a uniformly distributed load. The finite element model developed in Chapter 3 is used to solve Problems 1 and 2. The last two examples are aimed at assessing the validity of the torsional flexural response.

In all four examples, a validation study is performed by comparing the displacements, strains, and stresses within the beam, GFRP plate and adhesive layer based on the present theory to those based on FEA based on the 3D solid element C3D8 available within the ABAQUS simulation package.

4.2. Example 1: Cantilever under transverse point load

4.2.1. Statement of the Problem

A 1.5m span cantilever composite beam consists of a W150x13 beam (flange width $b_b = 100mm$, flange thickness $t_3 = 4.9mm$, depth $d = 148mm$ and web thickness $t_w = 4.3mm$) that is reinforced by a GFRP plate over the whole span (Fig. 4.1). The GFRP plate has a thickness $t_1 = 19mm$ and a width $b_p = 100mm$, while adhesive has a thickness $t_2 = 0.79mm$. Modulus of elasticity of steel is $E_s = 200GPa$ while that of GFRP is $E_p = 42GPa$. Shear modulus of adhesive is $G_a = 4.5GPa$, corresponding to a strong adhesive type (Table 1.1). Poisson's ratio of all three materials μ is 0.3. The cantilever is subjected to a transverse tip load $P = 15kN$ acting downward at the steel section centroid. It is required to compare (i) the transversal displacement at the free end, (ii) the maximum normal stress fields along the beam span for the wide flange beam and GFRP plate, and (iii) the average shear stress along the beam span for the adhesive layer as predicted by the closed form solution developed under Section 4.2.2 below, the finite element solution developed in Chapter 3, and a 3D FEA under ABAQUS.

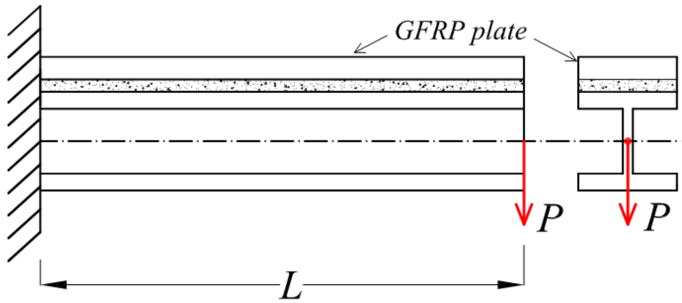

Figure 4.1. A cantilever under a transversely concentrated load applied at tip

4.2.2. Closed Form Solution-Enforcing Boundary Conditions

The closed form displacement field expressions obtained in Eq. 2.47 are

$$W_b(z) = C_1 + C_2 z + C_3 z^2 + C_4 e^{m_1 z} + C_5 e^{m_2 z}$$

$$W_p(z) = C_6 + C_7 z + C_3\left(-\frac{E_b A_b}{E_p A_p}\right) z^2 + C_4\left(-\frac{E_b A_b}{E_p A_p}\right) e^{m_1 z} + C_5\left(-\frac{E_b A_b}{E_p A_p}\right) e^{m_2 z}$$

$$V(z) = -C_1 \frac{c_1}{c_2} z - C_2 \frac{c_1}{2c_2} z^2 + C_7 \frac{c_1}{2c_2} z^2 + C_6 \frac{c_1}{c_2} z + C_3\left[\frac{2E_b A_b}{c_1 c_2 G_a A_a} z - c_1\left(\frac{E_b A_b + E_p A_p}{3c_2 E_p A_p}\right) z^3\right] +$$

$$+ C_4\left[m_1 \frac{E_b A_b}{c_1 c_2 G_a A_a} - c_1\left(\frac{E_b A_b + E_p A_p}{m_1 c_2 E_p A_p}\right)\right] e^{m_1 z} + C_5\left[m_2 \frac{E_b A_b}{c_1 c_2 G_a A_a} - c_1\left(\frac{E_b A_b + E_p A_p}{m_2 c_2 E_p A_p}\right)\right] e^{m_2 z} + C_8 \tag{4.1}$$

in which we recall that

$$m_1 = -m_2 = \sqrt{\frac{c_1^2 G_a A_a \left(E_b A_b + E_p A_p\right)\left(E_b I_{xxb} + E_p I_{xxp}\right) + c_2^2 G_a A_a E_b A_b E_p A_p}{E_b A_b E_p A_p \left(E_b I_{xxb} + E_p I_{xxp}\right)}},$$

and $C_1,\ldots,C_8$ are integration constants which are determined based on eight boundary conditions. For the present problem, the relevant boundary conditions are provided in Table 4.1.

Table 4.1 Boundary conditions for a cantilever problem under tip transverse load

Essential Boundary Condition	Natural Boundary Condition
$W_b(0)=0$ (4.2)	$E_b A_b W_b'(L)=0$ (4.3)
$W_p(0)=0$ (4.4)	$E_p A_p W_p'(L)=0$ (4.5)
$V'(0)=0$ (4.6)	$\left(E_b I_{xxb}+E_p I_{xxp}\right)V''(L)=0$ (4.7)
$V(0)=0$ (4.8)	$\left[c_1c_2G_aA_a\left(W_b-W_p\right)-\left(E_bI_{xxb}+E_pI_{xxp}\right)V'''+c_2^2G_aA_aV'\right]\Big\|_L=P$ (4.9)

From Eqs. (4.1) and (4.2), one obtains

$$C_1+C_4+C_5=0$$

From Eqs. (4.1) and (4.3), one obtains

$$C_2+2LC_3+m_1e^{m_1L}C_4+m_2e^{m_2L}C_5=0$$

From Eqs. (4.1) and (4.4), one obtains

$$-\left(\frac{E_bA_b}{E_pA_p}\right)C_4-\left(\frac{E_bA_b}{E_pA_p}\right)C_5+C_6=0$$

From Eqs. (4.1) and (4.5), one obtains

$$-2\left(\frac{E_bA_b}{E_pA_p}\right)LC_3-\left(\frac{E_bA_b}{E_pA_p}\right)m_1e^{m_1L}C_4-\left(\frac{E_bA_b}{E_pA_p}\right)m_2e^{m_2L}C_5+C_7=0$$

From Eqs. (4.1) and (4.6), one obtains

$$-\frac{c_1}{c_2}C_1+\frac{2E_bA_b}{c_1c_2G_aA_a}C_3+m_1\left[m_1\frac{E_bA_b}{c_1c_2G_aA_a}-c_1\left(\frac{E_bA_b+E_pA_p}{m_1c_2E_pA_p}\right)\right]C_4$$
$$+m_2\left[m_2\frac{E_bA_b}{c_1c_2G_aA_a}-c_1\left(\frac{E_bA_b+E_pA_p}{m_2c_2E_pA_p}\right)\right]C_5+\frac{c_1}{c_2}C_6=0$$

From Eqs. (4.1) and (4.7), one obtains

$$-\frac{c_1}{c_2}C_2-2c_1\left(\frac{E_bA_b+E_pA_p}{c_2E_pA_p}\right)LC_3+m_1^2\left[m_1\frac{E_bA_b}{c_1c_2G_aA_a}-c_1\left(\frac{E_bA_b+E_pA_p}{m_1c_2E_pA_p}\right)\right]e^{m_1L}C_4$$

$$+m_2^2\left[m_2\frac{E_bA_b}{c_1c_2G_aA_a}-c_1\left(\frac{E_bA_b+E_pA_p}{m_2c_2E_pA_p}\right)\right]e^{m_2L}C_5+\frac{c_1}{c_2}C_7=0$$

From Eqs. (4.1) and (4.8), one obtains

$$\left[m_1\frac{E_bA_b}{c_1c_2G_aA_a}-c_1\left(\frac{E_bA_b+E_pA_p}{m_1c_2E_pA_p}\right)\right]C_4+\left[m_2\frac{E_bA_b}{c_1c_2G_aA_a}-c_1\left(\frac{E_bA_b+E_pA_p}{m_2c_2E_pA_p}\right)\right]C_5+C_8=0$$

From Eqs. (4.1) and (4.9), one obtains

$$\left[c_1c_2G_aA_aL^2+\frac{E_bA_bc_1c_2G_aA_a}{E_pA_p}L^2+6\left(E_bI_{xxb}+E_pI_{xxp}\right)c_1\left(\frac{E_bA_b+E_pA_p}{3c_2E_pA_p}\right)\right.$$

$$\left.+\frac{2c_2E_bA_b}{c_1}-c_1c_2^2G_aA_a\left(\frac{E_bA_b+E_pA_p}{c_2E_pA_p}\right)L^2\right]C_3+\left\{c_1c_2G_aA_a+\frac{E_bA_bc_1c_2G_aA_a}{E_pA_p}+\right.$$

$$\left.-\left(E_bI_{xxb}+E_pI_{xxp}\right)m_1^3\left[\frac{m_1E_bA_b}{c_1c_2G_aA_a}-c_1\left(\frac{E_bA_b+E_pA_p}{m_1c_2E_pA_p}\right)\right]+c_2^2G_aA_am_1\left[\frac{m_1E_bA_b}{c_1c_2G_aA_a}-c_1\left(\frac{E_bA_b+E_pA_p}{m_1c_2E_pA_p}\right)\right]\right\}e^{m_1L}C_4$$

$$+\left\{c_1c_2G_aA_a+\frac{E_bA_bc_1c_2G_aA_a}{E_pA_p}-\left(E_bI_{xxb}+E_pI_{xxp}\right)m_2^3\left[m_2\frac{E_bA_b}{c_1c_2G_aA_a}-c_1\left(\frac{E_bA_b+E_pA_p}{m_2c_2E_pA_p}\right)\right]+\right.$$

$$\left.+c_2^2G_aA_am_2\left[m_2\frac{E_bA_b}{c_1c_2G_aA_a}-c_1\left(\frac{E_bA_b+E_pA_p}{m_2c_2E_pA_p}\right)\right]\right\}e^{m_2L}C_5=P$$

Equations from (4.2) to (4.9) are arranged in a matrix form as follows

$$[L]_{8\times8}\left\{\overline{C}\right\}_{8\times1}=\{P\}_{8\times1} \tag{4.10}$$

in which $[L]$ is a matrix of coefficients given by

$$[L]_{8\times8}=\begin{bmatrix} 1 & 0 & 0 & 1 & 1 & 0 & 0 & 0\\ 0 & 1 & 2L & m_1e^{m_1L} & m_2e^{m_2L} & 0 & 0 & 0\\ 0 & 0 & 0 & -f_1 & -f_1 & 1 & 0 & 0\\ 0 & 0 & -2f_1L & -f_1m_1e^{m_1L} & -f_1m_2e^{m_2L} & 0 & 1 & 0\\ -f_2 & 0 & 2f_3 & m_1f_5 & m_2f_6 & f_2 & 0 & 0\\ 0 & -f_2 & -6f_4L & m_1^2f_5e^{m_1L} & m_2^2f_6e^{m_2L} & 0 & f_2 & 0\\ 0 & 0 & 0 & f_5 & f_6 & 0 & 0 & 1\\ 0 & 0 & f_9 & f_{10}e^{m_1L} & f_{11}e^{m_2L} & 0 & 0 & 0 \end{bmatrix}$$

$\left\langle\overline{C}\right\rangle_{1\times8}^{T}=\left\langle C_1\quad C_2\quad C_3\quad C_4\quad C_5\quad C_6\quad C_7\quad C_8\right\rangle$ is a vector of unknown integration constants and the right hand-side vector is . In Eq. (4.10), the following terms have been defined

$$f_1=\frac{E_bA_b}{E_pA_p},\ f_2=\frac{c_1}{c_2},\ f_3=\frac{E_bA_b}{c_1c_2G_aA_a},\ f_4=c_1\left(\frac{E_bA_b+E_pA_p}{3c_2E_pA_p}\right),\ f_5=m_1\frac{E_bA_b}{c_1c_2G_aA_a}-c_1\left(\frac{E_bA_b+E_pA_p}{m_1c_2E_pA_p}\right),$$

$$f_6=m_2\frac{E_bA_b}{c_1c_2G_aA_a}-c_1\left(\frac{E_bA_b+E_pA_p}{m_2c_2E_pA_p}\right),$$

$$f_9=\left\{c_1c_2G_aA_aL^2+\frac{c_1c_2E_bA_bG_aA_a}{E_pA_p}L^2+6c_1\left(E_bI_{xxb}+E_pI_{xxp}\right)\left(\frac{E_bA_b+E_pA_p}{3c_2E_pA_p}\right)+\frac{2c_2E_bA_b}{c_1}+\right.$$

$$\left.-c_1c_2^2G_aA_a\left(\frac{E_bA_b+E_pA_p}{c_2E_pA_p}\right)L^2\right\},$$

$$f_{10}=\left\{c_1c_2G_aA_a+\frac{E_bA_bc_1c_2G_aA_a}{E_pA_p}-\left(E_bI_{xxb}+E_pI_{xxp}\right)m_1^3\left[\frac{m_1E_bA_b}{c_1c_2G_aA_a}-c_1\left(\frac{E_bA_b+E_pA_p}{m_1c_2E_pA_p}\right)\right]+\right.$$

$$\left.+c_2^2G_aA_am_1\left[\frac{m_1E_bA_b}{c_1c_2G_aA_a}-c_1\left(\frac{E_bA_b+E_pA_p}{m_1c_2E_pA_p}\right)\right]\right\},$$

$$f_{11}=\left\{c_1c_2G_aA_a+\frac{E_bA_bc_1c_2G_aA_a}{E_pA_p}-\left(E_bI_{xxb}+E_pI_{xxp}\right)m_2^3\left[m_2\frac{E_bA_b}{c_1c_2G_aA_a}-c_1\left(\frac{E_bA_b+E_pA_p}{m_2c_2E_pA_p}\right)\right]+\right.$$

$$\left.+c_2^2G_aA_am_2\left[m_2\frac{E_bA_b}{c_1c_2G_aA_a}-c_1\left(\frac{E_bA_b+E_pA_p}{m_2c_2E_pA_p}\right)\right]\right\}$$

Equation (4.10) is solved for the integration constants $\left\{\overline{C}\right\}_{8\times1}$ yielding $\left\{\overline{C}\right\}_{8\times1}=\left[L\right]_{8\times8}^{-1}\left\{P\right\}_{8\times1}$, and the vector of displacement functions can be obtained by substituting $\left\{\overline{C}\right\}_{8\times1}$ into Eqs. (4.1). A Matlab program was written to perform the solution as described above (Appendix B1).

4.2.3. Expressions for Strains and Stresses

Given the displacement field expressions, one recalls that the corresponding strains are given by (Eqs. 2.31-2.33) as

$$\varepsilon_{zb}=W_b'(z)-U_b''(z)X(s_b,n_b)-V''(z)Y(s_b,n_b)-\theta_z''(z)\Omega(s_b,n_b)$$

$$\varepsilon_{zp}=W_p'(z)-U_p''(z)x_p+V''(z)n_p+\theta_z''(z)n_px_p$$

$$\gamma_{zna}=\langle a_a\rangle_{1\times6}^{\mathrm{T}}\{\Delta_a\}_{6\times1},\gamma_{sna}=\langle a_{a1}\rangle_{1\times3}^{\mathrm{T}}\{U_o\}_{3\times1},\gamma_{sza}=-f(y_a)\theta'(z)$$

and stresses fields are given by (Eqs. 2.35) as

$$\sigma_{zb}=E_b\varepsilon_{zb}\ ,\ \sigma_{zp}=E_p\varepsilon_{zp}\ ;\ \tau_{sza}=G_a\gamma_{sza}\ ;\ \tau_{sna}=G_a\gamma_{sna}\ ;\ \tau_{zna}=G_a\gamma_{zna}$$

4.2.4. 3D Finite Element Model

The 8-node brick element C3D8R is selected from the ABAQUS library. The element has 24 degrees of freedom (with three translations at each of the eight nodes) and uses reduced integration to avoid volumetric locking. Thus, the element has a single integration point located at the element centroid. A mesh sensitivity study is performed to determine the mesh beyond which no improvement is attained in the solution. The mesh is fully defined by seven parameters $n_1,...,n_7$ as shown in Fig. 4.2. Various combinations for $n_1,...,n_7$ were investigated as presented in Table 4.2.

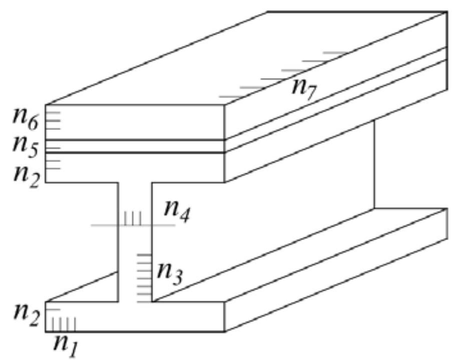

Figure 4.2 Parameters defining the FE mesh

Table 4.2. Meshes used in sensitivity study for Example 1

Mesh #	n1	n2	n3	n4	n5	n6	n7	#nodes	#DOFs
1	6	1	2	2	2	2	15	1,671	5,013
2	6	1	2	2	2	2	30	2,976	8,928
3	22	2	20	2	2	4	500	206,913	620,739
4	44	4	50	4	4	8	750	993,573	2,980,719
5	44	4	50	4	4	8	1,500	1,987,146	5,961,438

Figure 4.3a shows the displacement at the tip of the beam as function of the number of nodes. The displacement in Mesh 2 is 3.2% higher than that of Mesh 4 while that based on Mesh 3 is 0.05% higher than that of Mesh 4. Displacements based on Meshes 4 and 5 are identical.

Figure 4.3b shows the longitudinal normal stress at the bottom middle fiber of the steel beam while Fig. 4.3c shows the average shear stress at the GFRP and adhesive interface and Fig. 4.3d shows the longitudinal normal stress at the top middle fiber of GFRP plate (MPa). The normal stress (Figs. 4.3b and 4.3d) based on meshes 2 through 5 are observed to be identical except near the fixed end where further mesh refinements lead to higher stress predictions near the singularity points at the cantilever ends. Away from the singularity points (at about span/500) stresses are observed to be insensitive of finer mesh discretization. Figure 4.3c depicts the average shear stress τ_{nz} across the width for the adhesive-FRP interface as a function of the longitudinal coordinate z. The stresses based on Meshes 3 through 5 are nearly identical but somewhat differ from those based on Mesh 2. For practical purposes, Mesh 3 is acceptable for the stress and displacement predictions. However, in the present study, Mesh 4 was selected since it involves four layers of elements across the interlayer. This provides accurate values for the stresses at four sampling points across-height (the Gauss point at the centroid of each layer of elements). This provides the means to plot the shear strain profile as predicted by the FEA model across the beam interlayer depth and assess the validity of the assumption made in the present theory which postulates constant strain distribution across the adhesive layer (Section 2.4 in Chapter 2). The level of refinement of Mesh 5 was judged unnecessary given the computational time involved in running the problems.

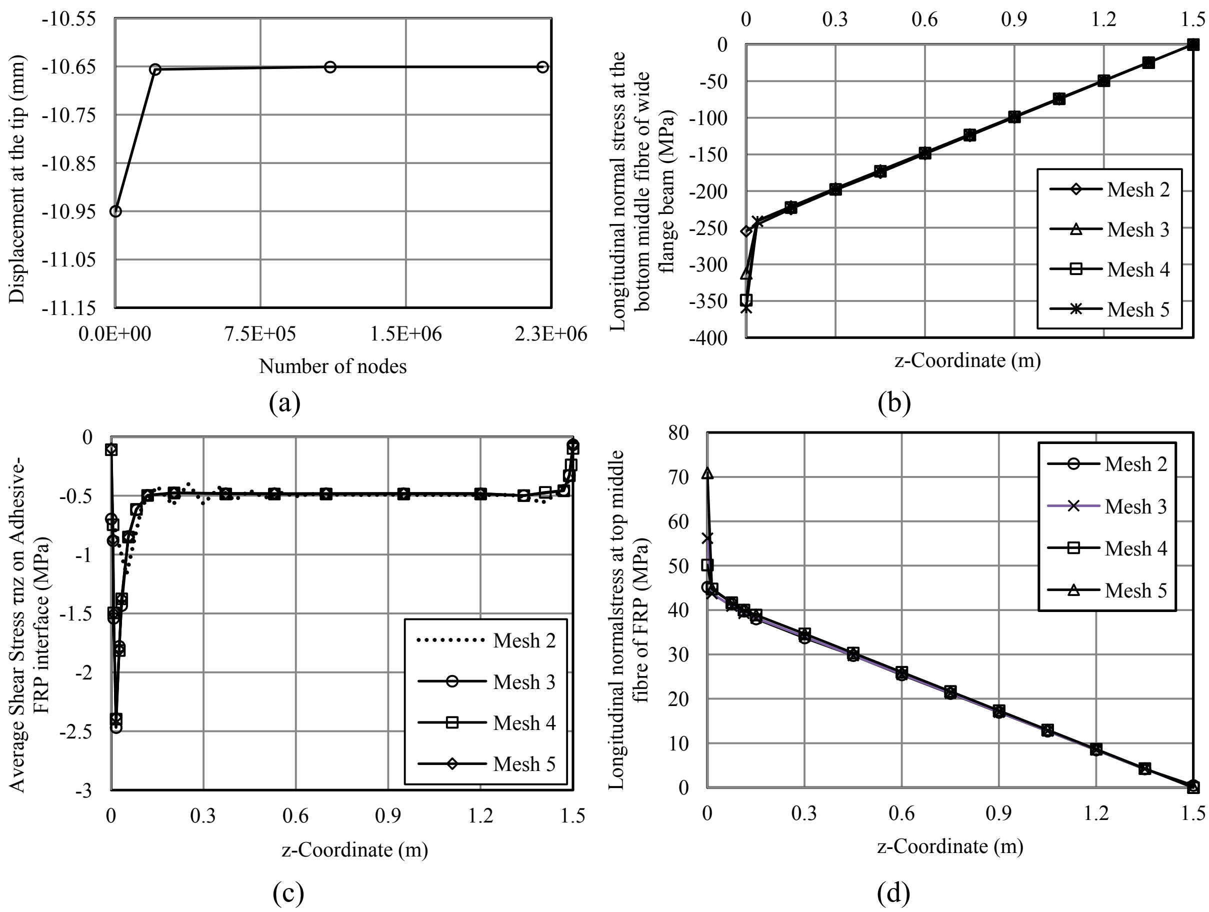

Figure 4.3 Mesh Sensitivity study for Example 1 (a) Displacement at the tip of wide flange beam (mm), (b) Longitudinal normal stress at the bottom middle fiber of the wide flange beam (MPa), (c) Average Shear Stress τ_{nz} across the width of Adhesive-FRP interface (MPa), and (d) Longitudinal normal stress at the top middle fiber of FRP plate (MPa).

4.2.5. Results

Displacements and stresses obtained from closed form solution, finite element solution with a single element, and finite element solution with 20-elements are observed to be equal as seen in the Table 4.3. The reason is that the finite element is based on exact shape functions. Therefore, it does not involve a discretization error and a single element is enough to achieve convergence.

Table 4.3 Convergence of finite element solution

Solution	Transversal displacement at tip (mm)	Longitudinal normal stress at bottom surface of wide flange beam (MPa)
Closed form solution	10.24	-248.8
Single element solution	10.24	-248.8
20-element solution	10.24	-248.8

Displacement and stress fields obtained from FEA and non-shear deformable theory are compared in Fig. 4.4. Figure 4.4a provides the displacement at the cantilever tip as a function of the shear modulus values of the adhesive. The 3D finite element solution is observed to have a slightly weaker stiffness than that based on the present study, and thus yields slightly higher displacement predictions. The percentage difference of displacement is about 4.3% on average. This is due to two reasons. The first reason relates to the shear deformation of wide flange beam and GFRP plate. The current study uses a non-shear deformable theory to derive longitudinal displacements (Eq. 2.15 in Chapter 2), while there is a small shear deformation contribution in the beam. This issue will be explained further under Example 4. The second reason is due to the adoption of the simplifying assumption of linear displacement fields within the adhesive layer under the present formulation. Figures 4.4b-c show the comparison of longitudinal normal stresses in the wide flange beam and FRP plate corresponding to the case $G_a = 4.5GPa$. The result shows an excellent match between the two solutions except near the end $L = 1.5m$ where the singularity at the fixed end due to the concentrated force is captured in the ABAQUS model but not under the present theory. Figure 4.4d shows the comparison of the shear stresses τ_{zn} averaged along the beam corresponding to the case $G_a = 4.5GPa$. The two solutions are observed to agree except within the small area near the free end where stress concentrations are not captured by the present theory. The shear stresses within the adhesive layer predicted from the current study are constant along the span, while the distribution of shear stresses as predicted by the ABAQUS model depicts some nonlinearity near the ends. In Figure

4.4d, ABAQUS shear stresses depicted are those averaged across the flange width at different values of the longitudinal coordinate z .

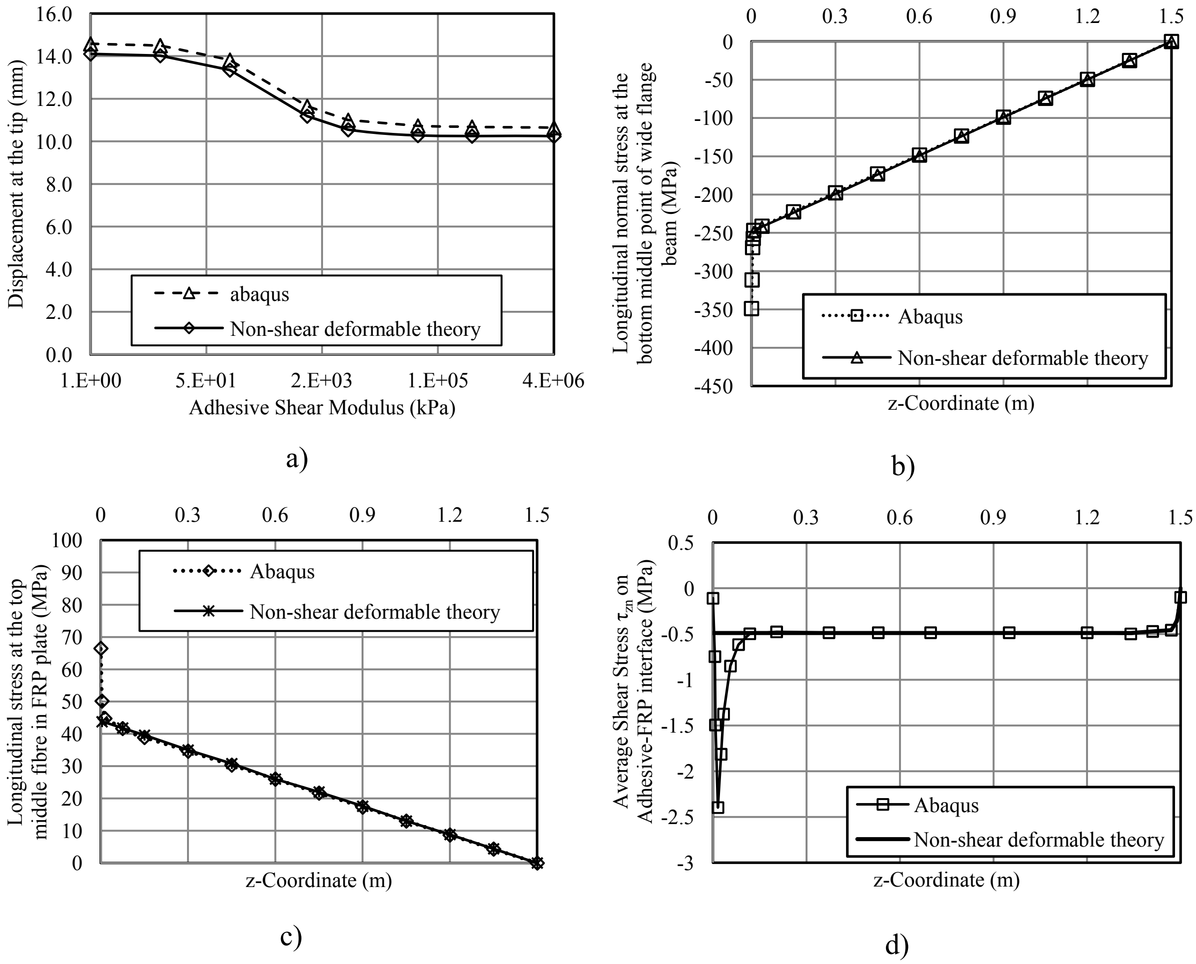

Figure 4.4. Result Comparison for Cantilever under transverse tip load (*a*) displacement at the tip, (*b*) longitudinal normal stress in the wide flange beam, (*c*) longitudinal normal stress in the FRP plate, (*d*) average shear tress τ_{nz} at the adhesive-FRP interface

Figure 4.5 shows the contour for the longitudinal normal stresses within the composite beam as predicted by the ABAQUS model. Figure 4.5a depicts the stress values for the GFRP plate. Figure 4.5b depicts the stress values in the adhesive layer. Figures 4.5c and d are top and bottom views of the steel section.

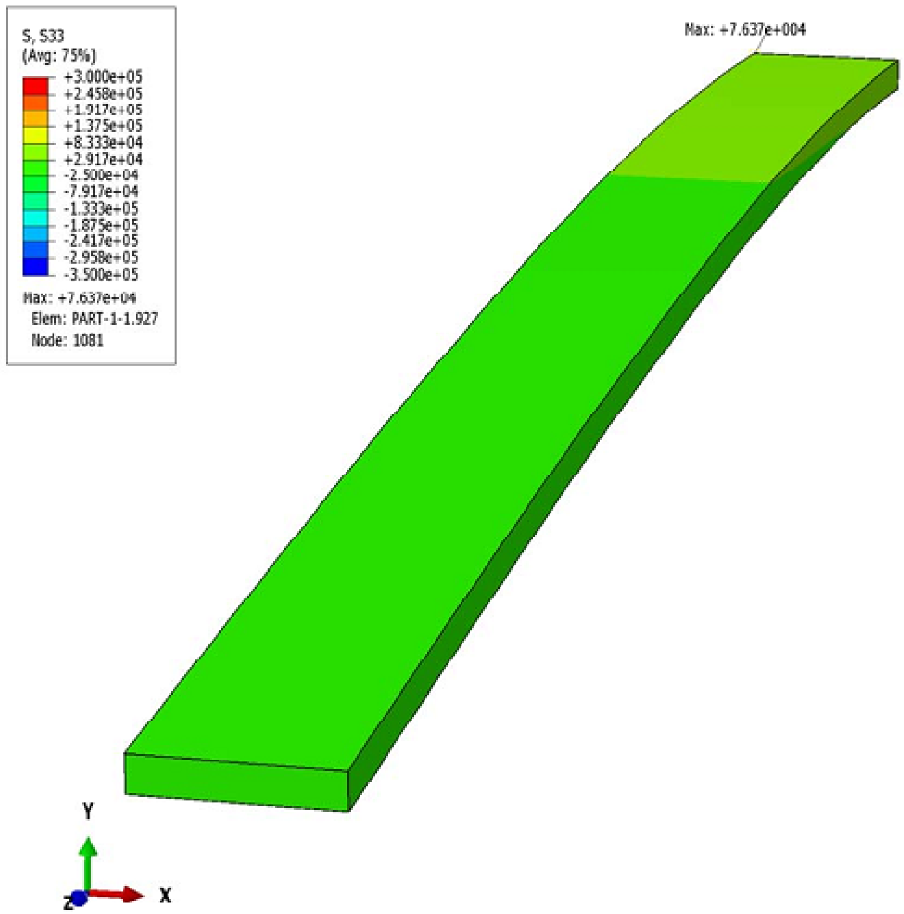
S, S33
(Avg: 75%)
+3.000e+05
+2.458e+05
+1.917e+05
+1.375e+05
+8.333e+04
+2.917e+04
-2.500e+04
-7.917e+04
-1.333e+05
-1.875e+05
-2.417e+05
-2.958e+05
-3.500e+05
Max: +7.637e+04
Elem: PART-1-1.927
Node: 1081
Max: +7.637e+004
Y
X
Z

(a)

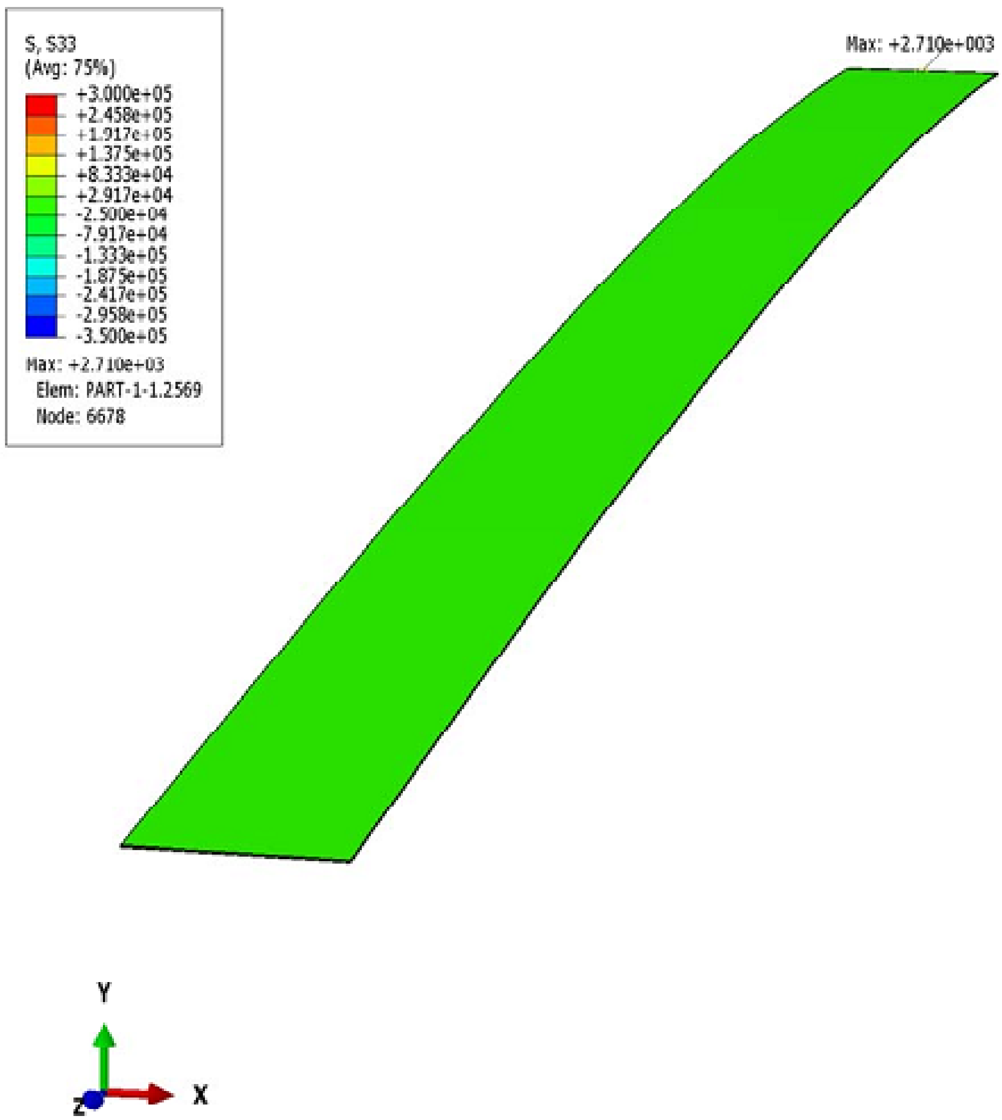
S, S33
(Avg: 75%)
+3.000e+05
+2.458e+05
+1.917e+05
+1.375e+05
+8.333e+04
+2.917e+04
-2.500e+04
-7.917e+04
-1.333e+05
-1.875e+05
-2.417e+05
-2.958e+05
-3.500e+05
Max: +2.710e+03
Elem: PART-1-1.2569
Node: 6678
Max: +2.710e+003
Y
X
Z

(b)

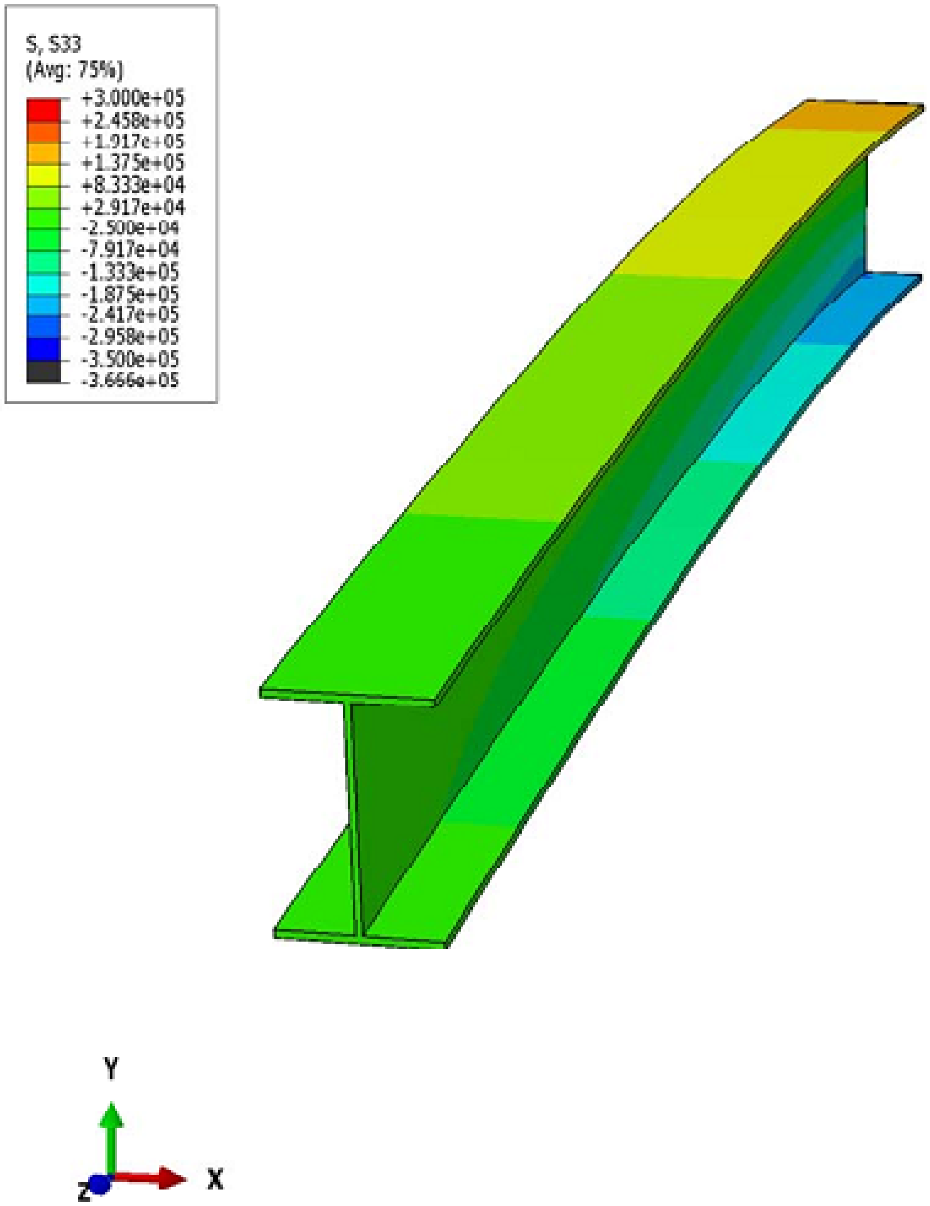
S, S33
(Avg: 75%)
+3.000e+05
+2.458e+05
+1.917e+05
+1.375e+05
+8.333e+04
+2.917e+04
-2.500e+04
-7.917e+04
-1.333e+05
-1.875e+05
-2.417e+05
-2.958e+05
-3.500e+05
-3.666e+05
Y
X
Z

(c)

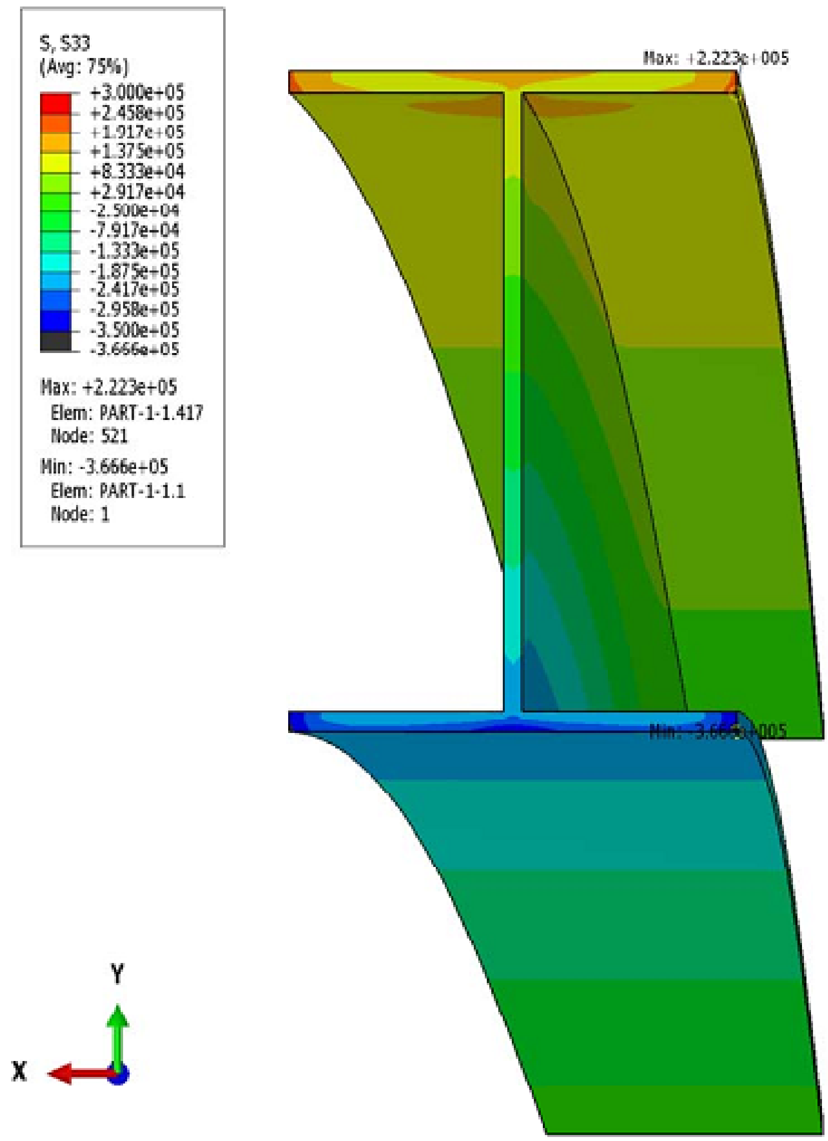

(d)

Figure 4.5. Longitudinal normal stress (KPa) contour based on ABAQUS model for (a) GFRP, (b) Adhesive Layer and (c) Top view of Steel beam looked following negative z-axis direction and (d) Bottom View of Steel Beam looked following positive z-axis direction.

The comparison of displacements and stresses above shows the excellent match between present study and 3D FEA.

Table 4.4 provides a comparison of computational running time and memory used for the present problem on a computer which possesses two processors Intel(R) Xeon(R) CPU E5-2430 0 at speeds 2.20GHz 2.21GHz, and 64.0GB memory (RAM). While the present study is performed in MATLAB software, the 3D FEA is performed in ABAQUS software. For the ABAQUS solution, the run time takes1832 seconds. This compares to 46 seconds using 2 elements under the present model, 50 seconds with 40 elements and 58 seconds with 200 elements. Also, when the beam span is longer (3m, 5m), the time consumed by ABAQUS is in the order of a few hours, while that based on the present is in the order of a few minutes. This will be illustrated in Example 3.

Table 4.4 Comparison of time consumption and Memory used in two solutions for problem 1

Number of element/Solution	Time consumption	Memory used
2-element/Present Study	46 seconds	698 MB
40-element/Present Study	50 seconds	709 MB
200-element/Present Study	58 seconds	732 MB
870000-element/ 3D FEA	1832 seconds	Minimum 2851 MB

4.2.6. Assessing the validity of the kinematic assumption of constant shear strain within the interlayer

The present model is based on the assumption of constant shear strain across the depth of the adhesive (Assumption (vii)). It is thus of interest to examine the validity of the assumption by examining the shear strain ε_{zn} distribution across the adhesive depth as predicted by ABAQUS (Fig. 4.6). Three cross-section locations are examined: near the cantilever root ($z = 40mm$), near mid-span ($z = 840mm$), and near the tip ($z = 1,484mm$). For each cross-section, two locations are considered: one at the center of the interlayer and another one at the edge. It is observed that in all cases, the shear strain is nearly constant, which is consistent with the assumption postulated in the present theory. It is noted however that at a given section, shear strains at the edge are consistently higher than those at the center of the adhesive layer. The present theory neglects this lateral variability in the shear stress. Nevertheless, as shown in Section 4.2.5, it is able to closely capture the global response of system.

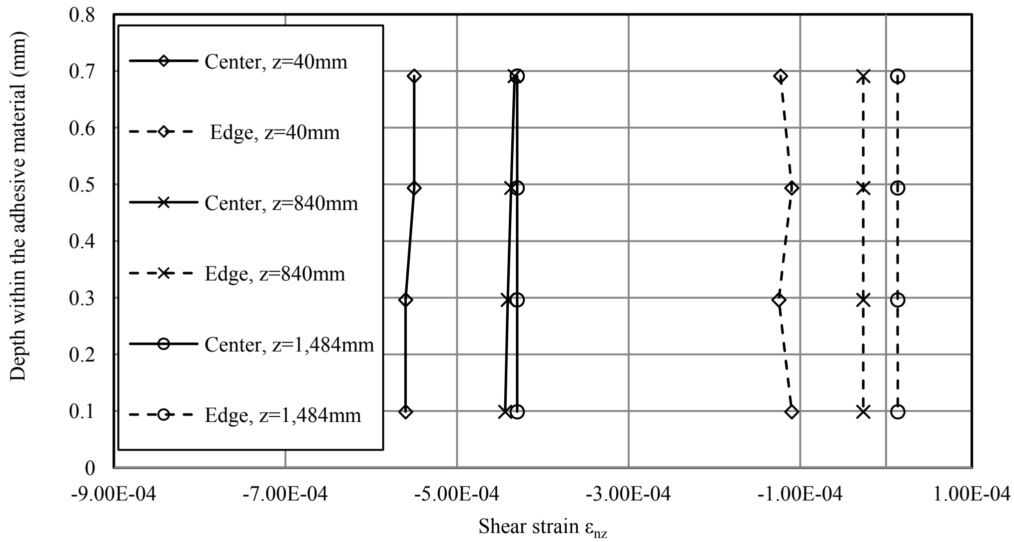

Figure 4.6 Shear strain ε_{nz} across the depth of adhesive layer for the case $G_a = 4.5GPa$ and $t_2 = 0.79mm$

4.3 Example 2: Simply supported beam under uniform pressure

4.3.1. Statement of the Problem

A 3m-simply supported beam reinforced by GFRP plate by using an adhesive layer is investigated in this example (Fig. 4.7). Dimensions of the composite section are identical to those of Example 1, i.e., the wide flange beam section is W150x13 and the GFRP plate has a thickness $t_1 = 19mm$ and a width $b_p = 100mm$, while adhesive has a thickness $t_2 = 0.79mm$. Modulus of elasticity of steel is $E_s = 200GPa$ while that of GFRP is $E_p = 42GPa$. Shear modulus of adhesive is $G_a = 0.4GPa$, corresponding to a low shear modulus adhesive type. Poisson's ratio of all three materials μ is 0.3. Transversely, the wide flange beam is simply supported. Longitudinally, the end $z = 0$ of the beam axis is restrained while at $z = L$, it is axially movable. Both ends of the GFRP plate are longitudinally free. The beam is subjected to a uniform pressure $p_u = 0.15\, N/mm^2$ applied to the un-reinforced flange surface.

The problem is to be solved using the finite element formulation developed in Chapter 3 and a 3D FEA solution based on ABAQUS. It is required to compare (i) the transversal displacement along the beam, (ii) maximum normal stress fields along the beam of the wide flange beam and GFRP plate, and (iii) the average shear stress along the beam of adhesive layer

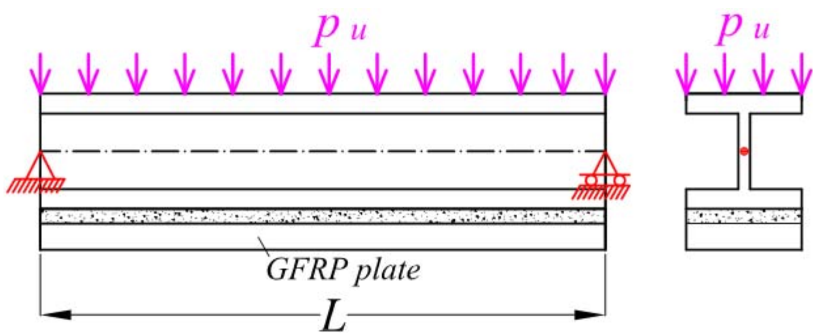

Figure 4.7. Simply supported beam under transverse uniform pressure

4.3.2. Finite Element Solution based on non- Shear Deformable Theory

The finite element formulation developed in the Chapter 3 is used. Starting with the energy equivalent load vector developed in Eq. 3.13, i.e.,

$$\left\{\tilde{Q}_1\right\}_{8\times1} = \left\{\tilde{\tilde{Q}}_{11}\right\}_{8\times1} + \left\{\tilde{\tilde{Q}}_{21}\right\}_{8\times1} \tag{4.11}$$

where $\left\langle\tilde{\tilde{Q}}_{11}\right\rangle^T_{1\times8} = \langle 0\rangle_{1\times8}$, and

$$\left\{\tilde{\tilde{Q}}_{21}\right\} = \int_L \left[\left[N_1(z)\right]^T_{8\times4}\{\rho_1\}_{4\times1} \;\vdots\; \left[N_1(z)\right]^T_{8\times4}\{\rho_3\}_{4\times1} \;\vdots\; \left[N_1(z)\right]'^T_{8\times4}\{\rho_3\}_{4\times1}\right]\left\{\tilde{p}_1\right\}_{3\times1} dz \text{ with}$$

$$\left\{\tilde{p}_1\right\}_{3\times1} = \int_{s_b}\left\{\begin{array}{c} p_z(s_b,z) \\ \hdashline p_v(s_b,z)\sin\alpha(s_b) - p_u(s_b,z)\cos\alpha(s_b) \\ \hdashline -p_z(s_b,z)Y(s_b,n_b) \end{array}\right\} ds_b$$

and noting that $p_z(s_b,z) = p_v(s_b,z) = 0$ and pressure $p_u(s_b,z) = -p$ uniformly applied at the outer surface of the un-reinforced flange, i.e., $\alpha(s_b) = \pi$. As a result, one has $\left\langle\tilde{p}_1\right\rangle^T_{1\times3} = \left\langle 0 \quad -\int_{b_b} p\,ds_b \quad 0\right\rangle$

and the load vector is given by $\left\{\tilde{\tilde{Q}}_{21}\right\} = q\int_L \left\{N_{3i}(z)\right\}_{8\times1} dz$, where $\left\{N_{3i}(z)\right\}_{8\times1}$ is the third column of Matrix $\left[N_1(z)\right]^T_{8\times4}$ and $q = -\int_{b_b} p\,ds_b$ is distributed line load. For the present problem, plots of all shape functions are provided in Appendix A5.

In this example, a single element solution and 100-element solution are found to give identical nodal displacement vector (i.e., slopes are $V' = 0.01025 rad$ at $Z = 0$ and $V' = -0.01025 rad$ at $Z = L$). In order to directly capture the mid-span displacements, four solutions are provided for 2, 8, 100, and

200 elements as presented in Table 4.4. Full agreement is observed. It is noted that the stresses are determined based on the procedure discussed under sub-section 3.5. This illustrates that, because the solution developed in Chapter 3 is based on exact shape functions, there are no discretization errors in the finite element developed.

Table 4.5 Convergence of finite element solution for Example 2

Number of elements	Deflection at mid-span(mm)	Longitudinal normal stress at top of upper flange (MPa)
2	-9.61	-186.51
8	-9.61	-186.51
100	-9.61	-186.51
200	-9.61	-186.51
3D FEA	-10.05	-186.57

4.3.3. 3D finite element model

The 8-node brick element C3D8R is also selected for the ABAQUS simulation as discussed in Example 1. Mesh sensitivity has shown that displacements and stresses converge when $n_1 = 20, n_2 = 4, n_3 = 70, n_4 = 4, n_5 = 4, n_6 = 8, n_7 = 750$.

4.3.4. Results

Figure 4.8 provides the transverse displacements obtained from non-shear deformable theory and ABAQUS as a function of the longitudinal-coordinate z. The difference between the mid–span displacement as predicted by the two solutions is 4.6%. As discussed in Example 1, the difference is caused by shear deformation effects omitted in the present solution and the simplifying assumption of linear displacement within the adhesive layer.

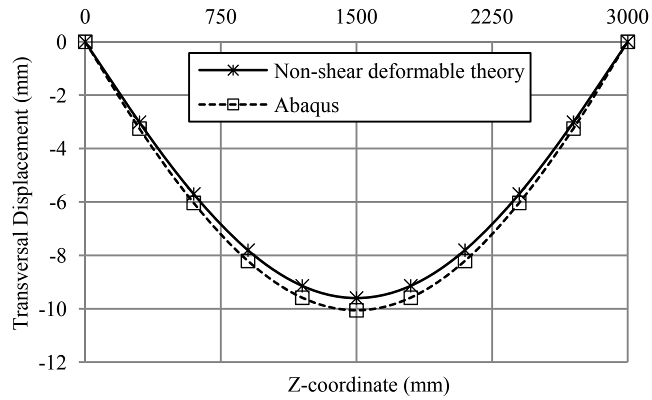

Figure 4.8 Transversal displacements against z coordinates

Figures 4.9a and b show the longitudinal normal stress at the top of upper and bottom of lower flanges, respectively. Also, Fig. 4.9c shows the longitudinal stress at the bottom surface of GFRP plate. The normal stresses show an excellent match between the two solutions. Figure 4.9d shows the shear stress τ_{nz} averaged over the adhesive width taken at different locations along the longitudinal coordinate z. For the central part of the span, very good agreement is obtained between the average shear stress τ_{nz} based on the two solutions with the exception of the two end regions where stress localizations are predicted by the 3D FEA but not captured by the present study.

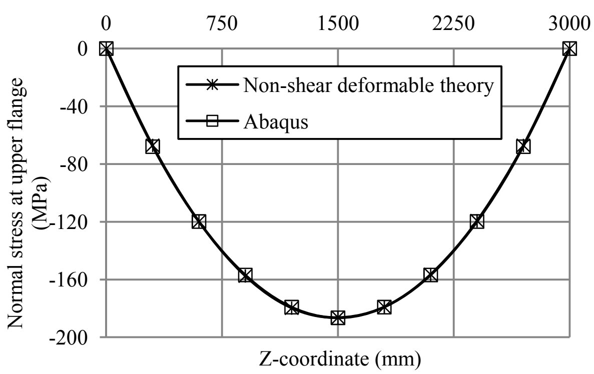

a)

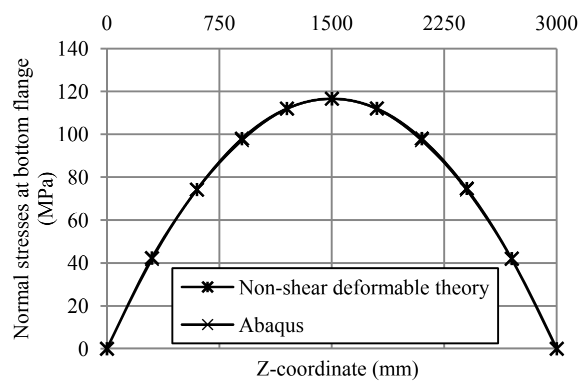

b)

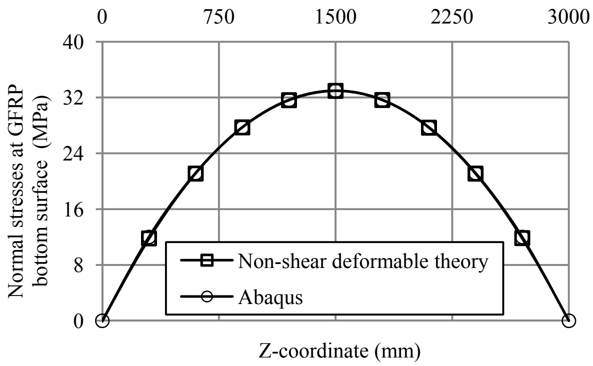

c)

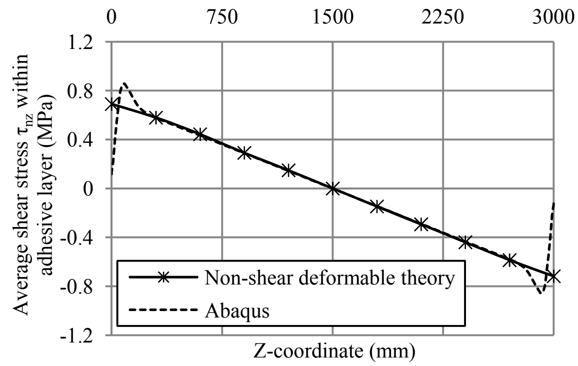

d)

Figure 4.9. Result comparison for simply-supported beam under transversal traction along the beam (*a*) longitudinal normal stress at top surface of upper flange of wide flange beam, (*b*) longitudinal normal stress at bottom surface of lower flange of wide flange beam, (*c*) longitudinal normal stress at bottom surface of the FRP plate, (*d*) average shear tress τ_{nz} at the adhesive-FRP interface.

4.4 Example 3: Cantilever under Weak Axis Bending

4.4.1. Statement of the Problem

A 5m span cantilever composite beam consists of a W410x85 beam (flange width $b_b = 181mm$, flange thickness $t_3 = 18.2mm$, depth $d = 417mm$ and web thickness $t_w = 10.9mm$) is reinforced by a GFRP plate over the whole span (Fig.4.10). The GFRP plate has a thickness $t_1 = 19mm$ and a width $b_p = 181mm$, while adhesive has a thickness $t_2 = 2mm$. Modulus of elasticity of steel is $E_s = 200GPa$ while that of GFRP is $E_p = 42GPa$. The shear modulus of the adhesive is $G_a = 0.4GPa$, corresponding to a low shear-modulus adhesive type (Table 1.1, Chapter 1). Poisson's ratio of all three materials μ is 0.3. The cantilever is subjected to lateral tractions $p_v = 1821.83\, kN/m^2$ acting at both steel flange surfaces in the X-positive direction at the tip so as to create an equivalent lateral resultant force $Q_x = 12kN$ acting at the beam centroid.

It is required to compare (i) the lateral displacement fields and twisting angle, (ii) the maximum normal stress fields along the beam of the wide flange beam and GFRP plate, and (iii) the average shear stress along the beam of adhesive layer as predicted by the closed form solution developed in Chapter 2, finite element solution developed in Chapter 3, to the 3D FEA analysis performed under ABAQUS.

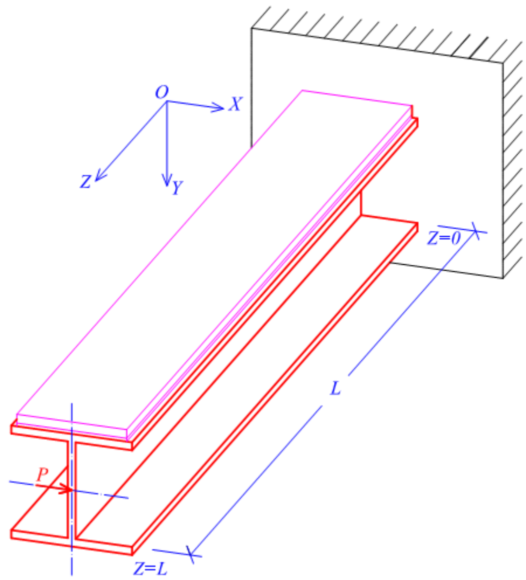

Figure 4.10. Cantilever under bending about weak axis

4.4.2 Closed Form Solution-Enforcing Boundary Conditions

The closed form expressions of the displacement fields related to the lateral torsional response were obtained in Eq. 2.48 of as

$$U_b = D_1 + D_2 z + D_3 z^2 + D_4 z^3 + \sum_{i=5}^{10} D_i e^{k_i z}$$

$$U_p = A_{51} + A_{52} z + D_3 z^2 + D_4 z^3 - \sum_{i=5}^{10} D_i \frac{E_b I_{yyb}}{E_p I_{yyp}} e^{k_i z} \tag{4.12}$$

$$\theta_z = -D_1 \frac{c_1}{c_2} - D_2 \frac{c_1}{c_2} z + D_{11} \frac{c_1}{c_2} + D_{12} \frac{c_1}{c_2} z + \sum_{i=5}^{10} D_i f_{6i} e^{k_i z}$$

in which

$$f_{6i} = \left[\frac{-E_b I_{yyb} E_p I_{yyp} k_i^4 + c_1^2 G_a I_{yya} \left(E_b I_{yyb} + E_p I_{yyp} \right) k_i^2 - c_1^2 G_a A_a \left(E_b I_{yyb} + E_p I_{yyp} \right)}{E_p I_{yyp} \left(c_1 c_3 G_a I_{yya} k_i^2 + c_1 c_2 G_a A_a \right)} \right], \; i = 5, 6, 7, \; 8, \; 9, \; 10$$

an k_i are defined in Eq. 2.49. Integration constants $D_1, \ldots, D_{12}$ are to be determined based on the twelve boundary conditions provided in Table 4.6. For conciseness, the symbols $B_2 = c_1^2 G_a A_a$; $B_3 = c_1 c_2 G_a A_a$; $B_7 = E_b I_{yyb}$; $B_8 = c_1^2 G_a I_{yya}$; $B_9 = c_1 c_3 G_a I_{yya}$; $B_{10} = E_p I_{yyp}$; $B_{11} = E_b I_{\omega\omega b} + E_p I_{\omega\omega p}$; $B_{12} = G_b J_b + G_p J_p + G_a J_a + c_3^2 G_a I_{yya}$ are used.

Table 4.6. Boundary conditions for a cantilever problem under lateral concentrated load at tip

Essential Boundary Condition	Natural Boundary Condition
$U'(0)=0$ (4.13)	$U_b'''(L)=0$ (4.14)
$U_b(0)=0$ (4.15)	$\left(-B_7U_b'''+B_8U_b'-B_8U_p'-B_9\theta'\right)\Big\vert_L-Q_x=0$ (4.16)
$U_p'(0)=0$ (4.17)	$U_p''(L)=0$ (4.18)
$U_p(0)=0$ (4.19)	$\left(-B_8U_b'-B_{10}U_p'''+B_8U_p'+B_9\theta'\right)\Big\vert_L=0$ (4.20)
$\theta'(0)=0$ (4.21)	$\theta''(L)=0$ (4.22)
$\theta(0)=0$ (4.23)	$\left(-B_9U_b'+B_9U_p'-B_{11}\theta'''+B_{12}\theta'\right)\Big\vert_L=0$ (4.24)

From Eqs. (4.12) and (4.13), one obtains

$$D_2+\sum_{i=5}^{10}D_ik_i=0 \tag{4.25}$$

From Eqs. (4.12) and (4.14), one obtains

$$2D_3+6D_4L+\sum_{i=5}^{10}D_ik_i^2e^{k_iL}=0 \tag{4.26}$$

From Eqs. (4.12) and (4.15), one obtains

$$D_1+\sum_{i=5}^{10}D_i=0 \tag{4.27}$$

From Eqs. (4.12) and (4.16), one obtains

$$\begin{gathered}-B_7\left(6D_4+\sum_{i=5}^{10}D_ik_i^3e^{k_iz}\right)+B_8\left(D_2+2D_3L+3D_4L^2+\sum_{i=5}^{10}D_ik_ie^{k_iL}\right)\\-B_8\left(D_{12}+2D_3L+3D_4L^2-\frac{B_7}{B_{10}}\sum_{i=5}^{10}D_ik_ie^{k_iL}\right)-B_9\left(-D_2\frac{B_2}{B_3}+D_{12}\frac{B_2}{B_3}+\sum_{i=5}^{10}D_i\,f_{6i}k_ie^{k_iz}\right)=Q_x\end{gathered} \tag{4.28}$$

From Eqs. (4.12) and(4.17), one obtains

$$-\frac{B_7}{B_{10}}\sum_{i=5}^{10}D_ik_i+D_{12}=0 \tag{4.29}$$

From Eqs.(4.12) and(4.18), one obtains

$$2D_3+6D_4L-\frac{B_7}{B_{10}}\sum_{i=5}^{10}D_ik_i^2e^{k_iL}=0 \tag{4.30}$$

From Eqs. (4.12) and (4.19), one obtains

$$D_{11}-\frac{B_7}{B_{10}}\sum_{i=5}^{10}D_i=0 \tag{4.31}$$

From Eqs. (4.12) and (4.20), one obtains

$$\begin{aligned}&-B_8\left(D_2+2D_3L+3D_4L^2+\sum_{i=5}^{10}D_ik_ie^{k_iL}\right)-B_{10}\left(6D_4-\frac{B_7}{B_{10}}\sum_{i=5}^{10}D_ik_i^3e^{k_iL}\right)\\&+B_8\left(D_{12}+2D_3L+3D_4L^2-\frac{B_7}{B_{10}}\sum_{i=5}^{10}D_ik_ie^{k_iL}\right)+B_9\left(-D_2\frac{B_2}{B_3}+D_{12}\frac{B_2}{B_3}+\sum_{i=5}^{10}D_i\,f_{6i}k_ie^{k_iL}\right)=0\end{aligned} \tag{4.32}$$

From Eqs. (4.12) and (4.21), one obtains

$$-\frac{B_2}{B_3}D_2+\sum_{i=5}^{10}D_i\,f_{6i}k_i+\frac{B_2}{B_3}D_{12}=0 \tag{4.33}$$

From Eqs. (4.12) and (4.22), one obtains

$$\sum_{i=5}^{10}D_i\,f_{6i}k_i^2e^{k_iz}=0 \tag{4.34}$$

From Eqs. (4.12) and (4.23), one obtains

$$-\frac{B_2}{B_3}D_1+\frac{B_2}{B_3}D_{11}+\sum_{i=5}^{10}D_i\,f_{8i}=0 \tag{4.35}$$

From Eqs. (4.12) and (4.24), one obtains

$$\begin{aligned}&-B_9\left(D_2+2D_3L+3D_4L^2+\sum_{i=5}^{10}D_ik_ie^{k_iL}\right)+B_9\left(D_{12}+2D_3L+3D_4L^2-\frac{B_7}{B_{10}}\sum_{i=5}^{10}D_ik_ie^{k_iL}\right)\\&-B_{11}\left(\sum_{i=5}^{10}D_i\,f_{6i}k_i^3e^{k_iL}\right)+B_{12}\left(-\frac{B_2}{B_3}D_2+\frac{B_2}{B_3}D_{12}+\sum_{i=5}^{10}D_i\,f_{6i}k_ie^{k_iL}\right)=0\end{aligned} \tag{4.36}$$

Eqs. (4.25)-(4.36) are arranged in a matrix form as

$$[F_2]_{12\times12}\left\{\overline{D}\right\}_{12\times1}=\{P\}_{12\times1} \tag{4.37}$$

in which

$\left\langle\overline{D}\right\rangle_{1\times12}^T=\langle D_1\quad D_2\quad D_3\quad D_4\quad D_5\quad D_6\quad D_7\quad D_8\quad D_9\quad D_{10}\quad D_{11}\quad D_{12}\rangle$ is a vector of integration constants and $\langle P\rangle_{1\times12}^T=\langle 0\quad 0\quad 0\quad Q_x\quad 0\quad 0\quad 0\quad 0\quad 0\quad 0\quad 0\quad 0\rangle$, and

$[F_2] =$

$$\begin{bmatrix} 0 & 1 & 0 & 0 & k_5 & k_6 & k_7 & k_8 & k_9 & k_{10} & 0 & 0 \\ 0 & 0 & 2 & 6L & k_5^2 e^{k_5 L} & k_6^2 e^{k_6 L} & k_7^2 e^{k_7 L} & k_8^2 e^{k_8 L} & k_9^2 e^{k_9 L} & k_{10}^2 e^{k_{10} L} & 0 & 0 \\ 1 & 0 & 0 & 0 & 1 & 1 & 1 & 1 & 1 & 1 & 0 & 0 \\ 0 & f_9 & 0 & -6B_7 & f_{105} & f_{106} & f_{107} & f_{108} & f_{109} & f_{1010} & 0 & -f_9 \\ 0 & 0 & 0 & 0 & -k_5 & -k_6 & -k_7 & -k_8 & -k_9 & -k_{10} & 0 & 1/f_7 \\ 0 & 0 & 2/f_7 & 6L/f_7 & -k_5^2 e^{k_5 L} & -k_6^2 e^{k_6 L} & -k_7^2 e^{k_7 L} & -k_8^2 e^{k_8 L} & -k_9^2 e^{k_9 L} & -k_{10}^2 e^{k_{10} L} & 0 & 0 \\ 0 & 0 & 0 & 0 & -1 & -1 & -1 & -1 & -1 & -1 & 1/f_7 & 0 \\ 0 & -f_9 & 0 & -6B_{10} & -f_{105} & -f_{106} & -f_{107} & -f_{108} & -f_{109} & -f_{1010} & 0 & f_9 \\ 0 & -f_2 & 0 & 0 & f_{65}k_5 & f_{66}k_6 & f_{67}k_7 & f_{68}k_8 & f_{69}k_9 & f_{610}k_{10} & 0 & f_2 \\ 0 & 0 & 0 & 0 & f_{115} & f_{116} & f_{117} & f_{118} & f_{119} & f_{1110} & 0 & 0 \\ -f_2 & 0 & 0 & 0 & f_{65} & f_{66} & f_{67} & f_{68} & f_{69} & f_{610} & f_2 & 0 \\ 0 & -f_{11} & 0 & 0 & f_{125} & f_{126} & f_{127} & f_{128} & f_{129} & f_{1210} & 0 & f_{11} \end{bmatrix}$$

with

$$f_2 = \frac{B_2}{B_3},\ f_7 = \frac{B_7}{B_{10}};\ f_9 = \frac{B_3 B_8 + B_2 B_9}{B_3},\ f_{10i} = \left(B_8 \frac{B_7 + B_{10}}{B_{10}} k_i - B_9 f_{6i} k_i - B_7 k_i^3 \right) e^{k_i L},\ f_{11} = \frac{B_3 B_9 + B_2 B_{12}}{B_3}$$

$$f_{11i} = f_{6i} k_i^2 e^{k_i L};\quad f_{12i} = \left[-B_9 \frac{B_7 + B_{10}}{B_{10}} k_i + B_{12} f_{6i} k_i - B_{11} f_{6i} k_i^3 \right] e^{k_i L};\ i = 5, 6, 7,\ 8,\ 9,\ 10$$

Equation (4.37) is solved for integration constants $\{\overline{D}\}_{12\times1}$ yielding $\{\overline{D}\}_{12\times1} = [F_2]_{12\times12}^{-1} \{P\}_{12\times1}$, and the vector of displacement functions can be obtained by substituting $\{\overline{D}\}_{12\times1}$ into Eqs. (4.12).

4.4.3. Expressions for Strains and Stresses

The stresses and strains can be obtained through the algorithm developed under Section 4.2.3.

4.4.4. Results

For comparison, the 8-node brick element C3D8R is also selected for FEA under ABAQUS. Displacements and stresses converge for the mesh $n_1 = 20, n_2 = 4, n_3 = 70, n_4 = 4, n_5 = 4, n_6 = 8,$ $n_7 = 3120$.

Figure 4.11(a) provides the lateral displacement at the wide flange beam centroid as a function of the longitudinal coordinate z. An excellent match is obtained between closed form solution/ finite element formulation derived based on non-shear deformable theory and FEA performed under

ABAQUS. Figure 4.11(b) shows the lateral displacement of GFRP centroid, while Figures 4.11(c-d) shows the lateral displacement at bottom flange centroid and top flange centroid, respectively. There is a slight difference (about 1.6%) between the two solutions. The twisting angle as determined from ABAQUS is obtained by dividing the difference between the lateral displacement of top flange centroid and the bottom flange centroid by the section height. As seen in Fig. 4.12, the non-shear deformable theory gives a significantly smaller angle of twist when compared to ABAQUS. The maximum difference of angle of twist is 66%. This suggests that the present study significantly overestimates the torsional stiffness of the composite system. A detailed discussion of this difference is discussed in detail in the Example 4. Nevertheless, for bending about weak axis in which the effect of twisting moments is small (as is the case in the present example), displacements obtained from non-shear deformable theory yield reasonable results when compared to the ABAQUS model.

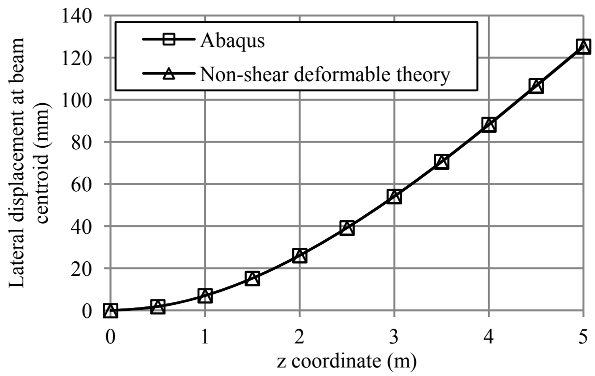

a)

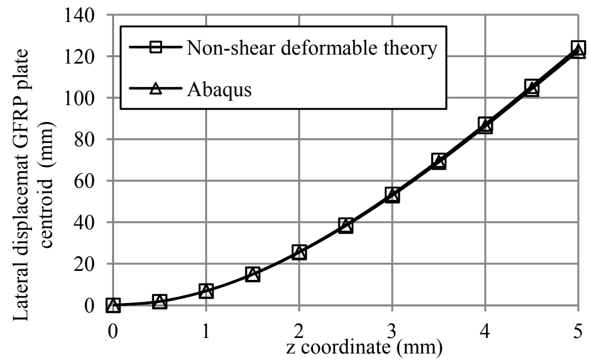

b)

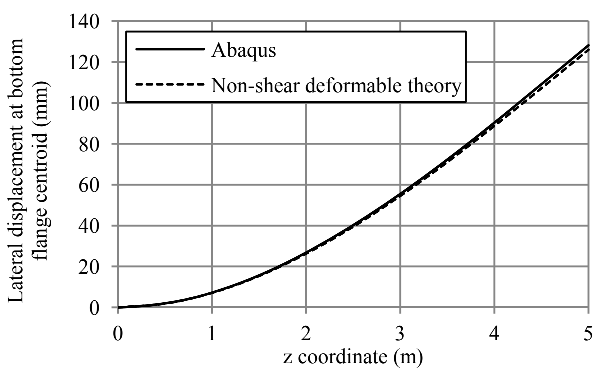

c)

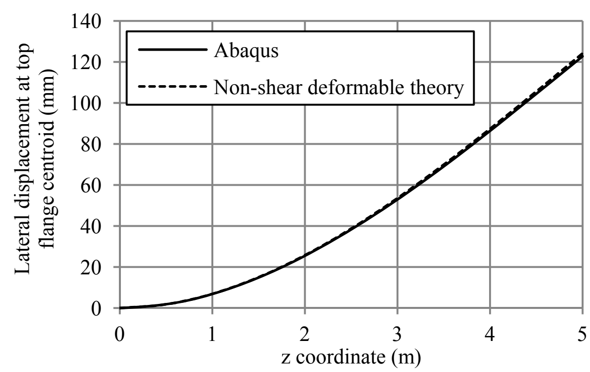

d)

Figure 4.11 Displacement comparison for cantilever under bending about weak axis (*a*) lateral displacement at wide flange beam centroid, (*b*) lateral displacement at GFRP plate centroid, (*c*) lateral displacement at bottom flange centroid, (*d*) lateral displacement at top flange centroid.

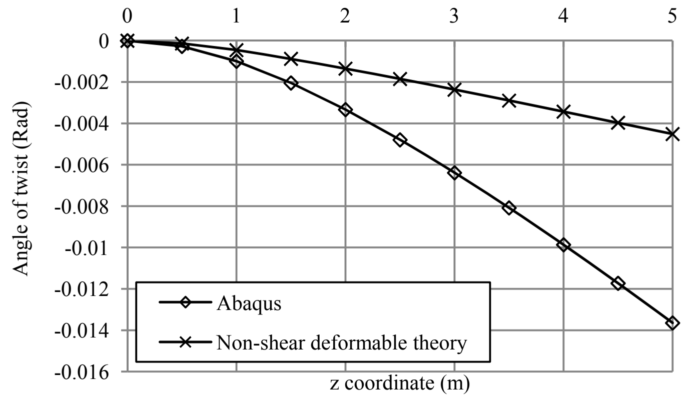

Figure 4.12 Angle of twist along the beam

Figure 4.13 (a) provides the longitudinal normal stress at middle point of left edge of bottom flange, while Fig. 4.13 (b) shows the longitudinal normal stress at top point of left edge of GFRP plate. As discussed in Example 1, the stress at singularity points located at the fixed end of the composite beam increases with a finer mesh. Except these singularity points, the stresses agree well between the two solutions. The maximum difference is about 4.9%. Again, because the effect of twisting moment in this case is small, the difference between the two solutions is also small. Figure 4.13 (c) provides the average shear stress τ_{sz} over the adhesive layer width while the figure 4.13 (d) shows the average shear tress τ_{sn} over the adhesive layer width. The present theory poorly predicts these shear stresses. Further discussion of the underlying reasons will be discussed in detail in Example 4.

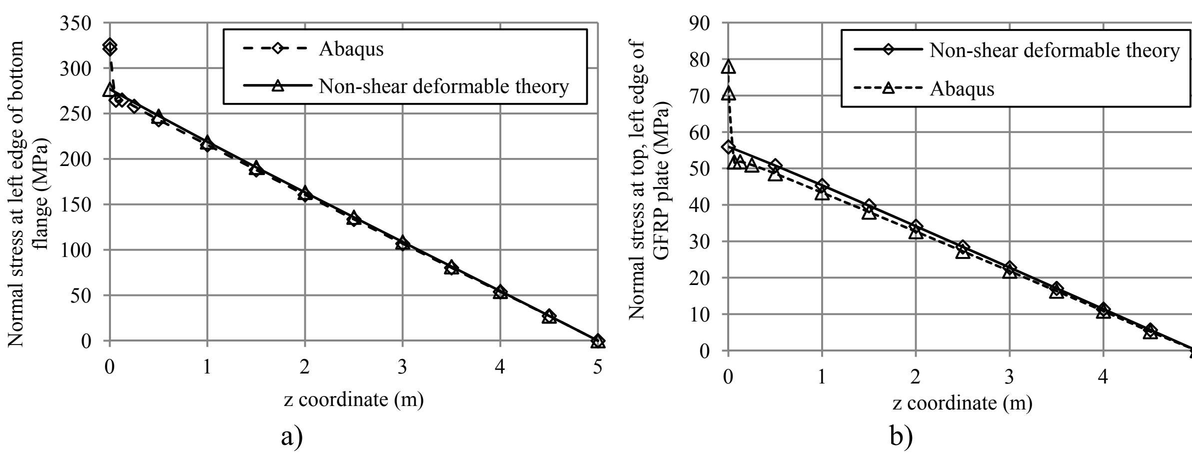

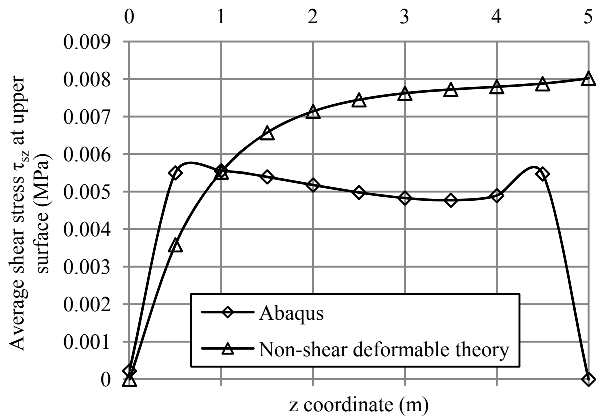

c)

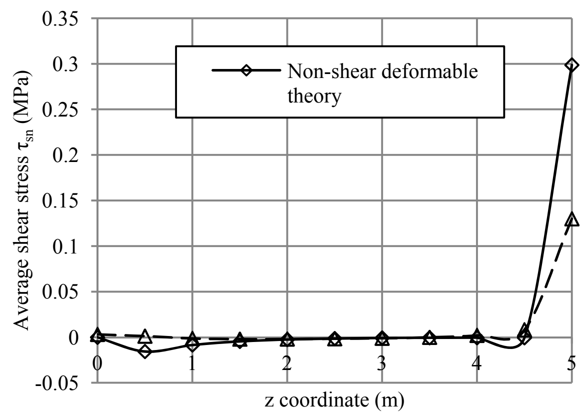

d)

Figure4.13. Stress comparison for cantilever under bending about weak axis (*a*) longitudinal normal stress at middle point of left edge of bottom flange, (*b*) longitudinal normal stress at top point of left edge of GFRP plate, (*c*) average shear stress τ_{sz} along the beam, (*d*) average shear tress τ_{sn} within adhesive layer.

Table 4.7 provides a comparison of computational running time and memory used for the problem 3 on a computer which possesses two processors Intel(R) Xeon(R) CPU E5-2430 0 at speeds 2.20GHz 2.20GHz, and 64.0GB RAM installed. While the present study is performed in MATLAB software, the 3D FEA is performed in ABAQUS software. For the ABAQUS solution, a running time of 4.31 hours of running were needed. This compares to 14 seconds using a single element under the present model, and 2 seconds under the closed form solution.

Table 4.7 Comparison of time consumption and Memory used in two solutions for problem 3

Number of element/Solution	Time consumption	Memory used
Single element/Present study	14 seconds	661 MB
Closed Form Solution	2.0 seconds	618 MB
2,995,200-element/ 3D FEA	4.31 hours	Minimum 8356 MB

4.5 Example 4-Twisting problem

4.5.1. Statement of the problem

The composite member in Example 3 is re-analyzed in this example. Instead of the two tangential tractions at bottom and top flange surfaces acting in the same direction, the member tip is subject to tangential tractions of equal magnitude $\tau_v = 2490 kN/m^2$ in opposite directions to induce a twisting moment about the wide flange centroid. The value of twisting moment is $T=-3.271kNm$. It is required (a) to compare the displacement fields U_b, U_p, θ_z at the free end by using the closed form solution developed under Sub-section 4.4.2, the finite element solution developed in Chapter 3, and a 3D FEA performed under ABAQUS and (b) investigate the shear stress distribution across the steel section, GFRP layer and adhesive material.

4.5.2. Result of displacement fields and Verification of assumptions

In the present example, the closed form solution developed in Section 4.4.2 is used with a different right hand side vector $\langle P\rangle^T_{1\times12}=\langle 0 \quad 0 \quad 0 \quad 0 \quad 0 \quad 0 \quad 0 \quad 0 \quad 0 \quad 0 \quad 0 \quad T\rangle$. The displacement fields obtained from the closed from solution/ Finite Element Formulation developed in Chapter 3 are compared to those obtained from FA analysis performed in ABAQUS. This comparison is presented in the Table 4.8. The difference in the beam displacement U_b is 34.5%, while that of U_p and θ_z are 53.6% and 54.2%, respectively. This shows that the present formulation significantly over-predicts the torsional stiffness of the composite system.

Table 4.8 Comparison of displacement at tip between ABAQUS and current study

Type of solution	Beam Displacement U_b (mm)	Plate Displacement U_p (mm)	Angle of twst θ_z (rad)
ABAQUS FEA (1)	1.878	-24.247	-0.124
Closed Form Solution and Finite Element Formulation (2)	1.230	-11.241	-0.0568
Percentage difference ((2) – (1))/(1)	34.5%	53.6%	54.2%

4.5.3. Verification of Kinematic Assumptions

4.5.3.1. Mid-surface Shear Strain distribution within GFRP and top flange mid-height

There are two main reasons for the observed discrepancy. The first reason relates to the postulated Vlasov assumption of zero shear strain at GFRP mid-height and top flange of the beam (Eq. 2.15), i.e,

$$\frac{\partial \overline{w}(s,z)}{\partial s}+\frac{\partial \overline{v}(s,z)}{\partial z}=0 \tag{4.38}$$

The validity of this assumption is assessed by extracting the shear strain (γ_{sz}) at integration points of the 3D FEA model for the beam flange, adhesive layer and GFRP plate. The strain values are observed at the six locations (Location 1($X = 0, Z = 500$), Location 2($X = -62.15, Z = 500$), Location 3($X = 0, Z = 2500$), Location 4($X = -62.15, Z = 2500$), Location 5($X = 0, Z = 4500$), Location 6($X = -62.15, Z = 4500$) as depicted in red in Fig. 4.14).

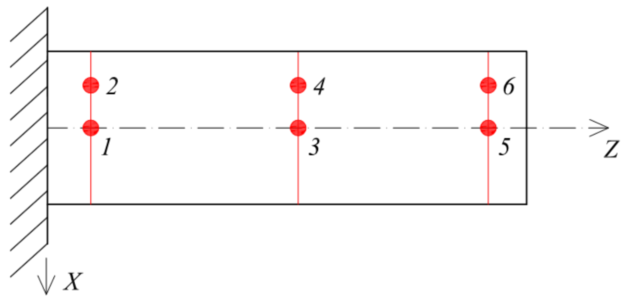

Figure4.14 Locations of selected locations to investigate shear strain distribution.

Each location captures the depth of upper flange, depth of adhesive layer and depth of GFRP plate. The results are shown in Fig.4.15.

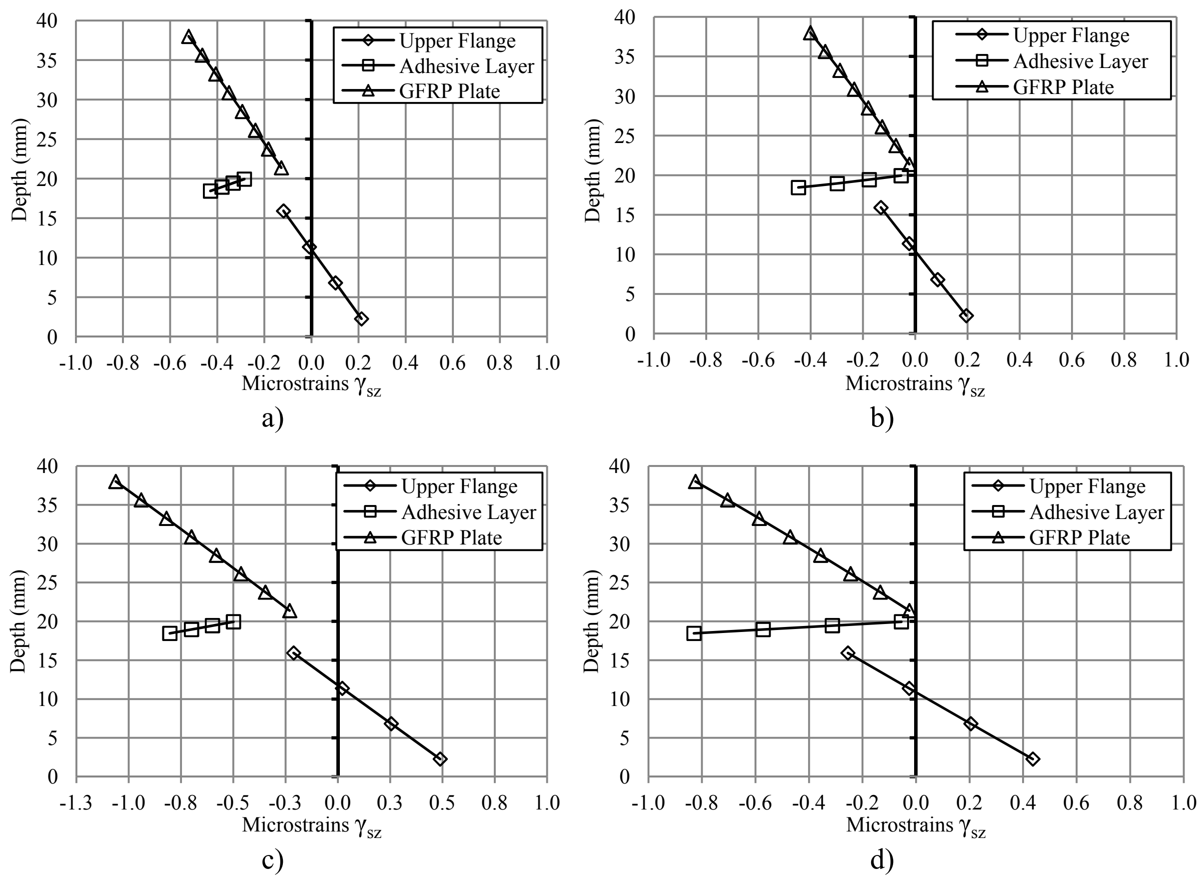

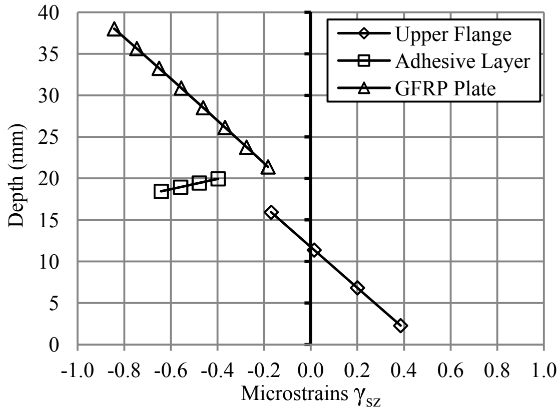

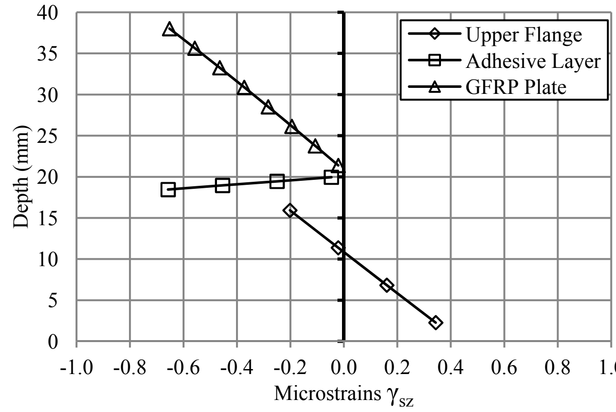

Figure 4.15 Shear strain γ_{sz} (Microstrains) distribution across the depths of upper flange, adhesive layer and GFRP plate at (a) Location 1, (b) Location 2, (c) Location 3, (d) Location 4, (e) Location 5, and (f) Location (6)

All six figures show that the shear strain distributions as predicted by ABAQUS FEA do not vanish at plate mid-height neither at top flange mid-height. Thus, the assumption of zero strain at GFRP mid-height (Assumption 2 in Sub-section 2.4 of Chapter 2) is unrealistic and leads to an overestimation of the twisting stiffness of the composite system. An improvement of the solutions developed in Chapters 2 and 3 would necessitate the use of more enriched kinematics accounting for shear deformations at plate mid-height. This will be the scope of the developments in Chapters 5-7 which focus on developing a shear deformable theory/solution.

4.5.3.2 Shear strain distribution across the adhesive layer depth

As stated under Section 2.4, the displacement fields within the adhesive layer were linearly interpolated between displacement fields of top of the wide flange beam and the underside of GFRP plate (see Eqs. 2.30). This results in a linear shear strain distribution γ_{sza} across the adhesive layer depth. Now, the assumption will be verified against the ABAQUS model. The adhesive shear strain γ_{sza} as expressed in Eqs. 2.33 is a linear function of the depth. It is observed from Figures 4.15(a)-(f) that, indeed, the shear strain γ_{sza} as predicted by ABAQUS is linear. Thus, in the shear deformable theory to be developed, a linear displacement distribution across the depth will be postulated.

4.5.3.3 Shear stress distribution across the width of the adhesive layer

Along the X direction, the shear strain γ_{sza} in the present formulation, and consequently the shear stress τ_{sza}, are constant. This is evident from Eqs. 2.33 The corresponding shear stress as predicted from the ABAQUS model is observed to be nonlinear. However, given the flat distribution observed in Fig. 4.16, such approximation is judged adequate and will be retained in the developments in Chapters 5-7.

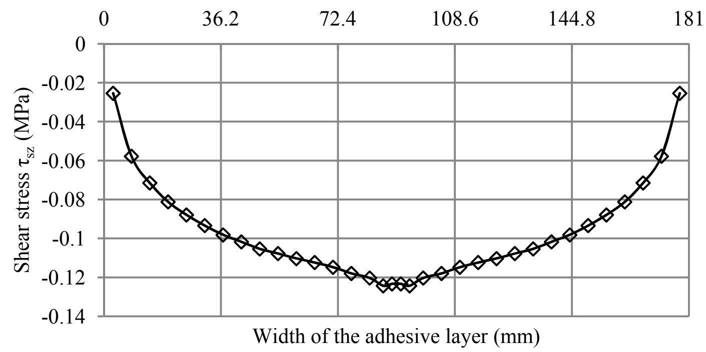

Figure 4.16 Shear stress τ_{sz} across the width of adhesive layer at $z = 2500mm$

4.5.3.3 Verification of the through-thickness shear stress distribution across the width of the adhesive layer

In Fig. 4.17(a), twelve locations are selected for the investigation corresponding to three longitudinal coordinate values ($Z = 500, 2500, 4500mm$), denoted by locations 1, 2, and 3 respectively and four lateral coordinate values ($X = -62.2, -33.8, -5.5, -1.4mm$). In the Y direction, shear stress τ_{sna} in ABAQUS model is observed to be almost constant (Figs. 4.17b- d).

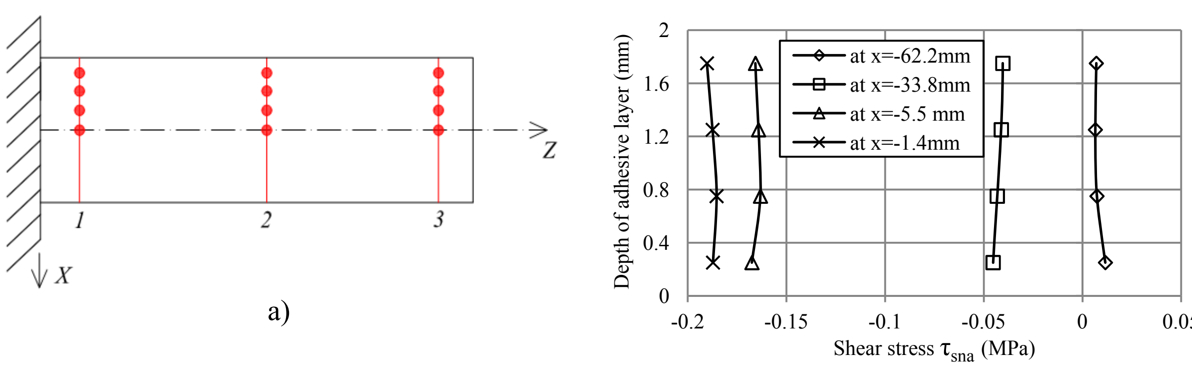

a)

b)

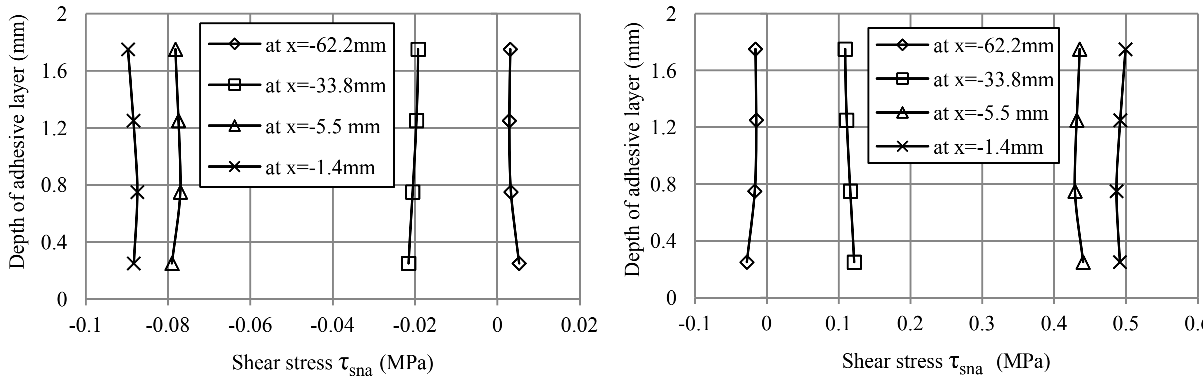

c) d)

Figure 4.17. (a) Selected locations for investigating τ_{sn} across the depth of adhesive layer, (b) Shear stress τ_{sna} distribution on cross-sections of adhesive layer at location 1, (c) Shear stress τ_{sna} distribution at location 2, (d) Shear stress τ_{sna} distribution at location 3.

Figure 4.18(a) shows a cross-section showing the number of elements taken to model the adhesive layer. The second element layer from bottom is selected for the investigation and the line passing through the Gauss points of this layer is denoted as "location 4". All shear stresses τ_{sna} at integration points are extracted. The shear stress τ_{sna} as expressed in Eqs. 2.35 is constant across the cross-section of adhesive layer. In the X direction, the shear stress in ABAQUS model is not constant. This can be verified in Figs.4.18b-d.

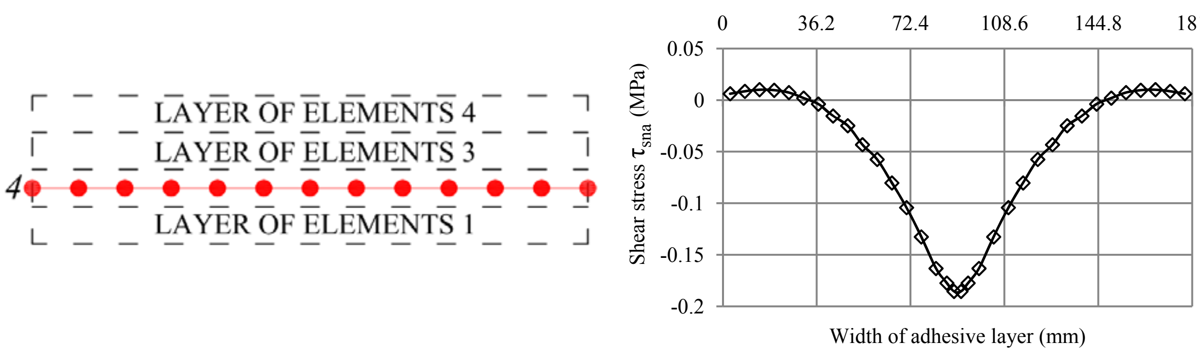

a) b)

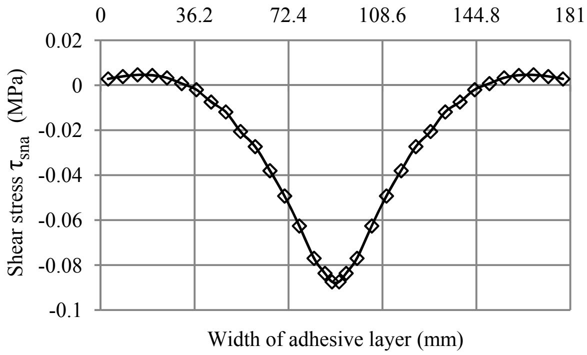

c)

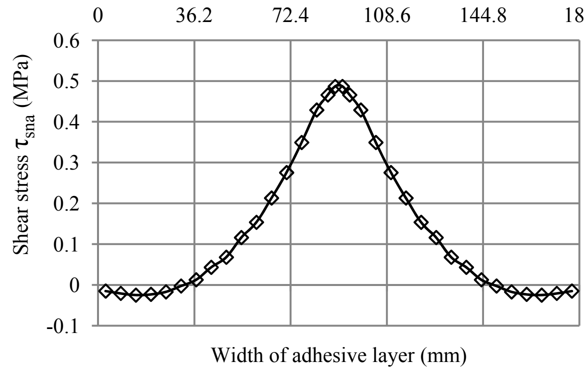

d)

Figure 4.18. (a) Location of Gauss points selected for extracting the shear stress τ_{sn} across the width of adhesive layer, (b) Shear stress τ_{sna} distribution on cross-sections of adhesive layer at location 1 and 4, (c) Shear stress τ_{sna} distribution on cross-sections of adhesive layer at location 2 and 4, (d) Shear stress τ_{sna} distribution on cross-sections of adhesive layer at location 3 and 4.

Figure 4.19 shows the contour for shear stress τ_{sn} (kPa) within the composite beam as predicted by the ABAQUS model. Figure 4.19a depicts the stress values within the composite beam, while Fig. 4.19b depicts the shear stress within the adhesive layer.

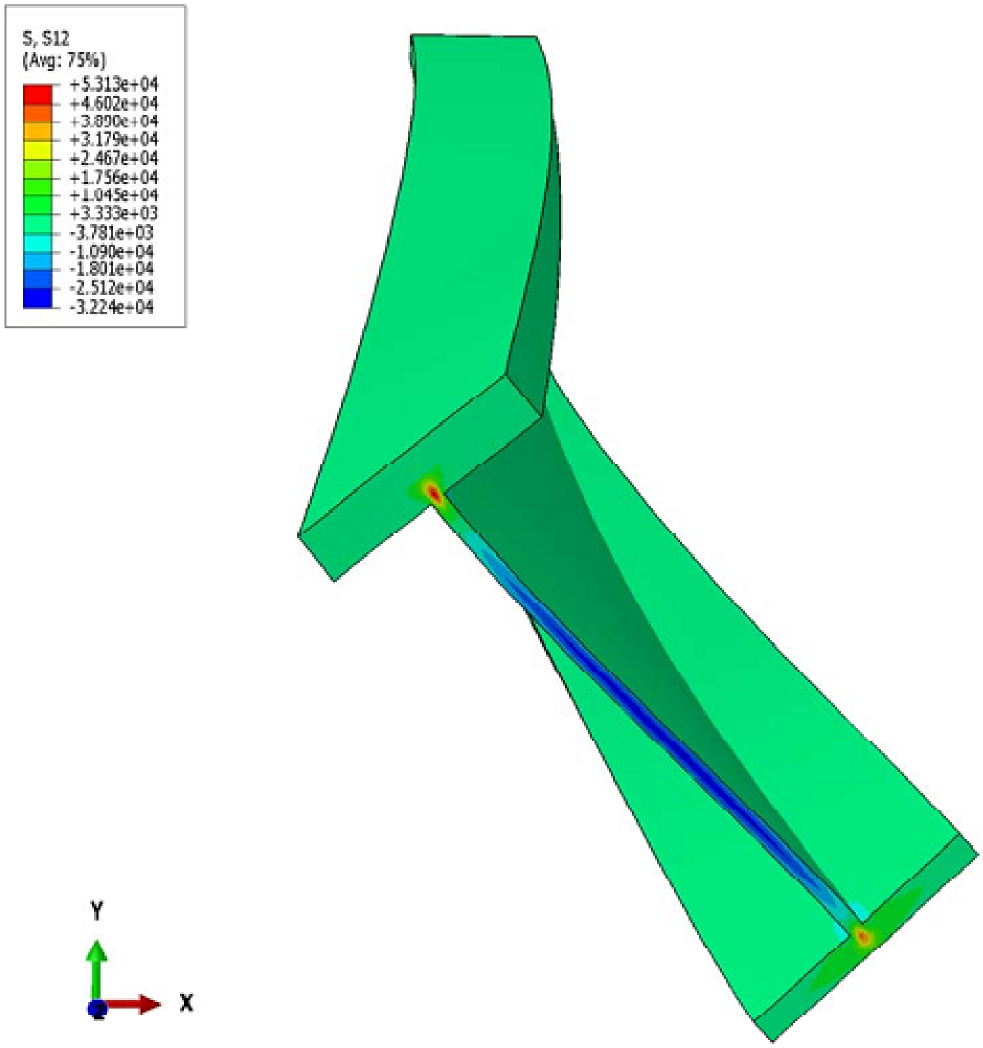
S, S12
(Avg: 75%)
+5.313e+04
+4.602e+04
+3.890e+04
+3.179e+04
+2.467e+04
+1.756e+04
+1.045e+04
+3.333e+03
-3.781e+03
-1.090e+04
-1.801e+04
-2.512e+04
-3.224e+04
Y
X

(a)

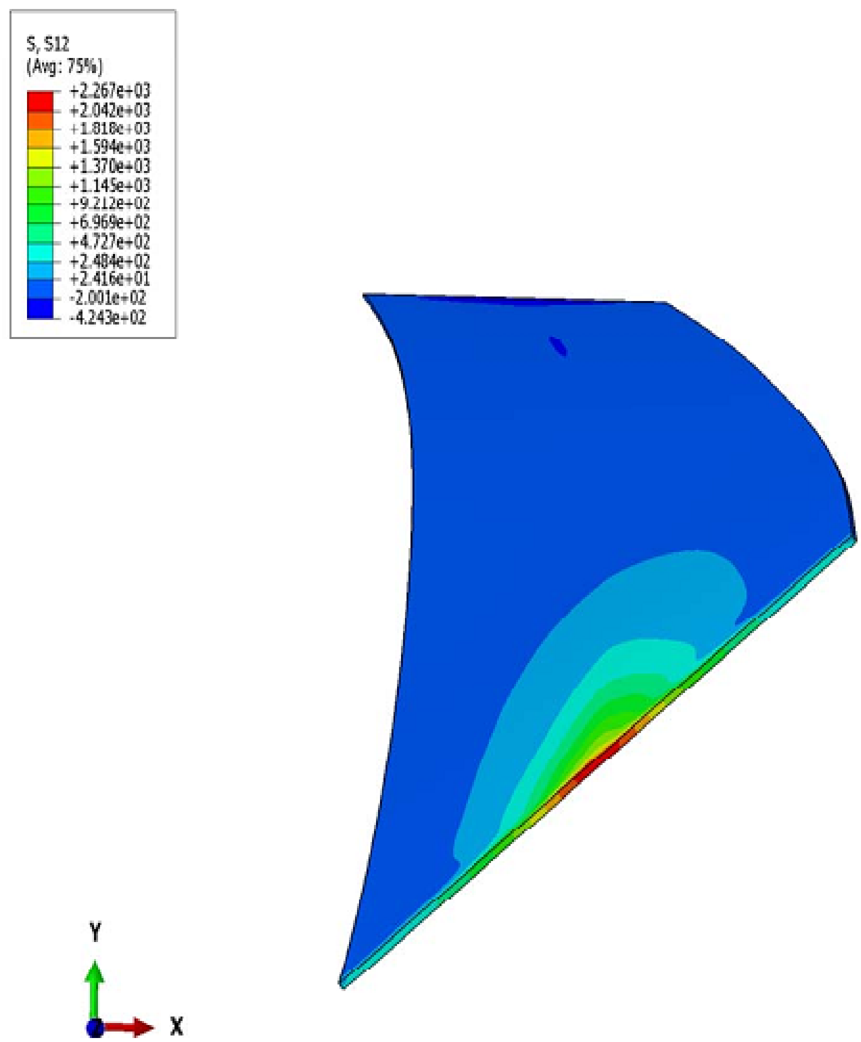

(b)

Figure 4.19. Shear stress τ_{sn} (kPa) distribution in (a) composite beam, (b) adhesive layer in ABAQUS model

Figure 4.20 shows the contour for longitudinal normal stress σ_z (kPa) within the composite beam as predicted by the ABAQUS model. Figure 4.20a depicts the stress values within the GFRP plate, Fig. 4.20b depicts the stress values within the adhesive layer, and Fig. 4.20c is bottom view of the composite beam.

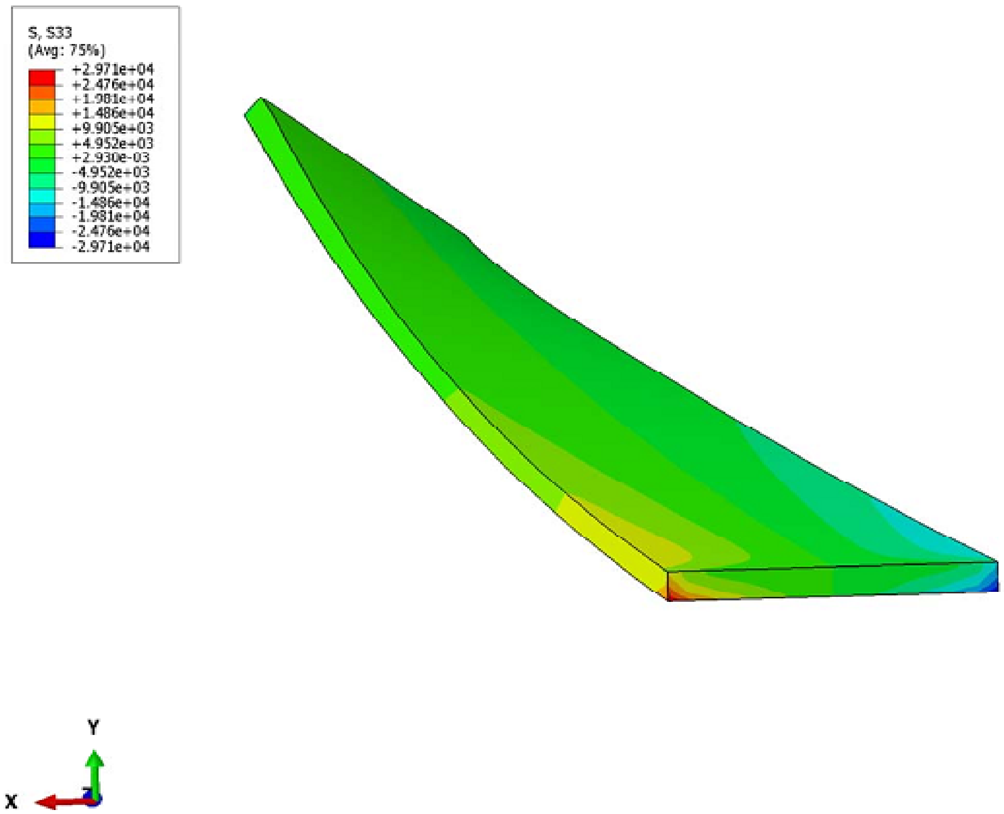
S, S33
(Avg: 75%)
+2.971e+04
+2.476e+04
+1.981e+04
+1.486e+04
+9.905e+03
+4.952e+03
+2.930e-03
-4.952e+03
-9.905e+03
-1.486e+04
-1.981e+04
-2.476e+04
-2.971e+04
Y
X

(a)

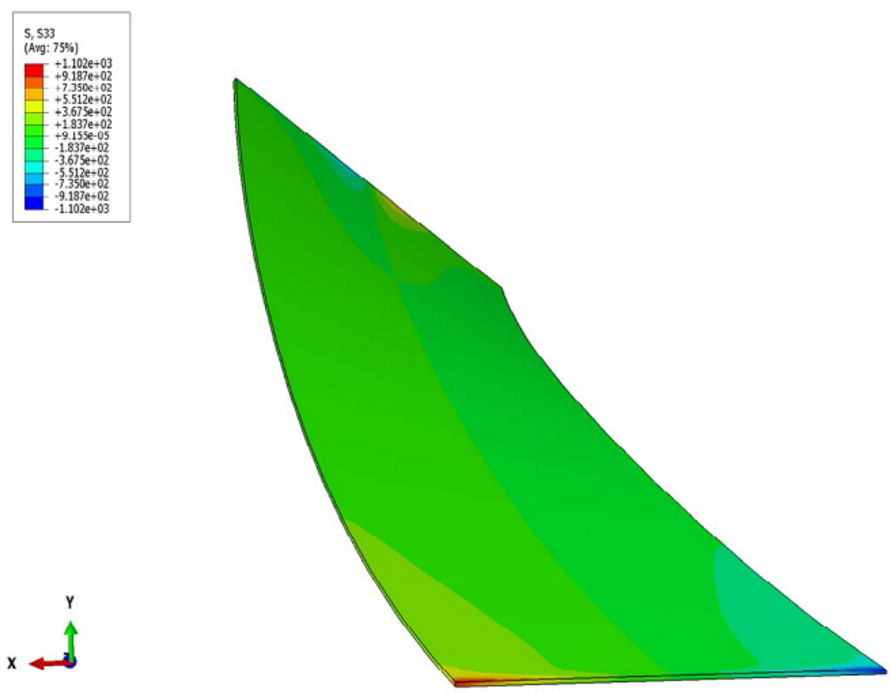
S, S33
(Avg: 75%)
+1.102e+03
+9.187e+02
+7.350e+02
+5.512e+02
+3.675e+02
+1.837e+02
+9.155e-05
-1.837e+02
-3.675e+02
-5.512e+02
-7.350e+02
-9.187e+02
-1.102e+03
Y
X

(b)

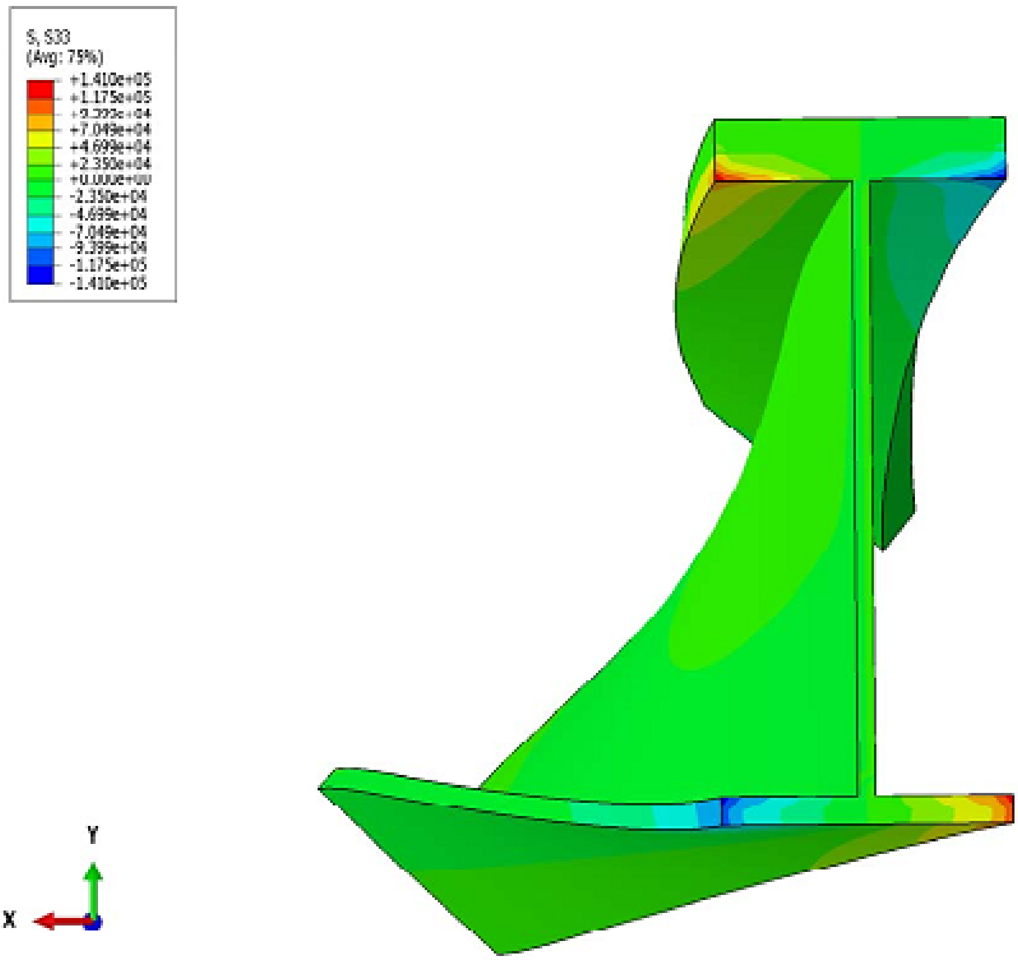

Figure 4.20. Normal stress σ_z (kPa) distribution in (a) GFRP plate, (b) adhesive layer, and (c) composite beam, in ABAQUS model

4.6 Summary and Conclusions

1. The non-shear deformable theory developed in Chapters 2 and 3 provides very good predictions of the longitudinal-transverse response of GFRP reinforced beams. When the response is predominantly lateral, the theory also provides reasonable results.
2. For the above class of problems, the predicted displacements are very close to those predicted by ABAQUS 3D FEA. Stress predictions are generally reliable, except at points of singularity, where the present theory does not capture localized stress concentrations.

3. The finite element developed in Chapter 3 was shown to be free from discretization errors and is able to model a beam with very few degrees of freedom.

4. The modeling and computational efforts involved in modeling composite systems in using the finite element developed in Chapter 3 is very small compared to that required in modeling the same problem using ABAQUS 3D modeling.

5. For predominantly torsional responses, the present theory grossly overestimates the stiffness of the composite system.

6. A systematic investigation of the kinematic assumptions used to develop the theory indicates that inclusion of shear deformation is needed to improve the present theory and expand its applicability to cases involving lateral-torsional response. This will be the scope of Chapters 5-7.

CHAPTER 5. SHEAR DEFORMABLE THEORY-FORMULATION

5.1. Introduction and Motivation

As discussed in Chapter 4, the assumption postulated in Chapter 2 that shear strains within the middle surface vanish, results in a significant overestimation of the torsional-flexural stiffness of the system. Also, three dimensional finite element analysis revealed that strain at the GFRP mid-surface do not vanish. Within this context, the present theory assumes a better kinematic model which captures the shear strains at the middle surface

5.2. Statement of the Problem

A steel wide flange section reinforced with a GFRP plate to one of the flanges is assumed to be subject to general loads. The GFRP plate is assumed to be connected the steel section through a thin layer of adhesive. It is required to formulate the governing field equations and boundary conditions based on shear deformable thin-walled beam. The assumptions of the formulation are presented in Section 5.3. The details of the formulation are presented in Section 5.4.

5.3. Assumptions

All assumptions made in Section 2.4 of Chapter 2 are valid except the assumption related to zero shear strain at the middle surface.

Assumptions related to kinematics

(i) The section contour does not deform in its own plane,

(ii) Each element behaves as a thin shell. This is in line of the Kirchhoff assumption of straight lines remaining normal to the section contour during a deformation.

(iii) Unlike the theory developed in Chapter 2, the assumption of zero shear strain is relaxed in the present theory by assuming that the section to undergo rotations θ_x and θ_y which are distinct from the derivatives of the corresponding displacement V', U' (in line with the Timoshenko beam) and warping deformation ψ which is also distinct from the derivative of the angle of twist θ_z' .

In addition, the following assumptions are made regarding the adhesive material

(iv) Perfect bond is assumed at interfaces between the adhesive and the GFRP plate and between the adhesive and the wide flange beam,

(v) The adhesive is assumed to act as a weak elastic material with a small modulus of elasticity when compared to those of the beam or GFRP. As a result, longitudinal stresses are considered negligible compared to the normal stresses in the GFRP plate and steel section,

(vi) The thickness of the adhesive layer is assumed to remain constant throughout deformation,

(vii) Displacement fields at any point within the Adhesive layer are linearly interpolated from those at the bottom surface of the GFRP plate and those at the top flange of the beam.

Also, the following assumption is made regarding the constitutive behaviour of the materials

(viii) All materials used are considered to be isotropic linearly elastic and.

5.4. Formulation

5.4.1. Kinematics

In the present theory, in addition to displacement fields $W_b(z)$, $W_p(z)$, $V(z)$, $U_b(z)$, $U_p(z)$, and $\theta_z(z)$, an additional six generalized displacements fields $\theta_{xb}(z), \theta_{xp}(z), \theta_{yb}(z), \theta_{yp}(z), \psi_b(z), \psi_p(z)$ are introduced to capture the effect of transverse shear deformation. While the transverse displacement fields $V(z), \theta_z(z)$ of the beam are common to the plate, the displacement fields $W_b(z), U_b(z)$ of the beam are assumed distinct from those of the plate $W_p(z), U_p(z)$. In general, the new six generated displacement fields are different from the first derivatives with respect to z of corresponding displacement fields, i.e., $\theta_x(z) \neq +V'(z)$ and $\theta_y(z) \neq +U'(z)$, and $\psi(z) \neq +\theta'(z)$. The angle of rotation of beam $\theta_{xb}(z)$ about the X-axis is assumed to be distinct from that of the plate $\theta_{xp}(z)$. Also, the angle of rotation of the beam $\theta_{yb}(z)$ about the Y-axis is assumed to be distinct from that of the plate $\theta_{yp}(z)$. In a similar manner, function $\psi_b(z)$ characterizing the warping deformation of the beam is assumed to be distinct from the warping deformation $\psi_p(z)$ for the plate. As a matter of convention, the angles of rotation $\theta_{xb}(z), \theta_{yb}(z), \theta_{yp}(z), \theta_z(z)$ follow the left hand rule sign convention as shown on Figures 5.1 and 5.2.

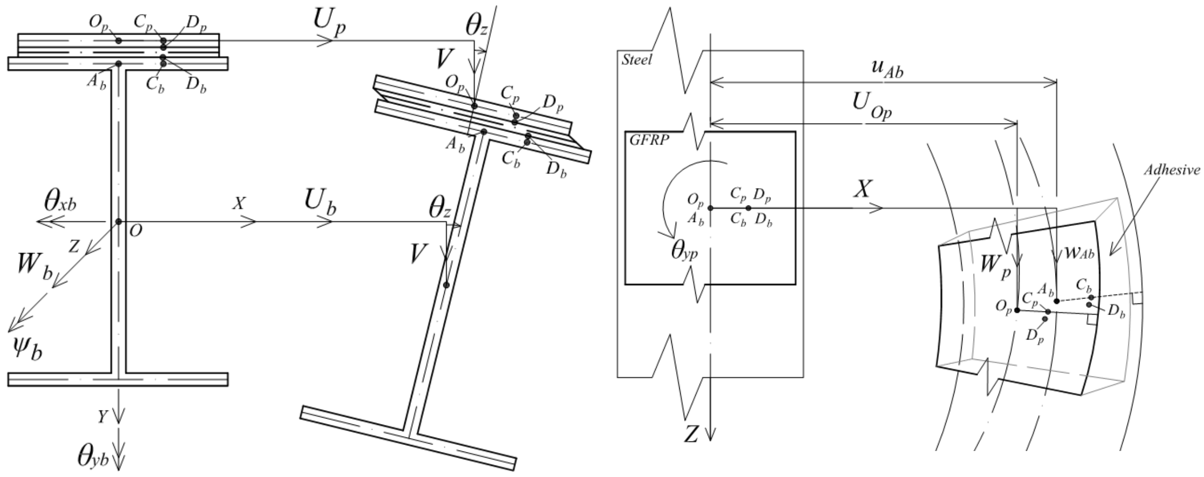

(a) Elevation View (b) Plan View

Figure 5.1. Kinematics of a GFRP strengthened wide flange beam

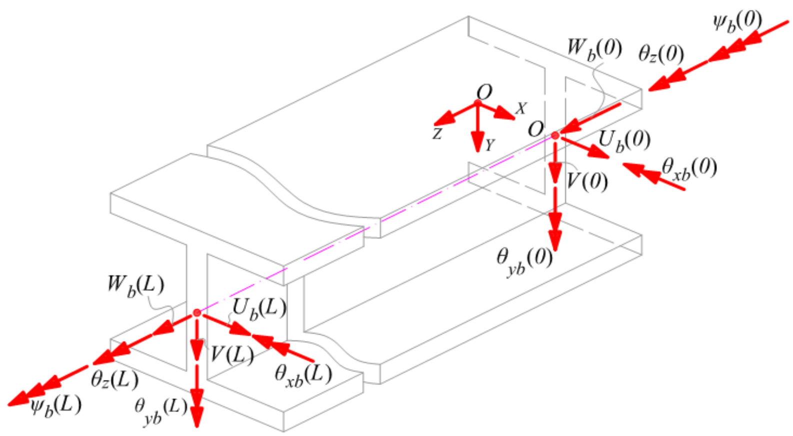

Figure 5.2. Governing displacement fields at member ends

5.4.2. Displacement fields within the plane of the cross-section

Based on Assumption (i) in Section 5.3, the displacement fields $\bar{u}(s,z)$ and $\bar{v}(s,z)$ within the plane of the cross-section for a Point lying on the mid-surface (based on Eqs. 2.9 and 2.10 in Chapter 2) are expressed as

$$\bar{u}(s,z) = U(z)\sin\alpha(s) - V(z)\cos\alpha(s) - q(s)\theta_z(z) \tag{5.1}$$

$$\bar{v}(s,z) = U(z)\cos\alpha(s) + V(z)\sin\alpha(s) + r(s)\theta_z(z) \tag{5.2}$$

in which $q(s_b) = x(s_b)\cos\alpha(s_b) + y(s_b)\sin\alpha(s_b)$; $r(s_b) = x(s_b)\sin\alpha(s_b) - y(s_b)\cos\alpha(s_b)$;

For a point offset from mid-surface within the cross section, the displacement fields $u(s,z,n)$ and $v(s,z,n)$ within the plane of the cross-section were given by Eqs. 2.13 and 2.14 in Chapter 2 as

$$u(s,z,n)=\bar{u}(s,z)=U(z)\sin\alpha(s)-V(z)\cos\alpha(s)-q(s)\theta_z(z) \tag{5.3}$$

$$v(s,z,n)=\{1-n[\alpha'(s)]\}U(z)\cos\alpha(s)+\{1-n[\alpha'(s)]\}V(z)\sin\alpha(s)+\theta_z(z)[r(s)+nq'(s)] \tag{5.4}$$

5.4.3. Longitudinal displacement field

In contrast to Eq. 2.16 in Chapter 2 resulting from the assumption zero transverse shear, the present theory assumed a more general expression for the displacement field at the middle surface

$$\bar{w}(s,z)=W(z)-\theta_y(z)x(s)-\ \theta_x(z)y(s)-\omega(s)\psi(z) \tag{5.5}$$

in which $\omega(s)=\int_0^s\left[\left(x(s)-x_o\right)\sin\alpha(s)-\left(y(s)-y_o\right)\cos\alpha(s)\right]ds=\int_0^s r(s)ds$, $\theta_x(z),\theta_y(z)$ are the angle of rotation about Y,X axes, respectively and $\psi(z)$ is a function which characterizes the warping deformation of the cross-section. Sign conventions for $\theta_x(z),\theta_y(z),\psi(z)$ are selected as shown in the Fig. 5.1. Since in general $\theta_x(z)\neq V'(z)$ and $\theta_y(z)\neq U'(z)$, and $\psi(z)\neq\theta_z'(z)$, the transverse shear strain γ_{sz} is non-zero, resulting in a more accurate representation of the kinematics of the problem.

For a Point offset from mid-surface within the cross section, the longitudinal displacement is given by

$$w(s,z,n)=\bar{w}(s,z)-n\frac{\partial\bar{u}(s,z)}{\partial z} \tag{5.6}$$

From Eq. (5.5), by substituting into Eq. (5.6), the longitudinal displacement of the Point B is obtained by

$$\begin{aligned}w(s,z,n)=&W(z)-x(s)\theta_y(z)-\ y(s)\theta_x(z)-\psi(z)\omega(s)\\&-n\sin\alpha(s)U'(z)+n\cos\alpha(s)V'(z)+nq(s)\theta_z'(z)\end{aligned} \tag{5.7}$$

5.4.4. Coordinates and Kinematics

Separate left-handed coordinate systems are defined for the wide flange beam (Fig. 5.3), GFRP plate (Fig. 5.4 and adhesive in a manner similar to Chapter 2.

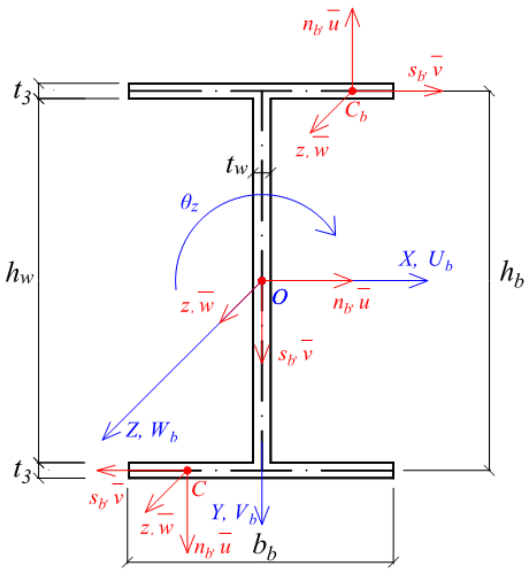

Figure 5.3. Local and global coordinates and dimensions of wide flange beam section

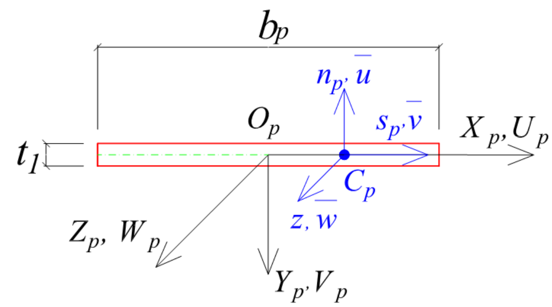

Figure 5.4. Local and global coordinates and dimensions of GFRP plate section

A global coordinate system $O_a X_a Y_a$ with Origin O_a is chosen at the Centroid of adhesive (Fig.5.5). Point $C_a\left(x_a\left(s_a\right), y_a\left(s_a\right)\right)$, in which $-b_p/2 \le x_a \le b_p/2$, lies is on the mid-surface of the adhesive layer. A local left-handed coordinate system $C_a n_a s_a z$ is selected for the layer, where coordinate s_a is oriented along the X_a direction, the n_a coordinate is normal to the contour, and the z coordinate is oriented along the Z axis. A transverse coordinate n_a , oriented upwards, is taken from centre line of the layer to a generic Point D (Fig 5.5).

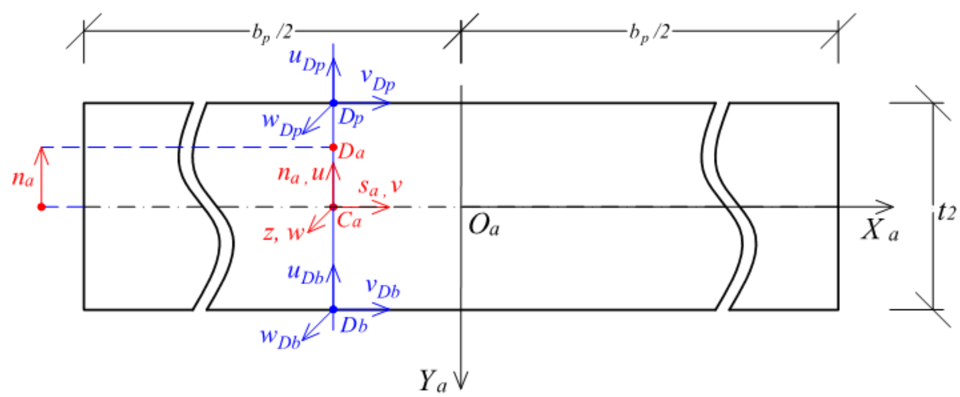

Figure 5.5. Cross-section of Adhesive layer and its coordinate system

5.4.5. Expression for Displacement Fields

5.4.5.1. Wide Flange Beam

From Eqs. (5.3), (5.4), and (5.7), one can express the displacement fields for Point $B_b(s_b,n_b,z)$ offset from the section contour within each part of the beam as:

$$u_b(s_b,n_b,z)=U_b(z)\sin\alpha(s_b)-V(z)\cos\alpha(s_b)-\theta_z(z)q(s_b) \tag{5.8}$$

$$v_b(s_b,n_b,z)=U_b(z)\cos\alpha(s_b)+V(z)\sin\alpha(s_b)+\theta_z(z)\left[r(s_b)+n_b q'(s_b)\right] \tag{5.9}$$

$$\begin{aligned} w_b(s_b,n_b,z)=&W_b(z)-x(s_b)\theta_{yb}(z)-y(s_b)\theta_{xb}(z)-\psi(z)\omega(s_b)\\ &-n_b\sin\alpha(s_b)U_b'(z)+n_b\cos\alpha(s_b)V'(z)+n_b q(s_b)\theta_z'(z)\end{aligned} \tag{5.10}$$

These displacement fields can be expressed in matrix form as

$$\begin{Bmatrix} u_b \\ v_b \\ w_b \end{Bmatrix}=\begin{bmatrix} 0 & \sin\alpha(s_b) & -\cos\alpha(s_b) & -q(s_b) & 0 & 0 & 0 \\ 0 & \cos\alpha(s_b) & \sin\alpha(s_b) & \left[r(s_b)+n_b q'(s_b)\right] & 0 & 0 & 0 \\ 1 & -n_b\sin\alpha(s_b)D & n_b\cos\alpha(s_b)D & n_b q(s_b)D & -x(s_b) & -y(s_b) & \omega(s_b) \end{bmatrix}\begin{Bmatrix} W_b(z) \\ U_b(z) \\ V(z) \\ \theta_z(z) \\ \theta_{by}(z) \\ \theta_{bx}(z) \\ \psi_b(z) \end{Bmatrix} \tag{5.11}$$

in which the operator $D=d/dz$ has been defined. By applying Eq. (5.11) for Point $D_b(s_b,(t_3/2),z)$ lying on top surface of the beam section and setting $\alpha=0^o$, one obtains

$$\begin{Bmatrix} u_b \\ v_b \\ w_b \end{Bmatrix}_{\left(n_b=\frac{t_3}{2}\right)}=\begin{bmatrix} 0 & 0 & -1 & -x(s_b) & 0 & 0 & 0 \\ 0 & 1 & 0 & \dfrac{h_b+t_3}{2} & 0 & 0 & 0 \\ 1 & 0 & \dfrac{t_3}{2}D & \dfrac{t_3}{2}x(s_b)D & -x(s_b) & \dfrac{h_b}{2} & -\dfrac{h_b}{2}x(s_b) \end{bmatrix}\begin{Bmatrix} W_b(z) \\ U_b(z) \\ V(z) \\ \theta_z(z) \\ \theta_{by}(z) \\ \theta_{bx}(z) \\ \psi_b(z) \end{Bmatrix} \tag{5.12}$$

5.4.5.2. GFRP Plate

Equations (5.3), (5.4), and (5.7) are specialized for the beam by setting $U=U_p, W=W_p$. The displacement fields for a Point $B_p(s_p,n_p,z)$ offset from the section contour are obtained as

$$u_p(s_p,n_p,z)=-V(z)-\theta_z(z)x(s_p) \tag{5.13}$$

$$v_p\left(s_p,n_p,z\right)=U_p\left(z\right)+\theta_z\left(z\right)n_p \tag{5.14}$$

$$w_p\left(s_p,n_p,z\right)=W_p\left(z\right)-x\left(s_p\right)\theta_{yp}\left(z\right)+n_pV'\left(z\right)+n_px\left(s_p\right)\theta'_z\left(z\right) \tag{5.15}$$

Displacement fields $\theta_{xp}\left(z\right),\psi_p\left(z\right)$ do not appear in Eqs. (5.13)-(5.15) since $y_p\left(s\right)=0,\omega_p\left(s\right)=0$.

In a matrix form, one has:

$$\begin{Bmatrix} u_p \\ v_p \\ w_p \end{Bmatrix}=\begin{bmatrix} 0 & 0 & -1 & -x_p\left(s_p\right) & 0 & 0 & 0 \\ 0 & 1 & 0 & n_p & 0 & 0 & 0 \\ 1 & 0 & n_pD & n_px\left(s_p\right)D & -x\left(s_p\right) & -y\left(s_p\right) & 0 \end{bmatrix}\begin{Bmatrix} W_p\left(z\right) \\ U_p\left(z\right) \\ V\left(z\right) \\ \theta_z\left(z\right) \\ \theta_{py}\left(z\right) \\ \theta_{px}\left(z\right) \\ \psi_p\left(z\right) \end{Bmatrix} \tag{5.16}$$

Therefore, displacement fields for Point $D_p\left(s_p,-\left(t_1/2\right),z\right)$ lying on bottom surface of the GFRP plate ($\alpha=0^o$) are expressed as

$$\begin{Bmatrix} u_p \\ v_p \\ w_p \end{Bmatrix}_{\left(n_p=-\frac{t_1}{2}\right)}=\begin{bmatrix} 0 & 0 & -1 & -x_p\left(s_p\right) & 0 & 0 & 0 \\ 0 & 1 & 0 & -\frac{t_1}{2} & 0 & 0 & 0 \\ 1 & 0 & -\frac{t_1}{2}D & -\frac{t_1}{2}x\left(s_p\right)D & -x\left(s_p\right) & 0 & 0 \end{bmatrix}\begin{Bmatrix} W_p\left(z\right) \\ U_p\left(z\right) \\ V\left(z\right) \\ \theta_z\left(z\right) \\ \theta_{py}\left(z\right) \\ \theta_{px}\left(z\right) \\ \psi_p\left(z\right) \end{Bmatrix} \tag{5.17}$$

5.4.5.3. Adhesive Layer

Coordinate n_a will be used to linearly interpolate displacement fields of the Point D_a as a function of Points D_p and D_b as shown in Fig.5.5. Since origins *O*, O_p , O_a are chosen to lie along the same vertical line, one has $s_a=s_b=s_p$, and thus $x_a\left(s_a\right)=x\left(s_b\right)=x_p\left(s_p\right)=x\left(s\right)$, where $-b_p/2\le x\left(s\right)\le b_p/2$. As stated under Section 5.3, Displacement fields $\langle u_a \quad v_a \quad w_a\rangle^T$ of Point D_a within the adhesive layer are determined by linear interpolation across the layer thickness, yielding

$$\begin{Bmatrix} u_a \\ v_a \\ w_a \end{Bmatrix}=\left(\frac{1}{2}+\frac{n_a}{t_2}\right)\begin{Bmatrix} u_p \\ v_p \\ w_p \end{Bmatrix}_{\left(n_p=-\frac{t_1}{2}\right)}+\left(\frac{1}{2}-\frac{n_a}{t_2}\right)\begin{Bmatrix} u_b \\ v_b \\ w_b \end{Bmatrix}_{\left(n_b=\frac{t_3}{2}\right)} \tag{5.18}$$

From Eqs. (5.12) and (5.17), by substituting into (5.18), the displacement fields at Point D_a are expressed as

$$u_{Da}\left(s_a,n_a,z\right)=\left(\frac{1}{2}+\frac{n_a}{t_2}\right)u_p(s_p,\frac{t_1}{2},z)+\left(\frac{1}{2}-\frac{n_a}{t_2}\right)u_b(s_b,-\frac{t_3}{2},z)$$

$$=\left(\frac{1}{2}+\frac{n_a}{t_2}\right)\left[-V\left(z\right)-\theta_z\left(z\right)x\left(s\right)\right]+\left(\frac{1}{2}-\frac{n_a}{t_2}\right)\left[-V\left(z\right)-\theta_z(z)x\left(s\right)\right]=-V\left(z\right)-\theta_z\left(z\right)x\left(s\right)$$

$$v_{Da}\left(s_z,n_a,z\right)=\left(\frac{1}{2}+\frac{n_a}{t_2}\right)v_p(s_p,\frac{t_3}{2},z)+\left(\frac{1}{2}-\frac{n_a}{t_2}\right)v_b(s_b,-\frac{t_1}{2},z)$$

$$=\left(\frac{1}{2}+\frac{n_a}{t_2}\right)\left[U_p\left(z\right)-\theta_z\left(z\right)\left(\frac{t_1}{2}\right)\right]+\left(\frac{1}{2}-\frac{n_a}{t_2}\right)\left[U_b\left(z\right)+\theta_z\left(z\right)\left(\frac{h_b+t_3}{2}\right)\right]$$

$$w_{Da}\left(s_a,n_a,z\right)=\left(\frac{1}{2}+\frac{n_a}{t_2}\right)w_{Dp}(s_p,\frac{t_1}{2},z)+\left(\frac{1}{2}-\frac{n_a}{t_2}\right)w_{Db}(s_b,-\frac{t_3}{2},z)$$

$$=\left(\frac{1}{2}+\frac{n_a}{t_2}\right)\left\{W_p\left(z\right)-x\left(s_p\right)\theta_{yp}\left(z\right)-\frac{t_1}{2}V'\left(z\right)-\frac{t_1}{2}x\left(s_p\right)\theta_z'\left(z\right)\right\}$$

$$+\left(\frac{1}{2}-\frac{n_a}{t_2}\right)\left\{W_b\left(z\right)-x\left(s_b\right)\theta_{yb}\left(z\right)+\frac{h_b}{2}\theta_{xb}\left(z\right)-\frac{h_b}{2}x\left(s_b\right)\psi\left(z\right)+\frac{t_3}{2}V'\left(z\right)+\frac{t_3}{2}x\left(s_b\right)\theta_z'\left(z\right)\right\}$$

5.4.6. Expressions for Strains

5.4.6.1. Wide Flange Beam

From the displacement fields expressed in Eqs. (5.8)-(5.10), the strain components are expressed as

$\varepsilon_{nb}=\varepsilon_{sb}=\gamma_{nsb}=\gamma_{znb}=0$, and

$$\gamma_{szb}=\frac{\partial v_b}{\partial z}+\frac{\partial w_b}{\partial s}=\left[U_b'\left(z\right)-\theta_{yb}\left(z\right)\right]\cos\alpha\left(s_b\right)+\left[V'\left(z\right)-\theta_{xb}\left(z\right)\right]\sin\alpha\left(s_b\right)+\left[\theta_z'\left(z\right)-\psi_b\left(z\right)\right]r\left(s_b\right)+2n_b\theta_z'\left(z\right)$$

and

$$\varepsilon_{zb}=W_b'\left(z\right)-x\left(s_b\right)\theta_{yb}'\left(z\right)-y\left(s_b\right)\theta_{xb}'\left(z\right)-\psi_b'\left(z\right)\omega\left(s_b\right)-n_b\sin\alpha\left(s_b\right)U_b''(z)+n_b\cos\alpha\left(s_b\right)V''\left(z\right)+$$
$$+n_bq\left(s_b\right)\theta_z''(z)$$

5.4.6.2. GFRP Plate

From the displacement fields expressed in Eqs. (5.13)-(5.15), the strain components are

$\varepsilon_{np}=\varepsilon_{sp}=\gamma_{nsp}=\gamma_{znp}=0$, and $\gamma_{szp}=\dfrac{\partial v_p}{\partial z}+\dfrac{\partial w_p}{\partial s}=U_p'\left(z\right)-\theta_{yp}\left(z\right)+2n_p\theta_z'\left(z\right)$,

$$\varepsilon_{zp}=W_p'\left(z\right)-x\left(s_p\right)\theta_{yp}'\left(z\right)+n_pV''\left(z\right)+n_px\left(s_p\right)\theta_z''(z)$$

5.4.6.3. Adhesive Layer

Because the cross-sectional area A_a and modulus of elasticity E_a of the adhesive layer are very small compared to those of the GFRP plate and the wide flange beam, the bending capacity of the layer is considered negligible (Assumption v). Therefore, the normal stresses $\sigma_{na}, \sigma_{za}, \sigma_{za}$ are considered negligible. Thus, the corresponding strains $\varepsilon_{na}, \varepsilon_{za}, \varepsilon_{za}$ will be assumed to have a negligible contribution to the strain energy expression. The remaining strains are

$$\gamma_{zna} = \langle a_{a1}(x)\rangle_{1\times 8}^{\mathrm{T}} \{\Delta_{a1}(z)\}_{8\times 1}, \gamma_{sna} = \langle a_{a2}\rangle_{1\times 3}^{\mathrm{T}} \{\Delta_{a2}(z)\}_{3\times 1}, \gamma_{sza} = \langle a_{a3}(n_a)\rangle_{1\times 6}^{\mathrm{T}} \{\Delta_{a3}(z)\}_{6\times 1} \quad (5.19)$$

in which

$$\langle a_{a1}(x)\rangle_{1\times 8}^{\mathrm{T}} = \langle -c_1 \quad c_1 \quad -c_3 \quad -c_2 \quad -c_2 x \quad c_1 x \quad -c_1 x \quad c_3 x\rangle, \ \langle a_{a2}\rangle_{1\times 3}^{\mathrm{T}} = \langle -c_1 \quad c_1 \quad -(c_2+c_3)\rangle,$$

$$\langle a_{a3}(n_a)\rangle_{1\times 6}^{T} = \left\langle \frac{1}{2}-\frac{n_a}{t_2} \;\middle|\; \frac{1}{2}+\frac{n_a}{t_2} \;\middle|\; \frac{h_b-2t_1+2t_3}{4} - \frac{h_b+2t_1+2t_3}{2t_2} n_a \;\middle|\; -\left(\frac{1}{2}-\frac{n_a}{t_2}\right) \;\middle|\; -\left(\frac{1}{2}+\frac{n_a}{t_2}\right) \;\middle|\; -\left(\frac{1}{2}-\frac{n_a}{t_2}\right)\frac{h_b}{2} \right\rangle \quad (5.20)$$

with $c_1 = \dfrac{1}{t_2}$, $c_2 = \dfrac{t_1+2t_2+t_3}{2t_2}$, $c_3 = \dfrac{h_b}{2t_2}$, and

$$\langle \Delta_{a1}(z)\rangle_{1\times 8}^{\mathrm{T}} = \langle W_b \quad W_p \quad \theta_{bx} \quad V' \quad \theta_z' \quad \theta_{yb} \quad \theta_{yp} \quad \psi_b\rangle$$

$$\langle \Delta_{a2}(z)\rangle_{1\times 3}^{\mathrm{T}} = \langle U_b \quad U_p \quad \theta_z\rangle$$

$$\langle \Delta_{a3}(z)\rangle_{1\times 6}^{T} = \langle U_b' \quad U_p' \quad \theta_z' \quad \theta_{yb} \quad \theta_{yp} \quad \psi_b\rangle$$

5.4.7. Expression for Stresses

The non-zero stresses can be related to the strains through

$\sigma_{zb} = E_b \varepsilon_{zb}$; $\tau_{szb} = G_b \gamma_{szb}$;

$\sigma_{zp} = E_p \varepsilon_{zp}$; $\tau_{szp} = G_p \gamma_{szp}$;

$\tau_{sza} = G_a \gamma_{sza}$; $\tau_{sna} = G_a \gamma_{sna}$; $\tau_{zna} = G_a \gamma_{zna}$

5.4.8. Variational Principle

5.4.8.1. General

The total potential energy π is the sum of internal strain energies stored within the steel beam U_b the GFRP plate U_p , the adhesive layer U_a minus the load potential energy loss by tractions at member ends V_1 and member tractions within the member V_2 , i.e.,

$$\pi = U_b + U_p + U_a - V_1 - V_2 \quad (5.21)$$

The details are presented in Appendix A6.

5.4.8.2. Internal Strain Energy

Contribution of the wide flange beam

The internal strain energy stored in the steel beam (Section A6.1 in Appendix A6) is given by

$$\begin{aligned} U_b = \int_L \Bigg(& \frac{1}{2}E_b A_b W_b'^{\,2} + \frac{1}{2}E_b I_{ssbf} V''^2 + \frac{1}{2}G_b A_{bw} V'^{\,2} - G_b A_{bw}\theta_{xb} V' + \frac{1}{2}E_b I_{xxb1}\theta_{xb}'^{\,2} + \frac{1}{2}G_b A_{bw}\theta_{xb}^2 + \\ & + \frac{1}{2}E_b I_{ssbw} U_b''^{\,2} + G_b A_{bf} U_b'^2 - 2G_b A_{bf}\theta_{yb} U_b' + \frac{1}{2}E_b I_{yybf}\theta_{yb}'^{\,2} + G_b A_{bf}\theta_{yb}^2 + \frac{1}{2}E_b I_{\omega\omega bl}\theta_z''^2 + \\ & + \frac{1}{2}G_b J_b \theta_z'^2 - \frac{h_b^2}{2}G_b A_{bf}\psi_b\theta_z' + \frac{1}{2}E_b I_{\omega\omega bg}\psi_b'^2 + \frac{h_b^2}{4}G_b A_{bf}\psi_b^{\,2} \Bigg) dz \end{aligned} \tag{5.22}$$

in which the following section properties have been defined

$$A_b = \sum_{i=1,3} b_i t_i;\; I_{xxb1} = \frac{t_w h_w^3}{12} + 2b_f t_3 \frac{h_b^2}{4};\; I_{ssbf} = 2\frac{b_f t_3^3}{12};\; A_{bw} = h_w t_w;\; I_{ssbw} = \frac{h_w t_w^3}{12};\; A_{bf} = b_f t_3;$$

$$I_{yybf} = 2\frac{t_3 b_f^3}{12}; \qquad I_{\omega\omega bl} = 2\frac{b_f^3 t_3^3}{144} + \frac{h_w^3 t_w^3}{144}; \qquad I_{\omega\omega bg} = \frac{h_b^2 b^3 t_3}{24}; \qquad J_b = \frac{h_w t_w^3}{3} + 2\frac{b_f t_3^3}{3} + \frac{h_b^2}{2}A_{bf};$$

Contribution of the plate

The internal strain energy stored in the GFRP plate (Section A6.2 in Appendix A6) is given by

$$\begin{aligned} U_p = \int_L \Bigg(& \frac{1}{2}E_p A_p W_p'^{\,2} + \frac{1}{2}E_p I_{xxp} V''^2 + \frac{1}{2}G_p A_p U_p'^{\,2} - G_p A_p \theta_{yp} U_p' \\ & + \frac{1}{2}E_p I_{yyp}\theta_{yp}'^{\,2} + \frac{1}{2}G_p A_p \theta_{yp}^2 + \frac{1}{2}E_p I_{\omega\omega p}\theta_z''^2 + \frac{1}{2}G_p J_p \theta_z'^{\,2} \Bigg) dz \end{aligned} \tag{5.23}$$

in which the following section properties are defined

$$A_p = t_1 b_p; \quad I_{xxp} = \frac{b_p t_1^3}{12}; \quad I_{yyp} = \frac{t_1 b_p^3}{12}; \quad I_{\omega\omega p} = \frac{b_p^3 t_1^3}{144}; \quad J_p = \frac{b_p t_1^3}{3}$$

Contribution of the adhesive layer

The internal strain energy stored in the adhesive layer (Section A6.3 in Appendix A6) is given by

$$\begin{aligned} U_a = & \frac{1}{2}G_a A_a \int_L \langle \Delta_{a11} \rangle_{1\times 4}^T \left[H_{a11} \right]_{4\times 4} \{\Delta_{a11}\}_{4\times 1} dz + \frac{1}{2}G_a I_{yya} \int_L \langle \Delta_{a12} \rangle_{1\times 4}^T \left[H_{a12} \right]_{4\times 4} \{\Delta_{a12}\}_{4\times 1} dz \\ & + \frac{1}{2}G_a A_a \int_L \langle \Delta_{a2} \rangle_{1\times 3}^T \left[H_{a2} \right]_{3\times 3} \{\Delta_{a2}\}_{3\times 1} dz + \frac{1}{24}G_a A_a \int_L \langle \Delta_{a3} \rangle_{1\times 6}^T \left[H_{a3} \right]_{6\times 6} \{\Delta_{a3}\}_{6\times 1} dz \end{aligned} \tag{5.24}$$

in which the following displacement vectors have been defined

$$\langle \Delta_{a11} \rangle_{1\times4}^{T} = \langle W_b \quad W_p \quad \theta_{xb} \quad V' \rangle;\ \langle \Delta_{a12} \rangle_{1\times4}^{T} = \langle \theta_z' \quad \theta_{yb} \quad \theta_{yp} \quad \psi_b \rangle;\ \langle \Delta_{a2} \rangle_{1\times3}^{T} = \langle U_b \quad U_p \quad \theta_z \rangle;$$

$$\Delta_{a3} = \langle U_b' \quad U_p' \quad \theta_z' \quad \theta_{yb} \quad \theta_{yp} \quad \psi_b \rangle;$$

Also, the following matrices have been defined

$$\left[H_{a11}\right]_{4\times4} = \begin{bmatrix} c_1^2 & -c_1^2 & c_1c_3 & c_1c_2 \\ -c_1^2 & c_1^2 & -c_1c_3 & -c_1c_2 \\ c_1c_3 & -c_1c_3 & c_3^2 & c_2c_3 \\ c_1c_2 & -c_1c_2 & c_2c_3 & c_2^2 \end{bmatrix};\left[H_{a12}\right]_{4\times4} = \begin{bmatrix} c_2^2 & -c_1c_2 & c_1c_2 & -c_2c_3 \\ -c_1c_2 & c_1^2 & -c_1^2 & c_1c_3 \\ c_1c_2 & -c_1^2 & c_1^2 & -c_1c_3 \\ -c_2c_3 & c_1c_3 & -c_1c_3 & c_3^2 \end{bmatrix};$$

$$\left[H_{a2}\right]_{3\times3} = \begin{bmatrix} c_1^2 & -c_1^2 & c_1(c_2+c_3) \\ -c_1^2 & c_1^2 & -c_1(c_2+c_3) \\ c_1(c_2+c_3) & -c_1(c_2+c_3) & (c_2+c_3)^2 \end{bmatrix};\ \left[\overline{H_{a3}}\right]_{6\times6} = \left[\begin{array}{ccc|ccc} 4 & 2 & 2c_4 & -4 & -2 & -2h_b \\ 2 & 4 & c_5 & -2 & -4 & -h_b \\ 2c_4 & c_5 & c_6 & -2c_4 & -c_5 & -c_4h_b \\ \hline -4 & -2 & -2c_4 & 4 & 2 & 2h_b \\ -2 & -4 & -c_5 & 2 & 4 & h_b \\ -2h_b & -h_b & -c_4h_b & 2h_b & h_b & h_b^2 \end{array}\right]$$

in which c_1, c_2, c_3 were already defined after Eq. (5.20) and $c_4 = h_b - t_1 + 2t_3$, $c_5 = h_b - 4t_1 + 2t_3$ and $c_6 = h_b^2 + 4t_1^2 + 4t_3^2 - 2h_bt_1 + 4h_bt_3 - 4t_1t_3$ and $I_{yya} = \int_{A_a} x^2 dA$

5.4.8.3. Load potential energy

The total potential energy loss $\tilde{V}$ is the sum of the potential energy lost $\tilde{V}$ by end tractions $\sigma_z(s_b, n_b, 0)$, $\tau_u(s_b, n_b, 0), \tau_v(s_b, n_b, 0), \sigma_z(s_b, n_b, L), \tau_u(s_b, n_b, L), \tau_v(s_b, n_b, L)$ at $z = 0, L$ (as defined in Fig. 5.6) and the potential energy lost $\tilde{V}$ by the member tractions $p_u(s_b, n_b, z), p_v(s_b, n_b, z), p_z(s_b, n_b, z)$.

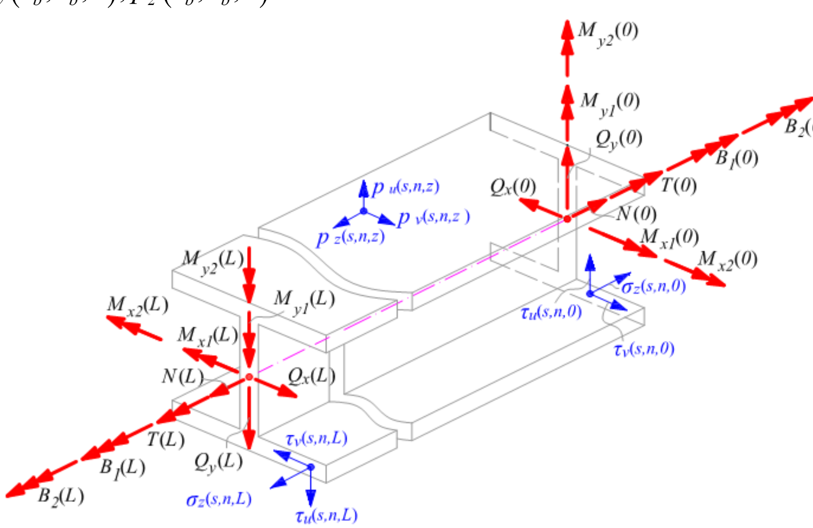

Figure 5.6. End and Member Tractions

5.4.5.3.1 Load potential due to loads acting at two ends

The total potential energy loss $\tilde{V}$ due to loads at the member ends are

$$V_1 = -\left[+\int_A \tau_v(s_b,n_b,0) v_b(s_b,n_b,0) dA + \int_A \tau_u(s_b,n_b,0) u_b(s_b,n_b,0) dA + \int_A \sigma_z(s_b,n_b,0) w_b(s_b,n_b,0) dA + \right.$$
$$\left. -\int_A \tau_v(s_b,n_b,L) v_b(s_b,n_b,L) dA - \int_A \tau_u(s_b,n_b,L) u_b(s_b,n_b,L) dA - \int_A \sigma_z(s_b,n_b,L) w_b(s_b,n_b,L) dA \right] \tag{5.25}$$

From Eqs. (5.8)-(5.10), by substituting into Eq.(5.25), and integrating over the area, one obtains (Section A6.4.1 in Appendix A6)

$$\begin{aligned} V_1 = -\big[& N(0)W_b(0) + Q_x(0)U_b(0) + Q_y(0)V(0) + M_{x1}(0)V'(0) + M_{x2}(0)\theta_{xb}(0) \\ & + M_{y1}(0)U_b'(0) + M_{y2}(0)\theta_{yb}(0) + T(0)\theta_z(0) + B_1(0)\theta_z'(0) + B_2(0)\psi_b(0) \\ & - N(L)W_b(L) - Q_x(L)U_b(L) - Q_y(L)V(L) - M_{x1}(L)V'(L) - M_{x2}(L)\theta_{xb}(L) \\ & - M_{y1}(L)U_b'(L) - M_{y2}(L)U_b'(L) - T(L)\theta_z(L) - B_1(L)\theta_z'(L) - B_2(L)\psi_b(L) \big] \end{aligned} \tag{5.26}$$

in which

$$\left\{ \begin{matrix} N(Z_e) \\ Q_x(Z_e) \\ Q_y(Z_e) \\ M_{x1}(Z_e) \\ M_{x2}(Z_e) \\ M_{y1}(Z_e) \\ M_{y2}(Z_e) \\ T(Z_e) \\ B_1(Z_e) \\ B_2(Z_e) \end{matrix} \right\} = \int_A \left\{ \begin{matrix} \sigma_z(s_b,n_b,Z_e) \\ \tau_v(s_b,n_b,Z_e)\cos\alpha(s_b) + \tau_u(s_b,n_b,Z_e)\sin\alpha(s_b) \\ \tau_v(s_b,n_b,Z_e)\sin\alpha(s_b) - \tau_u(s_b,n_b,Z_e)\cos\alpha(s_b) \\ \sigma_z(s_b,n_b,Z_e) n_b \cos\alpha(s_b) \\ -\sigma_z(s_b,n_b,Z_e) y(s_b) \\ -\sigma_z(s_b,n_b,Z_e) n_b \sin\alpha(s_b) \\ -\sigma_z(s_b,n_b,Z_e) x(s_b) \\ \tau_v(s_b,n_b,Z_e)\left[r(s_b) + nq'(s_b)\right] - \tau_u(s_b,n_b,Z_e) q(s_b) \\ \sigma_z(s_b,n_b,Z_e) n_b q(s_b) \\ -\sigma_z(s_b,n_b,Z_e)\omega(s_b) \end{matrix} \right\} dA, \quad Z_e = 0, L \tag{5.27}$$

Equation 2.41 in Chapter 2 differs from Eq.(5.27), since the generalized forces $M_x(0), M_y(0), B(0), M_x(L), M_y(L), B(L)$ are separated into $M_{x1}(0), M_{x2}(0), M_{y1}(0)$ $, M_{y2}(0), B_1(0), B_2(0), M_{x1}(L), M_{x2}(L), M_{y1}(L), M_{y2}(L), B_1(L), B_2(L)$ which are associated with the end generalized deformation $\big(V'(0), \theta_{xb}(0), U_b'(0), \theta_{yb}(0), \theta_z'(0),, \psi_b(0), V'(L), \theta_{xb}(L), U_b'(L),$ $\theta_{yb}(L), \theta_z'(L), \psi_b(L)\big)$ in the present theory. In contrast, under the non-shear deformable theory, they are assumed to undergo different generalized deformations $\big(V'(0), U_b'(0), \theta_z'(0), V'(L), U_b'(L),$

$\theta_z'(L))$. The difference is a natural outcome of the fact the shear deformations were suppressed in the former theory but incorporated in the present one.

5.4.5.3.2 Load potential due to member tractions

The total potential energy loss $\tilde{V}$ due to member tractions $p_u(s_b,n_b,z), p_v(s_b,n_b,z), p_z(s_b,n_b,z)$ is

$$V_2=\int_L\int_{s_b}\left[p_u(s_b,n_b,z)u_b(s_b,n_b,z)+p_v(s_b,n_b,z)v_b(s_b,n_b,z)+p_z(s_b,n_b,z)w_b(s_b,n_b,z)\right]ds_b dz \tag{5.28}$$

From Eqs. (5.8)-(5.10), by substituting into Eq.(5.28), grouping terms and performing integration by parts (A6.4.2 in the Appendix A6) one obtains

$$\begin{aligned}V_2=\int_L\Big[&q_{zb}(z)W_b(z)+q_{yb}(z)V(z)+m_{xb}(z)\theta_{xb}(z)+q_{xb}(z)U_b(z)+\\&+m_{yb}(z)\theta_{yb}(z)+m_{zb}(z)\theta_z(z)+b_b(z)\psi_b(z)\Big]dz\end{aligned} \tag{5.29}$$

in which the distributed members loads are related to the applied member tractions through the contour integrals (A6.4.2 in the Appendix A6)

$$\begin{Bmatrix}q_{zb}(z)\\q_{yb}(z)\\m_{xb}(z)\\q_{xb}(z)\\m_{yb}(z)\\m_{zb}(z)\\b_b(z)\end{Bmatrix}=\int_{s_b}\begin{Bmatrix}p_z(s_b,n_b,z)\\p_v(s_b,n_b,z)\sin\alpha(s_b)-p_u(s_b,n_b,z)\cos\alpha(s_b)-\{\partial/\partial z[p_z(s_b,n_b,z)]\}n_b\cos\alpha(s_b)\\-p_z(s_b,n_b,z)y(s_b)\\p_v(s_b,n_b,z)\cos\alpha(s_b)+p_u(s_b,n_b,z)\sin\alpha(s_b)+\{\partial/\partial z[p_z(s_b,n_b,z)]\}n_b\sin\alpha(s_b)\\-p_z(s_b,n_b,z)x(s_b)\\p_v(s_b,n_b,z)[r(s_b)+nq'(s_b)]-p_u(s_b,n_b,z)q(s_b)-\{\partial/\partial z[p_z(s_b,n_b,z)]\}n_bq(s_b)\\-p_z(s_b,n_b,z)\omega(s_b)\end{Bmatrix}ds_b \tag{5.30}$$

By comparing Eq. (5.30) with Eq. (2.43) in Chapter 2 one notices that, in addition to the four loading terms $q_{yb}(z),q_{xb}(z),q_{zb}(z),m_{zb}(z)$ which are common to both theories, the presence of new loads $m_{xb}(z),m_{yb}(z),b_b(z)$ arises. It is also noted that from equations of load potential energies (5.26) and(5.29), by setting $\theta_x(z)=V'(z)$, $\theta_y(z)=U'(z)$, $\psi(z)=\theta'(z)$, one recovers the load potential energy expressions in Chapter 2.

5.4.9. Longitudinal-Transverse Response

5.4.9.1. Potential Energy

From Eqs. 5.22-5.27, by omitting all torsional flexural terms, one obtains

$$\pi_1=\int_L\left[\frac{1}{2}E_bA_bW_b'^{\,2}+\frac{1}{2}E_bI_{ssbf}V''^2+\frac{1}{2}G_bA_{bw}V'^{\,2}-G_bA_{bw}\theta_{xb}V'+\frac{1}{2}E_bI_{xxb1}\theta_{xb}'^{\,2}+\frac{1}{2}G_bA_{bw}\theta_{xb}^2+\right.$$

$$\left.+\frac{1}{2}E_pA_pW_p'^{\,2}+\frac{1}{2}E_pI_{xxp}V''^2+\frac{1}{2}G_aA_a\left\langle\Delta_{a11}\right\rangle_{1\times4}^T\left[H_{a11}\right]_{4\times4}\left\{\Delta_{a11}\right\}_{4\times1}\right]dz+$$

$$+\left[N(0)W_b(0)+Q_y(0)V(0)+M_{x1}(0)V'(0)+M_{x2}(0)\theta_{xb}(0)-N(L)W_b(L)-Q_y(L)V(L)\right.$$

$$\left.-M_{x1}(L)V'(L)-M_{x2}(L)\theta_{xb}(L)\right]-\int_L q_z(z)W_b(z)dz-\int_L q_y(z)V(z)dz-\int_L m_{xb}(z)\theta_{xb}(z)dz \tag{5.31}$$

5.4.9.2. Variation of Potential Energy

From Eq. (5.31), by performing integration by parts, and grouping like terms (Appendix A7), one obtains

$$\delta\pi_1=\int_L\left[-E_bA_bW_b''+c_1^2G_aA_aW_b-c_1^2G_aA_aW_p+c_1c_2G_aA_aV'+c_1c_3G_aA_a\theta_{xb}-q_z(z)\right]\delta W_bdz+$$

$$+\int_L\left[-E_pA_pW_p''-c_1^2G_aA_aW_b+c_1^2G_aA_aW_p-c_1c_2G_aA_aV'-c_1c_3G_aA_a\theta_{xb}\right]\delta W_pdz+$$

$$+\int_L\left[-c_1c_2G_aA_aW_b'+c_1c_2G_aA_aW_p'+\left(E_bI_{ssbf}+E_pI_{xxp}\right)V''''-\left(G_bA_{bw}+c_2^2G_aA_a\right)V''\right.$$

$$\left.+\left(G_bA_{bw}-c_2c_3G_aA_a\right)\theta_{xb}'-q_y(z)\right]\delta Vdz+\int_L\left[c_1c_3G_aA_aW_b-c_1c_3G_aA_aW_p+\left(c_2c_3G_aA_a-G_bA_{bw}\right)V'+\right.$$

$$\left.-E_bI_{xxb1}\theta_{xb}''+\left(G_bA_{bw}+c_3^2G_aA_a\right)\theta_{xb}-m_{xb}(z)\right]\delta\theta_{xb}dz+E_bA_bW_b'\delta W_b\Big|_0^L+E_bI_{ssbf}V''\delta V'\Big|_0^L$$

$$-E_bI_{ssbf}V'''\delta V\Big|_0^L+G_bA_{bw}V'\delta V\Big|_0^L-G_bA_{bw}\theta_{xb}\delta V\Big|_0^L+E_bI_{xxb1}\theta_{xb}'\delta\theta_{xb}\Big|_0^L+E_pA_pW_p'\delta W_p\Big|_0^L$$

$$+E_pI_{xxp}V''\delta V'\Big|_0^L-E_pI_{xxp}V'''\delta V\Big|_0^L++\left(c_1c_2G_aA_aW_b-c_1c_2G_aA_aW_p+c_2c_3G_aA_a\theta_{xb}\right)\delta V\Big|_0^L$$

$$+c_2^2G_aA_aV'\delta V\Big|_0^L+-N(z)\delta W_b\Big|_0^L-M_{x1}(z)\delta V'\Big|_0^L-Q_y(z)\delta V\Big|_0^L-M_{x2}(z)\delta\theta_{xb}\Big|_0^L \tag{5.32}$$

5.4.9.3. Equilibrium equations and boundary conditions

From Eq. (5.32), one obtains a set of four coupled equilibrium equations and its ten boundary conditions.

$$-E_bA_bW_b''+c_1^2G_aA_aW_b-c_1^2G_aA_aW_p+c_1c_2G_aA_aV'+c_1c_3G_aA_a\theta_{xb}=q_{zb}(z) \tag{5.33}$$

$$-c_1^2G_aA_aW_b-E_pA_pW_p''+c_1^2G_aA_aW_p-c_1c_2G_aA_aV'-c_1c_3G_aA_a\theta_{xb}=0 \tag{5.34}$$

$$-c_1c_2G_aA_aW_b'+c_1c_2G_aA_aW_p'+\left(E_bI_{ssbf}+E_pI_{xxp}\right)V''''-\left(G_bA_{bw}+c_2^2G_aA_a\right)V''+\left(G_bA_{bw}-c_2c_3G_aA_a\right)\theta_{xb}'=q_{yb}(z) \tag{5.35}$$

$$c_1c_3G_aA_aW_b - c_1c_3G_aA_aW_p + \left(c_2c_3G_aA_a - G_bA_{bw}\right)V' - E_bI_{xxb1}\theta''_{xb} + \left(G_bA_{bw} + c_3^2G_aA_a\right)\theta_{xb} = m_{xb}(z) \quad (5.36)$$

The corresponding boundary conditions are

$$-\left[E_bA_bW_b'(0) - N(0)\right]\delta W_b(0) = 0 \quad (5.37)$$

$$\left[E_bA_bW_b'(L) - N(L)\right]\delta W_b(L) = 0 \quad (5.38)$$

$$-E_pA_pW_p'(0)\delta W_p(0) = 0 \quad (5.39)$$

$$E_pA_pW_p'(L)\delta W_p(L) = 0 \quad (5.40)$$

$$\begin{aligned}-\Big[&c_1c_2G_aA_aW_b(0) - c_1c_2G_aA_aW_p(0) - \left(E_bI_{ssbf} + E_pI_{xxp}\right)V'''(0) + \\ &+\left(G_bA_{bw} + c_2^2G_aA_a\right)V'(0) + \left(c_2c_3G_aA_a - G_bA_{bw}\right)\theta_{xb}(0) - Q_y(0)\Big]\delta V(0) = 0\end{aligned} \quad (5.41)$$

$$\begin{aligned}\Big[&c_1c_2G_aA_aW_b(L) - c_1c_2G_aA_aW_p(L) - \left(E_bI_{ssbf} + E_pI_{xxp}\right)V'''(L) + \\ &+\left(G_bA_{bw} + c_2^2G_aA_a\right)V'(L) + \left(c_2c_3G_aA_a - G_bA_{bw}\right)\theta_{xb}(L) - Q_y(L)\Big]\delta V(L) = 0\end{aligned} \quad (5.42)$$

$$-\left[\left(E_bI_{ssbf} + E_pI_{xxp}\right)V''(0) - M_{x1}(0)\right]\delta V'(0) = 0 \quad (5.43)$$

$$\left[\left(E_bI_{ssbf} + E_pI_{xxp}\right)V''(L) - M_{x1}(L)\right]\delta V'(L) = 0 \quad (5.44)$$

$$-\left[E_bI_{xxb1}\theta'_{xb}(0) - M_{x2}(0)\right]\delta\theta_{xb}(0) = 0 \quad (5.45)$$

$$\left[E_bI_{xxb1}\theta'_{xb}(L) - M_{x2}(L)\right]\delta\theta_{xb}(L) = 0 \quad (5.46)$$

5.4.10. Lateral-Torsional Response

5.4.10.1. Potential Energy

From Eqs. 5.22-5.27, by omitting all longitudinal-transverse terms (Appendix A7), one obtains

$$\begin{aligned}\pi_2 = \int_L \Big[\Big[&(1/2)E_bI_{ssbw}U_b''^2 + G_bA_{bf}U_b'^2 - 2G_bA_{bf}\theta_{yb}U_b' + (1/2)E_bI_{yybf}\theta_{yb}'^{\,2} + G_bA_{bf}\theta_{yb}^2 + \\ &+(1/2)E_bI_{\omega\omega bl}\theta_z''^2 + (1/2)G_bJ_b\theta_z'^2 - \left(h_b^2/2\right)G_bA_{bf}\psi_b\theta_z' + (1/2)E_bI_{\omega\omega bg}\psi_b'^2 + \left(h_b^2/4\right)G_bA_{bf}\psi_b^{\,2} + \\ &+(1/2)G_pA_pU_p'^{\,2} - G_pA_p\theta_{yp}U_p' + (1/2)E_pI_{yyp}\theta_{yp}'^{\,2} + (1/2)G_pA_p\theta_{yp}^2 + (1/2)E_pI_{\omega\omega p}\theta_z''^2 + (1/2)G_pJ_p\theta_z'^{\,2} + \\ &+(1/2)G_aI_{yya}\left\langle\Delta_{a12}\right\rangle_{1\times4}^T\left[\widetilde{H_{a12}}\right]_{4\times4}\left\{\Delta_{a12}\right\}_{4\times1} + (1/2)G_aA_a\left\langle\Delta_{a2}\right\rangle_{1\times3}^T\left[\widetilde{H_{a2}}\right]_{3\times3}\left\{\Delta_{a2}\right\}_{3\times1}dz + \\ &+(1/24)G_aA_a\left\langle\Delta_{a3}\right\rangle_{1\times6}^T\left[\widetilde{H_{a3}}\right]_{6\times6}\left\{\Delta_{a3}\right\}_{6\times1}\Big]dz + \Big[Q_x(0)U_b(0) + M_{y1}(0)U_b'(0) + M_{y2}(0)\theta_{yb}(0) + \\ &+T(0)\theta_z(0) + B_1(0)\theta_z'(0) + B_2(0)\psi_b(0) - Q_x(L)U_b(L) - M_{y1}(L)U_b'(L) - M_{y2}(L)\theta_{yb}(L)\end{aligned}$$

$$
-T(L)\theta_z(L)-B_1(L)\theta_z'(L)-B_2(L)\psi_b(L)\Big]-\int_L q_{xb}(z)U_b(z)dz-\int_L m_{yb}(z)\theta_{yb}(z)dz-\int_L m_{zb}(z)\theta_z(z)dz
$$

$$
-\int_L b_b(z)\psi_b(z)dz \tag{5.47}
$$

5.4.10.2. Variation of Potential energy

From Eq.(5.47), by performing integration by parts, and grouping like terms (Appendix A7), one obtains

$$
\begin{aligned}
\delta\pi_2 &= \int_L \Big[E_b I_{ssbw} U_b'''' - 2G_b A_{bf} U_b'' + 2G_b A_{bf}\theta_{yb}' + c_1^2 G_a A_a U_b - c_1^2 G_a A_a U_p + c_1(c_2+c_3)G_a A_a \theta_z + \\
&-(1/12)G_a A_a\left(4U_b''+2U_p''-4\theta_{yb}'-2\theta_{yp}'+2c_4\theta_z''-2h_b\psi_b'\right)-q_{xb}(z)\Big]\delta U_b dz+\int_L\Big[-G_p A_p\left(U_p''-\theta_{yp}'\right)-c_1^2 G_a A_a U_b \\
&+c_1^2 G_a A_a U_p - c_1(c_2+c_3)G_a A_a\theta_z-(1/12)G_a A_a\left(2U_b''+4U_p''-2\theta_{yb}'-4\theta_{yp}'+c_5\theta_z''-h_b\psi_b'\right)\Big]\delta U_p dz+ \\
&+\int_L\Big[-E_b I_{yybf}\theta_{yb}''+2G_b A_{bf}\theta_{yb}-2G_b A_{bf}U_b'+c_1^2 G_a I_{yya}\theta_{yb}-c_1^2 G_a I_{yya}\theta_{yp}-c_1c_2 G_a I_{yya}\theta_z'+c_1c_3 G_a I_{yya}\psi_b \\
&+(1/12)G_a A_a\left(-4U_b'-2U_p'+4\theta_{yb}+2\theta_{yp}-2c_4\theta_z'+2h_b\psi_b\right)-m_{yb}(z)\Big]\delta\theta_{yb}dz+ \\
&+\int_L\Big[-E_p I_{yyp}\theta_{yp}''+G_p A_p\theta_{yp}-G_p A_p U_p'-c_1^2 G_a I_{yya}\theta_{yb}+c_1^2 G_a I_{yya}\theta_{yp}+c_1c_2 G_a I_{yya}\theta_z'-c_1c_3 G_a I_{yya}\psi_b+ \\
&+(1/12)G_a A_a\left(-2U_b'-4U_p'+2\theta_{yb}+4\theta_{yp}-c_5\theta_z'+h_b\psi_b\right)\Big]\delta\theta_{yp}dz+\int_L\Big\{E_b I_{\omega\omega bl}\theta_z''''-G_b J_b\theta_z''+\left(h_b^2/4\right)G_b A_{bf}\psi_b'+ \\
&+E_p I_{\omega\omega p}\theta_z''''-G_p J_p\theta_z''+c_1c_2 G_a I_{yya}\theta_{yb}'-c_1c_2 G_a I_{yya}\theta_{yp}'-c_2^2 G_a I_{yya}\theta_z''+c_2c_3 G_a I_{yya}\psi_b'+c_1(c_2+c_3)G_a A_a U_b \\
&-(c_2+c_3)G_a A_a\left[c_1 U_p-(c_2+c_3)\theta_z\right]-G_a A_a\left(2c_4 U_b''+c_5 U_p''-2c_4\theta_{yb}'-c_5\theta_{yp}'+c_6\theta_z''-c_4 h_b\psi_b'\right)/12-m_{zb}(z)\Big\}\delta\theta_z dz \\
&+\int_L\Big[-E_b I_{\omega\omega bg}\psi_b''+\left(h_b^2/2\right)G_b A_{bf}\psi_b-\left(h_b^2/4\right)G_b A_{bf}\theta_z'+c_1c_3 G_a I_{yya}\theta_{yb}-c_1c_3 G_a I_{yya}\theta_{yp}-c_2c_3 G_a I_{yya}\theta_z'+ \\
&+c_3^2 G_a I_{yya}\psi_b+(1/12)G_a A_a\left(-2h_b U_b'-h_b U_p'+2h_b\theta_{yb}+h_b\theta_{yp}-c_4 h_b\theta_z'+h_b^2\psi_b\right)-b_b(z)\Big]\delta\psi_b dz+\Big[-E_b I_{ssbw}U_b'''+ \\
&-2G_b A_{bf}\theta_{yb}+2G_b A_{bf}U_b'+(1/12)G_a A_a\left(4U_b'+2U_p'-4\theta_{yb}-2\theta_{yp}+2c_4\theta_z'-2h_b\psi_b\right)\Big]\delta U_b\Big|_0^L+E_b I_{ssbw}U_b''\delta U_b'\Big|_0^L \\
&+\Big[G_p A_p\left(U_p'-\theta_{yp}\right)+(1/12)G_a A_a\left(2U_b'+4U_p'-2\theta_{yb}-4\theta_{yp}+c_5\theta_z'-h_b\psi_b\right)\Big]\delta U_p\Big|_0^L+E_b I_{yybf}\theta_{yb}'\delta\theta_{yb}\Big|_0^L+ \\
&+E_p I_{yyp}\theta_{yp}'\delta\theta_{yp}\Big|_0^L+E_b I_{\omega\omega bl}\theta_z''\delta\theta_z'\Big|_0^L+E_p I_{\omega\omega p}\theta_z''\delta\theta_z'\Big|_0^L+\Big[-E_b I_{\omega\omega bl}\theta_z'''+G_b J_b\theta_z'-\left(h_b^2/4\right)G_b A_{bf}\psi_b-E_p I_{\omega\omega p}\theta'''+ \\
&+G_p J_p\theta_z'-c_1c_2 G_a I_{yya}\theta_{yb}+c_1c_2 G_a I_{yya}\theta_{yp}+c_2^2 G_a I_{yya}\theta_z'-c_2c_3 G_a I_{yya}\psi_b+
\end{aligned}
$$

$$+(1/12)G_aA_a\left(2c_4U_b'+c_5U_p'-2c_4\theta_{yb}-c_5\theta_{yp}+c_6\theta_z'-c_4h_b\psi_b\right)\Big]\delta\theta_z\Big|_0^L+E_bI_{\omega\omega bg}\psi_b'\delta\psi_b\Big|_0^L+\Big[Q_x(0)\delta U_b(0)$$

$$+M_{y1}(0)\delta U_b'(0)+M_{y2}(0)\delta\theta_{yb}(0)+T(0)\delta\theta(0)+B_1(0)\delta\theta'(0)+B_2(0)\delta\psi_b(0)-Q_x(L)\delta U_b(L) \quad (5.48)$$

$$-M_{y1}(L)\delta U_b'(L)-M_{y2}(L)\delta\theta_{yb}(L)-T(L)\delta\theta(L)-B_1(L)\delta\theta'(L)-B_2(L)\delta\psi_b(L)\Big]$$

5.4.10.3. Equilibrium equations and boundary conditions

From Eq. (5.48), one obtains a set of coupled field equations and its corresponding boundary conditions. The field equations describe the lateral-torsional behavior of the system, and take the form

$$\begin{aligned}&E_bI_{ssbw}U_b''''-\left(2G_bA_{bf}+\frac{1}{3}G_aA_a\right)U_b''+c_1^2G_aA_aU_b-\frac{1}{6}G_aA_aU_p''-c_1^2G_aA_aU_p+\left(2G_bA_{bf}+\frac{1}{3}G_aA_a\right)\theta_{yb}'\\&+\frac{1}{6}G_aA_a\theta_{yp}'-\frac{1}{6}c_4G_aA_a\theta_z''+c_1(c_2+c_3)G_aA_a\theta_z+\frac{1}{6}h_bG_aA_a\psi_b'=q_{xb}(z)\end{aligned} \quad (5.49)$$

$$\begin{aligned}&-\frac{1}{6}G_aA_aU_b''-c_1^2G_aA_aU_b-\left(G_pA_p+\frac{1}{3}G_aA_a\right)U_p''+c_1^2G_aA_aU_p+\frac{1}{6}G_aA_a\theta_{yb}'\\&+\left(G_pA_p+\frac{1}{3}G_aA_a\right)\theta_{yp}'-\frac{1}{12}c_5G_aA_a\theta_z''-c_1(c_2+c_3)G_aA_a\theta_z+\frac{1}{12}h_bG_aA_a\psi_b'=0\end{aligned} \quad (5.50)$$

$$\begin{aligned}&-\left(2G_bA_{bf}+\frac{1}{3}G_aA_a\right)U_b'-\frac{1}{6}G_aA_aU_p'-E_bI_{yybf}\theta_{yb}''+\left(2G_bA_{bf}+c_1^2G_aI_{yya}+\frac{1}{3}G_aA_a\right)\theta_{by}\\&+\left(-c_1^2G_aI_{yya}+\frac{1}{6}G_aA_a\right)\theta_{yp}-\left(c_1c_2G_aI_{yya}+\frac{1}{6}c_4G_aA_a\right)\theta_z'+\left(c_1c_3G_aI_{yya}+\frac{1}{6}h_bG_aA_a\right)\psi_b=m_{yb}(z)\end{aligned} \quad (5.51)$$

$$\begin{aligned}&-\frac{1}{6}G_aA_aU_b'-\left(G_pA_p+\frac{1}{3}G_aA_a\right)U_p'+\left(-c_1^2G_aI_{yya}+\frac{1}{6}G_aA_a\right)\theta_{yb}-E_pI_{yyp}\theta_{yp}''\\&+\left(G_pA_p+c_1^2G_aI_{yya}+\frac{1}{3}G_aA_a\right)\theta_{yp}+\left(c_1c_2G_aI_{yya}-\frac{1}{12}c_5G_aA_a\right)\theta_z'+\left(-c_1c_3G_aI_{yya}+\frac{1}{12}h_bG_aA_a\right)\psi_b=0\end{aligned} \quad (5.52)$$

$$\begin{aligned}&-\frac{1}{6}c_4G_aA_aU_b''+c_1(c_2+c_3)G_aA_aU_b-\frac{1}{12}c_5G_aA_aU_p''-c_1(c_2+c_3)G_aA_aU_p+\left(c_1c_2G_aI_{yya}+\frac{1}{6}c_4G_aA_a\right)\theta_{yb}'\\&+\left(-c_1c_2G_aI_{yya}+\frac{1}{12}c_5G_aA_a\right)\theta_{yp}'+\left(E_bI_{\omega\omega bl}+E_pI_{\omega\omega p}\right)\theta_z''''-\left(G_bJ_b+G_pJ_p+c_2^2G_aI_{yya}+\frac{1}{12}c_6G_aA_a\right)\theta_z''\\&+(c_2+c_3)^2G_aA_a\theta_z+\left[\frac{h_b^2}{2}G_bA_{bf}+c_2c_3G_aI_{yya}+\frac{1}{12}c_4h_bG_aA_a\right]\psi_b'=m_{zb}(z)\end{aligned} \quad (5.53)$$

$$-\frac{1}{6}h_bG_aA_aU_b'-\frac{1}{12}h_bG_aA_aU_p'+\left(c_1c_3G_aI_{yya}+\frac{1}{6}h_bG_aA_a\right)\theta_{yb}+\left(-c_1c_3G_aI_{yya}+\frac{1}{12}h_bG_aA_a\right)\theta_{yp}$$

$$-\left(\frac{h_b^2}{2}G_bA_{bf}+c_2c_3G_aI_{yya}+\frac{1}{12}c_4h_bG_aA_a\right)\theta_z'-E_bI_{\omega\omega bg}\psi_b''+\left[\frac{h_b^2}{2}G_bA_{bf}+c_3^2G_aI_{yya}+\frac{1}{12}h_b^2G_aA_a\right]\psi_b=b_b(z) \tag{5.54}$$

The corresponding boundary conditions are

$$-\Big\{-E_bI_{ssbw}U_b'''(0)+2G_bA_{bf}U_b'(0)-2G_bA_{bf}\theta_{yb}(0)+$$
$$+\frac{1}{12}G_aA_a\left[4U_b'(0)+2U_p'(0)-4\theta_{yb}(0)-2\theta_{yp}(0)+2c_4\theta_z'(0)-2h_b\psi_b(0)\right]-Q_x(0)\Big\}\delta U_b(0)=0 \tag{5.55}$$

$$\Big\{-E_bI_{ssbw}U_b'''(L)+2G_bA_{bf}U_b'(L)-2G_bA_{bf}\theta_{yb}(L)+$$
$$+\frac{1}{12}G_aA_a\left[4U_b'(L)+2U_p'(L)-4\theta_{yb}(L)-2\theta_{yp}(L)+2c_4\theta_z'(L)-2h_b\psi_b(L)\right]-Q_x(L)\Big\}\delta U_b(L)=0 \tag{5.56}$$

$$-\left[E_bI_{ssbw}U_b''(0)-M_{y1}(0)\right]\delta U_b'(0)=0 \tag{5.57}$$

$$\left[E_bI_{ssbw}U_b''(L)-M_{y1}(L)\right]\delta U_b'(L)=0 \tag{5.58}$$

$$-\Big\{G_pA_pU_p'(0)-G_pA_p\theta_{yp}(0)+$$
$$\frac{1}{12}G_aA_a\left(2U_b'(0)+4U_p'(0)-2\theta_{yb}(0)-4\theta_{yp}(0)+c_5\theta_z'(0)-h_b\psi_b(0)\right)\Big\}\delta U_p(0)=0 \tag{5.59}$$

$$\Big\{G_pA_pU_p'(L)-G_pA_p\theta_{yp}(L)+$$
$$\frac{1}{12}G_aA_a\left(2U_b'(L)+4U_p'(L)-2\theta_{yb}(L)-4\theta_{yp}(L)+c_5\theta_z'(L)-h_b\psi_b(L)\right)\Big\}\delta U_p(L)=0 \tag{5.60}$$

$$-\left[E_bI_{yybf}\theta_{yb}'(0)-M_{y2}(0)\right]\delta\theta_{yb}(0)=0 \tag{5.61}$$

$$\left[E_bI_{yybf}\theta_{yb}'(L)-M_{y2}(L)\right]\delta\theta_{yb}(L)=0 \tag{5.62}$$

$$-E_pI_{yyp}\theta_{yp}'(0)\delta\theta_{yp}(0)=0 \tag{5.63}$$

$$E_pI_{yyp}\theta_{yp}'(L)\delta\theta_{yp}(L)=0 \tag{5.64}$$

$$-\Bigg\{-E_bI_{\omega\omega bl}\theta_z'''(0)+G_bJ_b\theta_z'(0)-\frac{h_b^2}{4}G_bA_{bf}\psi_b(0)-E_pI_{\omega\omega p}\theta_z'''(0)+G_pJ_p\theta_z'(0)+$$
$$+c_2^2G_aI_{yya}\theta_z'(0)-c_1c_2G_aI_{yya}\theta_{yb}(0)+c_1c_2G_aI_{yya}\theta_{yp}(0)-c_2c_3G_aI_{yya}\psi_b(0)+$$
$$+\frac{G_aA_a}{12}\left[2c_4U_b'(0)+c_5U_p'(0)+c_6\theta_z'(0)-2c_4\theta_{yb}(0)-c_5\theta_{yp}(0)-c_4h_b\psi_b(0)\right]-T(0)\Bigg\}\delta\theta_z(0)=0 \tag{5.65}$$

$$\begin{aligned}&\Big\{-E_b I_{\omega\omega bl}\theta_z'''(L)+G_bJ_b\theta_z'(L)-\left(h_b^2/4\right)G_bA_{bf}\psi_b(L)-E_pI_{\omega\omega p}\theta_z'''(L)+G_pJ_p\theta_z'(L)+\\&+c_2^2G_aI_{yya}\theta_z'(L)-c_1c_2G_aI_{yya}\theta_{yb}(L)+c_1c_2G_aI_{yya}\theta_{yp}(L)-c_2c_3G_aI_{yya}\psi_b(L)+\\&+\frac{G_aA_a}{12}\left[2c_4U_b'(L)+c_5U_p'(L)+c_6\theta_z'(L)-2c_4\theta_{yb}(L)-c_5\theta_{yp}(L)-c_4h_b\psi_b(L)\right]-T(L)\Big\}\delta\theta_z(L)=0\end{aligned} \quad (5.66)$$

$$-\left[\left(E_bI_{\omega\omega bl}+E_pI_{\omega\omega p}\right)\theta_z''(0)-B_1(0)\right]\delta\theta_z'(0)=0 \quad (5.67)$$

$$\left[\left(E_bI_{\omega\omega bl}+E_pI_{\omega\omega p}\right)\theta_z''(L)-B_1(L)\right]\delta\theta_z'(L)=0 \quad (5.68)$$

$$-\left[E_bI_{\omega\omega bg}\psi_b'(0)-B_2(0)\right]\delta\psi_b(0)=0 \quad (5.69)$$

$$\left[E_bI_{\omega\omega bg}\psi_b'(L)-B_2(L)\right]\delta\psi_b(L)=0 \quad (5.70)$$

5.4.11. Comparison between non-shear deformation and shear deformation theories

By comparing to the displacement fields and stress resultants expressed in non-shear deformation theory, one can see that the shear deformable theory has two types of moments. One is conjugate to the slope of the displacements and the other one is conjugate to the angle of rotations as shown in the Table 5.1.

Table 5.1. Comparison of stress resultants and conjugate generalized displacements obtained from non-shear deformation and shear deformation theories

Response	Non-shear Deformable Theory		Shear Deformable Theory	
	Stress resultant	Conjugate generalized displacement	Stress resultant	Conjugate generalized displacement
Longitudinal-Transverse	N	W	N	W
	Q_y	V	Q_y	V
	M_x	V'	M_{x1}	V'
			M_{x2}	θ_{xb}
Lateral-Torsional	Q_x	U_b	Q_x	U_b
	M_y	U_b'	M_{y1}	U_b'
			M_{y2}	θ_{yb}
	T	θ_z	T	θ_z
	B	θ_z'	B_1	θ_z'
			B_2	ψ_b

5.5. Summary

The theory developed in this chapter accounts for transverse shear deformation effect in composite beam analysis. The formulation covers the derivation of two longitudinal-transverse response and lateral-torsional responses (equilibrium equation systems and their boundary conditions). A comparison of the number of field variables, governing differential equations and the boundary conditions is summarized in Table 5.2.

Table 5.2. Comparsion of number of field variables and boundary conditions

Theory	Response	Number of field variables and field equations	Number of boundary conditions
Non-shear deformable	Longitudinal Transverse	3 (W_b, W_p, V)	8
	Lateral-Torsional	3 (U_b, U_p, θ_z)	12
	General	6 ($W_b, W_p, V, U_b, U_p, \theta_z$)	20
Shear deformable	Longitudinal Transverse	4 (W_b, W_p, V, θ_{xb})	10
	Lateral-Torsional	6 ($U_b, \theta_{yb}, U_p, \theta_{yp}, \theta_z, \psi_b$)	16
	General	10 ($W_b, W_p, V, \theta_{xb}, U_b, \theta_{yb}, U_p, \theta_{yp}, \theta_z, \psi_b$)	26

Given the large number of variables involved in the present theory, a closed form solution, while in principle attainable, is associated with two difficulties. For the lateral-torsional response, for example, the first difficulty is to solve the characteristic equation which has 16 roots. Since the system involves six field variables, each variable will then consist of the sum of 16 functions multiplied by a constant. This results in a total of 96 constants. Of these 96 constants, 80 are to be expressed in terms of the remaining 16 constants by back-substitution in the original system of equilibrium equations, resulting in lengthy algebraic manipulations. The second difficulty is to determine 16 integration constants based on 16 boundary conditions. To avoid these difficulties, two numerical methods will be developed. The first technique which solves the problem by using the Finite Difference Method presented in Chapter 6 and the second technique is the Finite Element Method formulation presented in Chapter 7.

CHAPTER 6. SHEAR DEFORMABLE THEORY - FINITE DIFFERENCE SOLUTION

The governing differential equations and associated boundary conditions developed in Chapter 5 are solved in the present chapter using the finite difference technique.

6.1. Background for the Finite Difference

The objective of finite difference technique is to transform the differential equations and boundary conditions into a set of algebraic equations. This is achieved by discretizing the domain into points, commonly taken equidistantly. A field variable $f(z)$ of a one dimensional domain $0 \le z \le L$ is subdivided into n segments, equidistantly spaced at a distance $\Delta = L/n$. One has $i = 0,1...n$ points. The value of a field variable $f(z)$ at a given point $z = z_i$ is denoted f_i .

The derivatives of a function $f(z)$ at a given point $z = z_i$ can be expressed into algebraic expressions in terms of the values of function f at the neighboring points $..., f_{i-2}, f_{i-1}, f_i, f_{i+1}, f_{i+2},...$. According to the central finite difference approximation (e.g., LeVeque (2007)), the first four derivatives of function f can be approximated as

$$\begin{aligned}
(f')_i &\approx \frac{f_{i+1} - f_{i-1}}{2\Delta}; \\
(f'')_i &\approx \frac{f_{i+1} - 2f_i + f_{i-1}}{\Delta^2}; \\
(f''')_i &\approx \frac{f_{i+2} - 2f_{i+1} + 2f_{i-1} - f_{i-2}}{2\Delta^3}; \\
(f'''')_i &\approx \frac{f_{i+2} - 4f_{i+1} + 6f_i - 4f_{i-1} + f_{i-2}}{\Delta^4}
\end{aligned} \tag{6.1}$$

6.2. Finite Difference Discretization for Longitudinal-Transversal Response

6.2.1. General

As seen in Chapter 5, the longitudinal-transverse response is described by four field variables W_b, W_p, V, θ_{bx}. Thus at a given point i $(i = 1,...,n+1)$, there are four unknowns $W_{bi}, W_{pi}, V_i, \theta_{bxi}$ (Fig. 6.1). Also, at the same point, one can write the discretized form for each of the equilibrium equations (Section 6.2.2), resulting into $4(n+1)$ field equations.

When expressing the field equations at the end nodes $i=1, i=n+1$, additional unknown values are introduced outside the domain $i=0,$ and $i=n+2$ for variables W_b, W_p, θ_{bx} . This is the case since the field equations contain derivatives up to the second order for variables W_b, W_p, θ_{bx}. In contrast, since for derivatives up to the fourth order for variable V appear in the field equations, four additional nodes $i=-1, i=0, i=n+1, i=n+2$ emerge in the discretized field equations. As seen in Fig. 6.1, the total number of unknowns becomes $4(n+1)+10$ unknowns. The remaining 10 equations needed to solve the system will come from writing the discretized form of the boundary conditions. These are developed in Section 6.2.3.

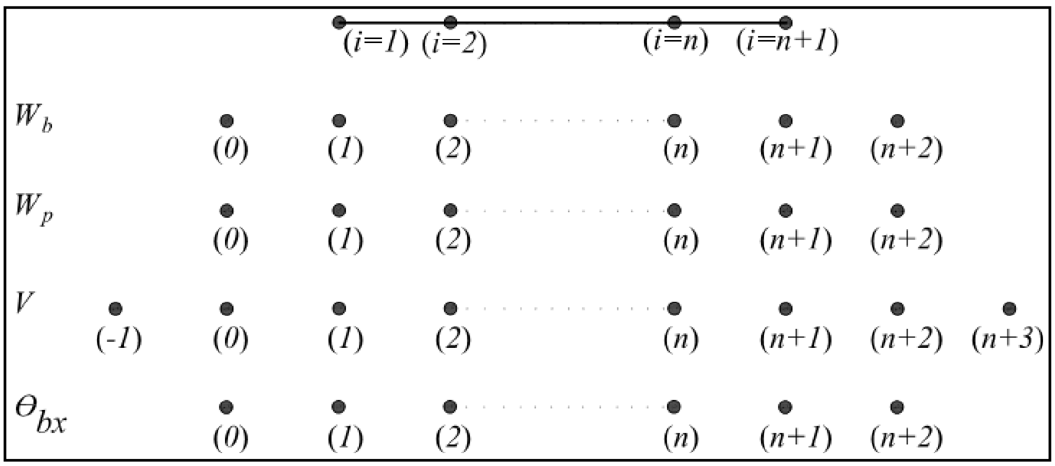

Figure 6.1. n subdivisions-discretized displacements

6.2.2. Discretized Equilibrium Equations

The finite difference discretization for Eqs. 5.33-5.36 at Point $i\,(i=1,2,\ldots,n+1)$ are

$$
\begin{aligned}
&-\left(\frac{E_b A_b}{\Delta^2}\right) W_{b(i-1)} + \left(\frac{2E_b A_b}{\Delta^2} + c_1^2 G_a A_a\right) W_{b(i)} - \left(\frac{E_b A_b}{\Delta^2}\right) W_{b(i+1)} - \left(c_1^2 G_a A_a\right) W_{p(i)} \\
&-\left(\frac{c_1 c_2 G_a A_a}{2\Delta}\right) V_{(i-1)} + \left(\frac{c_1 c_2 G_a A_a}{2\Delta}\right) V_{(i+1)} + \left(c_1 c_3 G_a A_a\right) \theta_{bx(i)} = q_{z(i)}
\end{aligned} \tag{6.2}
$$

$$
\begin{aligned}
&-\left(c_1^2 G_a A_a\right) W_{b(i)} - \left(\frac{E_p A_p}{\Delta^2}\right) W_{p(i-1)} + \left(c_1^2 G_a A_a + 2\frac{E_p A_p}{\Delta^2}\right) W_{p(i)} - \left(\frac{E_p A_p}{\Delta^2}\right) W_{p(i+1)} \\
&+\left(\frac{c_1 c_2 G_a A_a}{2\Delta}\right) V_{(i-1)} - \left(\frac{c_1 c_2 G_a A_a}{2\Delta}\right) V_{(i+1)} - \left(c_1 c_3 G_a A_a\right) \theta_{bx(i)} = 0
\end{aligned} \tag{6.3}
$$

$$\left(\frac{c_1c_2G_aA_a}{2\Delta}\right)W_{b(i-1)}-\left(\frac{c_1c_2G_aA_a}{2\Delta}\right)W_{b(i+1)}-\left(\frac{c_1c_2G_aA_a}{2\Delta}\right)W_{p(i-1)}+\left(\frac{c_1c_2G_aA_a}{2\Delta}\right)W_{p(i+1)}$$
$$+\left(\frac{E_bI_{ssbf}+E_pI_{xxp}}{\Delta^4}\right)V_{(i-2)}-\left(4\frac{E_bI_{ssbf}+E_pI_{xxp}}{\Delta^4}+\frac{G_bA_{bw}+c_2^2G_aA_a}{\Delta^2}\right)V_{(i-1)}$$
$$+\left(6\frac{E_bI_{ssbf}+E_pI_{xxp}}{\Delta^4}+2\frac{G_bA_{bw}+c_2^2G_aA_a}{\Delta^2}\right)V_{(i)}-\left(4\frac{E_bI_{ssbf}+E_pI_{xxp}}{\Delta^4}+\frac{G_bA_{bw}+c_2^2G_aA_a}{\Delta^2}\right)V_{(i+1)} \tag{6.4}$$
$$+\left(\frac{E_bI_{ssbf}+E_pI_{xxp}}{\Delta^4}\right)V_{(i+2)}-\left(\frac{G_bA_{bw}-c_2c_3G_aA_a}{2\Delta}\right)\theta_{xb(i-1)}+\left(\frac{G_bA_{bw}-c_2c_3G_aA_a}{2\Delta}\right)\theta_{xb(i+1)}=q_{y(i)}$$

$$\left(c_1c_3G_aA_a\right)W_{b(i)}-\left(c_1c_3G_aA_a\right)W_{p(i)}-\left(\frac{c_2c_3G_aA_a-G_bA_{bw}}{2\Delta}\right)V_{(i-1)}+\left(\frac{c_2c_3G_aA_a-G_bA_{bw}}{2\Delta}\right)V_{(i+1)}$$
$$-\left(\frac{E_bI_{xxb1}}{\Delta^2}\right)\theta_{xb(i-1)}+\left(2\frac{E_bI_{xxb1}}{\Delta^2}+G_bA_{bw}+c_3^2G_aA_a\right)\theta_{xb(i)}-\left(\frac{E_bI_{xxb1}}{\Delta^2}\right)\theta_{xb(i+1)}=m_{xb(i)} \tag{6.5}$$

6.2.3. Discretized Boundary Conditions

Ten finite difference discretizations for Eqs. 5.37-5.46 in Chapter 5 are

$$\left[-\left(\frac{E_bA_b}{2\Delta}\right)W_{b(0)}+\left(\frac{E_bA_b}{2\Delta}\right)W_{b(2)}-N_{(1)}\right]\delta W_{b(1)}=0 \tag{6.6}$$

$$\left[-\left(\frac{E_bA_b}{2\Delta}\right)W_{b(n)}+\left(\frac{E_bA_b}{2\Delta}\right)W_{b(n+2)}-N_{(n+1)}\right]\delta W_{b(n+1)}=0 \tag{6.7}$$

$$\frac{E_pA_p}{2\Delta}\left[-W_{p(0)}+W_{p(2)}\right]\delta W_{p(1)}=0 \tag{6.8}$$

$$\frac{E_pA_p}{2\Delta}\left[-W_{p(n)}+W_{p(n+2)}\right]\delta W_{p(n+1)}=0 \tag{6.9}$$

$$\Bigg[\left(c_1c_2G_aA_a\right)W_{b(1)}-\left(c_1c_2G_aA_a\right)W_{p(1)}+\left(\frac{E_bI_{ssbf}+E_pI_{xxp}}{2\Delta^3}\right)V_{(-1)}+$$
$$-\left(\frac{E_bI_{ssbf}+E_pI_{xxp}}{\Delta^3}+\frac{G_bA_{bw}+c_2^2G_aA_a}{2\Delta}\right)V_{(0)}+\left(\frac{E_bI_{ssbf}+E_pI_{xxp}}{\Delta^3}+\frac{G_bA_{bw}+c_2^2G_aA_a}{2\Delta}\right)V_{(2)}+ \tag{6.10}$$
$$-\left(\frac{E_bI_{ssbf}+E_pI_{xxp}}{2\Delta^3}\right)V_{(3)}+\left(c_2c_3G_aA_a-G_bA_{bw}\right)\theta_{bx(1)}-Q_{y(1)}\Bigg]\delta V_{(1)}=0$$

$$\left[(c_1 c_2 G_a A_a) W_{b(n+1)} - (c_1 c_2 G_a A_a) W_{p(n+1)} + \left(\frac{E_b I_{ssbf} + E_p I_{xxp}}{2\Delta^3} \right) V_{(n-1)} + \right.$$

$$- \left(\frac{E_b I_{ssbf} + E_p I_{xxp}}{\Delta^3} + \frac{G_b A_{bw} + c_2^2 G_a A_a}{2\Delta} \right) V_{(n)} + \left(\frac{E_b I_{ssbf} + E_p I_{xxp}}{\Delta^3} + \frac{G_b A_{bw} + c_2^2 G_a A_a}{2\Delta} \right) V_{(n+2)} + \quad (6.11)$$

$$\left. - \left(\frac{E_b I_{ssbf} + E_p I_{xxp}}{2\Delta^3} \right) V_{(n+3)} + (c_2 c_3 G_a A_a - G_b A_{bw}) \theta_{bx(n+1)} - Q_{y(n+1)} \right] \delta V_{(n+1)} = 0$$

$$\left[\left(\frac{E_b I_{ssbf} + E_p I_{xxp}}{\Delta^2} \right) \left[V_{(0)} - 2V_{(1)} + V_{(2)} \right] - M_{x1(1)} \right] \delta \frac{\left[-V_{(0)} + V_{(2)} \right]}{2\Delta} = 0 \quad (6.12)$$

$$\left[\left(\frac{E_b I_{ssbf} + E_p I_{xxp}}{\Delta^2} \right) \left[V_{(n)} - 2V_{(n+1)} + V_{(n+2)} \right] - M_{x1(n+1)} \right] \delta \frac{\left[-V_{(n)} + V_{(n+2)} \right]}{2\Delta} = 0 \quad (6.13)$$

$$\left[\frac{E_b I_{xxb1}}{2\Delta} \left(-\theta_{xb(0)} + \theta_{xb(2)} \right) - M_{x2(1)} \right] \delta \theta_{xb(1)} = 0 \quad (6.14)$$

$$\left[\frac{E_b I_{xxb1}}{2\Delta} \left(-\theta_{xb(n)} + \theta_{xb(n+2)} \right) - M_{x2(n+1)} \right] \delta \theta_{xb(n+1)} = 0 \quad (6.15)$$

Each of the four equations from (6.2) to (6.5) is expressed for $i = 1, 2, ..., n+1$. Therefore, there are $4(n+1)$ equations of unknown displacement values established. Also, from 10 boundary conditions, 10 discretized equations are established from Eqs. (6.6) to (6.15). In total, $4(n+1)+10$ independent discretized equations are written to solve for $4(n+1)+10$ unknown displacement values.

6.2.4. Finite Difference Expressions of Strains and Stresses

6.2.4.1. Wide Flange Beam

From the finite difference formula in Eq. (6.1), by substituting into displacement fields expressed in section 5.4.6.1 in Chapter 5, the strains within the wide flange beam are obtained as

$$\begin{aligned} \varepsilon_{zb(i)} = & \left[-\frac{1}{2\Delta} W_{b(i-1)} + \frac{1}{2\Delta} W_{b(i+1)} \right] + \left[\frac{1}{\Delta^2} V_{(i-1)} - \frac{2}{\Delta^2} V_{(i)} + \frac{1}{\Delta^2} V_{(i+1)} \right] n_b \cos\alpha(s_b) \\ & - \left[-\frac{1}{2\Delta} \theta_{xb(i-1)} + \frac{1}{2\Delta} \theta_{xb(i+1)} \right] y(s_b) \end{aligned} \quad (6.16)$$

and

$$\gamma_{szb(i)} = \left[-\frac{1}{2\Delta} V_{(i-1)} + \frac{1}{2\Delta} V_{(i+1)} - \theta_{xb(i)} \right] \sin \alpha (s_b) \tag{6.17}$$

The expressions for the corresponding stress fields are

$$\sigma_{zb(i)} = E_b \varepsilon_{zb(i)}, \tau_{szb(i)} = G_b \gamma_{szb(i)} \tag{6.18}$$

6.2.4.2. GFRP Plate

Also, for the GFRP plate

$$\varepsilon_{zp(i)} = \left[-\frac{1}{2\Delta} W_{p(i-1)} + \frac{1}{2\Delta} W_{p(i+1)} \right] + \left[\frac{1}{\Delta^2} V_{(i-1)} - \frac{2}{\Delta^2} V_{(i)} + \frac{1}{\Delta^2} V_{(i+1)} \right] n_p \tag{6.19}$$

$$\gamma_{szp(i)} = 0 \tag{6.20}$$

and the longitudinal normal stress is given by

$$\sigma_{zp(i)} = E_p \varepsilon_{zp(i)} \tag{6.21}$$

6.2.4.3. Adhesive Layer

From finite difference formula in Eq. (6.1), by substituting into displacement fields expressed in section 5.4.6.3, the finite difference formulations for strains within adhesive layer are obtained as

$$\begin{aligned} &\gamma_{zna(i)} = -c_1 W_{b(i)} + c_1 W_{p(i)} - c_2 \left[-\frac{1}{2\Delta} V_{(i-1)} + \frac{1}{2\Delta} V_{(i+1)} \right] - c_3 \theta_{xb(i)} \\ &\gamma_{sna(i)} = \gamma_{sza(i)} = 0 \end{aligned} \tag{6.22}$$

The expression for the corresponding stress fields is

$$\tau_{zna(i)} = G_a \gamma_{zna(i)} \tag{6.23}$$

6.3. Finite Difference Discretization for Lateral-Torsional Response

6.3.1. General

As seen in Fig. 6.3, when the number of subdivisions is n, each one of the displacement fields $U_p, \theta_{yb}, \theta_{yp}, \psi_b$ is discretized into $(n+1)+2$ unknown values while each one of the displacement fields U_b, θ_z is discretized into $(n+1)+4$ unknown values. In total, there are $6(n+1)+16$ unknown discretized displacement values. To obtain the unknown values, $6(n+1)+16$ independent equations should be established based on discretizing available differential equilibrium equations and their boundary conditions.

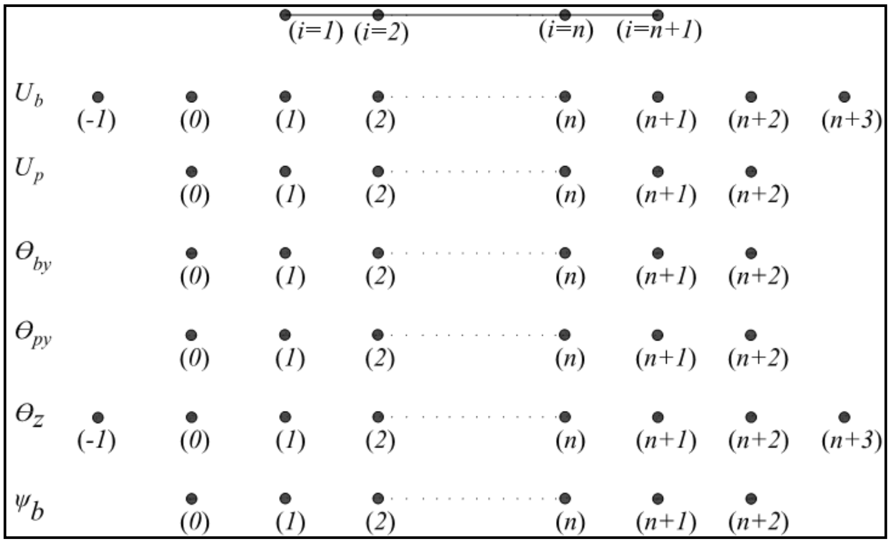

Figure 6.2. n -subdivisions- Discretized displacements

6.3.2. Discretized Equilibrium Equations

The finite difference discretization for Eqs. 5.49-5.54 at Point i ($i=1,2,...,n+1$) are

$$
\begin{aligned}
&\left(\frac{E_b I_{ssbw}}{\Delta^4}\right)U_{b(i-2)} - \left(\frac{4E_b I_{ssbw}}{\Delta^4} + \frac{2G_b A_{bf} + G_a A_a/3}{\Delta^2}\right)U_{b(i-1)} \\
&+\left(\frac{6E_b I_{ssbw}}{\Delta^4} + 2\frac{2G_b A_{bf} + G_a A_a/3}{\Delta^2} + c_1^2 G_a A_a\right)U_{b(i)} \\
&-\left(\frac{4E_b I_{ssbw}}{\Delta^4} + \frac{2G_b A_{bf} + G_a A_a/3}{\Delta^2}\right)U_{b(i+1)} + \left(\frac{E_b I_{ssbw}}{\Delta^4}\right)U_{b(i+2)} - \left(\frac{G_a A_a}{6\Delta^2}\right)U_{p(i-1)} + \left(2\frac{G_a A_a}{6\Delta^2} - c_1^2 G_a A_a\right)U_{p(i)} \\
&-\left(\frac{G_a A_a}{6\Delta^2}\right)U_{p(i+1)} - \left(\frac{2G_b A_{bf} + G_a A_a/3}{2\Delta}\right)\theta_{yb(i-1)} + \left(\frac{2G_b A_{bf} + G_a A_a/3}{2\Delta}\right)\theta_{yb(i+1)} - \left(\frac{G_a A_a}{12\Delta}\right)\theta_{yp(i-1)} \\
&+\left(\frac{G_a A_a}{12\Delta}\right)\theta_{yp(i+1)} - \left(\frac{c_4 G_a A_a}{6\Delta^2}\right)\theta_{z(i-1)} + \left[\frac{c_4 G_a A_a}{3\Delta^2} + c_1\left(c_2 + c_3\right)G_a A_a\right]\theta_{z(i)} - \left(\frac{c_4 G_a A_a}{6\Delta^2}\right)\theta_{z(i+1)} \\
&-\left(\frac{h_b G_a A_a}{12\Delta}\right)\psi_{b(i-1)} + \left(\frac{h_b G_a A_a}{12\Delta}\right)\psi_{b(i+1)} = q_{x(i)}
\end{aligned}
\tag{6.24}
$$

$$-\left(\frac{G_aA_a}{6\Delta^2}\right)U_{b(i-1)}+\left(\frac{G_aA_a}{3\Delta^2}-c_1^2G_aA_a\right)U_{b(i)}-\left(\frac{G_aA_a}{6\Delta^2}\right)U_{b(i+1)}-\left(\frac{G_pA_p+G_aA_a/3}{\Delta^2}\right)U_{p(i-1)}$$

$$+\left(2\frac{G_pA_p+G_aA_a/3}{\Delta^2}+c_1^2G_aA_a\right)U_{p(i)}-\left(\frac{G_pA_p+G_aA_a/3}{\Delta^2}\right)U_{p(i+1)}-\left(\frac{G_aA_a}{12\Delta}\right)\theta_{yb(i-1)}+\left(\frac{G_aA_a}{12\Delta}\right)\theta_{yb(i+1)}$$

$$-\left(\frac{G_pA_p+G_aA_a/3}{2\Delta}\right)\theta_{yp(i-1)}+\left(\frac{G_pA_p+G_aA_a/3}{2\Delta}\right)\theta_{yp(i+1)}-\left(\frac{c_5G_aA_a}{12\Delta^2}\right)\theta_{z(i-1)}$$

$$+\left[\frac{c_5G_aA_a}{6\Delta^2}-c_1\left(c_2+c_3\right)G_aA_a\right]\theta_{z(i)}-\left(\frac{c_5G_aA_a}{12\Delta^2}\right)\theta_{z(i+1)}-\left(\frac{h_bG_aA_a}{24\Delta}\right)\psi_{b(i-1)}+\left(\frac{h_bG_aA_a}{24\Delta}\right)\psi_{b(i+1)}=0 \tag{6.25}$$

$$\begin{aligned}
&\left(\frac{2G_bA_{bf}+G_aA_a/3}{2\Delta}\right)U_{b(i-1)}-\left(\frac{2G_bA_{bf}+G_aA_a/3}{2\Delta}\right)U_{b(i+1)}+\left(\frac{G_aA_a}{12\Delta}\right)U_{p(i-1)}\\
&-\left(\frac{G_aA_a}{12\Delta}\right)U_{p(i+1)}-\left(\frac{E_bI_{yybf}}{\Delta^2}\right)\theta_{yb(i-1)}+\left(2\frac{E_bI_{yybf}}{\Delta^2}+2G_bA_{bf}+c_1^2G_aI_{yya}+\frac{1}{3}G_aA_a\right)\theta_{yb(i)}\\
&-\left(\frac{E_bI_{yybf}}{\Delta^2}\right)\theta_{yb(i+1)}+\left(-c_1^2G_aI_{yya}+\frac{1}{6}G_aA_a\right)\theta_{yp(i)}+\left(\frac{c_1c_2G_aI_{yya}+c_4G_aA_a/6}{2\Delta}\right)\theta_{z(i-1)}\\
&-\left(\frac{c_1c_2G_aI_{yya}+c_4G_aA_a/6}{2\Delta}\right)\theta_{z(i+1)}+\left(c_1c_3G_aI_{yya}+\frac{1}{6}h_bG_aA_a\right)\psi_{b(i)}=m_{yb(i)}
\end{aligned} \tag{6.26}$$

$$\begin{aligned}
&\left(\frac{G_aA_a}{12\Delta}\right)U_{b(i-1)}-\left(\frac{G_aA_a}{12\Delta}\right)U_{b(i+1)}+\left(\frac{G_pA_p+G_aA_a/3}{2\Delta}\right)U_{p(i-1)}-\left(\frac{G_pA_p+G_aA_a/3}{2\Delta}\right)U_{p(i+1)}\\
&+\left(-c_1^2G_aI_{yya}+\frac{1}{6}G_aA_a\right)\theta_{yb(i)}-\left(\frac{E_pI_{yyp}}{\Delta^2}\right)\theta_{yp(i-1)}+\left(2\frac{E_pI_{yyp}}{\Delta^2}+G_pA_p+c_1^2G_aI_{yya}+\frac{1}{3}G_aA_a\right)\theta_{yp(i)}\\
&-\left(\frac{E_pI_{yyp}}{\Delta^2}\right)\theta_{yp(i+1)}-\left(\frac{c_1c_2G_aI_{yya}-c_5G_aA_a/12}{2\Delta}\right)\theta_{z(i-1)}+\left(\frac{c_1c_2G_aI_{yya}-c_5G_aA_a/12}{2\Delta}\right)\theta_{z(i+1)}\\
&+\left(-c_1c_3G_aI_{yya}+\frac{1}{12}h_bG_aA_a\right)\psi_{b(i)}=0
\end{aligned} \tag{6.27}$$

$$
\begin{aligned}
&-\left(\frac{c_4 G_a A_a}{6\Delta^2}\right)U_{b(i-1)}+\left[\frac{c_4 G_a A_a}{3\Delta^2}+c_1\left(c_2+c_3\right)G_a A_a\right]U_{b(i)}-\left(\frac{c_4 G_a A_a}{6\Delta^2}\right)U_{b(i+1)}\\
&-\left(\frac{c_5 G_a A_a}{12\Delta^2}\right)U_{p(i-1)}+\left[\frac{c_5 G_a A_a}{6\Delta^2}-c_1\left(c_2+c_3\right)G_a A_a\right]U_{p(i)}-\left(\frac{c_5 G_a A_a}{12\Delta^2}\right)U_{p(i+1)}\\
&-\left(\frac{c_1 c_2 G_a I_{yya}+c_4 G_a A_a/6}{2\Delta}\right)\theta_{yb(i-1)}+\left(\frac{c_1 c_2 G_a I_{yya}+c_4 G_a A_a/6}{2\Delta}\right)\theta_{yb(i+1)}\\
&-\left(\frac{-c_1 c_2 G_a I_{yya}+c_5 G_a A_a/12}{2\Delta}\right)\theta_{yp(i-1)}+\left(\frac{-c_1 c_2 G_a I_{yya}+c_5 G_a A_a/12}{2\Delta}\right)\theta_{yp(i+1)}+\left(\frac{E_b I_{\omega\omega bl}+E_p I_{\omega\omega p}}{\Delta^4}\right)\theta_{z(i-2)}\\
&-\left[4\frac{E_b I_{\omega\omega bl}+E_p I_{\omega\omega p}}{\Delta^4}+\frac{1}{\Delta^2}\left(G_b J_b+G_p J_p+c_2^2 G_a I_{yya}+\frac{1}{12}c_6 G_a A_a\right)\right]\theta_{z(i-1)}\\
&+\left[6\frac{E_b I_{\omega\omega bl}+E_p I_{\omega\omega p}}{\Delta^4}+2\frac{1}{\Delta^2}\left(G_b J_b+G_p J_p+c_2^2 G_a I_{yya}+\frac{1}{12}c_6 G_a A_a\right)+\left(c_2+c_3\right)^2 G_a A_a\right]\theta_{z(i)}\\
&-\left[4\frac{E_b I_{\omega\omega bl}+E_p I_{\omega\omega p}}{\Delta^4}+\frac{1}{\Delta^2}\left(G_b J_b+G_p J_p+c_2^2 G_a I_{yya}+\frac{1}{12}c_6 G_a A_a\right)\right]\theta_{z(i+1)}+\left(\frac{E_b I_{\omega\omega bl}+E_p I_{\omega\omega p}}{\Delta^4}\right)\theta_{z(i+2)}\\
&-\frac{1}{2\Delta}\left(\frac{h_b^2}{2}G_b A_{bf}+c_2 c_3 G_a I_{yya}+\frac{1}{12}c_4 h_b G_a A_a\right)\psi_{b(i-1)}\\
&+\frac{1}{2\Delta}\left(\frac{h_b^2}{2}G_b A_{bf}+c_2 c_3 G_a I_{yya}+\frac{1}{12}c_4 h_b G_a A_a\right)\psi_{b(i+1)}=m_{(i)}
\end{aligned}
\tag{6.28}
$$

$$
\begin{aligned}
&\left(\frac{h_b G_a A_a}{12\Delta}\right)U_{b(i-1)}-\left(\frac{h_b G_a A_a}{12\Delta}\right)U_{b(i+1)}+\left(\frac{h_b G_a A_a}{24\Delta}\right)U_{p(i-1)}-\left(\frac{h_b G_a A_a}{24\Delta}\right)U_{p(i+1)}\\
&+\left(c_1 c_3 G_a I_{yya}+\frac{1}{6}h_b G_a A_a\right)\theta_{yb(i)}+\left(-c_1 c_3 G_a I_{yya}+\frac{1}{12}h_b G_a A_a\right)\theta_{yp(i)}\\
&+\frac{1}{2\Delta}\left(\frac{h_b^2}{2}G_b A_{bf}+c_2 c_3 G_a I_{yya}+\frac{1}{12}c_4 h_b G_a A_a\right)\theta_{z(i-1)}-\frac{1}{2\Delta}\left(\frac{h_b^2}{2}G_b A_{bf}+c_2 c_3 G_a I_{yya}+\frac{1}{12}c_4 h_b G_a A_a\right)\theta_{z(i+1)}\\
&-\left(\frac{E_b I_{\omega\omega bg}}{\Delta^2}\right)\psi_{b(i-1)}+\left(2\frac{E_b I_{\omega\omega bg}}{\Delta^2}+\frac{h_b^2}{2}G_b A_{bf}+c_3^2 G_a I_{yya}+\frac{1}{12}h_b^2 G_a A_a\right)\psi_{b(i)}-\frac{E_b I_{\omega\omega bg}}{\Delta^2}\psi_{b(i+1)}=b_{(i)}
\end{aligned}
\tag{6.29}
$$

6.3.3. Discretized Boundary Conditions

The 16 boundary conditions in Eqs. 5.55-5.70 are written in a discretized form as

$$-\left[\left(\frac{E_b I_{ssbw}}{2\Delta^3}\right)U_{b(-1)}-\left(\frac{E_b I_{ssbw}}{\Delta^3}+\frac{G_b A_{bf}}{\Delta}+\frac{G_a A_a}{6\Delta}\right)U_{b(0)}+\left(\frac{E_b I_{ssbw}}{\Delta^3}+\frac{G_b A_{bf}}{\Delta}+\frac{G_a A_a}{6\Delta}\right)U_{b(2)}\right.$$

$$-\left(\frac{E_b I_{ssbw}}{2\Delta^3}\right)U_{b(3)}-\left(\frac{G_a A_a}{12\Delta}\right)U_{p(0)}+\left(\frac{G_a A_a}{12\Delta}\right)U_{p(2)}-\left(\frac{G_a A_a}{3}+2G_b A_{bf}\right)\theta_{yb(1)} \tag{6.30}$$

$$\left.-\left(\frac{G_a A_a}{6}\right)\theta_{yp(1)}-\left(\frac{c_4 G_a A_a}{12\Delta}\right)\theta_{z(0)}+\left(\frac{c_4 G_a A_a}{12\Delta}\right)\theta_{z(2)}-\left(\frac{h_b G_a A_a}{6}\right)\psi_{b(1)}-Q_{x(1)}\right]\delta U_{b(1)}=0$$

$$\left[\left(\frac{E_b I_{ssbw}}{2\Delta^3}\right)U_{b(n-1)}-\left(\frac{E_b I_{ssbw}}{\Delta^3}+\frac{G_b A_{bf}}{\Delta}+\frac{G_a A_a}{6\Delta}\right)U_{b(n)}+\left(\frac{E_b I_{ssbw}}{\Delta^3}+\frac{G_b A_{bf}}{\Delta}+\frac{G_a A_a}{6\Delta}\right)U_{b(n+2)}\right.$$

$$-\left(\frac{E_b I_{ssbw}}{2\Delta^3}\right)U_{b(n+3)}-\left(\frac{G_a A_a}{12\Delta}\right)U_{p(n)}+\left(\frac{G_a A_a}{12\Delta}\right)U_{p(n+2)}-\left(\frac{G_a A_a}{3}+2G_b A_{bf}\right)\theta_{yb(n+1)} \tag{6.31}$$

$$\left.-\left(\frac{G_a A_a}{6}\right)\theta_{yp(n+1)}-\left(\frac{c_4 G_a A_a}{12\Delta}\right)\theta_{z(n)}+\left(\frac{c_4 G_a A_a}{12\Delta}\right)\theta_{z(n+2)}-\left(\frac{h_b G_a A_a}{6}\right)\psi_{b(n+1)}-Q_{x(n+1)}\right]\delta U_{b(n+1)}=0$$

$$-\left[\frac{E_b I_{ssbw}}{\Delta^2}\left(U_{b(0)}-2U_{b(1)}+U_{b(2)}\right)-M_{y1(1)}\right]\delta\frac{\left[-U_{b(0)}+U_{b(2)}\right]}{2\Delta}=0 \tag{6.32}$$

$$\left[\frac{E_b I_{ssbw}}{\Delta^2}\left(U_{b(n)}-2U_{b(n+1)}+U_{b(n+2)}\right)-M_{y1(n+1)}\right]\delta\frac{\left[-U_{b(n)}+U_{b(n+2)}\right]}{2\Delta}=0 \tag{6.33}$$

$$-\left[-\left(\frac{G_a A_a}{12\Delta}\right)U_{b(0)}+\left(\frac{G_a A_a}{12\Delta}\right)U_{b(2)}-\left(\frac{G_p A_p}{2\Delta}+\frac{G_a A_a}{6\Delta}\right)U_{p(0)}+\left(\frac{G_p A_p}{2\Delta}+\frac{G_a A_a}{6\Delta}\right)U_{p(2)}-\left(\frac{G_a A_a}{6}\right)\theta_{yb(1)}\right.$$

$$\left.-\left(G_p A_p+\frac{G_a A_a}{3}\right)\theta_{yp(1)}-\left(\frac{c_5 G_a A_a}{24\Delta}\right)\theta_{z(0)}+\left(\frac{c_5 G_a A_a}{24\Delta}\right)\theta_{z(2)}-\left(\frac{h_b G_a A_a}{12}\right)\psi_{(1)}\right]\delta U_{p(1)}=0$$

$$\tag{6.34}$$

$$\left[-\left(\frac{G_a A_a}{12\Delta}\right)U_{b(n)}+\left(\frac{G_a A_a}{12\Delta}\right)U_{b(n+2)}-\left(\frac{G_p A_p}{2\Delta}+\frac{G_a A_a}{6\Delta}\right)U_{p(n)}+\left(\frac{G_p A_p}{2\Delta}+\frac{G_a A_a}{6\Delta}\right)U_{p(n+2)}-\left(\frac{G_a A_a}{6}\right)\theta_{yb(n+1)}\right.$$

$$\left.-\left(G_p A_p+\frac{G_a A_a}{3}\right)\theta_{yp(n+1)}-\left(\frac{c_5 G_a A_a}{24\Delta}\right)\theta_{z(n)}+\left(\frac{c_5 G_a A_a}{24\Delta}\right)\theta_{z(n+2)}-\left(\frac{h_b G_a A_a}{12}\right)\psi_{(n+1)}\right]\delta U_{p(n+1)}=0$$

$$\tag{6.35}$$

$$-\left[\frac{E_b I_{yybf}}{2\Delta}\left(-\theta_{yb(0)}+\theta_{yb(2)}\right)-M_{y2(1)}\right]\delta\theta_{yb(1)}=0 \tag{6.36}$$

$$\left[\frac{E_b I_{yybf}}{2\Delta}\left(-\theta_{yb(n)}+\theta_{yb(n+2)}\right)-M_{y2(n+1)}\right]\delta\theta_{yb(n+1)}=0 \tag{6.37}$$

$$-\frac{E_pI_{yyp}}{2\Delta}\left(-\theta_{yp(0)}+\theta_{yp(2)}\right)\delta\theta_{yp(1)}=0 \tag{6.38}$$

$$\frac{E_pI_{yyp}}{2\Delta}\left(-\theta_{yp(n)}+\theta_{yp(n+2)}\right)\delta\theta_{yp(n+1)}=0 \tag{6.39}$$

$$\begin{aligned}
&-\Bigg[-\left(\frac{c_4G_aA_a}{12\Delta}\right)U_{b(0)}+\left(\frac{c_4G_aA_a}{12\Delta}\right)U_{b(2)}-\left(\frac{c_5G_aA_a}{24\Delta}\right)U_{p(0)}+\left(\frac{c_5G_aA_a}{24\Delta}\right)U_{p(2)}\\
&-\left(c_1c_2G_aI_{yya}+\frac{c_4G_aA_a}{6}\right)\theta_{yb(1)}+\left(c_1c_2G_aI_{yya}-\frac{c_5G_aA_a}{12}\right)\theta_{yp(1)}+\left(\frac{E_bI_{\omega\omega bl}+E_pI_{\omega\omega p}}{2\Delta^3}\right)\theta_{z(-1)}\\
&-\left(\frac{E_bI_{\omega\omega bl}}{\Delta^3}+\frac{G_bJ_b}{2\Delta}+\frac{E_pI_{\omega\omega p}}{\Delta^3}+\frac{G_pJ_p}{2\Delta}+\frac{c_2^2G_aI_{yya}}{2\Delta}+\frac{c_6G_aA_a}{24\Delta}\right)\theta_{z(0)}\\
&+\left(\frac{E_bI_{\omega\omega bl}}{\Delta^3}+\frac{G_bJ_b}{2\Delta}+\frac{E_pI_{\omega\omega p}}{\Delta^3}+\frac{G_pJ_p}{2\Delta}+\frac{c_2^2G_aI_{yya}}{2\Delta}+\frac{c_6G_aA_a}{24\Delta}\right)\theta_{z(2)}-\left(\frac{E_bI_{\omega\omega bl}+E_pI_{\omega\omega p}}{2\Delta^3}\right)\theta_{z(3)}\\
&-\left(c_2c_3G_aI_{yya}+\frac{h_b^2}{4}G_bA_{bf}+\frac{c_4h_bG_aA_a}{12}\right)\psi_{(1)}-T_{(1)}\Bigg]\delta\theta_{z(1)}=0
\end{aligned} \tag{6.40}$$

$$\begin{aligned}
&\Bigg[-\left(\frac{c_4G_aA_a}{12\Delta}\right)U_{b(n)}+\left(\frac{c_4G_aA_a}{12\Delta}\right)U_{b(n+2)}-\left(\frac{c_5G_aA_a}{24\Delta}\right)U_{p(n)}+\left(\frac{c_5G_aA_a}{24\Delta}\right)U_{p(n+2)}\\
&-\left(c_1c_2G_aI_{yya}+\frac{c_4G_aA_a}{6}\right)\theta_{yb(n+1)}+\left(c_1c_2G_aI_{yya}-\frac{c_5G_aA_a}{12}\right)\theta_{yp(n+1)}+\left(\frac{E_bI_{\omega\omega bl}+E_pI_{\omega\omega p}}{2\Delta^3}\right)\theta_{z(n-1)}\\
&-\left(\frac{E_bI_{\omega\omega bl}}{\Delta^3}+\frac{G_bJ_b}{2\Delta}+\frac{E_pI_{\omega\omega p}}{\Delta^3}+\frac{G_pJ_p}{2\Delta}+\frac{c_2^2G_aI_{yya}}{2\Delta}+\frac{c_6G_aA_a}{24\Delta}\right)\theta_{z(n)}\\
&+\left(\frac{E_bI_{\omega\omega bl}}{\Delta^3}+\frac{G_bJ_b}{2\Delta}+\frac{E_pI_{\omega\omega p}}{\Delta^3}+\frac{G_pJ_p}{2\Delta}+\frac{c_2^2G_aI_{yya}}{2\Delta}+\frac{c_6G_aA_a}{24\Delta}\right)\theta_{z(n+2)}-\left(\frac{E_bI_{\omega\omega bl}+E_pI_{\omega\omega p}}{2\Delta^3}\right)\theta_{z(n+3)}\\
&-\left(c_2c_3G_aI_{yya}+\frac{h_b^2}{4}G_bA_{bf}+\frac{c_4h_bG_aA_a}{12}\right)\psi_{(n+1)}-T_{(n+1)}\Bigg]\delta\theta_{z(n+1)}=0
\end{aligned} \tag{6.41}$$

$$-\left[\frac{E_bI_{\omega\omega bl}+E_pI_{\omega\omega p}}{\Delta^2}\left(\theta_{z(0)}-2\theta_{z(1)}+\theta_{z(2)}\right)-B_{1(1)}\right]\delta\frac{\left[-\theta_{z(0)}+\theta_{z(1)}\right]}{2\Delta}=0 \tag{6.42}$$

$$\left[\frac{E_bI_{\omega\omega bl}+E_pI_{\omega\omega p}}{\Delta^2}\left(\theta_{z(n)}-2\theta_{z(n+1)}+\theta_{z(n+2)}\right)-B_{1(n+1)}\right]\delta\frac{\left[-\theta_{z(n)}+\theta_{z(n+1)}\right]}{2\Delta}=0 \tag{6.43}$$

$$-\left[\frac{E_b I_{\omega\omega bg}}{2\Delta}\left(-\psi_{b(0)}+\psi_{b(2)}\right)-B_{2(1)}\right]\delta\psi_{b(1)}=0 \tag{6.44}$$

$$\left[\frac{E_b I_{\omega\omega bg}}{2\Delta}\left(-\psi_{b(n)}+\psi_{b(n+2)}\right)-B_{2(n+1)}\right]\delta\psi_{b(n+1)}=0 \tag{6.45}$$

Each of the equations from (6.24) to (6.29) is expressed for $i=1,2,...,n+1$. Therefore, there are $6(n+1)$ equations. Also, the 16 discretized boundary equations established from Eqs. (6.30) to (6.45) are also added to the system of equations. This brings the number of equations $6(n+1)+16$

6.3.4. Finite Difference Formula of Strains, Stresses

6.3.4.1. Wide Flange Beam

From finite difference formula in Eq. (6.1), by substituting into displacement fields expressed in section 5.4.6.1, the strains within the wide flange beam can be expressed as

$$\begin{aligned}\varepsilon_{zb(i)}=&-\left[\frac{1}{\Delta^2}U_{b(i-1)}-\frac{2}{\Delta^2}U_{b(i)}+\frac{1}{\Delta^2}U_{b(i+1)}\right]n_b\sin\alpha\left(s_b\right)-\left[-\frac{1}{2\Delta}\theta_{yb(i-1)}+\frac{1}{2\Delta}\theta_{yb(i+1)}\right]x\left(s_b\right)\\&+\left[\frac{1}{\Delta^2}\theta_{z(i-1)}-\frac{2}{\Delta^2}\theta_{z(i)}+\frac{1}{\Delta^2}\theta_{z(i+1)}\right]n_b q\left(s_b\right)-\left[-\frac{1}{2\Delta}\psi_{b(i-1)}+\frac{1}{2\Delta}\psi_{b(i+1)}\right]\omega\left(s_b\right)\end{aligned} \tag{6.46}$$

and

$$\begin{aligned}\gamma_{szb(i)}=&\left[-\frac{1}{2\Delta}U_{b(i-1)}+\frac{1}{2\Delta}U_{b(i+1)}\right]\cos\alpha\left(s_b\right)-\theta_{yb(i)}\cos\alpha\left(s_b\right)\\&+\left[-\frac{1}{2\Delta}\theta_{z(i-1)}+\frac{1}{2\Delta}\theta_{z(i+1)}\right]\left[r\left(s_b\right)+2n_b\right]-\psi_{b(i)}r\left(s_b\right)\end{aligned} \tag{6.47}$$

The corresponding stresses are

$$\sigma_{zb(i)}=E_b\varepsilon_{zb(i)},\tau_{szb(i)}=G_b\gamma_{szb(i)} \tag{6.48}$$

6.3.4.2. GFRP Plate

From finite difference formula in Eq. (6.1), by substituting into displacement fields expressed in section 5.4.6.2, the strains within the GFRP plate can be expressed as

$$\varepsilon_{zp(i)}=-\left[-\frac{1}{2\Delta}\theta_{yp(i-1)}+\frac{1}{2\Delta}\theta_{yp(i+1)}\right]x\left(s_p\right)+\left[\frac{1}{\Delta^2}\theta_{z(i-1)}-\frac{2}{\Delta^2}\theta_{z(i)}+\frac{1}{\Delta^2}\theta_{z(i+1)}\right]n_p x\left(s_p\right) \tag{6.49}$$

$$\gamma_{szp(i)} = \left[-\frac{1}{2\Delta} U_{p(i-1)} + \frac{1}{2\Delta} U_{p(i+1)} \right] - \theta_{yp(i)} + 2\left[-\frac{1}{2\Delta} \theta_{z(i-1)} + \frac{1}{2\Delta} \theta_{z(i+1)} \right] n_p \qquad (6.50)$$

The corresponding stresses are

$$\sigma_{zp(i)} = E_p \varepsilon_{zp(i)}, \tau_{szp(i)} = G_p \gamma_{szp(i)} \qquad (6.51)$$

6.3.4.3. Adhesive Layer

From finite difference formula in Eq. (6.1), by substituting into displacement fields expressed in section 5.4.6.3 in Chapter 5, the strains within the GFRP plate can be expressed as

$$\begin{aligned}
\gamma_{zna(i)} &= c_1 \theta_{yb(i)} x - c_1 \theta_{yp(i)} x - c_2 \left[-\frac{1}{2\Delta} \theta_{z(i-1)} + \frac{1}{2\Delta} \theta_{z(i+1)} \right] x + c_3 \psi_{b(i)} x \\
\gamma_{sna(i)} &= -c_1 U_{b(i)} + c_1 U_{p(i)} - (c_2 + c_3) \theta_{z(i)} \\
\gamma_{sza(i)} &= \left(\frac{1}{2} - \frac{n_a}{t_2} \right) \left[-\frac{1}{2\Delta} U_{b(i-1)} + \frac{1}{2\Delta} U_{b(i+1)} \right] - \left(\frac{1}{2} - \frac{n_a}{t_2} \right) \theta_{yb(i)} + \left(\frac{1}{2} + \frac{n_a}{t_2} \right) \left[-\frac{1}{2\Delta} U_{p(i-1)} + \frac{1}{2\Delta} U_{p(i+1)} \right] \\
&\quad - \left(\frac{1}{2} + \frac{n_a}{t_2} \right) \theta_{yp(i)} + \left(\frac{h_b - 2t_1 + 2t_3}{4} - \frac{h_b + 2t_1 + 2t_3}{2t_2} n_a \right) \left[-\frac{1}{2\Delta} \theta_{z(i-1)} + \frac{1}{2\Delta} \theta_{z(i+1)} \right] - \left(\frac{1}{2} - \frac{n_a}{t_2} \right) \frac{h_b}{2} \psi_{b(i)}
\end{aligned}$$

(6.52)

The corresponding stresses are

$$\tau_{sza(i)} = G_a \gamma_{sza(i)}, \tau_{sna(i)} = G_a \gamma_{sna(i)}, \tau_{zna(i)} = G_a \gamma_{zna(i)} \qquad (6.53)$$

6.4. Summary

This chapter provided finite difference discretized equations for all field equations of the SDT and associated boundary conditions. Also, finite difference expressions for the resulting stresses have been developed. These equations will be used to implement solutions for practical problems and will be described in Chapter 8.

CHAPTER 7 – SHEAR DEFORMABLE THEORY – FINITE ELEMENT FORMULATION

7.1 Introduction and Scope

In this Chapter, a finite element formulation is developed based on the shear deformable theory developed in Chapter 5. In contrast to the treatment in Chapter 3 for the non-shear deformable theory in which the shape functions were chosen to satisfy the equilibrium equations of the system, the present treatment is based on approximate shape functions.

7.2 Expression for Total Potential Energy

From Eq. 5.21 in Chapter 5, the total potential energy π can be expressed as the sum of the total potential energy based on longitudinal-transverse response

$$\pi_1 = \pi_1\left(W_b, W_b', W_p, W_p', V, V', V'', \theta_{xb}, \theta_{xb}'\right)$$

and that based on the lateral torsional response

$$\pi_2 = \pi_2\left(U_b, U_b', U_b'', \theta_{yb}, \theta_{yb}', U_p, U_p', U_p'', \theta_{yp}, \theta_{yp}', \theta_z, \theta_z', \theta_z'', \psi_b, \psi_b'\right)$$, i.e.,

$$\pi = \pi_1 + \pi_2$$

in which

$$\begin{aligned}
\pi_1 = \int_L \Bigg[& \frac{1}{2}E_b A_b W_b'^{\,2} + \frac{1}{2}c_1^2 G_a A_a W_b^2 + \frac{1}{2}E_p A_p W_p'^{\,2} + \frac{1}{2}c_1^2 G_a A_a W_p^2 + \frac{1}{2}\left(E_b I_{ssbf} + E_p I_{xxp}\right)V''^2 \\
& + \frac{1}{2}\left(G_b A_{bw} + c_2^2 G_a A_a\right)V'^{\,2} + \frac{1}{2}E_b I_{xxb1}\theta_{xb}'^{\,2} + \frac{1}{2}\left(G_b A_{bw} + c_3^2 G_a A_a\right)\theta_{xb}^2 - c_1^2 G_a A_a W_b W_p + c_1 c_3 G_a A_a W_b \theta_{xb} \\
& + c_1 c_2 G_a A_a W_b V' - c_1 c_3 G_a A_a W_p \theta_{xb} - c_1 c_2 G_a A_a W_p V' + \left(c_2 c_3 G_a A_a - G_b A_{bw}\right)\theta_{xb} V' \Bigg] dz \\
& + \Big[Q_y(0)V(0) + N(0)W_b(0) + M_{x1}(0)V'(0) + M_{x2}(0)\theta_{xb}(0) - Q_y(L)V(L) - N(L)W_b(L) \\
& - M_{x1}(L)V'(L) - M_{x2}(L)\theta_{xb}(L)\Big] - \int_L \left[q_{zb}(z)W_b(z) + q_{yb}(z)V(z) + m_{xb}(z)\theta_{xb}(z)\right]dz
\end{aligned} \tag{7.1}$$

and

$$\pi_2=\int_L\left[\frac{1}{2}E_bI_{ssbw}U_b''^2+\left(G_bA_{bf}+\frac{1}{6}G_aA_a\right)U_b'^2+\frac{1}{2}c_1^2G_aA_aU_b^2+\frac{1}{2}E_bI_{yybf}\theta_{yb}'^2\right.$$

$$+\left(G_bA_{bf}+\frac{1}{2}c_1^2G_aI_{yya}+\frac{1}{6}G_aA_a\right)\theta_{yb}^2+\frac{1}{2}\left(G_pA_p+\frac{1}{3}G_aA_a\right)U_p'^2+\frac{1}{2}c_1^2G_aA_aU_p^2$$

$$+\frac{1}{2}E_pI_{yyp}\theta_{yp}'^2+\frac{1}{2}\left(G_pA_p+\frac{1}{3}G_aA_a+c_1^2G_aI_{yya}\right)\theta_{yp}^2+\frac{1}{2}\left(E_bI_{\omega\omega bl}+E_pI_{\omega\omega p}\right)\theta_z''^2$$

$$+\frac{1}{2}\left(G_bJ_b+G_pJ_p+c_2^2G_aI_{yya}+\frac{1}{12}c_6G_aA_a\right)\theta_z'^2+\frac{1}{2}\left(c_2+c_3\right)^2G_aA_a\theta_z^2+\frac{1}{2}E_bI_{\omega\omega bg}\psi_b'^2$$

$$+\frac{1}{2}\left(\frac{h_b^2}{2}G_bA_{bf}+c_3^2G_aI_{yya}+\frac{1}{12}h_b^2G_aA_a\right)\psi_b^2+\frac{1}{6}G_aA_aU_b'U_p'-c_1^2G_aA_aU_bU_p$$

$$-\left(2G_bA_{bf}+\frac{1}{3}G_aA_a\right)\theta_{yb}U_b'-\frac{1}{6}G_aA_aU_b'\theta_{yp}+\frac{1}{6}c_4G_aA_aU_b'\theta_z'+c_1\left(c_2+c_3\right)G_aA_aU_b\theta_z$$

$$-\frac{1}{6}h_bG_aA_aU_b'\psi_b-\left(G_pA_p+\frac{1}{3}G_aA_a\right)\theta_{yp}U_p'+\frac{1}{12}c_5G_aA_aU_p'\theta_z'-c_1\left(c_2+c_3\right)G_aA_aU_p\theta_z$$

$$-\frac{1}{6}G_aA_a\theta_{yb}U_p'-\frac{1}{12}h_bG_aA_aU_p'\psi_b-\left(c_1c_2G_aI_{yya}+\frac{1}{6}c_4G_aA_a\right)\theta_{yb}\theta_z'+\left(\frac{1}{6}G_aA_a-c_1^2G_aI_{yya}\right)\theta_{yb}\theta_{yp}$$

$$+\left(c_1c_3G_aI_{yya}+\frac{1}{6}h_bG_aA_a\right)\theta_{yb}\psi_b+\left(c_1c_2G_aI_{yya}-\frac{1}{12}c_5G_aA_a\right)\theta_{yp}\theta_z'+\left(\frac{1}{12}h_bG_aA_a-c_1c_3G_aI_{yya}\right)\theta_{yp}\psi_b$$

$$\left.-\left(\frac{h_b^2}{2}G_bA_{bf}+c_2c_3G_aI_{yya}+\frac{1}{12}c_4h_bG_aA_a\right)\theta_z'\psi_b\right]dz$$

$$+\left[Q_x(0)U_b(0)+T(0)\theta(0)+M_{y1}(0)U_b'(0)+B_1(0)\theta'(0)+M_{y2}(0)\theta_{yb}(0)+B_2(0)\psi_b(0)\right.$$

$$\left.-Q_x(L)U_b(L)-T(L)\theta(L)-M_{y1}(L)U_b'(L)-B_1(L)\theta'(L)-M_{y2}(L)U_b'(L)-B_2(L)\theta'(L)\right]$$

$$-\int_L\left[q_{xb}(z)U_b(z)+m_{yb}(z)\theta_{yb}(z)+m_{zb}(z)\theta_z(z)+b_b(z)\psi_b(z)\right]dz$$

(7.2)

7.3 Formulation for Longitudinal-Transverse Response

7.3.1 Shape Functions

The displacement fields $V(z), W_b(z), W_p(z), \theta_{xb}(z)$ are related to the relevant nodal displacements vectors $\langle D_V\rangle^T=\langle V(0)\quad V'(0)\quad V(L)\quad V'(L)\rangle$, $\langle D_{wb}\rangle_{1\times2}^T=\langle W_b(0)\quad W_b(L)\rangle$, $\langle D_{wp}\rangle_{1\times2}^T=\langle W_p(0)\quad W_p(L)\rangle$ and $\langle D_{\theta xb}\rangle_{1\times2}^T=\langle\theta_{xb}(0)\quad\theta_{xb}(L)\rangle$.

$$
\begin{aligned}
V(z) &= \langle H(z) \rangle_{1\times4}^{T} \{D_V\}_{4\times1} \\
W_b(z) &= \langle L(z) \rangle_{1\times2}^{T} \{D_{wb}\}_{2\times1} \\
W_p(z) &= \langle L(z) \rangle_{1\times2}^{T} \{D_{wp}\}_{2\times1} \\
\theta_{xb}(z) &= \langle L(z) \rangle_{1\times2}^{T} \{D_{\theta xb}\}_{2\times1}
\end{aligned}
\tag{7.3}
$$

in which $\langle H(z) \rangle_{1\times4}^{T} = \langle H_1(z) \quad H_2(z) \quad H_3(z) \quad H_4(z) \rangle$ is the vector of Hermitian interpolation shape functions $H_1(z) = 1 - 3\left(\frac{z}{L}\right)^2 + 2\left(\frac{z}{L}\right)^3$, $H_2(z) = z - 2\frac{z^2}{L} + \frac{z^3}{L^2}$, $H_3(z) = 3\left(\frac{z}{L}\right)^2 - 2\left(\frac{z}{L}\right)^3$, and $H_4(z) = \frac{z^3}{L^2} - \frac{z^2}{L}$ and $\langle L(z) \rangle_{1\times4}^{T} = \langle L_1(z) \quad L_2(z) \rangle$ is the vector of linear shape functions $L_1(z) = 1 - \left(\frac{z}{L}\right)$ and $L_2(z) = \left(\frac{z}{L}\right)$

7.3.2 Formulation of discrete equilibrium conditions

From Eqs. (7.3), by substituting into Eq. (7.1), the total potential energy is expressed as (See Eqs. A8.1, A8.7, and A8.11 in Appendix A8).

$$
\begin{aligned}
\pi_1 = {} & \frac{1}{2}\langle D_{wb} \rangle_{1\times2}^{T} [K_1]_{2\times2} \{D_{wb}\}_{2\times1} + \frac{1}{2}\langle D_{wp} \rangle_{1\times2}^{T} [K_2]_{2\times2} \{D_{wp}\}_{2\times1} \\
& + \frac{1}{2}\langle D_V \rangle_{1\times4}^{T} [K_3]_{4\times4} \{D_V\}_{4\times1} + \frac{1}{2}\langle D_{\theta xb} \rangle_{1\times2}^{T} [K_4]_{2\times2} \{D_{\theta xb}\}_{2\times1} \\
& + \langle D_{wb} \rangle_{1\times2}^{T} [K_5]_{2\times2} \{D_{wp}\}_{2\times1} + \langle D_{wb} \rangle_{1\times2}^{T} [K_6]_{2\times2} \{D_{\theta xb}\}_{2\times1} \\
& + \langle D_{wb} \rangle_{1\times2}^{T} [K_7]_{2\times4} \{D_V\}_{4\times1} + \langle D_{wp} \rangle_{1\times2}^{T} [K_8]_{2\times2} \{D_{\theta xb}\}_{2\times1} \\
& + \langle D_{wp} \rangle_{1\times2}^{T} [K_9]_{2\times4} \{D_V\}_{4\times1} + \langle D_V \rangle_{1\times4}^{T} [K_{10}]_{4\times2} \{D_{\theta xb}\}_{2\times1} \\
& - \langle \Delta_1 \rangle_{1\times10}^{T} \{\overline{Q}_1\}_{10\times1}
\end{aligned}
\tag{7.4}
$$

in which

$[K_1]_{2\times2} = E_b A_b \left[\widetilde{A_1}\right] + c_1^2 G_a A_a \left[\widetilde{A_2}\right]$, $[K_2]_{2\times2} = E_p A_p \left[\widetilde{A_1}\right] + c_1^2 G_a A_a \left[\widetilde{A_2}\right]$,

$[K_3]_{2\times2} = \left(E_b I_{ssbf} + E_p I_{xxp}\right)\left[\widetilde{A_3}\right] + \left(G_b A_{bw} + c_2^2 G_a A_a\right)\left[\widetilde{A_4}\right]$,

$[K_4]_{2\times2} = E_b I_{xxb1} \left[\widetilde{A_1}\right] + \left(G_b A_{bw} + c_3^2 G_a A_a\right)\left[\widetilde{A_2}\right]$

$$\left[K_5\right]_{4\times4} = -c_1^2 G_a A_a\left[\widetilde{A_2}\right],\ \left[K_6\right]_{2\times2} = c_1 c_3 G_a A_a\left[\widetilde{A_2}\right],\ \left[K_7\right]_{2\times4} = c_1 c_2 G_a A_a\left[\widetilde{A_5}\right],$$
$$\left[K_8\right]_{2\times4} = -c_1 c_3 G_a A_a\left[\widetilde{A_2}\right],$$

$$\left[K_9\right]_{2\times4} = -c_1 c_2 G_a A_a\left[\widetilde{A_5}\right],\ \left[K_{10}\right]_{4\times2} = \left(c_2 c_3 G_a A_a - G_b A_{bw}\right)\left[\widetilde{A_5}\right]^T$$

are stiffness matrix components, with

$$\left[\widetilde{A_1}\right]_{2\times2} = \frac{1}{L}\begin{bmatrix} 1 & -1 \\ -1 & 1 \end{bmatrix},\left[\widetilde{A_2}\right]_{2\times2} = \frac{L}{6}\begin{bmatrix} 2 & 1 \\ 1 & 2 \end{bmatrix}$$

$$\left[\widetilde{A_3}\right]_{4\times4} = \frac{1}{L^3}\begin{bmatrix} 12 & 6L & -12 & 6L \\ 6L & 4L^2 & -6L & 2L^2 \\ -12 & -6L & 12 & -6L \\ 6L & 2L^2 & -6L & 4L^2 \end{bmatrix},\left[\widetilde{A_4}\right]_{4\times4} = \frac{1}{30L}\begin{bmatrix} 36 & 3L & -36 & 3L \\ 3L & 4L^2 & -3L & -L^2 \\ -36 & -3L & 36 & -3L \\ 3L & -L^2 & -3L & 4L^2 \end{bmatrix}$$

$$\left[\widetilde{A_5}\right]_{2\times4} = \frac{1}{12}\begin{bmatrix} -6 & L & 6 & -L \\ -6 & -L & 6 & L \end{bmatrix} \tag{7.5}$$

$$\left[\widetilde{A_6}\right]_{4\times4} = \frac{1}{420}\begin{bmatrix} 156L & 22L^2 & 54L & -13L^2 \\ 22L^2 & 4L^3 & 13L^2 & -3L^3 \\ 54L & 13L^2 & 156L & -22L^2 \\ -13L^2 & -3L^3 & -22L^2 & 4L^3 \end{bmatrix},\left[\widetilde{A_7}\right]_{2\times2} = \frac{1}{2}\begin{bmatrix} -1 & 1 \\ -1 & 1 \end{bmatrix},$$

$\langle \Delta_1 \rangle^T_{1\times10} = \left\langle \langle D_{wb} \rangle^T_{1\times2} \,\vdots\, \langle D_{wp} \rangle^T_{1\times2} \,\vdots\, \langle D_V \rangle^T_{1\times4} \,\vdots\, \langle D_{\theta xb} \rangle^T_{1\times2} \right\rangle$ is the nodal displacement vector for the longitudinal transverse response, and the equivalent load vector is given in Section A8.2.3 in Appendix A8).

$$\left\{\overline{Q}_1\right\}_{10\times1} = \left\{\overline{\overline{Q}}_{11}\right\}_{10\times1} + \left\{\overline{\overline{Q}}_{21}\right\}_{10\times1} \tag{7.6}$$

in which

$$\left\langle \overline{\overline{Q}}_{11} \right\rangle^T_{1\times10} = \left\langle -N(0) \quad N(L) \,\vdots\, 0 \quad 0 \,\vdots\, -Q_y(0) \quad -M_{x1}(0) \quad Q_y(L) \quad M_{x1}(L) \,\vdots\, -M_{x2}(0) \quad M_{x2}(L) \right\rangle$$

is load vector at member ends and

$$\left\langle \overline{\overline{Q}}_{21} \right\rangle^T_{1\times10} = \left\langle \int_L q_{zb}(z)\langle L(z)\rangle^T_{1\times2} dz \,\vdots\, 0 \quad 0 \,\vdots\, \int_L q_{yb}(z)\langle H(z)\rangle^T_{1\times4} dz \,\vdots\, \int_L m_{xb}(z)\langle L(z)\rangle^T_{1\times2} dz \right\rangle$$

is the energy equivalent load vector. By taking variation of the Eq. (7.4) and grouping nodal displacement matrices, one obtains

$$\delta\pi_1 = \langle \delta\Delta_1 \rangle_{1\times 10}^T \left\{ \left[\overline{\overline{K}}_1 \right]_{10\times 10} \{\Delta_1\}_{10\times 1} - \left\{ \overline{Q}_1 \right\}_{10\times 1} \right\} = 0 \tag{7.7}$$

in which the total longitudinal-transverse stiffness matrix , displacement vector are

$$\left[\overline{\overline{K}}_1 \right]_{10\times 10} = \left[\begin{array}{c:c:c:c} [K_1] & [K_5] & [K_7] & [K_6] \\ \hdashline [K_5]^T & [K_2] & [K_9] & [K_8] \\ \hdashline [K_7]^T & [K_9]^T & [K_3] & [K_{10}] \\ \hdashline [K_6]^T & [K_8]^T & [K_{10}]^T & [K_4] \end{array} \right] \tag{7.8}$$

is the element stiffness matrix for the longitudinal transverse response.

7.4 Formulation for Lateral-Torsional Response

7.4.1 Shape Functions

The displacement fields $U_b(z), \theta_{yb}(z), U_p(z), \theta_{yp}(z), \theta_z(z), \psi_b(z)$ are related to the relevant nodal displacements vectors $\langle D_{ub} \rangle^T = \langle U_b(0) \quad U_b'(0) \quad U_b(L) \quad U_b'(L) \rangle$, $\langle D_{\theta yb} \rangle_{1\times 2}^T = \langle \theta_{yb}(0) \quad \theta_{yb}(L) \rangle$, $\langle D_{up} \rangle_{1\times 2}^T = \langle U_p(0) \quad U_p(L) \rangle$, $\langle D_{\theta yp} \rangle_{1\times 2}^T = \langle \theta_{yp}(0) \quad \theta_{yp}(L) \rangle$, $\langle D_{\theta z} \rangle_{1\times 4}^T = \langle \theta_z(0) \quad \theta_z'(0) \quad \theta_z(L) \quad \theta_z'(L) \rangle$, and $\langle D_{\psi b} \rangle_{1\times 2}^T = \langle \psi_b(0) \quad \psi_b(L) \rangle$ through

$$\begin{aligned} U_b(z) &= \langle H(z) \rangle_{1\times 4}^T \{D_{ub}\}_{4\times 1} \\ \theta_{yb}(z) &= \langle L(z) \rangle_{1\times 2}^T \{D_{\theta yb}\}_{2\times 1} \\ U_p(z) &= \langle L(z) \rangle_{1\times 2}^T \{D_{up}\}_{2\times 1} \\ \theta_{yp}(z) &= \langle L(z) \rangle_{1\times 2}^T \{D_{\theta yp}\}_{2\times 1} \\ \theta_z(z) &= \langle H(z) \rangle_{1\times 4}^T \{D_{\theta z}\}_{4\times 1} \\ \psi_b(z) &= \langle L(z) \rangle_{1\times 2}^T \{D_{\psi b}\}_{2\times 1} \end{aligned} \tag{7.9}$$

in which $\langle H(z) \rangle_{1\times 4}^T, \langle L(z) \rangle_{1\times 2}^T$ are the vector of Hermitian polynomial functions and the vector of linear shape function defined in Section 7.3.1.

7.4.2 Formulation of discrete equilibrium conditions

From Eqs. (7.9), by substituting into Eq. (7.2), the total potential energy is expressed (Eqs. A8.14, A8.19, and A8.22 in the Appendix A8)as

$$
\begin{aligned}
\pi_2 = & \frac{1}{2}\left\langle D_{ub}\right\rangle_{1\times 4}^{T}\left[\overline{K}_1\right]_{4\times 4}\left\{D_{ub}\right\}_{4\times 1}+\frac{1}{2}\left\langle D_{\theta yb}\right\rangle_{1\times 2}\left[\overline{K}_2\right]_{2\times 2}\left\{D_{\theta yb}\right\}_{2\times 1}+\frac{1}{2}\left\langle D_{up}\right\rangle_{1\times 2}\left[\overline{K}_3\right]_{2\times 2}\left\{D_{up}\right\}_{2\times 1} \\
& +\frac{1}{2}\left\langle D_{\theta yp}\right\rangle_{1\times 2}\left[\overline{K}_4\right]_{2\times 2}\left\{D_{\theta yp}\right\}_{2\times 1}+\frac{1}{2}\left\langle D_{\theta z}\right\rangle_{1\times 4}^{T}\left[\overline{K}_5\right]_{4\times 4}\left\{D_{\theta z}\right\}_{4\times 1}+\frac{1}{2}\left\langle D_{\psi b}\right\rangle_{1\times 2}\left[\overline{K}_6\right]_{2\times 2}\left\{D_{\psi b}\right\}_{2\times 1} \\
& +\left\langle D_{ub}\right\rangle_{1\times 4}\left[\overline{K}_7\right]_{4\times 2}\left\{D_{up}\right\}_{2\times 1}+\left\langle D_{ub}\right\rangle_{1\times 4}\left[\overline{K}_8\right]_{4\times 2}\left\{D_{\theta yb}\right\}_{2\times 1}+\left\langle D_{ub}\right\rangle_{1\times 4}\left[\overline{K}_9\right]_{4\times 2}\left\{D_{\theta yp}\right\}_{2\times 1} \\
& +\left\langle D_{ub}\right\rangle_{1\times 4}^{T}\left[\overline{K}_{10}\right]_{4\times 4}\left\{D_{\theta z}\right\}_{4\times 1}+\left\langle D_{ub}\right\rangle_{1\times 4}\left[\overline{K}_{11}\right]_{4\times 2}\left\{D_{\psi b}\right\}_{2\times 1}+\left\langle D_{up}\right\rangle_{1\times 2}\left[\overline{K}_{12}\right]_{2\times 2}\left\{D_{\theta yp}\right\}_{2\times 1} \qquad (7.10)\\
& +\left\langle D_{up}\right\rangle_{1\times 2}\left[\overline{K}_{13}\right]_{2\times 4}\left\{D_{\theta z}\right\}_{4\times 1}+\left\langle D_{\theta yb}\right\rangle_{1\times 2}\left[\overline{K}_{14}\right]_{2\times 2}\left\{D_{up}\right\}_{2\times 1}+\left\langle D_{up}\right\rangle_{1\times 2}\left[\overline{K}_{15}\right]_{2\times 2}\left\{D_{\psi b}\right\}_{2\times 1} \\
& +\left\langle D_{\theta yb}\right\rangle_{1\times 2}\left[\overline{K}_{16}\right]_{2\times 4}\left\{D_{\theta z}\right\}_{4\times 1}+\left\langle D_{\theta yb}\right\rangle_{1\times 2}\left[\overline{K}_{17}\right]_{2\times 2}\left\{D_{\theta yp}\right\}_{2\times 1}+\left\langle D_{\theta yb}\right\rangle_{1\times 2}\left[\overline{K}_{18}\right]_{2\times 2}\left\{D_{\psi b}\right\}_{2\times 1} \\
& +\left\langle D_{\theta yp}\right\rangle_{1\times 2}\left[\overline{K}_{19}\right]_{2\times 4}\left\{D_{\theta z}\right\}_{4\times 1}+\left\langle D_{\theta yp}\right\rangle_{1\times 2}\left[\overline{K}_{20}\right]_{2\times 2}\left\{D_{\psi b}\right\}_{2\times 1}+\left\langle D_{\theta z}\right\rangle_{1\times 4}\left[\overline{K}_{21}\right]_{4\times 2}\left\{D_{\psi b}\right\}_{2\times 1} \\
& -\left\langle \Delta_2\right\rangle_{1\times 16}^{T}\left\{\overline{Q}_2\right\}_{16\times 1}
\end{aligned}
$$

in which

$$\left[\overline{K}_1\right]_{4\times 4}=E_b I_{ssbw}\left[\widetilde{A}_3\right]_{4\times 4}+\left(2G_b A_{bf}+\frac{1}{3}G_a A_a\right)\left[\widetilde{A}_4\right]_{4\times 4}+c_1^2 G_a A_a\left[\widetilde{A}_6\right]_{4\times 4}$$

$$\left[\overline{K}_2\right]_{2\times 2}=E_b I_{yybf}\left[\widetilde{A}_1\right]_{2\times 2}+\left(2G_b A_{bf}+c_1^2 G_a I_{yya}+\frac{1}{3}G_a A_a\right)\left[\widetilde{A}_2\right]_{2\times 2}$$

$$\left[\overline{K}_3\right]_{2\times 2}=\left(G_p A_p+\frac{1}{3}G_a A_a\right)\left[\widetilde{A}_1\right]_{2\times 2}+c_1^2 G_a A_a\left[\widetilde{A}_2\right]_{2\times 2}$$

$$\left[\overline{K}_4\right]_{2\times 2}=E_p I_{yyp}\left[\widetilde{A}_1\right]_{2\times 2}+\left(G_p A_p+\frac{1}{3}G_a A_a+c_1^2 G_a I_{yya}\right)\left[\widetilde{A}_2\right]_{2\times 2}$$

$$\left[\overline{K}_5\right]_{4\times 4}=\left(E_b I_{\omega\omega bl}+E_p I_{\omega\omega p}\right)\left[\widetilde{A}_3\right]_{4\times 4}+\left(G_b J_b+G_p J_p+c_2^2 G_a I_{yya}+\frac{1}{12}c_6 G_a A_a\right)\left[\widetilde{A}_4\right]_{4\times 4}+\left(c_2+c_3\right)^2 G_a A_a\left[\widetilde{A}_6\right]_{4\times 4}$$

$$\left[\overline{K}_6\right]_{2\times 2}=E_b I_{\omega\omega bg}\left[\widetilde{A}_1\right]_{2\times 2}+\left(\frac{h_b^2}{2}G_b A_{bf}+c_3^2 G_a I_{yya}+\frac{1}{12}h_b^2 G_a A_a\right)\left[\widetilde{A}_2\right]_{2\times 2}$$

$$\left[\overline{K}_7\right]_{4\times 2}=\frac{1}{6}G_a A_a\left[\widetilde{A}_8\right]_{4\times 2}^{T}-c_1^2 G_a A_a\left[\widetilde{A}_9\right]_{4\times 2}^{T};\quad \left[\overline{K}_8\right]_{4\times 2}=-\left(2G_b A_{bf}+\frac{1}{3}G_a A_a\right)\left[\widetilde{A}_5\right]_{4\times 2}^{T}$$

$$\left[\overline{K}_9\right]_{4\times 2}=-\frac{1}{6}G_a A_a\left[\widetilde{A}_5\right]_{4\times 2}^{T};\quad \left[\overline{K}_{10}\right]_{4\times 4}=\frac{1}{6}c_4 G_a A_a\left[\widetilde{A}_4\right]_{4\times 4}^{T}+c_1\left(c_2+c_3\right)G_a A_a\left[\widetilde{A}_6\right]_{4\times 4}^{T}$$

$$\left[\overline{K}_{11}\right]_{4\times 2}=-\frac{1}{6}h_b G_a A_a\left[\widetilde{A}_5\right]_{4\times 2}^T;\quad \left[\overline{K}_{12}\right]_{2\times 2}=-\left(G_p A_p+\frac{1}{3}G_a A_a\right)\left[\widetilde{A}_7\right]_{2\times 2}^T$$

$$\left[\overline{K}_{13}\right]_{2\times 4}=\frac{1}{12}c_5 G_a A_a\left[\widetilde{A}_8\right]_{2\times 4}-c_1\left(c_2+c_3\right)G_a A_a\left[\widetilde{A}_9\right]_{2\times 4};\quad \left[\overline{K}_{14}\right]_{2\times 2}=-\frac{1}{6}G_a A_a\left[\widetilde{A}_7\right]_{2\times 2}$$

$$\left[\overline{K}_{15}\right]_{2\times 2}=-\frac{1}{12}h_b G_a A_a\left[\widetilde{A}_7\right]_{2\times 2}^T;\quad \left[\overline{K}_{16}\right]_{2\times 4}=-\left(c_1 c_2 G_a I_{yya}+\frac{1}{6}c_4 G_a A_a\right)\left[\widetilde{A}_5\right]_{2\times 4}$$

$$\left[\overline{K}_{17}\right]_{2\times 2}=\left(\frac{1}{6}G_a A_a-c_1^2 G_a I_{yya}\right)\left[\widetilde{A}_2\right]_{2\times 2}^T;\quad \left[\overline{K}_{18}\right]_{2\times 2}=\left(c_1 c_3 G_a I_{yya}+\frac{1}{6}h_b G_a A_a\right)\left[\widetilde{A}_2\right]_{2\times 2}^T$$

$$\left[\overline{K}_{19}\right]_{2\times 4}=\left(c_1 c_2 G_a I_{yya}-\frac{1}{12}c_5 G_a A_a\right)\left[\widetilde{A}_5\right]_{2\times 4};\quad \left[\overline{K}_{20}\right]_{2\times 2}=\left(\frac{1}{12}h_b G_a A_a-c_1 c_3 G_a I_{yya}\right)\left[\widetilde{A}_2\right]_{2\times 2}^T$$

$$\left[\overline{K}_{21}\right]_{4\times 2}=-\left(\frac{h_b^2}{2}G_b A_{bf}+c_2 c_3 G_a I_{yya}+\frac{1}{12}c_4 h_b G_a A_a\right)\left[\widetilde{A}_5\right]_{4\times 2}^T$$

in which matrices $\left[\widetilde{A}_i\right]_{i=\overline{1,7}}$ are defined as in Eq.(7.5) and

$$\left[\widetilde{A}_8\right]_{2\times 4}=\frac{1}{L}\begin{bmatrix}1 & 0 & -1 & 0\\ -1 & 0 & 1 & 0\end{bmatrix},\left[\widetilde{A}_9\right]_{2\times 4}=\frac{L}{60}\begin{bmatrix}21 & 3L & 9 & -2L\\ 9 & 2L & 21 & -3L\end{bmatrix}$$

and $\left\langle\Delta_2\right\rangle_{1\times 16}^T=\left\langle\left\langle D_{ub}\right\rangle_{1\times 4}^T \;\vdots\; \left\langle D_{\theta yb}\right\rangle_{1\times 2}^T \;\vdots\; \left\langle D_{up}\right\rangle_{1\times 2}^T \;\vdots\; \left\langle D_{\theta yp}\right\rangle_{1\times 2}^T \;\vdots\; \left\langle D_{\theta z}\right\rangle_{1\times 4}^T \;\vdots\; \left\langle D_{\psi b}\right\rangle_{1\times 2}^T\right\rangle$ is the nodal displacement vector related to the lateral torsional response, and the equivalent load vector is given by

$$\left\{\overline{Q}_2\right\}_{16\times 1}=\left\{\overline{\overline{Q}}_{12}\right\}_{16\times 1}+\left\{\overline{\overline{Q}}_{22}\right\}_{16\times 1} \tag{7.11}$$

in which

$$\left\langle\overline{\overline{Q}}_{12}\right\rangle_{1\times 16}^T=\left\langle -Q_x(0)\quad -M_{y1}(0)\quad Q_x(L)\quad M_{y1}(L)\;\vdots\; -M_{y2}(0)\quad M_{y2}(L)\;\vdots\right.$$

$$\left.\vdots\; 0\quad 0\;\vdots\; 0\quad 0\;\vdots\; -T(0)\quad -B_1(0)\quad T(L)\quad B_1(L)\;\vdots\; -B_2(0)\quad B_2(L)\right\rangle$$

is the vector of nodal forces and

$$\left\langle \overline{\overline{Q}}_{22} \right\rangle^T_{1\times16} =$$

$$\left\langle \int_L q_{xb}(z)\langle H(z)\rangle^T_{1\times4} dz \;\vdots\; \int_L m_{yb}(z)\langle L(z)\rangle^T_{1\times2} dz \;\vdots\; \langle 0\rangle^T_{1\times2} \;\vdots\; \langle 0\rangle^T_{1\times2} \;\vdots\; \int_L m_{zb}(z)\langle H(z)\rangle^T_{1\times4} dz \;\vdots\; \int_L b_b(z)\langle L(z)\rangle^T_{1\times2} dz \right\rangle$$

is the energy equivalent load vector due to member loads. By taking variation of the Eq. (7.4) and grouping nodal displacement matrices, one obtains

$$\delta\pi_2 = \langle \delta\Delta_2 \rangle^T_{1\times16} \left\{ \left[\overline{\overline{K}}_2 \right]_{16\times16} \{\Delta_2\}_{16\times1} - \left\{ \overline{Q}_2 \right\}_{16\times1} \right\} = 0 \tag{7.12}$$

in which

$$\langle \Delta_2 \rangle^T_{1\times16} = \left\langle \langle D_{ub} \rangle^T_{1\times4} \;\vdots\; \langle D_{\theta yb} \rangle^T_{1\times2} \;\vdots\; \langle D_{up} \rangle^T_{1\times2} \;\vdots\; \langle D_{\theta yp} \rangle^T_{1\times2} \;\vdots\; \langle D_{\theta z} \rangle^T_{1\times4} \;\vdots\; \langle D_{\psi b} \rangle^T_{1\times2} \right\rangle$$

is the nodal displacement vector, and

$$\left[\overline{\overline{K}}_2 \right]_{16\times16} = \begin{bmatrix} [K_1] & [K_8] & [K_7] & [K_9] & [K_{10}] & [K_{11}] \\ [K_8]^T & [K_2] & [K_{14}] & [K_{17}] & [K_{16}] & [K_{18}] \\ [K_7]^T & [K_{14}]^T & [K_3] & [K_{12}] & [K_{13}] & [K_{15}] \\ [K_9]^T & [K_{17}]^T & [K_{12}]^T & [K_4] & [K_{19}] & [K_{20}] \\ [K_{10}]^T & [K_{16}]^T & [K_{13}]^T & [K_{19}]^T & [K_5] & [K_{21}] \\ [K_{11}]^T & [K_{18}]^T & [K_{15}]^T & [K_{20}]^T & [K_{21}]^T & [K_6] \end{bmatrix}$$

(7.13)

is the element stiffness matrix for the lateral torsional response.

7.5. Strain and Stress Expressions

7.5.1 Longitudinal Normal Stress for Wide Flange Beam

As shown under the Sub-section 5.4.6.1, the longitudinal normal stress in a given finite element is determined by

$$\begin{aligned}\varepsilon_{zb} = {} & W_b'(z) - x(s_b)\theta_{yb}'(z) - y(s_b)\theta_{xb}'(z) - \psi_b'(z)\omega(s_b) - n_b \sin\alpha(s_b) U_b''(z) + \\ & n_b \cos\alpha(s_b) V''(z) + + n_b q(s_b)\theta_z''(z)\end{aligned} \tag{7.14}$$

In the present formulation, functions $W_b, \theta_{yb}, \theta_{xb}, \psi_b, U_b, V, \theta_z$ as determined from Eq. (7.3) and (7.9) are based on the assumed shape functions $\langle H(z)\rangle^T_{1\times4}, \langle L(z)\rangle^T_{1\times2}$. The direct substitution of these functions into Eq. (7.14) would lead to erroneous results since they do not include the load-dependent particular solution. Thus, in the following, an algorithm is developed to determine the strain ε_{zb} based on the nodal displacements and nodal forces for a given finite element.

From the boundary conditions for longitudinal-transverse response in Eqs.5.37-5.46 and lateral-torsional response in Eqs.5.55-5.70, expressions for the higher order derivatives of displacements at the element nodes can be developed by evaluating the nodal forces $\left\{\overline{\overline{Q}}_{11}\right\}_{10\times1}$ and $\left\{\overline{\overline{Q}}_{12}\right\}_{16\times1}$ for the element through the matrix multiplications $\left[\overline{\overline{K}}_{1}\right]_{10\times10}\left\{\Delta_1\right\}_{10\times1}$ and $\left[\overline{\overline{K}}_{2}\right]_{16\times16}\left\{\Delta_2\right\}_{16\times1}$. Once the nodal force vectors $\left\{\overline{\overline{Q}}_{11}\right\}_{10\times1}$, $\left\{\overline{\overline{Q}}_{12}\right\}_{16\times1}$ are determined, the higher order derivatives at the nodal displacements can be determined as follows:

The first derivative of W_b' can be obtained as

$$W_b'(0)=\frac{N(0)}{E_bA_b}, W_b'(L)=\frac{N(L)}{E_bA_b} \tag{7.15}$$

The first derivative of θ_{yb}' can be obtained as

$$\theta_{yb}'(0)=\frac{M_{y2}(0)}{E_bI_{yybf}}, \theta_{yb}'(L)=\frac{M_{y2}(L)}{E_bI_{yybf}} \tag{7.16}$$

The first derivative of θ_{xb}' can be obtained as

$$\theta_{xb}'(0)=\frac{M_{x2}(0)}{E_bI_{xxb1}}, \theta_{xb}'(L)=\frac{M_{x2}(L)}{E_bI_{xxb1}} \tag{7.17}$$

The first derivative of ψ_b' can be obtained as

$$\psi_b'(0)=\frac{B_2(0)}{E_bI_{\omega\omega bg}}, \psi_b'(L)=\frac{B_2(L)}{E_bI_{\omega\omega bg}} \tag{7.18}$$

The second derivative of U_b'' can be obtained as

$$U_b''(0)=\frac{M_{y1}(0)}{E_bI_{ssbw}}, U_b''(L)=\frac{M_{y1}(L)}{E_bI_{ssbw}} \tag{7.19}$$

The second derivative of V'' can be obtained as

$$V''(0)=\frac{M_{x1}(0)}{E_b I_{ssbf}+E_p I_{xxp}}, V''(L)=\frac{M_{x1}(L)}{E_b I_{ssbf}+E_p I_{xxp}} \tag{7.20}$$

The second derivative of θ_z'' can be obtained as

$$\theta_z''(0)=\frac{B_1(0)}{E_b I_{\omega\omega bl}+E_p I_{\omega\omega p}}, \theta_z''(L)=\frac{B_1(L)}{E_b I_{\omega\omega bl}+E_p I_{\omega\omega p}} \tag{7.21}$$

Equations (7.15)-(7.21) are substituted into Eq. (7.14), and by setting $z=0, L$, one obtains

$$\begin{aligned}
\varepsilon_{zb}(0)=&\frac{N(0)}{E_b A_b}-x(s_b)\frac{M_{y2}(0)}{E_b I_{yybf}}-y(s_b)\frac{M_{x2}(0)}{E_b I_{xxb1}}-\omega(s_b)\frac{B_2(0)}{E_b I_{\omega\omega bg}}-n_b\sin\alpha(s_b)\frac{M_{y1}(0)}{E_b I_{ssbw}}+\\
&+n_b\cos\alpha(s_b)\frac{M_{x1}(0)}{E_b I_{ssbf}+E_p I_{xxp}}+n_b q(s_b)\frac{B_1(0)}{E_b I_{\omega\omega bl}+E_p I_{\omega\omega p}},\\
\varepsilon_{zb}(L)=&\frac{N(L)}{E_b A_b}-x(s_b)\frac{M_{y2}(L)}{E_b I_{yybf}}-y(s_b)\frac{M_{x2}(L)}{E_b I_{xxb1}}-\omega(s_b)\frac{B_2(L)}{E_b I_{\omega\omega bg}}-n_b\sin\alpha(s_b)\frac{M_{y1}(L)}{E_b I_{ssbw}}+\\
&+n_b\cos\alpha(s_b)\frac{M_{x1}(L)}{E_b I_{ssbf}+E_p I_{xxp}}+n_b q(s_b)\frac{B_1(L)}{E_b I_{\omega\omega bl}+E_p I_{\omega\omega p}}
\end{aligned} \tag{7.22}$$

From the expression of strains in Eqs.(7.22), stresses are obtained by

$$\sigma_{zb}(0)=E_b\varepsilon_{zb}(0), \sigma_{zb}(L)=E_b\varepsilon_{zb}(L) \tag{7.23}$$

7.5.2 Longitudinal Normal Stress for GFRP plate

The longitudinal normal stress for the GFRP plate is expressed under the Item 5.4.6.2 as

$$\varepsilon_{zp}=W_p'(z)-x(s_p)\theta_{yp}'(z)+n_p V''(z)+n_p x(s_p)\theta_z''(z) \tag{7.24}$$

In the present developments, no loads were assumed to act on the GFRP plate, i.e., $N_p(0)=N_p(L)=M_{yp}(0)=M_{yp}(L)=0$, such terms do not appear in the boundary terms. If one incorporates these stress resultants in the finite element solution, the following equations would arise

$$W_p'(0)=\frac{N_p(0)}{E_p A_p}, W_p'(L)=\frac{N_p(L)}{E_p A_p} \tag{7.25}$$

and

$$\theta'_{yp}(0)=\frac{M_{yp}(0)}{E_p I_{yyp}},\theta'_{yp}(L)=\frac{M_{yp}(L)}{E_p I_{yyp}} \tag{7.26}$$

The derivatives of, while $V''(z)$ can be expressed as

$$V''(0)=\frac{M_{x1}(0)}{E_b I_{ssbf}+E_p I_{xxp}},V''(L)=\frac{M_{x1}(L)}{E_b I_{ssbf}+E_p I_{xxp}} \tag{7.27}$$

The second derivative of θ_z'' can be obtained as

$$\theta_z''(0)=\frac{B_1(0)}{E_b I_{\omega\omega bl}+E_p I_{\omega\omega p}},\theta_z''(L)=\frac{B_1(L)}{E_b I_{\omega\omega bl}+E_p I_{\omega\omega p}} \tag{7.28}$$

From Eqs. (7.27)-(7.28), by substituting into Eq.(7.24), and by setting $z=0,L$, one obtains

$$\begin{aligned}
\varepsilon_{zp}(0)&=\frac{N_p(0)}{E_p A_p}-x_p\frac{M_{yp}(0)}{E_p I_{yyp}}+n_p\frac{M_{x1}(0)}{E_b I_{ssbf}+E_p I_{xxp}}+n_p x_p\frac{B_1(0)}{E_b I_{\omega\omega bl}+E_p I_{\omega\omega p}}\\
\varepsilon_{zp}(L)&=\frac{N_p(L)}{E_p A_p}-x_p\frac{M_{yp}(L)}{E_p I_{yyp}}+n_p\frac{M_{x1}(L)}{E_b I_{ssbf}+E_p I_{xxp}}+n_p x_p\frac{B_1(L)}{E_b I_{\omega\omega bl}+E_p I_{\omega\omega p}}
\end{aligned} \tag{7.29}$$

From the expression of strains in Eqs.(7.29), stresses are obtained by

$$\sigma_{zp}(0)=E_p\varepsilon_{zp}(0),\sigma_{zp}(L)=E_p\varepsilon_{zp}(L) \tag{7.30}$$

7.5.3 Shear tresses within the adhesive layer

Shear strains as expressed in Eqs. 5.19 can be expanded as

$$\begin{aligned}
\gamma_{zna}&=-c_1W_b+c_1W_p-c_3\theta_{bx}-c_2V'-c_2x\theta_z'+c_1x\theta_{yb}-c_1x\theta_{yp}+c_3x\psi_b\\
\gamma_{sna}&=-c_1U_b+c_1U_p-(c_2+c_3)\theta_z\\
\gamma_{sza}&=\left(\frac{1}{2}-\frac{n_a}{t_2}\right)U_b'+\left(\frac{1}{2}+\frac{n_a}{t_2}\right)U_p'+\left(\frac{h_b-2t_1+2t_3}{4}-\frac{h_b+2t_1+2t_3}{2t_2}n_a\right)\theta_z'+\\
&-\left(\frac{1}{2}-\frac{n_a}{t_2}\right)\theta_{yb}-\left(\frac{1}{2}+\frac{n_a}{t_2}\right)\theta_{yp}-\left(\frac{1}{2}-\frac{n_a}{t_2}\right)\frac{h_b}{2}\psi_b
\end{aligned} \tag{7.31}$$

At both element ends, one has

$$\gamma_{zna}(0) = -c_1 W_b(0) + c_1 W_p(0) - c_3\theta_{bx}(0) - c_2 V'(0) - c_2 x\theta_z'(0) + c_1 x\theta_{yb}(0) - c_1 x\theta_{yp}(0) + c_3 x\psi_b(0)$$
$$\gamma_{sna}(0) = -c_1 U_b(0) + c_1 U_p(0) - (c_2 + c_3)\theta_z(0)$$
$$\gamma_{sza}(0) = \left(\frac{1}{2} - \frac{n_a}{t_2}\right)U_b'(0) + \left(\frac{1}{2} + \frac{n_a}{t_2}\right)U_p'(0) + \left(\frac{h_b - 2t_1 + 2t_3}{4} - \frac{h_b + 2t_1 + 2t_3}{2t_2}n_a\right)\theta_z'(0) +$$
$$-\left(\frac{1}{2} - \frac{n_a}{t_2}\right)\theta_{yb}(0) - \left(\frac{1}{2} + \frac{n_a}{t_2}\right)\theta_{yp}(0) - \left(\frac{1}{2} - \frac{n_a}{t_2}\right)\frac{h_b}{2}\psi_b(0)$$

(7.32)

and

$$\gamma_{zna}(L) = -c_1 W_b(L) + c_1 W_p(L) - c_3\theta_{bx}(L) - c_2 V'(L) - c_2 x\theta_z'(L) + c_1 x\theta_{yb}(L) - c_1 x\theta_{yp}(L) + c_3 x\psi_b(L)$$
$$\gamma_{sna}(L) = -c_1 U_b(L) + c_1 U_p(L) - (c_2 + c_3)\theta_z(L)$$
$$\gamma_{sza}(L) = \left(\frac{1}{2} - \frac{n_a}{t_2}\right)U_b'(L) + \left(\frac{1}{2} + \frac{n_a}{t_2}\right)U_p'(L) + \left(\frac{h_b - 2t_1 + 2t_3}{4} - \frac{h_b + 2t_1 + 2t_3}{2t_2}n_a\right)\theta_z'(L) +$$
$$-\left(\frac{1}{2} - \frac{n_a}{t_2}\right)\theta_{yb}(L) - \left(\frac{1}{2} + \frac{n_a}{t_2}\right)\theta_{yp}(L) - \left(\frac{1}{2} - \frac{n_a}{t_2}\right)\frac{h_b}{2}\psi_b(L)$$

(7.33)

The displacement fields $W_b(Z_e), W_p(Z_e), \theta_{xb}(Z_e), V'(Z_e), \theta_z'(Z_e), \theta_{yb}(Z_e), \theta_{yp}(Z_e), \psi_b$, $U_b'(Z_e)$, $U_b(Z_e)$, $U_p(Z_e), \theta_z(Z_e)$ with $Z_e = 0, L$ are determined from finite element solution. The value of $U_p'(Z_e)$ is determined based on boundary condition 5.59 and 5.60, i.e.,

$$U_p'(0) = \frac{Q_{xp}(0)}{(G_p A_p + G_a A_a/3)} + \theta_{yp}(0) - \frac{G_a A_a}{12(G_p A_p + G_a A_a/3)}\left(2U_b'(0) - 2\theta_{yb}(0) + c_5\theta_z'(0) - h_b\psi_b(0)\right)$$

$$U_p'(L) = \frac{Q_{xp}(L)}{(G_p A_p + G_a A_a/3)} + \theta_{yp}(L) - \frac{G_a A_a}{12(G_p A_p + G_a A_a/3)}\left(2U_b'(L) - 2\theta_{yb}(L) + c_5\theta_z'(L) - h_b\psi_b(L)\right)$$

CHAPTER 8-VALIDATION OF RESULTS FOR SHEAR-DEFORMABLE THEORY

8.1. Introduction

This chapter aims to assess the validity of the shear-deformable theory developed in Chapter 5, the finite difference solution developed in Chapter 6 and the finite element solution developed in Chapter 7. Three examples for composite systems are considered. These are:

1) A simply supported beam under uniformly distributed transverse load.
2) A cantilever subject to lateral tractions τ_v acting at both surfaces of beam flange sections at tip, inducing primarily weak axis bending.
3) A cantilever subject to equal and opposite lateral tractions τ_v acting at both surfaces of beam flange sections at tip, inducing primarily twisting.

These problems have been investigated in Chapter 4 based on non-shear deformation theory developed in Chapters 2 and 3 and 3D FEA analyses under ABAQUS. The objective of the present chapter is to quantify the improvement realized by incorporating shear deformation effects under the shear deformable theory developed in Chapters 5, 6 and 7.

8.2. Example 1-Simply supported beam

8.2.1 Statement of the Problem

The composite beam as described in the statement of Problem 2 in Chapter 4 is used, i.e., the wide flange beam section is W150x13 and the GFRP plate has a thickness $t_1 = 19mm$ and a width $b_p = 100mm$, while adhesive has a thickness $t_2 = 0.79mm$. Modulus of elasticity of steel is $E_s = 200GPa$ while that of GFRP is $E_p = 42GPa$. Shear modulus of adhesive is $G_a = 0.4GPa$ - corresponding to a low shear modulus adhesive type. Poisson's ratio of all three materials μ is 0.3. Transversely, the wide flange beam is simply supported. Longitudinally, the end $z = 0$ of the beam axis is restrained while at $z = L$, it is axially movable. Both ends of the GFRP plate are longitudinally free. The beam is subjected to a uniform pressure $p_u = 0.15\, N/mm^2$ applied to the un-reinforced flange surface. It is required to compare the displacements and stresses as predicted by the present theory, to those predicted by the non-shear deformable theory, and the 3D FEA analysis of Abaqus.

8.2.2 Present Finite Difference Solution

The finite difference discretized form of the four governing equilibrium equations of the longitudinal-transverse response was provided in Section 6.2. The load terms appearing in the right hand side of Field equations 6.2, 6.4, and 6.5 are $q_{z(i)} = 0$, $q_{y(i)} = q$, $m_{xb(i)} = 0$ in which $i = 1, 2, \ldots, (n+1)$. They involve $4(n+1)+10$ unknown displacements, n being the number of subdivisions taken in the problem. The four field equations are applied at $(n+1)$ points, resulting in $4(n+1)$ algebraic equations. The remaining 10 equations are obtained by writing the discretized form of the 10 boundary conditions of the problem. For the simply supported beam in this example, these equations are provided in Table 8.1.

Table 8.1. Discretized form of boundary conditions for example 1

$W_{b(1)} = 0$ (8.1)	$-\left(\frac{E_b A_b}{2\Delta}\right) W_{b(n)} + \left(\frac{E_b A_b}{2\Delta}\right) W_{b(n+2)} = 0$ (8.2)
$\frac{E_p A_p}{2\Delta}\left[-W_{p(0)} + W_{p(2)}\right] = 0$ (8.3)	$\frac{E_p A_p}{2\Delta}\left[-W_{p(n)} + W_{p(n+2)}\right] = 0$ (8.4)
$V_{(1)} = 0$ (8.5)	$V_{(n+1)} = 0$ (8.6)
$\left(\frac{E_b I_{ssbf} + E_p I_{xxp}}{\Delta^2}\right)\left[V_{(0)} - 2V_{(1)} + V_{(2)}\right] = 0$ (8.7)	$\left(\frac{E_b I_{ssbf} + E_p I_{xxp}}{\Delta^2}\right)\left[V_{(n)} - 2V_{(n+1)} + V_{(n+2)}\right] = 0$ (8.8)
$\frac{E_b I_{xxb1}}{2\Delta}\left(-\theta_{xb(0)} + \theta_{xb(2)}\right) = 0$ (8.9)	$\frac{E_b I_{xxb1}}{2\Delta}\left(-\theta_{xb(n)} + \theta_{xb(n+2)}\right) = 0$ (8.10)

Stresses and strains within the composite beam are determined based on Eqs.6.16-6.23, i.e.,

$$\begin{aligned}\varepsilon_{zb(i)} = &\left[-\frac{1}{2\Delta}W_{b(i-1)} + \frac{1}{2\Delta}W_{b(i+1)}\right] + \left[\frac{1}{\Delta^2}V_{(i-1)} - \frac{2}{\Delta^2}V_{(i)} + \frac{1}{\Delta^2}V_{(i+1)}\right] n_b \cos\alpha(s_b) \\ &-\left[-\frac{1}{2\Delta}\theta_{xb(i-1)} + \frac{1}{2\Delta}\theta_{xb(i+1)}\right] y(s_b)\end{aligned} \tag{8.11}$$

$$\varepsilon_{zp(i)} = \left[-\frac{1}{2\Delta}W_{p(i-1)} + \frac{1}{2\Delta}W_{p(i+1)}\right] + \left[\frac{1}{\Delta^2}V_{(i-1)} - \frac{2}{\Delta^2}V_{(i)} + \frac{1}{\Delta^2}V_{(i+1)}\right] n_p \tag{8.12}$$

$$\gamma_{zna(i)} = -c_1 W_{b(i)} + c_1 W_{p(i)} - c_2\left[-\frac{1}{2\Delta}V_{(i-1)} + \frac{1}{2\Delta}V_{(i+1)}\right] - c_3\theta_{xb(i)}$$
$$\gamma_{sna(i)} = \gamma_{sza(i)} = 0 \tag{8.13}$$

Expression for stress fields is

$$\sigma_{zb(i)} = E_b \varepsilon_{zb(i)}, \sigma_{zp(i)} = E_p \varepsilon_{zp(i)}, \tau_{zna(i)} = G_a \gamma_{zna(i)} \tag{8.14}$$

8.2.3 Present Finite Element Solution

By computing $q_{yb}(z) = q = \int_{s_b}\left[-p_u(s_b, n_b, z)\cos\alpha(s_b)\right]ds_b = -pb_b$ in Eq.5.30, the load vector is determined as $\left\langle \overline{\overline{Q}}_{21} \right\rangle^T_{1\times10} = \left\langle \langle 0\rangle^T_{1\times2} \; \middle| \; \langle 0\rangle^T_{1\times2} \; \middle| \; \left\langle \frac{qL}{2} \quad \frac{qL^2}{12} \quad \frac{qL}{2} \quad -\frac{qL^2}{12} \right\rangle_{1\times4} \; \middle| \; \langle 0\rangle^T_{1\times2} \right\rangle$.

Based on nodal displacement vector obtained from the finite element solution, the strains and stresses at two nodes of each element can be obtained as presented under Item 7.5.

8.2.4 Mesh sensitivity for finite difference and finite element solutions

Table 8.2 shows the convergence of the finite difference solution developed under Item 8.2.2. As observed, the deflection and stresses converge when 400 finite difference subdivisions are taken. The converged results differ from those based on the 3D FEA results. The meshing details of the 3D FEA were provided in Section 4.3.3. The difference in displacements is 1.1%, while that of stress are observed to agree within four significant digits.

Table 8.2. Mesh sensitivity of finite difference solution for example 1

Number of subdivisions	Deflection at mid-span (mm)	Longitudinal normal stress at top surface of upper flange (MPa)
100	-9.87	-185.17
200	-9.93	-186.22
300	-9.94	-186.42
400	-9.94	-186.54
500	-9.94	-186.55
3D FEA	-10.05	-186.57

For the same problem, the finite element formulation developed in Chapter 7 is used in the present example. Four finite element meshes are examined based on 10, 20, 30, and 40 elements and the results are presented in Table 8.3. Displacements and stresses are observed to converge with 30 elements. Again, when comparing to 3D FEA results, the difference in displacements is 1.1% between the present finite element formulation and that based on the 3D FEA analysis, while stresses are observed to agree within four significant digits.

It is noted that the FEA formulation presented in chapter 7 achieves convergence with significantly fewer degrees of freedom than the finite difference solution, which in turn has significantly less degrees of freedom than the 3D FEA in Abaqus.

Table 8.3. Mesh sensitivity of finite element solution for Problem 1

Number of elements	Deflection at mid-span(mm)	Longitudinal normal stress at top surface of upper flange (MPa)
10	-9.87	-186.42
20	-9.92	-186.54
30	-9.94	-186.56
40	-9.94	-186.56
3D FEA	-10.05	-186.57

8.2.5 Results

Figure 8.1 provides the transverse displacements obtained from the shear deformable theory, the non-shear deformable theory and ABAQUS as a function of the longitudinal-coordinate z. While the non-shear deformable theory has provided transverse displacement predictions in very good agreement with 3D FEA under Abaqus, the present shear deformable theory provides even better predictions. The maximum transverse displacement of shear deformable theory is -9.94mm, while that of ABAQUS model is -10.05mm, corresponding to a 1.1% difference. One recalls that the maximum displacement as predicted by the non-shear deformable theory is -9.60mm, corresponding to a difference of 4.6% from Abaqus. As discussed in Example 1 of Chapter 4, the difference is in part caused by the simplifying assumption of linear displacement within the adhesive layer.

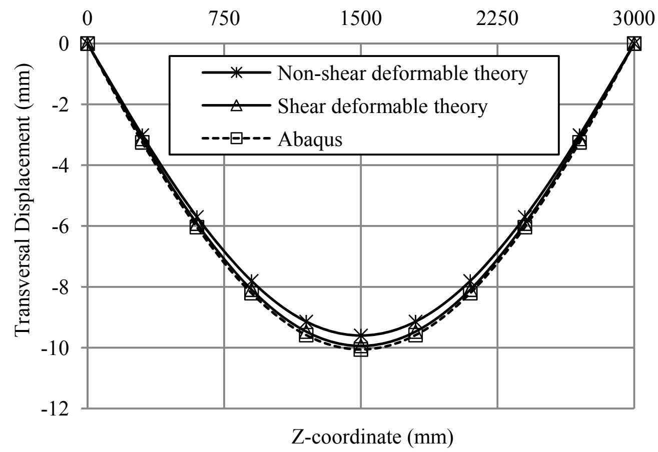

Figure 8.1 Transversal displacements against z coordinates

Figures 8.2a-c show the longitudinal normal stress distribution along the longitudinal coordinate z at top surface of the upper flange, and at the bottom surface of lower flange and at the bottom surface of GFRP plate, respectively. Figure 8.2d shows the shear stress τ_{nz} averaged over the width of the adhesive layer. The normal stresses show an excellent match between all three solutions. For the shear stress τ_{nz} within the adhesive layer, very good agreement is obtained except in the end regions where the localized stress distributions captured in the FEA are not captured within the two formulations in the present study. In these regions, the shear-deformable theory predicts slightly higher shear stress values than the non-shear deformable theory.

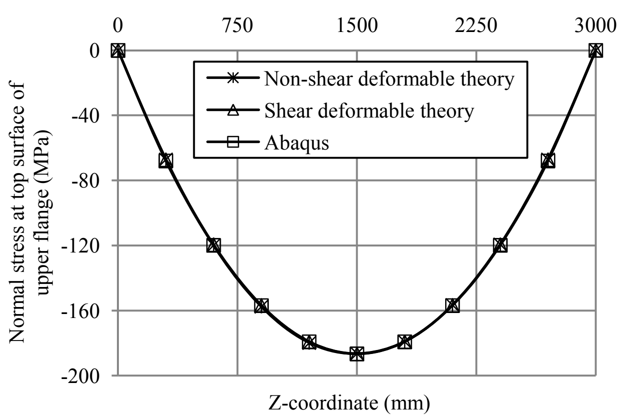

a)

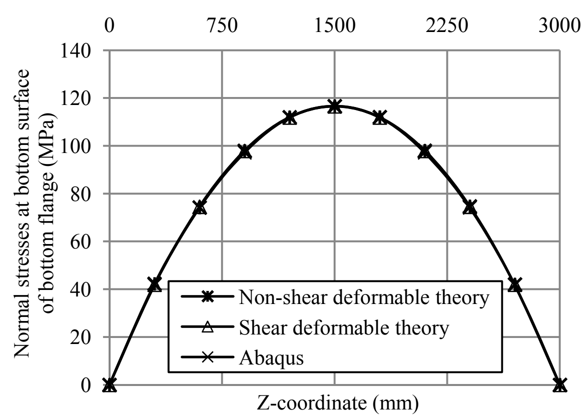

b)

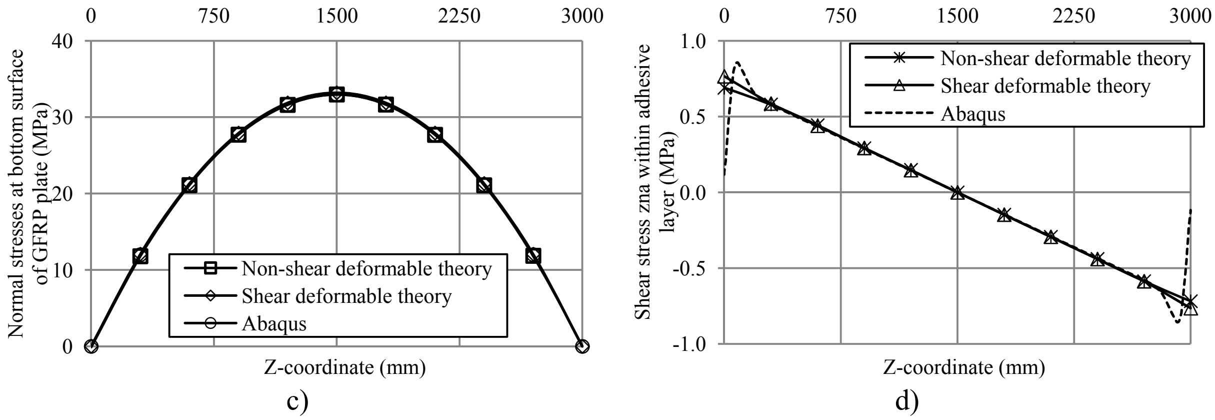

Figure 8.2 Comparison of results for simply-supported beam under uniformly distributed transverse tractions (*a*) normal stresses σ_{zb} at top surface of upper flange of wide flange beam, (*b*) normal stresses σ_{zb} at bottom surface of bottom flange of wide flange beam, (*c*) normal stresses σ_{zp} at bottom surface of the FRP plate, and (*d*) average shear tress τ_{nz} at the adhesive-FRP interface.

8.3. Example 2-Centilever under bending about weak axis

8.3.1 Statement of the Problem

The composite beam as described in the statement of Problem 3 in Chapter 4 is used, i.e., a 5m span cantilever composite beam consists of a W410x85 beam (flange width $b_b = 181mm$, flange thickness $t_3 = 18.2mm$, depth $d = 417mm$ and web thickness $t_w = 10.9mm$) that is reinforced by a GFRP plate over the whole span. The GFRP plate has a thickness $t_1 = 19mm$ and a width $b_p = 181mm$, while the adhesive has a thickness $t_2 = 2mm$. Modulus of elasticity of steel is $E_s = 200GPa$ while that of GFRP is $E_p = 42GPa$. The shear modulus of the adhesive is $G_a = 0.4GPa$ -corresponding to a low shear-modulus adhesive type (Table 1.1, Chapter 1). Poisson's ratio of all three materials μ is 0.3. The cantilever is subjected to two lateral tractions $p_v = 1821.83\,kN/m^2$ acting in the X-positive direction on two steel flange surfaces at the tip so as to create a total lateral resultant force $Q_x = 12kN$ at the beam centroid. It is required to compare the displacements and stresses as predicted by the present theory, to those predicted by the non-shear deformable theory, and the 3D FEA analysis of Abaqus.

8.3.2 Present Finite Difference Solution

The finite difference discretized form of the six governing equilibrium equations in the lateral-torsional response was provided in Section 6.3. The load terms appearing in the right hand side of the field equations 6.24, 6.26, 6.28, and 6.29 are $q_{x(i)} = m_{yb(i)} = m_{(i)} = b_{(i)} = 0$ in which $i = 1, 2, \ldots, (n+1)$. They involve $6(n+1)+16$ unknown displacements, n being the number of subdivisions taken in the problem. The six field equations are applied at $6(n+1)$ points, resulting in $6(n+1)$ algebraic equations. The remaining 16 equations are obtained by writing the discretized form of the 16 boundary conditions for the problem. For a cantilever beam, these equations are provided in following equations (Eqs. (8.15)-(8.30)).

$$U_{b(1)} = 0 \tag{8.15}$$

$$\begin{aligned}
&\left(\frac{E_b I_{ssbw}}{2\Delta^3}\right)U_{b(n-1)} - \left(\frac{E_b I_{ssbw}}{\Delta^3} + \frac{G_b A_{bf}}{\Delta} + \frac{G_a A_a}{6\Delta}\right)U_{b(n)} + \left(\frac{E_b I_{ssbw}}{\Delta^3} + \frac{G_b A_{bf}}{\Delta} + \frac{G_a A_a}{6\Delta}\right)U_{b(n+2)} \\
&-\left(\frac{E_b I_{ssbw}}{2\Delta^3}\right)U_{b(n+3)} - \left(\frac{G_a A_a}{12\Delta}\right)U_{p(n)} + \left(\frac{G_a A_a}{12\Delta}\right)U_{p(n+2)} - \left(\frac{G_a A_a}{3} + 2G_b A_{bf}\right)\theta_{yb(n+1)} \\
&-\left(\frac{G_a A_a}{6}\right)\theta_{yp(n+1)} - \left(\frac{c_4 G_a A_a}{12\Delta}\right)\theta_{z(n)} + \left(\frac{c_4 G_a A_a}{12\Delta}\right)\theta_{z(n+2)} - \left(\frac{h_b G_a A_a}{6}\right)\psi_{b(n+1)} - Q_{x(n+1)} = 0
\end{aligned} \tag{8.16}$$

$$\frac{1}{2\Delta}\left[-U_{b(0)} + U_{b(2)}\right] = 0 \tag{8.17}$$

$$\frac{E_b I_{ssbw}}{\Delta^2}\left(U_{b(n)} - 2U_{b(n+1)} + U_{b(n+2)}\right) - M_{y1(n+1)} = 0 \tag{8.18}$$

$$U_{p(1)} = 0 \tag{8.19}$$

$$\begin{aligned}
&-\left(\frac{G_a A_a}{12\Delta}\right)U_{b(n)} + \left(\frac{G_a A_a}{12\Delta}\right)U_{b(n+2)} - \left(\frac{G_p A_p}{2\Delta} + \frac{G_a A_a}{6\Delta}\right)U_{p(n)} + \left(\frac{G_p A_p}{2\Delta} + \frac{G_a A_a}{6\Delta}\right)U_{p(n+2)} - \left(\frac{G_a A_a}{6}\right)\theta_{yb(n+1)} \\
&-\left(G_p A_p + \frac{G_a A_a}{3}\right)\theta_{yp(n+1)} - \left(\frac{c_5 G_a A_a}{24\Delta}\right)\theta_{z(n)} + \left(\frac{c_5 G_a A_a}{24\Delta}\right)\theta_{z(n+2)} - \left(\frac{h_b G_a A_a}{12}\right)\psi_{(n+1)} = 0
\end{aligned} \tag{8.20}$$

$$\theta_{yb(1)} = 0 \tag{8.21}$$

$$\frac{E_b I_{yybf}}{2\Delta}\left(-\theta_{yb(n)} + \theta_{yb(n+2)}\right) - M_{y2(n+1)} = 0 \tag{8.22}$$

$$\theta_{yp(1)} = 0 \tag{8.23}$$

$$\frac{E_p I_{yyp}}{2\Delta}\left(-\theta_{yp(n)} + \theta_{yp(n+2)}\right) = 0 \tag{8.24}$$

$$\theta_{z(1)} = 0 \tag{8.25}$$

$$-\left(\frac{c_4 G_a A_a}{12\Delta}\right)U_{b(n)} + \left(\frac{c_4 G_a A_a}{12\Delta}\right)U_{b(n+2)} - \left(\frac{c_5 G_a A_a}{24\Delta}\right)U_{p(n)} + \left(\frac{c_5 G_a A_a}{24\Delta}\right)U_{p(n+2)}$$

$$-\left(c_1 c_2 G_a I_{yya} + \frac{c_4 G_a A_a}{6}\right)\theta_{yb(n+1)} + \left(c_1 c_2 G_a I_{yya} - \frac{c_5 G_a A_a}{12}\right)\theta_{yp(n+1)} + \left(\frac{E_b I_{\omega\omega bl} + E_p I_{\omega\omega p}}{2\Delta^3}\right)\theta_{z(n-1)}$$

$$-\left(\frac{E_b I_{\omega\omega bl}}{\Delta^3} + \frac{G_b J_b}{2\Delta} + \frac{E_p I_{\omega\omega p}}{\Delta^3} + \frac{G_p J_p}{2\Delta} + \frac{c_2^2 G_a I_{yya}}{2\Delta} + \frac{c_6 G_a A_a}{24\Delta}\right)\theta_{z(n)}$$

$$+\left(\frac{E_b I_{\omega\omega bl}}{\Delta^3} + \frac{G_b J_b}{2\Delta} + \frac{E_p I_{\omega\omega p}}{\Delta^3} + \frac{G_p J_p}{2\Delta} + \frac{c_2^2 G_a I_{yya}}{2\Delta} + \frac{c_6 G_a A_a}{24\Delta}\right)\theta_{z(n+2)} - \left(\frac{E_b I_{\omega\omega bl} + E_p I_{\omega\omega p}}{2\Delta^3}\right)\theta_{z(n+3)}$$

$$-\left(c_2 c_3 G_a I_{yya} + \frac{h_b^2}{4} G_b A_{bf} + \frac{c_4 h_b G_a A_a}{12}\right)\psi_{(n+1)} - T_{(n+1)} = 0$$

(8.26)

$$\frac{1}{2\Delta}\left[-\theta_{z(0)} + \theta_{z(1)}\right] = 0 \tag{8.27}$$

$$\frac{E_b I_{\omega\omega bl} + E_p I_{\omega\omega p}}{\Delta^2}\left(\theta_{z(n)} - 2\theta_{z(n+1)} + \theta_{z(n+2)}\right) - B_{1(n+1)} = 0 \tag{8.28}$$

$$\psi_{b(1)} = 0 \tag{8.29}$$

$$\frac{E_b I_{\omega\omega bg}}{2\Delta}\left(-\psi_{b(n)} + \psi_{b(n+2)}\right) - B_{2(n+1)} = 0 \tag{8.30}$$

The load terms in equations (6.24)-(6.29) are $q_{x(i)} = m_{yb(i)} = m_{(i)} = b_{(i)} = 0$ in which $i = 1, 2, \ldots, (n+1)$. Load terms in the boundary equations (8.15)-(8.30) are $M_{y1(n+1)} = M_{y2(n+1)} = T_{(n+1)} = B_{1(n+1)} = B_{2(n+1)} = 0$ and $Q_{x(n+1)} = 12kN$.

Stresses and strains within the composite beam are determined based on Eqs.6.46-6.53 in Chapter 6.

8.3.3 Present Finite Element Solution

The finite element solution for the lateral-torsional response was developed under Item 7.4, in which the load vector is set to

$$\left\langle \overline{\overline{Q}}_{12} \right\rangle_{1\times16}^{T} = \langle 0 \quad 0 \quad Q_x(L) \quad 0 \mid 0 \quad 0 \mid 0 \quad 0 \mid 0 \quad 0 \mid 0 \quad 0 \quad 0 \quad 0 \mid 0 \quad 0 \rangle$$

where $Q_x(L) = 12kN$. Based on the nodal displacement vector obtained from the finite element solution, the strains and stresses at two nodes of each element can be obtained as presented under Item 7.5.

8.3.4 Mesh sensitivity for finite difference and finite element solutions

Table 8.4 shows the convergence of the finite difference solution developed under Item 8.3.2. As observed, the displacements and stresses converge for the solution based on 200 subdivisions. Further refinements are observed to be unnecessary. When comparing the converged displacements to those based on the 3D FEA, the difference of displacement is 0.1%, while that of the longitudinal normal stress at mid-height of the left edge of bottom flange at the fixed end is 14.6%. However, the point at the fixed end in the 3D FEA is a singularity point where the normal stress is always increased when mesh is finer. This problem has been discussed in Example 1 of Chapter 4. The contour of the longitudinal normal stress distribution within a part of bottom flange near the fixed end of the cantilever is shown in Fig. 8.3. Another comparison of the normal stress is taken at longitudinal coordinate $z = 0.06m$ (near the fixed end) shows that the difference between two solutions is 3.6%. Further discussion of the normal stress distribution is being presented under Item 8.3.5.

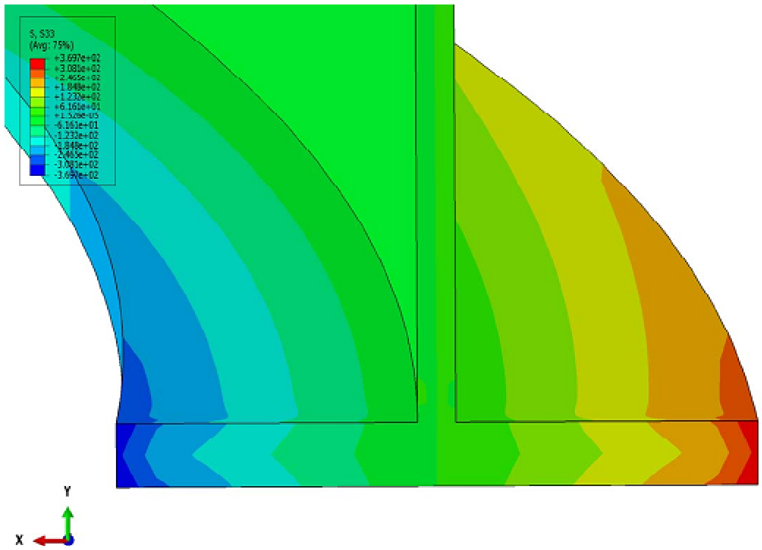

Figure 8.3 Contour of longitudinal normal stress from the fixed end of the bottom flange

Table 8.4. Mesh sensitivity for finite difference solution for Problem 2

Number of subdivisions	U_b at tip (mm)	Longitudinal normal stress at mid-hight of the left edge of upper flange (MPa)
30	129.7	280.1
50	128.1	279.9
100	126.1	278.5
200	125.4	278.3
300	125.4	278.3
3D FEA	125.5	325.7

Table 8.5 shows the results of a convergence study for the finite element solution. Meshes based on 20, 40, 80, 160, and 320 elements were attempted. As observed, the160-element solution attains convergence. When compared to 3D FEA results, the difference of displacement is 0.1%, while that of the longitudinal normal stress at mid-height of the left edge of bottom flange at the fixed end is 14.5%. The reason of the high difference of the normal stress has been discussed in previous paragraph. Another comparison of the normal stress is taken at longitudinal coordinate $z = 0.06m$ (near the fixed end) shows that the difference between two solutions is 3.5%.

Table 8.5. Mesh sensitivity of finite element solution for Problem 2

Number of elements	U_b at tip (mm)	Longitudinal normal stress at mid-point, left edge of upper flange (MPa)
20	111.3	274.0
40	122.7	276.5
80	124.7	277.7
160	125.1	278.4
320	125.3	278.6
3D FEA	125.45	325.7

8.3.5 Results

Figure 8.4 provides a comparison of the lateral displacements based on i) the present study, ii) the non-shear deformable theory, and iii) the 3D FEA analysis in Abaqus. Figure8.4a shows the lateral displacement at the wide flange beam centroid as a function of the longitudinal coordinate z. Figure 8.4b shows the lateral displacement at the GFRP centroid. Figure 8.4c shows the lateral displacement at the bottom flange centroid while Fig.8.4d shows the lateral displacement at the top flange centroid. While the non-shear deformable theory was shown to provide lateral displacement predictions in very good agreement with 3D FEA under Abaqus, the present shear deformable theory provides even predictions.

The maximum lateral displacement at the beam centroid of shear deformable theory is 125.3 mm, while that of ABAQUS model is 125.5mm, corresponding to a 0.1% difference. One recalls that the maximum displacement as predicted by the non-shear deformable theory is 125.1 mm, corresponding to a difference of 0.4% from Abaqus. As discussed in Example 3 of Chapter 4, the difference is in part caused by the simplifying assumption of linear displacement within the adhesive layer. As discussed in Section 4.4.5, the effect of twisting in this problem is very small and negligible. This is evidenced by the fact that the maximum displacement at the bottom flange of 126.9 mm is marginally higher than that of the top flange (123.7 mm). This slight difference is expected since the presence of the GFRP plate above the top flange introduces some asymmetry about the steel section centroid, and although the applied loading is symmetric with respect to the centroid of the steel cross-section, the response turns out to be slightly unsymmetrical.

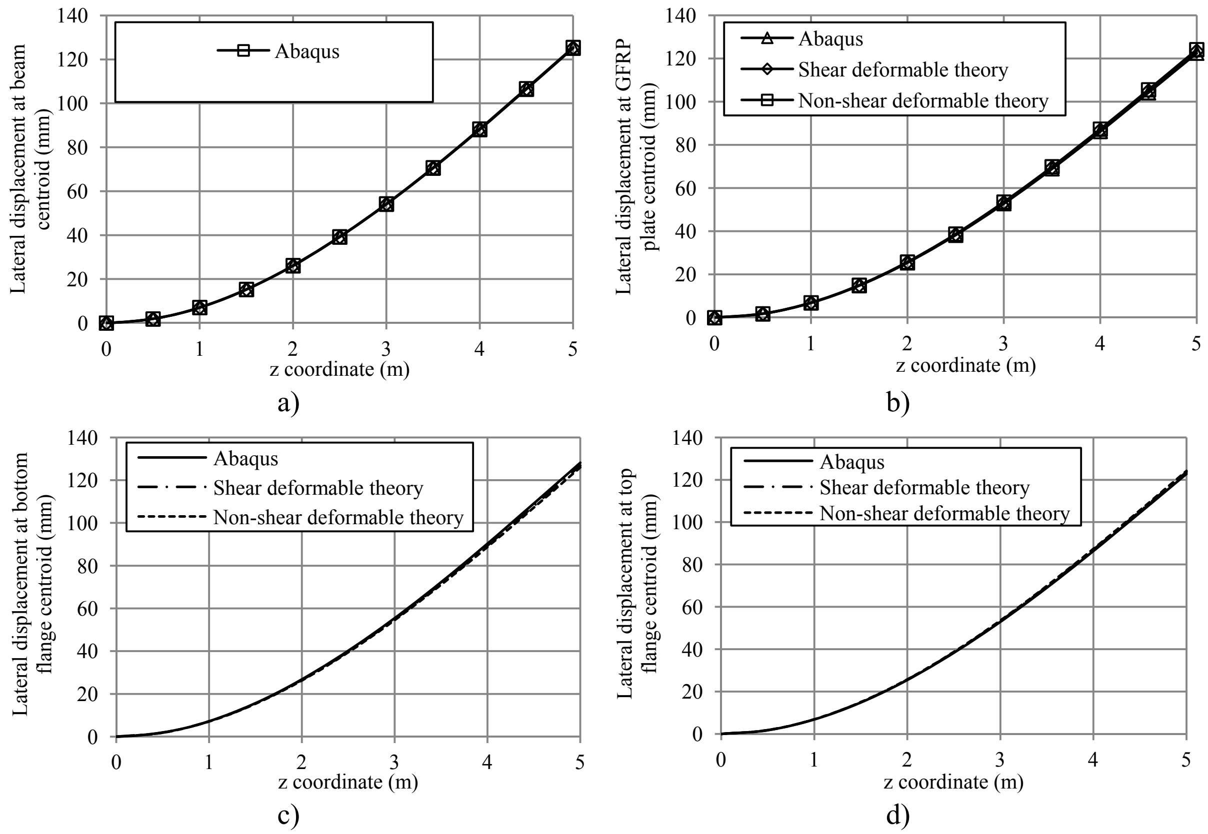

Figure 8.4 Displacement comparison for cantilever under bending about weak axis (*a*) lateral displacement at wide flange beam centroid, (*b*) lateral displacement at GFRP plate centroid, (*c*) lateral displacement at bottom flange centroid, (*d*) lateral displacement at top flange centroid.

Figures 8.5 a-b show the longitudinal normal stress distribution along the longitudinal coordinate z at the mid-height point of the left edge of the bottom flange, and at the top point of the left edge of the GFRP plate, respectively. As discussed in Example 1, the stress at singularity points located at the restrained ends of the composite always increases as the mesh is refined. With the exception of these singularity points, the stresses are observed to match well between the two solutions. The maximum difference between the normal stresses predictions is 4.2%, located at the top point of left edge of GFRP plate at the longitudinal coordinate $z = 0.06m$. Figure 8.5c provides the average shear stress τ_{sz} over the adhesive layer width, while Fig.8.5d shows the average shear stress τ_{sn} over the adhesive layer width. As discussed in Chapter 4, the non-shear deformable theory fails to predict these shear stresses. In this Chapter, when the shear-deformable theory is applied, the average shear stresses are much closer to those obtained from the FE analysis in ABAQUS. The maximum difference between the average shear stress τ_{sz} is as predicted by the two solutions is 18.2% which occurs at a longitudinal coordinate value $z = 500mm$, while that of average shear stress τ_{sn} is 35.0% which occurs at the tip. Except at these locations of stress localization, the average shear stresses predicted by the present theory agree well with those predicted by the Abaqus 3D FEA solution.

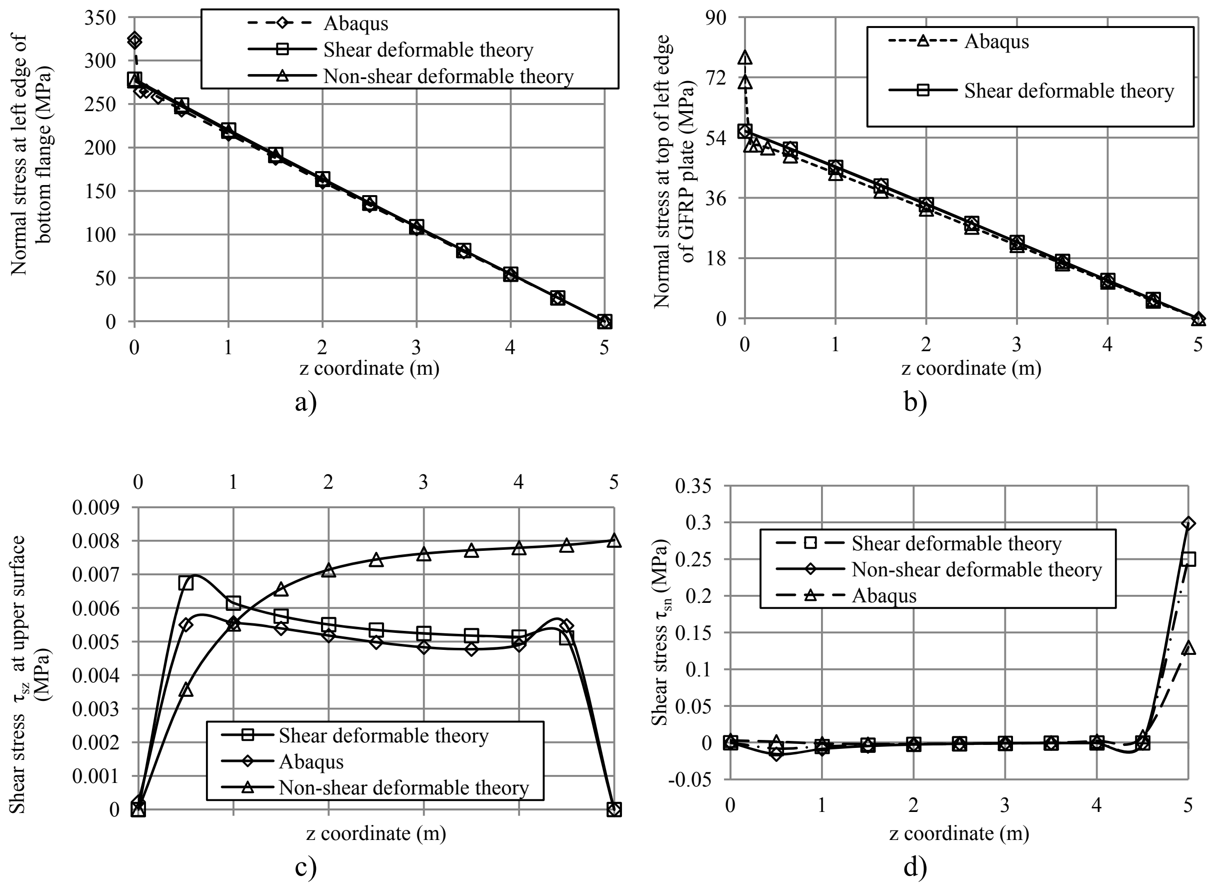

Figure 8.5 Stress comparison for cantilever under bending about weak axis: *a*) longitudinal normal stress at middle point of left edge of bottom flange, *b*) longitudinal normal stress at top point of left edge of GFRP plate, *c*) average shear stress τ_{sz} along the beam, *d*) average shear tress τ_{sn} within adhesive layer.

8.4. Example 3-Twisting problem

8.4.1. Twisting response of a beam with no GFRP plate

8.4.1.1. Statement of the problem

A cantilever has a 5m span. Its cross section is W410x85 (flange width $b_b = 181mm$, flange thickness $t_3 = 18.2mm$, depth $d = 417mm$ and web thickness $t_w = 10.9mm$). The modulus of elasticity of steel is $E_s = 200GPa$. The beam is subject to a twisting moment $T = 3.271kNm$ acting at the tip, which is induced by applying two opposite shear tractions $\tau_v = 2490kN/m^2$ at bottom and upper flange surfaces at the cantilever tip.

It is required to compare the (i) twisting angle, and (ii) longitudinal normal stress fields along the beam at mid-height left edge of the bottom flange by using the finite difference solution developed in Chapters 6, the finite element solution developed in Chapter 7, and the 3D FEA in ABAQUS.

8.4.1.2. Closed form solution based on Vlasov's theory

For a cantilever under of span L subject to a twisting moment T, acting at the tip, the twisting angle based on Vlasov's theory is determined by

$$\theta(z) = -\frac{T}{kGJ}\left[\tanh kL\left(1-\cosh kz\right)+\left(\sinh kz - kz\right)\right] \tag{8.31}$$

in which $k = \sqrt{GJ/EI_{\omega\omega}}$. In this example, $I_{\omega\omega} = 7.19E+11mm^6$ and $G = E/2\left(1+\mu\right) = 76.9GPa$. The value of the Saint-Venant constant J_e as determined based on the theory of elasticity (e.g. "Highly Flexible Structures, Modelling, computation and experimentation" by Pai (2007)) is determined by

$$J_e = \sum_{i=1,2,3}\frac{1}{3}b_i h_i^3\left(1-\frac{192h_i}{\pi^5 b_i}\sum_{n=1,3,...}^{\infty}\frac{1}{n^5}\tanh\frac{n\pi b_i}{2h_i}\right) = 845,100mm^4 \tag{8.32}$$

It is noted that the above value is slightly smaller than that based on the approximate value arising in Gjelsvik theory J, i.e,

$$J = \sum_{i=1,2,3}\frac{1}{3}b_i h_i^3 = 891,700mm^4 \tag{8.33}$$

Results based on both values are to be examined.

8.4.1.3 Solutions based on finite difference and finite element solutions

The above problem can be solved by setting $t_1 = t_2 = G_a = G_p = 0$ in the governing field equations based on the finite difference solution and the finite element solution developed in Chapters 6 and 7.

The finite difference solution for the cantilever is presented under the Item 8.3.2 with a change of load. The load terms in Eqs. (6.24)-(6.29) are $q_{x(i)} = m_{yb(i)} = m_{(i)} = b_{(i)} = 0$, respectively in which $i = 1, 2, \ldots, (n+1)$. Also, the load terms in the boundary Eqs. (8.15)-(8.30) are $M_{y1(n+1)} = M_{y2(n+1)} = Q_{x(n+1)} = B_{1(n+1)} = B_{2(n+1)} = 0$, and $T_{(n+1)} = 3.271 kNm$. Stresses and strains within the beam are determined based on Eqs. 6.46-6.53. By performing mesh sensitivity similar to that performed in Example 2, displacement and stress are observed to converge for 200 subdivisions.

Solution based on the finite element solution developed in Section 7.4 is used, in which the load vector for the problem is taken as $\left\langle \overline{\overline{Q}}_{12} \right\rangle^T_{1\times16} = \langle 0 \quad 0 \quad 0 \quad 0 \,\vdots\, 0 \quad 0 \,\vdots\, 0 \quad 0 \,\vdots\, 0 \quad 0 \,\vdots\, 0 \quad 0 \quad T \quad 0 \,\vdots\, 0 \quad 0 \rangle$ where

$T = 3.271 kNm$. Stresses and strains within the beam are determined based on the procedure developed under Section 7.5. By performing a mesh sensitivity analysis similar to that performed in Example 2, displacements and stresses are observed to converge for a 160-element mesh.

8.4.1.4 3D finite element model

The 8-node brick element C3D8R is also selected for FEA performed in ABAQUS. Displacements and stresses are converged for the mesh $n_1 = 20, n_2 = 4, n_3 = 70, n_4 = 4, n_7 = 3120$. Singularity points appear at the fixed end as discussed in Example 1 of Chapter 4.

8.4.1.5 Results

Figure 8.6 provides the angle of twist (*rad*) along the longitudinal coordinate z as obtained from the 3D FEA performed under ABAQUS. Overlaid on the same plot is the solution based on the Vlasov theory based on the value of J_e, and that based on J for comparison.

The twisting angle in the FE analysis is obtained by dividing the difference of lateral displacement between the top flange centroid and bottom flange centroid by the section depth between the two flange centroids. The angle of twist obtained from finite difference/ finite element solutions based on the shear-deformable theory and the angle of twist obtained based on Eq. 8.31 are observed to be nearly identical. This is a natural outcome of the fact that shear deformation (captured in the present shear deformable theory but not captured in the Vlasov theory) has a negligible effect for such a long span cantilever. As observed in Fig. 8.6, the maximum difference between the twisting angle based on the shear deformable theory based on the approximate Saint Venant expression J and ABAQUS is 11.9%, while that between based on the more exact value of Saint Venant expression J_e and ABAQUS is 8.0%. The example shows that for the torsion problems, the kinematics of the Vlasov theory and its variations (including shear deformation and/or local warping effects) overestimates the torsional stiffness of beams. The percentage difference in results is in the order of 8%-11.9%. It is thus expected that the present theory, based on similar kinematics will tend to overestimate the twisting stiffness of beams. This will be verified and illustrated in the second part of the example.

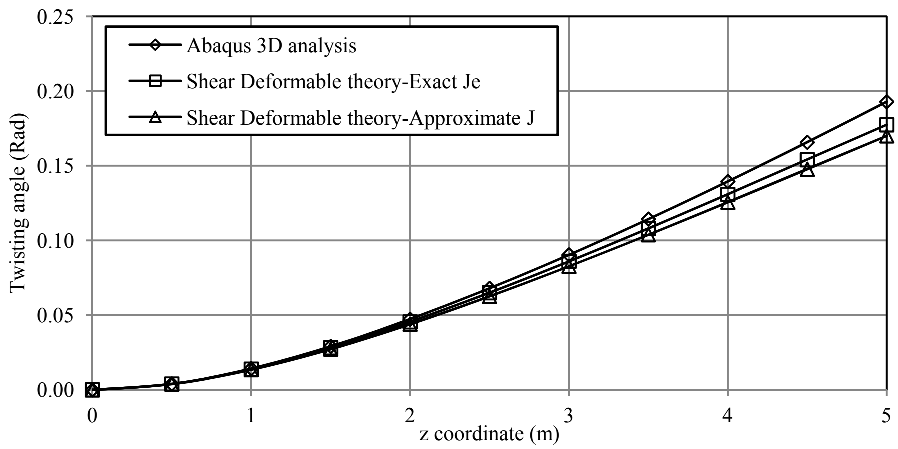

Figure 8.6 Angle of twist for cantilever subject to end twisting moment

Figure 8.7 shows the longitudinal normal stress (MPa), obtained from present study and FEA performed in ABAQUS, at the mid-height point of left edge of the bottom flange (as shown the cross-section in Fig. 8.7) along the longitudinal coordinate z (m). As discussed in Example 1 of Chapter 4, singularity points in the 3D FEA model appear at the fixed end, where the stresses are observed to increase as the finite element mesh gets finer. The maximum difference between the normal stresses between the two solutions at the singularity point at fixed end is 16.6%, while that at $z = 0.016m$ (very near the fixed end), the difference drops to only 1.8%. Also, near the tip, there is also a noticeable difference between two solutions. This difference reduces farther from the tip.

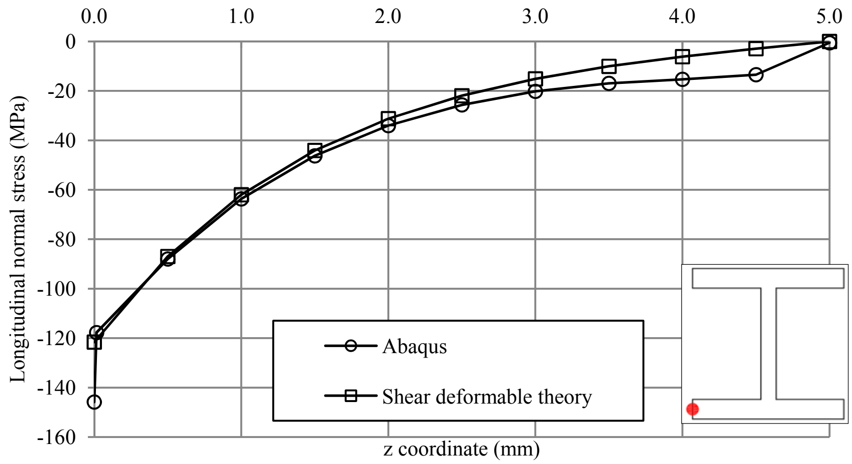

Figure 8.7 Longitudinal normal stresses at bottom flange mid-height.

8.4.2 Twisting a wide flange beam reinforced with a GFRP plate

8.4.2.1 Statement of the Problem

A GFRP with $E_p = 42GPa$ is connected to the section above. Two different values are considered for the shear modulus of adhesive $G_a = 5.0MPa$ (very weak) and $G_a = 0.4GPa$, a low shear modulus adhesive type (Table 1.1). Poisson's ratio of all materials μ is 0.3. The member is subjected to equal and opposite tangential tractions at the tip $\tau_v = 2490kN/m^2$ at both flange sections to induce a twisting moment $T = 3.2712kNm$ about wide flange centroid. It is required to compare the (i) displacement fields at the tip based on the shear-deformable theory developed in Chapters 5- 7 and FEA performed under ABAQUS for spans $L = 4.0m$, $L = 5.0m$, and $L = 6.0m$, (ii) Displacements and stresses as predicted by the non-shear deformable theory developed in Chapters 2 and 3, the shear-deformable theory developed in Chapters 5-7 and the 3D FE analysis in ABAQUS for the case $L = 5.0m$ and $G_a = 0.4GPa$, and (iii) Displacement and stresses as predicted by the non-shear deformable theory developed in Chapters 2 and 3, the shear-deformable theory developed in Chapters5-7 and the 3D FEA analysis performed in ABAQUS for the case $L = 5.0m$ and $G_a = 5.0MPa$.

8.4.2.2 Finite difference solution

The finite difference solution for the present problem is similar to that presented under Section 8.3.2 with a change of load terms. The load terms in the field equations (6.24)-(6.29) are set to

$q_{x(i)} = m_{yb(i)} = m_{(i)} = b_{(i)} = 0$ in which $i = 1, 2, \ldots, (n+1)$. Also, the load terms in the boundary equations (8.15)-(8.30) are taken as $M_{y1(n+1)} = M_{y2(n+1)} = Q_{x(n+1)} = B_{1(n+1)} = B_{2(n+1)} = 0$ and $T_{(n+1)} = 3.271 kNm$.

Stresses and strains within the beam are determined based on Eqs. 6.46-6.53. By performing a mesh sensitivity analysis, displacements and stress are found to converge for afor 200-subdivision solution.

Present Finite Element Solution

In the finite element solution, the load vector is taken as $\left\langle \overline{\overline{Q}}_{12} \right\rangle_{1\times16}^{T} = \langle 0 \quad 0 \quad 0 \quad 0 \mid 0 \quad 0 \mid 0 \quad 0 \mid 0 \quad 0 \mid 0 \quad 0 \quad T \quad 0 \mid 0 \quad 0 \rangle$ in which $T = 3.271 kNm$. Stresses and strains within the beam are determined based on the procedure developed under Section 7.5. By doing similar mesh sensitivity as performed in Example 2, displacement and stress are converged for 160-element solution.

8.4.2.3 3D-FEA Solution based on Abaqus

All elements are the 8-node brick element type C3D8R. For a span $L = 4.0m$, displacements and stresses are observed to converge for the mesh $n_1 = 20, n_2 = 4, n_3 = 70, n_4 = 4, n_5 = 4, n_6 = 8, n_7 = 2500$. For a span $L = 5.0m$, displacements and stresses are found to converge for the mesh $n_1 = 20, n_2 = 4, n_3 = 70, n_4 = 4, n_5 = 4, n_6 = 8, n_7 = 3120$ while for a span $L = 6.0m$, convergence is achieved for $n_1 = 20, n_2 = 4, n_3 = 70, n_4 = 4, n_5 = 4, n_6 = 8, n_7 = 3750$. Singularity points appear at the fixed end as discussed in Example 1 of Chapter 4.

The results based on the closed form solution based on the non-shear deformable theory, as performed in Example 4 of Chapter 4 are also provided for an applied twisting moment $T = 3.271 kNm$

8.4.2.4 Results

8.4.2.4.1 Requirement 1: Comparison of displacement fields

The displacements $U_b(L), U_p(L), \theta_z(L)$ obtained from the shear deformable theory and FEA performed under ABAQUS is shown in Table 8.6. As observed, the displacement difference between the two solutions decreases as the span increases.

This is due to three reasons. The first reason has been identified in the first part of the example which considered an unreinforced steel beam, in which it was concluded that the postulated Vlasov kinematics lead to overestimating the twisting stiffness. The second reason is the simplifying assumption of linear displacement within the adhesive layer thickness. As discussed in Example 4 of Chapter 4, the distribution of shear stress across the width of adhesive layer is nonlinear, leading to another slight overestimation of the stiffness of the system. The third reason lies in neglecting web distortion within the present theory, as per assumption (i) in Section 5.3 stating that the section contour does not deform in its own plane. In contrast, the 3D FEA model captures this type of deformation, as has been depicted in Fig.4.16a. Distortional effects were observed to increase for shorter beams, which explain why the difference between both solutions (3D FEA and shear deformable theory) decrease as the beam span decreases.

Table 8.6. Comparison of displacement fields at tip between shear deformable theory and 3D-FEA under Abaqus

Field	Span $L = 4.0m$			Span $L = 5.0m$			Span $L = 6.0m$		
	ABAQUS	Shear Deforma -ble Theory	Difference	ABAQUS	Shear Deforma -ble Theory	Difference	ABAQUS	Shear Deform -able Theory	Difference
$U_b(L)$	-1.27	-1.6	20.6%	-1.9	-2.2	13.6%	-2.5	-2.8	10.7%
$U_p(L)$	18.4	15.0	18.5%	24.3	20.3	15.7%	29.7	25.9	12.8%
$\theta_z(L)$	0.15	0.13	19%	0.124	0.103	17%	0.15	0.13	13%

8.4.2.4.2 Requirement 2: Results for the case $L = 5.0m$ and $G_a = 0.4GPa$

Figures 8.8 (a) and (b) provide the lateral displacement obtained from the 3D FEA under ABAQUS, the shear deformable theory and the non-shear deformable theory at the centroid of both flanges. As discussed in Chapter 4, the results obtained from non-shear deformable for twisting problem significantly overestimate the twisting resistance. A significant improvement is obtained in the case of the shear deformable theory compared to the 3D FEA solution for which the percentage difference for the lateral displacement at the top flange centroid is 17.1% and 15.4% for the lateral displacement at the bottom flange centroid. Figure 8.8 (c) shows the twisting angle along the beam. The twisting angle obtained from ABAQUS is determined by dividing the difference between lateral displacement of top flange centroid and bottom flange centroid by the section depth. The maximum difference at tip of twisting angle between two solutions is 16.6%. Figure 8.8(d) provides the lateral displacement of GFRP plate centroid. The maximum difference at the tip between the two solutions is 15.7%. The difference is most pronounced near the cantilever tip with better agreement obtained away from the cantilever tip.

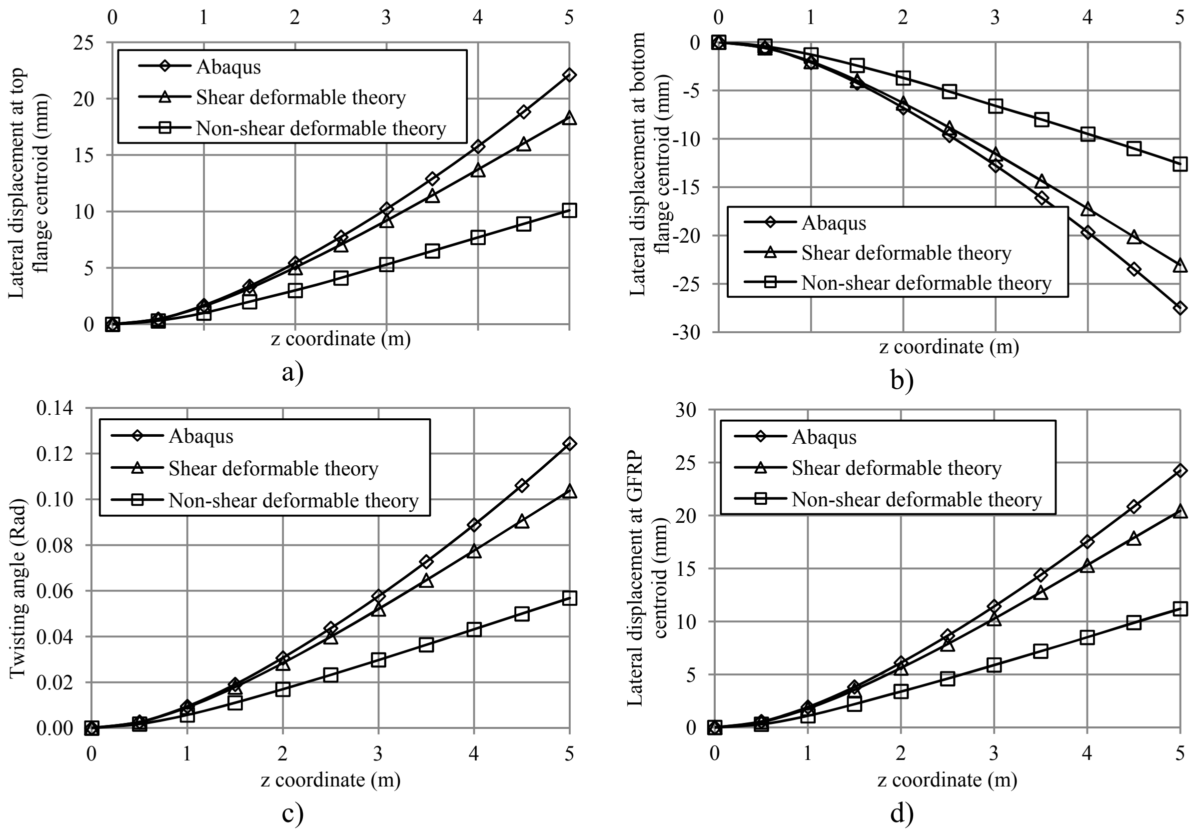

Figure 8.8 (a) Lateral displacement at top flange centroid, (b) Lateral displacement at bottom flange centroid, (c) Twisting angle, (d) Lateral displacement at GFRP plate centroid

Figure 8.9 provides the stress fields along longitudinal coordinate z obtained from non-shear deformable theory, shear deformable theory and 3D FEA performed in ABAQUS. Figure 8.9 (a)-(b) provides the longitudinal normal stress at middle height, left edge of the top flange, and at middle height, left edge of bottom flange, respectively along longitudinal coordinate z . These locations are shown in red points on cross-section. As analyzed for displacement fields, the maximum difference of the normal stresses also happens at the tip area. However, the stress values at the tip area are not important because they are not the maximum value which is located at the fixed end. As shown in the Example 1 of Chapter 4 that there are singularity points appearing at the fixed end. At longitudinal coordinate $z = 0.016m$ (very near the fixed end), the difference of longitudinal stress between two solutions is only 2.1%, while at the fixed end (where has the singularity points), the difference is up to 16.6%. Figure 8.9(c) provides the longitudinal normal stress at middle height, left edge of the GFRP plate along $z-$coordinate. At longitudinal coordinate $z = 0.016m$, the difference of longitudinal stress between two solutions is 1.6%, while at the fixed end (where has the singularity points), the difference is up to 22.9%. Figure 8.9(d) shows the average shear stress τ_{sz} at bottom adhesive surface. Shear stress at integration points of lowest element layer is averaged across the width of adhesive layer at each $z-$coordinate. As observed, the maximum difference between the two solutions is 29.3% at coordinate $z = 4.5m$.

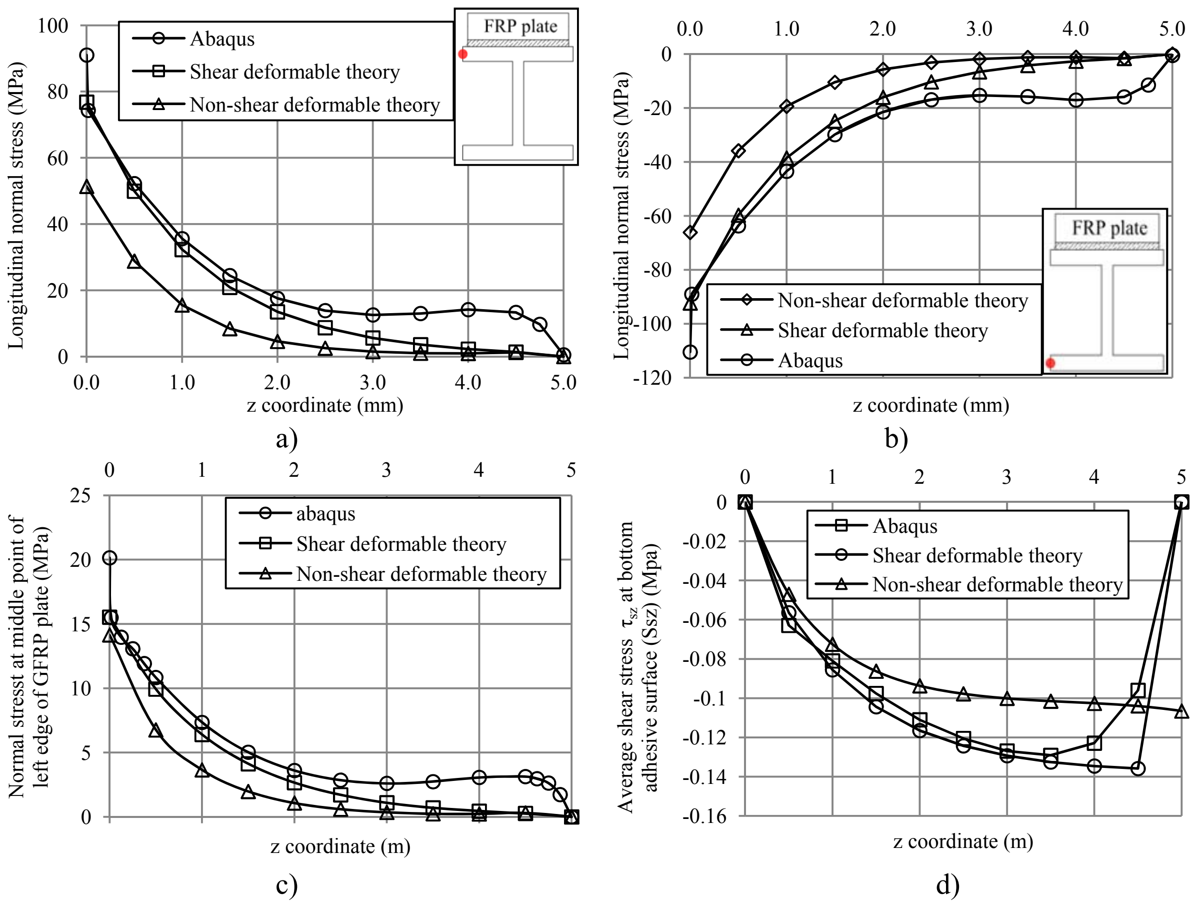

Figure 8.9 (a) Normal stress at middle height, left edge of top flange, (b) normal stress at middle height, left edge of bottom flange, (c) Normal stress at middle height, left edge of GFRP plate, and (d) Average shear stress τ_{sz} at bottom adhesive surface.

The results of displacements and stresses reflect a complexity of interaction between GFRP plate, adhesive layer and wide flange beam at the cantilever tip area. There are three reasons that may explain this problem.

The first one is caused by simplifying assumptions for normal-strains and shear-strains within the wide flange beam and GFRP plate, i.e., all strains exempt ε_z and γ_{sz} are assumed to be zero, while the simulation in ABAQUS is a 3D FEA model. This reason is verified under item 8.4.1- an example of a wide flange beam (without GFRP plate and adhesive layer) subject to a pure twisting moment. The maximum different between the present study (or Vlasov's theory) and ABAQUS is 8.0% for twisting angle, 16.6% for longitudinal normal stress at the tip and 1.8% for longitudinal normal stress at the longitudinal coordinate $z = 0.016m$ (very near the fixed end). To improve these differences, all strain components in all directions within the wide flange beam should be taken into account in total potential energy equation.

The second one is the simplifying assumption of linear displacement within the adhesive layer. As discussed in Example 4 of Chapter 4, the distribution of shear stress components across the width of adhesive layer is not linear, while the present study doesn't capture this characteristic. To improve the solution of displacements and stresses, the higher–order functions should be assumed to derive displacement fields within the adhesive layer instead of linear interpolation.

The third one is the effect of web distortion, especially at the tip. The effect in present study is eliminated by the assumption (i) in Item 5.3 that the section contour does not deform in its own plane, while the 3D model captures this kind of deformation. A picture of web distortion in ABAQUS model is shown in Fig.4.16a. The effect becomes larger when the beam span is shorter. The reason can be eliminated by installation of web stiffeners in 3D FEA model.

8.4.2.4.3 Results for the case $L = 5.0m$ and $G_a = 5MPa$

Figure 8.10 provides displacement fields along longitudinal coordinate z as predicted from non-shear deformable theory, the shear deformable theory, and the 3D FEA performed under ABAQUS. As observed, the results obtained from non-shear deformable slightly differ from those based on the shear-deformable theory. This contrasts with the large difference observed previously for the case of a strong adhesive layer. It is reasoned that, for a low adhesive shear modulus, the effect of shear deformation in the GFRP plate becomes small. This enables the non-shear deformable theory to reliably approximate the true behaviour of the system, as predicted by the 3D FEA in Abaqus. This is illustrated in Fig. 8.9, in which all three solutions are in close agreement.

Figures 8.10 (a) and (b) depict the lateral displacement along the longitudinal coordinate z at the centroids of both flanges. The maximum difference between the shear deformable theory and 3D

FEA is 8.6% for the lateral displacement at the top flange centroid at tip and 8.5% for lateral displacement at the bottom flange centroid at tip. Figure 8.10 (c) shows the twisting angle along the longitudinal coordinate z . The twisting angle obtained from ABAQUS is determined by dividing the difference between lateral displacements by the section depth. The maximum difference in the twisting angle between shear deformable theory and 3D FEA is 8.6% at tip. Figure 8.10(d) provides the lateral displacement of GFRP plate centroid. The maximum difference at the tip between the shear deformable theory and 3D FEA is 7.9%. Again, the maximum difference takes place near the cantilever tip, with better agreement away from the tip.

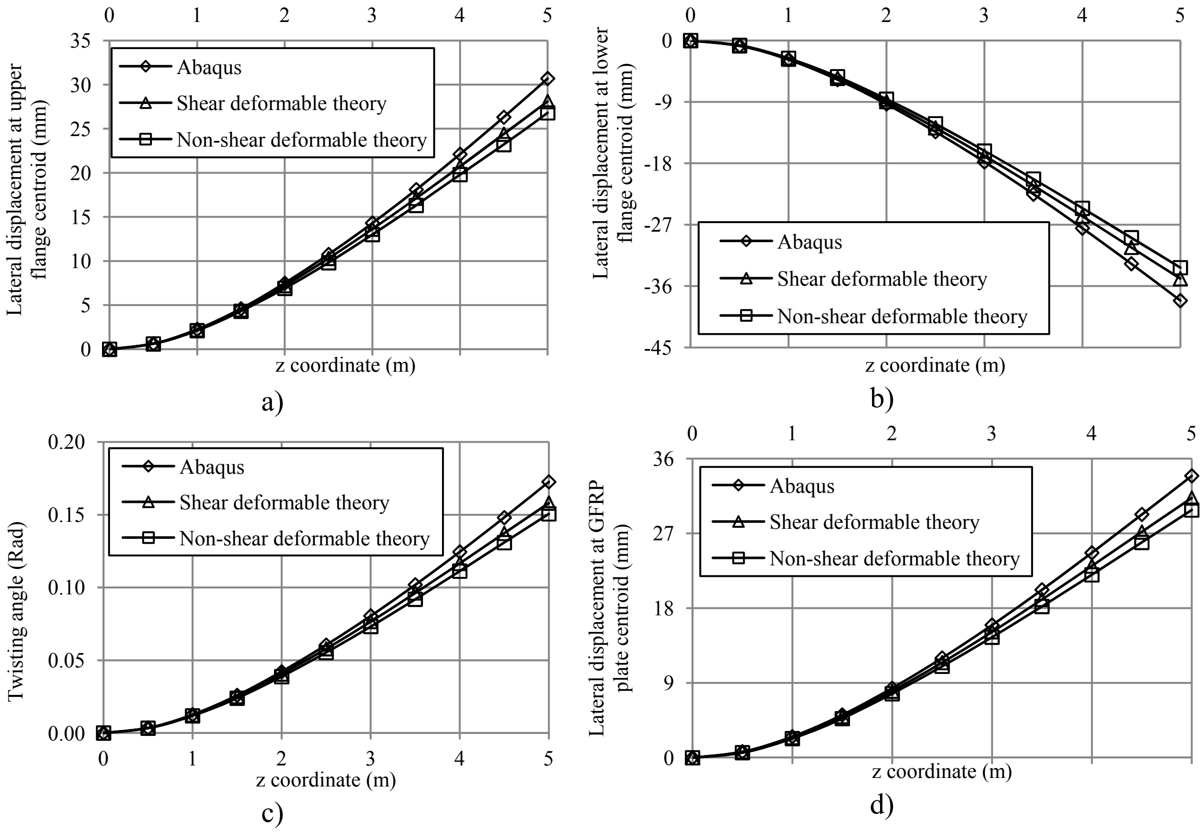

Figure 8.10 (a) Later displacement at top flange centroid, (b) Lateral displacement at bottom flange centroid, (c) Twisting angle, (d) Lateral displacement at GFRP plate centroid

Figure 8.11 shows the longitudinal normal stress fields along longitudinal coordinate z obtained from non-shear deformable theory, shear deformable theory, and 3D FEA performed under ABAQUS. As discussed for comparison of displacement, the stress field obtained from non-shear deformable is slightly different from that based on the shear deformable theory for the case of weak shear modulus.

Figure 8.11 provides the longitudinal normal stresses at the mid-height point of the, left edge of the bottom flange along $z-$coordinate (Fig. 8.11a), and at mid-height point of the left edge of the GFRP plate (Fig. 8.11b). The maximum difference in the normal stresses also happens near the tip area. However for stress fields, the stress values at the tip area are minimal and of no practical design interest At the longitudinal coordinate $z = 0.016m$ (near the fixed end), the difference between longitudinal stress between shear deformable theory and 3D FEA is only 2.6%, while at the cantilever tip (at singularity point) the difference is 16.3%.

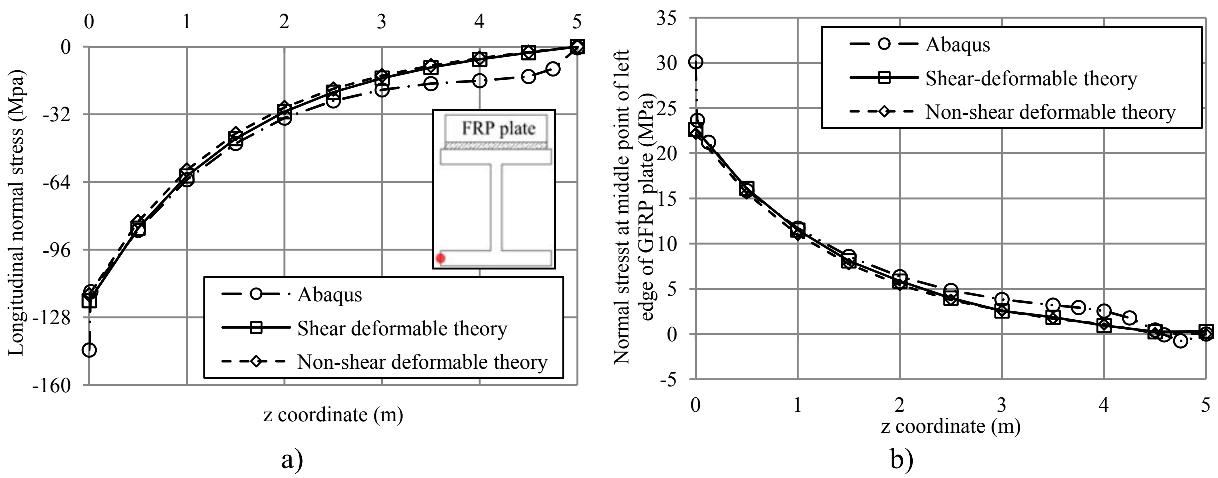

Figure 8.11 (a) Normal stress at middle height, left edge of bottom flange, (b) Normal stress at middle height, left edge of GFRP plate

Beside the comparison of displacement and stress between non-shear deformable theory, shear deformable theory and 3D FEA performed in ABAQUS, a comparison of time consumed and afford taken between the three solutions is also performed.

Table 8.7 provides a comparison of computational running time and memory used for the case $L = 5.0m$ on a computer with two processors Intel(R) Xeon(R) CPU E5-2430 0 at 2.20GHz 2.20GHz speeds, and an installed RAM of 64.0GB. While the analyses based on the present studies were implemented under MATLAB, the 3D FEA is performed under the ABAQUS simulation software. For the ABAQUS solution, 4.31 hours of running were needed. This compares to 14 seconds using a single element solution under the finite element solution developed based on non-shear deformable, 2.0 seconds using the closed form solution developed based on non-shear deformable theory, 26.2 seconds using 200 subdivisions of finite difference solution developed based on shear deformable theory, and 4.0 seconds using 160-element solution under the finite element solution developed based on shear deformable theory.

Table 8.7 Comparison of run-time and Memory used for Problem 3

Description of the solution	Run Time	Memory used
Non-shear deformable theory- FEA with a Single Element	14 seconds	661 MB
Non-shear deformable theory- Closed Form Solution	2.0 seconds	618 MB
Shear Deformable Theory Finite difference Solution (200 subdivisions)	26.2 seconds	722 MB
Shear Deformable Theory FEA with 160 elements	4.0 seconds	746 MB
3D FEA (Abaqus) 2,995,200-elements	4.31 hours	Minimum 8356 MB

8.5. Summary and Conclusions

The examples presented in this chapter illustrate the improvements achieved by implementing the shear deformable theory compared to the shear non-deformable theory. The shear deformable theory provides predictions which range from excellent agreement with Abaqus 3D FEA (for problems involving predominantly shear longitudinal-transverse response, lateral response, and twisting response with a low adhesive shear modulus) and very good agreement for problems involving predominantly twisting response with high shear modulus. The theory is able to reliably predict the displacements as well as shear stresses in the steel section, the GFRP plate and the adhesive material.

CHAPTER 9- SUMMARY, CONCLUSIONS AND RECOMMENDATIONS

9.1. Summary

The present thesis has focused on the analysis of composite beams consisting of steel wide flange sections reinforced with GFRP plates connected to one the flanges through a layer of adhesive. Towards this goal, the thesis has presented the following contributions

(1) A non-shear deformable theory was developed by extending the Gjelsvik theory for thin-walled beams for homogenous open-thin walled beams to the present composite system. The equilibrium equations and boundary conditions governing the longitudinal-transverse and lateral-torsional responses were developed by applying the principle of stationary potential energy.

(2) The theory describes the longitudinal-transverse response through a system of coupled differential equations relating three generalized displacement fields. Also, it describes the lateral-torsional response through another system of coupled differential equations relating an additional three generalized displacement fields.

(3) General closed form solutions were developed for the resulting coupled differential equations of equilibrium

(4) A super-convergent finite element was then developed based on shape functions which exactly satisfy the homogeneous form of the equilibrium equations.

(5) Results based on the non-shear deformable theory were assessed by comparisons with 3D FEA analysis under Abaqus. Except for cases involving predominantly twisting response, the theory was shown to provide reliable displacement and stress results.

(6) For cases involving predominantly twisting response, a careful examination of the 3D FEA results provided valuable insight on means of improving the theory.

(7) A more advanced shear deformable theory was then developed for the problem based on enriched kinematics. The new theory describes the longitudinal-transverse response through a system of coupled differential equations relating four displacement fields and the lateral-torsional response through a system of coupled differential equations relating an additional six displacement fields.

(8) A finite difference solution was developed for the shear deformable theory

(9) Also, a finite element formulation was developed for the shear deformable theory

9.2. Conclusions

(1) A major finding of the present study is establishing that shear deformation effects are key in attaining realistic predictions of the response of problems involving twist

(2) The non-shear deformable theory involves a small modelling and computational effort compared to 3D FEA modelling, and is suitable for predicting the static response of composite systems involving little or no twist

(3) The shear deformable theory, while more complex than the non-shear deformable theory, still involves a small modelling and computational effort compared to 3D FEA modelling, and is suitable for predicting the static response of composite systems under all loading cases examined, including those inducing significant twist.

(4) Like all beam theories, both theories developed in this research do not capture localizations captured in 3D FEA models. Outside regions of localization, both theories were generally able to reliably predict displacements and stresses within the steel member, the GFRP plate, and the adhesive layer.

9.3. Recommendations

The shear deformable theory was shown to capture the features necessary to reliably predict the static response of composite systems. Following are possible extensions for the theory

(1) The underlying kinematics can be extended to other types of analysis, including buckling analysis, and material and geometrically non-linear analyses.

(2) A closed form solution for the analysis for the static analysis theory can be attempted. If successful, a super-convergent finite element based on the shear deformable theory would add to the efficiency of the problem.

(3) The inertial forces can be incorporated into the analysis to capture she dynamic response of composite beams.

(4) It is recommended to extend the shear deformable theory to other steel section configurations and to involve multiple GFRP plates (e.g., connected to both flanges, web, etc.)

(5) A possible extension of the theory is to capture distortional effects of the web. This would improve the theory when predicting the response for short span members which are susceptible to web distortion.

REFERENCES

[1] Asik, M.Z. and Tezcan, S. (2005), A mathematical model for the behavior of laminated glass beams, Computers and Structures, 83 (21-22), 1742-1753

[2] Challamel, N. (2009), On lateral-torsional vibrations of elastic composite beam with interlayer slip, Journal of Sound and Vibration, 325(4-5), 1012-1022

[3] Challamel, N., Bernard, F. and Casandjian, C. (2010), Out-of-plane behavior of partially composite or sandwich beams by exact and finite element methods, Thin-Walled Structures, 48(8), 561-580

[4] Challamel, N. and Girhammar, U.A. (2012), Lateral-torsional buckling of vertically layered composite beams with interlayer slip under uniform moment, Engineering Structures, 34(46), 505-513

[5] Dall' Asta, A. (2001), Composite beams with weak shear connection, International Journal of Solids and Structures, 38(32-33), 5605-5624

[6] Deng, J., Lee, M. M. K. And Moy S.S.J. (2004), Stress analysis of steel beams reinforced with a bonded CFRP plate, Composite Structures, 65(2), 205-215

[7] Ditaranto, R.A. (1973), Static analysis of a laminated beam, Journal of Manufacturing Science and Engineering, 95(3), 755-761

[8] El Damatty, A.A. and Abushagur, M. (2003), Testing and modeling of shear and peel behavior for bonded steel/FRP connections, Thin-Walled Structures, 41(11), 987-1003

[9] El Damatty, A., Abushagur, M. and Youssef, M. A. (2003), Experiemental and analytical investigation of steel beams rehabilitated using GFRP sheets, Journal of Steel & Composite Structures 3(6), 421-438.

[10] Gara, F. , Ranzi, G. and Leoni, G. (2006), Displacement-based formulations for composite beams with longitudinal slip and vertical uplift, International Journal for Numerical Methods in Engineering, 65(8), 1197-1220

[11] Girhammar, U.A. and Pan, D.H. (2007), Exact static analysis of partially composite beams and beam-columns, International Journal of Mechanical Sciences, 49(2), 239-255

[12] Harries, A.K. and El-Tawil, S. (2008), Steel-FRP composite structural systems, International Conference on Composite Construction in Steel and Concrete 2008, Composite Construction in Steel and Concrete VI, Devil's Thumb Ranch, Tabernash, Colorado, United States, 703-716

[13] Koutsawa, Y., and Daya, E.M. (2007), Static and free vibration analysis of laminated glass beam on viscoelastic supports, International Journal of Solids and Structures, 44(25-26), 8735-8750

[14] Koziey B.L. and Mirza F.A. (1997), Consistent thick shell element, Computers and Structures, 65(12), 513–41.
[15] Lee, J. and Lee, S.-H. (2004), Flexural-torsional behavior of thin-walled composite beams, Thin-Walled Structures, 42(9), 1293-1305
[16] Lee, J., Kim, S.-E. and Hong, K. (2002), Lateral buckling of I-section composite beams, Engineering Structures, 24(7), 955-964.
[17] Linghoff, D. and Al-Emrani, M. (2010), Performance of steel beams strengthened with CFRP laminate – Part 2: Laboratory tests, Composites Part B, 41(7), 516-522
[18] Linghoff, D., Al-Emrani and Kliger, M. R. (2010), Performance of steel beams strengthened with CFRP laminate – Part 1: Laboratory tests, Composites Part B, 41(7), 509-515.
[19] Miller, C.T., Chajes J.M. and Hastings N.J. (2001), Strengthening of a steel bridge girder using CFRP plates, Journal of Bridge Engineering 6(6), 514-522.
[20] Nowzartash, F. and Mohareb, M. (2005), "Planar bending of sandwich beams with transverse loads off the centroidal axis", Journal of Structural Engineering, 131(4), 385-396
[21] Schnerch, D., Dawood, M., Rizkalla, S., Sumner, E. and Stanford, K. (2006), Bond behavior of CFRP strengthened steel structures, Advances in Structural Engineering, 9(6), 805-817
[22] Siddique, M.A.A. and El Damatty, A.A. (2012), Enhancement of buckling capacity of steel plates strengthened with GFRP plates, Thin-Walled Structures, 60(16), 154-162
[23] Siddique, M.A.A. and El Damatty, A.A. (2013), Improvement of local buckling behaviour of steel beams through bonding GFRP plates, Composite Structures, 96(6), 44-56
[24] Suresh, S.M and Shive, K.C (1999), Laminated composite open profile sections: First order shear deformation theory, Composite Structures, 45(2), 105-114
[25] Taljsten, B. (1997), Strengthening of beams by plate bonding, Journal of Materials in Civil Engineering, 9(4), 206-212.
[26] Tavakkolizadeh, M. and Saadatmanesh, H. (2003), Strengthening of steel-concrete composite girders using carbon fiber reinforced polymers sheets, Journal of Structural Engineering, 129(1), 30-40
[27] Vallabhan, D.G., Mohareb,M., Asik, M. and Bailey, J.R. (1993), Analysis of laminated glass units, Journal of Structural Engineering, 119(5), 1572–1585
[28] Zhao, X.-L. and Zhang, L. (2007), State-of-the-art review on FRP strengthened steel structures, Engineering Structures, 29(8), 1808-1823
[29] Finite Difference Methods for Ordinary and Partial Differential Equations: Steady-State and Time-dependent Problems (2007), author Randall LeVeque

APPENDICES A1-A8 RELATED TO THE DETAIL OF FORMULATION

AND

APPENDICES B1-B5 RELATED TO MATLAB PROGAMMING

APPENDIX A1–NON–SHEAR DEFORMABLE –THEORY TOTAL POTENTIAL ENERGY

The objective of this appendix is to provide the details for deriving the total potential energy of the system. As stated in Section 2.5.5.2, the total potential energy π is contributed by internal strain energies within the beam $\widetilde{U}_b$ (item A1.1 in Appendix A), GFRP plate (item A1.2) $\widetilde{U}_p$ and adhesive layer $\widetilde{U}_a$ (item A1.3) and load potential energy gained by tractions at member ends $\widetilde{V}_1$ and member tractions within the member $\widetilde{V}_2$, i.e.,

$$\pi = \widetilde{U}_b + \widetilde{U}_p + \widetilde{U}_a - \widetilde{V}_1 - \widetilde{V}_2 \tag{A1.1}$$

A1.1. Expression of Internal Strain Energy for the Beam

The internal strain energy of the beam has two contributions, i.e., $\widetilde{U}_b = \widetilde{U}_{b1} + \widetilde{U}_{b2}$ in which $\widetilde{U}_{b1}$ is due to the normal stresses and $\widetilde{U}_{b2}$ is due to shear stress. The first term $\widetilde{U}_{b1}$ is expressed as

$$\widetilde{U}_{b1} = \int_{V_b} \left(\frac{1}{2} \sigma_{zb} \varepsilon_{zb} \right) dV_b = \frac{1}{2} E_b \int_L \int_{A_b} \left[W_b' - X(s_b, n_b) U_b'' - Y(s_b, n_b) V'' - \Omega(s_b, n_b) \theta_z'' \right]^2 dA_b dz$$

By performing the area integrals and noting the coordinates chosen are orthogonal, i.e., $\int_{A_b} (X, Y, XY, X\Omega, Y\Omega) dA_b = (0,0,0,0,0)$, one obtains

$$\widetilde{U}_{b1} = \frac{1}{2} E_b A_b \int_L \left(W_b' \right)^2 dz + \frac{1}{2} E_b I_{yyb} \int_L \left(U_b'' \right)^2 dz + \frac{1}{2} E_b I_{xxb} \int_L \left(V_b'' \right)^2 dz + \frac{1}{2} E_b I_{\omega\omega b} \int_L \left(\theta_z'' \right)^2 dz \tag{A1.2}$$

in which $A_b = \sum_{i=\overline{1,3}} b_{ib} t_{ib}$; $I_{yyb} = \int_{A_b} \left[X(s_b, n_b) \right]^2 dA_b$; $I_{xxb} = \int_{A_b} \left[Y(s_b, n_b) \right]^2 dA_b$;

$I_{\omega\omega b} = \int_{A_b} \left[\Omega(s_b, n_b) \right]^2 dA_b$

The second term $\widetilde{U}_{b2}$ is expressed as

$$\widetilde{U}_{b2} = \int_{V_b} \left(\frac{1}{2} \tau_{szb} \gamma_{szb} \right) dV_b = \int_L \int_{A_b} \left\{ \frac{1}{2} G_b \left(2 n_b \theta' \right)^2 \right\} dA_b dz = \frac{1}{2} G_b J_b \int_L \left(\theta_z' \right)^2 dz \tag{A1.3}$$

in which $J_b = \int_{A_b} 4 n_b^2 dA_b = \sum_{i=\overline{1,3}} \int_{-\frac{t_i}{2}}^{\frac{t_i}{2}} \left(4 t_{ib}^2 b_{ib} \right) dt_{ib} = \sum_{i=\overline{1,3}} \frac{b_{ib} t_{ib}^3}{3}$ is the St. Venant torsional constant. In summary, the total strain energy in the beam is

$$\widetilde{U}_b = \frac{1}{2}\int_L \left(E_b A_b \ W_b'^2 + E_b I_{yyb} U_b''^2 + E_b I_{xxb} V_b''^2 + \ E_b I_{\omega\omega b} \theta_z''^2 + G_b J_b \theta_z'^2 \right) dz \qquad \text{(A1.4)}$$

A1.2. Expression of Internal Strain Energy for the GFRP plate

The internal strain energy of the plate has two contributions, i.e., $\widetilde{U}_p = \widetilde{U}_{p1} + \widetilde{U}_{p2}$ in which $\widetilde{U}_{p1}$ is the contribution due to normal stresses and $\widetilde{U}_{p2}$ is the contribution due to shear stress. The first term $\widetilde{U}_{p1}$ is expressed as

$$\widetilde{U}_{p1} = \int_{V_p} \left(\frac{1}{2} \sigma_{zp} \varepsilon_{zp} \right) dV_p = \frac{1}{2} E_p \int_L \int_{A_p} \left[W_p'(z) - U_p''(z) x_p + V''(z) n_p + \theta_z''(z) n_p x_p \right]^2 dA_p dz$$

By performing the area integrals and noting the coordinates chosen are orthogonal, i.e., $\int_{A_p} \left(x_p, n_p, x_p n_p, x_p^2 n_p, x_p n_p^2 \right) dA_p = (0,0,0,0,0)$, one obtains

$$\widetilde{U}_{p1} = \frac{1}{2} E_p \left(\int_L A_p W_p'^2 + I_{yyp} U_p''^2 + I_{xxp} V''^2 + I_{\omega\omega p} \theta_z''^2 \right) dz$$

(A1.5)

in which $A_p = b_p t_p$; $I_{yyp} = \int_{A_p} x_p^2 dA_p$; $I_{xxp} = \int_{A_p} n_p^2 dA_p$; $I_{\omega\omega p} = \int_{A_p} \left[n_p x_p (s_p) \right]^2 dA_p$;

The second term $\widetilde{U}_{p2}$ is expressed as:

$$\widetilde{U}_{p2} = \int_{V_p} \left(\frac{1}{2} \tau_{szp} \gamma_{szp} \right) dV_p = \frac{1}{2} \int_L \int_{A_p} G_p \left(2 n_p \theta_z' \right)^2 dA_p dz = \frac{1}{2} G_p J_p \int_L \left(\theta_z' \right)^2 dz \qquad \text{(A1.6)}$$

in which $J_p = \int_{A_p} 4 n_p^2 dA_p = \int_{-\frac{t_1}{2}}^{\frac{t_1}{2}} \left(4 t_p^2 b_p \right) dt_p = \frac{b_p t_p^3}{3}$ is the Saint-Venant torsional constant. In summary, the total strain energy in the GFRP plate is

$$\widetilde{U}_p = \frac{1}{2}\int_L \left(E_p A_p W_p'^2 + E_p I_{yyp} U_p''^2 + E_p I_{xxp} V''^2 + E_p I_{\omega\omega p} \theta_z''^2 + G_p J_p \theta_z'^2 \right) dz \qquad \text{(A1.7)}$$

A1.3. Expression of Internal Strain Energy for the Adhesive layer

The internal strain energy of the adhesive layer has three contributions, i.e., $\widetilde{U}_a = \widetilde{U}_{a1} + \widetilde{U}_{a2} + \widetilde{U}_{a3}$ in which $\widetilde{U}_{a1}$ is the contribution due to shear stress τ_{zna}, $\widetilde{U}_{a2}$ is the contribution due to the shear stress τ_{sna} , and $\widetilde{U}_{a3}$ is the contribution due to the shear stress τ_{sza} . The first term $\widetilde{U}_{a1}$ is expressed as

$$\widetilde{U}_{a1} = \frac{1}{2}\int_{V_a} \tau_{zna}\gamma_{zna} dV_a = \frac{1}{2} G_a \int_L \int_{A_a} \langle \Delta_a \rangle^{\mathrm{T}}_{1\times 6} \{a_a\}_{6\mathrm{x}1} \langle a_a \rangle^{\mathrm{T}}_{1\times 6} \{\Delta_a\}_{6\mathrm{x}1}\, dA_a dz$$

$$= \frac{1}{2} G_a \int_L \langle \Delta_a \rangle^{\mathrm{T}}_{1\times 6} \int_{A_a} \left[\begin{array}{cc|c|ccc} c_1^2 & -c_1^2 & c_1c_2 & -c_1^2 x & c_1^2 x & c_1c_3 x \\ -c_1^2 & c_1^2 & -c_1c_2 & c_1^2 x & -c_1^2 x & -c_1c_3 x \\ \hline c_1c_2 & -c_1c_2 & c_2^2 & -c_1c_2 x & c_1c_2 x & c_2c_3 x \\ \hline -c_1^2 x & c_1^2 x & -c_1c_2 x & c_1^2 x^2 & -c_1^2 x^2 & -c_1c_3 x^2 \\ c_1^2 x & -c_1^2 x & c_1c_2 x & -c_1^2 x^2 & c_1^2 x^2 & c_1c_3 x^2 \\ c_1c_3 x & -c_1c_3 x & c_2c_3 x & -c_1c_3 x^2 & c_1c_3 x^2 & c_3^2 x^2 \end{array}\right] dA_a \{\Delta_a\}_{6\mathrm{x}1}\, dz$$

$$= \frac{1}{2} G_a \int_L \left\langle \langle U_L \rangle^T_{1\times 2} \;\middle|\; V' \;\middle|\; \langle U_O \rangle'^T_{1\times 3} \right\rangle \left[\begin{array}{c|c|c} A_a c_1^2 [H_{a1}]_{2\times 2} & A_a c_1 c_2 \{H_{a3}\}_{2\times 1} & [0]_{2\times 3} \\ \hline A_a c_1 c_2 \langle H_{a3} \rangle^T_{1\times 2} & A_a c_2^2 & \langle 0 \rangle_{1\times 3} \\ \hline [0]_{3\times 2} & \{0\}_{3\times 1} & I_{yya} [H_{a2}]_{3\times 3} \end{array}\right] \left\{\begin{array}{c} \{U_L\}_{2\times 1} \\ \hline V' \\ \hline \{U_O\}'_{3\times 1} \end{array}\right\} dz$$

in which

$$\langle U_L \rangle^T_{1\times 2} = \langle W_b \quad W_p \rangle, \qquad \langle U_O \rangle^T_{1\times 3} = \langle U_b \quad U_p \quad \theta_z \rangle, \qquad [H_{a1}]_{2\times 2} = \begin{bmatrix} 1 & -1 \\ -1 & 1 \end{bmatrix},$$

$$[H_{a2}]_{3\times 3} = \begin{bmatrix} c_1^2 & -c_1^2 & -c_1c_3 \\ -c_1^2 & c_1^2 & c_1c_3 \\ -c_1c_3 & c_1c_3 & c_3^2 \end{bmatrix}, \qquad \langle H_{a3} \rangle^T_{1\times 2} = [1 \quad -1]$$

Note that all integrals $\int_{A_a} x dA_a = 0$. As a result, one obtains

$$\widetilde{U}_{a1} = \frac{1}{2} G_a A_a \int_L c_1^2 \langle U_L \rangle^T_{1\times 2} [H_{a1}]_{2\times 2} \{U_L\}_{2\times 1}\, dz + \frac{1}{2} G_a A_a \int_L \left[2c_1c_2 V' \left(W_b - W_p\right) + c_2^2 \left(V'\right)^2 \right] dz$$

$$+ \frac{1}{2} G_a I_{yya} \int_L \langle U_O \rangle'^{\mathrm{T}}_{1\times 3} [H_{a2}]_{3\times 3} \{U_O\}'\, dz$$

(A1.8)

The second term $\widetilde{U}_{a2}$ is expressed as

$$\widetilde{U}_{a2} = \frac{1}{2}\int_{V_a} \tau_{sna}\gamma_{sna} dV_a = \frac{1}{2} G_a \int_L \int_{A_a} \langle U_O \rangle^{\mathrm{T}}_{1\times 3} \{a_{a1}\}_{3\times 1} \langle a_{a1} \rangle^{\mathrm{T}}_{1\times 3} \{U_O\}_{3\times 1} dA_a dz$$

$$= \frac{1}{2} G_a \int_L \langle U_O \rangle^{\mathrm{T}}_{1\times 3} \int_{A_a} \begin{bmatrix} c_1^2 & -c_1^2 & c_1c_2 \\ -c_1^2 & c_1^2 & -c_1c_2 \\ c_1c_2 & -c_1c_2 & c_2^2 \end{bmatrix} dA_a \{U_O\}_{3\times 1} dz$$

in which $\langle U_O \rangle^T_{1\times 3} = \langle U_b \quad U_p \quad \theta \rangle$. By performing the area integrals, one obtains

$$\widetilde{U}_{a2}=\frac{1}{2}G_aA_a\int_L\left\langle U_O\right\rangle_{1\times3}^{\mathrm{T}}\left[H_{a4}\right]_{3\times3}\left\{U_O\right\}dz \tag{A1.9}$$

in which $\left[H_{a4}\right]_{3\times3}=\begin{bmatrix} c_1^2 & -c_1^2 & c_1c_2 \\ -c_1^2 & c_1^2 & -c_1c_2 \\ c_1c_2 & -c_1c_2 & c_2^2 \end{bmatrix}$

The third term $\widetilde{U}_{a3}$ is expressed as

$$\widetilde{U}_{a3}=\int_{V_a}\left(\frac{1}{2}\tau_{sza}\gamma_{sza}\right)dV_a=\int_L\int_{A_a}\left[\frac{1}{2}G_a\left(\gamma_{sza}\right)^2\right]dA_a dz=\frac{1}{2}G_aJ_a\int_L\left[\theta_z'\left(z\right)\right]^2dz \tag{A1.10}$$

in which

$$J_a=\frac{\left(t_1^2-t_1t_3+t_3^2\right)A_a}{3} \tag{A1.11}$$

From(A1.9), (A1.8) and (A1.10), the total internal strain energy in the Adhesive layer is

$$\begin{aligned}\widetilde{U}_a=&\frac{1}{2}G_aA_a\int_L c_1^2\left\langle U_L\right\rangle_{1\times2}^{T}\left[H_{a1}\right]_{2\times2}\left\{U_L\right\}_{2\times1}dz+\frac{1}{2}G_aA_a\int_L\left[2c_1c_2V'\left(W_b-W_p\right)+c_2^2V'^2\right]dz\\&+\frac{1}{2}G_aI_{yya}\int_L\left\langle U_O\right\rangle_{1\times3}^{\prime\mathrm{T}}\left[H_{a2}\right]_{3\times3}\left\{U_O\right\}'dz+\frac{1}{2}G_aA_a\int_L\left\langle U_O\right\rangle_{1\times3}^{\mathrm{T}}\left[H_{a4}\right]_{3\times3}\left\{U_O\right\}dz+\frac{1}{2}G_aJ_a\int_L\theta_z'^2dz\end{aligned} \tag{A1.12}$$

A1.4. Load potential energy

The total potential energy loss $\tilde{V}$ is the sum of the potential energy $\tilde{V}_1$ lost by end tractions $\sigma_z\left(s_b,n_b,0\right),\ \tau_u\left(s_b,n_b,0\right),\tau_v\left(s_b,n_b,0\right),\sigma_z\left(s_b,n_b,L\right),\tau_u\left(s_b,n_b,L\right),\tau_v\left(s_b,n_b,L\right)$ at $z=0,L$ and the potential energy $\tilde{V}_2$ lost by the member tractions $p_u\left(s_b,n_b,z\right),p_v\left(s_b,n_b,z\right),p_z\left(s_b,n_b,z\right)$.

A1.4.1. Load potential energy loss by end tractions

The total potential energy loss $\tilde{V}_1$ due to tractions at the member ends are

$$\begin{aligned}\widetilde{V}_1=-\Bigg[&\int_A\tau_v\left(s_b,n_b,0\right)v_b\left(s_b,n_b,0\right)dA+\int_A\tau_u\left(s_b,n_b,0\right)u_b\left(s_b,n_b,0\right)dA+\int_A\sigma_z\left(s_b,n_b,0\right)w_b\left(s_b,n_b,0\right)dA+\\&-\int_A\tau_v\left(s_b,n_b,L\right)v_b\left(s_b,n_b,L\right)dA-\int_A\tau_u\left(s_b,n_b,L\right)u_b\left(s_b,n_b,L\right)dA-\int_A\sigma_z\left(s_b,n_b,L\right)w_b\left(s_b,n_b,L\right)dA\Bigg]\end{aligned} \tag{A1.13}$$

in which:

$$u_b\left(s_b,n_b,z\right)=U_b\left(z\right)\sin\alpha\left(s_b\right)-V\left(z\right)\cos\alpha\left(s_b\right)-\theta_z\left(z\right)q\left(s_b\right)$$

$$v_b(s_b,n_b,z)=U_b(z)\cos\alpha(s_b)+V(z)\sin\alpha(s_b)+\theta_z(z)\left[r(s_b)+n_b q'(s_b)\right]$$

$$w_b(s_b,n_b,z)=W_b(z)-U_b'(z)X(s_b,n_b)-V'(z)Y(s_b,n_b)-\theta_z'(z)\Omega(s_b,n_b)$$

$$X(s_b,n_b)=x(s_b)+n_b\sin\alpha(s_b);\quad Y(s_b,n_b)=y(s_b)-n_b\cos\alpha(s_b)\ ;\ \Omega(s_b,n_b)=\omega_b(s_b)-n_b q(s_b);$$

$$q(s_b)=\left[x(s_b)\right]\cos\alpha(s_b)+\left[y(s_b)\right]\sin\alpha(s_b)\ ;\quad r(s_b)=\left[x(s_b)\right]\sin\alpha(s_b)-\left[y(s_b)\right]\cos\alpha(s_b);$$

By substituting the displacement fields in to Eq.(A1.13), one obtains

$$\begin{aligned}
\widetilde{V}_1=-\Bigg[&\int_A \tau_v(s_b,n_b,0)\left\{U_b(0)\cos\alpha(s_b)+V(0)\sin\alpha(s_b)+\theta_z(0)\left[r(s_b)+nq'(s_b)\right]\right\}dA+\\
&+\int_A \tau_u(s_b,n_b,0)\left\{U_b(0)\sin\alpha(s_b)-V(0)\cos\alpha(s_b)-\theta_z(0)q(s_b)\right\}dA+\\
&+\int_A \sigma_z(s_b,n_b,0)\left\{W_b(0)-U_b'(0)X(s_b,n_b)-V_b'(0)Y(s_b,n_b)-\theta_z'(0)\Omega(s_b,n_b)\right\}dA+\\
&-\int_A \tau_v(s_b,n_b,L)\left\{U_b(L)\cos\alpha(s_b)+V(L)\sin\alpha(s_b)+\theta_z(L)\left[r(s_b)+nq'(s_b)\right]\right\}dA+\\
&-\int_A \tau_u(s_b,n_b,L)\left\{U_b(L)\sin\alpha(s_b)\ \text{-}\ V(L)\cos\alpha(s_b)-\theta_z(L)q(s_b)\right\}dA+\\
&-\int_A \sigma_z(s_b,n_b,L)\left\{W_b(L)-U_b'(L)X(s_b,n_b)-V'(L)Y(s_b,n_b)-\theta_z'(L)\Omega(s_b,n_b)\right\}dA\Bigg]
\end{aligned}\tag{A1.14}$$

By re-group terms in Eq. (A1.14), one obtains

$$\begin{aligned}
\widetilde{V}_1=-\big[&N(0)W_b(0)+Q_x(0)U_b(0)+Q_y(0)V(0)+M_x(0)V'(0)+M_y(0)U_b'(0)+\\
&+T(0)\theta_z(0)+B(0)\theta_z'(0)-N(L)W_b(L)-Q_x(L)U_b(L)-Q_y(L)V(L)+\\
&-M_x(L)V'(L)-M_y(L)U_b'(L)-T(L)\theta_z(L)-B(L)\theta_z'(L)\big]
\end{aligned}\tag{A1.15}$$

in which

$$\begin{Bmatrix} N(Z_e)\\ Q_x(Z_e)\\ Q_y(Z_e)\\ M_x(Z_e)\\ M_y(Z_e)\\ T(Z_e)\\ B(Z_e)\end{Bmatrix}=\int_A\begin{Bmatrix}\sigma_z(s_b,n_b,Z_e)\\ \tau_v(s_b,n_b,Z_e)\cos\alpha(s_b)+\tau_u(s_b,n_b,Z_e)\sin\alpha(s_b)\\ \tau_v(s_b,n_b,Z_e)\sin\alpha(s_b)-\tau_u(s_b,n_b,Z_e)\cos\alpha(s_b)\\ -\sigma_z(s_b,n_b,Z_e)Y(s_b,n_b)\\ -\sigma_z(s_b,n_b,Z_e)X(s_b,n_b)\\ \tau_v(s_b,n_b,Z_e)\left[r(s_b)+nq'(s_b)\right]-\tau_u(s_b,n_b,Z_e)q(s_b)\\ -\sigma_z(s_b,n_b,Z_e)\Omega(s_b,n_b)\end{Bmatrix}dA,\quad Z_e=0,L \tag{A1.16}$$

A1.4.2. Load potential energy loss by member tractions

The total potential energy loss $\tilde{V}_2$ due to member tractions $p_u(s_b,n_b,z), p_v(s_b,n_b,z), p_z(s_b,n_b,z)$ is

$$\widetilde{V_2} = \int_L \int_{s_b} \left[p_v(s_b,n_b,z) v_b(s_b,n_b,z) + p_u(s_b,n_b,z) u_b(s_b,n_b,z) + p_z(s_b,n_b,z) w_b(s_b,n_b,z) \right] ds_b dz \quad \text{(A1.17)}$$

From Eqs. (2.20)-(2.22), by substituting into Eq.(A1.17), one obtains

$$\begin{aligned} \widetilde{V_2} &= \int_L \int_{s_b} p_v(s_b,n_b,0) \left\{ U_b(z)\cos\alpha(s_b) + V(z)\sin\alpha(s_b) + \theta_z(z)\left[r(s_b) + nq'(s_b) \right] \right\} ds_b dz + \\ &+ \int_L \int_{s_b} p_u(s_b,n_b,0) \left\{ U_b(z)\sin\alpha(s_b) - V(z)\cos\alpha(s_b) - \theta_z(z) q(s_b) \right\} ds_b dz + \\ &+ \int_L \int_{s_b} p_z(s_b,n_b,0) \left\{ W_b(z) - U_b'(z) X(s_b,n_b) - V'(z) Y(s_b,n_b) - \theta_z'(z) \Omega(s_b,n_b) \right\} ds_b dz \end{aligned} \quad \text{(A1.18)}$$

By grouping term in Eq.(A1.18), one obtains

$$\begin{aligned} \widetilde{V_2} &= -\int_L U_b'(z) \left[\int_{s_b} p_z(s_b,z) X(s_b,n_b) ds_b \right] dz + \int_L U_b(z) \left\{ \int_{s_b} \left[p_v(s_b,z)\cos\alpha(s_b) + p_u(s_b,z)\sin\alpha(s_b) \right] ds_b \right\} dz \\ &+ \int_L \theta_z(z) \left\{ \int_{s_b} \left\{ p_v(s_b,z)\left[r(s_b) + nq'(s_b) \right] - p_u(s_b,z) q(s_b) \right\} ds \right\} dz - \int_L \theta_z'(z) \left[\int_{s_b} p_z(s_b,z) \Omega(s_b,n_b) ds_b \right] dz \\ &+ \int_L V(z) \left\{ \int_{s_b} \left[p_v(s_b,z)\sin\alpha(s_b) - p_u(s_b,z)\cos(s_b) \right] ds_b \right\} dz - \int_L V'(z) \left[\int_{s_b} p_z(s_b,z) Y(s_b,n_b) ds_b \right] dz \\ &+ \int_L W_b(z) \left[\int_{s_b} p_z(s_b,z) ds_b \right] dz \end{aligned}$$

(A1.19)

By performing integration by parts from Eq.(A1.19), one obtains

$$\begin{aligned} \widetilde{V_2} &= \int_L U_b(z) \left\{ \int_{s_b} \left[p_v(s_b,z)\cos\alpha(s_b) + p_u(s_b,z)\sin\alpha(s_b) \right] ds_b \right\} dz + \int_L U_b(z) \left[\int_{s_b} \frac{\partial p_z(s_b,z)}{\partial z} X(s_b,n_b) ds_b \right] dz \\ &+ \int_L \theta_z(z) \left\{ \int_{s_b} \left\{ p_v(s_b,z)\left[r(s_b) + nq'(s_b) \right] - p_u(s_b,z) q(s_b) \right\} ds_b \right\} dz + \int_L \theta_z(z) \left[\int_{s_b} \frac{\partial p_z(s_b,z)}{\partial z} \Omega(s_b,n_b) ds_b \right] dz \\ &+ \int_L V(z) \left\{ \int_{s_b} \left[p_v(s_b,z)\sin\alpha(s_b) - p_u(s_b,z)\cos(s_b) \right] ds_b \right\} dz + \int_L V(z) \left[\int_{s_b} \frac{\partial p_z(s_b,z)}{\partial z} Y(s_b,n_b) ds_b \right] dz + \end{aligned}$$

$$+\int_L W_b(z)\left[\int_{s_b} p_z(s_b,z)\,ds_b\right]dz-\left\{U_b(z)\left[\int_{s_b} p_z(s_b,z)X(s_b,n_b)\,ds_b\right]\right\}\Bigg|_0^L-\left\{V(z)\left[\int_{s_b} p_z(s_b,z)Y(s_b,n_b)\,ds_b\right]\right\}\Bigg|_0^L$$

$$-\left\{\theta_z(z)\left[\int_{s_b} p_z(s_b,z)\Omega(s_b,n_b)\,ds_b\right]\right\}\Bigg|_0^L$$

The last three integrals pertain to the end tractions. Their effect has already been incorporated in the boundary terms when determining the load potential due to end tractions $\widetilde{V}_1$. Thus one obtains

$$\widetilde{V}_2=\int_L U_b(z)\left\{\int_{s_b}\left[p_v(s_b,z)\cos\alpha(s_b)+p_u(s_b,z)\sin\alpha(s_b)\right]ds_b\right\}dz+\int_L U_b(z)\left[\int_{s_b}\frac{\partial p_z(s_b,z)}{\partial z}X(s_b,n_b)\,ds_b\right]dz$$

$$+\int_L \theta_z(z)\left\{\int_{s_b}\left\{p_v(s_b,z)\left[r(s_b)+nq'(s_b)\right]-p_u(s_b,z)q(s_b)\right\}ds_b\right\}dz+\int_L \theta_z(z)\left[\int_{s_b}\frac{\partial p_z(s_b,z)}{\partial z}\Omega(s_b,n_b)\,ds_b\right]dz$$

$$+\int_L V(z)\left\{\int_{s_b}\left[p_v(s_b,z)\sin\alpha(s_b)-p_u(s_b,z)\cos(s_b)\right]ds_b\right\}dz+\int_L V(z)\left[\int_{s_b}\frac{\partial p_z(s_b,z)}{\partial z}Y(s_b,n_b)\,ds_b\right]dz$$

$$+\int_L W_b(z)\left[\int_{s_b} p_z(s_b,z)\,ds_b\right]dz$$

(A1.20)

In a concise form, the above expression can be expressed as

$$\widetilde{V}_2=\int_L q_{zb}(z)W_b(z)\,dz+\int_L q_{xb}(z)U_b(z)\,dz+\int_L q_{yb}(z)V(z)\,dz+\int_L m_{zb}(z)\theta_z(z)\,dz \tag{A1.21}$$

in which

$$\begin{Bmatrix} q_{zb}(z) \\ q_{xb}(z) \\ q_{yb}(z) \\ m_{zb}(z) \end{Bmatrix}=\int_{s_b}\begin{Bmatrix} p_z(s_b,z) \\ p_v(s_b,z)\cos\alpha(s_b)+p_u(s_b,z)\sin\alpha(s_b)+\left[\partial p_z(s_b,z)/\partial z\right]X(s_b,n_b) \\ p_v(s_b,z)\sin\alpha(s_b)-p_u(s_b,z)\cos\alpha(s_b)+\left[\partial p_z(s_b,z)/\partial z\right]Y(s_b,n_b) \\ p_v(s_b,z)\left[r(s_b)+nq'(s_b)\right]-p_u(s_b,z)q(s_b)+\left[\partial p_z(s_b,z)/\partial z\right]\Omega(s_b,n_b) \end{Bmatrix}ds_b \tag{A1.22}$$

APPENDIX A2- NON-SHEAR DEFORMABLE THEORY-VARIATION AND INTEGRATIONS BY PARTS

The variation of the total potential energy π of the composite system as given by Eq. (2.36) is

$$\delta\pi = \delta U_b + \delta U_p + \delta U_a - \delta V_1 - \delta V_2 \tag{A2.1}$$

in which U_b, U_p, U_a, V_1, V_2 are given by Eqs. 2.37, 2.38, 2.39, 2.40 and 2.42 of Chapter 2. This appendix sets the variation of the total potential energy of the system to zero and presents the details of integration by parts needed to recover the equilibrium equations and boundary conditions.

A2.1 Variation of the internal strain energy of the wide flange beam

By taking variation of the internal strain energy of the beam U_b in the Eq. 2.37, one has

$$\delta U_b = E_b A_b \int_L W_b' \delta W_b' dz + E_b I_{xxb} \int_L V'' \delta V'' dz + E_b I_{yyb} \int_L U_b'' \delta U_b'' dz + E_b I_{\omega\omega b} \int_L \theta_z'' \delta\theta_z'' dz + G_b J_b \int_L \theta_z' \delta\theta_z' dz \tag{A2.2}$$

By integrating Eq. (A2.2) by parts, one obtains

$$\begin{aligned}
\delta U_b = & -E_b A_b \int_L W_b'' \delta W_b dz + E_b I_{yyb} \int_L U_b'''' \delta U_b dz + E_b I_{xxb} \int_L V'''' \delta V dz + \int_L \left(E_b I_{\omega\omega b} \theta_z'''' - G_b J_b \theta_z'' \right) \delta\theta_z dz \\
& + E_b A_b W_b' \delta W_b \Big|_0^L + E_b I_{yyb} U_b'' \delta U_b' \Big|_0^L - E_b I_{yyb} U_b''' \delta U_b \Big|_0^L + E_b I_{xxb} V'' \delta V' \Big|_0^L - E_b I_{xxb} V''' \delta V \Big|_0^L \\
& + E_b I_{\omega\omega b} \theta_z'' \delta\theta_z' \Big|_0^L - E_b I_{\omega\omega b} \theta_z''' \delta\theta_z \Big|_0^L + G_b J_b \theta_z' \delta\theta_z \Big|_0^L
\end{aligned} \tag{A2.3}$$

A2.2. Variation of the internal strain energy of the GFRP plate

By taking variation of the internal strain energy of the beam U_p in the Eq. 2.38, one has

$$\delta U_p = E_p A_p \int_L W_p' \delta W_p' dz + E_p I_{xxp} \int_L V'' \delta V'' dz + E_p I_{yyp} \int_L U_p'' \delta U_p'' dz + E_p I_{\omega\omega p} \int_L \theta_z'' \delta\theta_z'' dz + G_p J_p \int_L \theta_z' \delta\theta_z' dz \tag{A2.4}$$

By integrating Eq. (A2.4) by parts, one obtains

$$\delta U_p = -E_pA_p\int_L W_p''\delta W_p dz + E_pI_{yyp}\int_L U_p''''\delta U_p dz + E_pI_{xxp}\int_L V''''\delta V dz + \int_L\left(E_pI_{\omega\omega p}\theta_z''''- G_pJ_p\theta_z''\right)\delta\theta_z dz$$

$$+E_pA_pW_p'\delta W_p\Big|_0^L + E_pI_{yyp}U_p''\delta U_p'\Big|_0^L - E_pI_{yyp}U_p'''\delta U_p\Big|_0^L + E_pI_{xxp}V''\delta V'\Big|_0^L - E_pI_{xxp}V'''\delta V\Big|_0^L$$

$$+E_pI_{\omega\omega p}\theta_z''\delta\theta_z'\Big|_0^L - E_pI_{\omega\omega p}\theta_z'''\delta\theta_z\Big|_0^L + G_pJ_p\theta_z'\delta\theta_z\Big|_0^L$$

(A2.5)

A2.3. Variation of the internal strain energy of the Adhesive layer

By taking variation of the internal strain energy of the adhesive U_a in the Eq. 2.39, one has

$$\delta U_a =$$

$$c_2^2G_aA_a\int_L V'\delta V'dz + G_aA_a\int_L\left\{c_1^2\left\langle U_L\right\rangle_{1\times2}^T\left[H_{a1}\right]_{2\times2}\delta\left\{U_L\right\}_{2\times1} + c_1c_2\left[V'\delta\left(W_b - W_p\right) + \left(W_b - W_p\right)\delta V'\right]\right\}dz +$$

$$+G_aJ_a\int_L\theta_z'\delta\theta_z'dz + G_a\int_L\left\{I_{yya}\left\langle U_O\right\rangle_{1\times3}^{\prime\mathrm{T}}\left[H_{a2}\right]_{3\times3}\delta\left\{U_O\right\}' + A_a\left\langle U_O\right\rangle_{1\times3}^{\mathrm{T}}\left[H_{a4}\right]_{3\times3}\delta\left\{U_O\right\}\right\}dz$$

(A2.6)

Equation (A2.6) is then integrated by parts yielding

$$\delta U_a =$$

$$-c_2^2G_aA_a\int_L V''\delta V dz + G_aA_a\int_L\left\{c_1^2\left\langle U_L\right\rangle_{1\times2}^T\left[H_{a1}\right]_{2\times2}\delta\left\{U_L\right\}_{2\times1} + c_1c_2\left[V'\delta\left(W_b - W_p\right) - \left(W_b' - W_p'\right)\delta V\right]\right\}dz$$

$$-G_aJ_a\int_L\theta_z''\delta\theta_z dz - G_a\int_L\left[I_{yya}\left\langle U_O\right\rangle_{1\times3}^{\prime\prime\mathrm{T}}\left[H_{a2}\right]_{3\times3}\delta\left\{U_O\right\}_{3\times1} - A_a\left\langle U_O\right\rangle_{1\times3}^{\mathrm{T}}\left[H_{a4}\right]_{3\times3}\delta\left\{U_O\right\}_{3\times1}\right]dz +$$

$$+\left[G_aA_ac_2^2V'\delta V\right]\Big|_0^L + \left[c_1c_2G_aA_a\left(W_b - W_p\right)\delta V\right]\Big|_0^L + \left[\left(G_aJ_a\right)\theta_z'\delta\theta_z\right]\Big|_0^L + \left[G_aI_{yya}\left\langle U_O\right\rangle_{1\times3}^{\prime\mathrm{T}}\left[H_{a2}\right]_{3\times3}\delta\left\{U_O\right\}_{3\times1}\right]\Big|_0^L$$

(A2.7)

From Eqs. (A2.3), (A2.5), (A2.7), (A1.15) and (A1.19), by substituting into Eq.(A2.1), the variation of the total potential energy $\delta\pi$ is expressed as

$$
\begin{aligned}
&\delta\pi = \\
&+\int_L \left[E_b A_b W_b' \delta W_b' + E_p A_p W_p' \delta W_p' + \left(E_b I_{xxb} + E_p I_{xxp} \right) V'' \delta V'' + G_a A_a c_2^2 V' \delta V' \right] dz \\
&+G_a A_a \int_L \left\{ c_1^2 \left\langle U_L \right\rangle_{1\times 2}^T \left[H_{a1} \right]_{2\times 2} \delta \left\{ U_L \right\}_{2\times 1} + c_1 c_2 \left[V' \delta \left(W_b - W_p \right) + \left(W_b - W_p \right) \delta V' \right] \right\} dz \\
&+\int_L \left[E_b I_{yyb} U_b'' \delta U_b'' + E_p I_{yyp} U_p'' \delta U_p'' + \left(E_b I_{\omega\omega b} + E_p I_{\omega\omega p} \right) \theta_z'' \delta \theta_z'' + \left(G_b J_b + G_p J_p + G_a J_a \right) \theta_z' \delta \theta_z' \right] dz \\
&+G_a \int_L \left\{ I_{yya} \left\langle U_O \right\rangle_{1\times 3}^{\prime \mathrm{T}} \left[H_{a2} \right]_{3\times 3} \delta \left\{ U_O \right\}' + A_a \left\langle U_O \right\rangle_{1\times 3}^{\mathrm{T}} \left[H_{a4} \right]_{3\times 3} \delta \left\{ U_O \right\} \right\} dz + N(0) \delta W_b(0) + Q_x(0) \delta U_b(0) \\
&+Q_y(0) \delta V(0) + M_x(0) \delta V'(0) + M_y(0) \delta U_b'(0) + T(0) \delta \theta_z(0) + B(0) \delta \theta_z'(0) - N(L) \delta W_b(L) \\
&-Q_x(L) \delta U_b(L) - Q_y(L) \delta V(L) - M_x(L) \delta V'(L) - M_y(L) \delta U_b'(L) - T(L) \delta \theta_z(L) - B(L) \delta \theta_z'(L) \\
&+\int_L \delta U_b'(z) \left[\int_{s_b} p_z(s_b, z) X(s_b, n_b) ds_b \right] dz - \int_L \delta U_b(z) \left\{ \int_{s_b} \left[p_v(s_b, z) \cos\alpha(s_b) + p_u(s_b, z) \sin\alpha(s_b) \right] ds_b \right\} dz \\
&-\int_L \delta \theta_z(z) \left\{ \int_{s_b} \left\{ p_v(s_b, z) \left[r(s_b) + n q'(s_b) \right] - p_u(s_b, z) q(s_b) \right\} ds_b \right\} dz + \int_L \delta \theta_z'(z) \left[\int_{s_b} p_z(s_b, z) \Omega(s_b, n_b) ds_b \right] dz \\
&-\int_L \delta V(z) \left\{ \int_s \left[p_v(s_b, z) \sin\alpha(s_b) - p_u(s_b, z) \cos\alpha(s_b) \right] ds \right\} dz + \int_L \delta V'(z) \left[\int_s p_z(s_b, z) Y(s_b, n_b) ds \right] dz \\
&-\int_L \delta W_b(z) \left[\int_s p_z(s_b, z) ds \right] dz
\end{aligned}
\tag{A2.8}
$$

Grouping like terms and rearranging, one obtains

$$
\begin{aligned}
&\delta\pi = \\
&\int_0^L \left(-E_b A_b W_b'' + c_1^2 G_a A_a W_b - c_1^2 G_a A_a W_p + c_1 c_2 G_a A_a V' - q_{zb}(z) \right) \delta W_b dz \\
&+\int_0^L \left(-c_1^2 G_a A_a W_b - E_p A_p W_p'' + c_1^2 G_a A_a W_p - c_1 c_2 G_a A_a V' \right) \delta W_p dz \\
&+\int_0^L \left[-c_1 c_2 G_a A_a W_b' + c_1 c_2 G_a A_a W_p' + \left(E_b I_{xxb} + E_p I_{xxp} \right) V'''' - c_2^2 G_a A_a V'' - q_{yb}(z) \right] \delta V dz \\
&+\int_0^L \Big[E_b I_{yyb} U_b'''' - c_1^2 G_a I_{yya} U_b'' + c_1^2 G_a A_a U_b + c_1^2 G_a I_{yya} U_p'' + \\
&\qquad -c_1^2 G_a A_a U_p + c_1 c_3 G_a I_{yya} \theta_z'' + c_1 c_2 G_a A_a \theta_z - q_{xb}(z) \Big] \delta U_b dz \\
&+\int_0^L \left[c_1^2 G_a I_{yya} U_b'' - c_1^2 G_a A_a U_b + E_p I_{yyp} U_p'''' - c_1^2 G_a I_{yya} U_p'' + c_1^2 G_a A_a U_p - c_1 c_3 G_a I_{yya} \theta_z'' - c_1 c_2 G_a A_a \theta_z \right] \delta U_p dz \\
&+\int_0^L \Big[c_1 c_3 G_a I_{yya} U_b'' + c_1 c_2 G_a A_a U_b - c_1 c_3 G_a I_{yya} U_p'' - c_1 c_2 G_a A_a U_p + \left(E_b I_{\omega\omega b} + E_p I_{\omega\omega p} \right) \theta_z'''' + \\
&\qquad -\left(G_b J_b + G_p J_p + G_a J_a + c_3^2 G_a I_{yya} \right) \theta_z'' + c_2^2 G_a A_a \theta_z - m_{zb}(z) \Big] \delta\theta_z dz \\
&+\left(E_b A_b W_b' - N(z) \right) \delta W_b \Big|_0^L + E_p A_p W_p' \delta W_p \Big|_0^L \\
&+\left[c_1 c_2 G_a A_a W_b - c_1 c_2 G_a A_a W_p - \left(E_b I_{xxb} + E_p I_{xxp} \right) V''' + c_2^2 G_a A_a V' - Q_y(z) + \int_{s_b} p_z(s_b, z) Y(s_b, n_b) ds_b \right] \delta V \Bigg|_0^L \\
&+\left[\left(E_b I_{xxb} + E_p I_{xxp} \right) V'' - M_x(z) \right] \delta V' \Big|_0^L \\
&+\left[-E_b I_{yyb} U_b''' + c_1^2 G_a I_{yya} U_b' - c_1^2 G_a I_{yya} U_p' - c_1 c_3 G_a I_{yya} \theta_z' - Q_x(z) + \int_{s_b} p_z(s_b, z) X(s_b, n_b) ds_b \right] \delta U_b \Bigg|_0^L \\
&+\left(-c_1^2 G_a I_{yya} U_b' - E_p I_{yyp} U_p''' \delta U_p + c_1^2 G_a I_{yya} U_p' + c_1 c_3 G_a I_{yya} \theta_z' \right) \delta U_p \Big|_0^L \\
&+\left(E_b I_{yyb} U_b'' - M_y(z) \right) \delta U_b' \Big|_0^L + \left(E_p I_{yyp} U_p'' \right) \delta U_p' \Big|_0^L \\
&+\Big[-c_1 c_3 G_a I_{yya} U_b' + c_1 c_3 G_a I_{yya} U_p' - \left(E_b I_{\omega\omega b} + E_p I_{\omega\omega p} \right) \theta_z''' + \left(G_b J_b + G_p J_p + G_a J_a + c_3^2 G_a I_{yya} \right) \theta_z' \\
&\quad -T(z) + \int_{s_b} p_z(s_b, z) \Omega(s_b, n_b) ds_b \Big] \delta\theta_z \Big|_0^L + \left[\left(E_b I_{\omega\omega b} + E_p I_{\omega\omega p} \right) \theta_z'' - B(z) \right] \delta\theta_z' \Big|_0^L = 0
\end{aligned}
\tag{A2.9}
$$

APPENDIX A3 NON-SHEAR DEFORMABLE THEORY- HOMOGENEOUS SOLUTION

The objective of this appendix is to formulate the homogeneous solution of the two systems of coupled equilibrium of equations. Section A2.1 provides the homogeneous solution for the longitudinal-transverse response, while Section A2.2 develops the homogeneous solution for torsional-flexural response.

A2.1. Solution for the Longitudinal-Transverse Response

The first set of coupled differential equations (2.39) describes longitudinal-transverse response of the composite system. Its homogeneous form is

$$\left[\begin{array}{c|c|c} -B_1D^2+B_2 & -B_2 & B_3D \\ \hline -B_2 & -B_4D^2+B_2 & -B_3D \\ \hline -B_3D & B_3D & B_5D^4-B_6D^2 \end{array}\right]\begin{Bmatrix} W_b \\ W_p \\ V \end{Bmatrix}=\begin{Bmatrix} 0 \\ 0 \\ 0 \end{Bmatrix} \tag{A3.1}$$

in which

$$B_1=E_bA_b;\ B_2=c_1^2G_aA_a;\ B_3=c_1c_2G_aA_a;\ B_4=E_pA_p;\ B_5=E_bI_{xxb}+E_pI_{xxp}\ B_6=c_2^2G_aA_a \tag{A3.2}$$

The solution of Eq. (A3.1) is assumed to take the exponential form

$$\begin{Bmatrix} W_b \\ W_p \\ V \end{Bmatrix}=\begin{Bmatrix} A_{1i} \\ A_{2i} \\ A_{3i} \end{Bmatrix}e^{m_iz} \tag{A3.3}$$

From Eqs. (A3.3), by substituting into Eqs. (A3.1), one obtains

$$\begin{bmatrix} -B_1m^2+B_2 & -B_2 & B_3m \\ -B_2 & -B_4m^2+B_2 & -B_3m \\ -B_3m & B_3m & B_5m^4-B_6m^2 \end{bmatrix}\begin{Bmatrix} A_{1i} \\ A_{2i} \\ A_{3i} \end{Bmatrix}e^{m_iz}=\begin{Bmatrix} 0 \\ 0 \\ 0 \end{Bmatrix}$$

For a non-trivial solution for $\langle A_{1i} \quad A_{2i} \quad A_{3i}\rangle_{1\times 3}$, the determinant of the above matrix must be vanish,

$$\text{i.e.,}\begin{vmatrix} \left(-B_1m^2+B_2\right) & \left(-B_2\right) & \left(B_3m\right) \\ \left(-B_2\right) & \left(-B_4m^2+B_2\right) & \left(-B_3m\right) \\ \left(-B_3m\right) & \left(B_3m\right) & \left(B_5m^4-B_6m^2\right) \end{vmatrix}=0$$

By expanding the above determinant, one obtains

$$\left[B_1B_4B_5m^4-\left(B_1B_2B_5+B_1B_4B_6+B_2B_4B_5\right)m^2+\left(B_2B_4B_6+B_1B_2B_6-B_1B_3^2-B_3^2B_4\right)\right]m^4=0 \tag{A3.4}$$

in which it can be shown that the coefficient of m^4 vanishes, i.e.,

$$B_2B_4B_6+B_1B_2B_6-B_1B_3^2-B_3^2B_4=\left(B_2B_6-B_3^2\right)\left(B_1+B_4\right)=\left(0\right)\left(B_1+B_4\right)=0$$

Therefore, equation (A3.4) is equivalent to

$$\left(m^2-C_1^2\right)m^6=0\,, C_1=\sqrt{\frac{c_1^2G_aA_a\left(E_bA_b+E_pA_p\right)\left(E_bI_{xxb}+E_pI_{xxp}\right)+c_2^2G_aA_aE_bA_bE_pA_p}{E_bA_bE_pA_p\left(E_bI_{xxb}+E_pI_{xxp}\right)}} \tag{A3.5}$$

Thus, the eight roots of the Eq. (A3.5) are $m_3=m_4=m_5=m_6=m_7=m_8=0$ and

$$m_1=-m_2=\sqrt{\frac{c_1^2G_aA_a\left(E_bA_b+E_pA_p\right)\left(E_bI_{xxb}+E_pI_{xxp}\right)+c_2^2G_aA_aE_bA_bE_pA_p}{E_bA_bE_pA_p\left(E_bI_{xxb}+E_pI_{xxp}\right)}}$$

Thus, the solution of Eq. (A3.3) takes to take the exponential form

$$\begin{Bmatrix} W_b \\ W_p \\ V \end{Bmatrix}=\begin{bmatrix} \left\langle A_1\right\rangle_{1\times8}^{\mathrm{T}} \\ \left\langle A_2\right\rangle_{1\times8}^{\mathrm{T}} \\ \left\langle A_3\right\rangle_{1\times8}^{\mathrm{T}} \end{bmatrix}\left\langle F\right\rangle_{8\times1} \tag{A3.6}$$

in which

$$\left\langle A_1\right\rangle_{1\times6}^{\mathrm{T}}=\left\langle A_{11}\quad A_{12}\quad A_{13}\quad A_{14}\quad A_{15}\quad A_{16}\quad A_{17}\quad A_{18}\right\rangle,$$

$$\left\langle A_2\right\rangle_{1\times6}^{\mathrm{T}}=\left\langle A_{21}\quad A_{22}\quad A_{23}\quad A_{24}\quad A_{25}\quad A_{26}\quad A_{27}\quad A_{28}\right\rangle,$$

$$\left\langle A_3\right\rangle_{1\times6}^{\mathrm{T}}=\left\langle A_{31}\quad A_{32}\quad A_{33}\quad A_{34}\quad A_{35}\quad A_{36}\quad A_{37}\quad A_{38}\right\rangle$$

$$\left\langle F\right\rangle_{1\times6}^{\mathrm{T}}=\left\langle 1\quad z\quad z^2\quad z^3\quad z^4\quad z^5\quad e^{m_7z}\quad e^{m_8z}\right\rangle,$$

There are 24 unknown factors in Eqs. (A3.6), but one only has 8 boundary conditions for the longitudinal-transverse response. Thus, 16 of the 24 unknown factors should be eliminated before enforcing the boundary conditions. This is done by substituting displacement fields in Eqs. (A3.6) into the three equilibrium equations in Eqs. (A3.1). From the first equilibrium equation, one has

$$-B_1D^2W_b+B_2W_b-B_2W_p+B_3DV=$$

$$\left(B_2A_{11}-2B_1A_{13}-B_2A_{21}+B_3A_{32}\right)+\left(B_2A_{12}-6B_1A_{14}-B_2A_{22}+2B_3A_{33}\right)z+$$

$$+\left(B_2A_{13}-12B_1A_{15}-B_2A_{23}+3B_3A_{34}\right)z^2+\left(B_2A_{14}-20B_1A_{16}-B_2A_{24}+4B_3A_{35}\right)z^3+$$

$$+\left(B_2A_{15}-B_2A_{25}+5B_3A_{36}\right)z^4+\left(B_2A_{16}-B_2A_{26}\right)z^5+\left(B_2A_{17}-m_1^2B_1A_{17}-B_2A_{27}+m_1B_3A_{37}\right)e^{m_1z}+$$

$$+\left(B_2A_{18}-m_2^2B_1A_{18}-B_2A_{28}+m_2B_3A_{38}\right)e^{m_2z}=0$$

The above equation must vanish for every value of z. This signifies that each of the coefficients of $z^0,z,z^2,z^3,z^4z^5,e^{m_1z},e^{m_2z}$ must vanish, leading to the following eight identities

$$B_2A_{11}-2B_1A_{13}-B_2A_{21}+B_3A_{32}=0 \tag{A3.7}$$

$$B_2A_{12}-6B_1A_{14}-B_2A_{22}+2B_3A_{33}=0 \tag{A3.8}$$

$$B_2A_{13}-12B_1A_{15}-B_2A_{23}+3B_3A_{34}=0 \tag{A3.9}$$

$$B_2A_{14}-20B_1A_{16}-B_2A_{24}+4B_3A_{35}=0 \tag{A3.10}$$

$$B_2A_{15}-B_2A_{25}+5B_3A_{36}=0 \tag{A3.11}$$

$$B_2A_{16}-B_2A_{26}=0 \tag{A3.12}$$

$$B_2A_{17}-m_1^2B_1A_{17}-B_2A_{27}+m_1B_3A_{37}=0 \tag{A3.13}$$

$$B_2A_{18}-m_2^2B_1A_{18}-B_2A_{28}+m_2B_3A_{38}=0 \tag{A3.14}$$

The second equilibrium equation in Eqs. (A3.1) is expanded into

$$-B_2W_b-B_4D^2W_p+B_2W_p-B_3DV=$$

$$\left(-B_2A_{11}+B_2A_{21}-2B_4A_{23}-B_3A_{32}\right)+\left(-B_2A_{12}+B_2A_{22}-6B_4A_{24}-2B_3A_{33}\right)z+$$

$$+\left(-B_2A_{13}+B_2A_{23}-12B_4A_{25}-3B_3A_{34}\right)z^2+\left(-B_2A_{14}+B_2A_{24}-20B_4A_{26}-4B_3A_{35}\right)z^3+$$

$$+\left(-B_2A_{15}+B_2A_{25}-5B_3A_{36}\right)z^4+\left(-B_2A_{16}+B_2A_{26}\right)z^5+\left(-B_2A_{17}+B_2A_{27}-m_1^2B_4A_{27}-m_1B_3A_{37}\right)e^{m_1z}+$$

$$+\left(-B_2A_{18}+B_2A_{28}-m_2^2B_4A_{28}-m_2B_3A_{38}\right)e^{m_2z}=0$$

which leads to the following eight identities

$$-B_2A_{11}+B_2A_{21}-2B_4A_{23}-B_3A_{32}=0 \tag{A3.15}$$

$$-B_2A_{12}+B_2A_{22}-6B_4A_{24}-2B_3A_{33}=0 \tag{A3.16}$$

$$-B_2A_{13}+B_2A_{23}-12B_4A_{25}-3B_3A_{34}=0 \tag{A3.17}$$

$$-B_2A_{14}+B_2A_{24}-20B_4A_{26}-4B_3A_{35}=0 \tag{A3.18}$$

$$-B_2A_{15}+B_2A_{25}-5B_3A_{36}=0 \tag{A3.19}$$

$$-B_2A_{16}+B_2A_{26}=0 \tag{A3.20}$$

$$-B_2A_{17}+B_2A_{27}-m_1^2B_4A_{27}-m_1B_3A_{37}=0 \tag{A3.21}$$

$$-B_2A_{18}+B_2A_{28}-m_2^2B_4A_{28}-m_2B_3A_{38}=0 \tag{A3.22}$$

In a similar manner, the third equilibrium equation in Eqs. (A3.1) leads to

$$\begin{aligned}
&-B_3DW_b+B_3DW_p+B_5D^4V-B_6D^2V= \\
&\left(-B_3A_{12}+B_3A_{22}-2B_6A_{33}+24B_5A_{35}\right) \\
&+\left(-2B_3A_{13}+2B_3A_{23}-6B_6A_{34}+120B_5A_{36}\right)z+\left(-3B_3A_{14}+3B_3A_{24}-12B_6A_{35}\right)z^2 \\
&+\left(-4B_3A_{15}+4B_3A_{25}-20B_6A_{36}\right)z^3+\left(-5B_3A_{16}+5B_3A_{26}\right)z^4 \\
&+\left(-m_1B_3A_{17}+m_1B_3A_{27}+m_1^4B_5A_{37}-m_1^2B_6A_{37}\right)e^{m_1z}+\left(-m_2B_3A_{18}+m_2B_3A_{28}+m_2^4B_5A_{38}-m_2^2B_6A_{38}\right)e^{m_2z}=0
\end{aligned}$$

leading to the following eight identities.

$$-B_3A_{12}+B_3A_{22}-2B_6A_{33}+24B_5A_{35}=0 \tag{A3.23}$$

$$-2B_3A_{13}+2B_3A_{23}-6B_6A_{34}+120B_5A_{36}=0 \tag{A3.24}$$

$$-3B_3A_{14}+3B_3A_{24}-12B_6A_{35}=0 \tag{A3.25}$$

$$-4B_3A_{15}+4B_3A_{25}-20B_6A_{36}=0 \tag{A3.26}$$

$$-5B_3A_{16}+5B_3A_{26}=0 \tag{A3.27}$$

$$-m_1B_3A_{17}+m_1B_3A_{27}+m_1^4B_5A_{37}-m_1^2B_6A_{37}=0 \tag{A3.28}$$

$$-m_2B_3A_{18}+m_2B_3A_{28}+m_2^4B_5A_{38}-m_2^2B_6A_{38}=0 \tag{A3.29}$$

From Eqs. (A3.12), (A3.20) and (A3.27), one obtains $A_{16} = A_{26}$

From Eqs. (A3.18) and (A3.25) and noting that $B_3/B_2 = B_6/B_3$, one obtains $A_{26} = 0$. Thus, one has

$$A_{16} = A_{26} = 0 \tag{A3.30}$$

By adding (A3.8) and (A3.16), one can express A_{14} in terms of A_{24}. Equation (A3.16) is divided by B_2 and Eq. (A3.23) is divided by B_3. Adding the two resulting equations and noting that $B_3/B_2 = B_6/B_3$, one obtains another expression of A_{35} in term of A_{24}. Then, by substituting the expressions of A_{14} and A_{35} into Eq. (A3.25), one obtains

$$A_{14} = A_{24} = A_{35} = 0 \tag{A3.31}$$

In a similar manner, by adding Eqs. (A3.9) and (A3.17), one can express A_{15} in term of A_{25}. Equation (A3.17) is divided by B_2 and Eq. (A3.24) is divided by B_3 and then both equations are added together. Noting that $B_3/B_2 = B_6/B_3$, one obtains another expression of A_{36} in term of A_{25}. By substituting the expressions of A_{14} and A_{35} in to Eq. (A3.26), one obtains

$$A_{15} = A_{25} = A_{36} = 0 \tag{A3.32}$$

From Eqs. (A3.7), (A3.15), (A3.16) and (A3.24), and noting that $A_{24} = A_{36} = 0$, one obtains the four relationships

$$A_{23} = -\frac{B_1}{B_4} A_{13} \tag{A3.33}$$

$$A_{32} = -\frac{B_2}{B_3}\left(A_{11} - A_{21}\right) + \frac{2B_1}{B_3} A_{13} \tag{A3.34}$$

$$A_{33} = -\frac{B_2}{2B_3} A_{12} + \frac{B_2}{2B_3} A_{22} \tag{A3.35}$$

$$A_{34} = -\left(\frac{B_1 B_2 + B_2 B_4}{3B_3 B_4}\right) A_{13} \tag{A3.36}$$

By solving equation systems (A3.13) and (A3.21) in term of A_{17}, one obtains

$$A_{27} = -\frac{B_1}{B_4} A_{17}$$
$$A_{37} = \left[m_1 \frac{B_1}{B_3} - \left(\frac{B_1 B_2 + B_2 B_4}{m_1 B_3 B_4} \right) \right] A_{17} \tag{A3.37}$$

By solving equation systems (A3.14) and (A3.22) in term of A_{18}, one obtains

$$A_{28} = -\frac{B_1}{B_4} A_{18}$$
$$A_{38} = \left[m_2 \frac{B_1}{B_3} - \left(\frac{B_1 B_2 + B_2 B_4}{m_2 B_3 B_4} \right) \right] A_{18} \tag{A3.38}$$

From equations from (A3.30) to (A3.38), by substituting in to (A3.3), and changing notations, the roots are obtained as

$$W_b(z) = C_1 + C_2 z + C_3 z^2 + C_4 e^{m_1 z} + C_5 e^{m_2 z}$$

$$W_p(z) = C_6 + C_7 z + C_3 \left(-\frac{E_b A_b}{E_p A_p} \right) z^2 + C_4 \left(-\frac{E_b A_b}{E_p A_p} \right) e^{m_1 z} + C_5 \left(-\frac{E_b A_b}{E_p A_p} \right) e^{m_2 z}$$

$$V(z) = -C_1 \frac{c_1}{c_2} z - C_2 \frac{c_1}{2c_2} z^2 + C_7 \frac{c_1}{2c_2} z^2 + C_6 \frac{c_1}{c_2} z + C_3 \left[\frac{2E_b A_b}{c_1 c_2 G_a A_a} z - c_1 \left(\frac{E_b A_b + E_p A_p}{3c_2 E_p A_p} \right) z^3 \right] +$$
$$+ C_4 \left[m_1 \frac{E_b A_b}{c_1 c_2 G_a A_a} - c_1 \left(\frac{E_b A_b + E_p A_p}{m_1 c_2 E_p A_p} \right) \right] e^{m_1 z} + C_5 \left[m_2 \frac{E_b A_b}{c_1 c_2 G_a A_a} - c_1 \left(\frac{E_b A_b + E_p A_p}{m_2 c_2 E_p A_p} \right) \right] e^{m_2 z} + C_8 \tag{A3.39}$$

in which we recall that

$$m_1 = -m_2 = \sqrt{\frac{c_1^2 G_a A_a \left(E_b A_b + E_p A_p\right)\left(E_b I_{xxb} + E_p I_{xxp}\right) + c_2^2 G_a A_a E_b A_b E_p A_p}{E_b A_b E_p A_p \left(E_b I_{xxb} + E_p I_{xxp}\right)}}$$

The eight constants $C_1, \ldots$ are to be determined based on eight corresponding boundary conditions. Equation (A3.39) corresponds to Eq. 2.47 in Chapter 2

A2.2. Solution for the Lateral-Torsional Response

As stated in the Item 2.5.6, the second set of coupled equations

$$\left[\begin{array}{c|c|c} B_7D^4-B_8D^2+B_2 & B_8D^2-B_2 & B_9D^2+B_3 \\ \hline B_8D^2-B_2 & B_{10}D^4-B_8D^2+B_2 & -B_9D^2-B_3 \\ \hline B_9D^2+B_3 & -B_9D^2-B_3 & B_{11}D^4-B_{12}D^2+B_6 \end{array}\right]\begin{Bmatrix} U_b \\ U_p \\ \theta_z \end{Bmatrix}=\begin{Bmatrix} 0 \\ 0 \\ 0 \end{Bmatrix} \quad \text{(A3.40)}$$

describes the lateral torsional response of the system, in which $B_7 = E_b I_{yyb}$; $B_8 = c_1^2 G_a I_{yya}$; $B_9 = c_1 c_3 G_a I_{yya}$; $B_{10} = E_p I_{yyp}$; $B_{11} = E_b I_{\omega\omega b} + E_p I_{\omega\omega p}$; and $B_{12} = G_b J_b + G_p J_p + G_a J_a + c_3^2 G_a I_{yya}$;

The roots of Equation System (A3.40) are assumed to take the exponential form

$$\begin{Bmatrix} U_b \\ U_p \\ \theta_z \end{Bmatrix}=\begin{Bmatrix} A_{4i} \\ A_{5i} \\ A_{6i} \end{Bmatrix} e^{k_i z} \quad \text{(A3.41)}$$

From Eq. (A3.41), by substituting into (A3.40) and note that $\langle A_{4i} \quad A_{4i} \quad A_{4i} \rangle_{1\times 3}$ does not vanish, leads to the conclusion that the determinant of the matrix must be vanish, i.e.,

$$\begin{vmatrix} \left(B_7k^4-B_8k^2+B_2\right) & \left(B_8k^2-B_2\right) & \left(B_9k^2+B_3\right) \\ \left(B_8k^2-B_2\right) & \left(B_{10}k^4-B_8k^2+B_2\right) & \left(-B_9k^2-B_3\right) \\ \left(B_9k^2+B_3\right) & \left(-B_9k^2-B_3\right) & \left(B_{11}k^4-B_{12}k^2+B_6\right) \end{vmatrix}=0$$

$$\begin{aligned} \Leftrightarrow &\left(B_7k^4-B_8k^2+B_2\right)\left[\left(B_{10}k^4-B_8k^2+B_2\right)\left(B_{11}k^4-B_{12}k^2+B_6\right)-\left(-B_9k^2-B_3\right)\left(-B_9k^2-B_3\right)\right]+ \\ &-\left(B_8k^2-B_2\right)\left[\left(B_8k^2-B_2\right)\left(B_{11}k^4-B_{12}k^2+B_6\right)-\left(-B_9k^2-B_3\right)\left(B_9k^2+B_3\right)\right]+ \\ &+\left(B_9k^2+B_3\right)\left[\left(B_8k^2-B_2\right)\left(-B_9k^2-B_3\right)-\left(B_9k^2+B_3\right)\left(B_{10}k^4-B_8k^2+B_2\right)\right]=0 \end{aligned} \quad \text{(A3.42)}$$

The first term in Eq. (A3.42) is expanded as

$$\left(B_7k^4-B_8k^2+B_2\right)\left[\left(B_{10}k^4-B_8k^2+B_2\right)\left(B_{11}k^4-B_{12}k^2+B_6\right)-\left(-B_9k^2-B_3\right)\left(-B_9k^2-B_3\right)\right]=$$

$$=\left(B_7k^4-B_8k^2+B_2\right)\begin{pmatrix}B_{10}B_{11}k^8-B_8B_{11}k^6+B_2B_{11}k^4-B_{10}B_{12}k^6+B_8B_{12}k^4-B_2B_{12}k^2\\+B_6B_{10}k^4-B_6B_8k^2+B_2B_6-B_9^2k^4-2B_3B_9k^2-B_3^2\end{pmatrix}$$

$$=\left(B_7k^4-B_8k^2+B_2\right)\begin{bmatrix}B_{10}B_{11}k^8-\left(B_8B_{11}+B_{10}B_{12}\right)k^6+\left(B_2B_{11}+B_8B_{12}+B_6B_{10}-B_9^2\right)k^4\\-\left(B_2B_{12}+B_6B_8+2B_3B_9\right)k^2\end{bmatrix}$$

$$=B_7B_{10}B_{11}k^{12}-B_8B_{10}B_{11}k^{10}+B_2B_{10}B_{11}k^8-\left(B_7B_8B_{11}+B_7B_{10}B_{12}\right)k^{10}+\left(B_8^2B_{11}+B_8B_{10}B_{12}\right)k^8+$$

$$-\left(B_2B_8B_{11}+B_2B_{10}B_{12}\right)k^6+\left(B_2B_7B_{11}+B_8B_7B_{12}+B_6B_7B_{10}-B_7B_9^2\right)k^8+$$

$$-\left(B_2B_8B_{11}+B_8^2B_{12}+B_6B_8B_{10}-B_8B_9^2\right)k^6\quad+\left(B_2^2B_{11}+B_2B_8B_{12}+B_2B_6B_{10}-B_2B_9^2\right)k^4+$$

$$-\left(B_2B_7B_{12}+B_6B_7B_8+2B_3B_7B_9\right)k^6\quad+\left(B_2B_8B_{12}+B_6B_8^2+2B_3B_8B_9\right)k^4-\left(B_2^2B_{12}+B_6B_2B_8+2B_2B_3B_9\right)k^2$$

$$=B_7B_{10}B_{11}k^{12}-\left(B_8B_{10}B_{11}+B_7B_8B_{11}+B_7B_{10}B_{12}\right)k^{10}+$$

$$+\left(B_2B_{10}B_{11}+B_8^2B_{11}+B_8B_{10}B_{12}+B_2B_7B_{11}+B_8B_7B_{12}+B_6B_7B_{10}-B_7B_9^2\right)k^8+$$

$$-\left(B_2B_8B_{11}+B_2B_{10}B_{12}+B_2B_8B_{11}+B_8^2B_{12}+B_6B_8B_{10}-B_8B_9^2+B_2B_7B_{12}+B_6B_7B_8+2B_3B_7B_9\right)k^6+$$

$$+\left(B_2^2B_{11}+B_2B_8B_{12}+B_2B_6B_{10}-B_2B_9^2+B_2B_8B_{12}+B_6B_8^2+2B_3B_8B_9\right)k^4+$$

$$-\left(B_2^2B_{12}+B_6B_2B_8+2B_2B_3B_9\right)k^2$$

The second term in Eq. (A3.42) is expanded as

$$-\left(B_8k^2-B_2\right)\left[\left(B_8k^2-B_2\right)\left(B_{11}k^4-B_{12}k^2+B_6\right)-\left(-B_9k^2-B_3\right)\left(B_9k^2+B_3\right)\right]=$$

$$=-\left(B_8k^2-B_2\right)\left(B_8k^2-B_2\right)\left(B_{11}k^4-B_{12}k^2+B_6\right)+\left(B_8k^2-B_2\right)\left(-B_9k^2-B_3\right)\left(B_9k^2+B_3\right)$$

$$=\left(-B_8^2k^4+2B_2B_8k^2-B_2^2\right)\left(B_{11}k^4-B_{12}k^2+B_6\right)+\left(B_8k^2-B_2\right)\left(-B_9^2k^4-2B_3B_9k^2-B_3^2\right)$$

$$=-B_8^2B_{11}k^8+2B_2B_8B_{11}k^6-B_2^2B_{11}k^4+B_8^2B_{12}k^6-2B_2B_8B_{12}k^4+B_2^2B_{12}k^2-B_6B_8^2k^4+2B_2B_6B_8k^2-B_2^2B_6+$$

$$-B_8B_9^2k^6+B_2B_9^2k^4-2B_3B_8B_9k^4+2B_2B_3B_9k^2-B_3^2B_8k^2+B_2B_3^2$$

$$=-B_8^2B_{11}k^8+\left(2B_2B_8B_{11}+B_8^2B_{12}-B_8B_9^2\right)k^6-\left(B_2^2B_{11}+2B_2B_8B_{12}+2B_3B_8B_9+B_6B_8^2-B_2B_9^2\right)k^4+$$

$$+\left(B_2^2B_{12}+2B_2B_6B_8+2B_2B_3B_9-B_3^2B_8\right)k^2$$

The third term in Eq. (A3.42) is expanded as

$$\left(B_9k^2+B_3\right)\left[\left(B_8k^2-B_2\right)\left(-B_9k^2-B_3\right)-\left(B_9k^2+B_3\right)\left(B_{10}k^4-B_8k^2+B_2\right)\right]=$$

$$=\left(B_9k^2+B_3\right)\left(B_8k^2-B_2\right)\left(-B_9k^2-B_3\right)-\left(B_9k^2+B_3\right)\left(B_9k^2+B_3\right)\left(B_{10}k^4-B_8k^2+B_2\right)$$

$$=\left(B_8k^2-B_2\right)\left(-B_9^2k^4-2B_3B_9k^2-B_3^2\right)+\left(-B_9^2k^4-2B_3B_9k^2-B_3^2\right)\left(B_{10}k^4-B_8k^2+B_2\right)$$

$$=-B_8B_9^2k^6+B_2B_9^2k^4-2B_3B_8B_9k^4+2B_2B_3B_9k^2-B_3^2B_8k^2+B_2B_3^2$$

$$-B_9^2B_{10}k^8-2B_3B_9B_{10}k^6-B_3^2B_{10}k^4+B_8B_9^2k^6+2B_3B_8B_9k^4+B_3^2B_8k^2-B_2B_9^2k^4-2B_2B_3B_9k^2-B_2B_3^2+$$

$$=-B_9^2B_{10}k^8+\left(B_8B_9^2-B_8B_9^2-2B_3B_9B_{10}\right)k^6+\left(B_2B_9^2-B_2B_9^2+2B_3B_8B_9-2B_3B_8B_9-B_3^2B_{10}\right)k^4$$

$$+\left(2B_2B_3B_9-B_3^2B_8+B_3^2B_8-2B_2B_3B_9\right)k^2$$

$$=-B_9^2B_{10}k^8+\left(-2B_3B_9B_{10}\right)k^6+\left(-B_3^2B_{10}\right)k^4$$

Therefore, Eq. (A3.42) is expanded as

$$\begin{aligned}
&B_7B_{10}B_{11}k^{12}-\left(B_8B_{10}B_{11}+B_7B_8B_{11}+B_7B_{10}B_{12}\right)k^{10}+\\
&+\left(B_2B_{10}B_{11}+B_8^2B_{11}+B_8B_{10}B_{12}+B_2B_7B_{11}+B_8B_7B_{12}+B_6B_7B_{10}-B_7B_9^2\right)k^8+\\
&-\left(B_2B_8B_{11}+B_2B_{10}B_{12}+B_2B_8B_{11}+B_8^2B_{12}+B_6B_8B_{10}-B_8B_9^2+B_2B_7B_{12}+B_6B_7B_8+2B_3B_7B_9\right)k^6+\\
&+\left(B_2^2B_{11}+B_2B_8B_{12}+B_2B_6B_{10}-B_2B_9^2+B_2B_8B_{12}+B_6B_8^2+2B_3B_8B_9\right)k^4+\\
&-\left(B_2^2B_{12}+B_6B_2B_8+2B_2B_3B_9\right)k^2-B_8^2B_{11}k^8+\left(2B_2B_8B_{11}+B_8^2B_{12}-B_8B_9^2\right)k^6\\
&-\left(B_2^2B_{11}+2B_2B_8B_{12}+2B_3B_8B_9+B_6B_8^2-B_2B_9^2\right)k^4+\left(B_2^2B_{12}+2B_2B_6B_8+2B_2B_3B_9-B_3^2B_8\right)k^2+\\
&-B_9^2B_{10}k^8+\left(-2B_3B_9B_{10}\right)k^6+\left(-B_3^2B_{10}\right)k^4=0
\end{aligned}\tag{A3.43}$$

The coefficients with the same power of k are grouped together noting that $B_2B_6=B_3^2$. Equation (A3.43) can be expressed as

$$B_7B_{10}B_{11}k^{12}-\left(B_8B_{10}B_{11}+B_7B_8B_{11}+B_7B_{10}B_{12}\right)k^{10}$$

$$+\left(B_2B_{10}B_{11}+B_8B_{10}B_{12}+B_2B_7B_{11}+B_8B_7B_{12}+B_6B_7B_{10}-B_7B_9^2-B_9^2B_{10}\right)k^8$$

$$-\left(B_2B_{10}B_{12}+B_6B_8B_{10}+B_2B_7B_{12}+B_6B_7B_8+2B_3B_7B_9+2B_3B_9B_{10}\right)k^6=0$$

$$\Leftrightarrow \qquad \left(k^6+F_1k^4+F_2k^2+F_3\right)k^6=0 \tag{A3.44}$$

in which

$$F_1 = -\frac{B_8 B_{10} B_{11} + B_7 B_8 B_{11} + B_7 B_{10} B_{12}}{B_7 B_{10} B_{11}},$$

$$F_2 = \frac{B_2 B_{10} B_{11} + B_8 B_{10} B_{12} + B_2 B_7 B_{11} + B_8 B_7 B_{12} + B_6 B_7 B_{10} - B_7 B_9^2 - B_9^2 B_{10}}{B_7 B_{10} B_{11}},$$

$$F_3 = -\frac{B_2 B_{10} B_{12} + B_6 B_8 B_{10} + B_2 B_7 B_{12} + B_6 B_7 B_8 + 2B_3 B_7 B_9 + 2B_3 B_9 B_{10}}{B_7 B_{10} B_{11}}$$

By substituting constants B_i in Eqs. (A3.2) into the expressions of F_1, F_2, F_3, one obtains

$$F_1 = -\frac{c_1^2 G_a I_{yya}\left(E_b I_{\omega\omega b} + E_p I_{\omega\omega p}\right)\left(E_b I_{yyb} + E_p I_{yyp}\right) + E_b I_{yyb} E_p I_{yyp}\left(G_b J_b + G_p J_p + G_a J_a + c_3^2 G_a I_{yya}\right)}{E_b I_{yyb} E_p I_{yyp}\left(E_b I_{\omega\omega b} + E_p I_{\omega\omega p}\right)}$$

$$F_2 = \frac{\left(E_b I_{yyb} + E_p I_{yyp}\right)\left[c_1^2 G_a A_a\left(E_b I_{\omega\omega b} + E_p I_{\omega\omega p}\right) + c_1^2 G_a I_{yya}\left(G_b J_b + G_p J_p + G_a J_a\right)\right] + c_2^2 G_a A_a E_b I_{yyb} E_p I_{yyp}}{E_b I_{yyb} E_p I_{yyp}\left(E_b I_{\omega\omega b} + E_p I_{\omega\omega p}\right)}$$

$$F_3 = -\frac{\left[c_1^2 G_a A_a\left(G_b J_b + G_p J_p + G_a J_a\right) + c_1^2\left(c_2 + c_3\right)^2 G_a A_a G_a I_{yya}\right]\left(E_b I_{yyb} + E_p I_{yyp}\right)}{E_b I_{yyb} E_p I_{yyp}\left(E_b I_{\omega\omega b} + E_p I_{\omega\omega p}\right)}$$

In summary, the 12 roots of (A3.44) include six zero roots

$$k_1 = k_2 = k_3 = k_4 = k_5 = k_6 = 0$$

and six roots $k_7,\ k_8,\ k_9,\ k_{10},\ k_{11},\ k_{12}$ obtained from Eq. (A3.45):

$$t^3 + F_1 t^2 + F_2 t + F_3 = 0, \quad t = k^2 \tag{A3.45}$$

After obtaining the six roots $k_7,\ k_8,\ k_9,\ k_{10},\ k_{11},\ k_{12}$, by substituting into Eq. (A3.41), one has

$$\begin{Bmatrix} U_b \\ U_p \\ \theta_z \end{Bmatrix} = \begin{bmatrix} \langle A_4 \rangle_{1\times 12}^{\mathrm{T}} \\ \langle A_5 \rangle_{1\times 12}^{\mathrm{T}} \\ \langle A_6 \rangle_{1\times 12}^{\mathrm{T}} \end{bmatrix} \langle F \rangle_{12\times 1} \tag{A3.46}$$

in which

$$\langle F \rangle_{1\times12}^{\mathrm{T}} = \langle 1 \quad z \quad z^2 \quad z^3 \quad z^4 \quad z^5 \quad e^{k_7 z} \quad e^{k_8 z} \quad e^{k_9 z} \quad e^{k_{10} z} \quad e^{k_{11} z} \quad e^{k_{12} z} \rangle,$$

$$\langle A_4 \rangle_{1\times12}^{\mathrm{T}} = \langle A_{41} \quad A_{42} \quad A_{43} \quad A_{44} \quad A_{45} \quad A_{46} \quad A_{47} \quad A_{48} \quad A_{49} \quad A_{410} \quad A_{411} \quad A_{412} \rangle,$$

$$\langle A_5 \rangle_{1\times12}^{\mathrm{T}} = \langle A_{51} \quad A_{52} \quad A_{53} \quad A_{54} \quad A_{55} \quad A_{56} \quad A_{57} \quad A_{58} \quad A_{59} \quad A_{510} \quad A_{511} \quad A_{512} \rangle,$$

$$\langle A_6 \rangle_{1\times12}^{\mathrm{T}} = \langle A_{61} \quad A_{62} \quad A_{63} \quad A_{64} \quad A_{65} \quad A_{66} \quad A_{67} \quad A_{68} \quad A_{69} \quad A_{610} \quad A_{611} \quad A_{612} \rangle$$

There are 36 unknown factors in Eqs. (A3.46), but one has only 12 boundary conditions. Thus, 24 unknown factors should be eliminated before using the boundary conditions. The unknown factors are now found by substituting the displacement fields in Eqs. (A3.46) into the three equilibrium equations in Eqs. (A3.40). From the first equilibrium equation, one has

$$\begin{aligned}
&\left(B_7 D^4 U_b - B_8 D^2 U_b + B_2 U_b\right) + \left(B_8 D^2 U_p - B_2 U_p\right) + \left(B_9 D^2 \theta + B_3 \theta\right) = 0 \\
\Leftrightarrow &\left(24 B_7 A_{45} - 2 B_8 A_{43} + B_2 A_{41} + 2 B_8 A_{53} - B_2 A_{51} + 2 B_9 A_{63} + B_3 A_{61}\right) \\
&+ \left(120 B_7 A_{46} - 6 B_8 A_{44} + B_2 A_{42} + 6 B_8 A_{54} - B_2 A_{52} + 6 B_9 A_{64} + B_3 A_{62}\right) z \\
&+ \left(-12 B_8 A_{45} + B_2 A_{43} + 12 B_8 A_{55} - B_2 A_{53} + 12 B_9 A_{65} + B_3 A_{63}\right) z^2 \\
&+ \left(-20 B_8 A_{46} + B_2 A_{44} + 20 B_8 A_{56} - B_2 A_{54} + 20 B_9 A_{66} + B_3 A_{64}\right) z^3 \\
&+ \left(B_2 A_{45} - B_2 A_{55} + B_3 A_{65}\right) z^4 + \left(B_2 A_{46} - B_2 A_{56} z^5 + B_3 A_{66}\right) z^5 \\
&+ \sum_{i=7}^{12} \left[\left(B_7 k_i^4 - B_8 k_i^2 + B_2\right) A_{4i} e^{k_i z} + \left(B_8 k_i^2 - B_2\right) A_{5i} e^{k_i z} + \left(B_9 k_i^2 + B_3\right) A_{6i} e^{k_i z} \right] = 0
\end{aligned}$$

To let the equation vanish for any z, the coefficients of $z^j\,(j = 0,1,\ldots,5)$ and $e^{k_i}\,(i = 7,8,\ldots,12)$ mush vanish. This leads to 12 equations:

$$B_2 A_{41} - 2 B_8 A_{43} + 24 B_7 A_{45} - B_2 A_{51} + 2 B_8 A_{53} + B_3 A_{61} + 2 B_9 A_{63} = 0 \tag{A3.47}$$

$$B_2 A_{42} - 6 B_8 A_{44} + 120 B_7 A_{46} - B_2 A_{52} + 6 B_8 A_{54} + B_3 A_{62} + 6 B_9 A_{64} = 0 \tag{A3.48}$$

$$B_2 A_{43} - 12 B_8 A_{45} - B_2 A_{53} + 12 B_8 A_{55} + B_3 A_{63} + 12 B_9 A_{65} = 0 \tag{A3.49}$$

$$B_2 A_{44} - 20 B_8 A_{46} - B_2 A_{54} + 20 B_8 A_{56} + B_3 A_{64} + 20 B_9 A_{66} = 0 \tag{A3.50}$$

$$B_2 A_{45} - B_2 A_{55} + B_3 A_{65} = 0 \tag{A3.51}$$

$$B_2 A_{46} - B_2 A_{56} + B_3 A_{66} = 0 \tag{A3.52}$$

$$\left[\left(B_7 k_i^4 - B_8 k_i^2 + B_2\right) A_{4i} + \left(B_8 k_i^2 - B_2\right) A_{5i} + \left(B_9 k_i^2 + B_3\right) A_{6i} \right]_{i=7,8\ldots,12} = 0 \tag{A3.53}$$

Note that Eqs. (A3.53) include six equations with respect to six values of *i*.

For the second equilibrium equation, one has

$$\left(B_8 D^2 U_b - B_2 U_b\right) + \left(B_{10} D^4 U_p - B_8 D^2 U_p + B_2 U_p\right) + \left(-B_9 D^2 \theta - B_3 \theta\right) = 0$$

$$\Leftrightarrow \left(-B_2 A_{41} + 2B_8 A_{43} + B_2 A_{51} - 2B_8 A_{53} + 24B_{10} A_{55} - B_3 A_{61} - 2B_9 A_{63}\right)$$

$$+\left(-B_2 A_{42} + 6B_8 A_{44} + B_2 A_{52} - 6B_8 A_{54} + 120B_{10} A_{56} - B_3 A_{62} - 6B_9 A_{64}\right) z$$

$$+\left(-B_2 A_{43} + 12B_8 A_{45} + B_2 A_{53} - 12B_8 A_{55} - B_3 A_{63} - 12B_9 A_{65}\right) z^2$$

$$+\left(-B_2 A_{44} + 20B_8 A_{46} + B_2 A_{54} - 20B_8 A_{56} - B_3 A_{64} - 20B_9 A_{66}\right) z^3$$

$$+\left(-B_2 A_{45} + B_2 A_{55} - B_3 A_{65}\right) z^4 + \left(-B_2 A_{46} + B_2 A_{56} - B_3 A_{66}\right) z^5$$

$$+\left(B_8 k_i^2 A_{4i} e^{k_i z} - B_2 A_{4i} e^{k_i z} + B_{10} k_i^4 A_{5i} e^{k_i z} - B_8 k_i^2 A_{5i} e^{k_i z} + B_2 A_{5i} e^{k_i z} - B_9 k_i^2 A_{6i} e^{k_i z} - B_3 A_{6i} e^{k_i z}\right)_{i=7,8,\dots,12} = 0$$

For the above equation to vanish for any z, the coefficients of $z^j\,(j = 0,1,\dots,5)$ and $e^{k_i}\,(i = 7,8,\dots,12)$ mush vanish. This leads to 12 equations:

$$-B_2 A_{41} + 2B_8 A_{43} + B_2 A_{51} - 2B_8 A_{53} + 24B_{10} A_{55} - B_3 A_{61} - 2B_9 A_{63} = 0 \qquad \text{(A3.54)}$$

$$-B_2 A_{42} + 6B_8 A_{44} + B_2 A_{52} - 6B_8 A_{54} + 120B_{10} A_{56} - B_3 A_{62} - 6B_9 A_{64} = 0 \qquad \text{(A3.55)}$$

$$-B_2 A_{43} + 12B_8 A_{45} + B_2 A_{53} - 12B_8 A_{55} - B_3 A_{63} - 12B_9 A_{65} = 0 \qquad \text{(A3.56)}$$

$$-B_2 A_{44} + 20B_8 A_{46} + B_2 A_{54} - 20B_8 A_{56} - B_3 A_{64} - 20B_9 A_{66} = 0 \qquad \text{(A3.57)}$$

$$-B_2 A_{45} + B_2 A_{55} - B_3 A_{65} \qquad \text{(A3.58)}$$

$$-B_2 A_{46} + B_2 A_{56} - B_3 A_{66} \qquad \text{(A3.59)}$$

$$\left[\left(B_8 k_i^2 - B_2\right) A_{4i} + \left(B_{10} k_i^4 - B_8 k_i^2 + B_2\right) A_{5i} - \left(B_9 k_i^2 + B_3\right) A_{6i}\right]_{i=7,8,\dots,12} = 0 \qquad \text{(A3.60)}$$

Note that Eqs. (A3.60) include six equations with respect to six values of *i*.

From the third equilibrium equation, one has

$$
\begin{aligned}
&\left(B_9 D^2 U_b + B_3 U_b\right) + \left(-B_9 D^2 U_p - B_3 U_p\right) + \left(B_{11} D^4 \theta - B_{12} D^2 \theta + B_6 \theta\right) = 0 \\
\Leftrightarrow &\left(+2B_9 A_{43} + B_3 A_{41} - 2B_9 A_{53} - B_3 A_{51} + 24B_{11} A_{65} - 2B_{12} A_{63} + B_6 A_{61}\right) \\
&+ \left(+6B_9 A_{44} + B_3 A_{42} - 6B_9 A_{54} - B_3 A_{52} + 120B_{11} A_{66} - 6B_{12} A_{64} + B_6 A_{62}\right) z \\
&+ \left(+12B_9 A_{45} + B_3 A_{43} - 12B_9 A_{55} - B_3 A_{53} - 12B_{12} A_{65} + B_6 A_{63}\right) z^2 \\
&+ \left(+20B_9 A_{46} + B_3 A_{44} - 20B_9 A_{56} - B_3 A_{54} - 20B_{12} A_{66} + B_6 A_{64}\right) z^3 \\
&+ \left(+B_3 A_{45} - B_3 A_{55} + B_6 A_{65}\right) z^4 + \left(+B_3 A_{46} - B_3 A_{56} + B_6 A_{66}\right) z^5 \\
&+ \left(+B_9 k_i^2 A_{4i} e^{k_i z} + B_3 A_{4i} e^{k_i z} - B_9 k_i^2 A_{5i} e^{k_i z} - B_3 A_{5i} e^{k_i z} + B_{11} k_i^4 A_{6i} e^{k_i z} - B_{12} k_i^2 A_{6i} e^{k_i z} + B_6 A_{6i} e^{k_i z}\right)_{i=7,8,\ldots,12} = 0
\end{aligned}
$$

For the above equation to vanish for any z, the coefficients of $z^j\,(j = 0,1,\ldots,5)$ and $e^{k_i}\,(i = 7,8,\ldots,12)$ mush vanish. This leads to 12 equations:

$$B_3 A_{41} + 2B_9 A_{43} - B_3 A_{51} - 2B_9 A_{53} + B_6 A_{61} - 2B_{12} A_{63} + 24B_{11} A_{65} = 0 \tag{A3.61}$$

$$B_3 A_{42} + 6B_9 A_{44} - B_3 A_{52} - 6B_9 A_{54} + B_6 A_{62} - 6B_{12} A_{64} + 120B_{11} A_{66} = 0 \tag{A3.62}$$

$$B_3 A_{43} + 12B_9 A_{45} - B_3 A_{53} - 12B_9 A_{55} + B_6 A_{63} - 12B_{12} A_{65} = 0 \tag{A3.63}$$

$$B_3 A_{44} + 20B_9 A_{46} - B_3 A_{54} - 20B_9 A_{56} + B_6 A_{64} - 20B_{12} A_{66} = 0 \tag{A3.64}$$

$$B_3 A_{45} - B_3 A_{55} + B_6 A_{65} = 0 \tag{A3.65}$$

$$B_3 A_{46} - B_3 A_{56} + B_6 A_{66} = 0 \tag{A3.66}$$

$$\left[\left(B_9 k_i^2 + B_3\right) A_{4i} - \left(B_9 k_i^2 + B_3\right) A_{5i} + \left(B_{11} k_i^4 - B_{12} k_i^2 + B_6\right) A_{6i}\right]_{i=7,8,\ldots,12} = 0 \tag{A3.67}$$

Note that Eqs. (A3.67) include six equations with respect to 6 values of *i*.

Equation (A3.63) divided by B_3 is added to Eq. (A3.49) divided by B_2, yielding

$$A_{45} - A_{55} = \left(\frac{B_2 B_{12} + B_3 B_9}{B_2 B_9 + B_3 B_8}\right) A_{65} \tag{A3.68}$$

From Eq. (A3.51) , one has

$$B_2 A_{45} - B_2 A_{55} + B_3 A_{65} = 0 \Leftrightarrow A_{45} - A_{55} = -\left(\frac{B_3}{B_2}\right) A_{65} \tag{A3.69}$$

From Eqs. (A3.68) and (A3.69), one has

$$A_{65} = 0 \text{ and } A_{45} = A_{55} \tag{A3.70}$$

Equation (A3.47) is added to Eq. (A3.54), which leads to:

$$A_{55} = -\frac{B_7}{B_{10}} A_{45} \tag{A3.71}$$

From Eqs. (A3.70) and (A3.71), one obtains

$$A_{45} = A_{55} = A_{65} = 0 \tag{A3.72}$$

Similarly, by adding Eq. (A3.64) divided by B_3 to Eq. (A3.50) divided by B_2, one obtains

$$A_{46} - A_{56} = \left(\frac{B_2 B_{12} + B_3 B_9}{B_2 B_9 + B_3 B_8} \right) A_{66} \tag{A3.73}$$

Equation (A3.52) can be expressed as

$$A_{46} - A_{56} = -\left(\frac{B_3}{B_2} \right) A_{66} \tag{A3.74}$$

From Eqs. (A3.73) and (A3.74), one has

$$A_{66} = 0 \text{ and } A_{46} = A_{56} \tag{A3.75}$$

Equation (A3.48) is added to Eq. (A3.55), which leads to:

$$A_{56} = -\frac{B_7}{B_{10}} A_{46} \tag{A3.76}$$

From Eqs. (A3.75) and(A3.76), one has

$$A_{46} = A_{56} = A_{66} = 0 \tag{A3.77}$$

Equation (A3.48) divided by B_3 is subtracted from Eq. (A3.62) divided by B_2. From Eqs. (A3.72) and (A3.77), one has

$$A_{44} - A_{54} = \left(\frac{B_2 B_{12} + B_3 B_9}{B_2 B_9 + B_3 B_8} \right) A_{64} \tag{A3.78}$$

Equation (A3.77) is substituted into Eq. (A3.50), which leads to

$$A_{44} - A_{54} = -\left(\frac{B_3}{B_2} \right) A_{64} \tag{A3.79}$$

From Eqs. (A3.78) and (A3.79), one obtains

$$A_{64} = 0 \text{ and } A_{44} = A_{54} \tag{A3.80}$$

Equation (A3.61) divided by B_3 is subtracted from Eq. (A3.47) divided by B_2. From Eqs. (A3.72) and (A3.77) , one has

$$A_{43} - A_{53} = \left(\frac{B_2 B_{12} + B_3 B_9}{B_2 B_9 + B_3 B_8} \right) A_{63} \tag{A3.81}$$

Equation (A3.72) is substituted into Eq. (A3.49), which leads to

$$A_{43} - A_{53} = -\left(\frac{B_3}{B_2} \right) A_{63} \tag{A3.82}$$

From Eqs. (A3.81) and (A3.82), one obtains

$$A_{63} = 0 \text{ and } A_{43} = A_{53} \tag{A3.83}$$

From Eqs. (A3.47) and (A3.48), and using equations (A3.72), (A3.77), (A3.80), and (A3.83), one obtains

$$\begin{aligned} A_{61} &= \frac{B_2}{B_3}\left(-A_{41} + A_{51}\right) \\ A_{62} &= \frac{B_2}{B_3}\left(-A_{42} + A_{52}\right) \end{aligned} \tag{A3.84}$$

From Eqs. (A3.53), (A3.60), and (A3.67), one has a system of the equations

$$\left[\left(B_7 k_i^4 - B_8 k_i^2 + B_2 \right) A_{4i} + \left(B_8 k_i^2 - B_2 \right) A_{5i} + \left(B_9 k_i^2 + B_3 \right) A_{6i} \right]_{i=7,8\ldots,12} = 0$$

$$\left[\left(B_8 k_i^2 - B_2 \right) A_{4i} + \left(B_{10} k_i^4 - B_8 k_i^2 + B_2 \right) A_{5i} - \left(B_9 k_i^2 + B_3 \right) A_{6i} \right]_{i=7,8\ldots.,12} = 0$$

$$\left[\left(B_9 k_i^2 + B_3 \right) A_{4i} - \left(B_9 k_i^2 + B_3 \right) A_{5i} + \left(B_{11} k_i^4 - B_{12} k_i^2 + B_6 \right) A_{6i} \right]_{i=7,8,\ldots,12} = 0$$

The equation system is solved and the results are expressed in terms of A_{4i}

$$\begin{aligned} A_{5i} &= -\frac{B_7}{B_{10}} A_{4i} \\ A_{6i} &= \left[\frac{-B_7 B_{10} k_i^4 + \left(B_7 B_8 + B_8 B_{10} \right) k_i^2 - B_2 \left(B_7 + B_{10} \right)}{B_{10} \left(B_9 k_i^2 + B_3 \right)} \right] A_{4i} = -\frac{\left(B_9 k_i^2 + B_3 \right)\left(B_7 + B_{10} \right)}{B_{10} \left(B_{11} k_i^4 - B_{12} k_i^2 + B_6 \right)} \end{aligned} \tag{A3.85}$$

in which $i = 7,\ 8,\ 9,\ 10,\ 11,\ 12$.

In summary, the equilibrium equation system in (A3.46) can now be expressed as

$$U_b = A_{41} + A_{42}z + A_{43}z^2 + A_{44}z^3 + \sum_{i=7}^{12} A_{4i}e^{k_i z}$$

$$U_p = A_{51} + A_{52}z + A_{53}z^2 + A_{54}z^3 + \sum_{i=7}^{12} A_{5i}e^{k_i z} \qquad \text{(A3.86)}$$

$$\theta_z = A_{61} + A_{62}z + \sum_{i=7}^{12} A_{6i}e^{k_i z}$$

in which

$$A_{53} = A_{43}, \quad A_{54} = A_{44}, \quad A_{61} = \frac{B_2}{B_3}(-A_{41} + A_{51}), \quad A_{62} = \frac{B_2}{B_3}(-A_{42} + A_{52})$$

$$A_{45} = A_{46} = A_{55} = A_{56} = A_{63} = A_{64} = A_{65} = A_{66} = 0 \qquad \text{(A3.87)}$$

$$A_{5i} = -\frac{B_7}{B_{10}}A_{4i}, \quad A_{6i} = \left[\frac{-B_7B_{10}k_i^4 + (B_7B_8 + B_8B_{10})k_i^2 - B_2(B_7 + B_{10})}{B_{10}(B_9k_i^2 + B_3)}\right]A_{4i}$$

$$i = 7,\ 8,\ 9,\ 10,\ 11,\ 12$$

Changing notation such that $A_{41} = D_1; A_{42} = D_2; A_{43} = D_3; A_{44} = D_4; A_{4i}(i = 7,12) = D_j\,(j = 5,10);$ $A_{51} = D_{11};\ A_{52} = D_{12}$, one can re-write Eqs. (A3.86) as

$$U_b = D_1 + D_2z + D_3z^2 + D_4z^3 + \sum_{i=5}^{10} D_i e^{k_i z}$$

$$U_p = A_{51} + A_{52}z + D_3z^2 + D_4z^3 - \sum_{i=5}^{10} D_i \frac{E_bI_{yyb}}{E_pI_{yyp}} e^{k_i z} \qquad \text{(A3.88)}$$

$$\theta_z = -D_1\frac{c_1}{c_2} - D_2\frac{c_1}{c_2}z + D_{11}\frac{c_1}{c_2} + D_{12}\frac{c_1}{c_2}z + \sum_{i=5}^{10} D_i f_{6i} e^{k_i z}$$

in which

$$f_{6i} = \left[\frac{-E_bI_{yyb}E_pI_{yyp}k_i^4 + c_1^2G_aI_{yya}\left(E_bI_{yyb} + E_pI_{yyp}\right)k_i^2 - c_1^2G_aA_a\left(E_bI_{yyb} + E_pI_{yyp}\right)}{E_pI_{yyp}\left(c_1c_3G_aI_{yya}k_i^2 + c_1c_2G_aA_a\right)}\right],\ i = 5,6,\ldots$$

and the values of k_i are obtained from the sixth order equation

$$k^6 + F_1k^4 + F_2k^2 + F_3 = 0 \qquad \text{(A3.89)}$$

with

$$F_1 = -\frac{c_1^2G_aI_{yya}\left(E_bI_{\omega\omega b} + E_pI_{\omega\omega p}\right)\left(E_bI_{yyb} + E_pI_{yyp}\right) + E_bI_{yyb}E_pI_{yyp}\left(G_bJ_b + G_pJ_p + G_aJ_a + c_3^2G_aI_{yya}\right)}{E_bI_{yyb}E_pI_{yyp}\left(E_bI_{\omega\omega b} + E_pI_{\omega\omega p}\right)}$$

$$F_2 = \frac{\left(E_b I_{yyb} + E_p I_{yyp}\right)\left[c_1^2 G_a A_a \left(E_b I_{\omega\omega b} + E_p I_{\omega\omega p}\right) + c_1^2 G_a I_{yya}\left(G_b J_b + G_p J_p + G_a J_a\right)\right] + c_2^2 G_a A_a E_b I_{yyb} E_p I_{yyp}}{E_b I_{yyb} E_p I_{yyp}\left(E_b I_{\omega\omega b} + E_p I_{\omega\omega p}\right)}$$

$$F_3 = -\frac{\left[c_1^2 G_a A_a \left(G_b J_b + G_p J_p + G_a J_a\right) + c_1^2 \left(c_2 + c_3\right)^2 G_a A_a G_a I_{yya}\right]\left(E_b I_{yyb} + E_p I_{yyp}\right)}{E_b I_{yyb} E_p I_{yyp}\left(E_b I_{\omega\omega b} + E_p I_{\omega\omega p}\right)}$$

APPENDIX A4-NON-SHEAR DEFORMATION THEORY- FORMULATION OF SITFFNESS MATRICES

A4.1 Scope

This Appendix shows the details for obtaining the stiffness matrices for longitudinal-transversal response and lateral-torsional response.

A4.2 Longitudinal-transverse response

A4.2.1 Expression of Total Potential Energy

The total potential energy in Eq. (3.1):

$$\pi_1 = \pi_{1b} + \pi_{1p} + \pi_{1a} - V_{11} - V_{21} \tag{A4.1}$$

in which

$$\pi_{1b} = \frac{1}{2} E_b \int_L \left(A_b W_b'^2 + I_{xxb} V''^2 \right) dz \tag{A4.2}$$

is the internal strain energy contribution of the wide flange beam,

$$\pi_{1p} = \frac{1}{2} E_p \int_L \left(A_p W_p'^2 + I_{xxp} V''^2 \right) dz \tag{A4.3}$$

is the internal strain energy contribution of the GFRP plate,

$$\pi_{1a} = \frac{1}{2} G_a A_a \int_L \left[c_2^2 V'^2 + c_1^2 W_b^2 + c_1^2 W_p^2 - 2c_1^2 W_b W_p + 2c_1 c_2 V' \left(W_b - W_p \right) \right] dz \tag{A4.4}$$

is the internal strain energy contribution of the adhesive layer,

$$V_{11} = \left\langle \Delta_{1N} \right\rangle_{1\times 8}^T \left\{ Q_{11} \right\}_{8\times 1} \tag{A4.5}$$

is the potential energy loss by the nodal generalized forces,

$\left\langle Q_{11} \right\rangle_{1\times 8}^T = \left\langle -N(0) \quad 0 \quad -Q_y(0) \quad -M_x(0) \quad N(L) \quad 0 \quad Q_y(L) \quad M_x(L) \right\rangle$ undergoing generalized nodal displacements $\left\langle \Delta_{1N} \right\rangle_{1\times 8}^T$ and

$$V_{21}=\int_L \langle W_b \quad V \quad V' \rangle_{1\times 3} \int_{s_b} \left\{ \begin{array}{c} p_z(s_b,z) \\ \hdashline p_v(s_b,z)\sin\alpha(s_b)-p_u(s_b,z)\cos\alpha(s_b) \\ \hdashline -p_z(s_b,z)Y(s_b,n_b) \end{array} \right\}_{3\times 1} ds_b dz \tag{A4.6}$$

is the load potential energy loss by the member tractions undergoing displacements

A4.2.2 Expression for Stiffness Matrices

From Eq. 3.8, by substituting into the expression of π_{1b} in Eq. (A4.2), one obtains the internal strain energy contribution of the wide flange beam as $\pi_{1b}=\frac{1}{2}\langle \Delta_{1N} \rangle_{1\times 8}^{T} \left[K_1 \right]_{8\times 8} \{\Delta_{1N}\}_{8\times 1}$ in which the stiffness matrix contribution $\left[K_1 \right]_{8\times 8}$ of the beam is given as

$$\begin{aligned}\left[K_1 \right]_{8\times 8} = E_b \left[L_1 \right]_{8\times 8}^{-1\ T} \Bigg[& A_b \int_L \left[Z_1(z) \right]_{8\times 4}^{\prime T} \{\rho_1\}_{4\times 1} \langle \rho_1 \rangle_{1\times 4}^{T} \left[Z_1(z) \right]_{4\times 8}^{\prime} dz + \\ & + I_{xxb} \int_L \left[Z_1(z) \right]_{8\times 4}^{\prime\prime T} \{\rho_3\}_{4\times 1} \langle \rho_3 \rangle_{1\times 4}^{T} \left[Z_1(z) \right]_{4\times 8}^{\prime\prime} dz \Bigg] \left[L_1 \right]_{8\times 8}^{-1}\end{aligned} \tag{A4.7}$$

From Eq. 3.8, by substituting into the expression of π_{1p} in Eq. (A4.3), one obtains the internal strain contribution of the GFRP plate as $\pi_{1p}=\frac{1}{2}\langle \Delta_{1N} \rangle_{1\times 8}^{T} \left[K_2 \right]_{8\times 8} \{\Delta_{1N}\}_{8\times 1}$ in which the stiffness matrix contribution of the plate as

$$\begin{aligned}\left[K_2 \right]_{8\times 8} = E_p \left[L_1 \right]_{8\times 8}^{-1\ T} \Bigg[& A_p \int_L \left[Z_1(z) \right]_{8\times 4}^{\prime T} \{\rho_2\}_{4\times 1} \langle \rho_2 \rangle_{1\times 4}^{T} \left[Z_1(z) \right]_{4\times 8}^{\prime} dz + \\ & + I_{xxp} \int_L \left[Z_1(z) \right]_{8\times 4}^{\prime\prime T} \{\rho_3\}_{4\times 1} \langle \rho_3 \rangle_{1\times 4}^{T} \left[Z_1(z) \right]_{4\times 8}^{\prime\prime} dz \Bigg] \left[L_1 \right]_{8\times 8}^{-1}\end{aligned} \tag{A4.8}$$

The stiffness contribution of the adhesive layer, π_{1a} is expressed as the sum of three contributions

$$\pi_{1a}=\pi_{1a1}+\pi_{1a2}+\pi_{1a3} \tag{A4.9}$$

in which

$$\pi_{1a1}=\frac{1}{2}c_2^2 G_a A_a \int_L V'^2 dz \tag{A4.10}$$

$$\pi_{1a2}=\frac{1}{2}G_a A_a \int_L \left(c_1^2 W_b^2 + c_1^2 W_p^2 - 2c_1^2 W_b W_p \right) dz \tag{A4.11}$$

which can be arranged in a matrix form as

$$\pi_{1a2} = \frac{1}{2} G_a A_a \int_L c_1^2 \left\langle W_b \quad W_p \right\rangle^T \begin{bmatrix} 1 & -1 \\ -1 & 1 \end{bmatrix} \begin{Bmatrix} W_b \\ W_p \end{Bmatrix} dz \tag{A4.12}$$

and

$$\pi_{1a3} = c_1 c_2 G_a A_a \int_L V' \left(W_b - W_p \right) dz \tag{A4.13}$$

From Eq. 3.8, by substituting into the expression of π_{1a1} in Eq. (A4.10), one obtains the first internal strain energy contribution of the adhesive layer as $\pi_{1a1} = \frac{1}{2} \langle \Delta_{1N} \rangle_{1\times 8}^T \left[K_{3a1} \right]_{8\times 8} \{ \Delta_{1N} \}_{8\times 1}$ in which the stiffness matrix contribution $\left[K_{3a1} \right]_{8\times 8}$ is given as

$$\left[K_{3a1} \right]_{8\times 8} = c_2^2 G_a A_a \left[L_1 \right]_{8\times 8}^{-1\,T} \left[\int_L \left[Z_1(z) \right]_{8\times 4}^{\prime T} \{ \rho_3 \}_{4\times 1} \langle \rho_3 \rangle_{1\times 4}^T \left[Z_1(z) \right]_{4\times 8}^{\prime} dz \right] \left[L_1 \right]_{8\times 8}^{-1} \tag{A4.14}$$

From Eq. 3.8, by substituting into the expression of π_{1a2} in Eq. (A4.11), one obtains the second internal strain energy contribution of adhesive layer as $\pi_{1a2} = \frac{1}{2} \langle \Delta_{1N} \rangle_{1\times 8}^T \left[K_{3a2} \right]_{8\times 8} \{ \Delta_{1N} \}_{8\times 1}$ in which the stiffness matrix contribution $\left[K_{3a2} \right]_{8\times 8}$ is given as

$$\left[K_{3a2} \right]_{8\times 8} = c_1^2 G_a A_a \left[L_1 \right]_{8\times 8}^{-1\,T} \left[\int_L \left[Z_1(z) \right]_{8\times 4}^{T} \left[\{ \rho_1 \}_{4\times 1} \;\vdots\; \{ \rho_2 \}_{4\times 1} \right] \begin{bmatrix} 1 & -1 \\ -1 & 1 \end{bmatrix} \begin{bmatrix} \langle \rho_1 \rangle_{1\times 4}^T \\ \hdashline \langle \rho_2 \rangle_{1\times 4}^T \end{bmatrix} \left[Z_1(z) \right]_{4\times 8} dz \right] \left[L_1 \right]_{8\times 8}^{-1} \tag{A4.15}$$

From Eq. 3.8, by substituting into the expression of π_{1a3} in Eq. (A4.13), one obtains the third internal strain energy contribution of adhesive layer as $\pi_{1a3} = \frac{1}{2} \langle \Delta_{1N} \rangle_{1\times 8}^T \left[K_{3a3} \right]_{8\times 8} \{ \Delta_{1N} \}_{8\times 1}$ in which the stiffness matrix contribution $\left[K_{3a3} \right]_{8\times 8}$ is given as

$$\begin{aligned} \pi_{1a3} &= c_1 c_2 G_a A_a \int_L \langle \Delta_{1N} \rangle_{1\times 8}^T \left[N_1(z) \right]_{8\times 4}^{\prime T} \{ \rho_3 \}_{4\times 1} \left(\langle \rho_1 \rangle_{1\times 4}^T - \langle \rho_2 \rangle_{1\times 4}^T \right) \left[N_1(z) \right]_{4\times 8} \{ \Delta_{1N} \}_{8\times 1} dz \\ &= c_1 c_2 G_a A_a \langle \Delta_{1N} \rangle_{1\times 8}^T \int_L \left\{ \left[N_1(z) \right]_{8\times 4}^{\prime T} \left[\{ \rho_3 \}_{4\times 1} \left(\langle \rho_1 \rangle_{1\times 4}^T - \langle \rho_2 \rangle_{1\times 4}^T \right) \right] \left[N_1(z) \right]_{4\times 8} \right\} dz \{ \Delta_{1N} \}_{8\times 1} \\ &= \langle \Delta_{1N} \rangle_{1\times 8}^T \left[M \right]_{8\times 8} \{ \Delta_{1N} \}_{8\times 1} \\ &= \frac{1}{2} \langle \Delta_{1N} \rangle_{1\times 8}^T \left(\left[M \right]_{8\times 8} + \left[M \right]_{8\times 8}^T \right) \{ \Delta_{1N} \}_{8\times 1} = \frac{1}{2} \langle \Delta_{1N} \rangle_{1\times 8}^T \left[K_{3a3} \right]_{8\times 8} \{ \Delta_{1N} \}_{8\times 1} \end{aligned} \tag{A4.16}$$

in which $\left[K_{3a3}\right]_{8\times 8}$ is the third stiffness contribution of adhesive layer

$$\left[K_{3a3}\right]_{8\times 8} = \left[M\right]_{8\times 8} + \left[M\right]_{8\times 8}^{T} \tag{A4.17}$$

and

$$\left[M\right]_{8\times 8} = c_1 c_2 G_a A_a \int_L \left\{ \left[N_1(z)\right]_{8\times 4}^{\prime T} \left[\left\{\rho_3\right\}_{4\times 1} \left(\left\langle \rho_1 \right\rangle_{1\times 4}^{T} - \left\langle \rho_2 \right\rangle_{1\times 4}^{T} \right) \right] \left[N_1(z)\right]_{4\times 8} \right\} dz \tag{A4.18}$$

From Eqs. (A4.14), (A4.15) and (A4.17), the total stiffness contribution of adhesive layer is

$$\left[K_3\right]_{8\times 8} = \left[K_{3a1}\right]_{8\times 8} + \left[K_{3a2}\right]_{8\times 8} + \left[K_{3a3}\right]_{8\times 8} \tag{A4.19}$$

The energy equivalent load vector is obtained by substituting Eqs. 3.8 into eq. (A4.6), yielding

$$V_{21} = \left\langle \Delta_{1N} \right\rangle_{1\times 8}^{T} \left\{Q_{21}\right\}_{8\times 1} \tag{A4.20}$$

in which the energy equivalent load vector $\left\{Q_{21}\right\}$ is given by

$$\left\{Q_{21}\right\} = \int_L \left[\left[N_1(z)\right]_{8\times 4}^{T} \left\{\rho_1\right\}_{4\times 1} \;\vdots\; \left[N_1(z)\right]_{8\times 4}^{T} \left\{\rho_3\right\}_{4\times 1} \;\vdots\; \left[N_1(z)\right]_{8\times 4}^{\prime T} \left\{\rho_3\right\}_{4\times 1} \right] \left\{p_1\right\}_{3\times 1} dz$$

with $$\left\{p_1\right\}_{3\times 1} = \int_{s_b} \left\{ \begin{array}{c} p_z(s_b, z) \\ \hdashline p_v(s_b, z)\sin\alpha(s_b) - p_u(s_b, z)\cos\alpha(s_b) \\ \hdashline -p_z(s_b, z) Y(s_b, n_b) \end{array} \right\} ds_b$$

A4.3 Torsional-flexural response

A4.3.1 Expression of Total Potential Energy

The total potential energy in Eq. (3.2)

$$\pi_2 = \pi_{2b} + \pi_{2p} + \pi_{2a} - V_{12} - V_{22} \tag{A4.21}$$

in which

$$\pi_{2b} = \frac{1}{2}\int_L \left(E_b I_{yyb} U_b''^{2} + E_b I_{\omega\omega b} \theta_z''^{2} + G_b J_b \theta_z'^{2} \right) dz \tag{A4.22}$$

is the internal strain energy contribution of the wide flange beam,

$$\pi_{2p} = \frac{1}{2}\int_L \left(E_p I_{yyp} U_p''^{2} + E_p I_{\omega\omega p} \theta_z''^{2} + G_p J_p \theta_z'^{2} \right) dz \tag{A4.23}$$

is the internal strain energy contribution of the GFRP plate,

$$\pi_{2a}=\frac{1}{2}\int_L\left\{G_aJ_a\theta'^2+G_aI_{yya}\langle U_O\rangle'^{\mathrm{T}}_{1\times3}\left[\overline{H}_{a1}\right]_{3\times3}\{U_O\}'+G_aA_a\langle U_O\rangle^{\mathrm{T}}_{1\times3}\left[\overline{H}_{a2}\right]_{3\times3}\{U_O\}\right\}dz \tag{A4.24}$$

is the internal strain energy contribution of the adhesive layer,

$$V_{12}=\langle\Delta_{2N}\rangle^T_{1\times12}\left\{Q_{12}\right\}_{12\times1} \tag{A4.25}$$

is the potential energy loss by the end forces,

$$\left\langle Q_{12}\right\rangle^T_{1\times8}=\langle -Q_x(0)\quad -M_y(0)\quad 0\quad 0\quad -T(0)\quad -B(0)\quad Q_x(L)\quad M_y(L)\quad 0\quad 0\quad T(L)\quad B(L)\rangle$$

undergoing generalized nodal displacements $\langle\Delta_{2N}\rangle^T_{1\times8}$ and

$$V_{22}=\int_0^L\langle U_b(z)\quad U_b'(z)\quad \theta_z(z)\quad \theta_z'(z)\rangle\int_{s_b}\left\{\begin{array}{c} p_v(s_b,z)\cos\alpha(s_b)+p_u(s_b,z)\sin\alpha(s_b)\\ \hdashline -p_z(s_b,z)X(s_b,n_b)\\ \hdashline p_v(s_b,z)\left[r(s_b)+nq'(s_b)\right]-p_u(s_b,z)q(s_b)\\ \hdashline -p_z(s_b,z)\Omega(s_b,n_b)\end{array}\right\}ds_bdz \tag{A4.26}$$

is the load potential energy loss by the member tractions undergoing displacements

A4.3.2 Expression for Stiffness Matrices

From Eq. 3.19, by substituting into the expression of π_{2b} in Eq. (A4.22), one obtains the internal strain energy contribution of the wide flange beam as $\pi_{2b}=\frac{1}{2}\langle\Delta_{2N}\rangle^T_{1\times12}\left[K_4\right]_{12\times12}\{\Delta_{2N}\}_{12\times1}$ in which the stiffness matrix contribution $\left[K_4\right]_{12\times12}$ of the beam is given as

$$\begin{aligned}\left[K_4\right]_{12\times12}=\left[L_2\right]^{-1\,T}_{12\times12}\Bigg[&E_bI_{yyb}\int_L\left[Z_2(z)\right]''^T_{12\times6}\{\rho_4\}_{6\times1}\langle\rho_4\rangle^T_{1\times6}\left[Z_2(z)\right]''_{6\times12}dz+\\ &+E_bI_{\omega\omega b}\int_L\left[Z_2(z)\right]''^T_{12\times6}\{\rho_6\}_{6\times1}\langle\rho_6\rangle^T_{1\times6}\left[Z_2(z)\right]''_{6\times12}dz+\\ &+G_bJ_b\int_L\left[Z_2(z)\right]'^T_{12\times6}\{\rho_6\}_{6\times1}\langle\rho_6\rangle^T_{1\times6}\left[Z_2(z)\right]'_{6\times12}dz\Bigg]\left[L_2\right]^{-1}_{12\times12}\end{aligned} \tag{A4.27}$$

From Eq. 3.19, by substituting into the expression of π_{2p} in Eq. (A4.23), one obtains the internal strain energy contribution of the wide flange beam as $\pi_{2p}=\frac{1}{2}\langle\Delta_{2N}\rangle^T_{1\times12}\left[K_5\right]_{12\times12}\{\Delta_{2N}\}_{12\times1}$ in which the stiffness matrix contribution $\left[K_5\right]_{12\times12}$ of the beam is given as

$$\left[K_5\right]_{12\times12}=\left[L_2\right]_{12\times12}^{-1\,T}\left[E_p I_{yyp}\int_L \left[Z_2(z)\right]_{3\times12}^{\prime\prime T}\left\{\rho_5\right\}_{6\times1}\left\langle\rho_5\right\rangle_{1\times6}^{T}\left[Z_2(z)\right]_{3\times12}^{\prime\prime}dz+\right.$$

$$+E_p I_{\omega\omega p}\int_L \left[Z_2(z)\right]_{3\times12}^{\prime\prime T}\left\{\rho_6\right\}_{6\times1}\left\langle\rho_6\right\rangle_{1\times6}^{T}\left[Z_2(z)\right]_{3\times12}^{\prime\prime}dz+ \tag{A4.28}$$

$$\left.+G_p J_p\int_L \left[Z_2(z)\right]_{3\times12}^{\prime T}\left\{\rho_6\right\}_{6\times1}\left\langle\rho_6\right\rangle_{1\times6}^{T}\left[Z_2(z)\right]_{3\times12}^{\prime}dz\right]\left[L_2\right]_{12\times12}^{-1}$$

From Eq. 3.19, by substituting into the expression of π_{2a} in Eq. (A4.24), one obtains the internal strain energy contribution of the wide flange beam as $\pi_{2a}=\frac{1}{2}\left\langle\Delta_{2N}\right\rangle_{1\times12}^{T}\left[K_6\right]_{12\times12}\left\{\Delta_{2N}\right\}_{12\times1}$ in which the stiffness matrix contribution $\left[K_6\right]_{12\times12}$ of the beam is given as

$$\left[K_6\right]_{12\times12}=\left[L_2\right]_{12\times12}^{-1\,T}\left[G_a J_a\int_L \left[Z_2\right]_{3\times12}^{\prime T}\left\{\rho_5\right\}_{6\times1}\left\langle\rho_5\right\rangle_{1\times6}^{T}\left[Z_2\right]_{3\times12}^{\prime}dz+\right.$$

$$+G_a I_{yya}\int_L \left[Z_2\right]_{12\times3}^{\prime T}\left[\overline{\rho}\right]_{6\times3}^{T}\left[\overline{H}_{a1}\right]_{3\times3}\left[\overline{\rho}\right]_{3\times6}\left[Z_2\right]_{3\times12}^{\prime}dz+ \tag{A4.29}$$

$$\left.+G_a A_a\int_L \left[Z_2\right]_{12\times3}^{T}\left[\overline{\rho}\right]_{6\times3}^{T}\left[\overline{H}_{a2}\right]_{3\times3}\left[\overline{\rho}\right]_{3\times6}\left[Z_2\right]_{3\times12}dz\right]\left[L_2\right]_{12\times12}^{-1}$$

in which $\left[\overline{\rho}\right]_{6\times3}^{T}=\left[\left\{\rho_4\right\}_{6\times1}\;\vdots\;\left\{\rho_5\right\}_{6\times1}\;\vdots\;\left\{\rho_6\right\}_{6\times1}\right]$

The energy equivalent load vector is obtained by substituting Eqs. 3.19 into eq.(A4.26), yielding

$$V_{22}=\left\langle\Delta_{2N}\right\rangle_{1\times12}^{T}\left\{Q_{22}\right\}_{12\times1} \tag{A4.30}$$

in which the energy equivalent load vector $\left\{Q_{22}\right\}$ is given by

$$\left\{Q_{22}\right\}=\int_0^L\left\langle\left[N_2(z)\right]_{12\times6}^{T}\left\{\rho_4\right\}_{6\times1}^{T}\;\vdots\;\left[N_2(z)\right]_{12\times6}^{\prime T}\left\{\rho_4\right\}_{6\times1}^{T}\;\vdots\;\left[N_2(z)\right]_{12\times6}^{T}\left\{\rho_6\right\}_{6\times1}^{T}\;\vdots\;\left[N_2(z)\right]_{12\times6}^{\prime T}\left\{\rho_6\right\}_{6\times1}^{T}\right\rangle\left\{p_2\right\}_{4\times1}dz$$

with $$\left\{p_2\right\}_{4\times1}=\int_{s_b}\left\{\begin{array}{c} p_v(s_b,z)\cos\alpha(s_b)+p_u(s_b,z)\sin\alpha(s_b)\\ \hdashline -p_z(s_b,z)X(s_b,n_b)\\ \hdashline p_v(s_b,z)\left[r(s_b)+nq'(s_b)\right]-p_u(s_b,z)q(s_b)\\ \hdashline -p_z(s_b,z)\Omega(s_b,n_b)\end{array}\right\}ds_b$$

APPENDIX A5 - SHAPE FUNCTION PLOTS FOR LONGITUDINAL-TRANSVERSE RESPONSE

A5.1 Introduction

Exact shape functions for the longitudinal-flexural response were first introduced in Eq. 3.7. They relate the displacement field vector $\langle \Delta_1(z) \rangle_{1\times 4}^T = \langle W_b(z) \quad W_p(z) \quad V(z) \quad V'(z) \rangle$ to the nodal displacement vector $\langle \Delta_{1N} \rangle_{1\times 8}^T = \langle W_b(0) \quad W_p(0) \quad V(0) \quad V'(0) \quad W_b(L) \quad W_p(L) \quad V(L) \quad V'(L) \rangle$ through

$$\{\Delta_1(z)\}_{4\times 1} = [N_1(z)]_{4\times 8} \{\Delta_{1N}\}_{8\times 1} \tag{A5.1}$$

In which we recall that

$$[N_1(z)]_{4\times 8} = [Z_1(z)]_{4\times 8} [L_1]_{8\times 8}^{-1} \tag{A5.2}$$

and

$$[Z_1(z)]_{4\times 8} = \left[\begin{array}{c:c:c:c:c:c:c:c} 1 & z & z^2 & e^{m_1 z} & e^{m_2 z} & 0 & 0 & 0 \\ \hdashline 0 & 0 & -f_1 z^2 & -f_1 e^{m_1 z} & -f_1 e^{m_2 z} & 1 & z & 0 \\ \hdashline -f_2 z & -f_2 z^2/2 & 2f_3 z - f_4 z^3 & f_5 e^{m_1 z} & f_6 e^{m_2 z} & f_2 z & f_2 z^2/2 & 1 \\ \hdashline -f_2 & -f_2 z & 2f_3 - 3f_4 z^2 & f_5 m_1 e^{m_1 z} & f_6 m_2 e^{m_2 z} & f_2 & f_2 z & 0 \end{array}\right]$$

with $f_1 = \dfrac{E_b A_b}{E_p A_p}$, $f_2 = \dfrac{c_1}{c_2}$, $f_3 = \dfrac{E_b A_b}{c_1 c_2 G_a A_a}$, $f_4 = \dfrac{c_1\left(E_b A_b + E_p A_p\right)}{3c_2 E_p A_p}$, $f_5 = m_1 \dfrac{E_b A_b}{c_1 c_2 G_a A_a} - \dfrac{c_1\left(E_b A_b + E_p A_p\right)}{m_1 c_2 E_p A_p}$,

$f_6 = m_2 \dfrac{E_b A_b}{c_1 c_2 G_a A_a} - \dfrac{c_1\left(E_b A_b + E_p A_p\right)}{m_2 E_p A_p}$

and $[L_1]_{8\times 8} = \left[\begin{array}{c} [Z_1(0)]_{4\times 8} \\ \hdashline [Z_1(L)]_{4\times 8} \end{array}\right]$

Matrix $[N_1(z)]_{4\times 8}$ can be expressed in a partitioned form as

$$\left[N_1(z)\right]_{4\times8} = \begin{bmatrix} \left\langle N_{1i}\right\rangle_{8\times1}^{T} \\ \hdashline \left\langle N_{2i}\right\rangle_{8\times1}^{T} \\ \hdashline \left\langle N_{3i}\right\rangle_{8\times1}^{T} \\ \hdashline \left\langle N_{4i}\right\rangle_{8\times1}^{T} \end{bmatrix} = \left[\begin{array}{c:c:c:c:c:c:c:c} N_{11} & N_{12} & N_{13} & N_{14} & N_{15} & N_{16} & N_{17} & N_{18} \\ \hdashline N_{21} & N_{22} & N_{23} & N_{24} & N_{25} & N_{26} & N_{27} & N_{28} \\ \hdashline N_{31} & N_{32} & N_{33} & N_{34} & N_{35} & N_{36} & N_{37} & N_{38} \\ \hdashline N_{41} & N_{42} & N_{43} & N_{44} & N_{45} & N_{46} & N_{47} & N_{48} \end{array}\right] \tag{A5.3}$$

In which $N_{1i}\left(i=1,\ldots,8\right)$ relate the longitudinal displacements $W_b\left(z\right)$ at the centroid of the wide flange beam to nodal displacement vector $\left\{\Delta_{1N}\right\}_{8\times1}$, N_{2i} relates the longitudinal displacements $W_p\left(z\right)$ at the centroid of the GFRP plate to nodal displacement vector $\left\{\Delta_{1N}\right\}_{8\times1}$, N_{3i} relates the transversal displacements $V\left(z\right)$ to nodal displacement vector $\left\{\Delta_{1N}\right\}_{8\times1}$, and N_{4i} relates the slope of transversal displacements $V'\left(z\right)$ to nodal displacement vector $\left\{\Delta_{1N}\right\}_{8\times1}$.

A5.2. Example of the Plot of Shape functions

For Problem 2 in Chapter 4, the exact shape function functions for 3m-long W150x13 simply supported beam used to interpolate the longitudinal displacements at the centroid of the wide flange beam are $\left\langle N_{1i}\right\rangle_{8\times1}^{T}$ and are depicted in Fig.A5.1. Also, the exact shape functions used to interpolate the longitudinal displacements at the centroid of the GFRP are $\left\langle N_{2i}\right\rangle_{8\times1}^{T}$ and are depicted in Fig. A5.2. The transverse displacement is interpolated by using the exact shape functions $\left\langle N_{3i}\right\rangle_{8\times1}^{T}$ and depicted in Fig. A5.3, while its slope along the longitudinal coordinate is interpolated by using the exact shape functions $\left\langle N_{4i}\right\rangle_{8\times1}^{T}$ and depicted in Fig. A5.4.

A5.2.1 Shape functions $\langle N_{1i}(z)\rangle_{1\times8}$

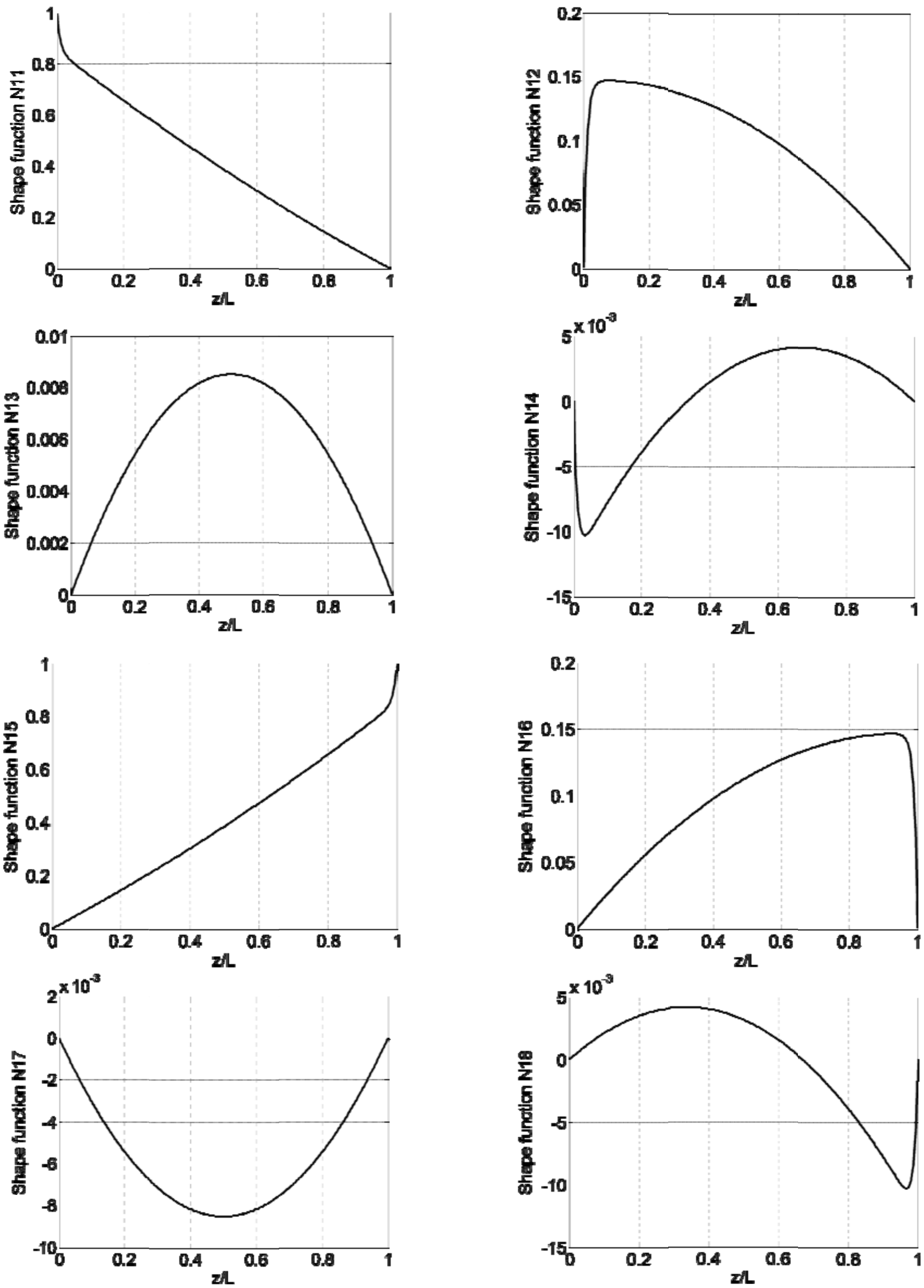

Figure A5.1. Shape functions $\langle N_{1i}(z)\rangle_{1\times8}$

A5.2.2 Shape functions $\langle N_{2i}(z) \rangle_{1\times8}$

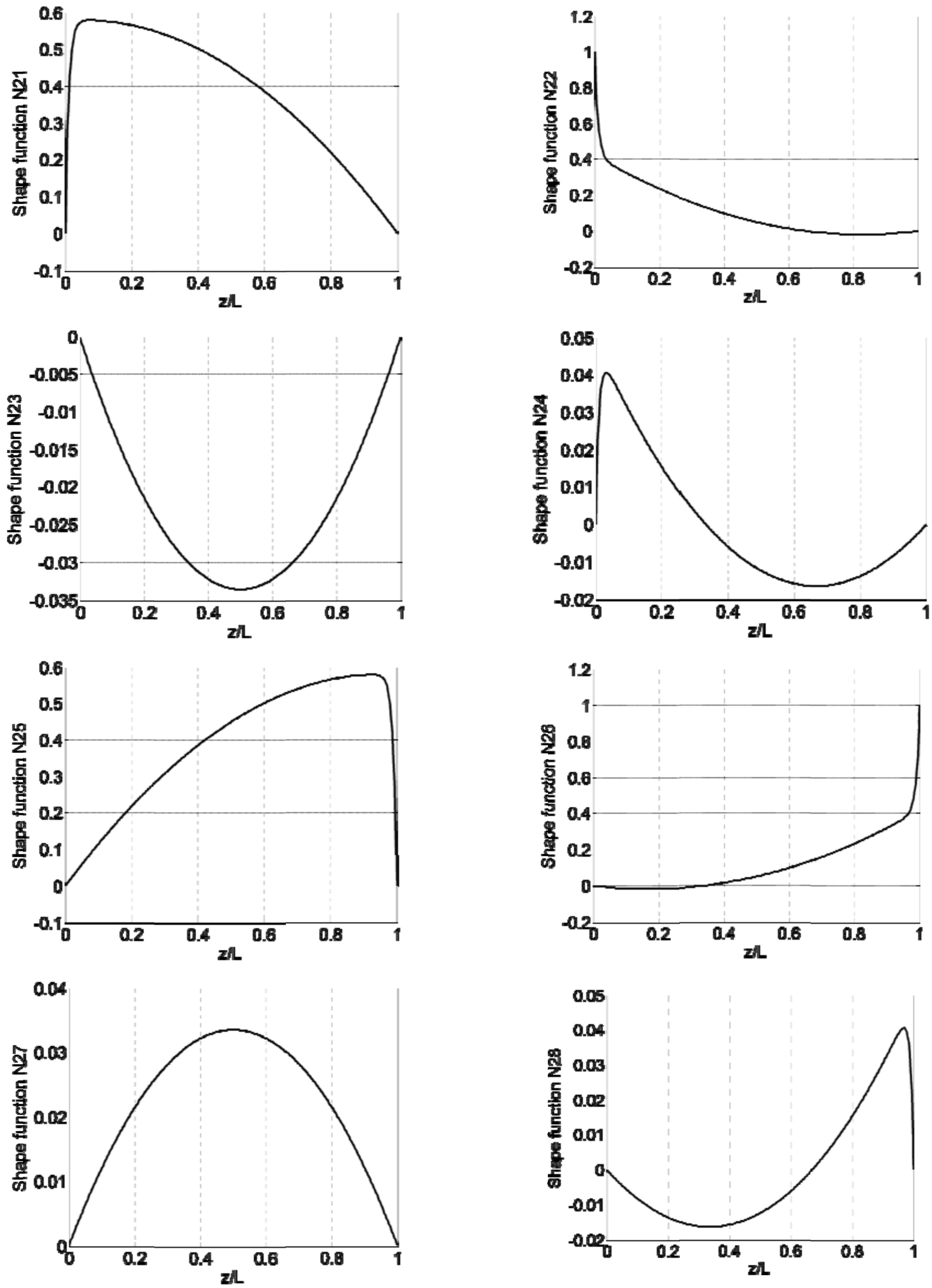

Figure A5.2. Shape functions $\langle N_{2i}(z) \rangle_{1\times8}$

A5.2.3. Shape functions $\left\langle N_{3i}(z) \right\rangle_{1\times 8}$

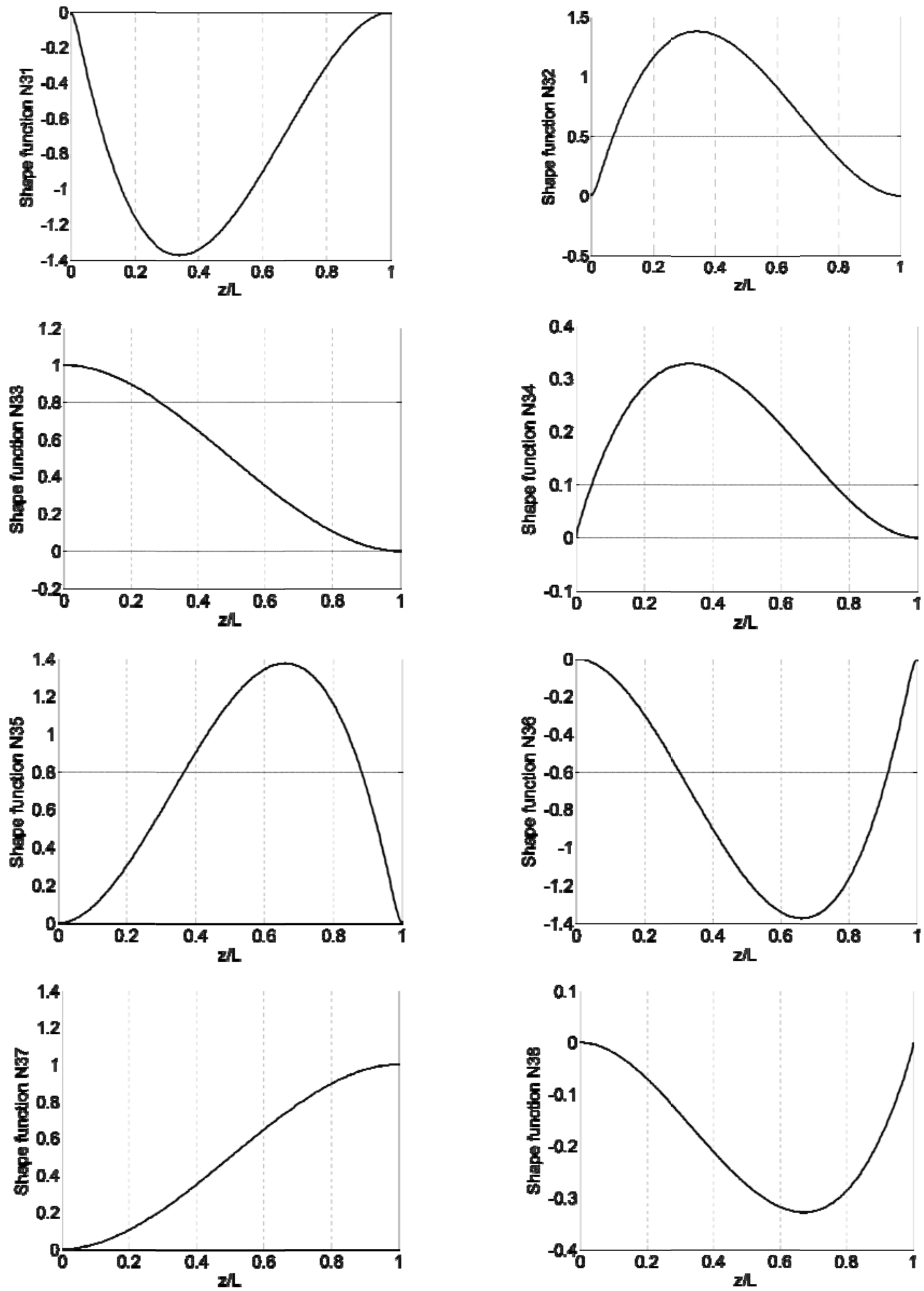

Figure A5.3. Shape functions $\left\langle N_{3i}(z) \right\rangle_{1\times 8}$

A5.2.4. Shape functions $\langle N_{4i}(z) \rangle_{1\times 8}$

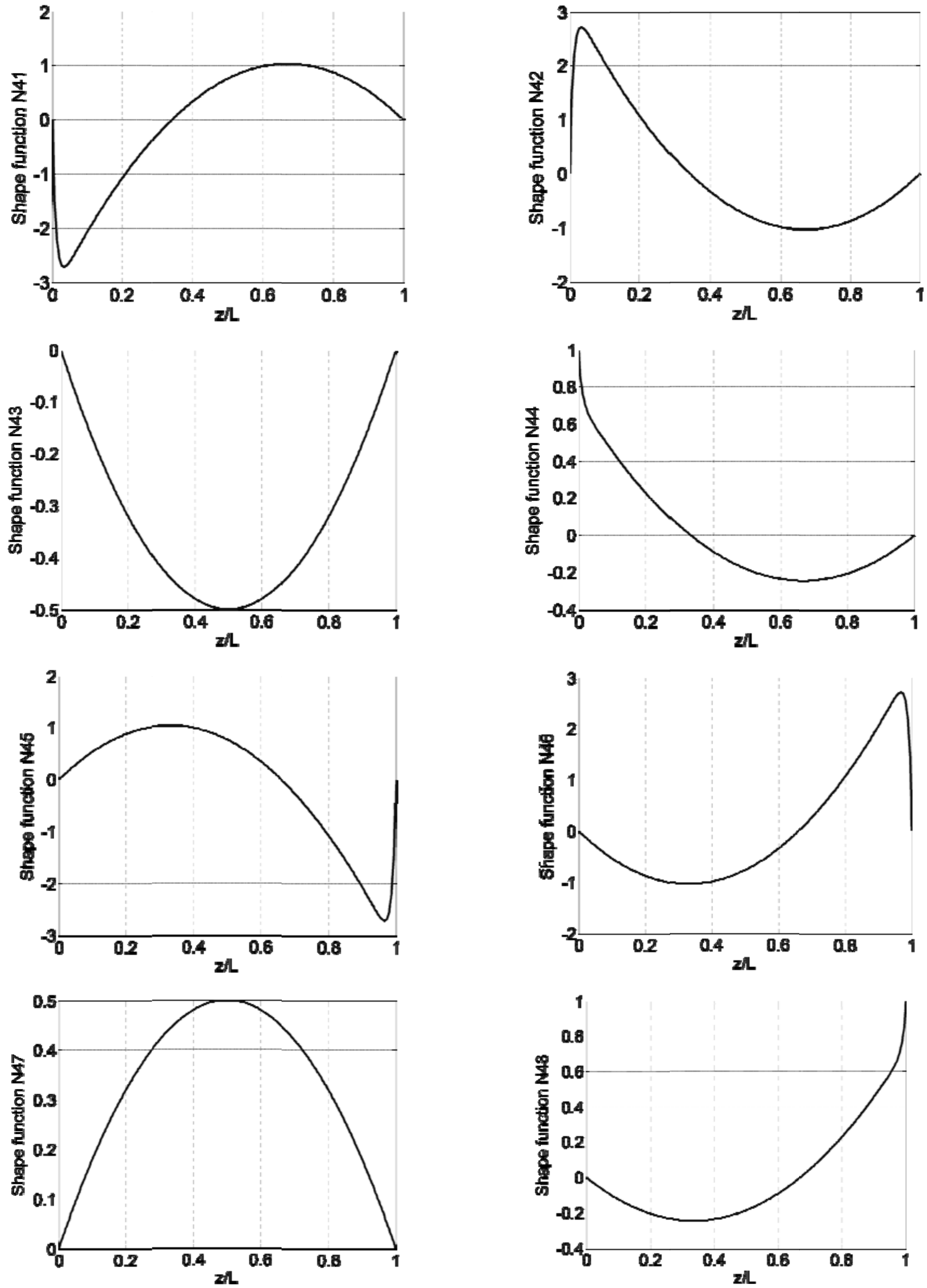

Figure A5.4. Shape functions $\langle N_{4i}(z) \rangle_{1\times 8}$

APPENDIX A6–SHEAR DEFORMABLE THEORY–TOTAL POTENTIAL ENERGY

The objective of this appendix is to provide the details for deriving the total potential energy of the system. As stated in Section 5.4.8.1, the total potential energy π is contributed by internal strain energies within the beam U_b (Item A6.1), GFRP plate U_p (Item A6.2), and adhesive layer U_a (Item A6.3), the load potential energy gained by tractions at member ends V_1 and member tractions within the member V_2. The energy components are expressed before getting the total potential energy. Thus, one has

$$\pi = U_b + U_p + U_a - V_1 - V_2 \tag{A6.1}$$

A6.1. Expression of Internal Strain Energy for the Beam

The internal strain energy of the beam has two contributions, i.e., $U_b = U_{b1} + U_{b2}$ in which U_{b1} is due to the normal stresses and U_{b2} is due to shear stresses. The first term U_{b1} is expressed as

$$U_{b1} = \int_{V_b} \left(\frac{1}{2} \sigma_{zb} \varepsilon_{zb} \right) dV_b = \frac{1}{2} E_b \int_L \int_{A_b} \Big[W_b'(z) - x(s_b)\theta_{yb}'(z) - y(s_b)\theta_{xb}'(z) - \psi'(z)\omega(s) + $$
$$ - n_b \sin\alpha(s_b) U_b''(z) + n_b \cos\alpha(s) V''(z) + n_b q(s_b) \theta_z''(z) \Big]^2 dA_b dz$$

By performing the area integrals and noting the coordinates chosen are orthogonal, i.e., $\int_{A_b} (x, y, xy, n, nx, ny, \omega, \omega x, \omega y, \omega n) dA_b = (0,0,0,0,0,0,0,0,0,0)$, one obtains

$$U_{b1} = \frac{1}{2} E_b \int_L \left(A_b W_b'^{\,2} + I_{ssbf} V''^2 + I_{xxb1} \theta_{xb}'^{\,2} + I_{ssbw} U_b''^2 + I_{yybf} \theta_{yb}'^{\,2} + I_{\omega\omega bl} \theta_z''^2 + I_{\omega\omega bg} \psi_b'^2 \right) dz \tag{A6.2}$$

in which

$$A_b = \sum_{i=1,3} b_i t_i; \;\; I_{xxb1} = \frac{t_w h_w^3}{12} + 2 b_f t_3 \frac{h_b^2}{4}; \;\; I_{ssbf} = 2\frac{b_f t_3^3}{12}; \;\; I_{ssbw} = \frac{h_w t_w^3}{12};$$

$$I_{yybf} = 2\frac{t_3 b_f^3}{12}; \qquad I_{\omega\omega bl} = 2\frac{b_f^3 t_3^3}{144} + \frac{h_w^3 t_w^3}{144}; \qquad I_{\omega\omega bg} = \frac{h_b^2 b^3 t_3}{24};$$

The second term U_{b2} is expressed as

$$U_{b2}=\int_{V_b}\left(\frac{1}{2}\tau_{szb}\gamma_{szb}\right)dV_b=$$

$$=\frac{1}{2}G_b\int_L\int_{A_b}\left\{\left[V'(z)-\ \theta_{xb}(z)\right]\sin\alpha(s_b)+\left[U_b'(z)-\theta_{yb}(z)\right]\cos\alpha(s_b)+\left[\theta_z'(z)-\psi(z)\right]r(s_b)+2n_b\theta_z'(z)\right\}^2 dA_b dz$$

By performing these integrals over the area A_b , one obtains

$U_{b2}=$

$$G_b\int_L\left(\frac{A_{bw}}{2}V'^{\,2}-A_{bw}\theta_{xb}V'+\frac{A_{bw}}{2}\theta_{xb}^2+A_{bf}U_b'^2-2A_{bf}\theta_{yb}U_b'+A_{bf}\theta_{yb}^2+\frac{J_b}{2}\theta_z'^2-\frac{h_b^2A_{bf}}{2}\psi_b\theta_z'+\frac{h_b^2A_{bf}}{2}\psi_b^{\,2}\right)dz \tag{A6.3}$$

in which $A_{bw}=h_wt_w$; $\quad A_{bf}=b_ft_3$; $\quad J_b=\dfrac{h_wt_w^3}{3}+2\dfrac{b_ft_3^3}{3}+\dfrac{h_b^2}{2}A_{bf}$;

In summary, the total strain energy in the beam is

$$\begin{aligned}U_b=\int_L\Bigg(&\frac{1}{2}E_bA_bW_b'^{\,2}+\frac{1}{2}E_bI_{ssbf}V''^2+\frac{1}{2}G_bA_{bw}V'^{\,2}-G_bA_{bw}\theta_{xb}V'+\frac{1}{2}E_bI_{xxb1}\theta_{xb}'^{\,2}+\frac{1}{2}G_bA_{bw}\theta_{xb}^2+\\&+\frac{1}{2}E_bI_{ssbw}U_b''^2+G_bA_{bf}U_b'^2-2G_bA_{bf}\theta_{yb}U_b'+\frac{1}{2}E_bI_{yybf}\theta_{yb}'^{\,2}+G_bA_{bf}\theta_{yb}^2+\frac{1}{2}E_bI_{\omega\omega bl}\theta_z''^2+\\&+\frac{1}{2}G_bJ_b\theta_z'^2-\frac{h_b^2}{2}G_bA_{bf}\psi_b\theta_z'+\frac{1}{2}E_bI_{\omega\omega bg}\psi_b'^2+\frac{h_b^2}{2}G_bA_{bf}\psi_b^{\,2}\Bigg)dz\end{aligned} \tag{A6.4}$$

Equation (A6.4) is Eq. (5.22) in Chapter 5.

A6.2. Expression of Internal Strain Energy for the GFRP plate

The internal strain energy of the plate has two contributions, i.e., $U_p=U_{p1}+U_{p2}$ in which U_{p1} is the contribution due to normal stresses and U_{p2} is the contribution due to shear stress. The first term U_{p1} is expressed as

$$U_{p1}=\int_{V_p}\left(\frac{1}{2}\sigma_{zp}\varepsilon_{zp}\right)dV_p=\frac{1}{2}E_p\int_L\int_{A_p}\left[W_p'(z)-x(s_p)\theta_{yp}'(z)+n_pV''(z)+n_px\left(s_p\right)\theta_z''(z)\right]^2dA_pdz$$

By performing the area integrals and noting the coordinates chosen are orthogonal, i.e., $\int_{A_p}\left(x,n_p,xn_p,x^2n_p,xn_p^2\right)dA_p=\left(0,0,0,0,0\right)$, one obtains

$$U_{p1}=\frac{1}{2}E_p\int_L\left(A_pW_p'^{\,2}+I_{xxp}V''^2+I_{yyp}\theta_{yp}'^{\,2}+I_{\omega\omega p}\theta_z''^2\right)dz \tag{A6.5}$$

in which $A_p = t_1 b_p$; $I_{xxp} = \dfrac{b_p t_1^3}{12}$; $I_{yyp} = \dfrac{t_1 b_p^3}{12}$; $I_{\omega\omega p} = \dfrac{b_p^3 t_1^3}{144}$

The second term U_{p2} is expressed as:

$$U_{p2} = \int_{V_p} \left(\frac{1}{2} \tau_{szp} \gamma_{szp} \right) dV_p = \frac{1}{2} G_p \int_L \int_{A_p} \left[U_p'(z) - \theta_{py}(z) + 2 n_p \theta_z'(z) \right]^2 dA_p dz \tag{A6.6}$$

By performing the area integrals and noting the coordinates chosen are orthogonal, i.e., $\int_{A_p} n_p dA_p = 0$, one obtains

$$U_{p2} = G_p \int_L \left(\frac{1}{2} A_p U_p'^2 - A_p \theta_{yp} U_p' + \frac{1}{2} A_p \theta_{yp}^2 + \frac{1}{2} J_p \theta_z'^2 \right) dz \tag{A6.7}$$

in which $J_p = \left(b_p t_1^3 / 3 \right)$ is the Saint Venant torsional constant. In summary, the total strain energy in the GFRP plate is

$$\begin{aligned} U_p = \int_L \Bigg(& \frac{1}{2} E_p A_p W_p'^2 + \frac{1}{2} E_p I_{xxp} V''^2 + \frac{1}{2} G_p A_p U_p'^2 - G_p A_p \theta_{yp} U_p' + \frac{1}{2} E_p I_{yyp} \theta_{yp}'^2 \\ & + \frac{1}{2} G_p A_p \theta_{yp}^2 + \frac{1}{2} E_p I_{\omega\omega p} \theta_z''^2 + \frac{1}{2} G_p J_p \theta_z'^2 \Bigg) dz \end{aligned} \tag{A6.8}$$

Equation (A6.8) is Eq. (5.23) in Chapter 5.

A6.3. Expression of Internal Strain Energy for the Adhesive layer

The internal strain energy of the adhesive layer has three contributions, i.e., $U_a = U_{a1} + U_{a2} + U_{a3}$ in which U_{a1} is the contribution due to shear stress τ_{zna}, U_{a2} is the contribution due to the shear stress τ_{sna}, and U_{a3} is the contribution due to the shear stress τ_{sza}. The first term U_{a1} is expressed as

$$U_{a1} = \frac{1}{2} \int_{V_a} \tau_{zna} \gamma_{zna} dV_a = \frac{1}{2} G_a \int_L \int_{\mathrm{A_a}} \left\langle \Delta_{a1}(z) \right\rangle_{1\times 8}^{\mathrm{T}} \left\{ a_{a1}(x) \right\}_{8\times 1} \left\langle a_{a1}(x) \right\rangle_{1\times 8}^{\mathrm{T}} \left\{ \Delta_{a1}(z) \right\}_{8\times 1} dA_a dz$$

$$=\frac{1}{2}G_a\int_L\left\langle\Delta_{a1}\right\rangle_{1\times8}^{\mathrm{T}}\int_{A_a}\left[\begin{array}{cccc|cccc} c_1^2 & -c_1^2 & c_1c_3 & c_1c_2 & c_1c_2x & -c_1^2x & c_1^2x & -c_1c_3x \\ -c_1^2 & c_1^2 & -c_1c_3 & -c_1c_2 & -c_1c_2x & c_1^2x & -c_1^2x & c_1c_3x \\ c_1c_3 & -c_1c_3 & c_3^2 & c_2c_3 & c_2c_3x & -c_1c_3x & c_1c_3x & -c_3^2x \\ c_1c_2 & -c_1c_2 & c_2c_3 & c_2^2 & c_2^2x & -c_1c_2x & c_1c_2x & -c_2c_3x \\ \hline c_1c_2x & -c_1c_2x & c_2c_3x & c_2^2x & c_2^2x^2 & -c_1c_2x^2 & c_1c_2x^2 & -c_2c_3x^2 \\ -c_1^2x & c_1^2x & -c_1c_3x & -c_1c_2x & -c_1c_2x^2 & c_1^2x^2 & -c_1^2x^2 & c_1c_3x^2 \\ c_1^2x & -c_1^2x & c_1c_3x & c_1c_2x & c_1c_2x^2 & -c_1^2x^2 & c_1^2x^2 & -c_1c_3x^2 \\ -c_1c_3x & c_1c_3x & -c_3^2x & -c_2c_3x & -c_2c_3x^2 & c_1c_3x^2 & -c_1c_3x^2 & c_3^2x^2 \end{array}\right]dA_a\left\{\Delta_{a1}\right\}_{8\text{x}1}dz$$

$$=\frac{1}{2}G_aA_a\int_L\left\langle\Delta_{a11}\right\rangle_{1\times4}^{T}\left[\widetilde{H_{a11}}\right]_{4\times4}\left\{\Delta_{a11}\right\}_{4\times1}dz+\frac{1}{2}G_aI_{yya}\int_L\left\langle\Delta_{a12}\right\rangle_{1\times4}^{T}\left[\widetilde{H_{a12}}\right]_{4\times4}\left\{\Delta_{a12}\right\}_{4\times1}dz$$

Noting that all integrals $\int_{A_a} x dA_a = 0$, one obtains

$$U_{a1}=\frac{1}{2}G_aA_a\int_L\left\langle\Delta_{a11}\right\rangle_{1\times4}^{T}\left[H_{a11}\right]_{4\times4}\left\{\Delta_{a11}\right\}_{4\times1}dz+\frac{1}{2}G_aI_{yya}\int_L\left\langle\Delta_{a12}\right\rangle_{1\times4}^{T}\left[H_{a12}\right]_{4\times4}\left\{\Delta_{a12}\right\}_{4\times1}dz$$

(A6.9)

in which $\left\langle\Delta_{a11}\right\rangle_{1\times4}^{T}=\left\langle W_b \quad W_p \quad \theta_{bx} \quad V'\right\rangle;\left\langle\Delta_{a12}\right\rangle_{1\times4}^{T}=\left\langle\theta_z' \quad \theta_{yb} \quad \theta_{yp} \quad \psi_b\right\rangle$ are displacement vectors, and

$$\left[H_{a11}\right]_{4\times4}=\begin{bmatrix} c_1^2 & -c_1^2 & c_1c_3 & c_1c_2 \\ -c_1^2 & c_1^2 & -c_1c_3 & -c_1c_2 \\ c_1c_3 & -c_1c_3 & c_3^2 & c_2c_3 \\ c_1c_2 & -c_1c_2 & c_2c_3 & c_2^2 \end{bmatrix};\quad \left[H_{a12}\right]_{4\times4}=\begin{bmatrix} c_2^2 & -c_1c_2 & c_1c_2 & -c_2c_3 \\ -c_1c_2 & c_1^2 & -c_1^2 & c_1c_3 \\ c_1c_2 & -c_1^2 & c_1^2 & -c_1c_3 \\ -c_2c_3 & c_1c_3 & -c_1c_3 & c_3^2 \end{bmatrix};$$

The second term U_{a2} is expressed as

$$U_{a2}=\frac{1}{2}\int_{V_a}\tau_{sna}\gamma_{sna}dV_a=\frac{1}{2}G_a\int_L\int_{A_a}\left\langle\Delta_{a2}(z)\right\rangle_{1\times3}^{\mathrm{T}}\left\{a_{a2}\right\}_{3\times1}\left\langle a_{a2}\right\rangle_{1\times3}^{\mathrm{T}}\left\{\Delta_{a2}(z)\right\}_{3\times1}dA_adz$$

$$=\frac{1}{2}G_a\int_L\left\langle\Delta_{a2}\right\rangle_{1\times3}^{\mathrm{T}}\int_{A_a}\begin{bmatrix} c_1^2 & -c_1^2 & c_1(c_2+c_3) \\ -c_1^2 & c_1^2 & -c_1(c_2+c_3) \\ c_1(c_2+c_3) & -c_1(c_2+c_3) & (c_2+c_3)^2 \end{bmatrix}dA_a\left\{\Delta_{a2}\right\}_{3\times1}dz$$

in which $\left\langle\Delta_{a2}\right\rangle_{1\times3}^{T}=\left\langle U_b \quad U_p \quad \theta\right\rangle$. By performing the area integrals, one obtains

$$U_{a2}=\frac{1}{2}G_aA_a\int_L\left\langle\Delta_{a2}\right\rangle_{1\times3}^{\mathrm{T}}\left[H_{a2}\right]_{3\times3}\left\{\Delta_{a2}\right\}dz \qquad \text{(A6.10)}$$

in which

$$\left[H_{a2}\right]_{3\times3}=\begin{bmatrix} c_1^2 & -c_1^2 & c_1(c_2+c_3) \\ -c_1^2 & c_1^2 & -c_1(c_2+c_3) \\ c_1(c_2+c_3) & -c_1(c_2+c_3) & (c_2+c_3)^2 \end{bmatrix}$$

The third term U_{a3} is expressed as

$$U_{a3} = \int_{V_a} \left(\frac{1}{2} \tau_{sza} \gamma_{sza} \right) dV_a = \int_L \int_{A_a} \left[\frac{1}{2} G_a \left(\gamma_{sza} \right)^2 \right] dA_a dz = \frac{1}{24} G_a A_a \int_L \left\langle \Delta_{a3} \right\rangle_{1\times 6}^T \left[H_{a3} \right]_{6\times 6} \left\{ \Delta_{a3} \right\}_{6\times 1} dz \qquad \text{(A6.11)}$$

in which $\Delta_{a3} = \left\langle U_b'(z) \quad U_p'(z) \quad \theta_z'(z) \quad \theta_{yb}(z) \quad \theta_{yp}(z) \quad \psi(z) \right\rangle$ is displacement vector, and

$$\left[H_{a3} \right]_{6\times 6} = \left[\begin{array}{ccc|ccc} 4 & 2 & 2c_4 & -4 & -2 & -2h_b \\ 2 & 4 & c_5 & -2 & -4 & -h_b \\ 2c_4 & c_5 & c_6 & -2c_4 & -c_5 & -c_4 h_b \\ \hline -4 & -2 & -2c_4 & 4 & 2 & 2h_b \\ -2 & -4 & -c_5 & 2 & 4 & h_b \\ -2h_b & -h_b & -c_4 h_b & 2h_b & h_b & h_b^2 \end{array} \right]$$

with $c_4 = h_b - t_1 + 2t_3; c_5 = h_b - 4t_1 + 2t_3;\ c_6 = h_b^2 + 4t_1^2 + 4t_3^2 - 2h_b t_1 + 4h_b t_3 - 4t_1 t_3$

From(A6.9), (A6.10), and (A6.11), the total internal strain energy in the adhesive layer is

$$\begin{aligned} U_a &= \frac{1}{2} G_a A_a \int_L \left\langle \Delta_{a11} \right\rangle_{1\times 4}^T \left[H_{a11} \right]_{4\times 4} \left\{ \Delta_{a11} \right\}_{4\times 1} dz + \frac{1}{2} G_a I_{yya} \int_L \left\langle \Delta_{a12} \right\rangle_{1\times 4}^T \left[H_{a12} \right]_{4\times 4} \left\{ \Delta_{a12} \right\}_{4\times 1} dz \\ &+ \frac{1}{2} G_a A_a \int_L \left\langle \Delta_{a2} \right\rangle_{1\times 3}^T \left[H_{a2} \right]_{3\times 3} \left\{ \Delta_{a2} \right\}_{3\times 1} dz + \frac{1}{24} G_a A_a \int_L \left\langle \Delta_{a3} \right\rangle_{1\times 6}^T \left[H_{a3} \right]_{6\times 6} \left\{ \Delta_{a3} \right\}_{6\times 1} dz \end{aligned} \qquad \text{(A6.12)}$$

Equation (A6.12) is Eq. 5.24 in Chapter 5.

A6.4. Load potential energy

The total potential energy $\tilde{V}$ loss is the sum of the potential energy $\tilde{V}$ lost by end tractions $\sigma_z(s_b, n_b, 0),\ \tau_u(s_b, n_b, 0), \tau_v(s_b, n_b, 0), \sigma_z(s_b, n_b, L), \tau_u(s_b, n_b, L), \tau_v(s_b, n_b, L)$ at $z = 0, L$ and the potential energy $\tilde{V}$ lost by the member tractions $p_u(s_b, n_b, z), p_v(s_b, n_b, z), p_z(s_b, n_b, z)$ (as defined in Fig. 5.6).

A6.4.1. Load potential energy loss by end tractions

The total potential energy $\tilde{V}$ loss due to tractions at the member ends are

$$\begin{aligned} V_1 = -\Bigg[&\int_A \tau_v(s_b, n_b, 0) v_b(s_b, n_b, 0) dA + \int_A \tau_u(s_b, n_b, 0) u_b(s_b, n_b, 0) dA + \int_A \sigma_z(s_b, n_b, 0) w_b(s_b, n_b, 0) dA + \\ &-\int_A \tau_v(s_b, n_b, L) v_b(s_b, n_b, L) dA - \int_A \tau_u(s_b, n_b, L) u_b(s_b, n_b, L) dA - \int_A \sigma_z(s_b, n_b, L) w_b(s_b, n_b, L) dA \Bigg] \end{aligned}$$

(A6.13)

in which:

$$
\begin{aligned}
u_b(s_b,n_b,z) &= U_b(z)\sin\alpha(s_b) - V(z)\cos\alpha(s_b) - \theta_z(z)q(s_b) \\
v_b(s_b,n_b,z) &= U_b(z)\cos\alpha(s_b) + V(z)\sin\alpha(s_b) + \theta_z(z)\left[r(s_b) + n_b q'(s_b)\right] \\
w_b(s_b,n_b,z) &= W_b(z) - x(s_b)\theta_{yb}(z) - y(s_b)\theta_{xb}(z) - \psi(z)\omega(s_b) \\
&\quad - n_b\sin\alpha(s_b)U_b'(z) + n_b\cos\alpha(s_b)V'(z) + n_b q(s_b)\theta_z'(z)
\end{aligned}
\qquad \text{(A6.14)}
$$

in which

$$
q(s_b) = \left[x(s_b)\right]\cos\alpha(s_b) + \left[y(s_b)\right]\sin\alpha(s_b) \;; \quad r(s_b) = \left[x(s_b)\right]\sin\alpha(s_b) - \left[y(s_b)\right]\cos\alpha(s_b)\;;
$$

From Eqs. (A6.14), by substituting into Eq.(A6.13), one obtains

$$
\begin{aligned}
V_1 = &-\int_A \tau_v(s_b,n_b,0)\left\{U_b(0)\cos\alpha(s_b) + V(0)\sin\alpha(s_b) + \theta_z(0)\left[r(s_b) + nq'(s_b)\right]\right\}dA + \\
&-\int_A \tau_u(s_b,n_b,0)\left[U_b(0)\sin\alpha(s_b) - V(0)\cos\alpha(s_b) - \theta_z(0)q(s_b)\right]dA + \\
&-\int_A \sigma_z(s_b,n_b,0)\left[W_b(0) - x(s_b)\theta_{yb}(0) - y(s_b)\theta_{xb}(0) - \psi_b(0)\omega(s_b) + \right. \\
&\qquad \left. - n_b\sin\alpha(s_b)U_b'(0) + n_b\cos\alpha(s_b)V'(0) + n_b q(s_b)\theta_z'(0)\right]dA + \\
&+\int_A \tau_v(s_b,n_b,L)\left\{U_b(L)\cos\alpha(s_b) + V(L)\sin\alpha(s_b) + \theta_z(L)\left[r(s_b) + nq'(s_b)\right]\right\}dA + \\
&+\int_A \tau_u(s_b,n_b,L)\left[U_b(L)\sin\alpha(s_b) - V(L)\cos\alpha(s_b) - \theta_z(L)q(s_b)\right]dA + \\
&+\int_A \sigma_z(s_b,n_b,L)\left[W_b(L) - x(s_b)\theta_{yb}(L) - y(s_b)\theta_{xb}(L) - \psi_b(L)\omega(s_b) + \right. \\
&\qquad \left. - n_b\sin\alpha(s_b)U_b'(L) + n_b\cos\alpha(s_b)V'(L) + n_b q(s_b)\theta_z'(L)\right]dA
\end{aligned}
\qquad \text{(A6.15)}
$$

By regrouping terms in Eq. (A6.15), one obtains

$$
\begin{aligned}
V_1 = -\Big[&N(0)W_b(0) + Q_x(0)U_b(0) + Q_y(0)V(0) + M_{x1}(0)V'(0) + M_{x2}(0)\theta_{xb}(0) \\
&+ M_{y1}(0)U_b'(0) + M_{y2}(0)\theta_{yb}(0) + T(0)\theta_z(0) + B_1(0)\theta_z'(0) + B_2(0)\psi_b(0) \\
&- N(L)W_b(L) - Q_x(L)U_b(L) - Q_y(L)V(L) - M_{x1}(L)V'(L) - M_{x2}(L)\theta_{xb}(L) \\
&- M_{y1}(L)U_b'(L) - M_{y2}(L)U_b'(L) - T(L)\theta_z(L) - B_1(L)\theta_z'(L) - B_2(L)\psi_b(L)\Big]
\end{aligned}
\qquad \text{(A6.16)}
$$

in which

$$\begin{Bmatrix} N(Z_e) \\ Q_x(Z_e) \\ Q_y(Z_e) \\ M_{x1}(Z_e) \\ M_{x2}(Z_e) \\ M_{y1}(Z_e) \\ M_{y2}(Z_e) \\ T(Z_e) \\ B_1(Z_e) \\ B_2(Z_e) \end{Bmatrix} = \int_A \begin{Bmatrix} \sigma_z(s_b,n_b,Z_e) \\ \tau_v(s_b,n_b,Z_e)\cos\alpha(s_b)+\tau_u(s_b,n_b,Z_e)\sin\alpha(s_b) \\ \tau_v(s_b,n_b,Z_e)\sin\alpha(s_b)-\tau_u(s_b,n_b,Z_e)\cos\alpha(s_b) \\ \sigma_z(s_b,n_b,Z_e)n_b\cos\alpha(s_b) \\ -\sigma_z(s_b,n_b,Z_e)y(s_b) \\ -\sigma_z(s_b,n_b,Z_e)n_b\sin\alpha(s_b) \\ -\sigma_z(s_b,n_b,Z_e)x(s_b) \\ \tau_v(s_b,n_b,Z_e)\left[r(s_b)+nq'(s_b)\right]-\tau_u(s_b,n_b,Z_e)q(s_b) \\ \sigma_z(s_b,n_b,Z_e)n_bq(s_b) \\ -\sigma_z(s_b,n_b,Z_e)\omega(s_b) \end{Bmatrix} dA, \quad Z_e=0,L \qquad \text{(A6.17)}$$

Equation (A6.17) is Eq. 5.27 in Chapter 5.

A6.4.2. Load potential energy loss by member tractions

The load potential energy $\tilde{V}$ loss due to member tractions $p_u(s_b,n_b,z), p_v(s_b,n_b,z), p_z(s_b,n_b,z)$ undergoing displacements u_b, v_b, w_b is

$$V_2 = \int_L \int_{s_b} \left[p_u(s_b,n_b,z)u_b(s_b,n_b,z) + p_v(s_b,n_b,z)v_b(s_b,n_b,z) + p_z(s_b,n_b,z)w_b(s_b,n_b,z) \right] ds_b dz \quad \text{(A6.18)}$$

From Eqs. (A6.14) by substituting into Eq.(A6.18), one obtains

$$\begin{aligned} V_2 = &\int_L \int_{s_b} p_u(s_b,n_b,z)\left\{U_b(z)\sin\alpha(s_b) - V(z)\cos\alpha(s_b) - \theta_z(z)q(s_b)\right\} ds_b dz + \\ &+\int_L \int_{s_b} p_v(s_b,n_b,z)\left\{U_b(z)\cos\alpha(s_b) + V(z)\sin\alpha(s_b) + \theta_z(z)\left[r(s_b)+nq'(s_b)\right]\right\} ds_b dz + \\ &+\int_L \int_{s_b} p_z(s_b,n_b,z)\left[W_b(z) - x(s_b)\theta_{by}(z) - y(s_b)\theta_{bx}(z) - \psi_b(z)\omega(s_b) + \right. \\ &\left. -n_b\sin\alpha(s_b)U_b'(z) + n_b\cos\alpha(s_b)V'(z) + n_bq(s_b)\theta_z'(z)\right] ds_b dz \end{aligned} \qquad \text{(A6.19)}$$

By grouping term in Eq.(A6.19), one obtains

$$V_2 = \int_L W_b(z)\left[\int_{s_b} p_z(s_b,n_b,z)\,ds_b\right]dz + \int_L V(z)\left\{\int_{s_b}\left[p_v(s_b,n_b,z)\sin\alpha(s_b) - p_u(s_b,z)\cos\alpha(s_b)\right]ds_b\right\}dz$$

$$+\int_L V'(z)\left[\int_{s_b} p_z(s_b,n_b,z)\,n_b\cos\alpha(s_b)\,ds_b\right]dz - \int_L \theta_{xb}(z)\left[\int_{s_b} p_z(s_b,n_b,z)\,y(s_b)\,ds_b\right]dz$$

$$-\int_L U_b'(z)\left[\int_{s_b} p_z(s_b,n_b,z)\,n_b\sin\alpha(s_b)\,ds_b\right]dz + \int_L U_b(z)\left\{\int_{s_b}\left[p_v(s_b,n_b,z)\cos\alpha(s_b) + p_u(s_b,n_b,z)\sin\alpha(s_b)\right]ds_b\right\}dz$$

$$-\int_L \theta_{yb}(z)\left[\int_{s_b} p_z(s_b,n_b,z)\,x(s_b)\,ds_b\right]dz + \int_L \theta_z(z)\left\{\int_{s_b}\left\{p_v(s_b,n_b,z)\left[r(s_b)+nq'(s_b)\right] - p_u(s_b,n_b,z)\,q(s_b)\right\}ds_b\right\}dz$$

$$+\int_L \theta_z'(z)\left[\int_{s_b} p_z(s_b,n_b,z)\,n_b q(s_b)\,ds_b\right]dz - \int_L \psi_b(z)\left[\int_{s_b} p_z(s_b,n_b,z)\,\omega(s_b)\,ds_b\right]dz$$

(A6.20)

By performing integration by parts in Eq.(A6.20), one obtains

$$V_2 = \int_L W_b(z)\left[\int_{s_b} p_z(s_b,n_b,z)\,ds_b\right]dz + \int_L V(z)\left\{\int_{s_b}\left[p_v(s_b,n_b,z)\sin\alpha(s_b) - p_u(s_b,z)\cos\alpha(s_b)\right]ds_b\right\}dz$$

$$-\int_L V(z)\left[\int_{s_b} \frac{\partial p_z(s_b,n_b,z)}{\partial z}\,n_b\cos\alpha(s_b)\,ds_b\right]dz - \int_L \theta_{xb}(z)\left[\int_{s_b} p_z(s_b,n_b,z)\,y(s_b)\,ds_b\right]dz$$

$$+\int_L U_b(z)\left[\int_{s_b} \frac{\partial p_z(s_b,n_b,z)}{\partial z}\,n_b\sin\alpha(s_b)\,ds_b\right]dz + \int_L U_b(z)\left\{\int_{s_b}\left[p_v(s_b,n_b,z)\cos\alpha(s_b) + p_u(s_b,n_b,z)\sin\alpha(s_b)\right]ds_b\right\}dz$$

$$-\int_L \theta_{yb}(z)\left[\int_{s_b} p_z(s_b,n_b,z)\,x(s_b)\,ds_b\right]dz + \int_L \theta_z(z)\left\{\int_{s_b}\left\{p_v(s_b,n_b,z)\left[r(s_b)+nq'(s_b)\right] - p_u(s_b,n_b,z)\,q(s_b)\right\}ds_b\right\}dz$$

$$-\int_L \theta_z(z)\left[\int_{s_b} \frac{\partial p_z(s_b,n_b,z)}{\partial z}\,n_b q(s_b)\,ds_b\right]dz - \int_L \psi_b(z)\left[\int_{s_b} p_z(s_b,n_b,z)\,\omega(s_b)\,ds_b\right]dz$$

$$-\left\{U_b(z)\left[\int_{s_b} p_z(s_b,n_b,z)\,n_b\sin\alpha(s_b)\,ds_b\right]\right\}\Bigg|_0^L + \left\{V(z)\left[\int_{s_b} p_z(s_b,n_b,z)\,n_b\cos\alpha(s_b)\,ds_b\right]\right\}\Bigg|_0^L$$

$$+\left\{\theta_z(z)\left[\int_{s_b} p_z(s_b,n_b,z)\,n_b q(s_b)\,ds_b\right]\right\}\Bigg|_0^L$$

The last three integrals pertain to the end tractions. Their effect has already been incorporated in the boundary terms when determining the load potential due to end tractions V_1 and thus can be discarded. Thus, one obtains

$$V_2 = \int_L W_b(z)\left[\int_{s_b} p_z(s_b,n_b,z)\,ds_b\right]dz + \int_L V(z)\left\{\int_{s_b}\left[p_v(s_b,n_b,z)\sin\alpha(s_b) - p_u(s_b,n_b,z)\cos\alpha(s_b)\right]ds_b\right\}dz$$

$$-\int_L V(z)\left[\int_{s_b}\frac{\partial p_z(s_b,n_b,z)}{\partial z}n_b\cos\alpha(s_b)\,ds\right]dz - \int_L \theta_{xb}(z)\left[\int_{s_b} p_z(s_b,n_b,z)\,y(s_b)\,ds_b\right]dz$$

$$+\int_L U_b(z)\left[\int_{s_b}\frac{\partial p_z(s_b,n_b,z)}{\partial z}n_b\sin\alpha(s_b)\,ds_b\right]dz + \int_L U_b(z)\left\{\int_{s_b}\left[p_v(s_b,n_b,z)\cos\alpha(s_b) + p_u(s_b,n_b,z)\sin\alpha(s_b)\right]ds_b\right\}dz$$

$$-\int_L \theta_{yb}(z)\left[\int_{s_b} p_z(s_b,n_b,z)\,x(s_b)\,ds_b\right]dz + \int_L \theta_z(z)\left\{\int_{s_b}\left\{p_v(s_b,n_b,z)\left[r(s_b)+nq'(s_b)\right] - p_u(s_b,n_b,z)\,q(s_b)\right\}ds_b\right\}dz$$

$$-\int_L \theta_z(z)\left[\int_{s_b}\frac{\partial p_z(s_b,n_b,z)}{\partial z}n_b q(s_b)\,ds_b\right]dz - \int_L \psi_b(z)\left[\int_{s_b} p_z(s_b,n_b,z)\,\omega(s_b)\,ds_b\right]dz$$

(A6.21)

In a concise form, the above expression can be expressed as

$$\begin{aligned} V_2 &= \int_L q_{zb}(z)W_b(z)dz + \int_L q_{yb}(z)V(z)dz + \int_L m_{xb}(z)\theta_{xb}(z)dz \\ &+\int_L q_{xb}(z)U_b(z)dz + \int_L m_{yb}(z)\theta_{yb}(z)dz + \int_L m_{zb}(z)\theta_z(z)dz + \int_L b_b(z)\psi_b(z)dz \end{aligned} \quad \text{(A6.22)}$$

in which

$$\begin{Bmatrix} q_{zb}(z) \\ q_{yb}(z) \\ m_{xb}(z) \\ q_{xb}(z) \\ m_{yb}(z) \\ m_{zb}(z) \\ b_b(z) \end{Bmatrix} = \int_{s_b}\begin{Bmatrix} p_z(s_b,n_b,z) \\ p_v(s_b,n_b,z)\sin\alpha(s_b) - p_u(s_b,n_b,z)\cos\alpha(s_b) - \left\{\partial/\partial z\left[p_z(s_b,n_b,z)\right]\right\}n_b\cos\alpha(s_b) \\ -p_z(s_b,n_b,z)\,y(s_b) \\ p_v(s_b,n_b,z)\cos\alpha(s_b) + p_u(s_b,n_b,z)\sin\alpha(s_b) + \left\{\partial/\partial z\left[p_z(s_b,n_b,z)\right]\right\}n_b\sin\alpha(s_b) \\ -p_z(s_b,n_b,z)\,x(s_b) \\ p_v(s_b,n_b,z)\left[r(s_b)+nq'(s_b)\right] - p_u(s_b,n_b,z)\,q(s_b) - \left\{\partial/\partial z\left[p_z(s_b,n_b,z)\right]\right\}n_b q(s_b) \\ -p_z(s_b,n_b,z)\,\omega(s_b) \end{Bmatrix} ds_b$$

(A6.23)

Equation (A6.23) is Eq. 5.30 in Chapter 5.

APPENDIX A7- SHEAR DEFORMABLE THEORY-VARIATION AND INTEGRATION

Starting with the Total Potential Energy for longitudinal transverse and lateral torsional responsed in Eq. 5. 31 and 5.47, respectively, the present appendix shows the steps to derive the field equations and boundary conditions.

A7.1 Longitudinal-Transverse Response

A7.1.1 Variation of the internal strain energy in the wide flange beam

By omitting lateral-torsional terms and taking variation of the internal strain energy of the beam U_b in the Eq. (5.22), one has

$$\begin{aligned}\delta U_b &= E_b A_b \int_L W_b' \delta W_b' dz + E_b I_{ssbf} \int_L V'' \delta V'' dz + G_b A_{bw} \int_L V' \delta V' dz - G_b A_{bw} \int_L \theta_{xb} \delta V' dz \\ &\quad - G_b A_{bw} \int_L V' \delta\theta_{xb} dz + E_b I_{xxb1} \int_L \theta_{xb}' \delta\theta_{xb}' dz + G_b A_{bw} \int_L \theta_{xb} \delta\theta_{xb} dz\end{aligned} \tag{A7.1}$$

From Eq. (A7.1), by integrating by parts, one obtains

$$\begin{aligned}\delta U_b &= E_b A_b W_b' \delta W_b \Big|_0^L - E_b A_b \int_L W_b'' \delta W_b dz + E_b I_{ssbf} V'' \delta V_b' \Big|_0^L - E_b I_{ssbf} V''' \delta V_b \Big|_0^L + E_b I_{ssbf} \int_L V'''' \delta V dz \\ &\quad + G_b A_{bw} V' \delta V_b \Big|_0^L - G_b A_{bw} \int_L V'' \delta V dz - G_b A_{bw} \theta_{xb} \delta V_b \Big|_0^L + G_b A_{bw} \int_L \theta_{xb}' \delta V dz \\ &\quad - G_b A_{bw} \int_L V' \delta\theta_{xb} dz + E_b I_{xxb1} \theta_{xb}' \delta\theta_{xb} \Big|_0^L - E_b I_{xxb1} \int_L \theta_{xb}'' \delta\theta_{xb} dz + G_b A_{bw} \int_L \theta_{xb} \delta\theta_{xb} dz\end{aligned} \tag{A7.2}$$

A7.1.2 Variation of the internal strain energy of the GFRP plate

By omitting lateral-torsional terms and taking variation of the internal strain energy of the beam U_p in the Eq. (5.23), one has

$$\delta U_p = E_p A_p \int_L W_p' \delta W_p' dz + E_p I_{xxp} \int_L V'' \delta V'' dz \tag{A7.3}$$

By integrating Eq. (A7.3) by parts, one obtains

$$\delta U_p = E_p A_p W_p' \delta W_p \Big|_0^L - E_p A_p \int_L W_p'' \delta W_p dz + E_p I_{xxp} V'' \delta V' \Big|_0^L - E_p I_{xxp} V''' \delta V \Big|_0^L + E_p I_{xxp} \int_L V'''' \delta V dz \tag{A7.4}$$

A7.1.3 Variation of the internal strain energy of the Adhesive layer

By omitting lateral-torsional terms in Eq. (5.24), internal strain energy of the adhesive U_a is expressed as

$$U_a = \frac{1}{2} G_a A_a \int_L \left\langle W_b \quad W_p \quad \theta_{bx} \;\vdots\; V' \right\rangle \left[\begin{array}{ccc:c} c_1^2 & -c_1^2 & c_1 c_3 & c_1 c_2 \\ -c_1^2 & c_1^2 & -c_1 c_3 & -c_1 c_2 \\ c_1 c_3 & -c_1 c_3 & c_3^2 & c_2 c_3 \\ \hdashline c_1 c_2 & -c_1 c_2 & c_2 c_3 & c_2^2 \end{array} \right] \left\{ \begin{array}{c} W_b \\ W_p \\ \theta_{bx} \\ \hline V' \end{array} \right\} dz \qquad \text{(A7.5)}$$

The expression in Eq. (A7.5) can be expanded as

$$U_a = \frac{1}{2} G_a A_a \int_L \left\langle W_b \quad W_p \quad \theta_{bx} \right\rangle \begin{bmatrix} c_1^2 & -c_1^2 & c_1 c_3 \\ -c_1^2 & c_1^2 & -c_1 c_3 \\ c_1 c_3 & -c_1 c_3 & c_3^2 \end{bmatrix} \begin{Bmatrix} W_b \\ W_p \\ \theta_{bx} \end{Bmatrix} dz + \frac{1}{2} G_a A_a \int_L \left\langle W_b \quad W_p \quad \theta_{bx} \right\rangle \begin{Bmatrix} c_1 c_2 \\ -c_1 c_2 \\ c_2 c_3 \end{Bmatrix} V' dz$$

$$+ \frac{1}{2} G_a A_a \int_L V' \left\langle c_1 c_2 \quad -c_1 c_2 \quad c_2 c_3 \right\rangle \begin{Bmatrix} W_b \\ W_p \\ \theta_{bx} \end{Bmatrix} dz + \frac{1}{2} G_a A_a c_2^2 \int_L V'^2 dz$$

(A7.6)

The variation δU_a is given by

$$\delta U_a = G_a A_a \int_L \left\langle W_b \quad W_p \quad \theta_{bx} \right\rangle \begin{bmatrix} c_1^2 & -c_1^2 & c_1 c_3 \\ -c_1^2 & c_1^2 & -c_1 c_3 \\ c_1 c_3 & -c_1 c_3 & c_3^2 \end{bmatrix} \begin{Bmatrix} \delta W_b \\ \delta W_p \\ \delta \theta_{bx} \end{Bmatrix} dz + \frac{G_a A_a}{2} \int_L \left\langle W_b \quad W_p \quad \theta_{bx} \right\rangle \begin{Bmatrix} c_1 c_2 \\ -c_1 c_2 \\ c_2 c_3 \end{Bmatrix} \delta V' dz$$

$$+ \frac{1}{2} G_a A_a \int_L V' \left\langle \delta W_b \quad \delta W_p \quad \delta \theta_{bx} \right\rangle \begin{Bmatrix} c_1 c_2 \\ -c_1 c_2 \\ c_2 c_3 \end{Bmatrix} dz + \frac{1}{2} G_a A_a \int_L V' \left\langle c_1 c_2 \quad -c_1 c_2 \quad c_2 c_3 \right\rangle \delta \begin{Bmatrix} \delta W_b \\ \delta W_p \\ \delta \theta_{bx} \end{Bmatrix} dz$$

$$+ \frac{1}{2} G_a A_a \int_L \left\langle c_1 c_2 \quad -c_1 c_2 \quad c_2 c_3 \right\rangle \begin{Bmatrix} W_b \\ W_p \\ \theta_{bx} \end{Bmatrix} \delta V' dz + G_a A_a c_2^2 \int_L V' \delta V' dz$$

(A7.7)

From Eq. (A7.7), by performing integration by parts, one obtains

$$\delta U_a =$$

$$\int_L \left(c_1^2 G_a A_a W_b - c_1^2 G_a A_a W_p + c_1 c_3 G_a A_a \theta_{bx} \right) \delta W_b dz + \int_L \left(-c_1^2 G_a A_a W_b + c_1^2 G_a A_a W_p - c_1 c_3 G_a A_a \theta_{bx} \right) \delta W_p dz +$$

$$+ \int_L \left(c_1 c_3 G_a A_a W_b - c_1 c_3 G_a A_a W_p + c_3^2 G_a A_a \theta_{bx} \right) \delta \theta_{bx} dz + \left(c_1 c_2 G_a A_a W_b - c_1 c_2 G_a A_a W_p + c_2 c_3 G_a A_a \theta_{bx} \right) \delta V \Big|_0^L$$

$$- \int_L \left(c_1 c_2 G_a A_a W_b' - c_1 c_2 G_a A_a W_p' + c_2 c_3 G_a A_a \theta_{bx}' \right) \delta V dz + c_1 c_2 G_a A_a \int_L V' \delta W_b dz - c_1 c_2 G_a A_a \int_L V' \delta W_p dz$$

$$+ c_2 c_3 G_a A_a \int_L V' \delta \theta_{bx} dz + c_2^2 G_a A_a V' \delta V \Big|_0^L - c_2^2 G_a A_a \int_L V'' \delta V dz$$

(A7.8)

A7.1.4 Variation of the Total Potential Energy

The variation of the total potential energy $\delta\pi_1 = \delta U_b + \delta U_p + \delta U_a - \delta V_1 - \delta V_2$ for the longitudinal-transverse response is obtained by adding Eqs. (A7.2), (A7.4), (A7.8), and variation of longitudinal-transverse load terms in Eqs. (5.27) and (5.30), yielding

$$
\begin{aligned}
\delta\pi_1 &= E_b A_b W_b' \delta W_b \Big|_0^L - E_b A_b \int_L W_b'' \delta W_b dz + E_b I_{ssbf} V'' \delta V_b' \Big|_0^L - E_b I_{ssbf} V''' \delta V_b \Big|_0^L + E_b I_{ssbf} \int_L V'''' \delta V dz \\
&+ G_b A_{bw} V' \delta V_b \Big|_0^L - G_b A_{bw} \int_L V'' \delta V dz - G_b A_{bw} \theta_{xb} \delta V_b \Big|_0^L + G_b A_{bw} \int_L \theta_{xb}' \delta V dz - G_b A_{bw} \int_L V' \delta\theta_{xb} dz \\
&+ E_b I_{xxb1} \theta_{xb}' \delta\theta_{xb} \Big|_0^L - E_b I_{xxb1} \int_L \theta_{xb}'' \delta\theta_{xb} dz + G_b A_{bw} \int_L \theta_{xb} \delta\theta_{xb} dz + E_p A_p W_p' \delta W_p \Big|_0^L - E_p A_p \int_L W_p'' \delta W_p dz \\
&+ E_p I_{xxp} \left(V'' \delta V' \Big|_0^L - V''' \delta V \Big|_0^L + \int_L V'''' \delta V dz \right) + \int_L \left(c_1^2 G_a A_a W_b - c_1^2 G_a A_a W_p + c_1 c_3 G_a A_a \theta_{bx} \right) \delta W_b dz \\
&+ G_a A_a \int_L \left(-c_1^2 W_b + c_1^2 W_p - c_1 c_3 \theta_{bx} \right) \delta W_p dz + \int_L \left(c_1 c_3 G_a A_a W_b - c_1 c_3 G_a A_a W_p + c_3^2 G_a A_a \theta_{bx} \right) \delta\theta_{bx} dz \\
&+ G_a A_a \left(c_1 c_2 W_b - c_1 c_2 W_p + c_2 c_3 \theta_{bx} \right) \delta V \Big|_0^L - \int_L \left(c_1 c_2 G_a A_a W_b' - c_1 c_2 G_a A_a W_p' + c_2 c_3 G_a A_a \theta_{bx}' \right) \delta V dz \\
&+ c_1 c_2 G_a A_a \left(\int_L V' \delta W_b dz - \int_L V' \delta W_p dz \right) + c_2 c_3 G_a A_a \int_L V' \delta\theta_{bx} dz + c_2^2 G_a A_a \left(V' \delta V \Big|_0^L - \int_L V'' \delta V dz \right) \\
&+ \Big[N(0) W_b(0) + Q_y(0) V(0) + M_{x1}(0) V'(0) + M_{x2}(0) \theta_{xb}(0) - N(L) W_b(L) - Q_y(L) V(L) \\
&- M_{x1}(L) V'(L) - M_{x2}(L) \theta_{xb}(L) \Big] - \int_L q_{zb}(z) W_b(z) dz - \int_L q_{yb}(z) V(z) dz - \int_L m_{xb}(z) \theta_{xb}(z) dz
\end{aligned}
\tag{A7.9}
$$

The terms in Eq. (A7.9) are re-arranged to give following expression

$$\delta\pi_1 = \int_L \left[-E_b A_b W_b'' + c_1^2 G_a A_a W_b - c_1^2 G_a A_a W_p + c_1 c_2 G_a A_a V' + c_1 c_3 G_a A_a \theta_{xb} - q_{zb}(z) \right] \delta W_b dz +$$

$$+\int_L \left[-E_p A_p W_p'' - c_1^2 G_a A_a W_b + c_1^2 G_a A_a W_p - c_1 c_2 G_a A_a V' - c_1 c_3 G_a A_a \theta_{xb} \right] \delta W_p dz +$$

$$+\int_L \left[-c_1 c_2 G_a A_a W_b' + c_1 c_2 G_a A_a W_p' + \left(E_b I_{ssbf} + E_p I_{xxp} \right) V'''' + \right.$$

$$\left. -\left(G_b A_{bw} + c_2^2 G_a A_a \right) V'' + \left(G_b A_{bw} - c_2 c_3 G_a A_a \right) \theta_{xb}' - q_{yb}(z) \right] \delta V dz +$$

$$+\int_L \left[c_1 c_3 G_a A_a W_b - c_1 c_3 G_a A_a W_p + \left(c_2 c_3 G_a A_a - G_b A_{bw} \right) V' + \right.$$

$$\left. -E_b I_{xxb1} \theta_{xb}'' + \left(G_b A_{bw} + c_3^2 G_a A_a \right) \theta_{xb} - m_{xb}(z) \right] \delta\theta_{xb} dz +$$

$$+ E_b A_b W_b' \delta W_b \Big|_0^L + E_b I_{ssbf} V'' \delta V_b' \Big|_0^L - E_b I_{ssbf} V''' \delta V \Big|_0^L + G_b A_{bw} V' \delta V \Big|_0^L$$

$$- G_b A_{bw} \theta_{xb} \delta V \Big|_0^L + E_b I_{xxb1} \theta_{xb}' \delta\theta_{xb} \Big|_0^L + E_p A_p W_p' \delta W_p \Big|_0^L + E_p I_{xxp} V'' \delta V' \Big|_0^L - E_p I_{xxp} V''' \delta V \Big|_0^L +$$

$$+ \left(c_1 c_2 G_a A_a W_b - c_1 c_2 G_a A_a W_p + c_2 c_3 G_a A_a \theta_{xb} \right) \delta V \Big|_0^L + c_2^2 G_a A_a V' \delta V \Big|_0^L +$$

$$+ N(0) \delta W_b(0) + Q_y(0) \delta V(0) + M_{x1}(0) \delta V'(0) + M_{x2}(0) \delta\theta_{xb}(0) +$$
$$- N(L) \delta W_b(L) - Q_y(L) \delta V(L) - M_{x1}(L) \delta V'(L) - M_{x2}(L) \delta\theta_{xb}(L) \qquad \text{(A7.10)}$$

Equation (A7.10) is Eq. 5.32 in Chapter 5.

A7.2 Lateral-Torsional Response

A7.2.1 Variation of the internal strain energy of the wide flange beam

By omitting longitudinal-transverse terms and taking variation of the internal strain energy of the beam U_b in the Eq. (5.22), one has

$$\delta U_b = E_b I_{ssbw} \int_L U_b'' \delta U_b'' dz + 2 G_b A_{bf} \int_L U_b' \delta U_b' dz - 2 G_b A_{bf} \int_L \theta_{yb} \delta U_b' dz + E_b I_{yybf} \int_L \theta_{yb}' \delta\theta_{yb}' dz$$
$$-2 G_b A_{bf} \int_L U_b' \delta\theta_{yb} dz + 2 G_b A_{bf} \int_L \theta_{yb} \delta\theta_{yb} dz + E_b I_{\omega\omega bl} \int_L \theta_z'' \delta\theta_z'' dz + G_b J_b \int_L \theta_z' \delta\theta_z' dz \qquad \text{(A7.11)}$$
$$-\frac{h_b^2}{4} G_b A_{bf} \int_L \psi_b \delta\theta_z' dz - \frac{h_b^2}{4} G_b A_{bf} \int_L \theta_z' \delta\psi_b dz + E_b I_{\omega\omega bg} \int_L \psi_b' \delta\psi_b' dz + \frac{h_b^2}{2} G_b A_{bf} \int_L \psi_b \delta\psi_b dz$$

By integrating Eq. (A7.11) by parts, one obtains

$$\delta U_b =$$

$$+\int_L \left(E_b I_{ssbw} U_b'''' - 2G_b A_{bf} U_b'' + 2G_b A_{bf} \theta_{yb}'\right)\delta U_b dz + \int_L \left(-E_b I_{yybf} \theta_{yb}'' + 2G_b A_{bf} \theta_{yb} - 2G_b A_{bf} U_b'\right)\delta\theta_{yb} dz$$

$$+\int_L \left(E_b I_{\omega\omega bl} \theta_z'''' - G_b J_b \theta_z'' + \frac{h_b^2}{4} G_b A_{bf} \psi_b'\right)\delta\theta_z dz + \int_L \left(-E_b I_{\omega\omega bg} \psi_b'' + \frac{h_b^2}{2} G_b A_{bf} \psi_b - \frac{h_b^2}{4} G_b A_{bf} \theta_z'\right)\delta\psi_b dz$$

$$-\left(E_b I_{ssbw} U_b''' + 2G_b A_{bf} \theta_{yb} - 2G_b A_{bf} U_b'\right)\delta U_b\Big|_0^L + E_b I_{ssbw} U_b'' \delta U_b'\Big|_0^L + E_b I_{yybf} \theta_{yb}' \delta\theta_{yb}\Big|_0^L + E_b I_{\omega\omega bl} \theta_z'' \delta\theta_z'\Big|_0^L$$

$$+\left(-E_b I_{\omega\omega bl} \theta_z''' + G_b J_b \theta_z' - \frac{h_b^2}{4} G_b A_{bf} \psi_b\right)\delta\theta_z\Bigg|_0^L + E_b I_{\omega\omega bg} \psi_b' \delta\psi_b\Big|_0^L \tag{A7.12}$$

A7.2.2 Variation of the internal strain energy of the GFRP plate

By omitting longitudinal-transverse terms and taking variation of the internal strain energy of the beam U_p in the Eq. (5.23), one has

$$\delta U_p = G_p A_p \int_L U_p' \delta U_p' dz - G_p A_p \int_L \theta_{yp} \delta U_p' dz + E_p I_{yyp} \int_L \theta_{yp}' \delta\theta_{yp}' dz$$
$$-G_p A_p \int_L U_p' \delta\theta_{yp} dz + G_p A_p \int_L \theta_{yp} \delta\theta_{yp} dz + E_p I_{\omega\omega p} \int_L \theta_z'' \delta\theta_z'' dz + G_p J_p \int_L \theta_z' \delta\theta_z' dz \tag{A7.13}$$

By integrating Eq. (A7.13) by parts, one obtains

$$\delta U_p = +\int_L \left(-G_p A_p U_p'' + G_p A_p \theta_{yp}'\right)\delta U_p dz + \int_L \left(-E_p I_{yyp} \theta_{yp}'' + G_p A_p \theta_{yp} - G_p A_p U_p'\right)\delta\theta_{yp} dz$$
$$+\int_L \left(E_p I_{\omega\omega p} \theta_z'''' - G_p J_p \theta_z''\right)\delta\theta_z dz + G_p A_p U_p' \delta U_p\Big|_0^L - G_p A_p \theta_{yp} \delta U_p\Big|_0^L \tag{A7.14}$$
$$+E_p I_{yyp} \theta_{yp}' \delta\theta_{yp}\Big|_0^L - E_p I_{\omega\omega p} \theta_z''' \delta\theta_z\Big|_0^L + E_p I_{\omega\omega p} \theta_z'' \delta\theta_z'\Big|_0^L + G_p J_p \theta_z' \delta\theta_z\Big|_0^L$$

A7.2.3 Variation of the internal strain energy of the Adhesive layer

By omitting longitudinal-transverse terms in Eq. (5.24), internal strain energy of the adhesive U_a is expressed as

$$U_a = U_{a1} + U_{a2} + U_{a3} = \frac{1}{2} G_a I_{yya} \int_L \langle \Delta_{a12} \rangle_{1\times4}^T \left[H_{a12}\right]_{4\times4} \{\Delta_{a12}\}_{4\times1} dz$$
$$+\frac{1}{2} G_a A_a \int_L \langle \Delta_{a2} \rangle_{1\times3}^T \left[H_{a2}\right]_{3\times3} \{\Delta_{a2}\}_{3\times1} dz + \frac{1}{24} G_a A_a \int_L \langle \Delta_{a3} \rangle_{1\times6}^T \left[H_{a3}\right]_{6\times6} \{\Delta_{a3}\}_{6\times1} dz \tag{A7.15}$$

The expression for the variation δU_{a1} is

$$\delta U_{a1} = G_a I_{yya} \int_L \left\langle \theta_z' \;\vdots\; \theta_{yb} \quad \theta_{yp} \quad \psi_b \right\rangle_{1\times 4} \left[\begin{array}{c:ccc} c_2^2 & -c_1c_2 & c_1c_2 & -c_2c_3 \\ \hdashline -c_1c_2 & c_1^2 & -c_1^2 & c_1c_3 \\ c_1c_2 & -c_1^2 & c_1^2 & -c_1c_3 \\ -c_2c_3 & c_1c_3 & -c_1c_3 & c_3^2 \end{array} \right] \left\{ \begin{array}{c} \delta\theta_z' \\ \hdashline \delta\theta_{yb} \\ \delta\theta_{yp} \\ \delta\psi_b \end{array} \right\} dA \tag{A7.16}$$

which can be expressed as

$$\begin{aligned} \delta U_{a1} = {} & G_a I_{yya} \int_L \theta_z' c_2^2 \delta\theta_z' dA + G_a I_{yya} \int_L \left\langle \theta_{yb} \quad \theta_{yp} \quad \psi_b \right\rangle \begin{bmatrix} c_1^2 & -c_1^2 & c_1c_3 \\ -c_1^2 & c_1^2 & -c_1c_3 \\ c_1c_3 & -c_1c_3 & c_3^2 \end{bmatrix} \begin{Bmatrix} \delta\theta_{yb} \\ \delta\theta_{yp} \\ \delta\psi_b \end{Bmatrix} dA \\ & + G_a I_{yya} \int_L \theta_z' \left\langle -c_1c_2 \quad c_1c_2 \quad -c_2c_3 \right\rangle \begin{Bmatrix} \delta\theta_{yb} \\ \delta\theta_{yp} \\ \delta\psi_b \end{Bmatrix} dA + G_a I_{yya} \int_L \left\langle \theta_{yb} \quad \theta_{yp} \quad \psi_b \right\rangle \begin{Bmatrix} -c_1c_2 \\ c_1c_2 \\ -c_2c_3 \end{Bmatrix} \delta\theta_z' dA \end{aligned} \tag{A7.17}$$

Equation (A7.17) is then integrated by parts yielding

$$\begin{aligned} \delta U_{a1} = {} & \int_L \left(c_1^2 G_a I_{yya} \theta_{yb} - c_1^2 G_a I_{yya} \theta_{yp} - c_1c_2 G_a I_{yya} \theta_z' + c_1c_3 G_a I_{yya} \psi_b \right) \delta\theta_{yb} dz \\ & + \int_L \left(-c_1^2 G_a I_{yya} \theta_{yb} + c_1^2 G_a I_{yya} \theta_{yp} + c_1c_2 G_a I_{yya} \theta_z' - c_1c_3 G_a I_{yya} \psi_b \right) \delta\theta_{yp} dz \\ & + \int_L \left(c_1c_2 G_a I_{yya} \theta_{yb}' - c_1c_2 G_a I_{yya} \theta_{yp}' - c_2^2 G_a I_{yya} \theta_z'' + c_2c_3 G_a I_{yya} \psi_b' \right) \delta\theta_z dz \\ & + \int_L \left(c_1c_3 G_a I_{yya} \theta_{yb} - c_1c_3 G_a I_{yya} \theta_{yp} - c_2c_3 G_a I_{yya} \theta_z' + c_3^2 G_a I_{yya} \psi_b \right) \delta\psi_b dz \\ & + \left(-c_1c_2 G_a I_{yya} \theta_{yb} + c_1c_2 G_a I_{yya} \theta_{yp} + c_2^2 G_a I_{yya} \theta_z' - c_2c_3 G_a I_{yya} \psi_b \right) \delta\theta_z \Big|_0^L \end{aligned} \tag{A7.18}$$

The variation δU_{a2} is written as

$$\delta U_{a2} = G_a A_a \int_L \left\langle U_b \quad U_p \quad \theta_z \right\rangle \begin{bmatrix} c_1^2 & -c_1^2 & c_1(c_2+c_3) \\ -c_1^2 & c_1^2 & -c_1(c_2+c_3) \\ c_1(c_2+c_3) & -c_1(c_2+c_3) & (c_2+c_3)^2 \end{bmatrix} \begin{Bmatrix} \delta U_b \\ \delta U_p \\ \delta\theta_z \end{Bmatrix} dz \tag{A7.19}$$

Equation (A7.19) is then expanded to give

$$\begin{aligned} \delta U_{a2} = {} & G_a A_a \int_L \left[c_1^2 U_b - c_1^2 U_p + c_1(c_2+c_3)\theta_z \right] \delta U_b dz + G_a A_a \int_L \left[-c_1^2 U_b + c_1^2 U_p - c_1(c_2+c_3)\theta_z \right] \delta U_p dz \\ & + G_a A_a \int_L \left[c_1(c_2+c_3) U_b - c_1(c_2+c_3) U_p + (c_2+c_3)^2 \theta_z \right] \delta\theta_z dz \end{aligned}$$

(A7.20)

The variation δU_{a3} is

$$\delta U_{a3}=\frac{1}{12}G_a A_a\int_L \langle \Delta_{sza}\rangle_{1\times 6}\left[\begin{array}{ccc|ccc} 4 & 2 & 2c_4 & -4 & -2 & -2h_b \\ 2 & 4 & c_5 & -2 & -4 & -h_b \\ 2c_4 & c_5 & c_6 & -2c_4 & -c_5 & -c_4h_b \\ \hline -4 & -2 & -2c_4 & 4 & 2 & 2h_b \\ -2 & -4 & -c_5 & 2 & 4 & h_b \\ -2h_b & -h_b & -c_4h_b & 2h_b & h_b & h_b^2 \end{array}\right]\{\delta\Delta_{sza}\}_{6\times 1}\,dz \qquad \text{(A7.21)}$$

in which $\langle \Delta_{sza}\rangle^T_{1\times 6}=\langle U_b' \quad U_p' \quad \theta_z' \quad \theta_{yb} \quad \theta_{yp} \quad \psi_b\rangle$

Equation (A7.21) is expanded as

$\delta U_{a3} =$

$$\frac{G_aA_a}{12}\int_L \langle U_b' \quad U_p' \quad \theta_z'\rangle\begin{bmatrix} 4 & 2 & 2c_4 \\ 2 & 4 & c_5 \\ 2c_4 & c_5 & c_6 \end{bmatrix}\begin{Bmatrix}\delta U_b' \\ \delta U_p' \\ \delta\theta_z'\end{Bmatrix}dz+\frac{G_aA_a}{12}\int_L \langle \theta_{yb} \quad \theta_{yp} \quad \psi_b\rangle\begin{bmatrix} -4 & -2 & -2c_4 \\ -2 & -4 & -c_5 \\ -2h_b & -h_b & -c_4h_b \end{bmatrix}\begin{Bmatrix}\delta U_b' \\ \delta U_p' \\ \delta\theta_z'\end{Bmatrix}dz$$

$$+\frac{G_aA_a}{12}\int_L \langle U_b' \quad U_p' \quad \theta_z'\rangle\begin{bmatrix} -4 & -2 & -2h_b \\ -2 & -4 & -h_b \\ -2c_4 & -c_5 & -c_4h_b \end{bmatrix}\begin{Bmatrix}\delta\theta_{yb} \\ \delta\theta_{yp} \\ \delta\psi_b\end{Bmatrix}dz+\frac{G_aA_a}{12}\int_L \langle \theta_{yb} \quad \theta_{yp} \quad \psi_b\rangle\begin{bmatrix} 4 & 2 & 2h_b \\ 2 & 4 & h_b \\ 2h_b & h_b & h_b^2 \end{bmatrix}\begin{Bmatrix}\delta\theta_{yb} \\ \delta\theta_{yp} \\ \delta\psi_b\end{Bmatrix}dz$$

(A7.22)

Equation (A7.22) is then integrated by parts yielding

$$
\begin{aligned}
\delta U_{a3} &= \frac{1}{12}G_a A_a\left(4U_b' + 2U_p' - 4\theta_{yb} - 2\theta_{yp} + 2c_4\theta_z' - 2h_b\psi_b\right)\delta U_b\Big|_0^L \\
&+ \frac{1}{12}G_a A_a\left(2U_b' + 4U_p' - 2\theta_{yb} - 4\theta_{yp} + c_5\theta_z' - h_b\psi_b\right)\delta U_p\Big|_0^L \\
&+ \frac{1}{12}G_a A_a\left(2c_4U_b' + c_5U_p' - 2c_4\theta_{yb} - c_5\theta_{yp} + c_6\theta_z' - c_4h_b\psi_b\right)\delta\theta_z\Big|_0^L \\
&- \frac{1}{12}G_a A_a\int_L\left(4U_b'' + 2U_p'' - 4\theta_{yb}' - 2\theta_{yp}' + 2c_4\theta_z'' - 2h_b\psi_b'\right)\delta U_b dz \\
&- \frac{1}{12}G_a A_a\int_L\left(2U_b'' + 4U_p'' - 2\theta_{yb}' - 4\theta_{yp}' + c_5\theta_z'' - h_b\psi_b'\right)\delta U_p dz \\
&+ \frac{1}{12}G_a A_a\int_L\left(-4U_b' - 2U_p' + 4\theta_{yb} + 2\theta_{yp} - 2c_4\theta_z' + 2h_b\psi_b\right)\delta\theta_{yb} dz \\
&+ \frac{1}{12}G_a A_a\int_L\left(-2U_b' - 4U_p' + 2\theta_{yb} + 4\theta_{yp} - c_5\theta_z' + h_b\psi_b\right)\delta\theta_{yp} dz \\
&- \frac{1}{12}G_a A_a\int_L\left(2c_4U_b'' + c_5U_p'' - 2c_4\theta_{yb}' - c_5\theta_{yp}' + c_6\theta_z'' - c_4h_b\psi_b'\right)\delta\theta_z dz \\
&+ \frac{1}{12}G_a A_a\int_L\left(-2h_bU_b' - h_bU_p' + 2h_b\theta_{yb} + h_b\theta_{yp} - c_4h_b\theta_z' + h_b^2\psi_b\right)\delta\psi_b dz
\end{aligned}
\tag{A7.23}
$$

A7.2.4 Total Potential Energy

The variation of the total potential energy $\delta\pi_2 = \delta U_b + \delta U_p + \delta U_a - \delta V_1 - \delta V_2$ for the lateral-torsional response is obtained by adding Eqs. (A7.12), (A7.14), (A7.18), (A7.20), (A7.23), and lateral-torsional load terms in Eqs. (5.27) and (5.30), yielding the Eq. 5.48 in Chapter 5, i.e.,

$$
\begin{aligned}
\delta\pi_2 = &\int_L \Big[E_b I_{ssbw} U_b'''' - 2G_b A_{bf} U_b'' + 2G_b A_{bf}\theta_{yb}' + c_1^2 G_a A_a U_b - c_1^2 G_a A_a U_p + c_1\left(c_2+c_3\right) G_a A_a \theta_z + \\
&- \frac{1}{12} G_a A_a \left(4U_b'' + 2U_p'' - 4\theta_{yb}' - 2\theta_{yp}' + 2c_4\theta_z'' - 2h_b\psi_b'\right) - q_{xb}(z)\Big]\delta U_b dz + \int_L \Big[-G_p A_p \left(U_p'' - \theta_{yp}'\right) - c_1^2 G_a A_a U_b \\
&+ c_1^2 G_a A_a U_p - c_1\left(c_2+c_3\right) G_a A_a \theta_z - \frac{1}{12} G_a A_a \left(2U_b'' + 4U_p'' - 2\theta_{yb}' - 4\theta_{yp}' + c_5\theta_z'' - h_b\psi_b'\right)\Big]\delta U_p dz + \\
&+ \int_L \Big[-E_b I_{yybf}\theta_{yb}'' + 2G_b A_{bf}\theta_{yb} - 2G_b A_{bf} U_b' + c_1^2 G_a I_{yya}\theta_{yb} - c_1^2 G_a I_{yya}\theta_{yp} - c_1 c_2 G_a I_{yya}\theta_z' + c_1 c_3 G_a I_{yya}\psi_b \\
&+ \frac{1}{12} G_a A_a \left(-4U_b' - 2U_p' + 4\theta_{yb} + 2\theta_{yp} - 2c_4\theta_z' + 2h_b\psi_b\right) - m_{yb}(z)\Big]\delta\theta_{yb} dz + \\
&+ \int_L \Big[-E_p I_{yyp}\theta_{yp}'' + G_p A_p \theta_{yp} - G_p A_p U_p' - c_1^2 G_a I_{yya}\theta_{yb} + c_1^2 G_a I_{yya}\theta_{yp} + c_1 c_2 G_a I_{yya}\theta_z' - c_1 c_3 G_a I_{yya}\psi_b + \\
&+ \frac{1}{12} G_a A_a \left(-2U_b' - 4U_p' + 2\theta_{yb} + 4\theta_{yp} - c_5\theta_z' + h_b\psi_b\right)\Big]\delta\theta_{yp} dz + \int_L \Big\{ E_b I_{\omega\omega bl}\theta_z'''' - G_b J_b \theta_z'' + \frac{h_b^2}{4} G_b A_{bf}\psi_b' + \\
&+ E_p I_{\omega\omega p}\theta_z'''' - G_p J_p \theta_z'' + c_1 c_2 G_a I_{yya}\theta_{yb}' - c_1 c_2 G_a I_{yya}\theta_{yp}' - c_2^2 G_a I_{yya}\theta_z'' + c_2 c_3 G_a I_{yya}\psi_b' + c_1\left(c_2+c_3\right) G_a A_a U_b \\
&- \left(c_2+c_3\right) G_a A_a \left[c_1 U_p - \left(c_2+c_3\right)\theta_z\right] - \frac{G_a A_a}{12}\left(2c_4 U_b'' + c_5 U_p'' - 2c_4\theta_{yb}' - c_5\theta_{yp}' + c_6\theta_z'' - c_4 h_b\psi_b'\right) - m_{zb}(z)\Big\}\delta\theta_z dz \\
&+ \int_L \Big[-E_b I_{\omega\omega bg}\psi_b'' + \frac{h_b^2}{2} G_b A_{bf}\psi_b - \frac{h_b^2}{4} G_b A_{bf}\theta_z' + c_1 c_3 G_a I_{yya}\theta_{yb} - c_1 c_3 G_a I_{yya}\theta_{yp} - c_2 c_3 G_a I_{yya}\theta_z' + \\
&+ c_3^2 G_a I_{yya}\psi_b + \frac{1}{12} G_a A_a \left(-2h_b U_b' - h_b U_p' + 2h_b\theta_{yb} + h_b\theta_{yp} - c_4 h_b\theta_z' + h_b^2\psi_b\right) - b(z)\Big]\delta\psi_b dz + \Big[-E_b I_{ssbw} U_b''' + \\
&- 2G_b A_{bf}\theta_{yb} + 2G_b A_{bf} U_b' + \frac{1}{12} G_a A_a \left(4U_b' + 2U_p' - 4\theta_{yb} - 2\theta_{yp} + 2c_4\theta_z' - 2h_b\psi_b\right)\Big]\delta U_b \Big|_0^L + E_b I_{ssbw} U_b'' \delta U_b' \Big|_0^L \\
&+ \Big[G_p A_p \left(U_p' - \theta_{yp}\right) + \frac{1}{12} G_a A_a \left(2U_b' + 4U_p' - 2\theta_{yb} - 4\theta_{yp} + c_5\theta_z' - h_b\psi_b\right)\Big]\delta U_p \Big|_0^L + E_b I_{yybf}\theta_{yb}'\delta\theta_{yb}\Big|_0^L + \\
&+ E_p I_{yyp}\,\theta_{yp}'\delta\theta_{yp}\Big|_0^L + E_b I_{\omega\omega bl}\theta_z''\,\delta\theta_z'\Big|_0^L + E_p I_{\omega\omega p}\,\theta_z''\delta\theta_z'\Big|_0^L + \Big[-E_b I_{\omega\omega bl}\theta_z''' + G_b J_b \theta_z' - \frac{h_b^2}{4} G_b A_{bf}\psi_b - E_p I_{\omega\omega p}\theta''' \\
&+ G_p J_p \theta_z' - c_1 c_2 G_a I_{yya}\theta_{yb} + c_1 c_2 G_a I_{yya}\theta_{yp} + c_2^2 G_a I_{yya}\theta_z' - c_2 c_3 G_a I_{yya}\psi_b \\
&+ \frac{1}{12} G_a A_a \left(2c_4 U_b' + c_5 U_p' - 2c_4\theta_{yb} - c_5\theta_{yp} + c_6\theta_z' - c_4 h_b\psi_b\right)\Big]\delta\theta_z\Big|_0^L + E_b I_{\omega\omega bg}\psi_b'\delta\psi_b\Big|_0^L + \Big[Q_x(0)\delta U_b(0) \\
&+ M_{y1}(0)\delta U_b'(0) + M_{y2}(0)\delta\theta_{yb}(0) + T(0)\delta\theta(0) + B_1(0)\delta\theta'(0) + B_2(0)\delta\psi_b(0) - Q_x(L)\delta U_b(L) \\
&- M_{y1}(L)\delta U_b'(L) - M_{y2}(L)\delta\theta_{yb}(L) - T(L)\delta\theta(L) - B_1(L)\delta\theta'(L) - B_2(L)\delta\psi_b(L)\Big]
\end{aligned}
\tag{A7.24}
$$

APPENDIX A8 - SHEAR DEFORMABLE THEORY-FORMULATION OF STIFFNESS MATRICES

A8.1 Scope

This appendix shows the method to obtain the stiffness matrices for longitudinal-transverse response and lateral-torsional response in which the effect of shear deformation is considered. The governing displacement fields in the total potential energy equation are substituted by expressions of shape functions and nodal displacement vectors. The shape functions are formed by assuming linear and cubic displacement functions. Based on the new expressions of energy terms, stiffness matrices as well as load vectors are determined for each response.

A8.2 For Longitudinal-Transverse Response

A8.2.1 Expression of Total Potential Energy

The total potential energy π_1 is contributed by

$$\pi_1 = U_1 - V_1 \tag{A8.1}$$

in which U_1 is total internal strain energy and V_1 is total potential energy loss.

$$\begin{aligned} U_1 = \int_L \Big[& \frac{1}{2} E_b A_b W_b'^{\,2} + \frac{1}{2} c_1^2 G_a A_a W_b^2 + \frac{1}{2} E_p A_p W_p'^{\,2} + \frac{1}{2} c_1^2 G_a A_a W_p^2 \\ & + \frac{1}{2}\left(E_b I_{ssbf} + E_p I_{xxp}\right) V''^2 + \frac{1}{2}\left(G_b A_{bw} + c_2^2 G_a A_a\right) V'^{\,2} + \frac{1}{2} E_b I_{xxb1} \theta_{xb}'^{\,2} \\ & + \frac{1}{2}\left(G_b A_{bw} + c_3^2 G_a A_a\right)\theta_{xb}^2 - c_1^2 G_a A_a W_b W_p + c_1 c_3 G_a A_a W_b \theta_{xb} + c_1 c_2 G_a A_a W_b V' \\ & - c_1 c_3 G_a A_a W_p \theta_{xb} - c_1 c_2 G_a A_a W_p V' + \left(c_2 c_3 G_a A_a - G_b A_{bw}\right)\theta_{xb} V' \Big] dz \end{aligned} \tag{A8.2}$$

$$\begin{aligned} V_1 = -\big[& Q_y(0)V(0) + N(0)W_b(0) + M_{x1}(0)V'(0) + M_{x2}(0)\theta_{xb}(0) - Q_y(L)V(L) - N(L)W_b(L) \\ & - M_{x1}(L)V'(L) - M_{x2}(L)\theta_{xb}(L)\big] + \int_L \left[q_{zb}(z)W_b(z) + q_{yb}(z)V(z) + m_{xb}(z)\theta_{xb}(z)\right] dz \end{aligned} \tag{A8.3}$$

A8.2.2 Derivation of Finite Element Formula

By substituting Eqs. (7.3) into Eq. (A8.2), one obtains

$$
\begin{aligned}
U_1 = &\langle D_{wb}\rangle_{1\times2}^T \left\{\frac{1}{2}E_bA_b\left[\widetilde{A_1}\right]\right\}\{D_{wb}\}_{2\times1} + \langle D_{wb}\rangle_{1\times2}^T \left\{\frac{1}{2}c_1^2G_aA_a\left[\widetilde{A_2}\right]\right\}\{D_{wb}\}_{2\times1} \\
&+\langle D_{wp}\rangle_{1\times2}^T \left\{\frac{1}{2}E_pA_p\left[\widetilde{A_1}\right]\right\}\{D_{wp}\}_{2\times1} + \langle D_{wp}\rangle_{1\times2}^T \left\{\frac{1}{2}c_1^2G_aA_a\left[\widetilde{A_2}\right]\right\}\{D_{wp}\}_{2\times1} \\
&+\langle D_V\rangle_{1\times4}^T \left\{\frac{1}{2}\left(E_bI_{ssbf}+E_pI_{xxp}\right)\left[\widetilde{A_3}\right]\right\}\{D_V\}_{4\times1} + \langle D_V\rangle_{1\times4}^T \left\{\frac{1}{2}\left(G_bA_{bw}+c_2^2G_aA_a\right)\left[\widetilde{A_4}\right]\right\}\{D_V\}_{4\times1} \\
&+\langle D_{\theta xb}\rangle_{1\times2}^T \left\{\frac{1}{2}E_bI_{xxb1}\left[\widetilde{A_1}\right]\right\}\{D_{\theta xb}\}_{2\times1} + \langle D_{\theta xb}\rangle_{1\times2}^T \left\{\frac{1}{2}\left(G_bA_{bw}+c_3^2G_aA_a\right)\left[\widetilde{A_2}\right]\right\}\{D_{\theta xb}\}_{2\times1} \qquad \text{(A8.4)} \\
&-\langle D_{wb}\rangle_{1\times2}^T \left\{c_1^2G_aA_a\left[\widetilde{A_2}\right]\right\}\{D_{wp}\}_{2\times1} + \langle D_{wb}\rangle_{1\times2}^T \left\{c_1c_3G_aA_a\left[\widetilde{A_2}\right]\right\}\{D_{\theta xb}\}_{2\times1} \\
&+\langle D_{wb}\rangle_{1\times2}^T \left\{c_1c_2G_aA_a\left[\widetilde{A_5}\right]\right\}\{D_V\}_{4\times1} - \langle D_{wp}\rangle_{1\times2}^T \left\{c_1c_3G_aA_a\left[\widetilde{A_2}\right]\right\}\{D_{\theta xb}\}_{2\times1} \\
&-\langle D_{wp}\rangle_{1\times2}^T \left\{c_1c_2G_aA_a\left[\widetilde{A_5}\right]\right\}\{D_V\}_{4\times1} + \langle D_V\rangle_{1\times4}^T \left\{\left(c_2c_3G_aA_a-G_bA_{bw}\right)\left[\widetilde{A_5}\right]^T\right\}\{D_{\theta xb}\}_{2\times1}
\end{aligned}
$$

in which

$$
\left[\widetilde{A_1}\right]_{2\times2} = \int_L \{L(z)\}_{2\times1}'\langle L(z)\rangle_{1\times2}^{T\,\prime}dz = \frac{1}{L}\begin{bmatrix}1 & -1\\ -1 & 1\end{bmatrix}, \left[\widetilde{A_2}\right]_{2\times2} = \int_L \{L(z)\}_{2\times1}\langle L(z)\rangle_{1\times2}^{T}dz = \frac{L}{6}\begin{bmatrix}2 & 1\\ 1 & 2\end{bmatrix},
$$

$$
\left[\widetilde{A_3}\right]_{4\times4} = \int_L \{H''(z)\}_{4\times1}\langle H''(z)\rangle_{1\times4}^{T}dz = \frac{1}{L^3}\begin{bmatrix}12 & 6L & -12 & 6L\\ 6L & 4L^2 & -6L & 2L^2\\ -12 & -6L & 12 & -6L\\ 6L & 2L^2 & -6L & 4L^2\end{bmatrix},
$$

$$
\left[\widetilde{A_4}\right]_{4\times4} = \int_L \{H'(z)\}_{4\times1}\langle H'(z)\rangle_{1\times4}^{T}dz = \frac{1}{30L}\begin{bmatrix}36 & 3L & -36 & 3L\\ 3L & 4L^2 & -3L & -L^2\\ -36 & -3L & 36 & -3L\\ 3L & -L^2 & -3L & 4L^2\end{bmatrix},
$$

$$
\left[\widetilde{A_5}\right]_{2\times4} = \int_L \{L(z)\}_{2\times1}\langle H'(z)\rangle_{1\times4}^{T}dz = \frac{1}{12}\begin{bmatrix}-6 & L & 6 & -L\\ -6 & -L & 6 & L\end{bmatrix},
$$

$$
\left[\widetilde{A_6}\right]_{4\times4} = \int_L \{H(z)\}_{4\times1}\langle H(z)\rangle_{1\times4}^{T}dz = \frac{1}{420}\begin{bmatrix}156L & 22L^2 & 54L & -13L^2\\ 22L^2 & 4L^3 & 13L^2 & -3L^3\\ 54L & 13L^2 & 156L & -22L^2\\ -13L^2 & -3L^3 & -22L^2 & 4L^3\end{bmatrix}, \qquad \text{(A8.5)}
$$

$$
\left[\widetilde{A_7}\right]_{2\times2} = \int_L \{L(z)\}_{2\times1}\langle L'(z)\rangle_{1\times2}^{T}dz = \frac{1}{2}\begin{bmatrix}-1 & 1\\ -1 & 1\end{bmatrix}
$$

From Eq. (A8.5), by grouping the terms which have identical nodal displacement matrix, one has

$$
\begin{aligned}
U_1 = & \left\langle D_{wb} \right\rangle_{1\times2}^{T} \left\{ \frac{1}{2} E_b A_b \left[\widetilde{A_1} \right] + \frac{1}{2} c_1^2 G_a A_a \left[\widetilde{A_2} \right] \right\} \left\{ D_{wb} \right\}_{2\times1} + \\
& + \left\langle D_{wp} \right\rangle_{1\times2}^{T} \left\{ \frac{1}{2} E_p A_p \left[\widetilde{A_1} \right] + \frac{1}{2} c_1^2 G_a A_a \left[\widetilde{A_2} \right] \right\} \left\{ D_{wp} \right\}_{2\times1} + \\
& + \left\langle D_V \right\rangle_{1\times4}^{T} \left\{ \frac{1}{2} \left(E_b I_{ssbf} + E_p I_{xxp} \right) \left[\widetilde{A_3} \right] + \frac{1}{2} \left(G_b A_{bw} + c_2^2 G_a A_a \right) \left[\widetilde{A_4} \right] \right\} \left\{ D_V \right\}_{4\times1} + \\
& + \left\langle D_{\theta xb} \right\rangle_{1\times2}^{T} \left\{ \frac{1}{2} E_b I_{xxb1} \left[\widetilde{A_1} \right] + \frac{1}{2} \left(G_b A_{bw} + c_3^2 G_a A_a \right) \left[\widetilde{A_2} \right] \right\} \left\{ D_{\theta xb} \right\}_{2\times1} + \\
& - \left\langle D_{wb} \right\rangle_{1\times2}^{T} \left\{ c_1^2 G_a A_a \left[\widetilde{A_2} \right] \right\} \left\{ D_{wp} \right\}_{2\times1} + \left\langle D_{wb} \right\rangle_{1\times2}^{T} \left\{ c_1 c_3 G_a A_a \left[\widetilde{A_2} \right] \right\} \left\{ D_{\theta xb} \right\}_{2\times1} + \\
& + \left\langle D_{wb} \right\rangle_{1\times2}^{T} \left\{ c_1 c_2 G_a A_a \left[\widetilde{A_5} \right] \right\} \left\{ D_V \right\}_{4\times1} - \left\langle D_{wp} \right\rangle_{1\times2}^{T} \left\{ c_1 c_3 G_a A_a \left[\widetilde{A_2} \right] \right\} \left\{ D_{\theta xb} \right\}_{2\times1} + \\
& - \left\langle D_{wp} \right\rangle_{1\times2}^{T} \left\{ c_1 c_2 G_a A_a \left[\widetilde{A_5} \right] \right\} \left\{ D_V \right\}_{4\times1} + \left\langle D_V \right\rangle_{1\times4}^{T} \left\{ \left(c_2 c_3 G_a A_a - G_b A_{bw} \right) \left[\widetilde{A_5} \right]^T \right\} \left\{ D_{\theta xb} \right\}_{2\times1}
\end{aligned}
\tag{A8.6}
$$

Equation (A8.6) is expressed according to stiffness matrix components as

$$
\begin{aligned}
U_1 = & \frac{1}{2} \left\langle D_{wb} \right\rangle_{1\times2}^{T} \left[K_1 \right]_{2\times2} \left\{ D_{wb} \right\}_{2\times1} + \frac{1}{2} \left\langle D_{wp} \right\rangle_{1\times2}^{T} \left[K_2 \right]_{2\times2} \left\{ D_{wp} \right\}_{2\times1} \\
& + \frac{1}{2} \left\langle D_V \right\rangle_{1\times4}^{T} \left[K_3 \right]_{4\times4} \left\{ D_V \right\}_{4\times1} + \frac{1}{2} \left\langle D_{\theta xb} \right\rangle_{1\times2}^{T} \left[K_4 \right]_{2\times2} \left\{ D_{\theta xb} \right\}_{2\times1} \\
& + \left\langle D_{wb} \right\rangle_{1\times2}^{T} \left[K_5 \right]_{2\times2} \left\{ D_{wp} \right\}_{2\times1} + \left\langle D_{wb} \right\rangle_{1\times2}^{T} \left[K_6 \right]_{2\times2} \left\{ D_{\theta xb} \right\}_{2\times1} \\
& + \left\langle D_{wb} \right\rangle_{1\times2}^{T} \left[K_7 \right]_{2\times4} \left\{ D_V \right\}_{4\times1} + \left\langle D_{wp} \right\rangle_{1\times2}^{T} \left[K_8 \right]_{2\times2} \left\{ D_{\theta xb} \right\}_{2\times1} \\
& + \left\langle D_{wp} \right\rangle_{1\times2}^{T} \left[K_9 \right]_{2\times4} \left\{ D_V \right\}_{4\times1} + \left\langle D_V \right\rangle_{1\times4}^{T} \left[K_{10} \right]_{4\times2} \left\{ D_{\theta xb} \right\}_{2\times1}
\end{aligned}
\tag{A8.7}
$$

in which

$$
\begin{aligned}
&\left[K_1\right]_{2\times2} = E_b A_b\left[\widetilde{A_1}\right] + c_1^2 G_a A_a\left[\widetilde{A_2}\right], \left[K_2\right]_{2\times2} = E_p A_p\left[\widetilde{A_1}\right] + c_1^2 G_a A_a\left[\widetilde{A_2}\right]\\
&\left[K_3\right]_{4\times4} = \left(E_b I_{ssbf} + E_p I_{xxp}\right)\left[\widetilde{A_3}\right] + \left(G_b A_{bw} + c_2^2 G_a A_a\right)\left[\widetilde{A_4}\right],\\
&\left[K_4\right]_{2\times2} = E_b I_{xxb1}\left[\widetilde{A_1}\right] + \left(G_b A_{bw} + c_3^2 G_a A_a\right)\left[\widetilde{A_2}\right],\\
&\left[K_5\right]_{2\times2} = -c_1^2 G_a A_a\left[\widetilde{A_2}\right], \left[K_6\right]_{2\times2} = c_1 c_3 G_a A_a\left[\widetilde{A_2}\right], \left[K_7\right]_{2\times4} = c_1 c_2 G_a A_a\left[\widetilde{A_5}\right],\\
&\left[K_8\right]_{2\times2} = -c_1 c_3 G_a A_a\left[\widetilde{A_2}\right], \left[K_9\right]_{2\times4} = -c_1 c_2 G_a A_a\left[\widetilde{A_5}\right], \left[K_{10}\right]_{4\times2} = \left(c_2 c_3 G_a A_a - G_b A_{bw}\right)\left[\widetilde{A_5}\right]^T
\end{aligned}
\tag{A8.8}
$$

are stiffness contributions of the structural system to the displacement fields.

A8.2.3 Load Vector and Finite Element Formula

From Eq. (A8.3), the potential energy loss by the end generalized forces is defined as

$$\overline{V}_{11} = \left\langle \Delta_1 \right\rangle_{1\times10}^T \left\{ \overline{\overline{Q}}_{11} \right\}_{10\times1} \tag{A8.9}$$

in which

$$\left\langle \overline{\overline{Q}}_{11} \right\rangle_{1\times10}^T = \left\langle -N(0) \quad N(L) \;\vdots\; 0 \quad 0 \;\vdots\; -Q_y(0) \quad -M_{x1}(0) \quad Q_y(L) \quad M_{x1}(L) \;\vdots\; -M_{x2}(0) \quad M_{x2}(L) \right\rangle$$

undergoing generalized nodal displacements $\left\langle \Delta_1 \right\rangle_{1\times10}^T$, and

the potential energy loss by member tractions is defined as

$$\overline{V}_{21} = \left\langle \Delta_1 \right\rangle_{1\times10}^T \left\{ \overline{\overline{Q}}_{21} \right\}_{10\times1} \tag{A8.10}$$

in which $\left\langle \overline{\overline{Q}}_{21} \right\rangle_{1\times10}^T = \left\langle \int_L q_{zb}(z)\left\langle L(z)\right\rangle_{1\times2}^T dz \;\vdots\; 0 \quad 0 \;\vdots\; \int_L q_{yb}(z)\left\langle H(z)\right\rangle_{1\times4}^T dz \;\vdots\; \int_L m_{xb}(z)\left\langle L(z)\right\rangle_{1\times2}^T dz \right\rangle$ is the energy equivalent load vector.

From Eqs. (A8.9) and (A8.10), by substituting into Eq.(A8.3), the discretized first variation of the total load potential energy is expressed as

$$V_1 = \overline{V}_{11} + \overline{V}_{21} = \left\langle \Delta_1 \right\rangle_{1\times10}^T \left\{ \overline{Q}_1 \right\}_{10\times1} \tag{A8.11}$$

in which

$$\left\{ \overline{Q}_1 \right\}_{10\times1} = \left\{ \overline{\overline{Q}}_{11} \right\}_{10\times1} + \left\{ \overline{\overline{Q}}_{21} \right\}_{10\times1} \tag{A8.12}$$

is equivalent load matrix.

From Eq.(A8.1), by assembling nodal displacement vectors in U_1 and minus to Eq. (A8.11), the discretized first variation of the total potential energy is expressed as

$$\partial \pi_1 = \langle \partial \Delta_1 \rangle_{1\times 10}^{T} \left\{ \left[\overline{\overline{K}}_1 \right]_{10\times 10} \{\Delta_1\}_{10\times 1} - \left\{ \overline{Q}_1 \right\}_{10\times 1} \right\} = 0 \quad \text{(A8.13)}$$

in which $\langle \Delta_1 \rangle_{1\times 10}^{T} = \left\langle \langle D_{wb} \rangle_{1\times 2}^{T} \;\vdots\; \langle D_{wp} \rangle_{1\times 2}^{T} \;\vdots\; \langle D_{V} \rangle_{1\times 4}^{T} \;\vdots\; \langle D_{\theta xb} \rangle_{1\times 2}^{T} \right\rangle$ is the nodal displacement vector, and

$$\left[\overline{\overline{K}}_1 \right]_{10\times 10} = \begin{bmatrix} [K_1] & [K_5] & [K_7] & [K_6] \\ [K_5]^T & [K_2] & [K_9] & [K_8] \\ [K_7]^T & [K_9]^T & [K_3] & [K_{10}] \\ [K_6]^T & [K_8]^T & [K_{10}]^T & [K_4] \end{bmatrix}$$ is the element stiffness matrix.

A8.3 For Lateral-Torsional Response

A8.3.1 Expression of Total Potential Energy

The total potential energy π_2 is contributed by

$$\pi_2 = U_2 - V_2 \quad \text{(A8.14)}$$

in which U_2 is total internal strain energy and V_2 is total potential energy loss.

$$U_2 = \int_L \left[\frac{1}{2} E_b I_{ssbw} U_b''^{\,2} + \left(G_b A_{bf} + \frac{1}{6} G_a A_a \right) U_b'^2 + \frac{1}{2} c_1^2 G_a A_a U_b^2 + \frac{1}{2} E_b I_{yybf} \theta_{yb}'^{\,2} \right.$$

$$+ \left(G_b A_{bf} + \frac{1}{2} c_1^2 G_a I_{yya} + \frac{1}{6} G_a A_a \right) \theta_{yb}^2 + \frac{1}{2} \left(G_p A_p + \frac{1}{3} G_a A_a \right) U_p'^2 + \frac{1}{2} c_1^2 G_a A_a U_p^2$$

$$+ \frac{1}{2} E_p I_{yyp} \theta_{yp}'^{\,2} + \frac{1}{2} \left(G_p A_p + \frac{1}{3} G_a A_a + c_1^2 G_a I_{yya} \right) \theta_{yp}^2 + \frac{1}{2} \left(E_b I_{\omega\omega bl} + E_p I_{\omega\omega p} \right) \theta_z''^2$$

$$+ \frac{1}{2} \left(G_b J_b + G_p J_p + c_2^2 G_a I_{yya} + \frac{1}{12} c_6 G_a A_a \right) \theta_z'^2 + \frac{1}{2} \left(c_2 + c_3 \right)^2 G_a A_a \theta_z^2 + \frac{1}{2} E_b I_{\omega\omega bg} \psi_b'^2$$

$$+ \frac{1}{2} \left(\frac{h_b^2}{2} G_b A_{bf} + c_3^2 G_a I_{yya} + \frac{1}{12} h_b^2 G_a A_a \right) \psi_b^2 + \frac{1}{6} G_a A_a U_b' U_p' - c_1^2 G_a A_a U_b U_p - \left(2 G_b A_{bf} + \frac{1}{3} G_a A_a \right) \theta_{yb} U_b'$$

$$- \frac{1}{6} G_a A_a U_b' \theta_{yp} + \frac{1}{6} c_4 G_a A_a U_b' \theta_z' + c_1 \left(c_2 + c_3 \right) G_a A_a U_b \theta_z - \frac{1}{6} h_b G_a A_a U_b' \psi_b - \left(G_p A_p + \frac{1}{3} G_a A_a \right) \theta_{yp} U_p'$$

$$+ \frac{1}{12} c_5 G_a A_a U_p' \theta_z' - c_1 \left(c_2 + c_3 \right) G_a A_a U_p \theta_z - \frac{1}{6} G_a A_a \theta_{yb} U_p' - \frac{1}{12} h_b G_a A_a U_p' \psi_b$$

$$- \left(c_1 c_2 G_a I_{yya} + \frac{1}{6} c_4 G_a A_a \right) \theta_{yb} \theta_z' + \left(\frac{1}{6} G_a A_a - c_1^2 G_a I_{yya} \right) \theta_{yb} \theta_{yp} + \left(c_1 c_3 G_a I_{yya} + \frac{1}{6} h_b G_a A_a \right) \theta_{yb} \psi_b$$

$$+ \left(c_1 c_2 G_a I_{yya} - \frac{1}{12} c_5 G_a A_a \right) \theta_{yp} \theta_z' + \left(\frac{1}{12} h_b G_a A_a - c_1 c_3 G_a I_{yya} \right) \theta_{yp} \psi_b$$

$$\left. - \left(\frac{h_b^2}{2} G_b A_{bf} + c_2 c_3 G_a I_{yya} + \frac{1}{12} c_4 h_b G_a A_a \right) \theta_z' \psi_b \right] dz$$

(A8.15)

$$V_2 = -\left[Q_x(0) U_b(0) + T(0) \theta_z(0) + M_{y1}(0) U_b'(0) + B_1(0) \theta_z'(0) + M_{y2}(0) \theta_{yb}(0) + B_2(0) \psi_b(0) \right.$$

$$\left. - Q_x(L) U_b(L) - T(L) \theta_z(L) - M_{y1}(L) U_b'(L) - B_1(L) \theta_z'(L) - M_{y2}(L) U_b'(L) - B_2(L) \psi_b(L) \right]$$

$$+ \int_L \left[q_{xb}(z) U_b(z) + m_{yb}(z) \theta_{yb}(z) + m_{zb}(z) \theta_z(z) + b_b(z) \psi_b(z) \right] dz$$

(A8.16)

A8.3.2 Derivation of Finite Element Formula

By substituting Eqs. 7.9 into Eq. (A8.15), one obtains

$$
\begin{aligned}
\pi = {} & \left(E_b I_{ssbw} / 2\right) \left\langle D_{ub} \right\rangle_{1\times4}^{T} \left[\widetilde{A_3}\right]_{4\times4} \left\{D_{ub}\right\}_{4\times1} + \left(G_b A_{bf} + G_a A_a / 6\right) \left\langle D_{ub} \right\rangle_{1\times4}^{T} \left[\widetilde{A_4}\right]_{4\times4} \left\{D_{ub}\right\}_{4\times1} \\
& + \left(c_1^2 G_a A_a / 2\right) \left\langle D_{ub} \right\rangle_{1\times4}^{T} \left[\widetilde{A_6}\right]_{4\times4} \left\{D_{ub}\right\}_{4\times1} + \left(E_b I_{yybf} / 2\right) \left\langle D_{\theta yb} \right\rangle_{1\times2} \left[\widetilde{A_1}\right]_{2\times2} \left\{D_{\theta yb}\right\}_{2\times1} \\
& + \left(G_b A_{bf} + c_1^2 G_a I_{yya} / 2 + G_a A_a / 6\right) \left\langle D_{\theta yb} \right\rangle_{1\times2} \left[\widetilde{A_2}\right]_{2\times2} \left\{D_{\theta yb}\right\}_{2\times1} \\
& + \left(G_p A_p / 2 + G_a A_a / 6\right) \left\langle D_{up} \right\rangle_{1\times2} \left[\widetilde{A_1}\right]_{2\times2} \left\{D_{up}\right\}_{2\times1} + \left(c_1^2 G_a A_a / 2\right) \left\langle D_{up} \right\rangle_{1\times2} \left[\widetilde{A_2}\right]_{2\times2} \left\{D_{up}\right\}_{2\times1} \\
& + \left(E_p I_{yyp} / 2\right) \left\langle D_{\theta yp} \right\rangle_{1\times2} \left[\widetilde{A_1}\right]_{2\times2} \left\{D_{\theta yp}\right\}_{2\times1} \\
& + \left(G_p A_p / 2 + G_a A_a / 6 + c_1^2 G_a I_{yya} / 2\right) \left\langle D_{\theta yp} \right\rangle_{1\times2} \left[\widetilde{A_2}\right]_{2\times2} \left\{D_{\theta yp}\right\}_{2\times1} \\
& + \left(E_b I_{\omega\omega bl} / 2 + E_p I_{\omega\omega p} / 2\right) \left\langle D_{\theta z} \right\rangle_{1\times4}^{T} \left[\widetilde{A_3}\right]_{4\times4} \left\{D_{\theta z}\right\}_{4\times1} \\
& + \left(G_b J_b / 2 + G_p J_p / 2 + c_2^2 G_a I_{yya} / 2 + c_6 G_a A_a / 24\right) \left\langle D_{\theta z} \right\rangle_{1\times4}^{T} \left[\widetilde{A_4}\right]_{4\times4} \left\{D_{\theta z}\right\}_{4\times1} \\
& + \left[\left(c_2 + c_3\right)^2 G_a A_a / 2\right] \left\langle D_{\theta z} \right\rangle_{1\times4}^{T} \left[\widetilde{A_6}\right]_{4\times4} \left\{D_{\theta z}\right\}_{4\times1} + \left(E_b I_{\omega\omega bg} / 2\right) \left\langle D_{\psi b} \right\rangle_{1\times2} \left[\widetilde{A_1}\right]_{2\times2} \left\{D_{\psi b}\right\}_{2\times1} \\
& + \left(h_b^2 G_b A_{bf} / 4 + c_3^2 G_a I_{yya} / 2 + h_b^2 G_a A_a / 24\right) \left\langle D_{\psi b} \right\rangle_{1\times2} \left[\widetilde{A_2}\right]_{2\times2} \left\{D_{\psi b}\right\}_{2\times1} \\
& + \left(G_a A_a / 6\right) \left\langle D_{ub} \right\rangle_{1\times4} \left[\widetilde{A_8}\right]_{4\times2}^{T} \left\{D_{up}\right\}_{2\times1} - c_1^2 G_a A_a \left\langle D_{ub} \right\rangle_{1\times4} \left[\widetilde{A_9}\right]_{4\times2}^{T} \left\{D_{up}\right\}_{2\times1} \\
& - \left(2 G_b A_{bf} + G_a A_a / 3\right) \left\langle D_{ub} \right\rangle_{1\times4} \left[\widetilde{A_5}\right]_{4\times2}^{T} \left\{D_{\theta yb}\right\}_{2\times1} - \left(G_a A_a / 6\right) \left\langle D_{ub} \right\rangle_{1\times4} \left[\widetilde{A_5}\right]_{4\times2}^{T} \left\{D_{\theta yp}\right\}_{2\times1} \\
& + \left(c_4 G_a A_a / 6\right) \left\langle D_{ub} \right\rangle_{1\times4}^{T} \left[\widetilde{A_4}\right]_{4\times4}^{T} \left\{D_{\theta z}\right\}_{4\times1} + c_1 \left(c_2 + c_3\right) G_a A_a \left\langle D_{ub} \right\rangle_{1\times4}^{T} \left[\widetilde{A_6}\right]_{4\times4}^{T} \left\{D_{\theta z}\right\}_{4\times1} \\
& - \left(h_b G_a A_a / 6\right) \left\langle D_{ub} \right\rangle_{1\times4} \left[\widetilde{A_5}\right]_{4\times2}^{T} \left\{D_{\psi b}\right\}_{2\times1} - \left(G_p A_p + G_a A_a / 3\right) \left\langle D_{up} \right\rangle_{1\times2} \left[\widetilde{A_7}\right]_{2\times2}^{T} \left\{D_{\theta yp}\right\}_{2\times1} \\
& + \left(c_5 G_a A_a / 12\right) \left\langle D_{up} \right\rangle_{1\times2}^{T} \left[\widetilde{A_8}\right]_{2\times4} \left\{D_{\theta z}\right\}_{4\times1} - c_1 \left(c_2 + c_3\right) G_a A_a \left\langle D_{up} \right\rangle_{1\times2}^{T} \left[\widetilde{A_9}\right]_{2\times4} \left\{D_{\theta z}\right\}_{4\times1} \\
& - \left(G_a A_a / 6\right) \left\langle D_{\theta yb} \right\rangle_{1\times2} \left[\widetilde{A_7}\right]_{2\times2} \left\{D_{up}\right\}_{2\times1} - \left(h_b G_a A_a / 12\right) \left\langle D_{up} \right\rangle_{1\times2} \left[\widetilde{A_7}\right]_{2\times2}^{T} \left\{D_{\psi b}\right\}_{2\times1} \\
& - \left(c_1 c_2 G_a I_{yya} + c_4 G_a A_a / 6\right) \left\langle D_{\theta yb} \right\rangle_{1\times2} \left[\widetilde{A_5}\right]_{2\times4} \left\{D_{\theta z}\right\}_{4\times1} \\
& + \left(G_a A_a / 6 - c_1^2 G_a I_{yya}\right) \left\langle D_{\theta yb} \right\rangle_{1\times2} \left[\widetilde{A_2}\right]_{2\times2}^{T} \left\{D_{\theta yp}\right\}_{2\times1} \\
& + \left(c_1 c_3 G_a I_{yya} + h_b G_a A_a / 6\right) \left\langle D_{\theta yb} \right\rangle_{1\times2} \left[\widetilde{A_2}\right]_{2\times2}^{T} \left\{D_{\psi b}\right\}_{2\times1} \\
& + \left(c_1 c_2 G_a I_{yya} - c_5 G_a A_a / 12\right) \left\langle D_{\theta yp} \right\rangle_{1\times2} \left[\widetilde{A_5}\right]_{2\times4} \left\{D_{\theta z}\right\}_{4\times1} \\
& + \left(h_b G_a A_a / 12 - c_1 c_3 G_a I_{yya}\right) \left\langle D_{\theta yp} \right\rangle_{1\times2} \left[\widetilde{A_2}\right]_{2\times2}^{T} \left\{D_{\psi b}\right\}_{2\times1} \\
& - \left(h_b^2 G_b A_{bf} / 2 + c_2 c_3 G_a I_{yya} + c_4 h_b G_a A_a / 12\right) \left\langle D_{\theta z} \right\rangle_{1\times4} \left[\widetilde{A_5}\right]_{4\times2}^{T} \left\{D_{\psi b}\right\}_{2\times1}
\end{aligned}
\tag{A8.17}
$$

in which $\left[\widetilde{A}_i\right]_{i=\overline{1,7}}$ are defined in Eq. (A8.5) and

$$\left[\widetilde{A}_8\right]_{2\times4} = \int_L \left\{L'(z)\right\}_{2\times1} \left\langle H'(z)\right\rangle^T_{1\times4} dz = \frac{1}{L}\begin{bmatrix} 1 & 0 & -1 & 0 \\ -1 & 0 & 1 & 0 \end{bmatrix},$$

$$\left[\widetilde{A}_9\right]_{2\times4} = \int_L \left\{L(z)\right\}_{2\times1} \left\langle H(z)\right\rangle^T_{1\times4} dz = \frac{L}{60}\begin{bmatrix} 21 & 3L & 9 & -2L \\ 9 & 2L & 21 & -3L \end{bmatrix}.$$

From Eq.(A8.17), by grouping the terms which have identical nodal displacement matrix, one has

$$U_2 = \left\langle D_{ub}\right\rangle^T_{1\times4}\left[\left(E_b I_{ssbw}/2\right)\left[\widetilde{A}_3\right]_{4\times4} + \left(G_b A_{bf} + G_a A_a/6\right)\left[\widetilde{A}_4\right]_{4\times4} + \left(c_1^2 G_a A_a/2\right)\left[\widetilde{A}_6\right]_{4\times4}\right]\left\{D_{ub}\right\}_{4\times1}$$

$$+\left\langle D_{\theta yb}\right\rangle_{1\times2}\left[\left(E_b I_{yybf}/2\right)\left[\widetilde{A}_1\right]_{2\times2} + \left(G_b A_{bf} + c_1^2 G_a I_{yya}/2 + G_a A_a/6\right)\left[\widetilde{A}_2\right]_{2\times2}\right]\left\{D_{\theta yb}\right\}_{2\times1}$$

$$+\left\langle D_{up}\right\rangle_{1\times2}\left[\left(G_p A_p/2 + G_a A_a/6\right)\left[\widetilde{A}_1\right]_{2\times2} + \left(c_1^2 G_a A_a/2\right)\left[\widetilde{A}_2\right]_{2\times2}\right]\left\{D_{up}\right\}_{2\times1}$$

$$+\left\langle D_{\theta yp}\right\rangle_{1\times2}\left[\frac{1}{2}E_p I_{yyp}\left[\widetilde{A}_1\right]_{2\times2} + \left(G_p A_p/2 + G_a A_a/6 + c_1^2 G_a I_{yya}/2\right)\left[\widetilde{A}_2\right]_{2\times2}\right]\left\{D_{\theta yp}\right\}_{2\times1}$$

$$+\left\langle D_{\theta z}\right\rangle^T_{1\times4}\left[\left(E_b I_{\omega\omega bl}/2 + E_p I_{\omega\omega p}/2\right)\left[\widetilde{A}_3\right]_{4\times4} + \left[\left(c_2 + c_3\right)^2 G_a A_a/2\right]\left[\widetilde{A}_6\right]_{4\times4} +\right.$$

$$\left. + \left(G_b J_b/2 + G_p J_p/2 + c_2^2 G_a I_{yya}/2 + c_6 G_a A_a/24\right)\left[\widetilde{A}_4\right]_{4\times4}\right]\left\{D_{\theta z}\right\}_{4\times1}$$

$$+\left\langle D_{\psi b}\right\rangle_{1\times2}\left[\left(E_b I_{\omega\omega bg}/2\right)\left[\widetilde{A}_1\right]_{2\times2} + \left(h_b^2 G_b A_{bf}/4 + c_3^2 G_a I_{yya}/2 + h_b^2 G_a A_a/24\right)\left[\widetilde{A}_2\right]_{2\times2}\right]\left\{D_{\psi b}\right\}_{2\times1}$$

$$+\left(G_a A_a/6\right)\left\langle D_{ub}\right\rangle_{1\times4}\left[\widetilde{A}_8\right]^T_{4\times2}\left\{D_{up}\right\}_{2\times1} - c_1^2 G_a A_a\left\langle D_{ub}\right\rangle_{1\times4}\left[\widetilde{A}_9\right]^T_{4\times2}\left\{D_{up}\right\}_{2\times1}$$

$$-\left(2G_b A_{bf} + G_a A_a/3\right)\left\langle D_{ub}\right\rangle_{1\times4}\left[\widetilde{A}_5\right]^T_{4\times2}\left\{D_{\theta yb}\right\}_{2\times1} - \left(G_a A_a/6\right)\left\langle D_{ub}\right\rangle_{1\times4}\left[\widetilde{A}_5\right]^T_{4\times2}\left\{D_{\theta yp}\right\}_{2\times1}$$

$$+\left(c_4 G_a A_a/6\right)\left\langle D_{ub}\right\rangle^T_{1\times4}\left[\widetilde{A}_4\right]^T_{4\times4}\left\{D_{\theta z}\right\}_{4\times1} + c_1\left(c_2 + c_3\right)G_a A_a\left\langle D_{ub}\right\rangle^T_{1\times4}\left[\widetilde{A}_6\right]^T_{4\times4}\left\{D_{\theta z}\right\}_{4\times1}$$

$$-\left(h_b G_a A_a/6\right)\left\langle D_{ub}\right\rangle_{1\times4}\left[\widetilde{A}_5\right]^T_{4\times2}\left\{D_{\psi b}\right\}_{2\times1} - \left(G_p A_p + G_a A_a/3\right)\left\langle D_{up}\right\rangle_{1\times2}\left[\widetilde{A}_7\right]^T_{2\times2}\left\{D_{\theta yp}\right\}_{2\times1}$$

$$+\left(c_5 G_a A_a/12\right)\left\langle D_{up}\right\rangle^T_{1\times2}\left[\widetilde{A}_8\right]_{2\times4}\left\{D_{\theta z}\right\}_{4\times1} - c_1\left(c_2 + c_3\right)G_a A_a\left\langle D_{up}\right\rangle^T_{1\times2}\left[\widetilde{A}_9\right]_{2\times4}\left\{D_{\theta z}\right\}_{4\times1}$$

$$-\left(G_a A_a/6\right)\left\langle D_{\theta yb}\right\rangle_{1\times2}\left[\widetilde{A}_7\right]_{2\times2}\left\{D_{up}\right\}_{2\times1} - \left(h_b G_a A_a/12\right)\left\langle D_{up}\right\rangle_{1\times2}\left[\widetilde{A}_7\right]^T_{2\times2}\left\{D_{\psi b}\right\}_{2\times1}$$

$$-\left(c_1 c_2 G_a I_{yya} + c_4 G_a A_a/6\right)\left\langle D_{\theta yb}\right\rangle_{1\times2}\left[\widetilde{A}_5\right]_{2\times4}\left\{D_{\theta z}\right\}_{4\times1} + \left(G_a A_a/6 - c_1^2 G_a I_{yya}\right)\left\langle D_{\theta yb}\right\rangle_{1\times2}\left[\widetilde{A}_2\right]^T_{2\times2}\left\{D_{\theta yp}\right\}_{2\times1}$$

$$+\left(c_1 c_3 G_a I_{yya} + h_b G_a A_a/6\right)\left\langle D_{\theta yb}\right\rangle_{1\times2}\left[\widetilde{A}_2\right]^T_{2\times2}\left\{D_{\psi b}\right\}_{2\times1} + \left(c_1 c_2 G_a I_{yya} - c_5 G_a A_a/12\right)\left\langle D_{\theta yp}\right\rangle_{1\times2}\left[\widetilde{A}_5\right]_{2\times4}\left\{D_{\theta z}\right\}_{4\times1}$$

$$+\left(h_b G_a A_a/12 - c_1 c_3 G_a I_{yya}\right)\left\langle D_{\theta yp}\right\rangle_{1\times2}\left[\widetilde{A}_2\right]^T_{2\times2}\left\{D_{\psi b}\right\}_{2\times1} +$$

$$-\left(h_b^2 G_b A_{bf}\ /\ 2 + c_2 c_3 G_a I_{yya} + c_4 h_b G_a A_a\ /\ 12\right)\left\langle D_{\theta z}\right\rangle_{1\times4}\left[\widetilde{A}_5\right]_{4\times2}^{T}\left\{D_{\psi b}\right\}_{2\times1} \tag{A8.18}$$

Equation (A8.18) is expressed according to stiffness matrix components as

$$\begin{aligned}\pi_2 = &\frac{1}{2}\left\langle D_{ub}\right\rangle_{1\times4}^{T}\left[\overline{K}_1\right]_{4\times4}\left\{D_{ub}\right\}_{4\times1} + \frac{1}{2}\left\langle D_{\theta yb}\right\rangle_{1\times2}\left[\overline{K}_2\right]_{2\times2}\left\{D_{\theta yb}\right\}_{2\times1} + \frac{1}{2}\left\langle D_{up}\right\rangle_{1\times2}\left[\overline{K}_3\right]_{2\times2}\left\{D_{up}\right\}_{2\times1}\\
&+\frac{1}{2}\left\langle D_{\theta yp}\right\rangle_{1\times2}\left[\overline{K}_4\right]_{2\times2}\left\{D_{\theta yp}\right\}_{2\times1} + \frac{1}{2}\left\langle D_{\theta z}\right\rangle_{1\times4}^{T}\left[\overline{K}_5\right]_{4\times4}\left\{D_{\theta z}\right\}_{4\times1} + \frac{1}{2}\left\langle D_{\psi b}\right\rangle_{1\times2}\left[\overline{K}_6\right]_{2\times2}\left\{D_{\psi b}\right\}_{2\times1}\\
&+\left\langle D_{ub}\right\rangle_{1\times4}\left[\overline{K}_7\right]_{4\times2}\left\{D_{up}\right\}_{2\times1} + \left\langle D_{ub}\right\rangle_{1\times4}\left[\overline{K}_8\right]_{4\times2}\left\{D_{\theta yb}\right\}_{2\times1} + \left\langle D_{ub}\right\rangle_{1\times4}\left[\overline{K}_9\right]_{4\times2}\left\{D_{\theta yp}\right\}_{2\times1}\\
&+\left\langle D_{ub}\right\rangle_{1\times4}^{T}\left[\overline{K}_{10}\right]_{4\times4}\left\{D_{\theta z}\right\}_{4\times1} + \left\langle D_{ub}\right\rangle_{1\times4}\left[\overline{K}_{11}\right]_{4\times2}\left\{D_{\psi b}\right\}_{2\times1} + \left\langle D_{up}\right\rangle_{1\times2}\left[\overline{K}_{12}\right]_{2\times2}\left\{D_{\theta yp}\right\}_{2\times1}\\
&+\left\langle D_{up}\right\rangle_{1\times2}\left[\overline{K}_{13}\right]_{2\times4}\left\{D_{\theta z}\right\}_{4\times1} + \left\langle D_{\theta yb}\right\rangle_{1\times2}\left[\overline{K}_{14}\right]_{2\times2}\left\{D_{up}\right\}_{2\times1} + \left\langle D_{up}\right\rangle_{1\times2}\left[\overline{K}_{15}\right]_{2\times2}\left\{D_{\psi b}\right\}_{2\times1}\\
&+\left\langle D_{\theta yb}\right\rangle_{1\times2}\left[\overline{K}_{16}\right]_{2\times4}\left\{D_{\theta z}\right\}_{4\times1} + \left\langle D_{\theta yb}\right\rangle_{1\times2}\left[\overline{K}_{17}\right]_{2\times2}\left\{D_{\theta yp}\right\}_{2\times1} + \left\langle D_{\theta yb}\right\rangle_{1\times2}\left[\overline{K}_{18}\right]_{2\times2}\left\{D_{\psi b}\right\}_{2\times1}\\
&+\left\langle D_{\theta yp}\right\rangle_{1\times2}\left[\overline{K}_{19}\right]_{2\times4}\left\{D_{\theta z}\right\}_{4\times1} + \left\langle D_{\theta yp}\right\rangle_{1\times2}\left[\overline{K}_{20}\right]_{2\times2}\left\{D_{\psi b}\right\}_{2\times1} + \left\langle D_{\theta z}\right\rangle_{1\times4}\left[\overline{K}_{21}\right]_{4\times2}\left\{D_{\psi b}\right\}_{2\times1}\end{aligned} \tag{A8.19}$$

In which

$$\left[\overline{K}_1\right]_{4\times4} = E_b I_{ssbw}\left[\widetilde{A}_3\right]_{4\times4} + \left(2G_b A_{bf} + \frac{1}{3}G_a A_a\right)\left[\widetilde{A}_4\right]_{4\times4} + c_1^2 G_a A_a\left[\widetilde{A}_6\right]_{4\times4}$$

$$\left[\overline{K}_2\right]_{2\times2} = E_b I_{yybf}\left[\widetilde{A}_1\right]_{2\times2} + \left(2G_b A_{bf} + c_1^2 G_a I_{yya} + \frac{1}{3}G_a A_a\right)\left[\widetilde{A}_2\right]_{2\times2}$$

$$\left[\overline{K}_3\right]_{2\times2} = \left(G_p A_p + \frac{1}{3}G_a A_a\right)\left[\widetilde{A}_1\right]_{2\times2} + c_1^2 G_a A_a\left[\widetilde{A}_2\right]_{2\times2}$$

$$\left[\overline{K}_4\right]_{2\times2} = E_p I_{yyp}\left[\widetilde{A}_1\right]_{2\times2} + \left(G_p A_p + \frac{1}{3}G_a A_a + c_1^2 G_a I_{yya}\right)\left[\widetilde{A}_2\right]_{2\times2}$$

$$\left[\overline{K}_5\right]_{4\times4} = \left(E_b I_{\omega\omega bl} + E_p I_{\omega\omega p}\right)\left[\widetilde{A}_3\right]_{4\times4} + \left(G_b J_b + G_p J_p + c_2^2 G_a I_{yya} + \frac{1}{12}c_6 G_a A_a\right)\left[\widetilde{A}_4\right]_{4\times4} + \left(c_2 + c_3\right)^2 G_a A_a\left[\widetilde{A}_6\right]_{4\times4}$$

$$\left[\overline{K}_6\right]_{2\times2} = E_b I_{\omega\omega bg}\left[\widetilde{A}_1\right]_{2\times2} + \left(\frac{h_b^2}{2}G_b A_{bf} + c_3^2 G_a I_{yya} + \frac{1}{12}h_b^2 G_a A_a\right)\left[\widetilde{A}_2\right]_{2\times2}$$

$$\left[\overline{K}_7\right]_{4\times2} = \frac{1}{6}G_a A_a\left[\widetilde{A}_8\right]_{4\times2}^{T} - c_1^2 G_a A_a\left[\widetilde{A}_9\right]_{4\times2}^{T};\quad \left[\overline{K}_8\right]_{4\times2} = -\left(2G_b A_{bf} + \frac{1}{3}G_a A_a\right)\left[\widetilde{A}_5\right]_{4\times2}^{T}$$

$$\left[\overline{K}_9\right]_{4\times2} = -\frac{1}{6}G_a A_a\left[\widetilde{A}_5\right]_{4\times2}^{T};\quad \left[\overline{K}_{10}\right]_{4\times4} = \frac{1}{6}c_4 G_a A_a\left[\widetilde{A}_4\right]_{4\times4}^{T} + c_1\left(c_2 + c_3\right)G_a A_a\left[\widetilde{A}_6\right]_{4\times4}^{T}$$

$$\left[\overline{K}_{11}\right]_{4\times 2}=-\frac{1}{6}h_b G_a A_a\left[\widetilde{A}_5\right]_{4\times 2}^T;\quad \left[\overline{K}_{12}\right]_{2\times 2}=-\left(G_p A_p+\frac{1}{3}G_a A_a\right)\left[\widetilde{A}_7\right]_{2\times 2}^T$$

$$\left[\overline{K}_{13}\right]_{2\times 4}=\frac{1}{12}c_5 G_a A_a\left[\widetilde{A}_8\right]_{2\times 4}-c_1\left(c_2+c_3\right)G_a A_a\left[\widetilde{A}_9\right]_{2\times 4};\quad \left[\overline{K}_{14}\right]_{2\times 2}=-\frac{1}{6}G_a A_a\left[\widetilde{A}_7\right]_{2\times 2}$$

$$\left[\overline{K}_{15}\right]_{2\times 2}=-\frac{1}{12}h_b G_a A_a\left[\widetilde{A}_7\right]_{2\times 2}^T;\quad \left[\overline{K}_{16}\right]_{2\times 4}=-\left(c_1 c_2 G_a I_{yya}+\frac{1}{6}c_4 G_a A_a\right)\left[\widetilde{A}_5\right]_{2\times 4}$$

$$\left[\overline{K}_{17}\right]_{2\times 2}=\left(\frac{1}{6}G_a A_a-c_1^2 G_a I_{yya}\right)\left[\widetilde{A}_2\right]_{2\times 2}^T;\quad \left[\overline{K}_{18}\right]_{2\times 2}=\left(c_1 c_3 G_a I_{yya}+\frac{1}{6}h_b G_a A_a\right)\left[\widetilde{A}_2\right]_{2\times 2}^T$$

$$\left[\overline{K}_{19}\right]_{2\times 4}=\left(c_1 c_2 G_a I_{yya}-\frac{1}{12}c_5 G_a A_a\right)\left[\widetilde{A}_5\right]_{2\times 4};\quad \left[\overline{K}_{20}\right]_{2\times 2}=\left(\frac{1}{12}h_b G_a A_a-c_1 c_3 G_a I_{yya}\right)\left[\widetilde{A}_2\right]_{2\times 2}^T$$

$$\left[\overline{K}_{21}\right]_{4\times 2}=-\left(\frac{h_b^2}{2}G_b A_{bf}+c_2 c_3 G_a I_{yya}+\frac{1}{12}c_4 h_b G_a A_a\right)\left[\widetilde{A}_5\right]_{4\times 2}^T$$

A8.3.3 Load Vector and Finite Element Formula

From Eq.(A8.16), the potential energy loss by the end generalized forces is defined as

$$\overline{V}_{12}=\langle\Delta_2\rangle_{1\times 16}^T\left\{\overline{\overline{Q}}_{12}\right\}_{16\times 1}\tag{A8.20}$$

in which

$$\left\langle\overline{\overline{Q}}_{12}\right\rangle_{1\times 16}^T=\langle -Q_x(0)\quad -M_{y1}(0)\quad Q_x(L)\quad M_{y1}(L)\ \vdots\ -M_{y2}(0)\quad M_{y2}(L)\ \vdots$$
$$\vdots\ 0\quad 0\ \vdots\ 0\quad 0\ \vdots\ -T(0)\quad -B_1(0)\quad T(L)\quad B_1(L)\ \vdots\ -B_2(0)\quad B_2(L)\rangle$$

undergoing generalized nodal displacements $\langle\Delta_2\rangle_{1\times 16}^T$, and

the potential energy loss by member tractions is defined as

$$\overline{V}_{22}=\langle\Delta_2\rangle_{1\times 16}^T\left\{\overline{\overline{Q}}_{22}\right\}_{16\times 1}\tag{A8.21}$$

in which

$$\left\langle\overline{\overline{Q}}_{22}\right\rangle_{1\times 16}^T=\left\langle\int_L q_x(z)\langle H(z)\rangle_{1\times 4}^T dz\ \vdots\ \int_L m_{yb}(z)\langle L(z)\rangle_{1\times 2}^T dz\ \vdots\ \langle 0\rangle_{1\times 2}^T\ \vdots\ \langle 0\rangle_{1\times 2}^T\ \vdots\ \int_L m(z)\langle H(z)\rangle_{1\times 4}^T dz\ \vdots\ \int_L b(z)\langle L(z)\rangle_{1\times 2}^T dz\right\rangle$$

is the energy equivalent load vector. Where $\langle 0\rangle_{1\times 2}^T=\langle 0\quad 0\rangle$.

From Eqs. (A8.20) and(A8.21), by substituting into Eq.(A8.16), the discretized first variation of the total load potential energy is expressed as

$$V_2 = \overline{V}_{21} + \overline{V}_{22} = \langle \Delta_2 \rangle_{1\times 16}^T \left\{ \overline{Q}_2 \right\}_{16\times 1} \tag{A8.22}$$

in which

$$\left\{ \overline{Q}_2 \right\}_{16\times 1} = \left\{ \overline{\overline{Q}}_{12} \right\}_{16\times 1} + \left\{ \overline{\overline{Q}}_{22} \right\}_{16\times 1} \tag{A8.23}$$

is equivalent load matrix.

From Eq.(A8.19), by assembling nodal displacement vectors in U_2 and minus to Eq. (A8.22), the discretized first variation of the total potential energy is expressed as

$$\partial \pi_2 = \langle \partial \Delta_2 \rangle_{1\times 16}^T \left\{ \left[\overline{\overline{K}}_2 \right]_{16\times 16} \{ \Delta_2 \}_{16\times 1} - \left\{ \overline{\overline{Q}}_2 \right\}_{16\times 1} \right\} = 0 \tag{A8.24}$$

in which $\langle \Delta_2 \rangle_{1\times 16}^T = \left\langle \langle D_{ub} \rangle_{1\times 4}^T \;\middle|\; \langle D_{\theta yb} \rangle_{1\times 2}^T \;\middle|\; \langle D_{up} \rangle_{1\times 2}^T \;\middle|\; \langle D_{\theta yp} \rangle_{1\times 2}^T \;\middle|\; \langle D_{\theta z} \rangle_{1\times 4}^T \;\middle|\; \langle D_{\psi b} \rangle_{1\times 2}^T \right\rangle$ is the nodal displacement vector, and

$$\left[\overline{\overline{K}}_2 \right]_{16\times 16} = \begin{bmatrix} [K_1] & [K_8] & [K_7] & [K_9] & [K_{10}] & [K_{11}] \\ [K_8]^T & [K_2] & [K_{14}] & [K_{17}] & [K_{16}] & [K_{18}] \\ [K_7]^T & [K_{14}]^T & [K_3] & [K_{12}] & [K_{13}] & [K_{15}] \\ [K_9]^T & [K_{17}]^T & [K_{12}]^T & [K_4] & [K_{19}] & [K_{20}] \\ [K_{10}]^T & [K_{16}]^T & [K_{13}]^T & [K_{19}]^T & [K_5] & [K_{21}] \\ [K_{11}]^T & [K_{18}]^T & [K_{15}]^T & [K_{20}]^T & [K_{21}]^T & [K_6] \end{bmatrix} \tag{A8.25}$$

is the element stiffness matrix, and $\left\{ \overline{\overline{Q}}_2 \right\}_{16\times 1}$ is the element load matrix.

APPENDIX B1 – PROGRAMMING OF PROBLEM 1 IN CHAPTER 4

B1.1 Input data

In each case study, its parameters $L, b_b, b_p, t_1, t_2, h_b, t_3, t_w, G_a, E_a, E_b, E_p, \mu$ are inputted in to a column of cells in sheet 1 of a spreadsheet named `'data21august.xlsx'`. The starting cell of inputting data is in the 6^{th} row and thus the ending cell is in the 18^{th} row. Twelve cases are inputted corresponding to twelve columns from C to N. As a result, all parameters of the twelve cases are listed in cells `'C6:N18'`. Values of the parameters as presented under the Statement of Problem 1 in Chapter 4 are inputted in the case 11^{th} (corresponding to the 11^{th} column of the total twelve columns).

B1.2 Programming in MATLAB

```
%--------------------------------------------------------------------------
-
%------------PROBLEM 1-CANTILEVEL COMPOSITE BEAM------------
-
%------------FINITE ELEMENT SOLUTION AND CLOSED FORM SOLUTION------------
-
%--------------------------------------------------------------------------
-
%Read data from spreadsheet file:
A=xlsread('data21august.xlsx',1,'C6:N18');
%Cases:
for i=11:11
  % i is column index of matrix A(12,10)
  disp(['CASE NUMBER ' num2str(i) ':']);
  disp('--------------')
  %------------------------------------------------------------
  %Input data of the case i:
  %------------------------------------------------------------
        L=[A(1,i)];    % Length of member
        bb=[A(2,i)];   % Width of beam flanges
        bp=[A(3,i)];   % Width of GFRP plate and Adhesive layer
        t1=[A(4,i)];   % Thickness(m) of the GFRP plate
        t2=[A(5,i)];   % Thickness(m) of the adhesive layer
        hb=[A(6,i)];   % Effective height (m) of the beam
        t3=[A(7,i)];   % Thickness(m) of the flanges
        tw=[A(8,i)];   % Thickness(m) of the web
        Ga=[A(9,i)];   % Module of shear(kN/m2) of adhesive
        Ea=[A(10,i)];  % Module of elasticity (kN/m2) of adhesive
        Eb=[A(11,i)];  % Module of elasticity(kN/m2)of the beam
        Ep=[A(12,i)];  % Module of elasticity(kN/m2) of the GFRP
```

```
      Muy=[A(13,i)]; % Poisson ratio
  %--------------------------------------------------------------
  % Calculation of section properties for the case i:
  %--------------------------------------------------------------
  % Shear module of steel beam:
  Gb=Eb/(2*(1+Muy));
  % Shear module of GFRP:
  Gp=Ep/(2*(1+Muy));
  %Calculation of section properties for wide flange beam:
  Ab=(t3*bb)*2+(hb-t3)*tw;
  Ixxb=((bb*(t3^3))/12+(t3*bb)*((hb/2)^2))*2+(tw*(hb-t3)^3)/12;
  Iyyb=(t3*(bb^3)/12)*2+((hb-t3)*tw^3)/12;
  Iwwb=(hb^2*bb^3*t3/24)+((t3^3)*(bb^3)/144)*2+(tw^3)*((hb-t3)^3)/144;
  Jb=(bb*(t3^3)/3)*2+(hb-t3)*(tw^3)/3;
  %Calculation of section properties for GFRP plate:
  Ap=t1*bp;
  Ixxp=bp*(t1^3)/12;
  Iyyp=t1*(bp^3)/12;
  Iwwp=(t1^3)*(bp^3)/144;
  Jp=bp*(t1^3)/3;
  %Calculation of section properties for adhesive layer:
  Aa=t2*bp;
  Ixxa=bp*(t2^3)/12;
  Iyya=t2*(bp^3)/12;
  Iwwa=(t2^3)*(bp^3)/144;
  Ja=((t1^2)-t1*t3+(t3^2))*Aa/3;
  %--------------------------------------------------------------------
  %   Determination of roots of characteristic equation for the case i
  %--------------------------------------------------------------------
  %Calculation of constants c1, c2 c3
  c1=1/t2;
  c2=(t1+2*t2+t3+hb)/(2*t2);
  c3=(t1+2*t2+t3-hb)/(2*t2);
  %Calculation of constant B1, B2,...,B12
  B1=Eb*Ab;
  B2=(c1^2)*Ga*Aa;
  B3=c1*c2*Ga*Aa;
  B4=Ep*Ap;
  B5=Eb*Ixxb+Ep*Ixxp;
  B6=(c2^2)*Ga*Aa;
  B7=Eb*Iyyb;
  B8=(c1^2)*Ga*Iyya;
  B9=c1*c3*Ga*Iyya;
  B10=Ep*Iyyp;
  B11=Eb*Iwwb+Ep*Iwwp;
  B12=Gb*Jb+Gp*Jp+Ga*Ja+(c3^2)*Ga*Iyya;
  % There are 6 zero roots and 2 non-zero roots.
  % The non-zero roots of characteristic equation are shown below.
  m1=sqrt((B1*B2*B5+B1*B4*B6+B2*B4*B5)/(B1*B4*B5));
  m2=-sqrt((B1*B2*B5+B1*B4*B6+B2*B4*B5)/(B1*B4*B5));
  %------------------------------------------------------------------------
-
  %            FINITE ELEMENT SOLUTION (1-Element solution)
  %------------------------------------------------------------------------
-
  % Determination of f values:
  f1=B1/B4;
```

```
  f2=B2/B3;
  f3=B1/B3;
  f4=(B1*B2+B2*B4)/(3*B3*B4);
  f5=m1*B1/B3-(B1*B2+B2*B4)/(m1*B3*B4);
  f6=m2*B1/B3-(B1*B2+B2*B4)/(m2*B3*B4);
  f9=B3*L^2+B1*B3*L^2/B4+6*B5*f4+2*B1*B6/B3-3*B6*L^2*f4;
  f10=B3+B1*B3/B4-B5*f5*m1^3+B6*f5*m1;
  f11=B3+B1*B3/B4-B5*f6*m2^3+B6*f6*m2;
  % Establishment of the matrix Z1(4x8):
  syms z
  z11=[1 z z^2 exp(m1*z) exp(m2*z) 0 0 0];
% first row of Z1
  z12=[0 0 -f1*z^2 -f1*exp(m1*z) -f1*exp(m2*z) 1 z 0];
% second row of Z1
  z13=[-f2*z -f2*(z^2)/2 (2*f3*z-f4*z^3) f5*exp(m1*z) f6*exp(m2*z) f2*z
f2*(z^2)/2 1]; % third row of Z2
  z14=diff(z13,z);
% fourth row of Z2
  % Matrix Z1:
  Z1=[z11; z12; z13; z14];
  % Transpore of matrix Z1:
  transpore_Z1=Z1';
  % First derivative of matrix Z1:
  first_diff_Z1=diff(Z1,z);
  % Transpore of the first derivative of matrix Z1:
  transpore_first_diff_Z1=(first_diff_Z1)';
  % Second derivative of matrix Z1:
  second_diff_Z1=diff(first_diff_Z1,z);
  % Transpore of the second derivative of matrix Z1:
  transpore_second_diff_Z1=(second_diff_Z1)';
  Z10=[z11; z12; z13; z14];  % Z1=Z10
  % Matrix Z1 at z=0:
  Z100=subs(Z10,0);
  % Matrix Z1 at z=L:
  Z10L=subs(Z10,L);
  % Matrix L1:
  L1=[Z100; Z10L];
  % Inverse matrix of L1:
  inverse_L1=inv(L1);
  % Transpore of inverse matrix of L1:
  transpore_of_inverse_L1=(inverse_L1)';
  % Unit matricies ro 1, 2, 3:
  ro1=[1;0;0;0];
  ro2=[0;1;0;0];
  ro3=[0;0;1;0];
  % Shape function matrix:
  N1z=Z10*inverse_L1;
  % Establishing stiffness matrix:
  %-------------------------------------------------------------------
-
  % First term of Prepare_K1:
  a1=transpore_first_diff_Z1*ro1*(ro1')*first_diff_Z1;
  first_term_of_K1=Eb*Ab*int(a1,z,0,L);
  % Second term of Prepare_K1:
  a2=transpore_first_diff_Z1*ro2*(ro2')*first_diff_Z1;
  second_term_of_K1=Ep*Ap*int(a2,z,0,L);
  % Third term of Prepare_K1:
```

```
  a3=transpore_second_diff_Z1*ro3*(ro3')*second_diff_Z1;
  third_term_of_K1=(Eb*Ixxb+Ep*Ixxp)*int(a3,z,0,L);
  % Fourth term of Prepare_K1:
  a4=transpore_first_diff_Z1*ro3*(ro3')*first_diff_Z1;
  fourth_term_of_K1=(Ga*Aa*(c2^2))*int(a4,z,0,L);
  % Fifth term of Prepare_K1:
  a5=transpore_Z1*[ro1 ro2]*[1 -1; -1 1]*[ro1'; ro2']*Z1;
  fifth_term_of_K1=(Ga*Aa*(c1^2))*int(a5,z,0,L);
  % Calculuate matrix T:
  a6=((diff(N1z,z))')*ro3*(ro1'-ro2')*N1z;
  integratez_within_T=int(a6,z,0,L);
  % Sum of integrations:

Sum_of_intergrations=first_term_of_K1+second_term_of_K1+third_term_of_K1+f
ourth_term_of_K1+fifth_term_of_K1;
  % Components of matrix K1:
  Prepare1_K1=(transpore_of_inverse_L1*Sum_of_intergrations*inverse_L1);
  T=integratez_within_T;
  %-----------------------------------------------------------------------
-
  % Element stiffness matrix K1: (8x8)
  K1=Prepare1_K1+c1*c2*Ga*Aa*(T+T');
  % Element stiffness matrix in brief form: (4x4)
  K11=[K1(5,5) K1(5,6) K1(5,7) K1(5,8)];
  K12=[K1(6,5) K1(6,6) K1(6,7) K1(6,8)];
  K13=[K1(7,5) K1(7,6) K1(7,7) K1(7,8)];
  K14=[K1(8,5) K1(8,6) K1(8,7) K1(8,8)];
  Small_K1=vpa([K11; K12; K13; K14],5);
  % Inverse matrix of the brief stiffness matrix:
  inverse_Small_K1=inv(Small_K1);
  % Element load matrix:
  Q1=[0; 0; 15; 0];
  %Nodal displacement vector:
  disp('Finite Element Solution:');
  disp('-----------------------');
  disp('* Nodal displacements at tip:');
  DeltaB=inverse_Small_K1*Q1;
  disp(DeltaB);
  %-----------------------------------------------------------------------
-
  %-----------------------------------------------------------------------
-
  % CLOSED FORM SOLUTION
  %-----------------------------------------------------------------------
-
  %-----------------------------------------------------------------------
-
  disp('Closed Form Solution:');
  disp('---------------------');
  % Matrix L=:
   zs1=[1 0 0 1 1 0 0 0];
   zs2=[0 1 2*L m1*exp(m1*L) m2*exp(m2*L) 0 0 0];
   zs3=[0 0 0 -f1 -f1 1 0 0];
   zs4=[0 0 -2*f1*L -f1*m1*exp(m1*L) -f1*m2*exp(m2*L) 0 1 0];
   zs5=[-f2 0 2*f3 m1*f5 m2*f6 f2 0 0];
   zs6=[0 -f2 -6*f4*L (m1^2)*f5*exp(m1*L) (m2^2)*f6*exp(m2*L) 0 f2 0];
   zs7=[0 0 0 f5 f6 0 0 1];
```

```
   zs8=[0 0 f9 f10*exp(m1*L) f11*exp(m2*L) 0 0 0];
   Zs00=[zs1; zs2; zs3; zs4; zs5; zs6; zs7; zs8];
   %Inverse of matrix Z00:
   inverse_Zs00=vpa(inv(Zs00),30);
   % Load matrix:
   PB=[0; 0; 0; 0; 0; 0; 0; 15];
   disp('* Displacement at tip obtained from closed form solution:');
   Root_A=inverse_Zs00*PB;
   displacement_V=[-f2*z -f2*(z^2)/2 (2*f3*z-f4*z^3) f5*exp(m1*z)
f6*exp(m2*z) f2*z f2*(z^2)/2 1]*Root_A;
   displacement_Wb=[1 z z^2 exp(m1*z) exp(m2*z) 0 0 0]*Root_A;
   displacement_Wp=[0 0 -f1*z^2 -f1*exp(m1*z) -f1*exp(m2*z) 1 z 0]*Root_A;
   disp('Displacement V:');
   displacement_V_values=subs(displacement_V,0:(L/10):L);
   % Display results on screen:
   fprintf('Z-coordinate(m) \t Value(kPa) \r');
   for k=1:11
       fprintf('%3.2e\t\t\t %3.2e\t\t\t\n', (k-1)*L/10,
displacement_V_values(1,k));
   end
   disp('----------------------------------------');
   disp('Displacement Wb:');
   displacement_Wb_values=subs(displacement_Wb,0:(L/10):L);
   % Display results on screen:
   fprintf('Z-coordinate(m) \t Value(kPa) \r');
   for k=1:11
       fprintf('%3.2e\t\t\t %3.2e\t\t\t\n', (k-1)*L/10,
displacement_Wb_values(1,k));
   end
   disp('----------------------------------------');
   disp('Displacement Wp:');
   displacment_Wp_values=subs(displacement_Wp,0:(L/10):L);
   % Display results on screen:
   fprintf('Z-coordinate(m) \t Value(kPa) \r');
   for k=1:11
       fprintf('%3.2e\t\t\t %3.2e\t\t\t\n', (k-1)*L/10,
displacment_Wp_values(1,k));
   end
   disp('----------------------------------------');
   %----------------------------------------------------------------------
-
   %-----------------------Output of stresses-----------------------------
-
   disp('Longitudinal normal stress at the bottom flange of the fixed
section in the wide flange beam:');
   epsilon_zb=diff(displacement_Wb,z)-
diff(diff(displacement_V,z),z)*(hb+t3)/2;
   normal_stress_at_bottom_in_beam=subs(epsilon_zb*Eb,0:(L/10):L);
   % Display results on screen:
   fprintf('Z-coordinate(m) \t Value(kPa) \r');
   for k=1:11
       fprintf('%3.2e\t\t\t %3.2e\t\t\t\n', (k-1)*L/10,
normal_stress_at_bottom_in_beam(1,k));
   end
   % Write to a spreadsheet file:
   name_of_stress={'Signma_zb:'};
   xlswrite('out_put_problem_1.xlsx',name_of_stress,i,'C2');
```

```
xlswrite('out_put_problem_1.xlsx',normal_stress_at_bottom_in_beam'/1000,i,
'C3:C13');
   disp('----------------------------------------');
   disp('Longitudinal normal stress at the top edge of fixed section in
the FRP plate:');
   epsilon_zp=diff(displacement_Wp,z)+diff(diff(displacement_V,z))*(t1/2);
   normal_stress_in_FRP_top=subs(epsilon_zp*Ep,0:(L/10):L);
   % Display results on screen:
   fprintf('Z-coordinate(m) \t Value(kPa) \r');
   for k=1:11
       fprintf('%3.2e\t\t\t %3.2e\t\t\t\n', (k-1)*L/10,
normal_stress_in_FRP_top(1,k));
   end
   % Write to a spreadsheet file:
   name_of_stress={'Signma_zp:'};
   xlswrite('out_put_problem_1.xlsx',name_of_stress,i,'e2');

xlswrite('out_put_problem_1.xlsx',normal_stress_in_FRP_top',i,'e3:e13');
   disp('----------------------------------------');
   disp('Shear stress gamma_sz in the adhesive layer:');
   a1=[-c1 c1 -c2 0 0 0];
   diff_V=diff(displacement_V,z);
   delta_a1=[displacement_Wb; displacement_Wp; diff_V; 0; 0; 0;];
   shear_strain_sz=a1*delta_a1;
   shear_stress_sz=subs(shear_strain_sz*Ga,0:(L/10):L);
   % Display results on screen:
   fprintf('Z-coordinate(m) \t Value(kPa) \r');
   for k=1:11
       fprintf('%3.2e\t\t\t %3.2e\t\t\t\n', (k-1)*L/10,
shear_stress_sz(1,k));
   end
   % Write to a spreadsheet file:
   name_of_stress={'Gamma_sz:'};
   xlswrite('out_put_problem_1.xlsx',name_of_stress,i,'g2');
   xlswrite('out_put_problem_1.xlsx',shear_stress_sz',i,'g3:g13');

disp('**************************************************************************
******************');
end
%--------------------------------------------------------------------------
-
%-------------------------End of problem 1-------------------------------
-
%--------------------------------------------------------------------------
-
```

B1.3 Outputs

```
CASE NUMBER 11:
--------------
Finite Element Solution:
------------------------
* Nodal displacements at tip:
 -.17465470481489906376997594286589e-3
```

```
  .68909816805728032867139004525470e-3
  .10246905278401764612910780488362e-1
  .10248387386718268468445073432818e-1

Closed Form Solution:
---------------------
* Displacement at tip obtained from closed form solution:
Displacement V:
Z-coordinate(m)          Value(m)
0.00e+000                0.00e+000
1.50e-001                1.49e-004
3.00e-001                5.74e-004
4.50e-001                1.24e-003
6.00e-001                2.13e-003
7.50e-001                3.20e-003
9.00e-001                4.42e-003
1.05e+000                5.77e-003
1.20e+000                7.21e-003
1.35e+000                8.71e-003
1.50e+000                1.02e-002
--------------------------------------
Displacement Wb:
Z-coordinate(m)          Value(m)
0.00e+000                -4.96e-024
1.50e-001                -3.32e-005
3.00e-001                -6.28e-005
4.50e-001                -8.90e-005
6.00e-001                -1.12e-004
7.50e-001                -1.31e-004
9.00e-001                -1.47e-004
1.05e+000                -1.59e-004
1.20e+000                -1.68e-004
1.35e+000                -1.73e-004
1.50e+000                -1.75e-004
--------------------------------------
Displacement Wp:
Z-coordinate(m)          Value(m)
0.00e+000                0.00e+000
1.50e-001                1.31e-004
3.00e-001                2.48e-004
4.50e-001                3.51e-004
6.00e-001                4.41e-004
7.50e-001                5.16e-004
9.00e-001                5.78e-004
1.05e+000                6.27e-004
1.20e+000                6.61e-004
1.35e+000                6.82e-004
1.50e+000                6.89e-004
--------------------------------------
Longitudinal normal stress at the bottom flange of the fixed section in
the wide flange beam:
Z-coordinate(m)          Value(kPa)
0.00e+000                -2.49e+005
1.50e-001                -2.24e+005
3.00e-001                -1.99e+005
4.50e-001                -1.74e+005
6.00e-001                -1.49e+005
```

```
7.50e-001              -1.24e+005
9.00e-001              -9.95e+004
1.05e+000              -7.46e+004
1.20e+000              -4.97e+004
1.35e+000              -2.49e+004
1.50e+000              1.46e-011
--------------------------------------
Longitudinal normal stress at the top edge of fixed section in the FRP
plate:
Z-coordinate(m)        Value(kPa)
0.00e+000              4.38e+004
1.50e-001              3.96e+004
3.00e-001              3.52e+004
4.50e-001              3.08e+004
6.00e-001              2.64e+004
7.50e-001              2.20e+004
9.00e-001              1.76e+004
1.05e+000              1.32e+004
1.20e+000              8.80e+003
1.35e+000              4.40e+003
1.50e+000              -9.90e-071
--------------------------------------
Shear stress gamma_sz in the adhesive layer:
Z-coordinate(m)        Value(kPa)
0.00e+000              5.68e-014
1.50e-001              -4.89e+002
3.00e-001              -4.89e+002
4.50e-001              -4.89e+002
6.00e-001              -4.89e+002
7.50e-001              -4.89e+002
9.00e-001              -4.89e+002
1.05e+000              -4.89e+002
1.20e+000              -4.89e+002
1.35e+000              -4.89e+002
1.50e+000              -4.89e+002
**************************************************************************
***
>>
```

APPENDIX B2 – PROGRAMMING OF PROBLEM 2 IN CHAPTER 4

B2.1 Input data

In each case study, its parameters $L, b_b, b_p, t_1, t_2, h_b, t_3, t_w, G_a, E_a, E_b, E_p, \mu$ are inputted in to a column of cells in sheet 1 of a spreadsheet named `'data21august.xlsx'`. The starting cell of inputting data is in the 6^{th} row and thus the ending cell is in the 18^{th} row. Thirteen cases are inputted corresponding to thirteen columns from C to O. As a result, all parameters of the thirteen cases are listed in cells `'C6:O18'`. Values of the parameters as presented under the Statement of Problem 2 in Chapter 4 are inputted in the case 13^{th} (corresponding to the 13^{th} column of the total thirteen columns).

B2.2 Programming in MATLAB

```
%-----------------------------------------------------------------------------
-
%--------------------PROBLEM 2-SIMPLY SUPPORTED BEAM-----------------------
-
%-----------------------FINITE ELEMENT SOLUTION----------------------------
-
%-----------------------------------------------------------------------------
-
%------------------------------------------------------------
% Input data shown in a Spreadsheet file
%------------------------------------------------------------
%Read data from spreadsheet file:
A=xlsread('data21august.xlsx',1,'C6:O18');
%Cases:
for k=13:13
  % k is index of a case in matrix A(13,10)
  disp(['CASE NUMBER ' num2str(k) ':']);
  disp('--------------')
  % Input Data for the case i:
        Ltotal=A(1,k);    % Length of member
        bb=A(2,k);   % Width of beam flanges
        bp=A(3,k);   % Width of GFRP plate and Adhesive layer
        t1=A(4,k);   % Thickness(m) of the GFRP plate
        t2=A(5,k);   % Thickness(m) of the adhesive layer
        hb=A(6,k);   % Effective height (m) of the beam
        t3=A(7,k);   % Thickness(m) of the flanges
        tw=A(8,k);   % Thickness(m) of the web
        Ga=A(9,k);   % Module of shear(kN/m2) of adhesive
        Ea=A(10,k);  % Module of elasticity (kN/m2) of adhesive
        Eb=A(11,k);  % Module of elasticity(kN/m2)of the beam
        Ep=A(12,k);  % Module of elasticity(kN/m2) of the GFRP
        Muy=A(13,k); % Poisson ratio
```

```
%--------------------------------------------------------------
% Calculation of section properties for the case i
%--------------------------------------------------------------
% Shear module of the beam:
Gb=Eb/(2*(1+Muy));
% Shear module of GFRP:
Gp=Ep/(2*(1+Muy));
% Geometry properties for the beam:
Ab=(t3*bb)*2+(hb-t3)*tw;
Ixxb=((bb*(t3^3))/12+(t3*bb)*((hb/2)^2))*2+(tw*(hb-t3)^3)/12;
Iyyb=(t3*(bb^3)/12)*2+((hb-t3)*tw^3)/12;
Iwwb=(hb^2*bb^3*t3/24)+((t3^3)*(bb^3)/144)*2+(tw^3)*((hb-t3)^3)/144;
Jb=(bb*(t3^3)/3)*2+(hb-t3)*(tw^3)/3;
% Geometry properties for GFRP plate:
Ap=t1*bp;
Ixxp=bp*(t1^3)/12;
Iyyp=t1*(bp^3)/12;
Iwwp=(t1^3)*(bp^3)/144;
Jp=bp*(t1^3)/3;
%Geometry properties for adhesive layer:
Aa=t2*bp;
Ixxa=bp*(t2^3)/12;
Iyya=t2*(bp^3)/12;
Iwwa=(t2^3)*(bp^3)/144;
Ja=((t1^2)-t1*t3+(t3^2))*Aa/3;
%-----------------------------------------------------------------------
-
%   Determination of roots of characteristic equation for the case i
%-----------------------------------------------------------------------
-
%Calculation of constants c1, c2 c3
c1=1/t2;
c2=(t1+2*t2+t3+hb)/(2*t2);
c3=(t1+2*t2+t3-hb)/(2*t2);
%Calculation of constant B1, B2,...,B12
B1=Eb*Ab;
B2=(c1^2)*Ga*Aa;
B3=c1*c2*Ga*Aa;
B4=Ep*Ap;
B5=Eb*Ixxb+Ep*Ixxp;
B6=(c2^2)*Ga*Aa;
B7=Eb*Iyyb;
B8=(c1^2)*Ga*Iyya;
B9=c1*c3*Ga*Iyya;
B10=Ep*Iyyp;
B11=Eb*Iwwb+Ep*Iwwp;
B12=Gb*Jb+Gp*Jp+Ga*Ja+(c3^2)*Ga*Iyya;
% There are 6 zero roots and 2 non-zero roots.
% The non-zero roots of characteristic equation in the normal solution
method are shown below.
m1=sqrt((B1*B2*B5+B1*B4*B6+B2*B4*B5)/(B1*B4*B5));
m2=-sqrt((B1*B2*B5+B1*B4*B6+B2*B4*B5)/(B1*B4*B5));
%-----------------------------------------------------------------------
-
%            FINITE ELEMENT SOLUTION (n-element solution)
%-----------------------------------------------------------------------
-
```

```
  n=input('Input number of elements n=');
  L=Ltotal/n;   % Length of one element
  syms z
  % Determination of f values:
  f1=B1/B4;
  f2=B2/B3;
  f3=B1/B3;
  f4=(B1*B2+B2*B4)/(3*B3*B4);
  f5=m1*B1/B3-(B1*B2+B2*B4)/(m1*B3*B4);
  f6=m2*B1/B3-(B1*B2+B2*B4)/(m2*B3*B4);
  f9=B3*L^2+B1*B3*L^2/B4+6*B5*f4+2*B1*B6/B3-3*B6*L^2*f4;
  f10=B3+B1*B3/B4-B5*f5*m1^3+B6*f5*m1;
  f11=B3+B1*B3/B4-B5*f6*m2^3+B6*f6*m2;
  % Establishment of the matrix Z1(4x8):
  syms z
  z11=[1 z z^2 exp(m1*z) exp(m2*z) 0 0 0];
% first row of Z1
  z12=[0 0 -f1*z^2 -f1*exp(m1*z) -f1*exp(m2*z) 1 z 0];
% second row of Z1
  z13=[-f2*z -f2*(z^2)/2 (2*f3*z-f4*z^3) f5*exp(m1*z) f6*exp(m2*z) f2*z
f2*(z^2)/2 1]; % third row of Z2
  z14=diff(z13,z);
% fourth row of Z2
  % Matrix Z1:
  Z1=[z11; z12; z13; z14];
  % Transpore of matrix Z1:
  transpore_Z1=Z1';
  % First derivative of matrix Z1:
  first_diff_Z1=diff(Z1,z);
  % Transpore of the first derivative of matrix Z1:
  transpore_first_diff_Z1=(first_diff_Z1)';
  % Second derivative of matrix Z1:
  second_diff_Z1=diff(first_diff_Z1,z);
  % Transpore of the second derivative of matrix Z1:
  transpore_second_diff_Z1=(second_diff_Z1)';
  Z10=[z11; z12; z13; z14];  % Z1=Z10
  % Matrix Z1 at z=0:
  Z100=subs(Z10,0);
  % Matrix Z1 at z=L:
  Z10L=subs(Z10,L);
  % Matrix L1:
  L1=[Z100; Z10L];
  % Inverse matrix of L1:
  inverse_L1=inv(L1);
  % Transpore of inverse matrix of L1:
  transpore_of_inverse_L1=(inverse_L1)';
  % Unit matricies ro 1, 2, 3:
  ro1=[1;0;0;0];
  ro2=[0;1;0;0];
  ro3=[0;0;1;0];
  % Shape function matrix:
  N1z=Z10*inverse_L1;
  %-------------------------------------------------------------------
-
  % Establishing element stiffness matrix:
  %-------------------------------------------------------------------
-
```

```
  % First term of Prepare_K1:
  a1=transpore_first_diff_Z1*ro1*(ro1')*first_diff_Z1;
  first_term_of_K1=Eb*Ab*int(a1,z,0,L);
  % Second term of Prepare_K1:
  a2=transpore_first_diff_Z1*ro2*(ro2')*first_diff_Z1;
  second_term_of_K1=Ep*Ap*int(a2,z,0,L);
  % Third term of Prepare_K1:
  a3=transpore_second_diff_Z1*ro3*(ro3')*second_diff_Z1;
  third_term_of_K1=(Eb*Ixxb+Ep*Ixxp)*int(a3,z,0,L);
  % Fourth term of Prepare_K1:
  a4=transpore_first_diff_Z1*ro3*(ro3')*first_diff_Z1;
  fourth_term_of_K1=(Ga*Aa*(c2^2))*int(a4,z,0,L);
  % Fifth term of Prepare_K1:
  a5=transpore_Z1*[ro1 ro2]*[1 -1; -1 1]*[ro1'; ro2']*Z1;
  fifth_term_of_K1=(Ga*Aa*(c1^2))*int(a5,z,0,L);
  % Calculuate matrix M:
  a6=((diff(N1z,z))')*ro3*(ro1'-ro2')*N1z;
  integratez_within_M=int(a6,z,0,L);
  % Sum of integrations:

Sum_of_intergrations=first_term_of_K1+second_term_of_K1+third_term_of_K1+f
ourth_term_of_K1+fifth_term_of_K1;
  % Components of matrix K1:
  Prepare1_K1=(transpore_of_inverse_L1*Sum_of_intergrations*inverse_L1);
  M=integratez_within_M;
  %
  % Element stiffness matrix K1: (8x8)
  K1=Prepare1_K1+c1*c2*Ga*Aa*(M+M');
  %-----------------------------------------------------------------------
-
  % Establishing sub-matrices KG11, KG22, KG12, and KG21 in order to form
  % global stiffness matrix for multi-element solution:
  %-----------------------------------------------------------------------
-
  KG11=zeros(4,4);
  for j=1:4
      for u=1:4
          KG11(j,u)=K1(j,u);
      end
  end
    KG22=zeros(4,4);
  for j=1:4
      for u=1:4
          KG22(j,u)=K1(j+4,u+4);
      end
  end
    KG12=zeros(4,4);
  for j=1:4
      for u=1:4
          KG12(j,u)=K1(j,u+4);
      end
  end
    KG21=zeros(4,4);
  for j=1:4
      for u=1:4
          KG21(j,u)=K1(j+4,u);
      end
```

```
  end
  %-----------------------------------------------------------------------
-
  % ESTABLISH THE GLOBAL STIFFNESS MATRIX
  %-----------------------------------------------------------------------
-
  Klocal=[(KG11+KG22) KG12; KG21 (KG11+KG22)];
  Kglobal1=zeros(n*4,n*4);
      for j=1:8
          for u=1:8
              Kglobal1(j,u)=Klocal(j,u);
          end
      end
      for j=5:4:(n*4-3)
          for u=j:(j+7)
              for p=j:(j+7)
                  Kglobal1(u,p)=Kglobal1(u-4,p-4);
              end
          end
      end
      for j=(n*4-3):(n*4)
          for u=(n*4-3):(n*4)
              Kglobal1(j,u)=KG22(j-(n*4-3)+1,u-(n*4-3)+1);
          end
      end
      Kglobal=zeros(4*(n+1),4*(n+1));
      for j=1:4
          for u=1:4
              Kglobal(j,u)=KG11(j,u);
          end
      end
      for j=1:4
          for u=1:4
              Kglobal(j+4,u)=KG21(j,u);
          end
      end
      for j=1:4
          for u=1:4
              Kglobal(j,u+4)=KG12(j,u);
          end
      end
      for j=1:(4*n)
          for p=1:(4*n)
              Kglobal(j+4,p+4)=Kglobal1(j,p);
          end
      end
      Kglobalsmall_1=zeros(4*(n+1)-3,4*(n+1));
      for i=1:(4*(n+1))
          Kglobalsmall_1(1,i)=Kglobal(2,i);
      end
      for i=4:(4*(n+1)-2)
          for j=1:(4*(n+1))
              Kglobalsmall_1(i-2,j)=Kglobal(i,j);
          end
      end
      for i=(4*(n+1)):(4*(n+1))
          for j=1:(4*(n+1))
```

```
            Kglobalsmall_1(i-3,j)=Kglobal(i,j);
        end
    end
Kglobalsmall=zeros(4*(n+1)-3,4*(n+1)-3);
    for i=1:(4*(n+1)-3)
        Kglobalsmall(i,1)=Kglobalsmall_1(i,2);
    end
    for i=4:(4*(n+1)-2)
        for j=1:(4*(n+1)-3)
            Kglobalsmall(j,i-2)=Kglobalsmall_1(j,i);
        end
    end
    for i=(4*(n+1)):(4*(n+1))
        for j=1:(4*(n+1)-3)
            Kglobalsmall(j,i-3)=Kglobalsmall_1(j,i);
        end
    end
Inverse_Kglobalsmall=inv(Kglobalsmall);
%-----------------------------------------------------------------------
-
% LOAD MATRIX
%-----------------------------------------------------------------------
-
% Uniformly distributed load:
q=-45/Ltotal;
% Shape functions:
N1z=Z10*inverse_L1;
ro1=[1; 0; 0; 0];
ro2=[0; 1; 0; 0];
ro3=[0; 0; 1; 0];
% Forming Q21:
Q211=int((N1z')*ro1, z, 0, L);
Q212=int((N1z')*ro3, z, 0, L);
Q213=int(((diff(N1z,z))')*ro3, z, 0, L);
preQ21=[Q211 Q212 Q213];
distributedload=[0; q; 0;];
Q21=preQ21*distributedload;
% Load matrix for n-element solution:
P=zeros(4*(n+1)-3,1);
for i=3:4:(4*(n+1)-9)
       P(i,1)=Q21(1,1)+Q21(5,1);
       P(i+1,1)=Q21(2,1)+Q21(6,1);
       P(i+2,1)=Q21(3,1)+Q21(7,1);
       P(i+3,1)=Q21(4,1)+Q21(8,1);
end
P(1,1)=Q21(2,1);
P(2,1)=Q21(4,1);
P(4*(n+1)-5,1)=Q21(5,1);
P(4*(n+1)-4,1)=Q21(6,1);
P(4*(n+1)-3,1)=Q21(8,1);
%-----------------------------------------------------------------------
-
% NODAL DISPLACEMENT VECTOR
%-----------------------------------------------------------------------
-
% Nodal displacement vector:
Displacement_field_small=Inverse_Kglobalsmall*P;
```

```
  % Full of nodal displacement vector (includes zero displacements at
  % constrains):
  Displacement_field=zeros(4*(n+1),1);
  Displacement_field(2,1)=Displacement_field_small(1,1);
  for i=4:(4*(n+1)-2)
      Displacement_field(i,1)=Displacement_field_small(i-2,1);
  end
    Displacement_field(4*(n+1),1)=Displacement_field_small(4*(n+1)-3,1);
  displacement_at_midspan=Displacement_field_small(4*n/2+3-2)
  Displacement_field;
  % Extracting transversal displacement field:
  displacement_Vtotal=zeros(n+1,1);
  for i=1:(n+1)
      displacement_Vtotal(i,1)=Displacement_field(3+4*(i-1),1);
  end
  %--------------------------------------------------------------------------
-
  % OUTPUT OF NODAL STRESSES
  %--------------------------------------------------------------------------
-
  % Longitudinal normal stress at bottom surface of bottom flange:
  normalstress_bottom_zb=zeros(n+1,1);
  % Longitudinal normal stress at top surface of GFRP plate:
  normalstress_top_zp=zeros(n+1,1);
  % Shear stress sigma_zn:
  shear_stress_zn=zeros(n+1,1);
  for i=1:n
      El_displacement=zeros(8,1);
      for j=1:8
      El_displacement(j,1)=Displacement_field(j+4*(i-1),1);
      end
      % Element nodal force vector:
      El_Force=vpa(K1*El_displacement-Q21,10);
      % Reaction forces:
      reactions=vpa(El_Force,10);
      % Normal stress_zb
      normalstress_bottom_zb(i,1)=Eb*[(-El_Force(1,1)/(Eb*Ab))-((-
El_Force(4,1)*((hb+t3)/2))/(Eb*Ixxb+Ep*Ixxp))];
      normalstress_bottom_zb(i+1,1)=Eb*[(El_Force(5,1)/(Eb*Ab))-
((El_Force(8,1)*((hb+t3)/2))/(Eb*Ixxb+Ep*Ixxp))];
      % Normal stress_zp
      normalstress_top_zp(i,1)=Ep*[(-El_Force(2,1)/(Ep*Ap))+((-
El_Force(4,1)*(t1/2))/(Eb*Ixxb+Ep*Ixxp))];

normalstress_top_zp(i+1,1)=Ep*[(El_Force(6,1)/(Ep*Ap))+((El_Force(8,1)*(t1
/2))/(Eb*Ixxb+Ep*Ixxp))];
      % Shear stress_zn
      shear_stress_zn(i,1)=Ga*[-
c1*El_displacement(1,1)+c1*El_displacement(2,1)-c2*El_displacement(4,1)];
      shear_stress_zn(i+1,1)=Ga*[-
c1*El_displacement(5,1)+c1*El_displacement(6,1)-c2*El_displacement(8,1)];
  end
%--------------------------------------------------------------------------
-
% DISPLAYING DISPLACEMENTS AND STRESSES
%--------------------------------------------------------------------------
-
```

```
disp('displacement_V:');
displacement_Vtotal_showed=zeros(11,1);
coordinate_z=zeros(11,1);
     displacement_Vtotal_showed(1,1)=displacement_Vtotal(1,1);
     coordinate_z(1,1)=0;
     displacement_Vtotal_showed(11,1)=displacement_Vtotal(n+1,1);
     coordinate_z(11,1)=Ltotal;
for i=1:9

displacement_Vtotal_showed(i+1,1)=displacement_Vtotal(round(n*i/10)+1,1);
     coordinate_z(i+1,1)=(round(n*i/10))*(Ltotal/n);
end
% Display results on screen:
   fprintf('Z-coordinate(m) \t Value(m) \r');
   for i=1:11
       fprintf('%3.2e\t\t\t %3.2e\t\t\t\n', coordinate_z(i,1),
displacement_Vtotal_showed(i,1));
   end
disp('----------------------------------------');
%----------------------------------------------------------------------------
-
%----------------------------------------------------------------------------
-
disp('normal_stress_bottom_zb:');
normalstress_bottom_zb_showed=zeros(11,1);
coordinate_zb=zeros(11,1);
     normalstress_bottom_zb_showed(1,1)=normalstress_bottom_zb(1,1);
     coordinate_zb(1,1)=0;
     normalstress_bottom_zb_showed(11,1)=normalstress_bottom_zb(n+1,1);
     coordinate_zb(11,1)=Ltotal;
for i=1:9

normalstress_bottom_zb_showed(i+1,1)=normalstress_bottom_zb(round(n*i/10)+
1,1);
     coordinate_zb(i+1,1)=(round(n*i/10))*(Ltotal/n);
end
% Display results on screen:
   fprintf('Z-coordinate(m) \t Value(kPa) \r');
   for i=1:11
       fprintf('%3.2e\t\t\t %3.2e\t\t\t\n', coordinate_zb(i,1),
normalstress_bottom_zb_showed(i,1));
   end
disp('----------------------------------------');
%----------------------------------------------------------------------------
-
%----------------------------------------------------------------------------
-
disp('normal_stress_top_zp:');
normalstress_top_zp_showed=zeros(11,1);
coordinate_zp=zeros(11,1);
     normalstress_top_zp_showed(1,1)=normalstress_top_zp(1,1);
     coordinate_zp(1,1)=0;
     normalstress_top_zp_showed(11,1)=normalstress_top_zp(n+1,1);
     coordinate_zp(11,1)=Ltotal;
for i=1:9

normalstress_top_zp_showed(i+1,1)=normalstress_top_zp(round(n*i/10)+1,1);
```

```
     coordinate_zp(i+1,1)=(round(n*i/10))*(Ltotal/n);
end
% Display results on screen:
   fprintf('Z-coordinate(m) \t Value(kPa) \r');
   for i=1:11
       fprintf('%3.2e\t\t\t %3.2e\t\t\t\n', coordinate_zp(i,1),
normalstress_top_zp_showed(i,1));
   end
disp('----------------------------------------');
%--------------------------------------------------------------------------
-
%--------------------------------------------------------------------------
-
disp('shear_stress_zn:');
shear_stress_zn_showed=zeros(11,1);
coordinate_zn=zeros(11,1);
     shear_stress_zn_showed(1,1)=shear_stress_zn(1,1);
     coordinate_zn(1,1)=0;
     shear_stress_zn_showed(11,1)=shear_stress_zn(n+1,1);
     coordinate_zn(11,1)=Ltotal;
for i=1:9
     shear_stress_zn_showed(i+1,1)=shear_stress_zn(round(n*i/10)+1,1);
     coordinate_zn(i+1,1)=(round(n*i/10))*(Ltotal/n);
end
% Display results on screen:
   fprintf('Z-coordinate(m) \t Value(kPa) \r');
   for i=1:11
       fprintf('%3.2e\t\t\t %3.2e\t\t\t\n', coordinate_zn(i,1),
shear_stress_zn_showed(i,1));
   end
disp('*************************************************************************
*');
end
%--------------------------------------------------------------------------
-
%-------------------------End of problem 2---------------------------------
-
%--------------------------------------------------------------------------
-
```

B2.3 Outputs

```
CASE NUMBER 13:
--------------
Input number of elements n=20

displacement_at_midspan =

   -0.0096

displacement_V:
Z-coordinate(m)          Value(m)
0.00e+000                0.00e+000
3.00e-001                -3.02e-003
```

```
6.00e-001                -5.70e-003
9.00e-001                -7.81e-003
1.20e+000                -9.15e-003
1.50e+000                -9.61e-003
1.80e+000                -9.15e-003
2.10e+000                -7.81e-003
2.40e+000                -5.70e-003
2.70e+000                -3.02e-003
3.00e+000                0.00e+000
----------------------------------------
normal_stress_bottom_zb:
Z-coordinate(m)           Value(kPa)
0.00e+000                -9.65e-007
3.00e-001                -6.72e+004
6.00e-001                -1.19e+005
9.00e-001                -1.57e+005
1.20e+000                -1.79e+005
1.50e+000                -1.87e+005
1.80e+000                -1.79e+005
2.10e+000                -1.57e+005
2.40e+000                -1.19e+005
2.70e+000                -6.72e+004
3.00e+000                -5.91e-007
----------------------------------------
normal_stress_top_zp:
Z-coordinate(m)          Value(kPa)
0.00e+000                6.94e-008
3.00e-001                1.19e+004
6.00e-001                2.11e+004
9.00e-001                2.77e+004
1.20e+000                3.17e+004
1.50e+000                3.30e+004
1.80e+000                3.17e+004
2.10e+000                2.77e+004
2.40e+000                2.11e+004
2.70e+000                1.19e+004
3.00e+000                1.43e-006
----------------------------------------
shear_stress_zn:
Z-coordinate(m)          Value(kPa)
0.00e+000                7.18e+002
3.00e-001                5.86e+002
6.00e-001                4.40e+002
9.00e-001                2.93e+002
1.20e+000                1.47e+002
1.50e+000                3.23e-009
1.80e+000                -1.47e+002
2.10e+000                -2.93e+002
2.40e+000                -4.40e+002
2.70e+000                -5.86e+002
3.00e+000                -7.18e+002
**********************************************************************
```

APPENDIX B3 – PROGRAMMING OF PROBLEMS 3 AND 4 IN CHAPTER 4

B3.1 Input data

In each case study, its parameters $L, b_b, b_p, t_1, t_2, h_b, t_3, t_w, G_a, E_a, E_b, E_p, \mu$ are inputted in to a column of cells in sheet 3 of a spreadsheet named `'data21august.xlsx'`. The starting cell of inputting data is in the 6^{th} row and thus the ending cell is in the 18^{th} row. Eighteen cases are inputted corresponding to eighteen columns from C to T. As a result, all parameters of the eighteen cases are listed in cells `'C6:T18'`. Values of the parameters as presented under the Statement of Problems 3 and 4 in Chapter 4 are inputted in the case 15^{th} (corresponding to the 15^{th} column of the total eighteen columns).

B3.2 Programming in MATLAB

```
%----------------------Non-shear deformable theory------------------------
-
%------------------------------------------------------------------------
-
%-----------PROBLEM 3-CANTILEVER UNDER BENDING ABOUT WEAK AXIS------------
-
%---------PROBLEM 4-CANTILEVER UNDER TWISTING ABOUT BEAM CENTROID---------
-
% The difference between two problems is load matrix. When running this
code, selecting load matrices named Q (Finite Element Solution) and F
(Closed Form Solution) corresponding to each problem should be done first.
%---------------------------------------------------------------
% Input data shown in a spreadsheet file
%---------------------------------------------------------------
%Read data from spreadsheet file:
A=xlsread('data21august.xlsx',3,'C6:T18');
% Case i:
for i=15:15
  % i is column index of matrix A(12,10)
  disp(['CASE NUMBER ' num2str(i) ':']);
  disp('--------------')
  % Input Data for the case i:
        L=[A(1,i)];     % Length of member
        bb=[A(2,i)];    % Width of beam flanges
        bp=[A(3,i)];    % Width of GFRP plate and Adhesive layer
        t1=[A(4,i)];    % Thickness(m) of the GFRP plate
        t2=[A(5,i)];    % Thickness(m) of the adhesive layer
        hb=[A(6,i)];    % Effective height (m) of the beam
        t3=[A(7,i)];    % Thickness(m) of the flanges
        tw=[A(8,i)];    % Thickness(m) of the web
        Ga=[A(9,i)];    % Module of shear(kN/m2) of adhesive
        Ea=[A(10,i)];   % Module of elasticity (kN/m2) of adhesive
        Eb=[A(11,i)];   % Module of elasticity(kN/m2)of the beam
```

```
      Ep=[A(12,i)];  % Module of elasticity(kN/m2) of the GFRP
      Muy=[A(13,i)]; % Poisson ratio
%-------------------------------------------------------------
% Calculation of section properties for the case i
%-------------------------------------------------------------
%disp('Start calculations');
%Calculation of shear modules
%disp('Calculation of shear modules:');
%disp('Shear module of the beam:');
Gb=Eb/(2*(1+Muy));
%disp('Shear module of GFRP:');
Gp=Ep/(2*(1+Muy));
%Calculation of section properties for wide flange beam:
Ab=(t3*bb)*2+(hb-t3)*tw;
Ixxb=((bb*(t3^3))/12+(t3*bb)*((hb/2)^2))*2+(tw*(hb-t3)^3)/12;
Iyyb=(t3*(bb^3)/12)*2+((hb-t3)*tw^3)/12;
Iwwb=(hb^2*bb^3*t3/24)+((t3^3)*(bb^3)/144)*2+(tw^3)*((hb-t3)^3)/144;
Jb=(bb*(t3^3)/3)*2+(hb-t3)*(tw^3)/3;
%Calculation of section properties for GFRP plate:
Ap=t1*bp;
Ixxp=bp*(t1^3)/12;
Iyyp=t1*(bp^3)/12;
Iwwp=(t1^3)*(bp^3)/144;
Jp=bp*(t1^3)/3;
%Calculation of section properties for adhesive layer:
Aa=t2*bp;
Ixxa=bp*(t2^3)/12;
Iyya=t2*(bp^3)/12;
Iwwa=(t2^3)*(bp^3)/144;
Ja=((t1^2)-t1*t3+(t3^2))*Aa/3;
%-------------------------------------------------------------------
%   Determination of roots of characteristic equation for the case i
%-------------------------------------------------------------------
%Calculation of constants c1, c2 c3:
c1=1/t2;
c2=(t1+2*t2+t3+hb)/(2*t2);
c3=(t1+2*t2+t3-hb)/(2*t2);
%Calculation of constant B1, B2,...,B12:
B1=Eb*Ab;
B2=(c1^2)*Ga*Aa;
B3=c1*c2*Ga*Aa;
B4=Ep*Ap;
B5=Eb*Ixxb+Ep*Ixxp;
B6=(c2^2)*Ga*Aa;
B7=Eb*Iyyb;
B8=(c1^2)*Ga*Iyya;
B9=c1*c3*Ga*Iyya;
B10=Ep*Iyyp;
B11=Eb*Iwwb+Ep*Iwwp;
B12=Gb*Jb+Gp*Jp+Ga*Ja+(c3^2)*Ga*Iyya;
% There are 6 zero roots and 6 non-zero roots.
% The non-zero roots of characteristic equation are shown below.
F1=-(B8*B10*B11+B7*B8*B11+B7*B10*B12)/(B7*B10*B11);
F2=(B2*B10*B11+B8*B10*B12+B2*B7*B11+B8*B7*B12+B6*B7*B10-B7*B9*B9-
  B9*B9*B10)/(B7*B10*B11);
```

```
  F3=-
    (B2*B10*B12+B6*B8*B10+B2*B7*B12+B6*B7*B8+2*B3*B7*B9+2*B3*B9*B10)/(B7*
    B10*B11);
  t=roots([1,F1,F2,F3]);
  k7=sqrt(t(1,:));
  k8=-sqrt(t(1,:));
  k9=sqrt(t(2,:));
  k10=-sqrt(t(2,:));
  k11=sqrt(t(3,:));
  k12=-sqrt(t(3,:));
  %-----------------------------------------------------------------------
-
  %             FINITE ELEMENT SOLUTION (1-Element solution)
  %-----------------------------------------------------------------------
-
  % Determination of f values
  f2=B2/B3;
  f7=B7/B10;
  f87=(-B7*B10*(k7)^4+(B7*B8+B8*B10)*(k7)^2-
     B2*(B7+B10))/(B10*(B9*(k7)^2+B3));
  f88=(-B7*B10*(k8)^4+(B7*B8+B8*B10)*(k8)^2-
     B2*(B7+B10))/(B10*(B9*(k8)^2+B3));
  f89=(-B7*B10*(k9)^4+(B7*B8+B8*B10)*(k9)^2-
     B2*(B7+B10))/(B10*(B9*(k9)^2+B3));
  f810=(-B7*B10*(k10)^4+(B7*B8+B8*B10)*(k10)^2-
     B2*(B7+B10))/(B10*(B9*(k10)^2+B3));
  f811=(-B7*B10*(k11)^4+(B7*B8+B8*B10)*(k11)^2-
     B2*(B7+B10))/(B10*(B9*(k11)^2+B3));
  f812=(-B7*B10*(k12)^4+(B7*B8+B8*B10)*(k12)^2-
     B2*(B7+B10))/(B10*(B9*(k12)^2+B3));
  % Establishment of the matrix Z2(6x12)
  syms z
  z21a=[1 z z^2 z^3 exp(k7*z) exp(k8*z) exp(k9*z) exp(k10*z) exp(k11*z)
exp(k12*z) 0 0];                                   % first row of Z2
  z22a=diff(z21a,z);
% second row of Z2
  z23a=[0 0 z^2 z^3 -f7*exp(k7*z) -f7*exp(k8*z) -f7*exp(k9*z) -
f7*exp(k10*z) -f7*exp(k11*z) -f7*exp(k12*z) 1 z];            % third row
of Z2
  z24a=diff(z23a,z);
% forth row of Z2
  z25a=[-f2 -f2*z 0 0 f87*exp(k7*z) f88*exp(k8*z) f89*exp(k9*z)
f810*exp(k10*z) f811*exp(k11*z) f812*exp(k12*z) f2 f2*z];     % fifth row
of Z2
  z26a=diff(z25a,z);
% sixth row of Z2
  % Matrix Z2:
  Z2a=[z21a; z22a; z23a; z24a; z25a; z26a];
  transpore_Z2a=Z2a';
  first_differential_Z2a=diff(Z2a,z);
  second_differential_Z2a=diff(first_differential_Z2a,z);
  transpore_first_diff_Z2a=(first_differential_Z2a)';
  transpore_second_diff_Z2a=( second_differential_Z2a)';
  Z2=[z21a; z22a; z23a; z24a; z25a; z26a];
  % Matrix Z2 at z=0:
  Z20=subs(Z2,0);
  % Matrix Z2 at z=l=L:
```

```
  Z2L=subs(Z2,L);
  % Matrix L2:
  L2=[Z20; Z2L];
  % Inverse matrix of L2:
  inverse_L2=inv(L2);
  % disp('Transpore of inverse matrix of L2:');
  transpore_of_inverse_L2=(inverse_L2)';
  % Input of matrices P1, P2, P3, P4, and P5:
  ro4=[1; 0; 0; 0; 0; 0;];
  ro5=[0; 0; 1; 0; 0; 0;];
  ro6=[0; 0; 0; 0; 1; 0;];
  traspore_robar=[ro4 ro5 ro6];
  Ha1bar=[c1^2 -c1^2 -c1*c3; -c1^2 c1^2 c1*c3; -c1*c3 c1*c3 c3^2];
  Ha2bar=[c1^2 -c1^2 c1*c2; -c1^2 c1^2 -c1*c2; c1*c2 -c1*c2 c2^2];
  % First term of Prepare_K2:
  a1=transpore_second_diff_Z2a*ro4*(ro4')*second_differential_Z2a;
  first_term_of_K2=Eb*Iyyb*int(a1,z,0,L);
  % Second term of Prepare_K2:
  a2=transpore_second_diff_Z2a*ro5*(ro5')*second_differential_Z2a;
  second_term_of_K2=Ep*Iyyp*int(a2,z,0,L);
  % Third term of Prepare_K2:
  a3=transpore_second_diff_Z2a*ro6*(ro6')*second_differential_Z2a;
  third_term_of_K2=(Eb*Iwwb+Ep*Iwwp)*int(a3,z,0,L);
  % Fourth term of Prepare_K2:
  a4=transpore_first_diff_Z2a*ro6*(ro6')*first_differential_Z2a;
  fourth_term_of_K2=(Gb*Jb+Gp*Jp)*int(a4,z,0,L);
  % Fifth term of Prepare_K2:

a5=transpore_first_diff_Z2a*traspore_robar*Ha1bar*(traspore_robar')*first_
differential_Z2a;
  fifth_term_of_K2=(Ga*Iyya)*int(a5,z,0,L);
  % Sixth term of Prepare_K2:
  a6=transpore_Z2a*traspore_robar*Ha2bar*(traspore_robar')*Z2a;
  sixth_term_of_K2=(Ga*Aa)*int(a6,z,0,L);
  % Stiffness matrix Prepare_K1:

Prepare_K2=first_term_of_K2+second_term_of_K2+third_term_of_K2+fourth_term
_of_K2+fifth_term_of_K2+sixth_term_of_K2;
  %-----------------------------------------------------------------------
-
  % Element stiffness matrix K1:
  K2=vpa(transpore_of_inverse_L2*Prepare_K2*inverse_L2);
  % Element stiffness matrix in brief form: (6x6)
  K21=[K2(7,7) K2(7,8) K2(7,9) K2(7,10) K2(7,11) K2(7,12)];
  K22=[K2(8,7) K2(8,8) K2(8,9) K2(8,10) K2(8,11) K2(8,12)];
  K23=[K2(9,7) K2(9,8) K2(9,9) K2(9,10) K2(9,11) K2(9,12)];
  K24=[K2(10,7) K2(10,8) K2(10,9) K2(10,10) K2(10,11) K2(10,12)];
  K25=[K2(11,7) K2(11,8) K2(11,9) K2(11,10) K2(11,11) K2(11,12)];
  K26=[K2(12,7) K2(12,8) K2(12,9) K2(12,10) K2(12,11) K2(12,12)];
  Small_K2=[K21; K22; K23; K24; K25; K26];
  % Inverse matrix of the brief stiffness matrix:
  inverse_Small_K2=inv(Small_K2);
  % Element load matrix for bending about weak axis:
  Q=[12; 0; 0; 0; 0; 0];
  % Element load matrix for twisting about the beam centroid:
  Q=[0; 0; 0; 0; -3.27118; 0];
  % Nodal displacement vector:
```

```
  disp('Finite Element Solution-1 element solution:');
  disp('------------------------');
  disp('Nodal displacement vector at tip:');
  Delta=inverse_Small_K2*Q
  %--------------------------------------------------------------------
-
  %--------------------------------------------------------------------
-
  % CLOSED FORM SOLUTION
  %--------------------------------------------------------------------
-
  %--------------------------------------------------------------------
-
  disp('Closed form solution:');
  disp('---------------------');
  f2=B2/B3;
  f7=B7/B10;
  f87=(-B7*B10*(k7)^4+(B7*B8+B8*B10)*(k7)^2-
     B2*(B7+B10))/(B10*(B9*(k7)^2+B3));
  f88=(-B7*B10*(k8)^4+(B7*B8+B8*B10)*(k8)^2-
     B2*(B7+B10))/(B10*(B9*(k8)^2+B3));
  f89=(-B7*B10*(k9)^4+(B7*B8+B8*B10)*(k9)^2-
     B2*(B7+B10))/(B10*(B9*(k9)^2+B3));
  f810=(-B7*B10*(k10)^4+(B7*B8+B8*B10)*(k10)^2-
     B2*(B7+B10))/(B10*(B9*(k10)^2+B3));
  f811=(-B7*B10*(k11)^4+(B7*B8+B8*B10)*(k11)^2-
     B2*(B7+B10))/(B10*(B9*(k11)^2+B3));
  f812=(-B7*B10*(k12)^4+(B7*B8+B8*B10)*(k12)^2-
     B2*(B7+B10))/(B10*(B9*(k12)^2+B3));
  f9=(B3*B8+B2*B9)/B3;
  f107=(B8*(B7+B10)*k7/B10-B9*f87*k7-B7*(k7)^3)*exp(k7*L);
  f108=(B8*(B7+B10)*k8/B10-B9*f88*k8-B7*(k8)^3)*exp(k8*L);
  f109=(B8*(B7+B10)*k9/B10-B9*f89*k9-B7*(k9)^3)*exp(k9*L);
  f1010=(B8*(B7+B10)*k10/B10-B9*f810*k10-B7*(k10)^3)*exp(k10*L);
  f1011=(B8*(B7+B10)*k11/B10-B9*f811*k11-B7*(k11)^3)*exp(k11*L);
  f1012=(B8*(B7+B10)*k12/B10-B9*f812*k12-B7*(k12)^3)*exp(k12*L);
  f11=(B3*B9+B2*B12)/B3;
  f127=(-B9*(B7+B10)*k7/B10+B12*f87*k7-B11*f87*(k7)^3)*exp(k7*L);
  f128=(-B9*(B7+B10)*k8/B10+B12*f88*k8-B11*f88*(k8)^3)*exp(k8*L);
  f129=(-B9*(B7+B10)*k9/B10+B12*f89*k9-B11*f89*(k9)^3)*exp(k9*L);
  f1210=(-B9*(B7+B10)*k10/B10+B12*f810*k10-B11*f810*(k10)^3)*exp(k10*L);
  f1211=(-B9*(B7+B10)*k11/B10+B12*f811*k11-B11*f811*(k11)^3)*exp(k11*L);
  f1212=(-B9*(B7+B10)*k12/B10+B12*f812*k12-B11*f812*(k12)^3)*exp(k12*L);
  % Establishment of the matrix Z(12x12) at z=0 and z=L:
  syms z
  z21=[1 0 0 0 1 1 1 1 1 1 0 0];
  z22=[0 0 0 0 -1 -1 -1 -1 -1 -1 1/f7 0];
  z23=[-f2 0 0 0 f87 f88 f89 f810 f811 f812 f2 0];
  z24=[0 1 0 0 k7 k8 k9 k10 k11 k12 0 0];
  z25=[0 0 0 0 -k7 -k8 -k9 -k10 -k11 -k12 0 1/f7];
  z26=[0 -f2 0 0 f87*k7 f88*k8 f89*k9 f810*k10 f811*k11 f812*k12 0 f2];
  z27=[0 0 2 6*L (k7^2)*exp(k7*L) (k8^2)*exp(k8*L) (k9^2)*exp(k9*L)
(k10^2)*exp(k10*L) (k11^2)*exp(k11*L) (k12^2)*exp(k12*L) 0 0];
  z28=[0 0 2/f7 6*L/f7 -(k7^2)*exp(k7*L) -(k8^2)*exp(k8*L) -
(k9^2)*exp(k9*L) -(k10^2)*exp(k10*L) -(k11^2)*exp(k11*L) -
(k12^2)*exp(k12*L) 0 0];
```

```
  z29=[0 0 0 0 f87*(k7^2)*exp(k7*L) f88*(k8^2)*exp(k8*L)
f89*(k9^2)*exp(k9*L) f810*(k10^2)*exp(k10*L) f811*(k11^2)*exp(k11*L)
f812*(k12^2)*exp(k12*L) 0 0];
  z210=[0 f9 0 -6*B7 f107 f108 f109 f1010 f1011 f1012 0 -f9];
  z211=[0 -f9 0 -6*B10 -f107 -f108 -f109 -f1010 -f1011 -f1012 0 f9];
  z212=[0 -f11 0 0 f127 f128 f129 f1210 f1211 f1212 0 f11];
  % disp('Z2 matrix:')
  Z_matrix=[z21; z22; z23; z24; z25; z26; z27; z28; z29; z210; z211;
z212];
  % Load matrix for bending about weak axis:
  F=[0; 0; 0; 0; 0; 0; 0; 0; 0; 12; 0; 0];
  % Load matrix for twisting about the beam centroid:
  F=[0; 0; 0; 0; 0; 0; 0; 0; 0; 0; 0; -3.27118];
  Root_A=Z_matrix\F;
    % Obtaining displacement and stresses
   displacement_Ub=[1 z z^2 z^3 exp(k7*z) exp(k8*z) exp(k9*z) exp(k10*z)
exp(k11*z) exp(k12*z) 0 0]*Root_A;
   displacement_Up=[0 0 z^2 z^3 -f7*exp(k7*z) -f7*exp(k8*z) -f7*exp(k9*z)
-f7*exp(k10*z) -f7*exp(k11*z) -f7*exp(k12*z) 1 z]*Root_A;
   displacement_theta=[-f2 -f2*z 0 0 f87*exp(k7*z) f88*exp(k8*z)
f89*exp(k9*z) f810*exp(k10*z) f811*exp(k11*z) f812*exp(k12*z) f2
f2*z]*Root_A;
   %-----------------------------------------------------------------------
-
   % Displacement fields:
   disp('Lateral deflection at beam centroid:');
   Lateral_displacement_Ub_vector=subs(displacement_Ub,0:(L/10):L);
    % Display results on screen:
   fprintf('Z-coordinate(m) \t Value(m) \r');
   for k=1:11
       fprintf('%3.2e\t\t\t %3.2e\t\t\t\n', (k-1)*L/10,
Lateral_displacement_Ub_vector(1,k));
   end
   disp('------------------------------------------------------------');
   disp('Lateral deflection at GFRP plate centroid:');
   Lateral_displacement_Up_vector=subs(displacement_Up,0:(L/10):L);
   % Display results on screen:
   fprintf('Z-coordinate(m) \t Value(m) \r');
   for k=1:11
       fprintf('%3.2e\t\t\t %3.2e\t\t\t\n', (k-1)*L/10,
Lateral_displacement_Up_vector(1,k));
   end
   disp('------------------------------------------------------------');
   disp('Twisting angle:');
   Lateral_displacement_theta_vector=subs(displacement_theta,0:(L/10):L);
   % Display results on screen:
   fprintf('Z-coordinate(m) \t Value(Rad) \r');
   for k=1:11
       fprintf('%3.2e\t\t\t %3.2e\t\t\t\n', (k-1)*L/10,
Lateral_displacement_theta_vector(1,k));
   end
   disp('----------------------------------------');
   %-----------------------------------------------------------------------
-
   %-------------------------Output of stresses----------------------------
-
```

```
   disp('Longitudinal normal stress S33 at the center point of left edge
of the beam:');
   epsilon_zb=diff(diff(displacement_Ub,z),z)*bb/2-
diff(diff(displacement_theta,z),z)*(hb*bb/4);
   max_normal_stress_in_beam=subs(Eb*epsilon_zb,0:(L/10):L);
   % Display results on screen:
   fprintf('Z-coordinate(m) \t Value(kPa) \r');
   for k=1:11
       fprintf('%3.2e\t\t\t %3.2e\t\t\t\n', (k-1)*L/10,
max_normal_stress_in_beam(1,k));
   end
   disp('----------------------------------------------------------');

   disp('Longitudinal normal stress S33 at the top point of left edge of
GFRP plate:');

epsilon_zp=diff(diff(displacement_Up,z),z)*(bp/2)+(diff(diff(displacement_
theta,z),z))*(-t1*bp/4);
   max_normal_stress_in_FRP=subs(Ep*epsilon_zp,0:(L/10):L);
   % Display results on screen:
   fprintf('Z-coordinate(m) \t Value(kPa) \r');
   for k=1:11
       fprintf('%3.2e\t\t\t %3.2e\t\t\t\n', (k-1)*L/10,
max_normal_stress_in_FRP(1,k));
   end
   disp('----------------------------------------------------------');

   disp('Shear stress gamma_nz in the adhesive layer at x=bp/2:');
   aa=[-c1 c1 -c2 c1*bp/2 -c1*bp/2 -c3*bp/2];
   deltaA_shear_zn=[0; 0; 0; diff(displacement_Ub,z);
diff(displacement_Up,z); diff(displacement_theta,z);];
   shear_strain_zn=aa*deltaA_shear_zn;
   shear_stress_zn=subs(shear_strain_zn*Ga,0:(L/10):L);
   % Display results on screen:
   fprintf('Z-coordinate(m) \t Value(kPa) \r');
   for k=1:11
       fprintf('%3.2e\t\t\t %3.2e\t\t\t\n', (k-1)*L/10,
shear_stress_zn(1,k));
   end
   disp('----------------------------------------------------------');

   disp('Shear stress gamma_sn in the adhesive layer:');
   aa1=[-c1 c1 -c2];
   deltaA_shear_sn=[displacement_Ub; displacement_Up;
displacement_theta;];
   shear_strain_sn=aa1*deltaA_shear_sn;
   shear_stress_sn=subs(shear_strain_sn*Ga,0:(L/10):L);
   % Display results on screen:
   fprintf('Z-coordinate(m) \t Value(kPa) \r');
   for k=1:11
       fprintf('%3.2e\t\t\t %3.2e\t\t\t\n', (k-1)*L/10,
shear_stress_sn(1,k));
   end
   disp('----------------------------------------------------------');

   disp('Maximum shear gamma_sz at upper surface in the adhesive layer:');
```

```
   fya=(t1+t3)*(t2/2)/t2+(t1-t3)/2;
   first_diff_of_theta_z=diff(displacement_theta,z);
   shear_strain_sza_upper=-fya*first_diff_of_theta_z;
   shear_stress_sz_upper=subs(Ga*shear_strain_sza_upper,0:(L/10):L);
   % Display results on screen:
   fprintf('Z-coordinate(m) \t Value(kPa) \r');
   for k=1:11
       fprintf('%3.2e\t\t\t %3.2e\t\t\t\n', (k-1)*L/10,
shear_stress_sz_upper(1,k));
   end
   disp('-----------------------------------------------------------');

   disp('Maximum shear stress gamma_sz at lower surface in the adhesive
layer:');
   fya1=(t1+t3)*(-t2/2)/t2+(t1-t3)/2;
   first_diff_of_theta_z=diff(displacement_theta,z);
   shear_strain_sza_lower=-fya1*first_diff_of_theta_z;
   shear_stress_sz_lower=subs(Ga*shear_strain_sza_lower,0:(L/10):L);
   % Display results on screen:
   fprintf('Z-coordinate(m) \t Value(kPa) \r');
   for k=1:11
       fprintf('%3.2e\t\t\t %3.2e\t\t\t\n', (k-1)*L/10,
shear_stress_sz_lower(1,k));
   end
   disp('---------------------------------------');


disp('********************************************************************
********************');
end
%-------------------------------------------------------------------------
-
%-------------------------End of problem 3--------------------------------
-
%-------------------------------------------------------------------------
-
```

B3.3 Outputs

B3.3.1 Problem 3-Bending about weak axis

CASE NUMBER 15:

Finite Element Solution – 1 element solution:

Nodal displacement vector at tip:
Delta =
.12510020874637546154407448212381-.22848134995411054195566995410546e-30*i
.37523067981824818143506131248161e-1+.62587495071424835903606539506242e-19*i
.12410947250115027870912842934745-.43385250809795323163729221910584e-20*i
.37296798235568895597756553155385e-1-.57465456692880484828741363666738e-18*i

-.45101368484806603425420926393994e-2+.45157199344522838280407711890175e-19*i
-.11020779186378404598903887480642e-2+.49845070389276979809804739844009e-19*i

Closed form solution:

Lateral deflection at beam centroid:

Z-coordinate(m)	Value(m)
0.00e+000	3.82e-020
5.00e-001	1.82e-003
1.00e+000	7.01e-003
1.50e+000	1.52e-002
2.00e+000	2.60e-002
2.50e+000	3.91e-002
3.00e+000	5.41e-002
3.50e+000	7.05e-002
4.00e+000	8.81e-002
4.50e+000	1.06e-001
5.00e+000	1.25e-001

Lateral deflection at GFRP plate centroid:

Z-coordinate(m)	Value(m)
0.00e+000	-5.49e-020
5.00e-001	1.79e-003
1.00e+000	6.91e-003
1.50e+000	1.50e-002
2.00e+000	2.57e-002
2.50e+000	3.87e-002
3.00e+000	5.35e-002
3.50e+000	6.99e-002
4.00e+000	8.73e-002
4.50e+000	1.06e-001
5.00e+000	1.24e-001

Twisting angle:

Z-coordinate(m)	Value(Rad)
0.00e+000	-1.41e-019
5.00e-001	-1.36e-004
1.00e+000	-4.55e-004
1.50e+000	-8.74e-004
2.00e+000	-1.35e-003
2.50e+000	-1.85e-003
3.00e+000	-2.37e-003
3.50e+000	-2.89e-003
4.00e+000	-3.43e-003
4.50e+000	-3.97e-003
5.00e+000	-4.51e-003

Longitudinal normal stress S33 at the center point of left edge of the beam:

Z-coordinate(m)	Value(kPa)
0.00e+000	2.77e+005
5.00e-001	2.47e+005
1.00e+000	2.19e+005
1.50e+000	1.91e+005
2.00e+000	1.63e+005
2.50e+000	1.36e+005
3.00e+000	1.09e+005
3.50e+000	8.15e+004
4.00e+000	5.44e+004
4.50e+000	2.72e+004
5.00e+000	-7.05e-012

Longitudinal normal stress S33 at the top point of left edge of GFRP plate:

Z-coordinate(m)	Value(kPa)
0.00e+000	5.59e+004
5.00e-001	5.08e+004
1.00e+000	4.53e+004
1.50e+000	3.98e+004
2.00e+000	3.41e+004
2.50e+000	2.85e+004
3.00e+000	2.28e+004
3.50e+000	1.71e+004
4.00e+000	1.14e+004
4.50e+000	5.68e+003
5.00e+000	4.83e-012

Shear stress gamma_nz in the adhesive layer at x=bp/2:

Z-coordinate(m)	Value(kPa)
0.00e+000	-3.17e-012
5.00e-001	3.66e+002
1.00e+000	5.65e+002
1.50e+000	6.73e+002
2.00e+000	7.31e+002
2.50e+000	7.63e+002
3.00e+000	7.80e+002
3.50e+000	7.91e+002
4.00e+000	7.99e+002
4.50e+000	8.07e+002
5.00e+000	5.29e+002

Shear stress gamma_sn in the adhesive layer:

Z-coordinate(m)	Value(kPa)
0.00e+000	-1.09e-011
5.00e-001	-1.57e+001
1.00e+000	-8.45e+000
1.50e+000	-4.57e+000
2.00e+000	-2.48e+000

2.50e+000	-1.36e+000
3.00e+000	-7.81e-001
3.50e+000	-5.06e-001
4.00e+000	-4.28e-001
4.50e+000	-5.63e-001
5.00e+000	2.99e+002

Maximum shear gamma_sz at upper surface in the adhesive layer:

Z-coordinate(m)	Value(kPa)
0.00e+000	-6.76e-016
5.00e-001	3.74e+000
1.00e+000	5.77e+000
1.50e+000	6.86e+000
2.00e+000	7.45e+000
2.50e+000	7.77e+000
3.00e+000	7.95e+000
3.50e+000	8.06e+000
4.00e+000	8.14e+000
4.50e+000	8.22e+000
5.00e+000	8.38e+000

Maximum shear stress gamma_sz at lower surface in the adhesive layer:

Z-coordinate(m)	Value(kPa)
0.00e+000	1.84e-015
5.00e-001	-3.59e+000
1.00e+000	-5.52e+000
1.50e+000	-6.57e+000
2.00e+000	-7.14e+000
2.50e+000	-7.45e+000
3.00e+000	-7.62e+000
3.50e+000	-7.72e+000
4.00e+000	-7.80e+000
4.50e+000	-7.87e+000
5.00e+000	-8.02e+000

****
****

B3.3.2 Problem 4- Twisting about the beam centroid

CASE NUMBER 15:

Finite Element Solution-1 element solution:

Nodal displacement vector at tip:

Delta =

.12294557880010806162779648111109e-2+.12309777276324320453196909989085e-19*i

```
 .27650310765621862350822901203337e-3+.72200367229563056689316141653517e-18*i
-.11241700426034599326267551472065e-1-.19632737288808860197253328728909e-18*i
-.25282447189032823294953659454420e-2-.66474095690903120495460598600246e-17*i
-.56804376345647978161134190769317e-1-.14309052284756047962855564949950e-29*i
-.14019922326351629088993934285957e-1+.45962028737444962140249507677004e-17*i

Closed form solution:
-------------------------------------------
Lateral deflection at beam centroid:
Z-coordinate(m)          Value(m)
0.00e+000                 8.50e-019
5.00e-001                 3.71e-005
1.00e+000                 1.24e-004
1.50e+000                 2.38e-004
2.00e+000                 3.67e-004
2.50e+000                 5.04e-004
3.00e+000                 6.45e-004
3.50e+000                 7.89e-004
4.00e+000                 9.35e-004
4.50e+000                 1.08e-003
5.00e+000                 1.23e-003
----------------------------------------------------------
Lateral deflection at GFRP plate centroid:
Z-coordinate(m)          Value(m)
0.00e+000                 3.54e-019
5.00e-001                -3.39e-004
1.00e+000                -1.14e-003
1.50e+000                -2.18e-003
2.00e+000                -3.36e-003
2.50e+000                -4.61e-003
3.00e+000                -5.90e-003
3.50e+000                -7.22e-003
4.00e+000                -8.55e-003
4.50e+000                -9.90e-003
5.00e+000                -1.12e-002
----------------------------------------------------------
Twisting angle:
Z-coordinate(m)          Value(Rad)
0.00e+000                -6.57e-019
5.00e-001                -1.70e-003
1.00e+000                -5.72e-003
1.50e+000                -1.10e-002
2.00e+000                -1.69e-002
2.50e+000                -2.32e-002
3.00e+000                -2.98e-002
3.50e+000                -3.64e-002
4.00e+000                -4.31e-002
4.50e+000                -4.99e-002
```

5.00e+000 -5.68e-002

Longitudinal normal stress S33 at the center point of left edge of the beam:

Z-coordinate(m)	Value(kPa)
0.00e+000	6.61e+004
5.00e-001	3.59e+004
1.00e+000	1.94e+004
1.50e+000	1.05e+004
2.00e+000	5.71e+003
2.50e+000	3.16e+003
3.00e+000	1.85e+003
3.50e+000	1.27e+003
4.00e+000	1.19e+003
4.50e+000	1.57e+003
5.00e+000	2.68e-012

Longitudinal normal stress S33 at the top point of left edge of GFRP plate:

Z-coordinate(m)	Value(kPa)
0.00e+000	-1.36e+004
5.00e-001	-6.44e+003
1.00e+000	-3.48e+003
1.50e+000	-1.88e+003
2.00e+000	-1.02e+003
2.50e+000	-5.67e+002
3.00e+000	-3.32e+002
3.50e+000	-2.28e+002
4.00e+000	-2.13e+002
4.50e+000	-2.93e+002
5.00e+000	5.00e-011

Shear stress gamma_nz in the adhesive layer at x=bp/2:

Z-coordinate(m)	Value(kPa)
0.00e+000	5.64e-011
5.00e-001	4.59e+003
1.00e+000	7.10e+003
1.50e+000	8.45e+003
2.00e+000	9.19e+003
2.50e+000	9.59e+003
3.00e+000	9.82e+003
3.50e+000	9.96e+003
4.00e+000	1.01e+004
4.50e+000	1.02e+004
5.00e+000	5.39e+003

Shear stress gamma_sn in the adhesive layer:

Z-coordinate(m)	Value(kPa)
0.00e+000	-5.46e-011
5.00e-001	-1.97e+002

```
1.00e+000                    -1.06e+002
1.50e+000                    -5.75e+001
2.00e+000                    -3.13e+001
2.50e+000                    -1.73e+001
3.00e+000                    -1.01e+001
3.50e+000                    -6.96e+000
4.00e+000                    -6.50e+000
4.50e+000                    -9.35e+000
5.00e+000                    5.16e+003
------------------------------------------------------------
Maximum shear gamma_sz at upper surface in the adhesive layer:
Z-coordinate(m)              Value(kPa)
0.00e+000                    -2.24e-014
5.00e-001                    4.71e+001
1.00e+000                    7.25e+001
1.50e+000                    8.62e+001
2.00e+000                    9.37e+001
2.50e+000                    9.78e+001
3.00e+000                    1.00e+002
3.50e+000                    1.02e+002
4.00e+000                    1.03e+002
4.50e+000                    1.04e+002
5.00e+000                    1.07e+002
------------------------------------------------------------
Maximum shear stress gamma_sz at lower surface in the adhesive layer:
Z-coordinate(m)              Value(kPa)
0.00e+000                    3.23e-014
5.00e-001                    -4.51e+001
1.00e+000                    -6.94e+001
1.50e+000                    -8.26e+001
2.00e+000                    -8.97e+001
2.50e+000                    -9.36e+001
3.00e+000                    -9.59e+001
3.50e+000                    -9.72e+001
4.00e+000                    -9.83e+001
4.50e+000                    -9.95e+001
5.00e+000                    -1.02e+002
------------------------------------------------------------
```

APPENDIX B4 – PROGRAMMING OF PROBLEM 1 IN CHAPTER 8

B4.1 Input data

In each case study, its parameters $L, b_b, b_p, t_1, t_2, h_b, t_3, t_w, G_a, E_a, E_b, E_p, \mu$ are inputted in to a column of cells in sheet 1 of a spreadsheet named `'data21august.xlsx'`. The starting cell of inputting data is in the 6^{th} row and thus the ending cell is in the 18^{th} row. Fourteen cases are inputted corresponding to fourteen columns from C to P. As a result, all parameters of the fourteen cases are listed in cells `'C6:P18'`. Values of the parameters as presented under the Statement of Problem 1 in Chapter 8 are inputted in the case 13^{th} (corresponding to the 13^{th} column of the total fourteen columns).

B4.2 Finite Difference Solution

B4.2.1 Programming in MATLAB

```
%---------------------------------------------------------------------------
%---------------------PROBLEM 1-SIMPLY SUPPORTED BEAM---------------------
%------------------------FINITE DIFFERENCE METHOD-------------------------
%-------------------------------------------------------------
% STEP1: Input data shown in a Spreadsheet file
%-------------------------------------------------------------
%Read data from spreadsheet file:
A=xlsread('data21august.xlsx',1,'C6:P18');
%Cases:
for k=13:13
  % k is column index of matrix A(13,10)
  disp(['CASE NUMBER ' num2str(k) ':']);
  disp('---------------')
  % Input Data for the case i:
        L=A(1,k);     % Length of member
        bb=A(2,k);    % Width of beam flanges
        bp=A(3,k);    % Width of GFRP plate and Adhesive layer
        t1=A(4,k);    % Thickness(m) of the GFRP plate
        t2=A(5,k);    % Thickness(m) of the adhesive layer
        hb=A(6,k);    % Effective height (m) of the beam
        t3=A(7,k);    % Thickness(m) of the flanges
        tw=A(8,k);    % Thickness(m) of the web
        Ga=A(9,k);    % Module of shear(kN/m2) of adhesive
        Ea=A(10,k);   % Module of elasticity (kN/m2) of adhesive
        Eb=A(11,k);   % Module of elasticity(kN/m2)of the beam
        Ep=A(12,k);   % Module of elasticity(kN/m2) of the GFRP
        Muy=A(13,k);  % Poisson ratio
  %-------------------------------------------------------------
  % STEP2: Calculation of section properties for the case i
  %-------------------------------------------------------------
```

```
% For wide flange beam
    % Geometrical properties:
    Ab=2*t3*bb+(hb-t3)*tw;
    Abf=t3*bb;
    Abw=(hb-t3)*tw;
    Iyy1=2*t3*(bb^3)/12;
    Ixxb1=tw*((hb-t3)^3)/12+2*bb*t3*(hb^2)/4;
    Iwwbg=(hb^2)*(bb^3)*t3/24;
    Issbw=(hb-t3)*(tw^3)/12;
    Issbf=2*bb*(t3^3)/12;
    Iwwbl=2*(bb^3)*(t3^3)/144+((hb-t3)^3)*(tw^3)/144;
    Jb=(bb*(t3^3)/3)*2+(hb-t3)*(tw^3)/3+(hb^2)*Abf/2;
    % Physical properties:
    Gb=Eb/(2*(1+Muy));
% For GFRP plate
    % Geometrical properties:
    Ap=t1*bp;
    Iyyp=t1*(bp^3)/12;
    Ixxp=bp*(t1^3)/12;
    Iwwp=(bp^3)*(t1^3)/144;
    Jp=bp*(t1^3)/3;
    % Physical properties:
    Gp=Ep/(2*(1+Muy));
% For Adhesive layer
Aa=t2*bb;
Iyya=t2*(bb^3)/12;
% Factors from c1 to c6:
c1=1/t2;
c2=(t1+2*t2+t3)/(2*t2);
c3=hb/(2*t2);
c4=hb-t1+2*t3;
c5=hb-4*t1+2*t3;
c6=hb^2+4*(t1^2)+4*(t3^2)-2*hb*t1+4*hb*t3-4*t1*t3;
%---------------------------------------------------------------
% STEP 3:  Finite differential codes
%---------------------------------------------------------------
% Input number of structural segments taken in to account:
 n=input('Input number of segments n=');
% Length of a segment (uniform length):
delta=L/n;
% Matrix M: Matrix of constant in the equilibrium equation system solved
% by finite differential method: M((n+1)*6+16,(n+1)*6+16);
%-------------------------------------------------------------------------
% Group of the first differential equations:
       %Expression for matrix of Wb in the first differential equations:
       Wb1=zeros(n+1,n+1+2);
        for i=1:(n+1)  % Number of specified points
            Wb1(i,i)=-Eb*Ab/(delta^2);   %Wb(i-1)
            Wb1(i,i+1)=2*Eb*Ab/(delta^2)+(c1^2)*Ga*Aa;   %Wb(i)
            Wb1(i,i+2)=-Eb*Ab/(delta^2);  %Wb(i+1)
        end
       %Expression for matrix of Wp in the first differential equations:
        Wp1=zeros(n+1,n+1+2);
        for i=1:(n+1)  % Number of specified points
            Wp1(i,i)=0;   %Wp(i-1)
            Wp1(i,i+1)=-(c1^2)*Ga*Aa;  %Wp(i)
            Wp1(i,i+2)=0;   %Wp(i+1)
```

```
          end
%Expression for matrix of V in the first differential equations:
          V1=zeros(n+1,n+1+4);
          for i=1:(n+1)  % Number of specified points
             V1(i,i)=0;  %V(i-2)
             V1(i,i+1)=-c1*c2*Ga*Aa/(2*delta);   %V(i-1)
             V1(i,i+2)=0;  %V(i)
             V1(i,i+3)=c1*c2*Ga*Aa/(2*delta);  %V(i+1)
             V1(i,i+4)=0;  %V(i+2)
          end
  %Expression for matrix of theta_bx in the first differential equations:
          Theta_bx1=zeros(n+1,n+1+2);
          for i=1:(n+1)  % Number of specified points
             Theta_bx1(i,i)=0;  %theta_bx(i-1)
             Theta_bx1(i,i+1)=c1*c3*Ga*Aa;   %theta_bx(i)
             Theta_bx1(i,i+2)=0;  %theta_bx(i+1)
          end
  % The first equilibrium equation expressed in all n+1 points:
  M1=[Wb1 Wp1 V1 Theta_bx1];
  %-----------------------------------------------------------------------
  % Group of the second differential equations:
         %Expression for matrix of Wb in the first differential equations:
         Wb2=zeros(n+1,n+1+2);
          for i=1:(n+1)  % Number of specified points
              Wb2(i,i)=0;   %Wb(i-1)
              Wb2(i,i+1)=-(c1^2)*Ga*Aa;   %Wb(i)
              Wb2(i,i+2)=0;  %Wb(i+1)
          end
         %Expression for matrix of Wp in the first differential equations:
          Wp2=zeros(n+1,n+1+2);
          for i=1:(n+1)  % Number of specified points
              Wp2(i,i)=-Ep*Ap/(delta^2);   %Wp(i-1)
              Wp2(i,i+1)=2*Ep*Ap/(delta^2)+(c1^2)*Ga*Aa;  %Wp(i)
              Wp2(i,i+2)=-Ep*Ap/(delta^2);   %Wp(i+1)
          end
          %Expression for matrix of V in the first differential equations:
          V2=zeros(n+1,n+1+4);
          for i=1:(n+1)  % Number of specified points
             V2(i,i)=0;  %V(i-2)
             V2(i,i+1)=c1*c2*Ga*Aa/(2*delta);   %V(i-1)
             V2(i,i+2)=0;  %V(i)
             V2(i,i+3)=-c1*c2*Ga*Aa/(2*delta);  %V(i+1)
             V2(i,i+4)=0;  %V(i+2)
          end
   %Expression for matrix of theta_bx in the first differential equations:
          Theta_bx2=zeros(n+1,n+1+2);
          for i=1:(n+1)  % Number of specified points
             Theta_bx2(i,i)=0;  %theta_bx(i-1)
             Theta_bx2(i,i+1)=-c1*c3*Ga*Aa;   %theta_bx(i)
             Theta_bx2(i,i+2)=0;  %theta_bx(i+1)
          end
  % The first equilibrium equation expressed in all n+1 points:
  M2=[Wb2 Wp2 V2 Theta_bx2];
  %-----------------------------------------------------------------------
  % Group of the third differential equations:
         %Expression for matrix of Wb in the first differential equations:
         Wb3=zeros(n+1,n+1+2);
```

```
          for i=1:(n+1)   % Number of specified points
              Wb3(i,i)=c1*c2*Ga*Aa/(2*delta);    %Wb(i-1)
              Wb3(i,i+1)=0;    %Wb(i)
              Wb3(i,i+2)=-c1*c2*Ga*Aa/(2*delta);  %Wb(i+1)
          end
         %Expression for matrix of Wp in the first differential equations:
          Wp3=zeros(n+1,n+1+2);
          for i=1:(n+1)   % Number of specified points
              Wp3(i,i)=-c1*c2*Ga*Aa/(2*delta);    %Wp(i-1)
              Wp3(i,i+1)=0;  %Wp(i)
              Wp3(i,i+2)=c1*c2*Ga*Aa/(2*delta);    %Wp(i+1)
          end
         %Expression for matrix of V in the first differential equations:
          V3=zeros(n+1,n+1+4);
          for i=1:(n+1)   % Number of specified points
             V3(i,i)=(Eb*Issbf+Ep*Ixxp)/(delta^4);  %V(i-2)
             V3(i,i+1)=-
(4*(Eb*Issbf+Ep*Ixxp)/(delta^4)+(Gb*Abw+(c2^2)*Ga*Aa)/(delta^2));    %V(i-
1)

V3(i,i+2)=6*(Eb*Issbf+Ep*Ixxp)/(delta^4)+2*(Gb*Abw+(c2^2)*Ga*Aa)/(delta^2)
;  %V(i)
             V3(i,i+3)=-
(4*(Eb*Issbf+Ep*Ixxp)/(delta^4)+(Gb*Abw+(c2^2)*Ga*Aa)/(delta^2));  %V(i+1)
             V3(i,i+4)=(Eb*Issbf+Ep*Ixxp)/(delta^4);  %V(i+2)
          end
   %Expression for matrix of theta_bx in the first differential equations:
          Theta_bx3=zeros(n+1,n+1+2);
          for i=1:(n+1)   % Number of specified points
             Theta_bx3(i,i)=-(Gb*Abw-c2*c3*Ga*Aa)/(2*delta);  %theta_bx(i-
1)
             Theta_bx3(i,i+1)=0;   %theta_bx(i)
             Theta_bx3(i,i+2)=(Gb*Abw-c2*c3*Ga*Aa)/(2*delta);
%theta_bx(i+1)
          end
  % The first equilibrium equation expressed in all n+1 points:
  M3=[Wb3 Wp3 V3 Theta_bx3];
%-------------------------------------------------------------------------
  % Group of the fourth differential equations:
         %Expression for matrix of Wb in the first differential equations:
         Wb4=zeros(n+1,n+1+2);
          for i=1:(n+1)   % Number of specified points
              Wb4(i,i)=0;    %Wb(i-1)
              Wb4(i,i+1)=c1*c3*Ga*Aa;    %Wb(i)
              Wb4(i,i+2)=0;   %Wb(i+1)
          end
         %Expression for matrix of Wp in the first differential equations:
          Wp4=zeros(n+1,n+1+2);
          for i=1:(n+1)   % Number of specified points
              Wp4(i,i)=0;    %Wp(i-1)
              Wp4(i,i+1)=-c1*c3*Ga*Aa;   %Wp(i)
              Wp4(i,i+2)=0;    %Wp(i+1)
          end
         %Expression for matrix of V in the first differential equations:
          V4=zeros(n+1,n+1+4);
          for i=1:(n+1)   % Number of specified points
             V4(i,i)=0;   %V(i-2)
```

```
            V4(i,i+1)=-(c2*c3*Ga*Aa-Gb*Abw)/(2*delta);   %V(i-1)
            V4(i,i+2)=0;  %V(i)
            V4(i,i+3)=(c2*c3*Ga*Aa-Gb*Abw)/(2*delta);  %V(i+1)
            V4(i,i+4)=0;  %V(i+2)
         end
   %Expression for matrix of theta_bx in the first differential equations:
         Theta_bx4=zeros(n+1,n+1+2);
         for i=1:(n+1)  % Number of specified points
            Theta_bx4(i,i)=-Eb*Ixxb1/(delta^2);  %theta_bx(i-1)
            Theta_bx4(i,i+1)=2*Eb*Ixxb1/(delta^2)+Gb*Abw+(c3^2)*Ga*Aa;
%theta_bx(i)
            Theta_bx4(i,i+2)=-Eb*Ixxb1/(delta^2);  %theta_bx(i+1)
         end
  % The first equilibrium equation expressed in all n+1 points:
  M4=[Wb4 Wp4 V4 Theta_bx4];
 %-----------------------------------------------------------------------
 %-----------------------------------------------------------------------
  % Boundary condition 1: Wb=0 at fixed end z=0:
  Wb5=zeros(1,n+1+2);
          Wb5(1,2)=1;
  Wp5=zeros(1,n+1+2);
  V5=zeros(1,n+1+4);
  Theta_bx5=zeros(1,n+1+2);
  % The 1st boundary condtion expressed in all n+1 points:
  M5=[Wb5 Wp5 V5 Theta_bx5];
  %----------------------------------------------------------------------
  % Boundary condition 2: W'b=0 at free end z=L:
  Wb6=zeros(1,n+1+2);
          Wb6(1,n+1)=-Eb*Ab/(2*delta);
          Wb6(1,n+1+2)=Eb*Ab/(2*delta);
  Wp6=zeros(1,n+1+2);
  V6=zeros(1,n+1+4);
  Theta_bx6=zeros(1,n+1+2);
  % The 2nd boundary condtion expressed in all n+1 points:
  M6=[Wb6 Wp6 V6 Theta_bx6];
%-----------------------------------------------------------------------
  % Boundary condition 3: W'p=0 at z=0:
  Wb7=zeros(1,n+1+2);
  Wp7=zeros(1,n+1+2);
              Wp7(1,1)=-Ep*Ap/(2*delta);
              Wp7(1,3)=Ep*Ap/(2*delta);
  V7=zeros(1,n+1+4);
  Theta_bx7=zeros(1,n+1+2);
  % The 3rd boundary condtion expressed in all n+1 points:
  M7=[Wb7 Wp7 V7 Theta_bx7];
%-----------------------------------------------------------------------
  % Boundary condition 4: W'p=0 at  z=L:
  Wb8=zeros(1,n+1+2);
  Wp8=zeros(1,n+1+2);
            Wp8(1,n+1)=-Ep*Ap/(2*delta);
            Wp8(1,n+1+2)=Ep*Ap/(2*delta);
  V8=zeros(1,n+1+4);
  Theta_bx8=zeros(1,n+1+2);
  % The 4th boundary condtion expressed in all n+1 points:
  M8=[Wb8 Wp8 V8 Theta_bx8];
 %-----------------------------------------------------------------------
   % Boundary condition 5: V=0 at z=0:
```

```
  Wb9=zeros(1,n+1+2);
  Wp9=zeros(1,n+1+2);
  V9=zeros(1,n+1+4);
       V9(1,3)=1;
  Theta_bx9=zeros(1,n+1+2);
  % The 5th boundary condtion expressed in all n+1 points:
  M9=[Wb9 Wp9 V9 Theta_bx9];
%------------------------------------------------------------------------
  % Boundary condition 6: V= at z=L:
  Wb10=zeros(1,n+1+2);
  Wp10=zeros(1,n+1+2);
  V10=zeros(1,n+1+4);
          V10(1,n+1+2)=1;  %V(i)
  Theta_bx10=zeros(1,n+1+2);
  % The 6th boundary condtion expressed in all n+1 points:
  M10=[Wb10 Wp10 V10 Theta_bx10];
%------------------------------------------------------------------------
   % Boundary condition 7: V''=0 at fixed end z=0:
  Wb11=zeros(1,n+1+2);
  Wp11=zeros(1,n+1+2);
  V11=zeros(1,n+1+4);
       V11(1,2)=1;
       V11(1,3)=-2;
       V11(1,4)=1;
  Theta_bx11=zeros(1,n+1+2);
  % The 7th boundary condtion expressed in all n+1 points:
  M11=[Wb11 Wp11 V11 Theta_bx11];
%------------------------------------------------------------------------
   % Boundary condition 8: V''=0 at free end z=L:
  Wb12=zeros(1,n+1+2);
  Wp12=zeros(1,n+1+2);
  V12=zeros(1,n+1+4);
        V12(1,n+1+1)=1;
        V12(1,n+1+2)=-2;
        V12(1,n+1+3)=1;
  Theta_bx12=zeros(1,n+1+2);
  % The 8th boundary condtion expressed in all n+1 points:
  M12=[Wb12 Wp12 V12 Theta_bx12];
%------------------------------------------------------------------------
   % Boundary condition 9: theta_bx'=0 at fixed end z=0:
  Wb13=zeros(1,n+1+2);
  Wp13=zeros(1,n+1+2);
  V13=zeros(1,n+1+4);
  Theta_bx13=zeros(1,n+1+2);
         Theta_bx13(1,1)=-1;
         Theta_bx13(1,3)=1;
  % The 9th boundary condtion expressed in all n+1 points:
  M13=[Wb13 Wp13 V13 Theta_bx13];
%------------------------------------------------------------------------
   % Boundary condition 10: theta_bx'=0 at free end z=L:
  Wb14=zeros(1,n+1+2);
  Wp14=zeros(1,n+1+2);
  V14=zeros(1,n+1+4);
  Theta_bx14=zeros(1,n+1+2);
       Theta_bx14(1,n+1)=-1;
       Theta_bx14(1,n+1+2)=1;
  % The 10th boundary condtion expressed in all n+1 points:
```

```
  M14=[Wb14 Wp14 V14 Theta_bx14];
%----------------------------------------------------------------------------
%----------------------------------------------------------------------------
  % STEP3: Grouping all Equilibrium Eqs. and Boundary Condition Eqs. in to
  % the matrix M:
%----------------------------------------------------------------------------
-
M=[M1; M2; M3; M4; M5; M6; M7; M8; M9; M10; M11; M12; M13; M14;];
%----------------------------------------------------------------------------
  % STEP4: Obtaining displacement fields
%----------------------------------------------------------------------------
% Inversing matrix M:
Inverse_M=inv(M);
% Load matrix:
q=-45/L;
Load_EquilEqs2=zeros(4*(n+1),1);
for i=1:(n+1)
    Load_EquilEqs2(2*(n+1)+i,1)=q;
end
Load_BC1=0;Load_BC2=0;Load_BC3=0;Load_BC4=0;Load_BC5=0;
Load_BC6=0;Load_BC7=0;Load_BC8=0;Load_BC9=0;Load_BC10=0;
Load=[Load_EquilEqs2; Load_BC1;
Load_BC2;Load_BC3;Load_BC4;Load_BC5;Load_BC6;Load_BC7;Load_BC8;Load_BC9;Lo
ad_BC10;];
% Displacement fields:
Displacement_Field=M\Load;
%disp('Displacement Wb at free end:');
%Wb_at_free_end=Displacement_Field(n+1+1,1)
%disp('Displacement Wp at free end:');
%Wp_at_free_end=Displacement_Field(2*(n+1)+3,1)
%disp('Displacement V at free end:');
%V_at_free_end=Displacement_Field(2*(n+1)+6+n/2+1,1)
%disp('Slope Theta_bx at free end:');
%Theta_bx_at_tip=Displacement_Field(4*(n+1)+9,1)
%----------------------------------------------------------------------------
   % STEP5: Stress fields
%----------------------------------------------------------------------------
% Obtaining 4 displacement matrices:
% Matrix of displacement Wb:
Matrix_Wb=zeros(n+1+2,1);
for i=1:(n+1+2)
Matrix_Wb(i,1)=Displacement_Field(i,1);
end
% Matrix of displacement Wp:
Matrix_Wp=zeros(n+1+2,1);
for i=1:(n+1+2)
Matrix_Wp(i,1)=Displacement_Field(n+1+2+i,1);
end
% Matrix of displacement V:
Matrix_V=zeros(n+1+4,1);
for i=1:(n+1+4)
Matrix_V(i,1)=Displacement_Field((n+1+2)*2+i,1);
end
%----------------------------------------------------------------------------
Matrix_V_showed=zeros(11,1);
coordinate_zb=zeros(11,1);
     Matrix_V_showed(1,1)=Matrix_V(3,1);
```

```
     coordinate_zb(1,1)=0;
for i=1:9
     Matrix_V_showed(i+1,1)=Matrix_V((round(n*i/10)+3),1);
     coordinate_zb(i+1,1)=(round(n*i/10))*(L/n);
end
     Matrix_V_showed(11,1)=Matrix_V(n+1+2,1);
     coordinate_zb(11,1)=L;
% Display results on screen:
   fprintf('Z-coordinate(m) \t Value(m) \r');
   for i=1:11
       fprintf('%3.2e\t\t\t %3.2e\t\t\t\n', coordinate_zb(i,1),
Matrix_V_showed(i,1));
   end
disp('-----------------------------------------------------------------');
% Write to a spreadsheet:
Nameofstress={'displacement_V:'};
coordinate_z_in_length={'Z_coord'};
value={'Value'};
xlswrite('new_theory_inplane_simply_supported_beam.xlsx',Nameofstress,k,'b
3');
xlswrite('new_theory_inplane_simply_supported_beam.xlsx',coordinate_z_in_l
ength,k,'b4');
xlswrite('new_theory_inplane_simply_supported_beam.xlsx',value,k,'c4');
xlswrite('new_theory_inplane_simply_supported_beam.xlsx',coordinate_zb,k,'
b5:b15');
xlswrite('new_theory_inplane_simply_supported_beam.xlsx',Matrix_V_showed,k
,'c5:c15');
%-------------------------------------------------------------------------
% Matrix of displacement theta_xb:
Matrix_theta_xb=zeros(n+1+2,1);
for i=1:(n+1+2)
Matrix_theta_xb(i,1)=Displacement_Field((n+1+2)*2+(n+1+4)+i,1);
end
%-------------------------------------------------------------------------
% Normal strain vector at the bottom surface of the steel beam:
epsilon_zb_bottom=zeros(n+1+2,1);
for i=2:(n+2)
epsilon_zb_bottom(i,1)=(-Matrix_Wb(i-1,1)+Matrix_Wb(i+1,1))/(2*delta)-
(t3/(2*(delta^2)))*(Matrix_V(i,1)-2*Matrix_V(i+1,1)+Matrix_V(i+2,1))-
(hb/(4*delta))*(-Matrix_theta_xb(i-1,1)+Matrix_theta_xb(i+1,1));
end
% Showing the normal strain vector above in a 10x1 sided matrix:
epsilon_zb_bottom_showed=zeros(11,1);
coordinate_zb=zeros(11,1);
     epsilon_zb_bottom_showed(1,1)=epsilon_zb_bottom(2,1);
     coordinate_zb(1,1)=0;
for i=1:9

epsilon_zb_bottom_showed(i+1,1)=epsilon_zb_bottom((round(n*i/10)+2),1);
     coordinate_zb(i+1,1)=(round(n*i/10))*(L/n);
end
     epsilon_zb_bottom_showed(11,1)=epsilon_zb_bottom(n+1+1,1);
     coordinate_zb(11,1)=L;
% Normal stress vector at the bottom surface of the steel beam:
normal_stress_zb_bottom=zeros(11,1);
for i=1:11
    normal_stress_zb_bottom(i,1)=Eb*epsilon_zb_bottom_showed(i,1);
```

```
end
disp('normal_stress_zb_bottom:');
% Display results on screen:
   fprintf('Z-coordinate(m) \t Value(kPa) \r');
   for i=1:11
       fprintf('%3.2e\t\t\t %3.2e\t\t\t\n', coordinate_zb(i,1),
normal_stress_zb_bottom(i,1));
   end
disp('-----------------------------------------------------------------');
% Write to a spreadsheet:
Nameofstress={'normal_stress_zb_bottom:'};
coordinate_z_in_length={'Z_coord'};
value={'Value'};
xlswrite('new_theory_inplane_simply_supported_beam.xlsx',Nameofstress,k,'e
3');
xlswrite('new_theory_inplane_simply_supported_beam.xlsx',coordinate_z_in_l
ength,k,'e4');
xlswrite('new_theory_inplane_simply_supported_beam.xlsx',value,k,'f4');
xlswrite('new_theory_inplane_simply_supported_beam.xlsx',coordinate_zb,k,'
e5:e15');
xlswrite('new_theory_inplane_simply_supported_beam.xlsx',normal_stress_zb_
bottom,k,'f5:f15');
%-------------------------------------------------------------------------
%-------------------------------------------------------------------------
% Normal strain vector at the top surface of the steel beam:
epsilon_zb_top=zeros(n+1+2,1);
for i=2:(n+2)
epsilon_zb_top(i,1)=(-Matrix_Wb(i-
1,1)+Matrix_Wb(i+1,1))/(2*delta)+(t3/(2*(delta^2)))*(Matrix_V(i,1)-
2*Matrix_V(i+1,1)+Matrix_V(i+2,1))+(hb/(4*delta))*(-Matrix_theta_xb(i-
1,1)+Matrix_theta_xb(i+1,1));
end
% Showing the normal strain vector above in a 10x1 sided matrix:
epsilon_zb_top_showed=zeros(11,1);
coordinate_zb=zeros(11,1);
     epsilon_zb_top_showed(1,1)=epsilon_zb_top(2,1);
     coordinate_zb(1,1)=0;
for i=1:9
     epsilon_zb_top_showed(i+1,1)=epsilon_zb_top((round(n*i/10)+2),1);
     coordinate_zb(i+1,1)=(round(n*i/10))*(L/n);
end
     epsilon_zb_top_showed(11,1)=epsilon_zb_top(n+1+1,1);
     coordinate_zb(11,1)=L;
% Normal stress vector at the bottom surface of the steel beam:
normal_stress_zb_top=zeros(11,1);
for i=1:11
    normal_stress_zb_top(i,1)=Eb*epsilon_zb_top_showed(i,1);
end
disp('normal_stress_zb_top=');
% Display results on screen:
   fprintf('Z-coordinate(m) \t Value(kPa) \r');
   for i=1:11
       fprintf('%3.2e\t\t\t %3.2e\t\t\t\n', coordinate_zb(i,1),
normal_stress_zb_top(i,1));
   end
disp('-----------------------------------------------------------------');
% Write to a spreadsheet:
```

```
Nameofstress={'normal_stress_zb_top:'};
coordinate_z_in_length={'Z_coord'};
value={'Value'};
xlswrite('new_theory_inplane_simply_supported_beam.xlsx',Nameofstress,k,'h
3');
xlswrite('new_theory_inplane_simply_supported_beam.xlsx',coordinate_z_in_l
ength,k,'h4');
xlswrite('new_theory_inplane_simply_supported_beam.xlsx',value,k,'i4');
xlswrite('new_theory_inplane_simply_supported_beam.xlsx',coordinate_zb,k,'
h5:h15');
xlswrite('new_theory_inplane_simply_supported_beam.xlsx',normal_stress_zb_
top,k,'i5:i15');
%--------------------------------------------------------------------------
% Normal strain vector at the top surface of the GFRP plate:
epsilon_zp_top=zeros(n+1+2,1);
for i=2:(n+2)
epsilon_zp_top(i,1)=(1/(2*delta))*(-Matrix_Wp(i-
1,1)+Matrix_Wp(i+1,1))+(t1/(2*(delta^2)))*(Matrix_V(i,1)-
2*Matrix_V(i+1,1)+Matrix_V(i+2,1));
end
% Showing the normal strain vector above in a 10x1 sided matrix:
epsilon_zp_top_showed=zeros(11,1);
coordinate_zp=zeros(11,1);
     epsilon_zp_top_showed(1,1)=epsilon_zp_top(2,1);
     coordinate_zp(1,1)=0;
for i=1:9
     epsilon_zp_top_showed(i+1,1)=epsilon_zp_top((round(n*i/10)+2),1);
     coordinate_zp(i+1,1)=(round(n*i/10))*(L/n);
end
     epsilon_zp_top_showed(11,1)=epsilon_zp_top(n+1+1,1);
     coordinate_zp(11,1)=L;
% Normal stress vector at the bottom surface of the steel beam:
normal_stress_zp_top=zeros(11,1);
for i=1:11
    normal_stress_zp_top(i,1)=Ep*epsilon_zp_top_showed(i,1);
end
disp('normal_stress_zp_top:');
% Display results on screen:
   fprintf('Z-coordinate(m) \t Value(kPa) \r');
   for i=1:11
       fprintf('%3.2e\t\t\t %3.2e\t\t\t\n', coordinate_zb(i,1),
normal_stress_zp_top(i,1));
   end
disp('------------------------------------------------------------');
% Write to a spreadsheet:
Nameofstress={'normal_stress_zp_top:'};
coordinate_z_in_length={'Z_coord'};
value={'Value'};
xlswrite('new_theory_inplane_simply_supported_beam.xlsx',Nameofstress,k,'k
3');
xlswrite('new_theory_inplane_simply_supported_beam.xlsx',coordinate_z_in_l
ength,k,'k4');
xlswrite('new_theory_inplane_simply_supported_beam.xlsx',value,k,'L4');
xlswrite('new_theory_inplane_simply_supported_beam.xlsx',coordinate_zp,k,'
k5:k15');
xlswrite('new_theory_inplane_simply_supported_beam.xlsx',normal_stress_zp_
top,k,'L5:L15');
```

```
%----------------------------------------------------------------------------
% Shear stress gamma_zna within the adhesive layer:
gamma_zna=zeros(n+1+2,1);
for i=2:(n+2)
gamma_zna(i,1)=-c1*Matrix_Wb(i,1)+c1*Matrix_Wp(i,1)-(c2/(2*delta))*(-
Matrix_V(i,1)+Matrix_V(i+2,1))-c3*Matrix_theta_xb(i,1);
end
% Showing the normal strain vector above in a 10x1 sided matrix:
gamma_zna_showed=zeros(11,1);
coordinate_zna=zeros(11,1);
     gamma_zna_showed(1,1)=gamma_zna(2,1);
     coordinate_zp(1,1)=0;
for i=1:9
     gamma_zna_showed(i+1,1)=gamma_zna((round(n*i/10)+2),1);
     coordinate_zna(i+1,1)=(round(n*i/10))*(L/n);
end
     gamma_zna_showed(11,1)=gamma_zna(n+1+1,1);
     coordinate_zna(11,1)=L;
% Normal stress vector at the bottom surface of the steel beam:
shear_stress_zna=zeros(11,1);
for i=1:11
    shear_stress_zna(i,1)=Ga*gamma_zna_showed(i,1);
end
disp('shear_stress_zna=');
% Display results on screen:
   fprintf('Z-coordinate(m) \t Value(kPa) \r');
   for i=1:11
       fprintf('%3.2e\t\t\t %3.2e\t\t\t\n', coordinate_zb(i,1),
shear_stress_zna(i,1));
   end
disp('-----------------------------------------------------------------');
% Write to a spreadsheet:
Nameofstress={'shear_stress_zna:'};
coordinate_z_in_length={'Z_coord'};
value={'Value'};
xlswrite('new_theory_inplane_simply_supported_beam.xlsx',Nameofstress,k,'N
3');
xlswrite('new_theory_inplane_simply_supported_beam.xlsx',coordinate_z_in_l
ength,k,'N4');
xlswrite('new_theory_inplane_simply_supported_beam.xlsx',value,k,'O4');
xlswrite('new_theory_inplane_simply_supported_beam.xlsx',coordinate_zna,k,
'N5:N15');
xlswrite('new_theory_inplane_simply_supported_beam.xlsx',shear_stress_zna,
k,'O5:O15');
%----------------------------------------------------------------------------
end
%----------------------------------------------------------------------------
%------------------END OF FINITE DIFFERENCE SOLUTION-----------------------
%----------------------------------------------------------------------------
```

B4.2.2 Outputs of the Finite Element Solution

CASE NUMBER 13:

Input number of segments n=400

Transverse displacement:

Z-coordinate(m)	Value(m)
0.00e+000	8.36e-011
3.00e-001	-3.14e-003
6.00e-001	-5.92e-003
9.00e-001	-8.09e-003
1.20e+000	-9.47e-003
1.50e+000	-9.94e-003
1.80e+000	-9.47e-003
2.10e+000	-8.09e-003
2.40e+000	-5.92e-003
2.70e+000	-3.14e-003
3.00e+000	4.26e-016

----

normal_stress_zb_bottom:

Z-coordinate(m)	Value(kPa)
0.00e+000	-2.77e-001
3.00e-001	-6.72e+004
6.00e-001	-1.19e+005
9.00e-001	-1.57e+005
1.20e+000	-1.79e+005
1.50e+000	-1.86e+005
1.80e+000	-1.79e+005
2.10e+000	-1.57e+005
2.40e+000	-1.19e+005
2.70e+000	-6.72e+004
3.00e+000	1.03e-005

----

normal_stress_zb_top:

Z-coordinate(m)	Value(kPa)
0.00e+000	2.77e-001
3.00e-001	4.19e+004
6.00e-001	7.45e+004
9.00e-001	9.79e+004
1.20e+000	1.12e+005
1.50e+000	1.17e+005
1.80e+000	1.12e+005
2.10e+000	9.79e+004
2.40e+000	7.45e+004
2.70e+000	4.19e+004
3.00e+000	-1.02e-005

----

normal_stress_zp_top:

Z-coordinate(m)	Value(kPa)
0.00e+000	1.87e-001
3.00e-001	1.21e+004
6.00e-001	2.13e+004
9.00e-001	2.79e+004
1.20e+000	3.19e+004
1.50e+000	3.32e+004
1.80e+000	3.19e+004

```
2.10e+000                    2.79e+004
2.40e+000                    2.13e+004
2.70e+000                    1.21e+004
3.00e+000                    -8.34e-006
------------------------------------------------------------------
shear_stress_zna:
Z-coordinate(m)              Value(kPa)
0.00e+000                    7.62e+002
3.00e-001                    5.86e+002
6.00e-001                    4.39e+002
9.00e-001                    2.93e+002
1.20e+000                    1.46e+002
1.50e+000                    -6.16e-005
1.80e+000                    -1.46e+002
2.10e+000                    -2.93e+002
2.40e+000                    -4.39e+002
2.70e+000                    -5.86e+002
3.00e+000                    -7.62e+002
------------------------------------------------------------------
>>
```

B4.3 Finite Element Solution

B4.3.1 Programming in MATLAB

```
%----------------------------------------------------------------------------
-
%---------------------PROBLEM 1-SIMPLY SUPPORTED BEAM---------------------
-
%-------------------------FINITE ELEMENT SOLUTION-------------------------
-
%--------------------------------------------------------------
% STEP1: Input data shown in a Spreadsheet file
%--------------------------------------------------------------
%Read data from spreadsheet file:
A=xlsread('data21august.xlsx',1,'C6:O18');
%Cases:
for k=13:13
  % k is column index of matrix A(13,10)
  disp(['CASE NUMBER ' num2str(k) ':']);
  disp('---------------')
  % Input Data for the case i:
        Ltotal=A(1,k);    % Length of member
        bb=A(2,k);    % Width of beam flanges
        bp=A(3,k);    % Width of GFRP plate and Adhesive layer
        t1=A(4,k);    % Thickness(m) of the GFRP plate
        t2=A(5,k);    % Thickness(m) of the adhesive layer
        hb=A(6,k);    % Effective height (m) of the beam
        t3=A(7,k);    % Thickness(m) of the flanges
        tw=A(8,k);    % Thickness(m) of the web
        Ga=A(9,k);    % Module of shear(kN/m2) of adhesive
        Ea=A(10,k);   % Module of elasticity (kN/m2) of adhesive
        Eb=A(11,k);   % Module of elasticity(kN/m2)of the beam
        Ep=A(12,k);   % Module of elasticity(kN/m2) of the GFRP
        Muy=A(13,k);  % Poisson ratio
  %--------------------------------------------------------------
  % STEP2: Calculation of section properties for the case i
  %--------------------------------------------------------------
  % For wide flange beam
      % Geometrical properties:
      Ab=2*t3*bb+(hb-t3)*tw;
      Abf=t3*bb;
      Abw=(hb-t3)*tw;
      Iyybf=2*t3*(bb^3)/12;
      Ixxb1=tw*((hb-t3)^3)/12+2*bb*t3*(hb^2)/4;
      Iwwbg=(hb^2)*(bb^3)*t3/24;
      Issbw=(hb-t3)*(tw^3)/12;
      Iyyb=Iyybf+Issbw;
      Issbf=2*bb*(t3^3)/12;
      Iwwbl=2*(bb^3)*(t3^3)/144+((hb-t3)^3)*(tw^3)/144;
      Jb=(bb*(t3^3)/3)*2+(hb-t3)*(tw^3)/3+(hb^2)*Abf/2;
      % Physical properties:
      Gb=Eb/(2*(1+Muy));
  % For GFRP plate:
      % Geometrical properties:
      Ap=t1*bp;
```

```
      Iyyp=t1*(bp^3)/12;
      Ixxp=bp*(t1^3)/12;
      Iwwp=(bp^3)*(t1^3)/144;
      Jp=bp*(t1^3)/3;
      % Physical properties:
      Gp=Ep/(2*(1+Muy));
  % For Adhesive layer:
  Aa=t2*bb;
  Iyya=t2*(bb^3)/12;
  % Factors from c1 to c6:
  c1=1/t2;
  c2=(t1+2*t2+t3)/(2*t2);
  c3=hb/(2*t2);
  c4=hb-t1+2*t3;
  c5=hb-4*t1+2*t3;
  c6=hb^2+4*(t1^2)+4*(t3^2)-2*hb*t1+4*hb*t3-4*t1*t3;
  %--------------------------------------------------------------
  % STEP 3:  Stiffness matrix
  %--------------------------------------------------------------
  n=input('Input number of segments n=');
  L=Ltotal/n;
  % element stiffness matrices:
  K1bar=(1/(L^3))*[12 6*L -12 6*L; 6*L 4*(L^2) -6*L 2*(L^2); -12 -6*L 12 -
6*L; 6*L 2*(L^2) -6*L 4*(L^2)];   %4x4
  K2bar=(1/(30*L))*[36 3*L -36 3*L; 3*L 4*(L^2) -3*L -(L^2); -36 -3*L 36 -
3*L; 3*L -(L^2) -3*L 4*(L^2)];      %4x4
  K3bar=(1/420)*[156*L 22*(L^2) 54*L -13*(L^2); 22*(L^2) 4*(L^3) 13*(L^2)
-3*(L^3); 54*L 13*(L^2) 156*L -22*(L^2); -13*(L^2) -3*(L^3) -22*(L^2)
4*(L^3)];  %4x4
  K4bar=(1/12)*[-6 L 6 -L; -6 -L 6 L];  %2x4
  K8bar=(1/L)*[1 0 -1 0; -1 0 1 0];    % 2x4
  K9bar=(L/60)*[21 3*L 9 -2*L; 9 2*L 21 -3*L]; %2x4
  K5bar=(L/6)*[2 1; 1 2];    %2x2
  K6bar=(1/2)*[-1 1; -1 1];  %2x2
  K7bar=(1/L)*[1 -1; -1 1];  %2x2
  % Stiffness elements in the global stifness matrix
  K1=Eb*Ab*K7bar/2+(c1^2)*Ga*Aa*K5bar/2;  %2x2
  K2=Ep*Ap*K7bar/2+(c1^2)*Ga*Aa*K5bar/2;   %2x2
  K3=(Eb*Issbf+Ep*Ixxp)*K1bar/2+(Gb*Abw+(c2^2)*Ga*Aa)*K2bar/2;     %2x2
  K4=Eb*Ixxb1*K7bar/2+(Gb*Abw+(c3^2)*Ga*Aa)*K5bar/2;  %2x2
  K5=-(c1^2)*Ga*Aa*K5bar; %4x4
  K6=c1*c3*Ga*Aa*K5bar;  %2x2
  K7=c1*c2*Ga*Aa*K4bar;  %2x4
  K8=-c1*c3*Ga*Aa*K5bar;   %2x4
  K9=-c1*c2*Ga*Aa*K4bar;  %2x4
  K10=(c2*c3*Ga*Aa-Gb*Abw)*K4bar;  %2x4
  % GLOBAL STIFFNESS MATRIX [K]:
  K=[2*K1 K5 K7 K6; K5' 2*K2 K9 K8; K7' K9' 2*K3 K10'; K6' K8' K10 2*K4];
  %Change position of rows:
  Kg1=zeros(10,10);
  for j=1:10
          Kg1(1,j)=K(1,j);  %row 1
          Kg1(2,j)=K(3,j);   %row 2
          Kg1(3,j)=K(5,j);   %row 3
          Kg1(4,j)=K(6,j);  %row 4
          Kg1(5,j)=K(9,j);   %row 5
          Kg1(6,j)=K(2,j);   %row 6
```

```
        Kg1(7,j)=K(4,j);  %row 7
        Kg1(8,j)=K(7,j);   %row 8
        Kg1(9,j)=K(8,j);   %row 9
        Kg1(10,j)=K(10,j);  %row 10
end
% Change position of rows and columns:
Kg=zeros(10,10);
for u=1:10
        Kg(u,1)=Kg1(u,1);  %column 1       Wb(0)
        Kg(u,2)=Kg1(u,3);   %column 2      Wp(0)
        Kg(u,3)=Kg1(u,5);   %column 3      V(0)
        Kg(u,4)=Kg1(u,6);  %column 4       V'(0)
        Kg(u,5)=Kg1(u,9);   %column 5      theta_xb(0)
        Kg(u,6)=Kg1(u,2);   %column 6      Wb(L)
        Kg(u,7)=Kg1(u,4);  %column 7       Wp(L)
        Kg(u,8)=Kg1(u,7);   %column 8      V(L))
        Kg(u,9)=Kg1(u,8);   %column 9      v'(L))
        Kg(u,10)=Kg1(u,10);  %column 10    theta_xb(L)
end
KG11=zeros(5,5);
for j=1:5
    for u=1:5
        KG11(j,u)=Kg(j,u);
    end
end
  KG22=zeros(5,5);
for j=1:5
    for u=1:5
        KG22(j,u)=Kg(j+5,u+5);
    end
end
  KG12=zeros(5,5);
for j=1:5
    for u=1:5
        KG12(j,u)=Kg(j,u+5);
    end
end
  KG21=zeros(5,5);
for j=1:5
    for u=1:5
        KG21(j,u)=Kg(j+5,u);
    end
end

%**************************************************************************
  % STEP 4: ESTABLISH THE GLOBAL STIFFNESS MATRIX

%**************************************************************************
  Klocal=[(KG11+KG22) KG12; KG21 (KG11+KG22)];
  %if n==1
   %   Kglobal=zeros(8,8);
    %  for j=1:8
     %     for u=1:8
      %        Kglobal(j,u)=KG22(j,u);
       %   end
     % end
  %else
```

```
    Kglobal1=zeros(n*5,n*5);
    for j=1:10
        for u=1:10
            Kglobal1(j,u)=Klocal(j,u);
        end
    end
    for j=6:5:(n*5-4)
        for u=j:(j+9)
            for p=j:(j+9)
                Kglobal1(u,p)=Kglobal1(u-5,p-5);
            end
        end
    end
    for j=(n*5-4):(n*5)
        for u=(n*5-4):(n*5)
            Kglobal1(j,u)=KG22(j-(n*5-4)+1,u-(n*5-4)+1);
        end
    end
    Kglobal=zeros(5*(n+1),5*(n+1));
    for j=1:5
        for u=1:5
            Kglobal(j,u)=KG11(j,u);
        end
    end
    for j=1:5
        for u=1:5
            Kglobal(j+5,u)=KG21(j,u);
        end
    end
    for j=1:5
        for u=1:5
            Kglobal(j,u+5)=KG12(j,u);
        end
    end
    for j=1:(5*n)
        for p=1:(5*n)
            Kglobal(j+5,p+5)=Kglobal1(j,p);
        end
    end
    Kglobalsmall_1=zeros(5*(n+1)-3,5*(n+1));
    for i=1:(5*(n+1))
        Kglobalsmall_1(1,i)=Kglobal(2,i);
    end
    for i=4:(5*(n+1)-3)
        for j=1:(5*(n+1))
            Kglobalsmall_1(i-2,j)=Kglobal(i,j);
        end
    end
    for i=(5*(n+1)-1):(5*(n+1))
        for j=1:(5*(n+1))
            Kglobalsmall_1(i-3,j)=Kglobal(i,j);
        end
    end
Kglobalsmall=zeros(5*(n+1)-3,5*(n+1)-3);
    for i=1:(5*(n+1)-3)
        Kglobalsmall(i,1)=Kglobalsmall_1(i,2);
    end
```

```
    for i=4:(5*(n+1)-3)
        for j=1:(5*(n+1)-3)
            Kglobalsmall(j,i-2)=Kglobalsmall_1(j,i);
        end
    end
    for i=(5*(n+1)-1):(5*(n+1))
        for j=1:(5*(n+1)-3)
            Kglobalsmall(j,i-3)=Kglobalsmall_1(j,i);
        end
    end

  %end
  %disp(Kglobal);
  Inverse_Kglobalsmall=inv(Kglobalsmall);

%*************************************************************************
  % Load matrix:

%*************************************************************************
  q=-45/Ltotal;
  Q21=zeros(10,1);
  Q21(3,1)=q*L/2;
  Q21(4,1)=q*(L^2)/12;
  Q21(8,1)=q*L/2;
  Q21(9,1)=-q*(L^2)/12;
  P=zeros(5*(n+1)-3,1);
  for i=6:5:(5*(n+1)-9)
         P(i,1)=Q21(3,1)+Q21(8,1);
         P(i+1,1)=Q21(4,1)+Q21(9,1);
  end
  P(2,1)=Q21(4,1);
  P(5*(n+1)-4,1)=Q21(9,1);
  %-----------------------------------------------------------------------
-
  % NODAL DISPLACEMENT VECTOR
  %-----------------------------------------------------------------------
-
  % Nodal displacement vector:
  Displacement_field_small=Inverse_Kglobalsmall*P;
  displacement_V_at_midspan=Displacement_field_small(5*n/2+3-2,1);
  % Full of nodal displacement vector (includes zero displacements at
  % constrains):
  Displacement_field=zeros(5*(n+1),1);
  Displacement_field(2,1)=Displacement_field_small(1,1);
  for i=4:(5*(n+1)-3)
      Displacement_field(i,1)=Displacement_field_small(i-2,1);
  end
    Displacement_field(5*(n+1)-1,1)=Displacement_field_small(5*(n+1)-3-
1,1);
    Displacement_field(5*(n+1),1)=Displacement_field_small(5*(n+1)-3,1);
  Displacement_field;
  % Extracting transversal displacement field:
  displacement_Vtotal=zeros(n+1,1);
  for i=1:(n+1)
      displacement_Vtotal(i,1)=Displacement_field(3+5*(i-1),1);
  end
```

```
  %------------------------------------------------------------------------
-
  % OUTPUT OF NODAL STRESSES
  %------------------------------------------------------------------------
-
  % Longitudinal normal stress at bottom surface of bottom flange:
  normalstress_bottom_zb=zeros(n+1,1);
  % Longitudinal normal stress at top surface of GFRP plate:
  normalstress_top_zp=zeros(n+1,1);
  % Shear stress sigma_zn:
  shear_stress_zn=zeros(n+1,1);
  for i=1:n
      El_displacement=zeros(10,1);
      for j=1:10
      El_displacement(j,1)=Displacement_field(j+5*(i-1),1);
      end
      % Element nodal force vector:
      El_Force=vpa(Kg*El_displacement-Q21,10);
      % Reaction forces:
      reactions=vpa(El_Force,10);
      % Normal stress_zb
      normalstress_bottom_zb(i,1)=Eb*[(-El_Force(1,1)/(Eb*Ab))-((-
El_Force(4,1)*(t3/2))/(Eb*Issbf+Ep*Ixxp))-((-
El_Force(5,1)*(hb/2))/(Eb*Ixxb1))];
      normalstress_bottom_zb(i+1,1)=Eb*[(El_Force(6,1)/(Eb*Ab))-
((El_Force(9,1)*(t3/2))/(Eb*Issbf+Ep*Ixxp))-
((El_Force(10,1)*(hb/2))/(Eb*Ixxb1))];
      % Normal stress_zp
      normalstress_top_zp(i,1)=Ep*[(-El_Force(2,1)/(Ep*Ap))+((-
El_Force(4,1)*(t1/2))/(Eb*Issbf+Ep*Ixxp))];

normalstress_top_zp(i+1,1)=Ep*[(El_Force(7,1)/(Ep*Ap))+((El_Force(9,1)*(t1
/2))/(Eb*Issbf+Ep*Ixxp))];
      % Shear stress_zn
      shear_stress_zn(i,1)=Ga*[-
c1*El_displacement(1,1)+c1*El_displacement(2,1)-c3*El_displacement(5,1)-
c2*El_displacement(4,1)];
      shear_stress_zn(i+1,1)=Ga*[-
c1*El_displacement(6,1)+c1*El_displacement(7,1)-c3*El_displacement(10,1)-
c2*El_displacement(9,1)];
  end
%-------------------------------------------------------------------------
-
% DISPLAYING DISPLACEMENTS AND STRESSES
%-------------------------------------------------------------------------
-
disp('displacement_V:');
displacement_Vtotal_showed=zeros(11,1);
coordinate_z=zeros(11,1);
     displacement_Vtotal_showed(1,1)=displacement_Vtotal(1,1);
     coordinate_z(1,1)=0;
     displacement_Vtotal_showed(11,1)=displacement_Vtotal(n+1,1);
     coordinate_z(11,1)=Ltotal;
for i=1:9

displacement_Vtotal_showed(i+1,1)=displacement_Vtotal(round(n*i/10)+1,1);
     coordinate_z(i+1,1)=(round(n*i/10))*(Ltotal/n);
```

```
end
% Display results on screen:
   fprintf('Z-coordinate(m) \t Value(m) \r');
   for i=1:11
       fprintf('%3.2e\t\t\t %3.2e\t\t\t\n', coordinate_z(i,1),
displacement_Vtotal_showed(i,1));
   end
disp('-----------------------------------------------------------------------
-');
%-----------------------------------------------------------------------
-
%-----------------------------------------------------------------------
-
disp('normal_stress_bottom_zb:');
normalstress_bottom_zb_showed=zeros(11,1);
coordinate_zb=zeros(11,1);
     normalstress_bottom_zb_showed(1,1)=normalstress_bottom_zb(1,1);
     coordinate_zb(1,1)=0;
     normalstress_bottom_zb_showed(11,1)=normalstress_bottom_zb(n+1,1);
     coordinate_zb(11,1)=Ltotal;
for i=1:9

normalstress_bottom_zb_showed(i+1,1)=normalstress_bottom_zb(round(n*i/10)+
1,1);
     coordinate_zb(i+1,1)=(round(n*i/10))*(Ltotal/n);
end
% Display results on screen:
   fprintf('Z-coordinate(m) \t Value(kPa) \r');
   for i=1:11
       fprintf('%3.2e\t\t\t %3.2e\t\t\t\n', coordinate_zb(i,1),
normalstress_bottom_zb_showed(i,1));
   end
disp('-----------------------------------------------------------------------
-');
%-----------------------------------------------------------------------
-
%-----------------------------------------------------------------------
-
disp('normal_stress_top_zp:');
normalstress_top_zp_showed=zeros(11,1);
coordinate_zp=zeros(11,1);
     normalstress_top_zp_showed(1,1)=normalstress_top_zp(1,1);
     coordinate_zp(1,1)=0;
     normalstress_top_zp_showed(11,1)=normalstress_top_zp(n+1,1);
     coordinate_zp(11,1)=Ltotal;
for i=1:9

normalstress_top_zp_showed(i+1,1)=normalstress_top_zp(round(n*i/10)+1,1);
     coordinate_zp(i+1,1)=(round(n*i/10))*(Ltotal/n);
end
% Display results on screen:
   fprintf('Z-coordinate(m) \t Value(kPa) \r');
   for i=1:11
       fprintf('%3.2e\t\t\t %3.2e\t\t\t\n', coordinate_zp(i,1),
normalstress_top_zp_showed(i,1));
   end
```

```
disp('-----------------------------------------------------------------
-');
%-----------------------------------------------------------------
-
%-----------------------------------------------------------------
-
disp('shear_stress_zn:');
shear_stress_zn_showed=zeros(11,1);
coordinate_zn=zeros(11,1);
     shear_stress_zn_showed(1,1)=shear_stress_zn(1,1);
     coordinate_zn(1,1)=0;
     shear_stress_zn_showed(11,1)=shear_stress_zn(n+1,1);
     coordinate_zn(11,1)=Ltotal;
for i=1:9
     shear_stress_zn_showed(i+1,1)=shear_stress_zn(round(n*i/10)+1,1);
     coordinate_zn(i+1,1)=(round(n*i/10))*(Ltotal/n);
end
% Display results on screen:
   fprintf('Z-coordinate(m) \t Value(kPa) \r');
   for i=1:11
       fprintf('%3.2e\t\t\t %3.2e\t\t\t\n', coordinate_zn(i,1),
shear_stress_zn_showed(i,1));
   end
disp('-----------------------------------------------------------------
-');
end
```

B4.3.2 Outputs of the Finite Element Solution

```
CASE NUMBER 13:
--------------
Input number of segments n=40
displacement_V:
Z-coordinate(m)          Value(m)
0.00e+000                0.00e+000
3.00e-001                -3.14e-003
6.00e-001                -5.92e-003
9.00e-001                -8.09e-003
1.20e+000                -9.47e-003
1.50e+000                -9.94e-003
1.80e+000                -9.47e-003
2.10e+000                -8.09e-003
2.40e+000                -5.92e-003
2.70e+000                -3.14e-003
3.00e+000                0.00e+000
-----------------------------------------------------------------
normal_stress_bottom_zb:
Z-coordinate(m)          Value(kPa)
0.00e+000                1.94e-007
3.00e-001                -6.72e+004
6.00e-001                -1.19e+005
9.00e-001                -1.57e+005
```

```
1.20e+000                    -1.79e+005
1.50e+000                    -1.87e+005
1.80e+000                    -1.79e+005
2.10e+000                    -1.57e+005
2.40e+000                    -1.19e+005
2.70e+000                    -6.72e+004
3.00e+000                    2.93e-009
-----------------------------------------------------------------
normal_stress_top_zp:
Z-coordinate(m)              Value(kPa)
0.00e+000                    -1.38e-007
3.00e-001                    1.21e+004
6.00e-001                    2.13e+004
9.00e-001                    2.79e+004
1.20e+000                    3.19e+004
1.50e+000                    3.32e+004
1.80e+000                    3.19e+004
2.10e+000                    2.79e+004
2.40e+000                    2.13e+004
2.70e+000                    1.21e+004
3.00e+000                    -3.48e-010
-----------------------------------------------------------------
shear_stress_zn:
Z-coordinate(m)              Value(kPa)
0.00e+000                    7.47e+002
3.00e-001                    5.74e+002
6.00e-001                    4.31e+002
9.00e-001                    2.87e+002
1.20e+000                    1.44e+002
1.50e+000                    -1.20e-010
1.80e+000                    -1.44e+002
2.10e+000                    -2.87e+002
2.40e+000                    -4.31e+002
2.70e+000                    -5.74e+002
3.00e+000                    -7.47e+002
-----------------------------------------------------------------
>>
```

APPENDIX B5 – PROGRAMMING OF PROBLEMS 2 AND 3 IN CHAPTER 8

B5.1 Input data

In each case study, its parameters $L, b_b, b_p, t_1, t_2, h_b, t_3, t_w, G_a, E_a, E_b, E_p, \mu$ are inputted in to a column of cells in sheet 3 of a spreadsheet named `'data21august.xlsx'`. The starting cell of inputting data is in the 6^{th} row and thus the ending cell is in the 18^{th} row. Eighteen cases are inputted corresponding to eighteen columns from C to T. As a result, all parameters of the eighteen cases are listed in cells `'C6:T18'`. Values of the parameters as presented under the Statement of Problems 2 and 3 in Chapter 8 are inputted in the case 15^{th} (corresponding to the 15^{th} column of the total eighteen columns).

B5.2 Finite Difference Solution

B5.2.1 Programming in MATLAB

```
%--------------------------------------------------------------------------
%-----------PROBLEM 2-CANTILEVER UNDER BENDING ABOUT WEAK AXIS------------
%-------PROBLEM 3-CANTILEVER UNDER TWISTING ABOUT THE BEAM CENTROID-------
%------------------------FINITE DIFFERENCE METHOD------------------------
% The difference between two problems is load matrix. When running this
code, selecting load matrices named Load (Finite Difference Solution)
corresponding to each problem should be done first.
%-------------------------------------------------------------
% STEP1: Input data shown in a Spreadsheet file
%-------------------------------------------------------------
%Read data from spreadsheet file:
A=xlsread('data21august.xlsx',3,'C6:T18');
%Cases:
for k=15:15
  % k is column index of matrix A(13,10)
  disp(['CASE NUMBER ' num2str(k) ':']);
  disp('--------------')
  % Input Data for the case i:
        L=A(1,k);     % Length of member
        bb=A(2,k);    % Width of beam flanges
        bp=A(3,k);    % Width of GFRP plate and Adhesive layer
        t1=A(4,k);    % Thickness(m) of the GFRP plate
        t2=A(5,k);    % Thickness(m) of the adhesive layer
        hb=A(6,k);    % Effective height (m) of the beam
        t3=A(7,k);    % Thickness(m) of the flanges
        tw=A(8,k);    % Thickness(m) of the web
        Ga=A(9,k);    % Module of shear(kN/m2) of adhesive
        Ea=A(10,k);   % Module of elasticity (kN/m2) of adhesive
        Eb=A(11,k);   % Module of elasticity(kN/m2)of the beam
        Ep=A(12,k);   % Module of elasticity(kN/m2) of the GFRP
```

```
        Muy=A(13,k); % Poisson ratio
  %--------------------------------------------------------------
  % STEP2: Calculation of section properties for the case i
  %--------------------------------------------------------------
  % For wide flange beam
      % Geometrical properties:
      Ab=2*t3*bb+(hb-t3)*tw;
      Aflange=t3*bb;
      Iyy1=2*t3*(bb^3)/12;
      Ixx1=tw*((hb-t3)^3)/12+2*bb*t3*(hb^2)/4;
      Iwwglobal=(hb^2)*(bb^3)*t3/24;
      Issweb=(hb-t3)*(tw^3)/12;
      Iss2flange=2*bb*(t3^3)/12;
      Iwwlocal=2*(bb^3)*(t3^3)/144+((hb-t3)^3)*(tw^3)/144;
      Jb=(bb*(t3^3)*0.3)*2+(hb-t3)*(tw^3)/3+(hb^2)*Aflange/2;
      % Physical properties:
      Gb=Eb/(2*(1+Muy));
  % For GFRP plate
      % Geometrical properties:
      Ap=t1*bp;
      Iyyp=t1*(bp^3)/12;
      Ixxp=bp*(t1^3)/12;
      Iwwp=(bp^3)*(t1^3)/144;
      Jp=bp*(t1^3)*0.3;
      % Physical properties:
      Gp=Ep/(2*(1+Muy));
  % For Adhesive layer
  Aa=t2*bb;
  Iyya=t2*(bb^3)/12;
  % Factors from c1 to c6:
  c1=1/t2;
  c2=(t1+2*t2+t3)/(2*t2);
  c3=hb/(2*t2);
  c4=hb-t1+2*t3;
  c5=hb-4*t1+2*t3;
  c6=hb^2+4*(t1^2)+4*(t3^2)-2*hb*t1+4*hb*t3-4*t1*t3;
  %--------------------------------------------------------------
  % STEP 3:  Finite differential codes
  %--------------------------------------------------------------
  % Input number of structural segments taken in to account:
   n=input('Input number of segments n=');
  % Length of a segment (uniform length):
  delta=L/n;
  % Matrix M: Matrix of constant in the equilibrium equation system solved
  % by finite differential method: M((n+1)*6+16,(n+1)*6+16);
  %------------------------------------------------------------------------
  % Group of the first differential equations:
         %Expression for matrix of Ub in the first differential equations:
         Ub1=zeros(n+1,n+1+4);
          for i=1:(n+1)  % Number of specified points
              Ub1(i,i)=Eb*Issweb/(delta)^4;   %Ub(i-2)
              Ub1(i,i+1)=-
(4*Eb*Issweb/(delta^4)+(2*Gb*Aflange+Ga*Aa/3)/(delta^2));   %Ub(i-1)

Ub1(i,i+2)=(6*Eb*Issweb/(delta^4)+2*(2*Gb*Aflange+Ga*Aa/3)/(delta^2)+(c1^2
)*Ga*Aa);  %Ub(i)
```

```
              Ub1(i,i+3)=-
(4*Eb*Issweb/(delta)^4+(2*Gb*Aflange+Ga*Aa/3)/(delta)^2);   %Ub(i+1)
              Ub1(i,i+4)=Eb*Issweb/(delta^4);   %Ub(i+2)
          end
         %Expression for matrix of Up in the first differential equations:
          Up1=zeros(n+1,n+1+2);
          for i=1:(n+1)   % Number of specified points
              Up1(i,i)=-Ga*Aa/(6*(delta^2));   %Up(i-1)
              Up1(i,i+1)=2*Ga*Aa/(6*(delta^2))-(c1^2)*Ga*Aa;  %Up(i)
              Up1(i,i+2)=-Ga*Aa/(6*(delta^2));   %Up(i+1)
          end
   %Expression for matrix of theta_by in the first differential equations:
          Theta_by1=zeros(n+1,n+1+2);
          for i=1:(n+1)   % Number of specified points
             Theta_by1(i,i)=-(2*Gb*Aflange+Ga*Aa/3)/(2*delta);
%theta_by(i-1)
             Theta_by1(i,i+1)=0;   %theta_by(i)
             Theta_by1(i,i+2)=(2*Gb*Aflange+Ga*Aa/3)/(2*delta);
%theta_by(i+1)
          end
   %Expression for matrix of theta_py in the first differential equations:
          Theta_py1=zeros(n+1,n+1+2);
          for i=1:(n+1)   % Number of specified points
             Theta_py1(i,i)=-Ga*Aa/(12*delta);  %theta_py(i-1)
             Theta_py1(i,i+1)=0;   %theta_py(i)
             Theta_py1(i,i+2)=Ga*Aa/(12*delta);  %theta_py(i+1)
          end
   %Expression for matrix of theta_z in the first differential equations:
          Theta_z1=zeros(n+1,n+1+4);
          for i=1:(n+1)   % Number of specified points
              Theta_z1(i,i)=0;  %theta_z(i-2)
              Theta_z1(i,i+1)=-c4*Ga*Aa/(6*(delta^2));   %theta_z(i-1)
              Theta_z1(i,i+2)=c4*Ga*Aa/(3*(delta^2))+c1*(c2+c3)*Ga*Aa;
%theta_z(i)
              Theta_z1(i,i+3)=-c4*Ga*Aa/(6*(delta^2));   %theta_z(i+1)
              Theta_z1(i,i+4)=0;  %theta_z(i+2)
          end
     %Expression for matrix of sai_b in the first differential equations:
          Sai_b1=zeros(n+1,n+1+2);
          for i=1:(n+1)   % Number of specified points
              Sai_b1(i,i)=-hb*Ga*Aa/(12*delta);   %sai_b(i-1)
              Sai_b1(i,i+1)=0;  %sai_b(i)
              Sai_b1(i,i+2)=hb*Ga*Aa/(12*delta);   %sai_b(i+1)
          end
  % The first equilibrium equation expressed in all n+1 points:
  M1=[Ub1 Up1 Theta_by1 Theta_py1 Theta_z1 Sai_b1];
  %-----------------------------------------------------------------------
  % Group of the second differential equations:
  % Expression for the matrix of Ub in the second differential equation:
  Ub2=zeros(n+1,n+1+4);
  for i=1:(n+1)   % Number of specified points
      Ub2(i,i)=0;   %Ub(i-2)
      Ub2(i,i+1)=-Ga*Aa/(6*delta^2);   %Ub(i-1)
      Ub2(i,i+2)=Ga*Aa/(3*delta^2)-(c1^2)*Ga*Aa;  %Ub(i)
      Ub2(i,i+3)=-Ga*Aa/(6*delta^2);   %Ub(i+1)
      Ub2(i,i+4)=0;   %Ub(i+2)
  end
```

```
   % Expression for the matrix of Up in the second differential equation:
  Up2=zeros(n+1,n+1+2);
  for i=1:(n+1)    % Number of specified points
      Up2(i,i)=-(Gp*Ap+Ga*Aa/3)/(delta^2);    %Up(i-1)
      Up2(i,i+1)=2*(Gp*Ap+Ga*Aa/3)/(delta^2)+(c1^2)*Ga*Aa;  %Up(i)
      Up2(i,i+2)=-(Gp*Ap+Ga*Aa/3)/(delta^2);    %Up(i+1)
  end
% Expression for the matrix of theta_by in the second differential
equation
  Theta_by2=zeros(n+1,n+1+2);
  for i=1:(n+1)    % Number of specified points
      Theta_by2(i,i)=-Ga*Aa/(12*delta);  %theta_by(i-1)
      Theta_by2(i,i+1)=0;   %theta_by(i)
      Theta_by2(i,i+2)=Ga*Aa/(12*delta);  %theta_by(i+1)
  end
  % Expression for the matrix of theta_py in the second differential
equation
  Theta_py2=zeros(n+1,n+1+2);
  for i=1:(n+1)    % Number of specified points
      Theta_py2(i,i)=-(Gp*Ap+Ga*Aa/3)/(2*delta);  %theta_py(i-1)
      Theta_py2(i,i+1)=0;  %theta_py(i)
      Theta_py2(i,i+2)=(Gp*Ap+Ga*Aa/3)/(2*delta);   %theta_py(i+1)
  end
  % Expression for the matrix of theta_z in the second differential
equation
  Theta_z2=zeros(n+1,n+1+4);
  for i=1:(n+1)    % Number of specified points
      Theta_z2(i,i)=0;  %theta_z(i-2)
      Theta_z2(i,i+1)=-c5*Ga*Aa/(12*(delta^2));   %theta_z(i-1)
      Theta_z2(i,i+2)=c5*Ga*Aa/(6*(delta^2))-c1*(c2+c3)*Ga*Aa;
%theta_z(i)
      Theta_z2(i,i+3)=-c5*Ga*Aa/(12*(delta^2));   %theta_z(i+1)
      Theta_z2(i,i+4)=0;  %theta_z(i+2)
  end
  % Expression for the matrix of sai_b in the second differential equation
  Sai_b2=zeros(n+1,n+1+2);
  for i=1:(n+1)    % Number of specified points
      Sai_b2(i,i)=-hb*Ga*Aa/(24*delta);   %sai_b(i-1)
      Sai_b2(i,i+1)=0;  %sai_b(i)
      Sai_b2(i,i+2)=hb*Ga*Aa/(24*delta);   %sai_b(i+1)
  end
  % The second equilibrium equation expressed in all n+1 points:
  M2=[Ub2 Up2 Theta_by2 Theta_py2 Theta_z2 Sai_b2];
  %-----------------------------------------------------------------------
  % Group of the third differential equations:
  % Expression for the matrix of Ub in the third differential equation:
  Ub3=zeros(n+1,n+1+4);
  for i=1:(n+1)    % Number of specified points
      Ub3(i,i)=0;   %Ub(i-2)
      Ub3(i,i+1)=(2*Gb*Aflange+Ga*Aa/3)/(2*delta);   %Ub(i-1)
      Ub3(i,i+2)=0;  %Ub(i)
      Ub3(i,i+3)=-(2*Gb*Aflange+Ga*Aa/3)/(2*delta);   %Ub(i+1)
      Ub3(i,i+4)=0;   %Ub(i+2)
  end
    % Expression for the matrix of Up in the third differential equation:
  Up3=zeros(n+1,n+1+2);
  for i=1:(n+1)    % Number of specified points
```

```
    Up3(i,i)=Ga*Aa/(12*delta);   %Up(i-1)
    Up3(i,i+1)=0;  %Up(i)
    Up3(i,i+2)=-Ga*Aa/(12*delta);   %Up(i+1)
  end
   % Expression for the matrix of theta_by in the third differential
equation:
  Theta_by3=zeros(n+1,n+1+2);
  for i=1:(n+1)   % Number of specified points
    Theta_by3(i,i)=-Eb*Iyy1/(delta^2);  %theta_by(i-1)

Theta_by3(i,i+1)=2*Eb*Iyy1/(delta^2)+2*Gb*Aflange+(c1^2)*Ga*Iyya+Ga*Aa/3;
%theta_by(i)
    Theta_by3(i,i+2)=-Eb*Iyy1/(delta^2);  %theta_by(i+1)
  end
   % Expression for the matrix of theta_py in the third differential
equation:
  Theta_py3=zeros(n+1,n+1+2);
  for i=1:(n+1)   % Number of specified points
    Theta_py3(i,i)=0;  %theta_py(i-1)
    Theta_py3(i,i+1)=-(c1^2)*Ga*Iyya+Ga*Aa/6;   %theta_py(i)
    Theta_py3(i,i+2)=0;  %theta_py(i+1)
  end
   % Expression for the matrix of theta_z in the third differential
equation:
  Theta_z3=zeros(n+1,n+1+4);
  for i=1:(n+1)   % Number of specified points
    Theta_z3(i,i)=0;  %theta_z(i-2)
    Theta_z3(i,i+1)=(c1*c2*Ga*Iyya+c4*Ga*Aa/6)/(2*delta);   %theta_z(i-
1)
    Theta_z3(i,i+2)=0;   %theta_z(i)
    Theta_z3(i,i+3)=-(c1*c2*Ga*Iyya+c4*Ga*Aa/6)/(2*delta);
%theta_z(i+1)
    Theta_z3(i,i+4)=0;  %theta_z(i+2)
  end
   % Expression for the matrix of Sai in the third differential equation:
  Sai_b3=zeros(n+1,n+1+2);
  for i=1:(n+1)   % Number of specified points
     Sai_b3(i,i)=0;   %sai_b(i-1)
     Sai_b3(i,i+1)=c1*c3*Ga*Iyya+hb*Ga*Aa/6;  %sai_b(i)
     Sai_b3(i,i+2)=0;   %sai_b(i+1)
  end
  % The third equilibrium equation expressed in all n+1 points:
  M3=[Ub3 Up3 Theta_by3 Theta_py3 Theta_z3 Sai_b3];
%-----------------------------------------------------------------------
 % Group of the fourth differential equations:
 % Expression for the matrix of Ub in the fourth differential equation:
  Ub4=zeros(n+1,n+1+4);
  for i=1:(n+1)   % Number of specified points
    Ub4(i,i)=0;   %Ub(i-2)
    Ub4(i,i+1)=Ga*Aa/(12*delta);   %Ub(i-1)
    Ub4(i,i+2)=0;  %Ub(i)
    Ub4(i,i+3)=-Ga*Aa/(12*delta);   %Ub(i+1)
    Ub4(i,i+4)=0;   %Ub(i+2)
  end
   % Expression for the matrix of Up in the fourth differential equation:
  Up4=zeros(n+1,n+1+2);
  for i=1:(n+1)   % Number of specified points
```

```
        Up4(i,i)=(Gp*Ap+Ga*Aa/3)/(2*delta);    %Up(i-1)
        Up4(i,i+1)=0;  %Up(i)
        Up4(i,i+2)=-(Gp*Ap+Ga*Aa/3)/(2*delta);    %Up(i+1)
    end
% Expression for the matrix of theta_by in the fourth differential
equation:
  Theta_by4=zeros(n+1,n+1+2);
  for i=1:(n+1)    % Number of specified points
      Theta_by4(i,i)=0;  %theta_by(i-1)
      Theta_by4(i,i+1)=-(c1^2)*Ga*Iyya+Ga*Aa/6;    %theta_by(i)
      Theta_by4(i,i+2)=0;  %theta_by(i+1)
  end
   % Expression for the matrix of theta_py in the fourth differential
equation:
  Theta_py4=zeros(n+1,n+1+2);
  for i=1:(n+1)    % Number of specified points
      Theta_py4(i,i)=-Ep*Iyyp/(delta^2);  %theta_py(i-1)
      Theta_py4(i,i+1)=2*Ep*Iyyp/(delta^2)+Gp*Ap+(c1^2)*Ga*Iyya+Ga*Aa/3;
%theta_py(i)
      Theta_py4(i,i+2)=-Ep*Iyyp/(delta^2);  %theta_py(i+1)
  end
   % Expression for the matrix of theta_z in the fourth differential
equation:
  Theta_z4=zeros(n+1,n+1+4);
  for i=1:(n+1)    % Number of specified points
      Theta_z4(i,i)=0;  %theta_z(i-2)
      Theta_z4(i,i+1)=-(c1*c2*Ga*Iyya-c5*Ga*Aa/12)/(2*delta);
%theta_z(i-1)
      Theta_z4(i,i+2)=0;   %theta_z(i)
      Theta_z4(i,i+3)=(c1*c2*Ga*Iyya-c5*Ga*Aa/12)/(2*delta);
%theta_z(i+1)
      Theta_z4(i,i+4)=0;  %theta_z(i+2)
  end
   % Expression for the matrix of Sai in the fourth differential equation:
  Sai_b4=zeros(n+1,n+1+2);
  for i=1:(n+1)    % Number of specified points
      Sai_b4(i,i)=0;   %sai_b(i-1)
      Sai_b4(i,i+1)=-c1*c3*Ga*Iyya+hb*Ga*Aa/12;  %sai_b(i)
      Sai_b4(i,i+2)=0;   %sai_b(i+1)
  end
  % The fourth equilibrium equation expressed in all n+1 points:
  M4=[Ub4 Up4 Theta_by4 Theta_py4 Theta_z4 Sai_b4];
 %-------------------------------------------------------------------------
 % Group of the fifth differential equations:
 % Expression for the matrix of Ub in the fifth differential equation:
 Ub5=zeros(n+1,n+1+4);
  for i=1:(n+1)    % Number of specified points
      Ub5(i,i)=0;   %Ub(i-2)
      Ub5(i,i+1)=-c4*Ga*Aa/(6*delta^2);    %Ub(i-1)
      Ub5(i,i+2)=c4*Ga*Aa/(3*delta^2)+c1*(c2+c3)*Ga*Aa;  %Ub(i)
      Ub5(i,i+3)=-c4*Ga*Aa/(6*delta^2);    %Ub(i+1)
      Ub5(i,i+4)=0;   %Ub(i+2)
  end
  % Expression for the matrix of Up in the fifth differential equation:
  Up5=zeros(n+1,n+1+2);
  for i=1:(n+1)    % Number of specified points
      Up5(i,i)=-c5*Ga*Aa/(12*delta^2);   %Up(i-1)
```

```
      Up5(i,i+1)=c5*Ga*Aa/(6*delta^2)-c1*(c2+c3)*Ga*Aa;  %Up(i)
      Up5(i,i+2)=-c5*Ga*Aa/(12*delta^2);   %Up(i+1)
  end
  % Expression for the matrix of theta_by in the fifth differential
equation:
  Theta_by5=zeros(n+1,n+1+2);
  for i=1:(n+1)   % Number of specified points
      Theta_by5(i,i)=-(c1*c2*Ga*Iyya+c4*Ga*Aa/6)/(2*delta);  %theta_by(i-
1)
      Theta_by5(i,i+1)=0;   %theta_by(i)
      Theta_by5(i,i+2)=(c1*c2*Ga*Iyya+c4*Ga*Aa/6)/(2*delta);
%theta_by(i+1)
  end
  % Expression for the matrix of theta_py in the fifth differential
equation:
  Theta_py5=zeros(n+1,n+1+2);
  for i=1:(n+1)   % Number of specified points
      Theta_py5(i,i)=-(-c1*c2*Ga*Iyya+c5*Ga*Aa/12)/(2*delta);
%theta_py(i-1)
      Theta_py5(i,i+1)=0;   %theta_py(i)
      Theta_py5(i,i+2)=(-c1*c2*Ga*Iyya+c5*Ga*Aa/12)/(2*delta);
%theta_py(i+1)
  end
  % Expression for the matrix of theta_z in the fifth differential
equation:
  Theta_z5=zeros(n+1,n+1+4);
  for i=1:(n+1)   % Number of specified points
      Theta_z5(i,i)=(Eb*Iwwlocal+Ep*Iwwp)/(delta^4);  %theta_z(i-2)
      Theta_z5(i,i+1)=-
(4*(Eb*Iwwlocal+Ep*Iwwp)/(delta^4)+(Gb*Jb+Gp*Jp+(c2^2)*Ga*Iyya+c6*Ga*Aa/12
)/(delta^2));   %theta_z(i-1)

Theta_z5(i,i+2)=(6*(Eb*Iwwlocal+Ep*Iwwp)/(delta^4)+2*(Gb*Jb+Gp*Jp+(c2^2)*G
a*Iyya+c6*Ga*Aa/12)/(delta^2)+((c2+c3)^2)*Ga*Aa);   %theta_z(i)
      Theta_z5(i,i+3)=-
(4*(Eb*Iwwlocal+Ep*Iwwp)/(delta^4)+(Gb*Jb+Gp*Jp+(c2^2)*Ga*Iyya+c6*Ga*Aa/12
)/(delta^2));   %theta_z(i+1)
      Theta_z5(i,i+4)=(Eb*Iwwlocal+Ep*Iwwp)/(delta^4);  %theta_z(i+2)
  end
  % Expression for the matrix of Sai in the fifth differential equation:
  Sai_b5=zeros(n+1,n+1+2);
  for i=1:(n+1)   % Number of specified points
      Sai_b5(i,i)=-
((hb^2)*Gb*Aflange/2+c2*c3*Ga*Iyya+c4*hb*Ga*Aa/12)/(2*delta);   %sai_b(i-
1)
      Sai_b5(i,i+1)=0;  %sai_b(i)

Sai_b5(i,i+2)=((hb^2)*Gb*Aflange/2+c2*c3*Ga*Iyya+c4*hb*Ga*Aa/12)/(2*delta)
;   %sai_b(i+1)
  end
  % The fifth equilibrium equation expressed in all n+1 points:
  M5=[Ub5 Up5 Theta_by5 Theta_py5 Theta_z5 Sai_b5];
  %-----------------------------------------------------------------------
  % Group of the sixth differential equations:
  % Expression for the matrix of Ub in the sixth differential equation:
  Ub6=zeros(n+1,n+1+4);
  for i=1:(n+1)   % Number of specified points
```

```
      Ub6(i,i)=0;   %Ub(i-2)
      Ub6(i,i+1)=hb*Ga*Aa/(12*delta);   %Ub(i-1)
      Ub6(i,i+2)=0;  %Ub(i)
      Ub6(i,i+3)=-hb*Ga*Aa/(12*delta);   %Ub(i+1)
      Ub6(i,i+4)=0;   %Ub(i+2)
  end
  % Expression for the matrix of Up in the sixth differential equation:
  Up6=zeros(n+1,n+1+2);
  for i=1:(n+1)   % Number of specified points
      Up6(i,i)=hb*Ga*Aa/(24*delta);   %Up(i-1)
      Up6(i,i+1)=0;  %Up(i)
      Up6(i,i+2)=-hb*Ga*Aa/(24*delta);   %Up(i+1)
  end
  % Expression for the matrix of theta_by in the sixth differential
equation:
  Theta_by6=zeros(n+1,n+1+2);
  for i=1:(n+1)   % Number of specified points
      Theta_by6(i,i)=0;  %theta_by(i-1)
      Theta_by6(i,i+1)=(c1*c3*Ga*Iyya+hb*Ga*Aa/6);   %theta_by(i)
      Theta_by6(i,i+2)=0;  %theta_by(i+1)
  end
  % Expression for the matrix of theta_py in the sixth differential
equation:
  Theta_py6=zeros(n+1,n+1+2);
  for i=1:(n+1)   % Number of specified points
      Theta_py6(i,i)=0;  %theta_py(i-1)
      Theta_py6(i,i+1)=(-c1*c3*Ga*Iyya+hb*Ga*Aa/12);   %theta_py(i)
      Theta_py6(i,i+2)=0;  %theta_py(i+1)
  end
  % Expression for the matrix of theta_z in the sixth differential
equation:
  Theta_z6=zeros(n+1,n+1+4);
  for i=1:(n+1)   % Number of specified points
      Theta_z6(i,i)=0;  %theta_z(i-2)

Theta_z6(i,i+1)=((hb^2)*Gb*Aflange/2+c2*c3*Ga*Iyya+c4*hb*Ga*Aa/12)/(2*delt
a);   %theta_z(i-1)
      Theta_z6(i,i+2)=0;   %theta_z(i)
      Theta_z6(i,i+3)=-
((hb^2)*Gb*Aflange/2+c2*c3*Ga*Iyya+c4*hb*Ga*Aa/12)/(2*delta);
%theta_z(i+1)
      Theta_z6(i,i+4)=0;  %theta_z(i+2)
  end
  % Expression for the matrix of Sai in the sixth differential equation:
  Sai_b6=zeros(n+1,n+1+2);
  for i=1:(n+1)   % Number of specified points
      Sai_b6(i,i)=-Eb*Iwwglobal/(delta^2);   %sai_b(i-1)

Sai_b6(i,i+1)=2*Eb*Iwwglobal/(delta^2)+(hb^2)*Gb*Aflange/2+(c3^2)*Ga*Iyya+
(hb^2)*Ga*Aa/12;  %sai_b(i)
      Sai_b6(i,i+2)=-Eb*Iwwglobal/(delta^2);   %sai_b(i+1)
  end
  % The sixth equilibrium equation expressed in all n+1 points:
  M6=[Ub6 Up6 Theta_by6 Theta_py6 Theta_z6 Sai_b6];
  %-------------------------------------------------------------------------
  % Boundary condition 1: Ub=0 at fixed end z=0:
  Ub7=zeros(1,n+1+4);
```

```
        Ub7(1,3)=1;
  Up7=zeros(1,n+1+2);
  Theta_by7=zeros(1,n+1+2);
  Theta_py7=zeros(1,n+1+2);
  Theta_z7=zeros(1,n+1+4);
  Sai_b7=zeros(1,n+1+2);
  % The 1st boundary condtion expressed in all n+1 points:
  M7=[Ub7 Up7 Theta_by7 Theta_py7 Theta_z7 Sai_b7];
  %-----------------------------------------------------------------------
  % Boundary condition 2: at free end z=L:
  Ub8=zeros(1,n+1+4);
      Ub8(1,n+1)=Eb*Issweb/(2*(delta^3));   %Ub(i-2)
      Ub8(1,n+1+1)=-
(Eb*Issweb/(delta^3)+Gb*Aflange/delta+Ga*Aa/(6*delta));   %Ub(i-1)
      Ub8(1,n+1+2)=0;  %Ub(i)
      Ub8(1,n+1+3)=(Eb*Issweb/(delta^3)+Gb*Aflange/delta+Ga*Aa/(6*delta));
%Ub(i+1)
      Ub8(1,n+1+4)=-Eb*Issweb/(2*(delta^3));   %Ub(i+2)
  Up8=zeros(1,n+1+2);
      Up8(1,n+1)=-Ga*Aa/(12*delta);   %Up(i-1)
      Up8(1,n+1+1)=0;  %Up(i)
      Up8(1,n+1+2)=Ga*Aa/(12*delta);   %Up(i+1)
  Theta_by8=zeros(1,n+1+2);
      Theta_by8(1,n+1)=0;  %theta_by(i-1)
      Theta_by8(1,n+1+1)=-(Ga*Aa/3+2*Gb*Aflange);   %theta_by(i)
      Theta_by8(1,n+1+2)=0;  %theta_by(i+1)
  Theta_py8=zeros(1,n+1+2);
      Theta_py8(1,n+1)=0;  %theta_py(i-1)
      Theta_py8(1,n+1+1)=-Ga*Aa/6;   %theta_py(i)
      Theta_py8(1,n+1+2)=0;  %theta_py(i+1)
  Theta_z8=zeros(1,n+1+4);
      Theta_z8(1,n+1)=0;  %theta_z(i-2)
      Theta_z8(1,n+1+1)=-c4*Ga*Aa/(12*delta);   %theta_z(i-1)
      Theta_z8(1,n+1+2)=0;   %theta_z(i)
      Theta_z8(1,n+1+3)=c4*Ga*Aa/(12*delta);   %theta_z(i+1)
      Theta_z8(1,n+1+4)=0;  %theta_z(i+2)
  Sai_b8=zeros(1,n+1+2);
      Sai_b8(1,n+1)=0;   %sai_b(i-1)
      Sai_b8(1,n+1+1)=-hb*Ga*Aa/6;  %sai_b(i)
      Sai_b8(1,n+1+2)=0;   %sai_b(i+1)
% The 2nd boundary condtion expressed in all n+1 points:
  M8=[Ub8 Up8 Theta_by8 Theta_py8 Theta_z8 Sai_b8];
%-------------------------------------------------------------------------
% Boundary condition 3: U'b(0)=0 at fixed end z=0:
 Ub9=zeros(1,n+1+4);
      Ub9(1,2)=-1/(2*delta);   %Ub(i-1)
      Ub9(1,4)=1/(2*delta);   %Ub(i+1)
  Up9=zeros(1,n+1+2);
  Theta_by9=zeros(1,n+1+2);
  Theta_py9=zeros(1,n+1+2);
  Theta_z9=zeros(1,n+1+4);
  Sai_b9=zeros(1,n+1+2);
% The 3rd boundary condtion expressed in all n+1 points:
  M9=[Ub9 Up9 Theta_by9 Theta_py9 Theta_z9 Sai_b9];
%-------------------------------------------------------------------------
% Boundary condition 4: U''b(0)=0 at fixed end z=L:
  Ub10=zeros(1,n+1+4);
```

```
      Ub10(1,n+1+1)=1/(delta^2);   %Ub(i-1)
      Ub10(1,n+1+2)=-2/(delta^2);   %Ub(i)
      Ub10(1,n+1+3)=1/(delta^2);   %Ub(i+1)
  Up10=zeros(1,n+1+2);
  Theta_by10=zeros(1,n+1+2);
  Theta_py10=zeros(1,n+1+2);
  Theta_z10=zeros(1,n+1+4);
  Sai_b10=zeros(1,n+1+2);
% The 4th boundary condtion expressed in all n+1 points:
  M10=[Ub10 Up10 Theta_by10 Theta_py10 Theta_z10 Sai_b10];
 %---------------------------------------------------------------------------
 % Boundary condition 5: Up(0)=0 at fixed end z=0:
  Ub11=zeros(1,n+1+4);
  Up11=zeros(1,n+1+2);
         Up11(1,2)=1;
  Theta_by11=zeros(1,n+1+2);
  Theta_py11=zeros(1,n+1+2);
  Theta_z11=zeros(1,n+1+4);
  Sai_b11=zeros(1,n+1+2);
% The 5th boundary condtion expressed in all n+1 points:
  M11=[Ub11 Up11 Theta_by11 Theta_py11 Theta_z11 Sai_b11];
%----------------------------------------------------------------------------
% Boundary condition 6: at free end z=L:
Ub12=zeros(1,n+1+4);
      Ub12(1,n+1)=0;   %Ub(i-2)
      Ub12(1,n+1+1)=-Ga*Aa/(12*delta);   %Ub(i-1)
      Ub12(1,n+1+2)=0;  %Ub(i)
      Ub12(1,n+1+3)=Ga*Aa/(12*delta);   %Ub(i+1)
      Ub12(1,n+1+4)=0;   %Ub(i+2)
  Up12=zeros(1,n+1+2);
      Up12(1,n+1)=-(Gp*Ap/(2*delta)+Ga*Aa/(6*delta));   %Up(i-1)
      Up12(1,n+1+1)=0;  %Up(i)
      Up12(1,n+1+2)=(Gp*Ap/(2*delta)+Ga*Aa/(6*delta));   %Up(i+1)
  Theta_by12=zeros(1,n+1+2);
      Theta_by12(1,n+1)=0;  %theta_by(i-1)
      Theta_by12(1,n+1+1)=-Ga*Aa/6;   %theta_by(i)
      Theta_by12(1,n+1+2)=0;  %theta_by(i+1)
  Theta_py12=zeros(1,n+1+2);
      Theta_py12(1,n+1)=0;  %theta_py(i-1)
      Theta_py12(1,n+1+1)=-(Gp*Ap+Ga*Aa/3);   %theta_py(i)
      Theta_py12(1,n+1+2)=0;  %theta_py(i+1)
  Theta_z12=zeros(1,n+1+4);
      Theta_z12(1,n+1)=0;  %theta_z(i-2)
      Theta_z12(1,n+1+1)=-c5*Ga*Aa/(24*delta);   %theta_z(i-1)
      Theta_z12(1,n+1+2)=0;   %theta_z(i)
      Theta_z12(1,n+1+3)=c5*Ga*Aa/(24*delta);   %theta_z(i+1)
      Theta_z12(1,n+1+4)=0;  %theta_z(i+2)
  Sai_b12=zeros(1,n+1+2);
      Sai_b12(1,n+1)=0;   %sai_b(i-1)
      Sai_b12(1,n+1+1)=-hb*Ga*Aa/12;  %sai_b(i)
      Sai_b12(1,n+1+2)=0;   %sai_b(i+1)
% The 6th boundary condtion expressed in all n+1 points:
  M12=[Ub12 Up12 Theta_by12 Theta_py12 Theta_z12 Sai_b12];
%----------------------------------------------------------------------------
 % Boundary condition 7: Theta_by(0)=0 at fixed end z=0:
  Ub13=zeros(1,n+1+4);
  Up13=zeros(1,n+1+2);
```

```
  Theta_by13=zeros(1,n+1+2);
        Theta_by13(1,2)=1;
  Theta_py13=zeros(1,n+1+2);
  Theta_z13=zeros(1,n+1+4);
  Sai_b13=zeros(1,n+1+2);
% The 7th boundary condtion expressed in all n+1 points:
  M13=[Ub13 Up13 Theta_by13 Theta_py13 Theta_z13 Sai_b13];
%---------------------------------------------------------------------------
 % Boundary condition 8: Theta_by'(0)=0 at free end z=L:
  Ub14=zeros(1,n+1+4);
  Up14=zeros(1,n+1+2);
  Theta_by14=zeros(1,n+1+2);
      Theta_by14(1,n+1)=-1/(2*delta);  %theta_by(i-1)
      Theta_by14(1,n+1+2)=1/(2*delta);  %theta_by(i+1)
  Theta_py14=zeros(1,n+1+2);
  Theta_z14=zeros(1,n+1+4);
  Sai_b14=zeros(1,n+1+2);
% The 8th boundary condtion expressed in all n+1 points:
  M14=[Ub14 Up14 Theta_by14 Theta_py14 Theta_z14 Sai_b14];
%---------------------------------------------------------------------------
 % Boundary condition 9: Theta_py(0)=0 at fixed end z=0:
  Ub15=zeros(1,n+1+4);
  Up15=zeros(1,n+1+2);
  Theta_by15=zeros(1,n+1+2);
  Theta_py15=zeros(1,n+1+2);
        Theta_py15(1,2)=1;
  Theta_z15=zeros(1,n+1+4);
  Sai_b15=zeros(1,n+1+2);
% The 9th boundary condtion expressed in all n+1 points:
  M15=[Ub15 Up15 Theta_by15 Theta_py15 Theta_z15 Sai_b15];
%---------------------------------------------------------------------------
 % Boundary condition 10: Theta_py'(0)=0 at free end z=L:
  Ub16=zeros(1,n+1+4);
  Up16=zeros(1,n+1+2);
  Theta_by16=zeros(1,n+1+2);
  Theta_py16=zeros(1,n+1+2);
      Theta_py16(1,n+1)=-1/(2*delta);  %theta_by(i-1)
      Theta_py16(1,n+1+2)=1/(2*delta);  %theta_by(i+1)
  Theta_z16=zeros(1,n+1+4);
  Sai_b16=zeros(1,n+1+2);
% The 10th boundary condtion expressed in all n+1 points:
  M16=[Ub16 Up16 Theta_by16 Theta_py16 Theta_z16 Sai_b16];
%---------------------------------------------------------------------------
 % Boundary condition 11: Theta_z(0)=0 at fixed end z=0:
  Ub17=zeros(1,n+1+4);
  Up17=zeros(1,n+1+2);
  Theta_by17=zeros(1,n+1+2);
  Theta_py17=zeros(1,n+1+2);
  Theta_z17=zeros(1,n+1+4);
          Theta_z17(1,3)=1;
  Sai_b17=zeros(1,n+1+2);
% The 11th boundary condtion expressed in all n+1 points:
  M17=[Ub17 Up17 Theta_by17 Theta_py17 Theta_z17 Sai_b17];
%---------------------------------------------------------------------------
% Boundary condition 12: at free end z=L:
  Ub18=zeros(1,n+1+4);
      Ub18(1,n+1)=0;   %Ub(i-2)
```

```
       Ub18(1,n+1+1)=-c4*Ga*Aa/(12*delta);   %Ub(i-1)
       Ub18(1,n+1+2)=0;  %Ub(i)
       Ub18(1,n+1+3)=c4*Ga*Aa/(12*delta);   %Ub(i+1)
       Ub18(1,n+1+4)=0;   %Ub(i+2)
  Up18=zeros(1,n+1+2);
       Up18(1,n+1)=-c5*Ga*Aa/(24*delta);   %Up(i-1)
       Up18(1,n+1+1)=0;  %Up(i)
       Up18(1,n+1+2)=c5*Ga*Aa/(24*delta);   %Up(i+1)
  Theta_by18=zeros(1,n+1+2);
       Theta_by18(1,n+1)=0;  %theta_by(i-1)
       Theta_by18(1,n+1+1)=-(c1*c2*Ga*Iyya+c4*Ga*Aa/6);   %theta_by(i)
       Theta_by18(1,n+1+2)=0;  %theta_by(i+1)
  Theta_py18=zeros(1,n+1+2);
       Theta_py18(1,n+1)=0;  %theta_py(i-1)
       Theta_py18(1,n+1+1)=c1*c2*Ga*Iyya-c5*Ga*Aa/12;   %theta_py(i)
       Theta_py18(1,n+1+2)=0;  %theta_py(i+1)
  Theta_z18=zeros(1,n+1+4);
       Theta_z18(1,n+1)=(Eb*Iwwlocal+Ep*Iwwp)/(2*delta^3);  %theta_z(i-2)
       Theta_z18(1,n+1+1)=-
(Eb*Iwwlocal/(delta^3)+Gb*Jb/(2*delta)+Ep*Iwwp/(delta^3)+Gp*Jp/(2*delta)+(
c2^2)*Ga*Iyya/(2*delta)+c6*Ga*Aa/(24*delta));   %theta_z(i-1)
       Theta_z18(1,n+1+2)=0;   %theta_z(i)

Theta_z18(1,n+1+3)=(Eb*Iwwlocal/(delta^3)+Gb*Jb/(2*delta)+Ep*Iwwp/(delta^3
)+Gp*Jp/(2*delta)+(c2^2)*Ga*Iyya/(2*delta)+c6*Ga*Aa/(24*delta));
%theta_z(i+1)
       Theta_z18(1,n+1+4)=-(Eb*Iwwlocal+Ep*Iwwp)/(2*delta^3);
%theta_z(i+2)
  Sai_b18=zeros(1,n+1+2);
       Sai_b18(1,n+1)=0;   %sai_b(i-1)
       Sai_b18(1,n+1+1)=-
(c2*c3*Ga*Iyya+(hb^2)*Gb*Aflange/2+c4*hb*Ga*Aa/12);  %sai_b(i)
       Sai_b18(1,n+1+2)=0;   %sai_b(i+1)
% The 12th boundary condtion expressed in all n+1 points:
  M18=[Ub18 Up18 Theta_by18 Theta_py18 Theta_z18 Sai_b18];
%------------------------------------------------------------------------
 % Boundary condition 13: Theta_z'(0)=0 at fixed end z=0:
  Ub19=zeros(1,n+1+4);
  Up19=zeros(1,n+1+2);
  Theta_by19=zeros(1,n+1+2);
  Theta_py19=zeros(1,n+1+2);
  Theta_z19=zeros(1,n+1+4);
           Theta_z19(1,2)=-1/(2*delta); %theta_z(i-1)
           Theta_z19(1,4)=1/(2*delta);  %theta_z(i+1)
  Sai_b19=zeros(1,n+1+2);
% The 13th boundary condtion expressed in all n+1 points:
  M19=[Ub19 Up19 Theta_by19 Theta_py19 Theta_z19 Sai_b19];
%------------------------------------------------------------------------
 % Boundary condition 14: Theta_py'(0)=0 at free end z=L:
  Ub20=zeros(1,n+1+4);
  Up20=zeros(1,n+1+2);
  Theta_by20=zeros(1,n+1+2);
  Theta_py20=zeros(1,n+1+2);
  Theta_z20=zeros(1,n+1+4);
         Theta_z20(1,n+1+1)=1/(delta^2);  %theta_z(i-1)
         Theta_z20(n+1+2)=-2/(delta^2);   %theta_z(i)
         Theta_z20(n+1+3)=1/(delta^2);  %theta_z(i+1)
```

```
  Sai_b20=zeros(1,n+1+2);
% The 14th boundary condtion expressed in all n+1 points:
  M20=[Ub20 Up20 Theta_by20 Theta_py20 Theta_z20 Sai_b20];
%--------------------------------------------------------------------------
 % Boundary condition 15: Sai_b(0)=0 at fixed end z=0:
  Ub21=zeros(1,n+1+4);
  Up21=zeros(1,n+1+2);
  Theta_by21=zeros(1,n+1+2);
  Theta_py21=zeros(1,n+1+2);
  Theta_z21=zeros(1,n+1+4);
  Sai_b21=zeros(1,n+1+2);
        Sai_b21(1,2)=1;
% The 15th boundary condtion expressed in all n+1 points:
  M21=[Ub21 Up21 Theta_by21 Theta_py21 Theta_z21 Sai_b21];
%--------------------------------------------------------------------------
 % Boundary condition 16: Sai_b'(0)=0 at free end z=L:
  Ub22=zeros(1,n+1+4);
  Up22=zeros(1,n+1+2);
  Theta_by22=zeros(1,n+1+2);
  Theta_py22=zeros(1,n+1+2);
  Theta_z22=zeros(1,n+1+4);
  Sai_b22=zeros(1,n+1+2);
      Sai_b22(1,n+1)=-1/(2*delta);  %Sai_b(i-1)
      Sai_b22(1,n+1+2)=1/(2*delta);  %Sai_b(i+1)
% The 16th boundary condtion expressed in all n+1 points:
  M22=[Ub22 Up22 Theta_by22 Theta_py22 Theta_z22 Sai_b22];
%--------------------------------------------------------------------------
  % STEP3: Grouping all Equilibrium Eqs. and Boundary Condition Eqs. in to
  % the matrix M:
%--------------------------------------------------------------------------
M=[M1; M2; M3; M4; M5; M6; M7; M8; M9; M10; M11; M12; M13; M14; M15; M16;
M17; M18; M19; M20; M21; M22];
%--------------------------------------------------------------------------
  % STEP4: Obtaining displacement fields
%--------------------------------------------------------------------------
% Inversing matrix M:
%Inverse_M=inv(M);
% Load matrix:
%--------------------------------------------------------------------------
% ATTENTION!
% For bending about weak axis: Load_BC2=12, all others equal zero
% For twisting about the beam centroid: Load_BC12=3.27118013, all others
equal zero
%--------------------------------------------------------------------------
Load_EquilEqs2=zeros(6*(n+1),1);
Load_BC1=0;
Load_BC2=12;Load_BC3=0;Load_BC4=0;Load_BC5=0;Load_BC6=0;Load_BC7=0;Load_BC
8=0;Load_BC9=0;
Load_BC10=0;Load_BC11=0;Load_BC12=0;Load_BC13=0;Load_BC14=0;Load_BC15=0;Lo
ad_BC16=0;
Load=[Load_EquilEqs2; Load_BC1;
Load_BC2;Load_BC3;Load_BC4;Load_BC5;Load_BC6;Load_BC7;Load_BC8;Load_BC9;Lo
ad_BC10;Load_BC11;Load_BC12;Load_BC13;Load_BC14;Load_BC15;Load_BC16;];
% Displacement fields:
Displacement_Field=M\Load;
%disp('Displacement Ub at free end:');
%Ub_at_free_end=Displacement_Field(n+1+2,1)
```

```
%disp('Displacement Up at free end:');
%Up_at_free_end=Displacement_Field(n+1+4+n+1+1,1)
%disp('Twisting angle at free end:');
%Theta_z_at_tip=Displacement_Field((n+1)*5+12,1)
%-------------------------------------------------------------------------
  %STEP5: Stress output
%-------------------------------------------------------------------------
% Obtaining displacement fields:
% Obtaining vector of Ub:
Matrix_Ub=zeros(n+1+4,1);
for i=1:(n+1+4)
    Matrix_Ub(i,1)=Displacement_Field(i,1);
end
%---------------------------------------------------------
disp('---------------------------------------------------------');
disp('Matrix Ub');
Matrix_Ub_showed=zeros(11,1);
coordinate_zub=zeros(11,1);
     Matrix_Ub_showed(1,1)=Matrix_Ub(3,1);
     coordinate_zub(1,1)=0;
     Matrix_Ub_showed(11,1)=Matrix_Ub(n+3,1);
     coordinate_zub(11,1)=L;
for i=1:9
     Matrix_Ub_showed(i+1,1)=Matrix_Ub((round(n*i/10)+3),1);
     coordinate_zub(i+1,1)=(round(n*i/10))*(L/n);
end
% Display results on screen:
   fprintf('Z-coordinate(m) \t Value(m) \r');
   for i=1:11
       fprintf('%3.2e\t\t\t %3.2e\t\t\t\n', coordinate_zub(i,1),
Matrix_Ub_showed(i,1));
   end
disp('---------------------------------------------------------');
% Write to a spreadsheet:
displacement_matrix_Ub={'Matrix_Ub:'};
coordinate_z_in_length={'Z_coord'};
value={'Value'};
xlswrite('FDM_out_of_plane_new_theory_bending.xlsx',displacement_matrix_Ub
,k,'B3');
xlswrite('FDM_out_of_plane_new_theory_bending.xlsx',coordinate_z_in_length
,k,'B4');
xlswrite('FDM_out_of_plane_new_theory_bending.xlsx',value,k,'C4');
xlswrite('FDM_out_of_plane_new_theory_bending.xlsx',coordinate_zub,k,'B5:B
15');
xlswrite('FDM_out_of_plane_new_theory_bending.xlsx',Matrix_Ub_showed,k,'C5
:C15');
%-------------------------------------------------------------------------
% Obtaining vector of Up:
Matrix_Up=zeros(n+1+2,1);
for i=1:(n+1+2)
    Matrix_Up(i,1)=Displacement_Field(n+1+4+i,1);
end
%---------------------------------------------------------
disp('---------------------------------------------------------');
disp('Matrix Up');
Matrix_Up_showed=zeros(11,1);
coordinate_zup=zeros(11,1);
```

```
     Matrix_Up_showed(1,1)=Matrix_Up(2,1);
     coordinate_zup(1,1)=0;
     Matrix_Up_showed(11,1)=Matrix_Up(n+2,1);
     coordinate_zup(11,1)=L;
for i=1:9
     Matrix_Up_showed(i+1,1)=Matrix_Up(round(n*i/10)+2,1);
     coordinate_zup(i+1,1)=(round(n*i/10))*(L/n);
end
% Display results on screen:
   fprintf('Z-coordinate(m) \t Value(m) \r');
   for i=1:11
       fprintf('%3.2e\t\t\t %3.2e\t\t\t\n', coordinate_zup(i,1),
Matrix_Up_showed(i,1));
   end
disp('-----------------------------------------------------------');
% Write to a spreadsheet:
displacement_matrix_Up={'Matrix_Up:'};
coordinate_z_in_length={'Z_coord'};
value={'Value'};
xlswrite('FDM_out_of_plane_new_theory_bending.xlsx',displacement_matrix_Up
,k,'e3');
xlswrite('FDM_out_of_plane_new_theory_bending.xlsx',coordinate_z_in_length
,k,'e4');
xlswrite('FDM_out_of_plane_new_theory_bending.xlsx',value,k,'f4');
xlswrite('FDM_out_of_plane_new_theory_bending.xlsx',coordinate_zup,k,'e5:e
15');
xlswrite('FDM_out_of_plane_new_theory_bending.xlsx',Matrix_Up_showed,k,'f5
:f15');
%--------------------------------------------------------------------------
% Obtaining vector of theta_yb:
% Obtaining vector of theta_yb:
Matrix_theta_yb=zeros(n+1+2,1);
for i=1:(n+1+2)
   Matrix_theta_yb(i,1)=Displacement_Field(n+1+4+n+1+2+i,1);
end
%---------------------------------------------------------
disp('Matrix theta_yb');
Matrix_theta_yb_showed=zeros(11,1);
coordinate_ztheta_yb=zeros(11,1);
     Matrix_theta_yb_showed(1,1)=Matrix_theta_yb(2,1);
     coordinate_ztheta_yb(1,1)=0;
     Matrix_theta_yb_showed(11,1)=Matrix_theta_yb(n+2,1);
     coordinate_ztheta_yb(11,1)=L;
for i=1:9
     Matrix_theta_yb_showed(i+1,1)=Matrix_theta_yb(round(n*i/10)+2,1);
     coordinate_ztheta_yb(i+1,1)=(round(n*i/10))*(L/n);
end
% Display results on screen:
   fprintf('Z-coordinate(m) \t Value(Rad) \r');
   for i=1:11
       fprintf('%3.2e\t\t\t %3.2e\t\t\t\n', coordinate_ztheta_yb(i,1),
Matrix_theta_yb_showed(i,1));
   end
disp('-----------------------------------------------------------');
% Write to a spreadsheet:
displacement_matrix_theta_yb={'Matrix_theta_yb:'};
coordinate_z_in_length={'Z_coord'};
```

```
value={'Value'};
xlswrite('FDM_out_of_plane_new_theory_bending.xlsx',displacement_matrix_th
eta_yb,k,'h3');
xlswrite('FDM_out_of_plane_new_theory_bending.xlsx',coordinate_z_in_length
,k,'h4');
xlswrite('FDM_out_of_plane_new_theory_bending.xlsx',value,k,'i4');
xlswrite('FDM_out_of_plane_new_theory_bending.xlsx',coordinate_ztheta_yb,k
,'h5:h15');
xlswrite('FDM_out_of_plane_new_theory_bending.xlsx',Matrix_theta_yb_showed
,k,'i5:i15');
%-------------------------------------------------------------------------
% Obtaining vector of theta_yp:
Matrix_theta_yp=zeros(n+1+2,1);
for i=1:(n+1+2)
    Matrix_theta_yp(i,1)=Displacement_Field(n+1+4+(n+1+2)*2+i,1);
end
%-------------------------------------------------------
disp('Matrix theta_yp');
Matrix_theta_yp_showed=zeros(11,1);
coordinate_ztheta_yp=zeros(11,1);
     Matrix_theta_yp_showed(1,1)=Matrix_theta_yp(2,1);
     coordinate_ztheta_yp(1,1)=0;
     Matrix_theta_yp_showed(11,1)=Matrix_theta_yp(n+2,1);
     coordinate_ztheta_yp(11,1)=L;
for i=1:9
     Matrix_theta_yp_showed(i+1,1)=Matrix_theta_yp(round(n*i/10)+2,1);
     coordinate_ztheta_yp(i+1,1)=(round(n*i/10))*(L/n);
end
% Display results on screen:
   fprintf('Z-coordinate(m) \t Value(Rad) \r');
   for i=1:11
       fprintf('%3.2e\t\t\t %3.2e\t\t\t\n', coordinate_ztheta_yp(i,1),
Matrix_theta_yp_showed(i,1));
   end
disp('----------------------------------------------------------');
% Write to a spreadsheet:
displacement_matrix_theta_yp={'Matrix_theta_yp:'};
coordinate_z_in_length={'Z_coord'};
value={'Value'};
xlswrite('FDM_out_of_plane_new_theory_bending.xlsx',displacement_matrix_th
eta_yp,k,'k3');
xlswrite('FDM_out_of_plane_new_theory_bending.xlsx',coordinate_z_in_length
,k,'k4');
xlswrite('FDM_out_of_plane_new_theory_bending.xlsx',value,k,'L4');
xlswrite('FDM_out_of_plane_new_theory_bending.xlsx',coordinate_ztheta_yp,k
,'k5:k15');
xlswrite('FDM_out_of_plane_new_theory_bending.xlsx',Matrix_theta_yp_showed
,k,'L5:L15');
%-------------------------------------------------------------------------
% Obtaining vector of theta_z:
Matrix_theta_z=zeros(n+1+4,1);
for i=1:(n+1+4)
    Matrix_theta_z(i,1)=Displacement_Field((n+1+4)+(n+1+2)*3+i,1);
end
%-------------------------------------------------------
disp('Matrix theta_z');
Matrix_theta_z_showed=zeros(11,1);
```

```
coordinate_ztheta_z=zeros(11,1);
     Matrix_theta_z_showed(1,1)=Matrix_theta_z(3,1);
     coordinate_ztheta_z(1,1)=0;
     Matrix_theta_z_showed(11,1)=Matrix_theta_z(n+3,1);
     coordinate_ztheta_z(11,1)=L;
for i=1:9
     Matrix_theta_z_showed(i+1,1)=Matrix_theta_z(round(n*i/10)+3,1);
     coordinate_ztheta_z(i+1,1)=(round(n*i/10))*(L/n);
end
% Display results on screen:
   fprintf('Z-coordinate(m) \t Value(Rad) \r');
   for i=1:11
       fprintf('%3.2e\t\t\t %3.2e\t\t\t\n', coordinate_ztheta_z(i,1),
Matrix_theta_z_showed(i,1));
   end
disp('-----------------------------------------------------------');
% Write to a spreadsheet:
displacement_matrix_theta_z={'Matrix_theta_z:'};
coordinate_z_in_length={'Z_coord'};
value={'Value'};
xlswrite('FDM_out_of_plane_new_theory_bending.xlsx',displacement_matrix_th
eta_z,k,'N3');
xlswrite('FDM_out_of_plane_new_theory_bending.xlsx',coordinate_z_in_length
,k,'N4');
xlswrite('FDM_out_of_plane_new_theory_bending.xlsx',value,k,'O4');
xlswrite('FDM_out_of_plane_new_theory_bending.xlsx',coordinate_ztheta_z,k,
'N5:N15');
xlswrite('FDM_out_of_plane_new_theory_bending.xlsx',Matrix_theta_z_showed,
k,'O5:O15');
%-------------------------------------------------------------------------
% Obtaining vector of Sai_b:
Matrix_sai_b=zeros(n+1+2,1);
for i=1:(n+1+2)
    Matrix_sai_b(i,1)=Displacement_Field((n+1+4)*2+(n+1+2)*3+i,1);
end
%---------------------------------------------------------
disp('Matrix_sai_b');
Matrix_sai_b_showed=zeros(11,1);
coordinate_zsai_b=zeros(11,1);
     Matrix_sai_b_showed(1,1)=Matrix_sai_b(2,1);
     coordinate_zsai_b(1,1)=0;
     Matrix_sai_b_showed(11,1)=Matrix_sai_b(n+2,1);
     coordinate_zsai_b(11,1)=L;
for i=1:9
     Matrix_sai_b_showed(i+1,1)=Matrix_sai_b(round(n*i/10)+2,1);
     coordinate_zsai_b(i+1,1)=(round(n*i/10))*(L/n);
end
% Display results on screen:
   fprintf('Z-coordinate(m) \t Value \r');
   for i=1:11
       fprintf('%3.2e\t\t\t %3.2e\t\t\t\n', coordinate_zsai_b(i,1),
Matrix_sai_b_showed(i,1));
   end
disp('-----------------------------------------------------------');
% Write to a spreadsheet:
displacement_matrix_sai_b={'Matrix_sai_b:'};
coordinate_z_in_length={'Z_coord'};
```

```
value={'Value'};
xlswrite('FDM_out_of_plane_new_theory_bending.xlsx',displacement_matrix_sa
i_b,k,'q3');
xlswrite('FDM_out_of_plane_new_theory_bending.xlsx',coordinate_z_in_length
,k,'q4');
xlswrite('FDM_out_of_plane_new_theory_bending.xlsx',value,k,'r4');
xlswrite('FDM_out_of_plane_new_theory_bending.xlsx',coordinate_zsai_b,k,'q
5:q15');
xlswrite('FDM_out_of_plane_new_theory_bending.xlsx',Matrix_sai_b_showed,k,
'r5:r15');
%-----------------------------------------------------------------------
%-----------------------------------------------------------------------
% Obtaining normal stress at left,center point of upper flange of the
beam:
epsilon_zb_left_upper=zeros(n+1+2,1);
for i=2:(n+1+1)
epsilon_zb_left_upper(i,1)=(bb/(4*delta))*(-Matrix_theta_yb(i-
1,1)+Matrix_theta_yb(i+1,1))-(hb*bb/(8*delta))*(-Matrix_sai_b(i-
1,1)+Matrix_sai_b(i+1,1));%-(bb*t3/(4*(delta^2)))*(Matrix_theta_z(i,1)-
2*Matrix_theta_z(i+1,1)+Matrix_theta_z(i+2,1));
end
epsilon_zb_left_upper_showed=zeros(11,1);
coordinate_zb=zeros(11,1);
     epsilon_zb_left_upper_showed(1,1)=epsilon_zb_left_upper(2,1);
     coordinate_zb(1,1)=0;
for i=1:9

epsilon_zb_left_upper_showed(i+1,1)=epsilon_zb_left_upper((round(n*i/10)+2
),1);
     coordinate_zb(i+1,1)=(round(n*i/10))*(L/n);
end
     epsilon_zb_left_upper_showed(11,1)=epsilon_zb_left_upper(n+1+1,1);
     coordinate_zb(11,1)=L;
% Normal stress vector at left,center point of upper flange of the beam:
normal_stress_zb_left_upper=zeros(11,1);
for i=1:11
    normal_stress_zb_left_upper(i,1)=Eb*epsilon_zb_left_upper_showed(i,1);
end
disp('normal_stress_zb_left_upper=');
% Display results on screen:
   fprintf('Z-coordinate(m) \t Value(kPa) \r');
   for i=1:11
       fprintf('%3.2e\t\t\t %3.2e\t\t\t\n', coordinate_zb(i,1),
normal_stress_zb_left_upper(i,1));
   end
disp('-----------------------------------------------------------');
% Write to a spreadsheet:
stresses={'normal_stress_zb_left_upper:'};
coordinate_z_in_length={'Z_coord'};
value={'Value'};
xlswrite('FDM_out_of_plane_new_theory_bending.xlsx',stresses,k,'t3');
xlswrite('FDM_out_of_plane_new_theory_bending.xlsx',coordinate_z_in_length
,k,'t4');
xlswrite('FDM_out_of_plane_new_theory_bending.xlsx',value,k,'u4');
xlswrite('FDM_out_of_plane_new_theory_bending.xlsx',coordinate_zb,k,'t5:t1
5');
```

```
xlswrite('FDM_out_of_plane_new_theory_bending.xlsx',normal_stress_zb_left_
upper,k,'u5:u15');
%---------------------------------------------------------------------------
%---------------------------------------------------------------------------
% Obtaining normal stress at left,top point of GFRP plate:
epsilon_zp_left_upper=zeros(n+1+2,1);
for i=2:(n+1+1)
epsilon_zp_left_upper(i,1)=((-Matrix_theta_yp(i-
1,1)+Matrix_theta_yp(i+1,1))/(2*delta))*(bp/2)+(1/delta^2)*(Matrix_theta_z
(i,1)-2*Matrix_theta_z(i+1,1)+Matrix_theta_z(i+2,1))*(-t1*bp/4);
end
epsilon_zp_left_upper_showed=zeros(11,1);
coordinate_zp=zeros(11,1);
     epsilon_zp_left_upper_showed(1,1)=epsilon_zp_left_upper(2,1);
     coordinate_zp(1,1)=0;
for i=1:9

epsilon_zp_left_upper_showed(i+1,1)=epsilon_zp_left_upper((round(n*i/10)+2
),1);
     coordinate_zp(i+1,1)=(round(n*i/10))*(L/n);
end
     epsilon_zp_left_upper_showed(11,1)=epsilon_zp_left_upper(n+1+1,1);
     coordinate_zp(11,1)=L;
% Normal stress vector at left,top point of GFRP plate
normal_stress_zp_left_upper=zeros(11,1);
for i=1:11
    normal_stress_zp_left_upper(i,1)=Ep*epsilon_zp_left_upper_showed(i,1);
end
disp('normal_stress_zp_left_upper=');
% Display results on screen:
   fprintf('Z-coordinate(m) \t Value(kPa) \r');
   for i=1:11
       fprintf('%3.2e\t\t\t %3.2e\t\t\t\n', coordinate_zp(i,1),
normal_stress_zp_left_upper(i,1));
   end
disp('------------------------------------------------------------');
% Write to a spreadsheet:
stresses={'normal_stress_zp_left_upper:'};
coordinate_z_in_length={'Z_coord'};
value={'Value'};
xlswrite('FDM_out_of_plane_new_theory_bending.xlsx',stresses,k,'w3');
xlswrite('FDM_out_of_plane_new_theory_bending.xlsx',coordinate_z_in_length
,k,'w4');
xlswrite('FDM_out_of_plane_new_theory_bending.xlsx',value,k,'x4');
xlswrite('FDM_out_of_plane_new_theory_bending.xlsx',coordinate_zp,k,'w5:w1
5');
xlswrite('FDM_out_of_plane_new_theory_bending.xlsx',normal_stress_zp_left_
upper,k,'x5:x15');
%---------------------------------------------------------------------------
%---------------------------------------------------------------------------
% Obtaining shear stress gamma zna at left point of adhesive layer:
gamma_zna_left_upper=zeros(n+1+2,1);
for i=2:(n+1+1)
gamma_zna_left_upper(i,1)=c1*Matrix_theta_yb(i,1)*(-bp/2)-
c1*Matrix_theta_yp(i,1)*(-bp/2)-(c2/(2*delta))*(-
Matrix_theta_z(i,1)+Matrix_theta_z(i+2,1))*(-bp/2)+c3*Matrix_sai_b(i,1)*(-
bp/2);
```

```
end
gamma_zna_left_upper_showed=zeros(11,1);
coordinate_zna=zeros(11,1);
     gamma_zna_left_upper_showed(1,1)=gamma_zna_left_upper(2,1);
     coordinate_zna(1,1)=0;
for i=1:9

gamma_zna_left_upper_showed(i+1,1)=gamma_zna_left_upper((round(n*i/10)+2),
1);
     coordinate_zna(i+1,1)=(round(n*i/10))*(L/n);
end
     gamma_zna_left_upper_showed(11,1)=gamma_zna_left_upper(n+1+1,1);
     coordinate_zna(11,1)=L;
% Shear stress vector at left,top point of GFRP plate
shear_stress_zna_left_upper=zeros(11,1);
for i=1:11
    shear_stress_zna_left_upper(i,1)=Ga*gamma_zna_left_upper_showed(i,1);
end
disp('shear_stress_zna_left_upper=');
% Display results on screen:
   fprintf('Z-coordinate(m) \t Value(kPa) \r');
   for i=1:11
       fprintf('%3.2e\t\t\t %3.2e\t\t\t\n', coordinate_zna(i,1),
shear_stress_zna_left_upper(i,1));
   end
disp('----------------------------------------------------------');
% Write to a spreadsheet:
stresses={'shear_stress_zna_left_upper:'};
coordinate_z_in_length={'Z_coord'};
value={'Value'};
xlswrite('FDM_out_of_plane_new_theory_bending.xlsx',stresses,k,'z3');
xlswrite('FDM_out_of_plane_new_theory_bending.xlsx',coordinate_z_in_length
,k,'z4');
xlswrite('FDM_out_of_plane_new_theory_bending.xlsx',value,k,'aa4');
xlswrite('FDM_out_of_plane_new_theory_bending.xlsx',coordinate_zna,k,'z5:z
15');
xlswrite('FDM_out_of_plane_new_theory_bending.xlsx',shear_stress_zna_left_
upper,k,'aa5:aa15');
%-------------------------------------------------------------------------
%-------------------------------------------------------------------------
% Obtaining shear stress gamma sna:
gamma_sna_left_upper=zeros(n+1+2,1);
for i=2:(n+1+1)
gamma_sna_left_upper(i,1)=-c1*Matrix_Ub(i+1,1)+c1*Matrix_Up(i,1)-
(c2+c3)*Matrix_theta_z(i+1,1);
end
gamma_sna_left_upper_showed=zeros(11,1);
coordinate_sna=zeros(11,1);
     gamma_sna_left_upper_showed(1,1)=gamma_sna_left_upper(2,1);
     coordinate_sna(1,1)=0;
for i=1:9

gamma_sna_left_upper_showed(i+1,1)=gamma_sna_left_upper((round(n*i/10)+2),
1);
     coordinate_sna(i+1,1)=(round(n*i/10))*(L/n);
end
     gamma_sna_left_upper_showed(11,1)=gamma_sna_left_upper(n+1+1,1);
```

```
     coordinate_sna(11,1)=L;
% Shear stress vector:
shear_stress_sna_left_upper=zeros(11,1);
for i=1:11
    shear_stress_sna_left_upper(i,1)=Ga*gamma_sna_left_upper_showed(i,1);
end
disp('shear_stress_sna_left_upper=');
% Display results on screen:
   fprintf('Z-coordinate(m) \t Value(kPa) \r');
   for i=1:11
       fprintf('%3.2e\t\t\t %3.2e\t\t\t\n', coordinate_sna(i,1),
shear_stress_sna_left_upper(i,1));
   end
disp('-----------------------------------------------------------');
% Write to a spreadsheet:
stresses={'shear_stress_sna_left_upper:'};
coordinate_z_in_length={'Z_coord'};
value={'Value'};
xlswrite('FDM_out_of_plane_new_theory_bending.xlsx',stresses,k,'ac3');
xlswrite('FDM_out_of_plane_new_theory_bending.xlsx',coordinate_z_in_length
,k,'ac4');
xlswrite('FDM_out_of_plane_new_theory_bending.xlsx',value,k,'ad4');
xlswrite('FDM_out_of_plane_new_theory_bending.xlsx',coordinate_sna,k,'ac5:
ac15');
xlswrite('FDM_out_of_plane_new_theory_bending.xlsx',shear_stress_sna_left_
upper,k,'ad5:ad15');
%-----------------------------------------------------------------------
%-----------------------------------------------------------------------
% Obtaining shear stress gamma sza at upper surface of adhesive layer:
gamma_sza_upper=zeros(n+1+2,1);
for i=2:(n+1+1)
gamma_sza_upper(i,1)=(1/(2*delta))*(-Matrix_Up(i-1,1)+Matrix_Up(i+1,1))-
Matrix_theta_yp(i,1)+(((hb-2*t1+2*t3)/4-
(hb+2*t1+2*t3)*(t2/2)/(2*t2))/(2*delta))*(-
Matrix_theta_z(i,1)+Matrix_theta_z(i+2,1));
end
gamma_sza_upper_showed=zeros(11,1);
coordinate_sza_upper=zeros(11,1);
     gamma_sza_upper_showed(1,1)=gamma_sza_upper(2,1);
     coordinate_sza_upper(1,1)=0;
for i=1:9
     gamma_sza_upper_showed(i+1,1)=gamma_sza_upper((round(n*i/10)+2),1);
     coordinate_sza_upper(i+1,1)=(round(n*i/10))*(L/n);
end
     gamma_sza_left_upper(11,1)=gamma_sza_upper(n+1+1,1);
     coordinate_sza_upper(11,1)=L;
% Shear stress vector at upper surface of adhesive layer:
shear_stress_sza_upper=zeros(11,1);
for i=1:11
    shear_stress_sza_upper(i,1)=Ga*gamma_sza_upper_showed(i,1);
end
disp('shear_stress_sza_upper=');
% Display results on screen:
   fprintf('Z-coordinate(m) \t Value(kPa) \r');
   for i=1:11
       fprintf('%3.2e\t\t\t %3.2e\t\t\t\n',
coordinate_sza_upper(i,1),shear_stress_sza_upper(i,1));
```

```
   end
disp('------------------------------------------------------------');
% Write to a spreadsheet:
stresses={'shear_stress_sza_upper:'};
coordinate_z_in_length={'Z_coord'};
value={'Value'};
xlswrite('FDM_out_of_plane_new_theory_bending.xlsx',stresses,k,'af3');
xlswrite('FDM_out_of_plane_new_theory_bending.xlsx',coordinate_z_in_length
,k,'af4');
xlswrite('FDM_out_of_plane_new_theory_bending.xlsx',value,k,'ag4');
xlswrite('FDM_out_of_plane_new_theory_bending.xlsx',coordinate_sza_upper,k
,'af5:af15');
xlswrite('FDM_out_of_plane_new_theory_bending.xlsx',shear_stress_sza_upper
,k,'ag5:ag15');
%--------------------------------------------------------------------------
%--------------------------------------------------------------------------
% Obtaining shear stress gamma sza at bottom surface of adhesive layer:
gamma_sza_bottom=zeros(n+1+2,1);
for i=2:(n+1+1)
gamma_sza_bottom(i,1)=(1/(2*delta))*(-Matrix_Ub(i,1)+Matrix_Ub(i+2,1))-
Matrix_theta_yb(i,1)+(((hb-2*t1+2*t3)/4-(hb+2*t1+2*t3)*(-
t2/2)/(2*t2))/(2*delta))*(-
Matrix_theta_z(i,1)+Matrix_theta_z(i+2,1))+hb*Matrix_sai_b(i,1)/2;
end
gamma_sza_bottom_showed=zeros(11,1);
coordinate_sza=zeros(11,1);
     gamma_sza_bottom_showed(1,1)=gamma_sza_bottom(2,1);
     coordinate_sza(1,1)=0;
for i=1:9
     gamma_sza_bottom_showed(i+1,1)=gamma_sza_bottom((round(n*i/10)+2),1);
     coordinate_sza(i+1,1)=(round(n*i/10))*(L/n);
end
     gamma_sza_left_bottom(11,1)=gamma_sza_bottom(n+1+1,1);
     coordinate_sza(11,1)=L;
% Shear stress vector at bottom surface of adhesive layer:
shear_stress_sza_bottom=zeros(11,1);
for i=1:11
    shear_stress_sza_bottom(i,1)=Ga*gamma_sza_bottom_showed(i,1);
end
disp('shear_stress_sza_bottom=');
% Display results on screen:
   fprintf('Z-coordinate(m) \t Value(kPa) \r');
   for i=1:11
       fprintf('%3.2e\t\t\t %3.2e\t\t\t\n',
coordinate_sza(i,1),shear_stress_sza_bottom(i,1));
   end
disp('------------------------------------------------------------');
% Write to a spreadsheet:
stresses={'shear_stress_sza_bottom:'};
coordinate_z_in_length={'Z_coord'};
value={'Value'};
xlswrite('FDM_out_of_plane_new_theory_bending.xlsx',stresses,k,'ai3');
xlswrite('FDM_out_of_plane_new_theory_bending.xlsx',coordinate_z_in_length
,k,'ai4');
xlswrite('FDM_out_of_plane_new_theory_bending.xlsx',value,k,'aj4');
xlswrite('FDM_out_of_plane_new_theory_bending.xlsx',coordinate_sza,k,'ai5:
ai15');
```

```
xlswrite('FDM_out_of_plane_new_theory_bending.xlsx',shear_stress_sza_botto
m,k,'aj5:aj15');
%-------------------------------------------------------------------------
end
%-------------------------------------------------------------------------
%------------------END OF FINITE DIFFERENCE SOLUTION----------------------
%-------------------------------------------------------------------------
```

B5.2.2 Outputs of the Finite Difference Method

B5.2.2.1 Problem 2-Bending about weak axis

CASE NUMBER 15:

Input number of segments n=200

Matrix Ub:

Z-coordinate(m)	Value(m)
0.00e+000	4.20e-016
5.00e-001	1.83e-003
1.00e+000	7.05e-003
1.50e+000	1.53e-002
2.00e+000	2.61e-002
2.50e+000	3.92e-002
3.00e+000	5.42e-002
3.50e+000	7.07e-002
4.00e+000	8.83e-002
4.50e+000	1.07e-001
5.00e+000	1.25e-001

Matrix Up

Z-coordinate(m)	Value(m)
0.00e+000	1.57e-013
5.00e-001	1.79e-003
1.00e+000	6.89e-003
1.50e+000	1.50e-002
2.00e+000	2.56e-002
2.50e+000	3.85e-002
3.00e+000	5.33e-002
3.50e+000	6.96e-002
4.00e+000	8.70e-002
4.50e+000	1.05e-001
5.00e+000	1.24e-001

Matrix theta_yb

Z-coordinate(m)	Value(Rad)
0.00e+000	3.90e-012
5.00e-001	7.15e-003
1.00e+000	1.35e-002
1.50e+000	1.92e-002

2.00e+000	2.41e-002
2.50e+000	2.82e-002
3.00e+000	3.16e-002
3.50e+000	3.42e-002
4.00e+000	3.61e-002
4.50e+000	3.72e-002
5.00e+000	3.76e-002

Matrix theta_yp

Z-coordinate(m)	Value(Rad)
0.00e+000	-1.60e-012
5.00e-001	7.00e-003
1.00e+000	1.33e-002
1.50e+000	1.89e-002
2.00e+000	2.37e-002
2.50e+000	2.78e-002
3.00e+000	3.12e-002
3.50e+000	3.38e-002
4.00e+000	3.57e-002
4.50e+000	3.68e-002
5.00e+000	3.72e-002

Matrix theta_z

Z-coordinate(m)	Value(Rad)
0.00e+000	8.10e-016
5.00e-001	-2.04e-004
1.00e+000	-7.07e-004
1.50e+000	-1.41e-003
2.00e+000	-2.23e-003
2.50e+000	-3.14e-003
3.00e+000	-4.10e-003
3.50e+000	-5.10e-003
4.00e+000	-6.11e-003
4.50e+000	-7.14e-003
5.00e+000	-8.17e-003

Matrix_sai_b

Z-coordinate(m)	Value
0.00e+000	-1.09e-013
5.00e-001	-7.52e-004
1.00e+000	-1.24e-003
1.50e+000	-1.56e-003
2.00e+000	-1.77e-003
2.50e+000	-1.90e-003
3.00e+000	-1.98e-003
3.50e+000	-2.04e-003
4.00e+000	-2.07e-003
4.50e+000	-2.09e-003
5.00e+000	-2.10e-003

----

normal_stress_zb_left_upper=

Z-coordinate(m)	Value(kPa)
0.00e+000	2.78e+005
5.00e-001	2.49e+005
1.00e+000	2.21e+005
1.50e+000	1.92e+005
2.00e+000	1.64e+005
2.50e+000	1.37e+005
3.00e+000	1.09e+005
3.50e+000	8.19e+004
4.00e+000	5.46e+004
4.50e+000	2.73e+004
5.00e+000	-6.89e-005

----

normal_stress_zp_left_upper=

Z-coordinate(m)	Value(kPa)
0.00e+000	5.59e+004
5.00e-001	5.06e+004
1.00e+000	4.52e+004
1.50e+000	3.96e+004
2.00e+000	3.40e+004
2.50e+000	2.84e+004
3.00e+000	2.28e+004
3.50e+000	1.71e+004
4.00e+000	1.14e+004
4.50e+000	5.70e+003
5.00e+000	-1.08e-005

----

shear_stress_zna_left_upper=

Z-coordinate(m)	Value(kPa)
0.00e+000	-9.92e-005
5.00e-001	-1.77e+002
1.00e+000	-2.90e+002
1.50e+000	-3.63e+002
2.00e+000	-4.11e+002
2.50e+000	-4.42e+002
3.00e+000	-4.61e+002
3.50e+000	-4.74e+002
4.00e+000	-4.82e+002
4.50e+000	-4.86e+002
5.00e+000	-3.90e+002

----

shear_stress_sna_left_upper=

Z-coordinate(m)	Value(kPa)
0.00e+000	3.13e-005
5.00e-001	-8.05e+000
1.00e+000	-5.23e+000
1.50e+000	-3.40e+000
2.00e+000	-2.20e+000
2.50e+000	-1.42e+000
3.00e+000	-9.09e-001
3.50e+000	-5.66e-001

4.00e+000	-3.30e-001
4.50e+000	-1.59e-001
5.00e+000	2.51e+002

----

shear_stress_sza_upper=

Z-coordinate(m)	Value(kPa)
0.00e+000	-6.92e+000
5.00e-001	-6.77e+000
1.00e+000	-6.16e+000
1.50e+000	-5.76e+000
2.00e+000	-5.50e+000
2.50e+000	-5.33e+000
3.00e+000	-5.23e+000
3.50e+000	-5.16e+000
4.00e+000	-5.12e+000
4.50e+000	-5.09e+000
5.00e+000	0.00e+000

----

shear_stress_sza_bottom=

Z-coordinate(m)	Value(kPa)
0.00e+000	-5.87e-007
5.00e-001	-4.05e+000
1.00e+000	-1.72e+000
1.50e+000	-1.98e-001
2.00e+000	7.87e-001
2.50e+000	1.43e+000
3.00e+000	1.84e+000
3.50e+000	2.10e+000
4.00e+000	2.25e+000
4.50e+000	2.34e+000
5.00e+000	0.00e+000

>>

B5.2.2.2 Problem 3-Twisting about the beam centroid for the case $L = 5.0m$ **and** $G_a = 0.4GPa$

Twisting:

CASE NUMBER 15:

Input number of segments n=200

Matrix Ub

Z-coordinate(m)	Value(m)
0.00e+000	-2.90e-015
5.00e-001	-1.03e-004
1.00e+000	-3.77e-004
1.50e+000	-7.85e-004
2.00e+000	-1.30e-003
2.50e+000	-1.90e-003
3.00e+000	-2.56e-003

3.50e+000	-3.29e-003
4.00e+000	-4.05e-003
4.50e+000	-4.85e-003
5.00e+000	-5.66e-003

Matrix Up

Z-coordinate(m)	Value(m)
0.00e+000	-2.04e-012
5.00e-001	4.58e-004
1.00e+000	1.57e-003
1.50e+000	3.09e-003
2.00e+000	4.85e-003
2.50e+000	6.75e-003
3.00e+000	8.73e-003
3.50e+000	1.08e-002
4.00e+000	1.28e-002
4.50e+000	1.48e-002
5.00e+000	1.68e-002

Matrix theta_yb

Z-coordinate(m)	Value(Rad)
0.00e+000	-2.71e-011
5.00e-001	-3.66e-004
1.00e+000	-6.51e-004
1.50e+000	-8.79e-004
2.00e+000	-1.06e-003
2.50e+000	-1.21e-003
3.00e+000	-1.33e-003
3.50e+000	-1.42e-003
4.00e+000	-1.50e-003
4.50e+000	-1.55e-003
5.00e+000	-1.57e-003

Matrix theta_yp

Z-coordinate(m)	Value(Rad)
0.00e+000	3.97e-011
5.00e-001	1.44e-003
1.00e+000	2.33e-003
1.50e+000	2.87e-003
2.00e+000	3.18e-003
2.50e+000	3.35e-003
3.00e+000	3.44e-003
3.50e+000	3.48e-003
4.00e+000	3.48e-003
4.50e+000	3.48e-003
5.00e+000	3.36e-003

Matrix theta_z

Z-coordinate(m)	Value(Rad)
0.00e+000	1.43e-013
5.00e-001	2.55e-003

1.00e+000	8.86e-003
1.50e+000	1.76e-002
2.00e+000	2.80e-002
2.50e+000	3.93e-002
3.00e+000	5.14e-002
3.50e+000	6.38e-002
4.00e+000	7.65e-002
4.50e+000	8.94e-002
5.00e+000	1.02e-001

Matrix_sai_b

Z-coordinate(m)	Value
0.00e+000	1.72e-012
5.00e-001	9.42e-003
1.00e+000	1.55e-002
1.50e+000	1.95e-002
2.00e+000	2.21e-002
2.50e+000	2.38e-002
3.00e+000	2.49e-002
3.50e+000	2.55e-002
4.00e+000	2.60e-002
4.50e+000	2.62e-002
5.00e+000	2.63e-002

----

normal_stress_zb_left_upper=

Z-coordinate(m)	Value(kPa)
0.00e+000	-9.77e+004
5.00e-001	-6.61e+004
1.00e+000	-4.46e+004
1.50e+000	-3.03e+004
2.00e+000	-2.09e+004
2.50e+000	-1.44e+004
3.00e+000	-1.00e+004
3.50e+000	-6.84e+003
4.00e+000	-4.46e+003
4.50e+000	-2.55e+003
5.00e+000	-3.67e-003

----

normal_stress_zp_left_upper=

Z-coordinate(m)	Value(kPa)
0.00e+000	1.28e+004
5.00e-001	8.02e+003
1.00e+000	4.87e+003
1.50e+000	2.87e+003
2.00e+000	1.61e+003
2.50e+000	8.38e+002
3.00e+000	3.75e+002
3.50e+000	1.11e+002
4.00e+000	-2.77e+001
4.50e+000	-9.36e+001
5.00e+000	-7.64e-004

---

shear_stress_zna_left_upper=

Z-coordinate(m)	Value(kPa)
0.00e+000	1.20e-003
5.00e-001	2.21e+003
1.00e+000	3.63e+003
1.50e+000	4.55e+003
2.00e+000	5.14e+003
2.50e+000	5.53e+003
3.00e+000	5.78e+003
3.50e+000	5.94e+003
4.00e+000	6.03e+003
4.50e+000	6.09e+003
5.00e+000	3.92e+003

---

shear_stress_sna_left_upper=

Z-coordinate(m)	Value(kPa)
0.00e+000	-4.13e-004
5.00e-001	1.01e+002
1.00e+000	6.55e+001
1.50e+000	4.26e+001
2.00e+000	2.76e+001
2.50e+000	1.78e+001
3.00e+000	1.14e+001
3.50e+000	7.13e+000
4.00e+000	4.19e+000
4.50e+000	2.10e+000
5.00e+000	-5.65e+003

---

shear_stress_sza_upper=

Z-coordinate(m)	Value(kPa)
0.00e+000	-1.78e+001
5.00e-001	-2.17e+001
1.00e+000	-2.94e+001
1.50e+000	-3.44e+001
2.00e+000	-3.76e+001
2.50e+000	-3.97e+001
3.00e+000	-4.11e+001
3.50e+000	-4.19e+001
4.00e+000	-4.24e+001
4.50e+000	-4.27e+001
5.00e+000	0.00e+000

---

shear_stress_sza_bottom=

Z-coordinate(m)	Value(kPa)
0.00e+000	9.28e-006
5.00e-001	-5.58e+001
1.00e+000	-8.50e+001
1.50e+000	-1.04e+002
2.00e+000	-1.16e+002
2.50e+000	-1.24e+002

3.00e+000	-1.30e+002
3.50e+000	-1.33e+002
4.00e+000	-1.35e+002
4.50e+000	-1.36e+002
5.00e+000	0.00e+000

B5.3 Finite Element Solution

B5.3.1 Programming in MATLAB

```
%--------------------------------------------------------------------------
%-----------PROBLEM 2-CANTILEVER UNDER BENDING ABOUT WEAK AXIS------------
%-------PROBLEM 3-CANTILEVER UNDER TWISTING ABOUT THE BEAM CENTROID-------
%--------------------------FINITE ELEMENT METHOD-------------------------
% The difference between two problems is load matrix. When running this
code, selecting load matrices named P (Finite Element Solution)
corresponding to each problem should be done first.
%--------------------------------------------------------------
% STEP1: Input data shown in a Spreadsheet file
%--------------------------------------------------------------
%Read data from spreadsheet file:
A=xlsread('data21august.xlsx',3,'C6:T18');
%Cases:
for k=15:15
  % k is column index of matrix A(13,10)
  disp(['CASE NUMBER ' num2str(k) ':']);
  disp('--------------')
  % Input Data for the case i:
        Ltotal=A(1,k);    % Length of member
        bb=A(2,k);   % Width of beam flanges
        bp=A(3,k);   % Width of GFRP plate and Adhesive layer
        t1=A(4,k);   % Thickness(m) of the GFRP plate
        t2=A(5,k);   % Thickness(m) of the adhesive layer
        hb=A(6,k);   % Effective height (m) of the beam
        t3=A(7,k);   % Thickness(m) of the flanges
        tw=A(8,k);   % Thickness(m) of the web
        Ga=A(9,k);   % Module of shear(kN/m2) of adhesive
        Ea=A(10,k);  % Module of elasticity (kN/m2) of adhesive
        Eb=A(11,k);  % Module of elasticity(kN/m2)of the beam
        Ep=A(12,k);  % Module of elasticity(kN/m2) of the GFRP
        Muy=A(13,k); % Poisson ratio
  %--------------------------------------------------------------
  % STEP2: Calculation of section properties for the case i
  %--------------------------------------------------------------
  % For wide flange beam
      % Geometrical properties:
      Ab=2*t3*bb+(hb-t3)*tw;
      Abf=t3*bb;
      Iyybf=2*t3*(bb^3)/12;
      Ixx1=tw*((hb-t3)^3)/12+2*bb*t3*(hb^2)/4;
      Iwwbg=(hb^2)*(bb^3)*t3/24;
```

```
      Issbw=(hb-t3)*(tw^3)/12;
      Iyyb=Iyybf+Issbw;
      Issbf=2*bb*(t3^3)/12;
      Iwwbl=2*(bb^3)*(t3^3)/144+((hb-t3)^3)*(tw^3)/144;
      Jb=(bb*(t3^3)*0.312)*2+(hb-t3)*(tw^3)/3+(hb^2)*Abf/2;
      % Physical properties:
      Gb=Eb/(2*(1+Muy));
  % For GFRP plate
      % Geometrical properties:
      Ap=t1*bp;
      Iyyp=t1*(bp^3)/12;
      Ixxp=bp*(t1^3)/12;
      Iwwp=(bp^3)*(t1^3)/144;
      Jp=bp*(t1^3)*0.300;
      % Physical properties:
      Gp=Ep/(2*(1+Muy));
  % For Adhesive layer
  Aa=t2*bb;
  Iyya=t2*(bb^3)/12;
  % Factors from c1 to c6:
  c1=1/t2;
  c2=(t1+2*t2+t3)/(2*t2);
  c3=hb/(2*t2);
  c4=hb-t1+2*t3;
  c5=hb-4*t1+2*t3;
  c6=hb^2+4*(t1^2)+4*(t3^2)-2*hb*t1+4*hb*t3-4*t1*t3;
  %--------------------------------------------------------------
  % STEP 3:  Stiffness matrix
  %--------------------------------------------------------------
  n=input('Input number of segments n=');
  L=Ltotal/n;
  % element stiffness matrices:
  K1bar=(1/(L^3))*[12 6*L -12 6*L; 6*L 4*(L^2) -6*L 2*(L^2); -12 -6*L 12 -
6*L; 6*L 2*(L^2) -6*L 4*(L^2)];   %4x4
  K2bar=(1/(30*L))*[36 3*L -36 3*L; 3*L 4*(L^2) -3*L -(L^2); -36 -3*L 36 -
3*L; 3*L -(L^2) -3*L 4*(L^2)];      %4x4
  K3bar=(1/420)*[156*L 22*(L^2) 54*L -13*(L^2); 22*(L^2) 4*(L^3) 13*(L^2)
-3*(L^3); 54*L 13*(L^2) 156*L -22*(L^2); -13*(L^2) -3*(L^3) -22*(L^2)
4*(L^3)];  %4x4
  K4bar=(1/12)*[-6 L 6 -L; -6 -L 6 L];  %2x4
  K8bar=(1/L)*[1 0 -1 0; -1 0 1 0];   % 2x4
  K9bar=(L/60)*[21 3*L 9 -2*L; 9 2*L 21 -3*L]; %2x4
  K5bar=(L/6)*[2 1; 1 2];   %2x2
  K6bar=(1/2)*[-1 1; -1 1];  %2x2
  K7bar=(1/L)*[1 -1; -1 1];  %2x2
  % Stiffness elements in the global stifness matrix
  K1=Eb*Issbw*K1bar/2+(Gb*Abf+Ga*Aa/6)*K2bar+(c1^2)*Ga*Aa*K3bar/2;  %4x4
  K2=Eb*Iyybf*K7bar/2+(Gb*Abf+(c1^2)*Ga*Iyya/2+Ga*Aa/6)*K5bar;   %2x2
  K3=(Gp*Ap+Ga*Aa/3)*K7bar/2+(c1^2)*Ga*Aa*K5bar/2;     %2x2
  K4=Ep*Iyyp*K7bar/2+(Gp*Ap+Ga*Aa/3+(c1^2)*Ga*Iyya)*K5bar/2;  %2x2

K5=(Eb*Iwwbl+Ep*Iwwp)*K1bar/2+((c2+c3)^2)*Ga*Aa*K3bar/2+(Gb*Jb+Gp*Jp+(c2^2
)*Ga*Iyya+c6*Ga*Aa/12)*K2bar/2; %4x4

K6=Eb*Iwwbg*K7bar/2+((hb^2)*Gb*Abf/2+(c3^2)*Ga*Iyya+(hb^2)*Ga*Aa/12)*K5bar
/2;  %2x2
  K7=Ga*Aa*K8bar/6-(c1^2)*Ga*Aa*K9bar;  %2x4
```

```
  K8=-(2*Gb*Abf+Ga*Aa/3)*K4bar;    %2x4
  K9=-Ga*Aa*K4bar/6;  %2x4
  K10=c4*Ga*Aa*K2bar/6+c1*(c2+c3)*Ga*Aa*K3bar;  %%4x4
  K11=-hb*Ga*Aa*K4bar/6;  %2x4
  K12=-(Gp*Ap+Ga*Aa/3)*K6bar;  %2x2
  K13=c5*Ga*Aa*K8bar/12-c1*(c2+c3)*Ga*Aa*K9bar;  %2x4
  K14=-Ga*Aa*K6bar/6;   %2x2
  K15=-hb*Ga*Aa*K6bar/12;  %2x2
  K16=-(c1*c2*Ga*Iyya+c4*Ga*Aa/6)*K4bar; %2x4
  K17=(Ga*Aa/6-(c1^2)*Ga*Iyya)*K5bar; %2x2
  K18=(c1*c3*Ga*Iyya+hb*Ga*Aa/6)*K5bar;  %2x2
  K19=(c1*c2*Ga*Iyya-c5*Ga*Aa/12)*K4bar;  %2x4
  K20=(hb*Ga*Aa/12-c1*c3*Ga*Iyya)*K5bar;  %2x2
  K21=-((hb^2)*Gb*Abf/2+c2*c3*Ga*Iyya+c4*hb*Ga*Aa/12)*K4bar; %4x4
  % GLOBAL STIFFNESS MATRIX [K]:
  K=[2*K1 K8' K7' K9' K10' K11'; K8 2*K2 K14 K17' K16 K18'; K7 K14' 2*K3
K12' K13 K15'; K9 K17 K12 2*K4 K19 K20'; K10 K16' K13' K19' 2*K5 K21'; K11
K18 K15 K20 K21 2*K6];
  %Change position of rows:
  Kg1=zeros(16,16);
  for j=1:16
          Kg1(1,j)=K(1,j);  %row 1
          Kg1(2,j)=K(2,j);   %row 2
          Kg1(3,j)=K(5,j);   %row 3
          Kg1(4,j)=K(7,j);  %row 4
          Kg1(5,j)=K(9,j);   %row 5
          Kg1(6,j)=K(11,j);   %row 6
          Kg1(7,j)=K(12,j);  %row 7
          Kg1(8,j)=K(15,j);   %row 8
          Kg1(9,j)=K(3,j);   %row 9
          Kg1(10,j)=K(4,j);  %row 10
          Kg1(11,j)=K(6,j);   %row 11
          Kg1(12,j)=K(8,j);   %row 12
          Kg1(13,j)=K(10,j);  %row 13
          Kg1(14,j)=K(13,j);   %row 14
          Kg1(15,j)=K(14,j);   %row 15
          Kg1(16,j)=K(16,j);   %row 16
  end
  % Change position of rows and columns:
  Kg=zeros(16,16);
  for u=1:16
          Kg(u,1)=Kg1(u,1);  %column 1       Ub(0)
          Kg(u,2)=Kg1(u,2);   %column 2      Ub'(0)
          Kg(u,3)=Kg1(u,5);   %column 3      theta_yb(0)
          Kg(u,4)=Kg1(u,7);  %column 4       Up(0)
          Kg(u,5)=Kg1(u,9);   %column 5      theta_yp(0)
          Kg(u,6)=Kg1(u,11);   %column 6     theta_z(0)
          Kg(u,7)=Kg1(u,12);  %column 7      theta_z'(0)
          Kg(u,8)=Kg1(u,15);   %column 8     sai(0)
          Kg(u,9)=Kg1(u,3);   %column 9      Ub(L)
          Kg(u,10)=Kg1(u,4);  %column 10     Ub'(L)
          Kg(u,11)=Kg1(u,6);   %column 11    theta_yb(L)
          Kg(u,12)=Kg1(u,8);   %column 12    Up(L)
          Kg(u,13)=Kg1(u,10);  %column 13    theta_yp(L)
          Kg(u,14)=Kg1(u,13);   %column 14   theta_z(L)
          Kg(u,15)=Kg1(u,14);   %column 15   theta_z'(L)
          Kg(u,16)=Kg1(u,16);   %column 16   sai(L)
```

```
  end
  KG11=zeros(8,8);
  for j=1:8
      for u=1:8
          KG11(j,u)=Kg(j,u);
      end
  end
    KG22=zeros(8,8);
  for j=1:8
      for u=1:8
          KG22(j,u)=Kg(j+8,u+8);
      end
  end
    KG12=zeros(8,8);
  for j=1:8
      for u=1:8
          KG12(j,u)=Kg(j,u+8);
      end
  end
    KG21=zeros(8,8);
  for j=1:8
      for u=1:8
          KG21(j,u)=Kg(j+8,u);
      end
  end

%*************************************************************************
  % STEP 4: ESTABLISH THE GLOBAL STIFFNESS MATRIX

%*************************************************************************
  Klocal=[(KG11+KG22) KG12; KG21 (KG11+KG22)];
  %if n==1
   %   Kglobal=zeros(8,8);
    %  for j=1:8
     %     for u=1:8
      %       Kglobal(j,u)=KG22(j,u);
       %   end
     % end
  %else
      Kglobal1=zeros(n*8,n*8);
      for j=1:16
          for u=1:16
              Kglobal1(j,u)=Klocal(j,u);
          end
      end
      for j=9:8:(n*8-7)
          for u=j:(j+15)
              for p=j:(j+15)
                  Kglobal1(u,p)=Kglobal1(u-8,p-8);
              end
          end
      end
      for j=(n*8-7):(n*8)
          for u=(n*8-7):(n*8)
              Kglobal1(j,u)=KG22(j-(n*8-7)+1,u-(n*8-7)+1);
          end
      end
```

```
      Kglobal=zeros(8*n,8*n);
      for j=1:(8*n)
          for p=1:(8*n)
              Kglobal(j,p)=Kglobal1(j,p);
          end
      end
  %end
  %disp(Kglobal);
  Inverse_Kgobal=inv(Kglobal);

%*************************************************************************
  % Load matrix:

%*************************************************************************
  P=zeros(8*n,1);
      P((8*n-7),1)=12; %Apply lateral load at shear center of wide flange
beam at free end
      %P((8*n-2),1)=3.27118; %Apply twisting moment at free end about
shear center of wide flange beam
  % DISPLACEMENT FIELD:
  Displacement_field=Kglobal\P;
  displacement_at_free_end=[Displacement_field(8*n-
7);Displacement_field(8*n-6);Displacement_field(8*n-
5);Displacement_field(8*n-4);Displacement_field(8*n-
3);Displacement_field(8*n-2);Displacement_field(8*n-
1);Displacement_field(8*n);];
    %----------------------------------------------------------------------
  % NODAL DISPLACEMENT VECTOR
  %-----------------------------------------------------------------------
  % Nodal displacement vector:
  Displacement_field_small=Inverse_Kgobal*P;

  % Full of nodal displacement vector (includes zero displacements at
  % constrains):
  Displacement_field=zeros(8*(n+1),1);
  for i=1:8
      Displacement_field(i,1)=0;
  end
  Displacement_field(2,1)=Displacement_field_small(1,1);
  for i=9:(8*(n+1))
      Displacement_field(i,1)=Displacement_field_small(i-8,1);
  end
  Displacement_field;
  % Extracting lateral displacement field at the beam centroid:
  displacement_Utotal=zeros(n+1,1);
  for i=1:(n+1)
      displacement_Utotal(i,1)=Displacement_field(1+8*(i-1),1);
  end
  % Extracting twisting angle:
  theta_ztotal=zeros(n+1,1);
  for i=1:(n+1)
      theta_ztotal(i,1)=Displacement_field(6+8*(i-1),1);
  end
  %-----------------------------------------------------------------------
  % OUTPUT OF NODAL STRESSES
  %-----------------------------------------------------------------------
```

```
  % Longitudinal normal stress at bottom surface of bottom flange:
  normalstress_bottom_zb=zeros(n+1,1);
  % Longitudinal normal stress at top surface of GFRP plate:
  normalstress_top_zp=zeros(n+1,1);
  % Shear stress sigma_sna
  sigma_sna=zeros(n+1,1);
  % Shear stress sigma_sza at top surface
  sigma_sza_top=zeros(n+1,1);
  for i=1:n
      El_displacement=zeros(16,1);
      for j=1:16
      El_displacement(j,1)=Displacement_field(j+8*(i-1),1);
      end
      % Element nodal force vector:
      El_Force=vpa(Kg*El_displacement,10);
      % Reaction forces:
      reactions=vpa(El_Force,10);
      % Normal stress_zb
      normalstress_bottom_zb(i,1)=Eb*((bb/2)*(-El_Force(3,1))/(Eb*Iyybf)-
(hb*bb/4)*(-El_Force(8,1))/(Eb*Iwwbg));
      normalstress_bottom_zb(i+1,1)=Eb*((bb/2)*El_Force(11,1)/(Eb*Iyybf)-
(hb*bb/4)*El_Force(16,1)/(Eb*Iwwbg));
      % Normal stress_zp
      normalstress_top_zp(i,1)=Ep*(-(-bb/2)*(-El_Force(5,1))/(Ep*Iyyp)+(-
t1*bb/4)*(-El_Force(7,1))/(Eb*Iwwbl+Ep*Iwwp));
      normalstress_top_zp(i+1,1)=Ep*(-(-bb/2)*El_Force(13,1)/(Ep*Iyyp)+(-
t1*bb/4)*El_Force(15,1)/(Eb*Iwwbl+Ep*Iwwp));
      % Shear stress sigma_sna
      sigma_sna(i,1)=Ga*(-c1*El_displacement(1,1)+c1*El_displacement(4,1)-
(c2+c3)*El_displacement(6,1));
      sigma_sna(i+1,1)=Ga*(-
c1*El_displacement(9,1)+c1*El_displacement(12,1)-
(c2+c3)*El_displacement(14,1));
      % Shear stress sigma_sza
      Up_prime0=((-El_Force(4,1)))/(Gp*Ap+Ga*Aa/3)+El_displacement(5,1)-
((Ga*Aa)/(12*(Gp*Ap+Ga*Aa/3)))*(2*El_displacement(2,1)-
2*El_displacement(3,1)+c5*El_displacement(7,1)-hb*El_displacement(8,1));
      Up_primeL=((El_Force(12,1)))/(Gp*Ap+Ga*Aa/3)+El_displacement(13,1)-
((Ga*Aa)/(12*(Gp*Ap+Ga*Aa/3)))*(2*El_displacement(10,1)-
2*El_displacement(11,1)+c5*El_displacement(15,1)-
hb*El_displacement(16,1));
      sigma_sza_top(i,1)=Ga*(Up_prime0+(-t1)*El_displacement(7,1)-
El_displacement(5,1));
      %sigma_sza_top(i+1,1)=Ga*(-Up_primeL-(-
t1)*El_displacement(15,1)+El_displacement(13,1));
  end
%-----------------------------------------------------------------------
% DISPLAYING DISPLACEMENTS AND STRESSES
%-----------------------------------------------------------------------
disp('displacement_Ub:');
displacement_Ub_showed=zeros(11,1);
coordinate_z=zeros(11,1);
     displacement_Ub_showed(1,1)=displacement_Utotal(1,1);
     coordinate_z(1,1)=0;
     displacement_Ub_showed(11,1)=displacement_Utotal(n+1,1);
     coordinate_z(11,1)=Ltotal;
for i=1:9
```

```
     displacement_Ub_showed(i+1,1)=displacement_Utotal(round(n*i/10)+1,1);
     coordinate_z(i+1,1)=(round(n*i/10))*(Ltotal/n);
end
% Display results on screen:
   fprintf('Z-coordinate(m) \t Value(m) \r');
   for i=1:11
       fprintf('%3.2e\t\t\t %3.2e\t\t\t\n', coordinate_z(i,1),
displacement_Ub_showed(i,1));
   end
disp('-----------------------------------------------------------');
%--------------------------------------------------------------------------
%--------------------------------------------------------------------------
disp('normal_stress_bottom_zb:');
normalstress_bottom_zb_showed=zeros(11,1);
coordinate_zb=zeros(11,1);
     normalstress_bottom_zb_showed(1,1)=normalstress_bottom_zb(1,1);
     coordinate_zb(1,1)=0;
     normalstress_bottom_zb_showed(11,1)=normalstress_bottom_zb(n+1,1);
     coordinate_zb(11,1)=Ltotal;
for i=1:9

normalstress_bottom_zb_showed(i+1,1)=normalstress_bottom_zb(round(n*i/10)+
1,1);
     coordinate_zb(i+1,1)=(round(n*i/10))*(Ltotal/n);
end
% Display results on screen:
   fprintf('Z-coordinate(m) \t Value(kPa) \r');
   for i=1:11
       fprintf('%3.2e\t\t\t %3.2e\t\t\t\n', coordinate_zb(i,1),
normalstress_bottom_zb_showed(i,1));
   end
disp('-----------------------------------------------------------');
%--------------------------------------------------------------------------
%--------------------------------------------------------------------------
disp('normal_stress_top_zp:');
normalstress_top_zp_showed=zeros(11,1);
coordinate_zp=zeros(11,1);
     normalstress_top_zp_showed(1,1)=normalstress_top_zp(1,1);
     coordinate_zp(1,1)=0;
     normalstress_top_zp_showed(11,1)=normalstress_top_zp(n+1,1);
     coordinate_zp(11,1)=Ltotal;
for i=1:9

normalstress_top_zp_showed(i+1,1)=normalstress_top_zp(round(n*i/10)+1,1);
     coordinate_zp(i+1,1)=(round(n*i/10))*(Ltotal/n);
end
% Display results on screen:
   fprintf('Z-coordinate(m) \t Value(kPa) \r');
   for i=1:11
       fprintf('%3.2e\t\t\t %3.2e\t\t\t\n', coordinate_zp(i,1),
normalstress_top_zp_showed(i,1));
   end
disp('-----------------------------------------------------------');
%--------------------------------------------------------------------------
%--------------------------------------------------------------------------
disp('shear_stress_sn:');
sigma_sna_showed=zeros(11,1);
```

```
coordinate_sn=zeros(11,1);
     sigma_sna_showed(1,1)=sigma_sna(1,1);
     coordinate_sn(1,1)=0;
     sigma_sna_showed(11,1)=sigma_sna(n+1,1);
     coordinate_sn(11,1)=Ltotal;
for i=1:9
     sigma_sna_showed(i+1,1)=sigma_sna(round(n*i/10)+1,1);
     coordinate_sn(i+1,1)=(round(n*i/10))*(Ltotal/n);
end
% Display results on screen:
   fprintf('Z-coordinate(m) \t Value(kPa) \r');
   for i=1:11
       fprintf('%3.2e\t\t\t %3.2e\t\t\t\n', coordinate_sn(i,1),
sigma_sna_showed(i,1));
   end
disp('-----------------------------------------------------------');
%--------------------------------------------------------------------------
%--------------------------------------------------------------------------
disp('shear_stress_sz:');
sigma_sza_top_showed=zeros(11,1);
coordinate_sz=zeros(11,1);
     sigma_sza_top_showed(1,1)=sigma_sza_top(1,1);
     coordinate_sz(1,1)=0;
     sigma_sza_top_showed(11,1)=sigma_sza_top(n+1,1);
     coordinate_sz(11,1)=Ltotal;
for i=1:9
     sigma_sza_top_showed(i+1,1)=sigma_sza_top(round(n*i/10)+1,1);
     coordinate_sz(i+1,1)=(round(n*i/10))*(Ltotal/n);
end
% Display results on screen:
   fprintf('Z-coordinate(m) \t Value(kPa) \r');
   for i=1:11
       fprintf('%3.2e\t\t\t %3.2e\t\t\t\n', coordinate_sz(i,1),
sigma_sza_top_showed(i,1));
   end
disp('-----------------------------------------------------------');
end
%--------------------------------------------------------------------------
%----------------------END OF FINITE ELEMENT SOLUTION----------------------
%--------------------------------------------------------------------------
-
```

B5.3.2 Outputs of the Finite Element Solution

B5.3.2.1 Problem 2-Bending about weak axis

CASE NUMBER 15:

Input number of segments n=160
----
displacement_Ub:

Z-coordinate(m)	Value(m)
0.00e+000	0.00e+000
5.00e-001	1.83e-003

1.00e+000	7.03e-003
1.50e+000	1.52e-002
2.00e+000	2.61e-002
2.50e+000	3.91e-002
3.00e+000	5.41e-002
3.50e+000	7.05e-002
4.00e+000	8.81e-002
4.50e+000	1.06e-001
5.00e+000	1.25e-001

----

normal_stress_bottom_zb:

Z-coordinate(m)	Value(kPa)
0.00e+000	2.78e+005
5.00e-001	2.49e+005
1.00e+000	2.20e+005
1.50e+000	1.92e+005
2.00e+000	1.64e+005
2.50e+000	1.36e+005
3.00e+000	1.09e+005
3.50e+000	8.17e+004
4.00e+000	5.44e+004
4.50e+000	2.72e+004
5.00e+000	-1.36e-007

----

normal_stress_top_zp:

Z-coordinate(m)	Value(kPa)
0.00e+000	5.59e+004
5.00e-001	5.11e+004
1.00e+000	4.56e+004
1.50e+000	4.00e+004
2.00e+000	3.43e+004
2.50e+000	2.87e+004
3.00e+000	2.29e+004
3.50e+000	1.72e+004
4.00e+000	1.15e+004
4.50e+000	5.74e+003
5.00e+000	-6.73e-008

----

shear_stress_sn:

Z-coordinate(m)	Value(kPa)
0.00e+000	0.00e+000
5.00e-001	-2.24e+002
1.00e+000	-1.98e+002
1.50e+000	-1.72e+002
2.00e+000	-1.47e+002
2.50e+000	-1.23e+002
3.00e+000	-9.80e+001
3.50e+000	-7.35e+001
4.00e+000	-4.90e+001
4.50e+000	-2.45e+001
5.00e+000	2.51e+002

----
shear_stress_sz:

Z-coordinate(m)	Value(kPa)
0.00e+000	0.00e+000
5.00e-001	6.82e+000
1.00e+000	6.21e+000
1.50e+000	5.82e+000
2.00e+000	5.57e+000
2.50e+000	5.40e+000
3.00e+000	5.30e+000
3.50e+000	5.23e+000
4.00e+000	5.19e+000
4.50e+000	5.17e+000
5.00e+000	0.00e+000

>>

B5.3.2.2 Problem 3-Twisting about the beam centroid for the case $L = 5.0m$ and $G_a = 0.4GPa$

CASE NUMBER 15:

Input number of segments n=160
----
displacement_Ub:

Z-coordinate(m)	Value(m)
0.00e+000	0.00e+000
5.00e-001	-5.63e-005
1.00e+000	-1.95e-004
1.50e+000	-3.87e-004
2.00e+000	-6.14e-004
2.50e+000	-8.63e-004
3.00e+000	-1.13e-003
3.50e+000	-1.40e-003
4.00e+000	-1.68e-003
4.50e+000	-1.96e-003
5.00e+000	-2.24e-003

----
normal_stress_bottom_zb:

Z-coordinate(m)	Value(kPa)
0.00e+000	-9.23e+004
5.00e-001	-5.98e+004
1.00e+000	-3.86e+004
1.50e+000	-2.49e+004
2.00e+000	-1.60e+004
2.50e+000	-1.03e+004
3.00e+000	-6.63e+003
3.50e+000	-4.23e+003
4.00e+000	-2.66e+003
4.50e+000	-1.61e+003
5.00e+000	-1.85e-008

----

normal_stress_top_zp:

Z-coordinate(m)	Value(kPa)
0.00e+000	1.25e+004
5.00e-001	9.51e+003
1.00e+000	6.13e+003
1.50e+000	3.96e+003
2.00e+000	2.55e+003
2.50e+000	1.64e+003
3.00e+000	1.06e+003
3.50e+000	6.74e+002
4.00e+000	4.24e+002
4.50e+000	2.56e+002
5.00e+000	4.90e-009

----

shear_stress_sn:

Z-coordinate(m)	Value(kPa)
0.00e+000	0.00e+000
5.00e-001	5.30e+001
1.00e+000	3.42e+001
1.50e+000	2.21e+001
2.00e+000	1.42e+001
2.50e+000	9.16e+000
3.00e+000	5.88e+000
3.50e+000	3.76e+000
4.00e+000	2.36e+000
4.50e+000	1.47e+000
5.00e+000	-5.73e+003

----

shear_stress_sz:

Z-coordinate(m)	Value(kPa)
0.00e+000	1.41e+001
5.00e-001	2.22e+001
1.00e+000	2.98e+001
1.50e+000	3.47e+001
2.00e+000	3.78e+001
2.50e+000	3.98e+001
3.00e+000	4.11e+001
3.50e+000	4.20e+001
4.00e+000	4.25e+001
4.50e+000	4.28e+001
5.00e+000	0.00e+000

APPENDIX B6-ABAQUS PARAMETERIZED INPUT FILES

B6.1 Cantilever composite beam under transverse point load applied at tip

```
*Heading
Cantilever beam under transverse point load applied at tip
SI units (kg, mm, s, N)
*PARAMETER
##############################################################
L   = 1500   # Total length of the beam
########################################
h   = 138.2 # Depth of the web
tw  = 4.3    # Thickness of the web
t3  = 4.9     # Thickness of the flange
bb  = 100    # Width of flange
Eb  = 200.E3  # Modulus of elasticity of steel (N/mm2)
v   = 0.3     # Poisson's ratio
########################################
bp  = 100    # With of GFRP plate
t1  = 19.0     # Thickness of GFRP plate
Ep  = 42.E3  # Modulus of elasticity of FRP (N/mm2)
########################################
t2  = 0.79   # Thickness of adhesive layer
Ea  = 11.7E3   # Modulus of elasticity of adhesive (N/mm2)
##############################################################
n1  = 22   # Number of elements on the X-direction for a half of flange cantilevel
n2  = 4    # Number of elements on the X-direction for the web
n3  = 4    # Number of elements on the Y-direction for the flange
n4  = 50    # Number of elements on the Y-direction for the web
n5  = 4    # Number of elements on the Y-direction for the adhesive layer
n6  = 8    # Number of elements on the Y-direction for the GFRP plate
n7  = 750   # Number of elements on the Z-direction 1
##############################################################
b1=(bb-tw)/2  # Width of one flange cantilever
b2=b1+tw
h1=t3+h
h2=h+2*t3
h3=h2+t2
h4=h3+t1
ha=h2+t2/n5
### Increment in nodel numbers
###
nflange1x=1           # Increment in node numbers for the flange cantilevel 1 (x-direction)
nflange1y=2*n1+n2+1    # Increment in node numbers for the flange cantilevel 1 (y-direction)
nflange1z=2000        # Increment in node numbers for the flange cantilevel 1 (z-direction)
```

```
###
nwebx=1          # Increment in node numbers for the web (x-direction)
nweby=n2+1       # Increment in node numbers for the web (y-direction)
nwebz=2000       # Increment in node numbers for the web (z-direction)
###
### Increment in element numbers
###
elflange1x=1         # Increment in element numbers for the flange cantilevel 1 (x-direction)
elflange1y=2*n1+n2   # Increment in element numbers for the flange cantilevel 1 (y-direction)
elflange1z=2000      # Increment in element numbers for the flange cantilevel 1 (z-direction)
###
elwebx=1         # Increment in element numbers for the web (x-direction)
elweby=n2        # Increment in element numbers for the web (y-direction)
elwebz=2000      # Increment in element numbers for the web (z-direction)
################################################################################
### Number of generating nodes
### For the I beam
## At Z=0
A1bo = 1
A2bo = n1+1
A3bo = n1+n2+1
A4bo = 2*n1+n2+1
A5bo = (2*n1+n2+1)*n3+1
A6bo = (2*n1+n2+1)*(n3+1)-(n1+n2)
A7bo = (2*n1+n2+1)*(n3+1)-n1
A8bo = (2*n1+n2+1)*(n3+1)
A9bo1 = A8bo+1
A10bo1= A8bo+1+n2
A9bo2 = A8bo+(n2+1)*(n4-1)-n2
A10bo2= A8bo+(n2+1)*(n4-1)
A11bo= A10bo2+1
A12bo= A10bo2+n1+1
A13bo= A10bo2+n1+n2+1
A14bo= A10bo2+2*n1+n2+1
A15bo= A10bo2+(2*n1+n2+1)*(n3+1)-(2*n1+n2)
A16bo= A10bo2+(2*n1+n2+1)*(n3+1)-(n1+n2)
A17bo= A10bo2+(2*n1+n2+1)*(n3+1)-n1
A18bo= A10bo2+(2*n1+n2+1)*(n3+1)
## At Z=L
A1bl = 2000*n7+1
A2bl = 2000*n7+n1+1
A3bl = 2000*n7+n1+n2+1
A4bl = 2000*n7+2*n1+n2+1
A5bl = 2000*n7+(2*n1+n2+1)*n3+1
A6bl = 2000*n7+(2*n1+n2+1)*(n3+1)-(n1+n2)
A7bl = 2000*n7+(2*n1+n2+1)*(n3+1)-n1
A8bl = 2000*n7+(2*n1+n2+1)*(n3+1)
A9bl1 = A8bl+1
```

```
A10bl1= A8bl+1+n2
A9bl2 = A8bl+(n2+1)*(n4-1)-n2
A10bl2= A8bl+(n2+1)*(n4-1)
A11bl= A10bl2+1
A12bl= A10bl2+n1+1
A13bl= A10bl2+n1+n2+1
A14bl= A10bl2+2*n1+n2+1
A15bl= A10bl2+(2*n1+n2+1)*(n3+1)-(2*n1+n2)
A16bl= A10bl2+(2*n1+n2+1)*(n3+1)-(n1+n2)
A17bl= A10bl2+(2*n1+n2+1)*(n3+1)-n1
A18bl= A10bl2+(2*n1+n2+1)*(n3+1)
### For the adhesive layer
## At Z=0
A1ao = A18bo+1
A2ao = A18bo+1+n1
A3ao = A18bo+1+n1+n2
A4ao = A18bo+1+n1+n2+n1
A5ao = A15bo+(2*n1+n2+1)*n5
A6ao = A15bo+(2*n1+n2+1)*n5+n1
A7ao = A15bo+(2*n1+n2+1)*n5+n1+n2
A8ao = A15bo+(2*n1+n2+1)*n5+2*n1+n2
## At Z=L
A1al = A18bl+1
A2al = A18bl+1+n1
A3al = A18bl+1+n1+n2
A4al = A18bl+1+n1+n2+n1
A5al = A15bl+(2*n1+n2+1)*n5
A6al = A15bl+(2*n1+n2+1)*n5+n1
A7al = A15bl+(2*n1+n2+1)*n5+n1+n2
A8al = A15bl+(2*n1+n2+1)*n5+2*n1+n2
### For the GFRP plate
## At Z=0
A1po = A5ao
A2po = A6ao
A3po = A7ao
A4po = A8ao
A5po = A5ao+(2*n1+n2+1)*n6
A6po = A5ao+(2*n1+n2+1)*n6+n1
A7po = A5ao+(2*n1+n2+1)*n6+n1+n2
A8po = A5ao+(2*n1+n2+1)*n6+2*n1+n2
## At Z=L
A1pl = A5al
A2pl = A6al
A3pl = A7al
A4pl = A8al
A5pl = A5al+(2*n1+n2+1)*n6
A6pl = A5al+(2*n1+n2+1)*n6+n1
A7pl = A5al+(2*n1+n2+1)*n6+n1+n2
```

```
A8pl = A5al+(2*n1+n2+1)*n6+2*n1+n2
###########################################################################
### Define the Y-coordinate of nodes 9, 10
YA9bo1 = t3+h/n4
YA10bo1= t3+h/n4
YA9bo2 = t3+h-h/n4
YA10bo2= t3+h-h/n4
### Number of node row in Y-direction for center web part
NRYCW=n4-2
### Number of node row in Y-direction for adhesive upper part
NRYUAD=n5-1
###########################################################################
### elements of final layer at z=L
firstelementwebatL=2000*(n7-1)+(2*n1+n2)*n3+1
secondelementwebatL=2000*(n7-1)+(2*n1+n2)*n3+n2*n4
###########################################################################
### Nodes of master element of bottom layer the bottom flange
Nmeblbf1=1
Nmeblbf2=2001
Nmeblbf3=2002
Nmeblbf4=2
Nmeblbf5=2*n1+n2+1+1
Nmeblbf6=2000+2*n1+n2+1+1
Nmeblbf7=2000+2*n1+n2+1+2
Nmeblbf8=2*n1+n2+1+2
### Nodes of master element of upper layerS the bottom flange
Nmeulbf1=2*n1+n2+1+1
Nmeulbf2=2000+2*n1+n2+1+1
Nmeulbf3=2000+2*n1+n2+1+2
Nmeulbf4=2*n1+n2+1+2
Nmeulbf5=(2*n1+n2+1)*2+1
Nmeulbf6=2000+(2*n1+n2+1)*2+1
Nmeulbf7=2000+(2*n1+n2+1)*2+1+1
Nmeulbf8=(2*n1+n2+1)*2+1+1
### Nodes of master element of the bottom web
Nmebw1=A6bo
Nmebw2=2000+A6bo
Nmebw3=2000+A6bo+1
Nmebw4=A6bo+1
Nmebw5=(2*n1+n2+1)*(n3+1)+1
Nmebw6=2000+(2*n1+n2+1)*(n3+1)+1
Nmebw7=2000+(2*n1+n2+1)*(n3+1)+2
Nmebw8=(2*n1+n2+1)*(n3+1)+2
### Nodes of master element of the center web
Nmecw1=(2*n1+n2+1)*(n3+1)+1
Nmecw2=2000+(2*n1+n2+1)*(n3+1)+1
Nmecw3=2000+(2*n1+n2+1)*(n3+1)+1+1
Nmecw4=(2*n1+n2+1)*(n3+1)+1+1
```

```
Nmecw5=(2*n1+n2+1)*(n3+1)+1+n2+1
Nmecw6=2000+(2*n1+n2+1)*(n3+1)+1+n2+1
Nmecw7=2000+(2*n1+n2+1)*(n3+1)+1+n2+2
Nmecw8=(2*n1+n2+1)*(n3+1)+1+n2+2
### Nodes of master element of the top web
Nmetw1=A9bo2
Nmetw2=2000+A9bo2
Nmetw3=2000+A9bo2+1
Nmetw4=A9bo2+1
Nmetw5=A12bo
Nmetw6=2000+A12bo
Nmetw7=2000+A12bo+1
Nmetw8=A12bo+1
### Nodes of master element of the top flange
Nmetf1=A11bo
Nmetf2=2000+A11bo
Nmetf3=2000+A11bo+1
Nmetf4=A11bo+1
Nmetf5=A11bo+2*n1+n2+1
Nmetf6=2000+A11bo+2*n1+n2+1
Nmetf7=2000+A11bo+2*n1+n2+1+1
Nmetf8=A11bo+2*n1+n2+1+1
### Nodes of master element of the adhesive layer
Nmeal1=A15bo
Nmeal2=2000+A15bo
Nmeal3=2000+A15bo+1
Nmeal4=A15bo+1
Nmeal5=A15bo+2*n1+n2+1
Nmeal6=2000+A15bo+2*n1+n2+1
Nmeal7=2000+A15bo+2*n1+n2+1+1
Nmeal8=A15bo+2*n1+n2+1+1
### Nodes of master element of the FRP plate
Nmefp1=A5ao
Nmefp2=2000+A5ao
Nmefp3=2000+A5ao+1
Nmefp4=A5ao+1
Nmefp5=A5ao+2*n1+n2+1
Nmefp6=2000+A5ao+2*n1+n2+1
Nmefp7=2000+A5ao+2*n1+n2+1+1
Nmefp8=A5ao+2*n1+n2+1+1
################################################################################
### Master element number
### Master element 1 for bottom flange
Mael1=1
### Master element 1 for bottom web
Mael2=(2*n1+n2)*n3+1
### Master element 1 for center web
Mael3=(2*n1+n2)*n3+1+n2
```

```
### Master element 1 for top web
Mael4=(2*n1+n2)*n3+n2*(n4-1)+1
### Master element 1 for top flange
Mael5=(2*n1+n2)*n3+n2*n4+1
### Master element 1 for adhesive layer
Mael6=(2*n1+n2)*n3*2+n2*n4+1
### Master element 1 for bottom flange
Mael7=(2*n1+n2)*n3*2+n2*n4+(2*n1+n2)*n5+1
##############################################################################
### Element numbers needs to be generated in Y direction
### For upper layers of bottom flange
numberulbfy=n3-1
### For center web
numbercw=n4-2
### Elements numbers needs to be generated in X direction for the flanges
numberelbfx=2*n1+n2
### Parameters related to the NCOPY command
### For right bottom flange part 2
c1=n1+n2
### For left + right flange
c2=A10bo2
##############################################################################
###eloutput11=(2*n1+n2)*n3+(n4*n2)+1+2000*(n7-2340)
###eloutput21=(2*n1+n2)*n3+(n4*n2)+(2*n1+n2)*n5+2000*(n7-2340)
###eloutput12=(2*n1+n2)*n3+(n4*n2)+1+2000*(n7-1560)
###eloutput22=(2*n1+n2)*n3+(n4*n2)+(2*n1+n2)*n5+2000*(n7-1560)
###eloutput13=(2*n1+n2)*n3+(n4*n2)+1+2000*(n7-780)
###eloutput23=(2*n1+n2)*n3+(n4*n2)+(2*n1+n2)*n5+2000*(n7-780)
##############################################################################
beamcentroidat0=(2*n1+n2+1)*(n3+1)+(n2+1)*(n4/2)-n2/2
beamcentroidatL=2000*n7+(2*n1+n2+1)*(n3+1)+(n2+1)*(n4)/2-n2/2
bottomflangecentroidat0=(2*n1+n2+1)*((n3/2)+1)-n1-n2/2
bottomflangecentroidatL=2000*n7+(2*n1+n2+1)*((n3/2)+1)-n1-n2/2
upperflangecentroidat0=(2*n1+n2+1)*(n3+1)+(n2+1)*(n4-1)+(2*n1+n2+1)*((n3/2)+1)-n1-n2/2
upperflangecentroidatL=2000*n7+(2*n1+n2+1)*(n3+1)+(n2+1)*(n4-1)+(2*n1+n2+1)*((n3/2)+1)-n1-
n2/2
GFRPcentroidat0=(2*n1+n2+1)*(n3+1)*2+(n2+1)*(n4-1)+(2*n1+n2+1)*(n5-
1)+(2*n1+n2+1)*((n6/2)+1)-n1-n2/2
GFRPcentroidatL=2000*n7+(2*n1+n2+1)*(n3+1)*2+(n2+1)*(n4-1)+(2*n1+n2+1)*(n5-
1)+(2*n1+n2+1)*((n6/2)+1)-n1-n2/2
##############################################################################
*PREPRINT, ECHO=YES, MODEL=YES, HISTORY=YES
**
**Model denifition
*NODE
<A1bo>, 0.0, 0.0, 0.0
<A2bo>, <b1>, 0.0, 0.0
<A3bo>, <b2>, 0.0, 0.0
```

```
<A4bo>, <bb>, 0.0, 0.0
<A5bo>, 0.0, <t3>, 0.0
<A6bo>, <b1>, <t3>, 0.0
<A7bo>, <b2>, <t3>, 0.0
<A8bo>, <bb>, <t3>, 0.0
<A9bo1>, <b1>, <YA9bo1>, 0.0
<A10bo1>, <b2>, <YA10bo1>, 0.0
<A9bo2>, <b1>, <YA9bo2>, 0.0
<A10bo2>, <b2>, <YA10bo2>, 0.0
<A11bo>, 0.0, <h1>, 0.0
<A12bo>, <b1>, <h1>, 0.0
<A13bo>, <b2>, <h1>, 0.0
<A14bo>, <bb>, <h1>, 0.0
<A15bo>, 0.0, <h2>, 0.0
<A16bo>, <b1>, <h2>, 0.0
<A17bo>, <b2>, <h2>, 0.0
<A18bo>, <bb>, <h2>, 0.0
**
<A1ao>, 0.0, <ha>, 0.0
<A2ao>, <b1>, <ha>, 0.0
<A3ao>, <b2>, <ha>, 0.0
<A4ao>, <bb>, <ha>, 0.0
<A5ao>, 0.0, <h3>, 0.0
<A6ao>, <b1>, <h3>, 0.0
<A7ao>, <b2>, <h3>, 0.0
<A8ao>, <bb>, <h3>, 0.0
**
<A5po>, 0.0, <h4>, 0.0
<A6po>, <b1>, <h4>, 0.0
<A7po>, <b2>, <h4>, 0.0
<A8po>, <bb>, <h4>, 0.0
**
<A1bl>, 0.0, 0.0, <L>
<A2bl>, <b1>, 0.0, <L>
<A3bl>, <b2>, 0.0, <L>
<A4bl>, <bb>, 0.0, <L>
<A5bl>, 0.0, <t3>, <L>
<A6bl>, <b1>, <t3>, <L>
<A7bl>, <b2>, <t3>, <L>
<A8bl>, <bb>, <t3>, <L>
<A9bl1>, <b1>, <YA9bo1>, <L>
<A10bl1>, <b2>, <YA10bo1>, <L>
<A9bl2>, <b1>, <YA9bo2>, <L>
<A10bl2>, <b2>, <YA10bo2>, <L>
<A11bl>, 0.0, <h1>, <L>
<A12bl>, <b1>, <h1>, <L>
<A13bl>, <b2>, <h1>, <L>
<A14bl>, <bb>, <h1>, <L>
```

```
<A15bl>, 0.0, <h2>, <L>
<A16bl>, <b1>, <h2>, <L>
<A17bl>, <b2>, <h2>, <L>
<A18bl>, <bb>, <h2>, <L>
**
<A1al>, 0.0, <ha>, <L>
<A2al>, <b1>, <ha>, <L>
<A3al>, <b2>, <ha>, <L>
<A4al>, <bb>, <ha>, <L>
<A5al>, 0.0, <h3>, <L>
<A6al>, <b1>, <h3>, <L>
<A7al>, <b2>, <h3>, <L>
<A8al>, <bb>, <h3>, <L>
**
<A5pl>, 0.0, <h4>, <L>
<A6pl>, <b1>, <h4>, <L>
<A7pl>, <b2>, <h4>, <L>
<A8pl>, <bb>, <h4>, <L>
**
**Node set of left bottom edge of bottom flange 1 along z axis
*NGEN, NSET=LBEBF1
<A1bo>, <A1bl>, 2000
**Node set of left upper edge of bottom flange 1 along z axis
*NGEN, NSET=LUEBF1
<A5bo>, <A5bl>, 2000
**Node set of left surface of bottom flange 1 along z axis
*NFILL, NSET=LSBF1
LBEBF1, LUEBF1, <n3>, <nflange1y>
**
**Node set of right bottom edge of bottom flange 1 along z axis
*NGEN, NSET=RBEBF1
<A2bo>, <A2bl>, 2000
**Node set of right upper edge of bottom flange 1 along z axis
*NGEN, NSET=RUEBF1
<A6bo>, <A6bl>, 2000
**Node set of right surface of bottom flange 1 along z axis
*NFILL, NSET=RSBF1
RBEBF1, RUEBF1, <n3>, <nflange1y>
**
**Node set of bottom flange block 1
*NFILL, NSET=BFB1
LSBF1, RSBF1, <n1>, 1
**
**Node set of bottom flange block 2
*NCOPY, OLDSET=BFB1, CHANGENUMBER=<c1>, NEWSET=BFB2, SHIFT
<b2>, 0.0, 0.0
0.0, 0.0, 0.0, 0.0, 0.0, 1.0, 0.0
**Node set of center bottom flange part
```

```
*NSET, NSET=abc1, GENERATE
<A3bo>, <A3bl>, 2000
*NSET, NSET=abc2, GENERATE
<A7bo>, <A7bl>, 2000
*NFILL, NSET=bottomweb1
RBEBF1, abc1, <n2>, 1
*NFILL, NSET=upperbottomweb2
RUEBF1, abc2, <n2>, 1
*NFILL, NSET=centerbottomflange
bottomweb1, upperbottomweb2, <n3>, <nflange1y>
**
**Bottom flange
*NSET, NSET=bottomflange
BFB1, centerbottomflange, BFB2
**Node set of unpper flange
*NCOPY, OLDSET=bottomflange, CHANGENUMBER=<c2>, NEWSET=upperflange, SHIFT
0.0, <h1>, 0.0
0.0, 0.0, 0.0, 0.0, 0.0, 1.0, 0.0
**Node set for the center Web
** Node line at left upper edge of the center web
*NGEN, NSET=LUECW
<A9bo2>, <A9bl2>, 2000
** Node line at right upper edge of the center web
*NGEN, NSET=RUECW
<A10bo2>, <A10bl2>, 2000
** Node set at upper surface of the center web
*NFILL, NSET=USCW
LUECW, RUECW, <n2>, 1
**
** Node line at left bottom edge of the center web
*NGEN, NSET=LBECW
<A9bo1>, <A9bl1>, 2000
** Node line at right bottom edge of the center web
*NGEN, NSET=RBECW
<A10bo1>, <A10bl1>, 2000
** Node set at bottom surface of the center web
*NFILL, NSET=BSCW
LBECW, RBECW, <n2>, 1
** Forming node set for the center web
*NFILL, NSET=centerweb
BSCW, USCW, <NRYCW>, <nweby>
**
**Node set for adhesive layer
**
**Bottom surface:
**Node line A1a, left bottom edge of adhesive layer
*NGEN, NSET=LBEAL
<A1ao>, <A1al>, 2000
```

```
*NGEN, NSET=lineA2a
<A2ao>, <A2al>, 2000
*NFILL, NSET=firstsurfacead
LBEAL, lineA2a, <n1>, 1
**
**Node line A3a, left bottom edge of adhesive layer
*NGEN, NSET=lineA3a
<A3ao>, <A3al>, 2000
*NFILL, NSET=secondsurfacead
lineA2a, lineA3a, <n2>, 1
**
**Node line A4a, left bottom edge of adhesive layer
*NGEN, NSET=lineA4a
<A4ao>, <A4al>, 2000
*NFILL, NSET=thirdsurfacead
lineA3a, lineA4a, <n1>, 1
**
**Bottom surface of adhesive layer
*NSET, NSET=BSAL
firstsurfacead, secondsurfacead, thirdsurfacead
**
**Upper surface:
**Node line A5a, left top edge of adhesive layer
*NGEN, NSET=LTEAL
<A5ao>, <A5al>, 2000
**Node line A6a
*NGEN, NSET=lineA6a
<A6ao>, <A6al>, 2000
**Node line A7a
*NGEN, NSET=lineA7a
<A7ao>, <A7al>, 2000
**Node line A8a, right top edge of adhesive layer
*NGEN, NSET=RTEAL
<A8ao>, <A8al>, 2000
**Node surface formed by A5a and A6a, A6a and A7a, A7a and A8a
*NFILL, NSET=SFA5aA6a
LTEAL, lineA6a, <n1>, 1
*NFILL, NSET=SFA6aA7a
lineA6a, lineA7a, <n2>, 1
*NFILL, NSET=SFA7aA8a
lineA7a, RTEAL, <n1>, 1
*NSET, NSET=uppersurfacead
SFA5aA6a, SFA6aA7a, SFA7aA8a
**
**Node set for adhesive layer:
*NFILL, NSET=adhesivelayernodeset
BSAL, uppersurfacead, <NRYUAD>, <nflange1y>
**
```

```
**Node set for GFRP plate
**
**Upper surface:
**Node line A5p, left top edge of GFRP plate
*NGEN, NSET=LTEGFRP
<A5po>, <A5pl>, 2000
**Node line A6p
*NGEN, NSET=lineA6p
<A6po>, <A6pl>, 2000
**Node line A7p
*NGEN, NSET=lineA7p
<A7po>, <A7pl>, 2000
**Node line A8p, right top edge of GFRP plate
*NGEN, NSET=RTEGFRP
<A8po>, <A8pl>, 2000
**Node surface formed by A5p and A6p, A6p and A7p, A7p and A8p
*NFILL, NSET=SFA5pA6p
LTEGFRP, lineA6p, <n1>, 1
*NFILL, NSET=SFA6pA7p
lineA6p, lineA7p, <n2>, 1
*NFILL, NSET=SFA7pA8p
lineA7p, RTEGFRP, <n1>, 1
*NSET, NSET=uppersurfacegfrp
SFA5pA6p, SFA6pA7p, SFA7pA8p
**Node set for GFRP plate:
*NFILL, NSET=gfrpplatenodeset
uppersurfacead, uppersurfacegfrp, <n6>, <nflange1y>
**Element generation
**Bottom flange:
**Creating master element for bottom flange
*ELEMENT, TYPE=C3D8R, ELSET=MAELBF
1, <Nmeblbf1>, <Nmeblbf2>, <Nmeblbf3>, <Nmeblbf4>, <Nmeblbf5>, <Nmeblbf6>, <Nmeblbf7>,
<Nmeblbf8>
**Creating element for bottom flange
*ELGEN, ELSET=elbottomflange
1, <numberelbfx>, <nflange1x>, <elflange1x>, <n3>, <nflange1y>, <elflange1y>, <n7>, <nflange1z>,
<elflange1z>
**
**Bottom web part:
**Creating master element for bottom web part
*ELEMENT, TYPE=C3D8R, ELSET=MAELBW
<Mael2>, <Nmebw1>, <Nmebw2>, <Nmebw3>, <Nmebw4>, <Nmebw5>, <Nmebw6>, <Nmebw7>,
<Nmebw8>
**Creating element for bottom web part
*ELGEN, ELSET=elebottomweb
<Mael2>, <n2>, <nwebx>, <elwebx>, 1, <nweby>, <elweby>, <n7>, <nwebz>, <elwebz>
**
**Center web part:
```

```
**Creating master element for center web part
*ELEMENT, TYPE=C3D8R, ELSET=MAELCW
<Mael3>, <Nmecw1>, <Nmecw2>, <Nmecw3>, <Nmecw4>, <Nmecw5>, <Nmecw6>, <Nmecw7>,
<Nmecw8>
**Creating element for center web part
*ELGEN, ELSET=elecenterweb
<Mael3>, <n2>, <nwebx>, <elwebx>, <numbercw>, <nweby>, <elweby>, <n7>, <nwebz>, <elwebz>
**
**Top web part:
**Creating master element for top web part
*ELEMENT, TYPE=C3D8R, ELSET=MAELTW
<Mael4>, <Nmetw1>, <Nmetw2>, <Nmetw3>, <Nmetw4>, <Nmetw5>, <Nmetw6>, <Nmetw7>,
<Nmetw8>
**Creating element for top web part
*ELGEN, ELSET=eletopweb
<Mael4>, <n2>, <nwebx>, <elwebx>, 1, <nweby>, <elweby>, <n7>, <nwebz>, <elwebz>
**
**Top flange:
**Creating master element for top flange
*ELEMENT, TYPE=C3D8R, ELSET=MAELTF
<Mael5>, <Nmetf1>, <Nmetf2>, <Nmetf3>, <Nmetf4>, <Nmetf5>, <Nmetf6>, <Nmetf7>, <Nmetf8>
**Creating element for top flange
*ELGEN, ELSET=eltopflange
<Mael5>, <numberelbfx>, <nflange1x>, <elflange1x>, <n3>, <nflange1y>, <elflange1y>, <n7>,
<nflange1z>, <elflange1z>
**
*ELSET, ELSET=wideflangebeam
elbottomflange, elebottomweb, elecenterweb, eletopweb, eltopflange
**
**Adhesive layer:
**Creating master element for adhesive layer
*ELEMENT, TYPE=C3D8R, ELSET=MAELAd
<Mael6>, <Nmeal1>, <Nmeal2>, <Nmeal3>, <Nmeal4>, <Nmeal5>, <Nmeal6>, <Nmeal7>,
<Nmeal8>
**Creating element for adhesive layer
*ELGEN, ELSET=eladhesivelayer
<Mael6>, <numberelbfx>, <nflange1x>, <elflange1x>, <n5>, <nflange1y>, <elflange1y>, <n7>,
<nflange1z>, <elflange1z>
**
**GFRP plate:
**Creating master element for GFRP plate
*ELEMENT, TYPE=C3D8R, ELSET=MAELGFRP
<Mael7>, <Nmefp1>, <Nmefp2>, <Nmefp3>, <Nmefp4>, <Nmefp5>, <Nmefp6>, <Nmefp7>,
<Nmefp8>
**Creating element for adhesive layer
*ELGEN, ELSET=elGFRPplate
<Mael7>, <numberelbfx>, <nflange1x>, <elflange1x>, <n6>, <nflange1y>, <elflange1y>, <n7>,
<nflange1z>, <elflange1z>
```

```
**
**Defining nodes that is fixed at z=0
*NSET, NSET=Startsection, GENERATE
1, <A8po>, 1
**
**Defining the surface where loads are applied
*ELSET, ELSET=websurfaceatL, GENERATE
<firstelementwebatL>, <secondelementwebatL>, 1
*SURFACE, TYPE=ELEMENT, NAME=WEBSURFACEATCOORDL
websurfaceatL, S4
**
**Defining output set for adhesive layer
**ELSET, ELSET=adhesiveoutputsets, GENERATE
**<eloutput11>, <eloutput21>, 1
**<eloutput12>, <eloutput22>, 1
**<eloutput13>, <eloutput23>, 1
**
**Defining output dipslcement of nodes
*NSET, NSET=beamcentroid, GENERATE
<beamcentroidat0>, <beamcentroidatL>, 2000
*NSET, NSET=bottomflangecentroid, GENERATE
<bottomflangecentroidat0>, <bottomflangecentroidatL>, 2000
*NSET, NSET=upperflangecentroid, GENERATE
<upperflangecentroidat0>, <upperflangecentroidatL>, 2000
*NSET, NSET=GFRPcentroid, GENERATE
<GFRPcentroidat0>, <GFRPcentroidatL>, 2000
**
*SOLID SECTION, ELSET=wideflangebeam, MATERIAL=STEEL
*MATERIAL, NAME=STEEL
*ELASTIC, TYPE=ISOTROPIC
<Eb>, <v>
*SOLID SECTION, ELSET=eladhesivelayer, MATERIAL=ADHESIVE
*MATERIAL, NAME=ADHESIVE
*ELASTIC, TYPE=ISOTROPIC
<Ea>, <v>
*SOLID SECTION, ELSET=elGFRPplate, MATERIAL=FRPmat
*MATERIAL, NAME=FRPmat
*ELASTIC, TYPE=ISOTROPIC
<Ep>, <v>
**
** History data
**
*STEP
*STATIC
*DSLOAD
WEBSURFACEATCOORDL, TRSHR, -25241.48, 0.0, 1.0, 0.0
*BOUNDARY
Startsection,1,3
```

```
*NODE PRINT
U,
RF,
*NODE PRINT, NSET=beamcentroid
U,
*NODE PRINT, NSET=bottomflangecentroid
U,
*NODE PRINT, NSET=upperflangecentroid
U,
*NODE PRINT, NSET=GFRPcentroid
U,
*EL PRINT
S,
**EL PRINT, ELSET=adhesiveoutputsets
**E,
*END STEP
```

B6.2 Simply supported composite beam under transverse tractions applied along the bottom flange

```
*Heading
Simply supported beam under transverse tractions
SI units (kg, mm, s, N)
*PARAMETER
###############################################################
L  = 3000   # Total length of the beam
########################################
h   = 138.2  # Depth of the web
tw  = 4.3    # Thickness of the web
t3  = 4.9    # Thickness of the flange
bb  = 100   # Width of flange
Eb  = 200.E3  # Modulus of elasticity of steel (N/mm2)
v   = 0.3    # Poisson's ratio
########################################
bp  = 100   # With of GFRP plate
t1  = 19.0    # Thickness of GFRP plate
Ep  = 42.E3  # Modulus of elasticity of FRP (N/mm2)
########################################
t2  = 0.79  # Thickness of adhesive layer
Ea  = 1.04E3   # Modulus of elasticity of adhesive (N/mm2)
###############################################################
n1  = 20   # Number of elements on the X-direction for a half of flange cantilevel
n2  = 4    # Number of elements on the X-direction for the web
n3  = 4    # Number of elements on the Y-direction for the flange
n4  = 70    # Number of elements on the Y-direction for the web
n5  = 4    # Number of elements on the Y-direction for the adhesive layer
n6  = 16    # Number of elements on the Y-direction for the GFRP plate
n7  = 2500   # Number of elements on the Z-direction 1
###############################################################
b1=(bb-tw)/2  # Width of one flange cantilever
b2=b1+tw
h1=t3+h
h2=h+2*t3
h3=h2+t2
h4=h3+t1
ha=h2+t2/n5
### Increment in nodel numbers
###
nflange1x=1          # Increment in node numbers for the flange cantilevel 1 (x-direction)
nflange1y=2*n1+n2+1    # Increment in node numbers for the flange cantilevel 1 (y-direction)
nflange1z=2000        # Increment in node numbers for the flange cantilevel 1 (z-direction)
###
nwebx=1          # Increment in node numbers for the web (x-direction)
nweby=n2+1        # Increment in node numbers for the web (y-direction)
nwebz=2000        # Increment in node numbers for the web (z-direction)
```

```
###
### Increment in element numbers
###
elflange1x=1          # Increment in element numbers for the flange cantilevel 1 (x-direction)
elflange1y=2*n1+n2    # Increment in element numbers for the flange cantilevel 1 (y-direction)
elflange1z=2000       # Increment in element numbers for the flange cantilevel 1 (z-direction)
###
elwebx=1         # Increment in element numbers for the web (x-direction)
elweby=n2        # Increment in element numbers for the web (y-direction)
elwebz=2000      # Increment in element numbers for the web (z-direction)
###############################################################################
############
### Number of generating nodes
### For the I beam
## At Z=0
A1bo = 1
A2bo = n1+1
A3bo = n1+n2+1
A4bo = 2*n1+n2+1
A5bo = (2*n1+n2+1)*n3+1
A6bo = (2*n1+n2+1)*(n3+1)-(n1+n2)
A7bo = (2*n1+n2+1)*(n3+1)-n1
A8bo = (2*n1+n2+1)*(n3+1)
A9bo1 = A8bo+1
A10bo1= A8bo+1+n2
A9bo2 = A8bo+(n2+1)*(n4-1)-n2
A10bo2= A8bo+(n2+1)*(n4-1)
A11bo= A10bo2+1
A12bo= A10bo2+n1+1
A13bo= A10bo2+n1+n2+1
A14bo= A10bo2+2*n1+n2+1
A15bo= A10bo2+(2*n1+n2+1)*(n3+1)-(2*n1+n2)
A16bo= A10bo2+(2*n1+n2+1)*(n3+1)-(n1+n2)
A17bo= A10bo2+(2*n1+n2+1)*(n3+1)-n1
A18bo= A10bo2+(2*n1+n2+1)*(n3+1)
## At Z=L
A1bl = 2000*n7+1
A2bl = 2000*n7+n1+1
A3bl = 2000*n7+n1+n2+1
A4bl = 2000*n7+2*n1+n2+1
A5bl = 2000*n7+(2*n1+n2+1)*n3+1
A6bl = 2000*n7+(2*n1+n2+1)*(n3+1)-(n1+n2)
A7bl = 2000*n7+(2*n1+n2+1)*(n3+1)-n1
A8bl = 2000*n7+(2*n1+n2+1)*(n3+1)
A9bl1 = A8bl+1
A10bl1= A8bl+1+n2
A9bl2 = A8bl+(n2+1)*(n4-1)-n2
A10bl2= A8bl+(n2+1)*(n4-1)
```

```
A11bl= A10bl2+1
A12bl= A10bl2+n1+1
A13bl= A10bl2+n1+n2+1
A14bl= A10bl2+2*n1+n2+1
A15bl= A10bl2+(2*n1+n2+1)*(n3+1)-(2*n1+n2)
A16bl= A10bl2+(2*n1+n2+1)*(n3+1)-(n1+n2)
A17bl= A10bl2+(2*n1+n2+1)*(n3+1)-n1
A18bl= A10bl2+(2*n1+n2+1)*(n3+1)
### For the adhesive layer
## At Z=0
A1ao = A18bo+1
A2ao = A18bo+1+n1
A3ao = A18bo+1+n1+n2
A4ao = A18bo+1+n1+n2+n1
A5ao = A15bo+(2*n1+n2+1)*n5
A6ao = A15bo+(2*n1+n2+1)*n5+n1
A7ao = A15bo+(2*n1+n2+1)*n5+n1+n2
A8ao = A15bo+(2*n1+n2+1)*n5+2*n1+n2
## At Z=L
A1al = A18bl+1
A2al = A18bl+1+n1
A3al = A18bl+1+n1+n2
A4al = A18bl+1+n1+n2+n1
A5al = A15bl+(2*n1+n2+1)*n5
A6al = A15bl+(2*n1+n2+1)*n5+n1
A7al = A15bl+(2*n1+n2+1)*n5+n1+n2
A8al = A15bl+(2*n1+n2+1)*n5+2*n1+n2
### For the GFRP plate
## At Z=0
A1po = A5ao
A2po = A6ao
A3po = A7ao
A4po = A8ao
A5po = A5ao+(2*n1+n2+1)*n6
A6po = A5ao+(2*n1+n2+1)*n6+n1
A7po = A5ao+(2*n1+n2+1)*n6+n1+n2
A8po = A5ao+(2*n1+n2+1)*n6+2*n1+n2
## At Z=L
A1pl = A5al
A2pl = A6al
A3pl = A7al
A4pl = A8al
A5pl = A5al+(2*n1+n2+1)*n6
A6pl = A5al+(2*n1+n2+1)*n6+n1
A7pl = A5al+(2*n1+n2+1)*n6+n1+n2
A8pl = A5al+(2*n1+n2+1)*n6+2*n1+n2
##########################################################################
### Define the Y-coordinate of nodes 9, 10
```

```
YA9bo1 = t3+h/n4
YA10bo1= t3+h/n4
YA9bo2 = t3+h-h/n4
YA10bo2= t3+h-h/n4
### Number of node row in Y-direction for center web part
NRYCW=n4-2
### Number of node row in Y-direction for adhesive upper part
NRYUAD=n5-1
##########################################################################
### elements of final layer at z=L
firstelementatL=2000*(n7-1)+1
secondelementatL=2000*(n7-1)+(2*n1+n2)*n3
thirdelementatL=2000*(n7-1)+(2*n1+n2)*n3+n2*n4+1
fourthelementatL=2000*(n7-1)+(2*n1+n2)*n3*2+n2*n4
##########################################################################
### Nodes of master element of bottom layer the bottom flange
Nmeblbf1=1
Nmeblbf2=2001
Nmeblbf3=2002
Nmeblbf4=2
Nmeblbf5=2*n1+n2+1+1
Nmeblbf6=2000+2*n1+n2+1+1
Nmeblbf7=2000+2*n1+n2+1+2
Nmeblbf8=2*n1+n2+1+2
### Nodes of master element of upper layerS the bottom flange
Nmeulbf1=2*n1+n2+1+1
Nmeulbf2=2000+2*n1+n2+1+1
Nmeulbf3=2000+2*n1+n2+1+2
Nmeulbf4=2*n1+n2+1+2
Nmeulbf5=(2*n1+n2+1)*2+1
Nmeulbf6=2000+(2*n1+n2+1)*2+1
Nmeulbf7=2000+(2*n1+n2+1)*2+1+1
Nmeulbf8=(2*n1+n2+1)*2+1+1
### Nodes of master element of the bottom web
Nmebw1=A6bo
Nmebw2=2000+A6bo
Nmebw3=2000+A6bo+1
Nmebw4=A6bo+1
Nmebw5=(2*n1+n2+1)*(n3+1)+1
Nmebw6=2000+(2*n1+n2+1)*(n3+1)+1
Nmebw7=2000+(2*n1+n2+1)*(n3+1)+2
Nmebw8=(2*n1+n2+1)*(n3+1)+2
### Nodes of master element of the center web
Nmecw1=(2*n1+n2+1)*(n3+1)+1
Nmecw2=2000+(2*n1+n2+1)*(n3+1)+1
Nmecw3=2000+(2*n1+n2+1)*(n3+1)+1+1
Nmecw4=(2*n1+n2+1)*(n3+1)+1+1
Nmecw5=(2*n1+n2+1)*(n3+1)+1+n2+1
```

```
Nmecw6=2000+(2*n1+n2+1)*(n3+1)+1+n2+1
Nmecw7=2000+(2*n1+n2+1)*(n3+1)+1+n2+2
Nmecw8=(2*n1+n2+1)*(n3+1)+1+n2+2
### Nodes of master element of the top web
Nmetw1=A9bo2
Nmetw2=2000+A9bo2
Nmetw3=2000+A9bo2+1
Nmetw4=A9bo2+1
Nmetw5=A12bo
Nmetw6=2000+A12bo
Nmetw7=2000+A12bo+1
Nmetw8=A12bo+1
### Nodes of master element of the top flange
Nmetf1=A11bo
Nmetf2=2000+A11bo
Nmetf3=2000+A11bo+1
Nmetf4=A11bo+1
Nmetf5=A11bo+2*n1+n2+1
Nmetf6=2000+A11bo+2*n1+n2+1
Nmetf7=2000+A11bo+2*n1+n2+1+1
Nmetf8=A11bo+2*n1+n2+1+1
### Nodes of master element of the adhesive layer
Nmeal1=A15bo
Nmeal2=2000+A15bo
Nmeal3=2000+A15bo+1
Nmeal4=A15bo+1
Nmeal5=A15bo+2*n1+n2+1
Nmeal6=2000+A15bo+2*n1+n2+1
Nmeal7=2000+A15bo+2*n1+n2+1+1
Nmeal8=A15bo+2*n1+n2+1+1
### Nodes of master element of the FRP plate
Nmefp1=A5ao
Nmefp2=2000+A5ao
Nmefp3=2000+A5ao+1
Nmefp4=A5ao+1
Nmefp5=A5ao+2*n1+n2+1
Nmefp6=2000+A5ao+2*n1+n2+1
Nmefp7=2000+A5ao+2*n1+n2+1+1
Nmefp8=A5ao+2*n1+n2+1+1
#################################################################################
### Master element number
### Master element 1 for upper bottom flange part
Mael1=2*n1+n2+1
### Master element 1 for bottom web
Mael2=(2*n1+n2)*n3+1
### Master element 1 for center web
Mael3=(2*n1+n2)*n3+1+n2
### Master element 1 for top web
```

```
Mael4=(2*n1+n2)*n3+n2*(n4-1)+1
### Master element 1 for top flange
Mael5=(2*n1+n2)*n3+n2*n4+1
### Master element 1 for adhesive layer
Mael6=(2*n1+n2)*n3*2+n2*n4+1
### Master element 1 for bottom flange
Mael7=(2*n1+n2)*n3*2+n2*n4+(2*n1+n2)*n5+1
################################################################################
### Element numbers needs to be generated in Y direction
### For upper layers of bottom flange
numberulbfy=n3-1
### For center web
numberelcw=n4-2
### Elements numbers needs to be generated in X direction for the flanges
numberelbfx=2*n1+n2
### Parameters related to the NCOPY command
### For right bottom flange part 2
c1=n1+n2
### For left + right flange
c2=A10bo2
################################################################################
###eloutput11=(2*n1+n2)*n3+(n4*n2)+1+2000*(n7-2340)
###eloutput21=(2*n1+n2)*n3+(n4*n2)+(2*n1+n2)*n5+2000*(n7-2340)
###eloutput12=(2*n1+n2)*n3+(n4*n2)+1+2000*(n7-1560)
###eloutput22=(2*n1+n2)*n3+(n4*n2)+(2*n1+n2)*n5+2000*(n7-1560)
###eloutput13=(2*n1+n2)*n3+(n4*n2)+1+2000*(n7-780)
###eloutput23=(2*n1+n2)*n3+(n4*n2)+(2*n1+n2)*n5+2000*(n7-780)
################################################################################
beamcentroidat0=(2*n1+n2+1)*(n3+1)+(n2+1)*(n4/2)-n2/2
beamcentroidatL=2000*n7+(2*n1+n2+1)*(n3+1)+(n2+1)*(n4)/2-n2/2
bottomflangecentroidat0=(2*n1+n2+1)*((n3/2)+1)-n1-n2/2
bottomflangecentroidatL=2000*n7+(2*n1+n2+1)*((n3/2)+1)-n1-n2/2
upperflangecentroidat0=(2*n1+n2+1)*(n3+1)+(n2+1)*(n4-1)+(2*n1+n2+1)*((n3/2)+1)-n1-n2/2
upperflangecentroidatL=2000*n7+(2*n1+n2+1)*(n3+1)+(n2+1)*(n4-1)+(2*n1+n2+1)*((n3/2)+1)-n1-
n2/2
GFRPcentroidat0=(2*n1+n2+1)*(n3+1)*2+(n2+1)*(n4-1)+(2*n1+n2+1)*(n5-
1)+(2*n1+n2+1)*((n6/2)+1)-n1-n2/2
GFRPcentroidatL=2000*n7+(2*n1+n2+1)*(n3+1)*2+(n2+1)*(n4-1)+(2*n1+n2+1)*(n5-
1)+(2*n1+n2+1)*((n6/2)+1)-n1-n2/2
################################################################################
support1at0=(2*n1+n2+1)*(n3+1)+(n2+1)*(n4/2)-n2
support2at0=(2*n1+n2+1)*(n3+1)+(n2+1)*(n4/2)
support1atL=2000*n7+(2*n1+n2+1)*(n3+1)+(n2+1)*(n4/2)-n2
support2atL=2000*n7+(2*n1+n2+1)*(n3+1)+(n2+1)*(n4/2)
################################################################################
*PREPRINT, ECHO=YES, MODEL=YES, HISTORY=YES
**
**Model denifition
```

```
*NODE
<A1bo>, 0.0, 0.0, 0.0
<A2bo>, <b1>, 0.0, 0.0
<A3bo>, <b2>, 0.0, 0.0
<A4bo>, <bb>, 0.0, 0.0
<A5bo>, 0.0, <t3>, 0.0
<A6bo>, <b1>, <t3>, 0.0
<A7bo>, <b2>, <t3>, 0.0
<A8bo>, <bb>, <t3>, 0.0
<A9bo1>, <b1>, <YA9bo1>, 0.0
<A10bo1>, <b2>, <YA10bo1>, 0.0
<A9bo2>, <b1>, <YA9bo2>, 0.0
<A10bo2>, <b2>, <YA10bo2>, 0.0
<A11bo>, 0.0, <h1>, 0.0
<A12bo>, <b1>, <h1>, 0.0
<A13bo>, <b2>, <h1>, 0.0
<A14bo>, <bb>, <h1>, 0.0
<A15bo>, 0.0, <h2>, 0.0
<A16bo>, <b1>, <h2>, 0.0
<A17bo>, <b2>, <h2>, 0.0
<A18bo>, <bb>, <h2>, 0.0
**
<A1ao>, 0.0, <ha>, 0.0
<A2ao>, <b1>, <ha>, 0.0
<A3ao>, <b2>, <ha>, 0.0
<A4ao>, <bb>, <ha>, 0.0
<A5ao>, 0.0, <h3>, 0.0
<A6ao>, <b1>, <h3>, 0.0
<A7ao>, <b2>, <h3>, 0.0
<A8ao>, <bb>, <h3>, 0.0
**
<A5po>, 0.0, <h4>, 0.0
<A6po>, <b1>, <h4>, 0.0
<A7po>, <b2>, <h4>, 0.0
<A8po>, <bb>, <h4>, 0.0
**
<A1bl>, 0.0, 0.0, <L>
<A2bl>, <b1>, 0.0, <L>
<A3bl>, <b2>, 0.0, <L>
<A4bl>, <bb>, 0.0, <L>
<A5bl>, 0.0, <t3>, <L>
<A6bl>, <b1>, <t3>, <L>
<A7bl>, <b2>, <t3>, <L>
<A8bl>, <bb>, <t3>, <L>
<A9bl1>, <b1>, <YA9bo1>, <L>
<A10bl1>, <b2>, <YA10bo1>, <L>
<A9bl2>, <b1>, <YA9bo2>, <L>
<A10bl2>, <b2>, <YA10bo2>, <L>
```

```
<A11bl>, 0.0, <h1>, <L>
<A12bl>, <b1>, <h1>, <L>
<A13bl>, <b2>, <h1>, <L>
<A14bl>, <bb>, <h1>, <L>
<A15bl>, 0.0, <h2>, <L>
<A16bl>, <b1>, <h2>, <L>
<A17bl>, <b2>, <h2>, <L>
<A18bl>, <bb>, <h2>, <L>
**
<A1al>, 0.0, <ha>, <L>
<A2al>, <b1>, <ha>, <L>
<A3al>, <b2>, <ha>, <L>
<A4al>, <bb>, <ha>, <L>
<A5al>, 0.0, <h3>, <L>
<A6al>, <b1>, <h3>, <L>
<A7al>, <b2>, <h3>, <L>
<A8al>, <bb>, <h3>, <L>
**
<A5pl>, 0.0, <h4>, <L>
<A6pl>, <b1>, <h4>, <L>
<A7pl>, <b2>, <h4>, <L>
<A8pl>, <bb>, <h4>, <L>
**
**Node set of left bottom edge of bottom flange 1 along z axis
*NGEN, NSET=LBEBF1
<A1bo>, <A1bl>, 2000
**Node set of left upper edge of bottom flange 1 along z axis
*NGEN, NSET=LUEBF1
<A5bo>, <A5bl>, 2000
**Node set of left surface of bottom flange 1 along z axis
*NFILL, NSET=LSBF1
LBEBF1, LUEBF1, <n3>, <nflange1y>
**
**Node set of right bottom edge of bottom flange 1 along z axis
*NGEN, NSET=RBEBF1
<A2bo>, <A2bl>, 2000
**Node set of right upper edge of bottom flange 1 along z axis
*NGEN, NSET=RUEBF1
<A6bo>, <A6bl>, 2000
**Node set of right surface of bottom flange 1 along z axis
*NFILL, NSET=RSBF1
RBEBF1, RUEBF1, <n3>, <nflange1y>
**
**Node set of bottom flange block 1
*NFILL, NSET=BFB1
LSBF1, RSBF1, <n1>, 1
**
**Node set of bottom flange block 2
```

```
*NCOPY, OLDSET=BFB1, CHANGENUMBER=<c1>, NEWSET=BFB2, SHIFT
<b2>, 0.0, 0.0
0.0, 0.0, 0.0, 0.0, 0.0, 1.0, 0.0
**Node set of center bottom flange part
*NSET, NSET=abc1, GENERATE
<A3bo>, <A3bl>, 2000
*NSET, NSET=abc2, GENERATE
<A7bo>, <A7bl>, 2000
*NFILL, NSET=bottomweb1
RBEBF1, abc1, <n2>, 1
*NFILL, NSET=upperbottomweb2
RUEBF1, abc2, <n2>, 1
*NFILL, NSET=centerbottomflange
bottomweb1, upperbottomweb2, <n3>, <nflange1y>
**
**Bottom flange
*NSET, NSET=bottomflange
BFB1, centerbottomflange, BFB2
**Node set of unpper flange
*NCOPY, OLDSET=bottomflange, CHANGENUMBER=<c2>, NEWSET=upperflange, SHIFT
0.0, <h1>, 0.0
0.0, 0.0, 0.0, 0.0, 0.0, 1.0, 0.0
**Node set for the center Web
** Node line at left upper edge of the center web
*NGEN, NSET=LUECW
<A9bo2>, <A9bl2>, 2000
** Node line at right upper edge of the center web
*NGEN, NSET=RUECW
<A10bo2>, <A10bl2>, 2000
** Node set at upper surface of the center web
*NFILL, NSET=USCW
LUECW, RUECW, <n2>, 1
**
** Node line at left bottom edge of the center web
*NGEN, NSET=LBECW
<A9bo1>, <A9bl1>, 2000
** Node line at right bottom edge of the center web
*NGEN, NSET=RBECW
<A10bo1>, <A10bl1>, 2000
** Node set at bottom surface of the center web
*NFILL, NSET=BSCW
LBECW, RBECW, <n2>, 1
** Forming node set for the center web
*NFILL, NSET=centerweb
BSCW, USCW, <NRYCW>, <nweby>
**
**
**
```

```
**Node set for adhesive layer
**
**Bottom surface:
**Node line A1a, left bottom edge of adhesive layer
*NGEN, NSET=LBEAL
<A1ao>, <A1al>, 2000
*NGEN, NSET=lineA2a
<A2ao>, <A2al>, 2000
*NFILL, NSET=firstsurfacead
LBEAL, lineA2a, <n1>, 1
**
**Node line A3a, left bottom edge of adhesive layer
*NGEN, NSET=lineA3a
<A3ao>, <A3al>, 2000
*NFILL, NSET=secondsurfacead
lineA2a, lineA3a, <n2>, 1
**
**Node line A4a, left bottom edge of adhesive layer
*NGEN, NSET=lineA4a
<A4ao>, <A4al>, 2000
*NFILL, NSET=thirdsurfacead
lineA3a, lineA4a, <n1>, 1
**
**Bottom surface of adhesive layer
*NSET, NSET=BSAL
firstsurfacead, secondsurfacead, thirdsurfacead
**
**Upper surface:
**Node line A5a, left top edge of adhesive layer
*NGEN, NSET=LTEAL
<A5ao>, <A5al>, 2000
**Node line A6a
*NGEN, NSET=lineA6a
<A6ao>, <A6al>, 2000
**Node line A7a
*NGEN, NSET=lineA7a
<A7ao>, <A7al>, 2000
**Node line A8a, right top edge of adhesive layer
*NGEN, NSET=RTEAL
<A8ao>, <A8al>, 2000
**Node surface formed by A5a and A6a, A6a and A7a, A7a and A8a
*NFILL, NSET=SFA5aA6a
LTEAL, lineA6a, <n1>, 1
*NFILL, NSET=SFA6aA7a
lineA6a, lineA7a, <n2>, 1
*NFILL, NSET=SFA7aA8a
lineA7a, RTEAL, <n1>, 1
*NSET, NSET=uppersurfacead
```

```
SFA5aA6a, SFA6aA7a, SFA7aA8a
**
**Node set for adhesive layer:
*NFILL, NSET=adhesivelayernodeset
BSAL, uppersurfacead, <NRYUAD>, <nflange1y>
**
**Node set for GFRP plate
**
**Upper surface:
**Node line A5p, left top edge of GFRP plate
*NGEN, NSET=LTEGFRP
<A5po>, <A5pl>, 2000
**Node line A6p
*NGEN, NSET=lineA6p
<A6po>, <A6pl>, 2000
**Node line A7p
*NGEN, NSET=lineA7p
<A7po>, <A7pl>, 2000
**Node line A8p, right top edge of GFRP plate
*NGEN, NSET=RTEGFRP
<A8po>, <A8pl>, 2000
**Node surface formed by A5p and A6p, A6p and A7p, A7p and A8p
*NFILL, NSET=SFA5pA6p
LTEGFRP, lineA6p, <n1>, 1
*NFILL, NSET=SFA6pA7p
lineA6p, lineA7p, <n2>, 1
*NFILL, NSET=SFA7pA8p
lineA7p, RTEGFRP, <n1>, 1
*NSET, NSET=uppersurfacegfrp
SFA5pA6p, SFA6pA7p, SFA7pA8p
**
**Node set for GFRP plate:
*NFILL, NSET=gfrpplatenodeset
uppersurfacead, uppersurfacegfrp, <n6>, <nflange1y>
**
**Element generation
**
**Bottom flange:
**Creating master element for bottom flange layer
*ELEMENT, TYPE=C3D8R, ELSET=MAELBF1
1, <Nmeblbf1>, <Nmeblbf2>, <Nmeblbf3>, <Nmeblbf4>, <Nmeblbf5>, <Nmeblbf6>, <Nmeblbf7>,
<Nmeblbf8>
**Creating element for bottom flange
*ELGEN, ELSET=elbottomflange1
1, <numberelbfx>, <nflange1x>, <elflange1x>, 1, <nflange1y>, <elflange1y>, <n7>, <nflange1z>,
<elflange1z>
**Creating master element for upper bottom flange layers
*ELEMENT, TYPE=C3D8R, ELSET=MAELBF2
```

```
<Mael1>, <Nmeulbf1>, <Nmeulbf2>, <Nmeulbf3>, <Nmeulbf4>, <Nmeulbf5>, <Nmeulbf6>,
<Nmeulbf7>, <Nmeulbf8>
**Creating element for upper bottom flange layers
*ELGEN, ELSET=elbottomflange2
<Mael1>, <numberelbfx>, <nflange1x>, <elflange1x>, <numberulbfy>, <nflange1y>, <elflange1y>,
<n7>, <nflange1z>, <elflange1z>
**
**Bottom web part:
**Creating master element for bottom web part
*ELEMENT, TYPE=C3D8R, ELSET=MAELBW
<Mael2>, <Nmebw1>, <Nmebw2>, <Nmebw3>, <Nmebw4>, <Nmebw5>, <Nmebw6>, <Nmebw7>,
<Nmebw8>
**Creating element for bottom web part
*ELGEN, ELSET=elebottomweb
<Mael2>, <n2>, <nwebx>, <elwebx>, 1, <nweby>, <elweby>, <n7>, <nwebz>, <elwebz>
**
**Center web part:
**Creating master element for center web part
*ELEMENT, TYPE=C3D8R, ELSET=MAELCW
<Mael3>, <Nmecw1>, <Nmecw2>, <Nmecw3>, <Nmecw4>, <Nmecw5>, <Nmecw6>, <Nmecw7>,
<Nmecw8>
**Creating element for center web part
*ELGEN, ELSET=elecenterweb
<Mael3>, <n2>, <nwebx>, <elwebx>, <numberelcw>, <nweby>, <elweby>, <n7>, <nwebz>,
<elwebz>
**
**Top web part:
**Creating master element for top web part
*ELEMENT, TYPE=C3D8R, ELSET=MAELTW
<Mael4>, <Nmetw1>, <Nmetw2>, <Nmetw3>, <Nmetw4>, <Nmetw5>, <Nmetw6>, <Nmetw7>,
<Nmetw8>
**Creating element for top web part
*ELGEN, ELSET=eletopweb
<Mael4>, <n2>, <nwebx>, <elwebx>, 1, <nweby>, <elweby>, <n7>, <nwebz>, <elwebz>
**
**Top flange:
**Creating master element for top flange
*ELEMENT, TYPE=C3D8R, ELSET=MAELTF
<Mael5>, <Nmetf1>, <Nmetf2>, <Nmetf3>, <Nmetf4>, <Nmetf5>, <Nmetf6>, <Nmetf7>, <Nmetf8>
**Creating element for top flange
*ELGEN, ELSET=eltopflange
<Mael5>, <numberelbfx>, <nflange1x>, <elflange1x>, <n3>, <nflange1y>, <elflange1y>, <n7>,
<nflange1z>, <elflange1z>
**
*ELSET, ELSET=wideflangebeam
elbottomflange1, elbottomflange2, elebottomweb, elecenterweb, eletopweb, eltopflange
**
**Adhesive layer:
```

```
**Creating master element for adhesive layer
*ELEMENT, TYPE=C3D8R, ELSET=MAELAd
<Mael6>, <Nmeal1>, <Nmeal2>, <Nmeal3>, <Nmeal4>, <Nmeal5>, <Nmeal6>, <Nmeal7>,
<Nmeal8>
**Creating element for adhesive layer
*ELGEN, ELSET=eladhesivelayer
<Mael6>, <numberelbfx>, <nflange1x>, <elflange1x>, <n5>, <nflange1y>, <elflange1y>, <n7>,
<nflange1z>, <elflange1z>
**
**GFRP plate:
**Creating master element for GFRP plate
*ELEMENT, TYPE=C3D8R, ELSET=MAELGFRP
<Mael7>, <Nmefp1>, <Nmefp2>, <Nmefp3>, <Nmefp4>, <Nmefp5>, <Nmefp6>, <Nmefp7>,
<Nmefp8>
**Creating element for adhesive layer
*ELGEN, ELSET=elGFRPplate
<Mael7>, <numberelbfx>, <nflange1x>, <elflange1x>, <n6>, <nflange1y>, <elflange1y>, <n7>,
<nflange1z>, <elflange1z>
**
**Defining boundary conditions
** Simply supported at two ends:
** Node set at 0
*NSET, NSET=SSBat0, GENERATE
<support1at0>, <support2at0>, 1
**Node set at L
*NSET, NSET=SSBatL, GENERATE
<support1atL>, <support2atL>, 1
** Constraint conditions:
** Constraint u3: at bottom and upper flange at z=0:
** Flanges:
** Constraint u1 at z=0:
*NSET, NSET=verticalcenteredge0, GENERATE
23, 203, 45
593, 1673, 45
228, 568, 5
**
** Constraint u3: at bottom and upper flange at z=L:
** Flanges:
**
** Constraint u1 at z=0:
*NSET, NSET=verticalcenteredgeL, GENERATE
5000023, 5000203, 45
5000593, 50001673, 45
5000228, 5000568, 5
**
**Defining the bottom surface where uniform traction is applied
*ELSET, ELSET=elementwebbottomsurface, GENERATE
21, 4998021, 2000
```

```
22, 4998022, 2000
23, 4998023, 2000
24, 4998024, 2000
*SURFACE, TYPE=ELEMENT, NAME=BOTTOMWEBSURFACE
elementwebbottomsurface, S1
**
**Defining output set for adhesive layer
**ELSET, ELSET=adhesiveoutputsets, GENERATE
**<eloutput11>, <eloutput21>, 1
**<eloutput12>, <eloutput22>, 1
**<eloutput13>, <eloutput23>, 1
**
**Defining output dipslcement of nodes
*NSET, NSET=beamcentroid, GENERATE
<beamcentroidat0>, <beamcentroidatL>, 2000
*NSET, NSET=bottomflangecentroid, GENERATE
<bottomflangecentroidat0>, <bottomflangecentroidatL>, 2000
*NSET, NSET=upperflangecentroid, GENERATE
<upperflangecentroidat0>, <upperflangecentroidatL>, 2000
*NSET, NSET=GFRPcentroid, GENERATE
<GFRPcentroidat0>, <GFRPcentroidatL>, 2000
**
*SOLID SECTION, ELSET=wideflangebeam, MATERIAL=STEEL
*MATERIAL, NAME=STEEL
*ELASTIC, TYPE=ISOTROPIC
<Eb>, <v>
*SOLID SECTION, ELSET=eladhesivelayer, MATERIAL=ADHESIVE
*MATERIAL, NAME=ADHESIVE
*ELASTIC, TYPE=ISOTROPIC
<Ea>, <v>
*SOLID SECTION, ELSET=elGFRPplate, MATERIAL=FRPmat
*MATERIAL, NAME=FRPmat
*ELASTIC, TYPE=ISOTROPIC
<Ep>, <v>
**
** History data
**
*STEP
*STATIC
*DSLOAD
BOTTOMWEBSURFACE, P, 3.48837209
*BOUNDARY
SSBat0, 2, 3
SSBatL, 2
verticalcenteredge0, 1
verticalcenteredgeL, 1
*NODE PRINT, NSET=beamcentroid
U,
```

```
*NODE PRINT, NSET=bottomflangecentroid
U,
*NODE PRINT, NSET=upperflangecentroid
U,
*NODE PRINT, NSET=GFRPcentroid
U,
**EL PRINT, ELSET=adhesiveoutputsets
**E,
*END STEP
```

B6.3 The cantilever composite beam under twisting moment about the beam centroid

It should be noted that this code can be applied to the case of bending about weak axis by simply changing the sign of load values in *DSLOAD. Below is the code for the cantilever composite beam under twisting moment about the beam centroid.

```
*Heading
The composite beam under twisting about the beam centroid
SI units (kg, mm, s, N)
*PARAMETER
##############################################################
L   = 5000   # Total length of the beam
########################################
h   = 380.6  # Depth of the web
tw  = 10.9    # Thickness of the web
t3  = 18.2     # Thickness of the flange
bb  = 181.0    # Width of flange
Eb  = 200.E3  # Modulus of elasticity of steel (N/mm2)
v   = 0.3     # Poisson's ratio
########################################
bp  = 181.0    # With of GFRP plate
t1  = 19.0     # Thickness of GFRP plate
Ep  = 42.E3  # Modulus of elasticity of FRP (N/mm2)
########################################
t2  = 2.0   # Thickness of adhesive layer
Ea  = 0.013E3   # Modulus of elasticity of adhesive (N/mm2)
##############################################################
n1  = 15   # Number of elements on the X-direction for a half of flange cantilevel
n2  = 4    # Number of elements on the X-direction for the web
n3  = 4    # Number of elements on the Y-direction for the flange
n4  = 70    # Number of elements on the Y-direction for the web
n5  = 4    # Number of elements on the Y-direction for the adhesive layer
n6  = 8    # Number of elements on the Y-direction for the GFRP plate
n7  = 3120   # Number of elements on the Z-direction 1
```

```
#############################################################
b1=(bb-tw)/2  # Width of one flange cantilever
b2=b1+tw
h1=t3+h
h2=h+2*t3
h3=h2+t2
h4=h3+t1
ha=h2+t2/n5
### Increment in nodel numbers
###
nflange1x=1          # Increment in node numbers for the flange cantilevel 1 (x-direction)
nflange1y=2*n1+n2+1    # Increment in node numbers for the flange cantilevel 1 (y-direction)
nflange1z=2000        # Increment in node numbers for the flange cantilevel 1 (z-direction)
###
nwebx=1          # Increment in node numbers for the web (x-direction)
nweby=n2+1        # Increment in node numbers for the web (y-direction)
nwebz=2000        # Increment in node numbers for the web (z-direction)
###
### Increment in element numbers
###
elflange1x=1          # Increment in element numbers for the flange cantilevel 1 (x-direction)
elflange1y=2*n1+n2     # Increment in element numbers for the flange cantilevel 1 (y-direction)
elflange1z=1000       # Increment in element numbers for the flange cantilevel 1 (z-direction)
###
elwebx=1         # Increment in element numbers for the web (x-direction)
elweby=n2         # Increment in element numbers for the web (y-direction)
elwebz=1000       # Increment in element numbers for the web (z-direction)
################################################################################
############
### Number of generating nodes
### For the I beam
## At Z=0
A1bo = 1
A2bo = n1+1
A3bo = n1+n2+1
A4bo = 2*n1+n2+1
A5bo = (2*n1+n2+1)*n3+1
A6bo = (2*n1+n2+1)*(n3+1)-(n1+n2)
A7bo = (2*n1+n2+1)*(n3+1)-n1
A8bo = (2*n1+n2+1)*(n3+1)
A9bo1 = A8bo+1
A10bo1= A8bo+1+n2
A9bo2 = A8bo+(n2+1)*(n4-1)-n2
A10bo2= A8bo+(n2+1)*(n4-1)
A11bo= A10bo2+1
A12bo= A10bo2+n1+1
A13bo= A10bo2+n1+n2+1
A14bo= A10bo2+2*n1+n2+1
```

```
A15bo= A10bo2+(2*n1+n2+1)*(n3+1)-(2*n1+n2)
A16bo= A10bo2+(2*n1+n2+1)*(n3+1)-(n1+n2)
A17bo= A10bo2+(2*n1+n2+1)*(n3+1)-n1
A18bo= A10bo2+(2*n1+n2+1)*(n3+1)
## At Z=L
A1bl = 2000*n7+1
A2bl = 2000*n7+n1+1
A3bl = 2000*n7+n1+n2+1
A4bl = 2000*n7+2*n1+n2+1
A5bl = 2000*n7+(2*n1+n2+1)*n3+1
A6bl = 2000*n7+(2*n1+n2+1)*(n3+1)-(n1+n2)
A7bl = 2000*n7+(2*n1+n2+1)*(n3+1)-n1
A8bl = 2000*n7+(2*n1+n2+1)*(n3+1)
A9bl1 = A8bl+1
A10bl1= A8bl+1+n2
A9bl2 = A8bl+(n2+1)*(n4-1)-n2
A10bl2= A8bl+(n2+1)*(n4-1)
A11bl= A10bl2+1
A12bl= A10bl2+n1+1
A13bl= A10bl2+n1+n2+1
A14bl= A10bl2+2*n1+n2+1
A15bl= A10bl2+(2*n1+n2+1)*(n3+1)-(2*n1+n2)
A16bl= A10bl2+(2*n1+n2+1)*(n3+1)-(n1+n2)
A17bl= A10bl2+(2*n1+n2+1)*(n3+1)-n1
A18bl= A10bl2+(2*n1+n2+1)*(n3+1)
### For the adhesive layer
## At Z=0
A1ao = A18bo+1
A2ao = A18bo+1+n1
A3ao = A18bo+1+n1+n2
A4ao = A18bo+1+n1+n2+n1
A5ao = A15bo+(2*n1+n2+1)*n5
A6ao = A15bo+(2*n1+n2+1)*n5+n1
A7ao = A15bo+(2*n1+n2+1)*n5+n1+n2
A8ao = A15bo+(2*n1+n2+1)*n5+2*n1+n2
## At Z=L
A1al = A18bl+1
A2al = A18bl+1+n1
A3al = A18bl+1+n1+n2
A4al = A18bl+1+n1+n2+n1
A5al = A15bl+(2*n1+n2+1)*n5
A6al = A15bl+(2*n1+n2+1)*n5+n1
A7al = A15bl+(2*n1+n2+1)*n5+n1+n2
A8al = A15bl+(2*n1+n2+1)*n5+2*n1+n2
### For the GFRP plate
## At Z=0
A1po = A5ao
A2po = A6ao
```

```
A3po = A7ao
A4po = A8ao
A5po = A5ao+(2*n1+n2+1)*n6
A6po = A5ao+(2*n1+n2+1)*n6+n1
A7po = A5ao+(2*n1+n2+1)*n6+n1+n2
A8po = A5ao+(2*n1+n2+1)*n6+2*n1+n2
## At Z=L
A1pl = A5al
A2pl = A6al
A3pl = A7al
A4pl = A8al
A5pl = A5al+(2*n1+n2+1)*n6
A6pl = A5al+(2*n1+n2+1)*n6+n1
A7pl = A5al+(2*n1+n2+1)*n6+n1+n2
A8pl = A5al+(2*n1+n2+1)*n6+2*n1+n2
##########################################################################
### Define the Y-coordinate of nodes 9, 10
YA9bo1 = t3+h/n4
YA10bo1= t3+h/n4
YA9bo2 = t3+h-h/n4
YA10bo2= t3+h-h/n4
### Number of node row in Y-direction for center web part
NRYCW=n4-2
### Number of node row in Y-direction for adhesive upper part
NRYUAD=n5-1
##########################################################################
### elements of final layer at z=L
firstelementatL=1000*(n7-1)+1
secondelementatL=1000*(n7-1)+(2*n1+n2)*n3
thirdelementatL=1000*(n7-1)+(2*n1+n2)*n3+n2*n4+1
fourthelementatL=1000*(n7-1)+(2*n1+n2)*n3*2+n2*n4
##########################################################################
### Nodes of master element of bottom layer the bottom flange
Nmeblbf1=1
Nmeblbf2=2001
Nmeblbf3=2002
Nmeblbf4=2
Nmeblbf5=2*n1+n2+1+1
Nmeblbf6=2000+2*n1+n2+1+1
Nmeblbf7=2000+2*n1+n2+1+2
Nmeblbf8=2*n1+n2+1+2
### Nodes of master element of upper layerS the bottom flange
Nmeulbf1=2*n1+n2+1+1
Nmeulbf2=2000+2*n1+n2+1+1
Nmeulbf3=2000+2*n1+n2+1+2
Nmeulbf4=2*n1+n2+1+2
Nmeulbf5=(2*n1+n2+1)*2+1
Nmeulbf6=2000+(2*n1+n2+1)*2+1
```

```
Nmeulbf7=2000+(2*n1+n2+1)*2+1+1
Nmeulbf8=(2*n1+n2+1)*2+1+1
### Nodes of master element of the bottom web
Nmebw1=A6bo
Nmebw2=2000+A6bo
Nmebw3=2000+A6bo+1
Nmebw4=A6bo+1
Nmebw5=(2*n1+n2+1)*(n3+1)+1
Nmebw6=2000+(2*n1+n2+1)*(n3+1)+1
Nmebw7=2000+(2*n1+n2+1)*(n3+1)+2
Nmebw8=(2*n1+n2+1)*(n3+1)+2
### Nodes of master element of the center web
Nmecw1=(2*n1+n2+1)*(n3+1)+1
Nmecw2=2000+(2*n1+n2+1)*(n3+1)+1
Nmecw3=2000+(2*n1+n2+1)*(n3+1)+1+1
Nmecw4=(2*n1+n2+1)*(n3+1)+1+1
Nmecw5=(2*n1+n2+1)*(n3+1)+1+n2+1
Nmecw6=2000+(2*n1+n2+1)*(n3+1)+1+n2+1
Nmecw7=2000+(2*n1+n2+1)*(n3+1)+1+n2+2
Nmecw8=(2*n1+n2+1)*(n3+1)+1+n2+2
### Nodes of master element of the top web
Nmetw1=A9bo2
Nmetw2=2000+A9bo2
Nmetw3=2000+A9bo2+1
Nmetw4=A9bo2+1
Nmetw5=A12bo
Nmetw6=2000+A12bo
Nmetw7=2000+A12bo+1
Nmetw8=A12bo+1
### Nodes of master element of the top flange
Nmetf1=A11bo
Nmetf2=2000+A11bo
Nmetf3=2000+A11bo+1
Nmetf4=A11bo+1
Nmetf5=A11bo+2*n1+n2+1
Nmetf6=2000+A11bo+2*n1+n2+1
Nmetf7=2000+A11bo+2*n1+n2+1+1
Nmetf8=A11bo+2*n1+n2+1+1
### Nodes of master element of the adhesive layer
Nmeal1=A15bo
Nmeal2=2000+A15bo
Nmeal3=2000+A15bo+1
Nmeal4=A15bo+1
Nmeal5=A15bo+2*n1+n2+1
Nmeal6=2000+A15bo+2*n1+n2+1
Nmeal7=2000+A15bo+2*n1+n2+1+1
Nmeal8=A15bo+2*n1+n2+1+1
### Nodes of master element of the FRP plate
```

```
Nmefp1=A5ao
Nmefp2=2000+A5ao
Nmefp3=2000+A5ao+1
Nmefp4=A5ao+1
Nmefp5=A5ao+2*n1+n2+1
Nmefp6=2000+A5ao+2*n1+n2+1
Nmefp7=2000+A5ao+2*n1+n2+1+1
Nmefp8=A5ao+2*n1+n2+1+1
################################################################################
### Master element number
### Master element 1 for bottom flange
Mael1=1
### Master element 1 for bottom web
Mael2=(2*n1+n2)*n3+1
### Master element 1 for center web
Mael3=(2*n1+n2)*n3+1+n2
### Master element 1 for top web
Mael4=(2*n1+n2)*n3+n2*(n4-1)+1
### Master element 1 for top flange
Mael5=(2*n1+n2)*n3+n2*n4+1
### Master element 1 for adhesive layer
Mael6=(2*n1+n2)*n3*2+n2*n4+1
### Master element 1 for bottom flange
Mael7=(2*n1+n2)*n3*2+n2*n4+(2*n1+n2)*n5+1
################################################################################
### Element numbers needs to be generated in Y direction
### For upper layers of bottom flange
numberulbfy=n3-1
### For center web
numberulbfy=n4-2
### Elements numbers needs to be generated in X direction for the flanges
numberelbfx=2*n1+n2
### Parameters related to the NCOPY command
### For right bottom flange part 2
c1=n1+n2
### For left + right flange
c2=A10bo2
################################################################################
eloutput11=(2*n1+n2)*n3+(n4*n2)+1+1000*(n7-2340)
eloutput21=(2*n1+n2)*n3+(n4*n2)+(2*n1+n2)*n5+1000*(n7-2340)
eloutput12=(2*n1+n2)*n3+(n4*n2)+1+1000*(n7-1560)
eloutput22=(2*n1+n2)*n3+(n4*n2)+(2*n1+n2)*n5+1000*(n7-1560)
eloutput13=(2*n1+n2)*n3+(n4*n2)+1+1000*(n7-780)
eloutput23=(2*n1+n2)*n3+(n4*n2)+(2*n1+n2)*n5+1000*(n7-780)
################################################################################
beamcentroidat0=(2*n1+n2+1)*(n3+1)+(n2+1)*(n4/2)-n2/2
beamcentroidatL=2000*n7+(2*n1+n2+1)*(n3+1)+(n2+1)*(n4)/2-n2/2
bottomflangecentroidat0=(2*n1+n2+1)*((n3/2)+1)-n1-n2/2
```

```
bottomflangecentroidatL=2000*n7+(2*n1+n2+1)*((n3/2)+1)-n1-n2/2
upperflangecentroidat0=(2*n1+n2+1)*(n3+1)+(n2+1)*(n4-1)+(2*n1+n2+1)*((n3/2)+1)-n1-n2/2
upperflangecentroidatL=2000*n7+(2*n1+n2+1)*(n3+1)+(n2+1)*(n4-1)+(2*n1+n2+1)*((n3/2)+1)-n1-
n2/2
GFRPcentroidat0=(2*n1+n2+1)*(n3+1)*2+(n2+1)*(n4-1)+(2*n1+n2+1)*(n5-
1)+(2*n1+n2+1)*((n6/2)+1)-n1-n2/2
GFRPcentroidatL=2000*n7+(2*n1+n2+1)*(n3+1)*2+(n2+1)*(n4-1)+(2*n1+n2+1)*(n5-
1)+(2*n1+n2+1)*((n6/2)+1)-n1-n2/2
#################################################################################
*PREPRINT, ECHO=YES, MODEL=YES, HISTORY=YES
**
**Model denifition
*NODE
<A1bo>, 0.0, 0.0, 0.0
<A2bo>, <b1>, 0.0, 0.0
<A3bo>, <b2>, 0.0, 0.0
<A4bo>, <bb>, 0.0, 0.0
<A5bo>, 0.0, <t3>, 0.0
<A6bo>, <b1>, <t3>, 0.0
<A7bo>, <b2>, <t3>, 0.0
<A8bo>, <bb>, <t3>, 0.0
<A9bo1>, <b1>, <YA9bo1>, 0.0
<A10bo1>, <b2>, <YA10bo1>, 0.0
<A9bo2>, <b1>, <YA9bo2>, 0.0
<A10bo2>, <b2>, <YA10bo2>, 0.0
<A11bo>, 0.0, <h1>, 0.0
<A12bo>, <b1>, <h1>, 0.0
<A13bo>, <b2>, <h1>, 0.0
<A14bo>, <bb>, <h1>, 0.0
<A15bo>, 0.0, <h2>, 0.0
<A16bo>, <b1>, <h2>, 0.0
<A17bo>, <b2>, <h2>, 0.0
<A18bo>, <bb>, <h2>, 0.0
**
<A1ao>, 0.0, <ha>, 0.0
<A2ao>, <b1>, <ha>, 0.0
<A3ao>, <b2>, <ha>, 0.0
<A4ao>, <bb>, <ha>, 0.0
<A5ao>, 0.0, <h3>, 0.0
<A6ao>, <b1>, <h3>, 0.0
<A7ao>, <b2>, <h3>, 0.0
<A8ao>, <bb>, <h3>, 0.0
**
<A5po>, 0.0, <h4>, 0.0
<A6po>, <b1>, <h4>, 0.0
<A7po>, <b2>, <h4>, 0.0
<A8po>, <bb>, <h4>, 0.0
**
```

```
<A1bl>, 0.0, 0.0, <L>
<A2bl>, <b1>, 0.0, <L>
<A3bl>, <b2>, 0.0, <L>
<A4bl>, <bb>, 0.0, <L>
<A5bl>, 0.0, <t3>, <L>
<A6bl>, <b1>, <t3>, <L>
<A7bl>, <b2>, <t3>, <L>
<A8bl>, <bb>, <t3>, <L>
<A9bl1>, <b1>, <YA9bo1>, <L>
<A10bl1>, <b2>, <YA10bo1>, <L>
<A9bl2>, <b1>, <YA9bo2>, <L>
<A10bl2>, <b2>, <YA10bo2>, <L>
<A11bl>, 0.0, <h1>, <L>
<A12bl>, <b1>, <h1>, <L>
<A13bl>, <b2>, <h1>, <L>
<A14bl>, <bb>, <h1>, <L>
<A15bl>, 0.0, <h2>, <L>
<A16bl>, <b1>, <h2>, <L>
<A17bl>, <b2>, <h2>, <L>
<A18bl>, <bb>, <h2>, <L>
**
<A1al>, 0.0, <ha>, <L>
<A2al>, <b1>, <ha>, <L>
<A3al>, <b2>, <ha>, <L>
<A4al>, <bb>, <ha>, <L>
<A5al>, 0.0, <h3>, <L>
<A6al>, <b1>, <h3>, <L>
<A7al>, <b2>, <h3>, <L>
<A8al>, <bb>, <h3>, <L>
**
<A5pl>, 0.0, <h4>, <L>
<A6pl>, <b1>, <h4>, <L>
<A7pl>, <b2>, <h4>, <L>
<A8pl>, <bb>, <h4>, <L>
**
**Node set of left bottom edge of bottom flange 1 along z axis
*NGEN, NSET=LBEBF1
<A1bo>, <A1bl>, 2000
**Node set of left upper edge of bottom flange 1 along z axis
*NGEN, NSET=LUEBF1
<A5bo>, <A5bl>, 2000
**Node set of left surface of bottom flange 1 along z axis
*NFILL, NSET=LSBF1
LBEBF1, LUEBF1, <n3>, <nflange1y>
**
**Node set of right bottom edge of bottom flange 1 along z axis
*NGEN, NSET=RBEBF1
<A2bo>, <A2bl>, 2000
```

```
**Node set of right upper edge of bottom flange 1 along z axis
*NGEN, NSET=RUEBF1
<A6bo>, <A6bl>, 2000
**Node set of right surface of bottom flange 1 along z axis
*NFILL, NSET=RSBF1
RBEBF1, RUEBF1, <n3>, <nflange1y>
**
**Node set of bottom flange block 1
*NFILL, NSET=BFB1
LSBF1, RSBF1, <n1>, 1
**
**Node set of bottom flange block 2
*NCOPY, OLDSET=BFB1, CHANGENUMBER=<c1>, NEWSET=BFB2, SHIFT
<b2>, 0.0, 0.0
0.0, 0.0, 0.0, 0.0, 0.0, 1.0, 0.0
**Node set of center bottom flange part
*NSET, NSET=abc1, GENERATE
<A3bo>, <A3bl>, 2000
*NSET, NSET=abc2, GENERATE
<A7bo>, <A7bl>, 2000
*NFILL, NSET=bottomweb1
RBEBF1, abc1, <n2>, 1
*NFILL, NSET=upperbottomweb2
RUEBF1, abc2, <n2>, 1
*NFILL, NSET=centerbottomflange
bottomweb1, upperbottomweb2, <n3>, <nflange1y>
**
**Bottom flange
*NSET, NSET=bottomflange
BFB1, centerbottomflange, BFB2
**Node set of unpper flange
*NCOPY, OLDSET=bottomflange, CHANGENUMBER=<c2>, NEWSET=upperflange, SHIFT
0.0, <h1>, 0.0
0.0, 0.0, 0.0, 0.0, 0.0, 1.0, 0.0
**Node set for the center Web
** Node line at left upper edge of the center web
*NGEN, NSET=LUECW
<A9bo2>, <A9bl2>, 2000
** Node line at right upper edge of the center web
*NGEN, NSET=RUECW
<A10bo2>, <A10bl2>, 2000
** Node set at upper surface of the center web
*NFILL, NSET=USCW
LUECW, RUECW, <n2>, 1
**
** Node line at left bottom edge of the center web
*NGEN, NSET=LBECW
<A9bo1>, <A9bl1>, 2000
```

```
** Node line at right bottom edge of the center web
*NGEN, NSET=RBECW
<A10bo1>, <A10bl1>, 2000
** Node set at bottom surface of the center web
*NFILL, NSET=BSCW
LBECW, RBECW, <n2>, 1
** Forming node set for the center web
*NFILL, NSET=centerweb
BSCW, USCW, <NRYCW>, <nweby>
**
**Node set for adhesive layer
**
**Bottom surface:
**Node line A1a, left bottom edge of adhesive layer
*NGEN, NSET=LBEAL
<A1ao>, <A1al>, 2000
*NGEN, NSET=lineA2a
<A2ao>, <A2al>, 2000
*NFILL, NSET=firstsurfacead
LBEAL, lineA2a, <n1>, 1
**
**Node line A3a, left bottom edge of adhesive layer
*NGEN, NSET=lineA3a
<A3ao>, <A3al>, 2000
*NFILL, NSET=secondsurfacead
lineA2a, lineA3a, <n2>, 1
**
**Node line A4a, left bottom edge of adhesive layer
*NGEN, NSET=lineA4a
<A4ao>, <A4al>, 2000
*NFILL, NSET=thirdsurfacead
lineA3a, lineA4a, <n1>, 1
**
**Bottom surface of adhesive layer
*NSET, NSET=BSAL
firstsurfacead, secondsurfacead, thirdsurfacead
**
**Upper surface:
**Node line A5a, left top edge of adhesive layer
*NGEN, NSET=LTEAL
<A5ao>, <A5al>, 2000
**Node line A6a
*NGEN, NSET=lineA6a
<A6ao>, <A6al>, 2000
**Node line A7a
*NGEN, NSET=lineA7a
<A7ao>, <A7al>, 2000
**Node line A8a, right top edge of adhesive layer
```

```
*NGEN, NSET=RTEAL
<A8ao>, <A8al>, 2000
**Node surface formed by A5a and A6a, A6a and A7a, A7a and A8a
*NFILL, NSET=SFA5aA6a
LTEAL, lineA6a, <n1>, 1
*NFILL, NSET=SFA6aA7a
lineA6a, lineA7a, <n2>, 1
*NFILL, NSET=SFA7aA8a
lineA7a, RTEAL, <n1>, 1
*NSET, NSET=uppersurfacead
SFA5aA6a, SFA6aA7a, SFA7aA8a
**
**Node set for adhesive layer:
*NFILL, NSET=adhesivelayernodeset
BSAL, uppersurfacead, <NRYUAD>, <nflange1y>
**
**Node set for GFRP plate
**
**Upper surface:
**Node line A5p, left top edge of GFRP plate
*NGEN, NSET=LTEGFRP
<A5po>, <A5pl>, 2000
**Node line A6p
*NGEN, NSET=lineA6p
<A6po>, <A6pl>, 2000
**Node line A7p
*NGEN, NSET=lineA7p
<A7po>, <A7pl>, 2000
**Node line A8p, right top edge of GFRP plate
*NGEN, NSET=RTEGFRP
<A8po>, <A8pl>, 2000
**Node surface formed by A5p and A6p, A6p and A7p, A7p and A8p
*NFILL, NSET=SFA5pA6p
LTEGFRP, lineA6p, <n1>, 1
*NFILL, NSET=SFA6pA7p
lineA6p, lineA7p, <n2>, 1
*NFILL, NSET=SFA7pA8p
lineA7p, RTEGFRP, <n1>, 1
*NSET, NSET=uppersurfacegfrp
SFA5pA6p, SFA6pA7p, SFA7pA8p
**
**Node set for GFRP plate:
*NFILL, NSET=gfrpplatenodeset
uppersurfacead, uppersurfacegfrp, <n6>, <nflange1y>
**
**Element generation
**
**Bottom flange:
```

```
**Creating master element for bottom flange
*ELEMENT, TYPE=C3D8R, ELSET=MAELBF
1, <Nmeblbf1>, <Nmeblbf2>, <Nmeblbf3>, <Nmeblbf4>, <Nmeblbf5>, <Nmeblbf6>, <Nmeblbf7>,
<Nmeblbf8>
**Creating element for bottom flange
*ELGEN, ELSET=elbottomflange
1, <numberelbfx>, <nflange1x>, <elflange1x>, <n3>, <nflange1y>, <elflange1y>, <n7>, <nflange1z>,
<elflange1z>
**
**Bottom web part:
**Creating master element for bottom web part
*ELEMENT, TYPE=C3D8R, ELSET=MAELBW
<Mael2>, <Nmebw1>, <Nmebw2>, <Nmebw3>, <Nmebw4>, <Nmebw5>, <Nmebw6>, <Nmebw7>,
<Nmebw8>
**Creating element for bottom web part
*ELGEN, ELSET=elebottomweb
<Mael2>, <n2>, <nwebx>, <elwebx>, 1, <nweby>, <elweby>, <n7>, <nwebz>, <elwebz>
**
**Center web part:
**Creating master element for center web part
*ELEMENT, TYPE=C3D8R, ELSET=MAELCW
<Mael3>, <Nmecw1>, <Nmecw2>, <Nmecw3>, <Nmecw4>, <Nmecw5>, <Nmecw6>, <Nmecw7>,
<Nmecw8>
**Creating element for center web part
*ELGEN, ELSET=elecenterweb
<Mael3>, <n2>, <nwebx>, <elwebx>, <numberulbfy>, <nweby>, <elweby>, <n7>, <nwebz>,
<elwebz>
**
**Top web part:
**Creating master element for top web part
*ELEMENT, TYPE=C3D8R, ELSET=MAELTW
<Mael4>, <Nmetw1>, <Nmetw2>, <Nmetw3>, <Nmetw4>, <Nmetw5>, <Nmetw6>, <Nmetw7>,
<Nmetw8>
**Creating element for top web part
*ELGEN, ELSET=eletopweb
<Mael4>, <n2>, <nwebx>, <elwebx>, 1, <nweby>, <elweby>, <n7>, <nwebz>, <elwebz>
**
**Top flange:
**Creating master element for top flange
*ELEMENT, TYPE=C3D8R, ELSET=MAELTF
<Mael5>, <Nmetf1>, <Nmetf2>, <Nmetf3>, <Nmetf4>, <Nmetf5>, <Nmetf6>, <Nmetf7>, <Nmetf8>
**Creating element for top flange
*ELGEN, ELSET=eltopflange
<Mael5>, <numberelbfx>, <nflange1x>, <elflange1x>, <n3>, <nflange1y>, <elflange1y>, <n7>,
<nflange1z>, <elflange1z>
**
*ELSET, ELSET=wideflangebeam
elbottomflange, elebottomweb, elecenterweb, eletopweb, eltopflange
```

```
**
**Adhesive layer:
**Creating master element for adhesive layer
*ELEMENT, TYPE=C3D8R, ELSET=MAELAd
<Mael6>, <Nmeal1>, <Nmeal2>, <Nmeal3>, <Nmeal4>, <Nmeal5>, <Nmeal6>, <Nmeal7>,
<Nmeal8>
**Creating element for adhesive layer
*ELGEN, ELSET=eladhesivelayer
<Mael6>, <numberelbfx>, <nflange1x>, <elflange1x>, <n5>, <nflange1y>, <elflange1y>, <n7>,
<nflange1z>, <elflange1z>
**
**GFRP plate:
**Creating master element for GFRP plate
*ELEMENT, TYPE=C3D8R, ELSET=MAELGFRP
<Mael7>, <Nmefp1>, <Nmefp2>, <Nmefp3>, <Nmefp4>, <Nmefp5>, <Nmefp6>, <Nmefp7>,
<Nmefp8>
**Creating element for adhesive layer
*ELGEN, ELSET=elGFRPplate
<Mael7>, <numberelbfx>, <nflange1x>, <elflange1x>, <n6>, <nflange1y>, <elflange1y>, <n7>,
<nflange1z>, <elflange1z>
**
**Defining nodes that is fixed at z=0
*NSET, NSET=Startsection, GENERATE
1, <A8po>, 1
**
**Defining the 1st surface where loads are applied
*ELSET, ELSET=bottomflangeatfreeend, GENERATE
<firstelementatL>, <secondelementatL>, 1
*SURFACE, TYPE=ELEMENT, NAME=BOTTOMFLANGESURFACE
bottomflangeatfreeend, S4
**
**Defining the 2st surface where loads are applied
*ELSET, ELSET=upperflangeatfreeend, GENERATE
<thirdelementatL>, <fourthelementatL>, 1
*SURFACE, TYPE=ELEMENT, NAME=UPPERFLANGESURFACE
upperflangeatfreeend, S4
**
**Defining output set for adhesive layer
*ELSET, ELSET=adhesiveoutputsets, GENERATE
<eloutput11>, <eloutput21>, 1
<eloutput12>, <eloutput22>, 1
<eloutput13>, <eloutput23>, 1
**
**Defining output dipslcement of nodes
*NSET, NSET=beamcentroid, GENERATE
<beamcentroidat0>, <beamcentroidatL>, 2000
*NSET, NSET=bottomflangecentroid, GENERATE
<bottomflangecentroidat0>, <bottomflangecentroidatL>, 2000
```

```
*NSET, NSET=upperflangecentroid, GENERATE
<upperflangecentroidat0>, <upperflangecentroidatL>, 2000
*NSET, NSET=GFRPcentroid, GENERATE
<GFRPcentroidat0>, <GFRPcentroidatL>, 2000
**
*SOLID SECTION, ELSET=wideflangebeam, MATERIAL=STEEL
*MATERIAL, NAME=STEEL
*ELASTIC, TYPE=ISOTROPIC
<Eb>, <v>
*SOLID SECTION, ELSET=eladhesivelayer, MATERIAL=ADHESIVE
*MATERIAL, NAME=ADHESIVE
*ELASTIC, TYPE=ISOTROPIC
<Ea>, <v>
*SOLID SECTION, ELSET=elGFRPplate, MATERIAL=FRPmat
*MATERIAL, NAME=FRPmat
*ELASTIC, TYPE=ISOTROPIC
<Ep>, <v>
**
** History data
**
*STEP
*STATIC
*DSLOAD
BOTTOMFLANGESURFACE, TRSHR, 2490, 1.0, 0.0, 0.0
UPPERFLANGESURFACE, TRSHR, -2490, 1.0, 0.0, 0.0
*BOUNDARY
Startsection,1,3
*NODE PRINT
U,
RF,
*NODE PRINT, NSET=beamcentroid
U,
*NODE PRINT, NSET=bottomflangecentroid
U,
*NODE PRINT, NSET=upperflangecentroid
U,
*NODE PRINT, NSET=GFRPcentroid
U,
*EL PRINT
S,
*EL PRINT, ELSET=adhesiveoutputsets
E,
*END STEP
```